



University of HUDDERSFIELD

University of Huddersfield Repository

Asim, Taimoor

Computational Fluid Dynamics Based Diagnostics and Optimal Design of Hydraulic Capsule Pipelines

Original Citation

Asim, Taimoor (2013) Computational Fluid Dynamics Based Diagnostics and Optimal Design of Hydraulic Capsule Pipelines. Doctoral thesis, University of Huddersfield.

This version is available at <http://eprints.hud.ac.uk/id/eprint/17805/>

The University Repository is a digital collection of the research output of the University, available on Open Access. Copyright and Moral Rights for the items on this site are retained by the individual author and/or other copyright owners. Users may access full items free of charge; copies of full text items generally can be reproduced, displayed or performed and given to third parties in any format or medium for personal research or study, educational or not-for-profit purposes without prior permission or charge, provided:

- The authors, title and full bibliographic details is credited in any copy;
- A hyperlink and/or URL is included for the original metadata page; and
- The content is not changed in any way.

For more information, including our policy and submission procedure, please contact the Repository Team at: E.mailbox@hud.ac.uk.

<http://eprints.hud.ac.uk/>

COMPUTATIONAL FLUID DYNAMICS BASED DIAGNOSTICS AND OPTIMAL DESIGN OF HYDRAULIC CAPSULE PIPELINES

A THESIS SUBMITTED IN PARTIAL FULFILMENT OF THE REQUIREMENTS FOR THE
DEGREE OF DOCTOR OF PHILOSOPHY AT THE UNIVERSITY OF HUDDERSFIELD

by

Taimoor Asim

B.Eng. National University of Sciences and Technology, PAK, 2007

M.Sc. University of Huddersfield, UK, 2008

Director of Research: Prof. Rakesh Mishra

Leader of Energy, Emissions and the Environment Research Group

School of Computing and Engineering

University of Huddersfield

UK

February 2013

In memory of my beloved mother Mrs. Khushnood Aftab (late)



ABSTRACT

Scarcity of fossil fuels and rapid escalation in the energy prices around the world is affecting efficiency of established modes of cargo transport within transportation industry. Extensive research is being carried out on improving efficiency of existing modes of cargo transport, as well as to develop alternative means of transporting goods. One such alternative method can be through the use of energy contained within fluid flowing in pipelines in order to transfer goods from one place to another. Although the concept of using fluid pipelines for transportation purposes has been in practice for more than a millennium now, but the detailed knowledge of the flow behaviour in such pipelines is still a subject of active research. This is due to the fact that most of the studies conducted on transporting goods in pipelines are based on experimental measurements of global flow parameters, and only a rough approximation of the local flow behaviour within these pipelines has been reported. With the emergence of sophisticated analytical tools and the use of high performance computing facilities being installed throughout the globe, it is now possible to simulate the flow conditions within these pipelines and get better understanding of the underlying flow phenomena.

The present study focuses on the use of advanced modelling tools to simulate the flow within Hydraulic Capsule Pipelines (HCPs) in order to quantify the flow behaviour within such pipelines. Hydraulic Capsule Pipeline is the term which refers to the transport of goods in hollow containers, typically of spherical or cylindrical shapes, termed as capsules, being carried along the pipeline by water. A novel modelling technique has been employed to carry out the investigations under various geometric and flow conditions within HCPs.

Both qualitative and quantitative flow diagnostics has been carried out on the flow of both spherical and cylindrical shaped capsules in a horizontal HCP for on-shore applications. A train of capsules consisting of a single to multiple capsules per unit length of the pipeline has been modelled for practical flow velocities within HCPs. It has been observed that the flow behaviour within HCP depends on a number of fluid and geometric parameters. The pressure drop in such pipelines cannot be predicted from established methods. Development of a predictive tool for such applications is one of the aims that is been achieved in this study. Furthermore, investigations have been conducted on vertical pipelines as well, which are very important for off-shore applications of HCPs. The energy requirements for vertical HCPs are significantly higher than horizontal HCPs. It has been shown that a minimum average flow velocity is required to transport a capsule in a vertical HCP, depending upon the geometric and physical properties of the capsules. The concentric propagation, along the centreline of pipe, of heavy density capsules in vertical HCPs marks a significant variation from horizontal HCPs transporting heavy density capsules.

Bends are an integral part of pipeline networks. In order to design any pipeline, it is essential to consider the effects of the bends on the overall energy requirements within the pipelines. In order to accurately design both horizontal and vertical HCPs, analysis of the flow behaviour and energy requirements, of varying geometric configurations, has been carried out. A novel modelling technique has been incorporated in order to accurately predict the velocity, trajectory and orientation of the capsules in pipe bends.

Optimisation of HCPs plays a crucial role towards worldwide commercial acceptability of such pipelines. Based on Least-Cost Principle, an optimisation methodology has been developed for single stage HCPs for both on-shore and off-shore applications. The input to the optimisation model is the solid throughput required from the system, and the outputs are the optimal diameter of the HCPs and the pumping requirements for the capsule transporting system. The optimisation model presented in the present study is both robust and user-friendly.

A complete flow diagnostics and design, including optimisation, of Hydraulic Capsule Pipelines has been presented in this study. The advanced computational skills being incorporated in this study has made it possible to map and analyse the flow structure within HCPs. Detailed analysis on even the smallest scale flow variations in HCPs has led to a better understanding of the flow behaviour.

DECLARATION

- The author of this thesis (including any appendices and/or schedules to this thesis) owns any copyright in it (the “Copyright”) and he has given The University of Huddersfield the right to use such Copyright for any administrative, promotional, educational and/or teaching purposes.
- Copies of this thesis, either in full or in extracts, may be made only in accordance with the regulations of the University Library. Details of these regulations may be obtained from the Librarian. This page must form part of any such copies made.
- The ownership of any patents, designs, trademarks and any and all other intellectual property rights except for the Copyright (the “Intellectual Property Rights”) and any reproductions of copyright works, for example graphs and tables (“Reproductions”), which may be described in this thesis, may not be owned by the author and may be owned by third parties. Such Intellectual Property Rights and Reproductions cannot and must not be made available for use without the prior written permission of the owner(s) of the relevant Intellectual Property Rights and/or Reproductions.

ACKNOWLEDGEMENTS

It is a great pleasure to acknowledge the efforts and support of those who have, directly or indirectly, contributed towards the creation of this thesis. Foremost, I would like to thank almighty Allah for giving me the opportunity to be on this planet and contribute in whatever capacity I can, towards the betterment of the human race. Secondly, I would like to acknowledge the contributions made by my parents, Mr. and Mrs. Aftab Iqbal, in terms of moral, emotional and financial support throughout my growing years and especially my mother who always took great interest in my academic carrier.

No other person, living or dead, has directly contributed more than my supervisor Prof. Rakesh Mishra towards making this thesis a reality. His constant efforts, guidance and support have always been iconic to me. His dynamic nature, versatile skills and command over Fluid Dynamics helped me learn a lot from him. I would like to thank him for teaching me scientific writing skills and for the opportunity of participation in various international conferences. One simply could not wish a better or friendlier supervisor.

I would like to acknowledge the support and friendship of my colleagues at the Energy, Emissions and Environment Research group at the University of Huddersfield, especially my co-supervisor Prof. Vasudeva Rao for his considerable help in the modelling and design of fluid flows. I would like to acknowledge the support provided by other research groups such as Diagnostics, CPT and HPC to name a few of them. I would also like to acknowledge the support of the administrative staff at the School of Computing and Engineering and the technicians in both the Technology and Canal Side buildings at the University of Huddersfield. Furthermore, I would like to acknowledge the researchers around the globe whose work has been reproduced in this thesis without permission, in the form of figures (mostly in Chapter 2). I presume that they wouldn't have disagreed to reproduce their work if I would have contacted them, which I wouldn't able to do due to shortage of time and in some cases due to insufficient contact information.

Last but not least, I would like to thank my better half, Somia Taimoor, and my son, Arham Taimoor, for their patience and constant support throughout my PhD journey. Without their help, I wouldn't be able to achieve this.

CONTENTS

ABSTRACT	iv
DECLARATION	vi
ACKNOWLEDGEMENTS	vii
CONTENTS	viii
LIST OF FIGURES	xiv
LIST OF TABLES	xxviii
NOMENCLATURE	xxx
SYMBOLS	xxxii
SUBSCRIPTS	xxxiii
CHAPTER 1 INTRODUCTION	1
1.1. Pipeline Transport	2
1.2. Pressure Drop Considerations in Hydraulic Pipelines.....	3
1.2.1. Horizontal Pipelines	4
1.2.2. Vertical Pipelines.....	5
1.2.3. Pipeline Bends	6
1.3. Transport of Capsules in Pipelines	6
1.4. History of Hydraulic Capsule Pipelines	7
1.5. Components of a Hydraulic Capsule Pipeline	9
1.5.1. Pump.....	9
1.5.2. Capsules.....	10
1.5.3. Capsule Injection System	10
1.5.4. Capsule Ejection System	11
1.6. Mechanics of Transportation of Solids in Pipelines	11
1.6.1. Design Considerations for Pipelines Transporting Capsules.....	12
1.7. Pressure Drop Considerations in Hydraulic Capsule Pipelines	14
1.7.1. Horizontal Pipelines	15
1.7.2. Vertical Pipelines.....	15

1.7.3.	Pipeline Bends	16
1.8.	Motivation	17
1.9.	Research Aims.....	18
1.10.	Organization of Thesis.....	19
CHAPTER 2	LITERATURE REVIEW	21
2.1.	Horizontal HCPs.....	22
2.1.1.	Summary of Literature regarding Horizontal HCPs.....	28
2.2.	Vertical HCPs.....	28
2.2.1.	Summary of Literature regarding Vertical HCPs	31
2.3.	HCP Bends	32
2.3.1.	Summary of Literature regarding HCP Bends.....	34
2.4.	HCP's Optimisation.....	35
2.4.1.	Summary of Literature regarding Optimisation of HCPs.....	37
2.5.	Scope of Research	37
2.6.	Specific Research Objectives	38
CHAPTER 3	CFD MODELLING OF HYDRAULIC CAPSULE PIPELINES	39
3.1.	Pre-Processing	40
3.1.1.	Pipe and Bend Geometries	40
3.1.2.	Capsule Geometries.....	41
3.1.3.	Meshing of the Flow Domain.....	44
3.2.	Solver Execution	45
3.2.1.	Selection of the Physical Models.....	45
3.2.2.	Defining Material Properties and Operating Conditions	47
3.2.3.	Boundary Conditions.....	47
3.2.4.	Capsule Velocities in Horizontal HCPs.....	48
3.2.5.	Capsule Velocities in Vertical HCPs.....	53
3.2.6.	Capsule Velocities in Bends	54
3.2.7.	Solver Settings.....	55
3.2.8.	Convergence Criteria.....	56
CHAPTER 4	ANALYSIS OF HORIZONTAL PIPELINES TRANSPORTING CAPSULES	57
4.1.	Analysis of Single Phase Flow in a Horizontal Pipe	58
4.2.	Analysis of Horizontal Pipelines Transporting Capsules	63

4.3.	Mesh Independence Tests.....	63
4.4.	Benchmark Tests	64
4.5.	Analysis of the Flow of Equi-Density Spherical Capsules in a Horizontal HCP	65
4.5.1.	Average Flow Velocity Effects	68
4.5.2.	Capsule Diameter Effects	70
4.5.3.	Capsule Concentration Effects	71
4.5.4.	Effects of Spacing between the Capsules	72
4.6.	Analysis of the Flow of Equi-Density Cylindrical Capsules in a Horizontal HCP	76
4.6.1.	Average Flow Velocity Effects	78
4.6.2.	Length of the Capsule Effects	80
4.6.3.	Capsule Diameter Effects	81
4.6.4.	Capsule Concentration Effects	81
4.6.5.	Effects of Spacing between the Capsules	83
4.7.	Analysis of the Flow of Heavy-Density Spherical Capsules in a Horizontal HCP	87
4.7.1.	Average Flow Velocity Effects	90
4.7.2.	Capsule Diameter Effects	91
4.7.3.	Capsule Concentration Effects	92
4.7.4.	Effects of Spacing between the Capsules	93
4.8.	Analysis of the Flow of Heavy-Density Cylindrical Capsules in a Horizontal HCP	96
4.8.1.	Average Flow Velocity Effects	99
4.8.2.	Length of the Capsule Effects	100
4.8.3.	Capsule Diameter Effects	101
4.8.4.	Capsule Concentration Effects	102
4.8.5.	Effects of Spacing between the Capsules	103
4.9.	Prediction Models.....	107
4.10.	Summary of the Analysis of a Horizontal HCP.....	110
CHAPTER 5		
	ANALYSIS OF VERTICAL PIPELINES TRANSPORTING CAPSULES	112
5.1.	Analysis of Single Phase Flow in a Vertical Pipe	113
5.2.	Analysis of the Flow of Equi-Density Spherical Capsules in a Vertical HCP	116
5.2.1.	Average Flow Velocity Effects	119
5.2.2.	Capsule Diameter Effects	120
5.2.3.	Capsule Concentration Effects	121

5.2.4.	Effects of Spacing between the Capsules	123
5.3.	Analysis of the Flow of Equi-Density Cylindrical Capsules in a Vertical HCP	126
5.3.1.	Average Flow Velocity Effects	128
5.3.2.	Length of the Capsule Effects	130
5.3.3.	Capsule Diameter Effects	131
5.3.4.	Capsule Concentration Effects	131
5.3.5.	Effects of Spacing between the Capsules	132
5.4.	Analysis of the Flow of Heavy-Density Spherical Capsules in a Vertical HCP	136
5.4.1.	Average Flow Velocity Effects	140
5.4.2.	Capsule Diameter Effects	141
5.4.3.	Capsule Concentration Effects	142
5.4.4.	Effects of Spacing between the Capsules	144
5.5.	Analysis of the Flow of Heavy-Density Cylindrical Capsules in a Vertical HCP.....	146
5.5.1.	Average Flow Velocity Effects	149
5.5.2.	Length of the Capsule Effects	151
5.5.3.	Capsule Diameter Effects	152
5.5.4.	Capsule Concentration Effects	153
5.5.5.	Effects of Spacing between the Capsules	154
5.6.	Prediction Models.....	157
5.7.	Summary of the Analysis of a Vertical HCP	160
CHAPTER 6	ANALYSIS OF BENDS TRANSPORTING CAPSULES.....	161
6.1.	Analysis of Single Phase Flow in Horizontal Bends	162
6.1.1.	Average Flow Velocity Effects	162
6.1.2.	Effects of Radius of Curvature	163
6.2.	Analysis of the Flow of Equi-Density Capsules in Horizontal Bends.....	164
6.2.1.	Average Flow Velocity Effects	164
6.2.2.	Capsule Diameter Effects	165
6.2.3.	Capsule Concentration Effects	166
6.2.4.	Effects of Spacing between the Capsules	166
6.2.5.	Effects of Radius of Curvature of the Bend.....	167
6.2.6.	Capsule Shape Effects	168
6.2.7.	Length of the Capsule Effects	168

6.3.	Analysis of the Flow of Heavy-Density Capsules in Horizontal Bends.....	169
6.3.1.	Average Flow Velocity Effects	170
6.3.2.	Capsule Diameter Effects	171
6.3.3.	Capsule Concentration Effects	171
6.3.4.	Effects of Spacing between the Capsules	172
6.3.5.	Effects of Radius of Curvature of the Bend.....	173
6.3.6.	Capsule Shape Effects	173
6.3.7.	Length of the Capsule Effects	174
6.4.	Analysis of Single Phase Flow in Vertical Bends	175
6.4.1.	Average Flow Velocity Effects	175
6.4.2.	Effects of Radius of Curvature	176
6.5.	Analysis of the Flow of Equi-Density Capsules in Vertical Bends.....	177
6.5.1.	Average Flow Velocity Effects	178
6.5.2.	Capsule Diameter Effects	178
6.5.3.	Capsule Concentration Effects	179
6.5.4.	Effects of Spacing between the Capsules	180
6.5.5.	Effects of Radius of Curvature of the Bend.....	180
6.5.6.	Capsule Shape Effects	181
6.5.7.	Length of the Capsule Effects	182
6.6.	Analysis of the Flow of Heavy-Density Capsules in Vertical Bends.....	182
6.6.1.	Average Flow Velocity Effects	183
6.6.2.	Capsule Diameter Effects	184
6.6.3.	Capsule Concentration Effects	184
6.6.4.	Effects of Spacing between the Capsules	185
6.6.5.	Effects of Radius of Curvature of the Bend.....	186
6.6.6.	Capsule Shape Effects	186
6.6.7.	Length of the Capsule Effects	187
6.7.	Prediction Models.....	188
6.8.	Summary of the Analysis of a HCP Bends.....	191
CHAPTER 7	OPTIMISATION OF HCPS.....	193
7.1.	Introduction	194
7.2.	Optimisation of HCPS.....	194

7.3.	Cost of Pipes.....	195
7.4.	Cost of Capsules	195
7.5.	Cost of Power	195
7.6.	Mixture Flow Rate.....	196
7.7.	Total Pressure Drop.....	196
7.8.	Solid Throughput.....	197
7.9.	Working of the Optimisation Model	198
7.10.	Limitations of the Optimisation Model	201
7.11.	Design Example for On-Shore Applications	201
7.11.1.	Comparison of the Optimisation Model w.r.t. Agarwal et. al.'s [66] Optimisation Model.....	205
7.11.2.	Capsule Shape Effects	206
7.11.3.	Effects of the Density of the Capsules.....	211
7.12.	Design Example for Off-Shore Applications	215
7.12.1.	Capsule Shape Effects	219
7.12.2.	Effects of the Density of the Capsules.....	223
7.13.	Summary of HCP's Optimisation.....	226
CHAPTER 8	CONCLUSIONS	228
8.1.	Research Problem Synopsis.....	229
8.2.	Research Aims and Major Achievements.....	229
8.3.	Thesis Conclusions.....	232
8.4.	Thesis Contributions.....	236
8.5.	Recommendations for Future Work	237
REFERENCES	239
APPENDICES	247
A-1:	Computational Fluid Dynamics	247
A-2:	Capsule Velocities.....	253
A-3:	Pressure Drop in Horizontal HCPs.....	280
A-4:	Pressure Drop in Vertical HCPs.....	290
A-5:	Pressure Drop in HCP Bends	300
A-6:	Expressions for Capsule Velocities and Friction Factor in HCPs.....	305
LIST OF PUBLICATIONS	309

LIST OF FIGURES

Figure 1.1. Flow in a Horizontal Pipe	3
Figure 1.2. The Lilo-1 system [12]	8
Figure 1.3. Sumitomo Metal Industries [13]	8
Figure 1.4. Magplane Technology [15]	9
Figure 1.5. Top View of Pump for Pipelines transporting Capsules [16]	10
Figure 1.6. Capsule Injection System (a) Side View (b) Top View [18]	11
Figure 2.1. Prediction of Holdup in Equi-Density Spherical Capsules [24]	23
Figure 2.2. Relation between $\Delta P/L_m$ and Re of Mixture based on Experiments [26]	24
Figure 2.3. Characteristics near Capsule for (a) Elastic and (b) Rigid Capsule Models [32]	26
Figure 2.4. The Predicted Effect of k on the Holdup at various Solid Throughputs	27
Figure 2.5. The Relation between the Balance Velocity and the Inclination Angle (a) $k = 0.664$ (b) $k = 0.507$ (c) $k = 0.403$ [46]	29
Figure 2.6. Distributions of Turbulent Intensity (a) $k = 0.9$ (b) $k = 0.67$ [47]	30
Figure 2.7. Pneumatic, Steadily Moving Capsule [50]	31
Figure 2.8. Effect of Bend Central Angle on Velocity Ratio of Capsule in Bend [53]	32
Figure 2.9. Pressure Losses through Various Regions in a Horizontal Bend [57]	33
Figure 2.10. Single and Multiphase Pressure Drop [61]	34
Figure 2.11. Operation of TLIM Capsule Pump [63]	35
Figure 2.12. Hoist Description [65]	36
Figure 3.1. Geometry of the Pipe	40
Figure 3.2. Geometry of the Bends	41
Figure 3.3. Geometry of Equi-Density Spherical Capsules	42

Figure 3.4. Geometry of Heavy-Density Cylindrical Capsules	42
Figure 3.5. Trajectory of Heavy-Density Spherical Capsules in HCP Bends	43
Figure 3.6. Trajectory of Equi-Density Cylindrical Capsules in HCP Bends	44
Figure 3.7. Meshing of the Flow Domain	45
Figure 3.8. Experimental data for Equi-Density Spherical Capsule in a Horizontal Pipeline	48
Figure 3.9. Curve fitting on the experimental data for Equi-Density Spherical Capsule in a Horizontal Pipeline	
Figure 3.10. Experimental data for Heavy-Density Spherical Capsule in a Horizontal Pipeline	50
Figure 3.11. Curve fitting for Heavy-Density Spherical Capsule in a Horizontal Pipeline	51
Figure 3.12. Experimental data for Heavy-Density Cylindrical Capsule in a Horizontal Pipeline	52
Figure 3.13. Curve fitting for Heavy-Density Cylindrical Capsule in a Horizontal Pipeline	53
Figure 4.1. Pressure Variations for Water Flow in a Horizontal Pipe	58
Figure 4.2. Variations in C_p for Water Flow in a Horizontal Pipe	59
Figure 4.3. Velocity Distribution for Water Flow in a Horizontal Pipe	61
Figure 4.4. Velocity Profile for Water Flow in a Horizontal Pipe	61
Figure 4.5. Entrance Length Effects for Water Flow in a Horizontal Pipe	62
Figure 4.6. Analysis Line for the flow of (a) An Equi-Density Spherical Capsule (b) A Heavy-Density Cylindrical Capsule, in a Horizontal Pipe	63
Figure 4.7. Validation of the CFD results w.r.t. the Experimental results, for the Pressure Drop in a Horizontal Pipe, Transporting Equi-Density Spherical Capsules, at Various Flow Velocities	65
Figure 4.8. Variations in (a) Pressure and (b) Velocity, for a Single Spherical Capsule of $k = 0.5$ in a Horizontal Pipe at $V_{av} = 1\text{m/sec}$	66
Figure 4.9. (a) Variations in C_p for a Single Spherical Capsule of $k = 0.5$ in a Horizontal Pipe at $V_{av} = 1\text{m/sec}$ (b) Variations in u/u_{max} for a Single Spherical Capsule of $k = 0.5$ in a Horizontal Pipe at $V_{av} = 1\text{m/sec}$	67
Figure 4.10. Variations in the Cross-Sectional Velocity Profiles for a Single Spherical Capsule of $k = 0.5$ in a Horizontal Pipe at $V_{av} = 1\text{m/sec}$ at (a) Upstream and (b) Downstream of the Capsule	68
Figure 4.11. Development of Velocity Profile in the Presence of a Single Spherical Capsule in a Horizontal Pipe having Density Equal to Water	68

Figure 4.12. Variations in (a) Pressure and (b) Velocity, for a Single Spherical Capsule of $k = 0.5$ in a Horizontal Pipe at $V_{av} = 4\text{m/sec}$	69
Figure 4.13. (a) Variations in C_p for a Single Spherical Capsule of $k = 0.5$ in a Horizontal Pipe at $V_{av} = 4\text{m/sec}$ (b) Variations in u/u_{max} for a Single Spherical Capsule of $k = 0.5$ in a Horizontal Pipe at $V_{av} = 4\text{m/sec}$	69
Figure 4.14. Variations in (a) Pressure and (b) Velocity, for a Single Spherical Capsule of $k = 0.9$ in a Horizontal Pipe at $V_{av} = 1\text{m/sec}$	70
Figure 4.15. (a) Variations in C_p for a Single Spherical Capsule of $k = 0.5$ in a Horizontal Pipe at $V_{av} = 1\text{m/sec}$ (b) Variations in u/u_{max} for a Single Spherical Capsule of $k = 0.5$ in a Horizontal Pipe at $V_{av} = 1\text{m/sec}$	71
Figure 4.16. Variations in (a) Pressure and (b) Velocity, for Three Spherical Capsules of $k = 0.5$ and $Sc = 1 * d$ in a Horizontal Pipe at $V_{av} = 1\text{m/sec}$	71
Figure 4.17. (a) Variations in C_p for Three Spherical Capsules of $k = 0.5$ and $Sc = 1 * d$ in a Horizontal Pipe at $V_{av} = 1\text{m/sec}$ (b) Variations in u/u_{max} for Three Spherical Capsules of $k = 0.5$ and $Sc = 1 * d$ in a Horizontal Pipe at $V_{av} = 1\text{m/sec}$	72
Figure 4.18. Variations in (a) Pressure and (b) Velocity, for Three Spherical Capsules of $k = 0.5$ and $Sc = 5 * d$ in a Horizontal Pipe at $V_{av} = 1\text{m/sec}$	73
Figure 4.19. (a) Variations in C_p for Three Spherical Capsules of $k = 0.5$ and $Sc = 5 * d$ in a Horizontal Pipe at $V_{av} = 1\text{m/sec}$ (b) Variations in u/u_{max} for Three Spherical Capsules of $k = 0.5$ and $Sc = 5 * d$ in a Horizontal Pipe at $V_{av} = 1\text{m/sec}$	73
Figure 4.20. Variations in Normalised Pressure Drop for a Single Equi-Density Spherical Capsule in a Horizontal Pipe	74
Figure 4.21. Variations in Normalised Pressure Drop for Three Equi-Density Spherical Capsules in a Horizontal Pipe	75
Figure 4.22. Variations in Normalised Pressure Drop for Three Spherical Capsules of $k = 0.7$ in a Horizontal Pipe	75
Figure 4.23. Variations in (a) Pressure and (b) Velocity, for a Cylindrical Capsule of $k = 0.5$ and $L_c = 1 * d$ in a Horizontal Pipe at $V_{av} = 1\text{m/sec}$	76
Figure 4.24. (a) Variations in C_p for a Cylindrical Capsule of $k = 0.5$ and $L_c = 1 * d$ in a Horizontal Pipe at $V_{av} = 1\text{m/sec}$ (b) Variations in u/u_{max} for a Cylindrical Capsule of $k = 0.5$ and $L_c = 1 * d$ in a Horizontal Pipe at $V_{av} = 1\text{m/sec}$	77
Figure 4.25. Variations in the Cross-Sectional Velocity Profiles for a Single Cylindrical Capsule of $k = 0.5$ and $L_c = 1 * d$ in a Horizontal Pipe at $V_{av} = 1\text{m/sec}$ at (a) Upstream and (b) Downstream of the Capsule	78
Figure 4.26. Development of Velocity Profile in the Presence of a Single Cylindrical Capsule in a Horizontal Pipe having Density Equal to Water	78

Figure 4.27. Variations in (a) Pressure and (b) Velocity, for a Cylindrical Capsule of $k = 0.5$ and $L_c = 1 * d$ in a Horizontal Pipe at $V_{av} = 4m/sec$	79
Figure 4.28. (a) Variations in C_p for a Cylindrical Capsule of $k = 0.5$ and $L_c = 1 * d$ in a Horizontal Pipe at $V_{av} = 4m/sec$ (b) Variations in u/u_{max} for a Cylindrical Capsule of $k = 0.5$ and $L_c = 1 * d$ in a Horizontal Pipe at $V_{av} = 4m/sec$	79
Figure 4.29. Variations in (a) Pressure and (b) Velocity, for a Single Cylindrical Capsule of $k = 0.5$ and $L_c = 5 * d$ in a Horizontal Pipe at $V_{av} = 1m/sec$	80
Figure 4.30. (a) Variations in C_p for a Single Cylindrical Capsule of $k = 0.5$ and $L_c = 5 * d$ in a Horizontal Pipe at $V_{av} = 1m/sec$ (b) Variations in u/u_{max} for a Single Cylindrical Capsule of $k = 0.5$ and $L_c = 5 * d$ in a Horizontal Pipe at $V_{av} = 1m/sec$	80
Figure 4.31. (a) Variations in Pressure for a Single Cylindrical Capsule of $k = 0.9$ and $L_c = 5 * d$ in a Horizontal Pipe at $V_{av} = 1m/sec$ (b) Variations in C_p for a Single Cylindrical Capsule of $k = 0.9$ and $L_c = 5 * d$ in a Horizontal Pipe at $V_{av} = 1m/sec$	81
Figure 4.32. Variations in (a) Pressure and (b) Velocity, for Two Cylindrical Capsules of $k = 0.5$, Sc and $L_c = 1 * d$ in a Horizontal Pipe at $V_{av} = 1m/sec$	82
Figure 4.33. (a) Variations in C_p for Two Cylindrical Capsules of $k = 0.5$, Sc and $L_c = 1 * d$ in a Horizontal Pipe at $V_{av} = 1m/sec$ (b) Variations in u/u_{max} for Two Cylindrical Capsules of $k = 0.5$, Sc and $L_c = 1 * d$ in a Horizontal Pipe at $V_{av} = 1m/sec$	82
Figure 4.34. Variations in (a) Pressure and (b) Velocity, for Two Cylindrical Capsules of $k = 0.5$, $Sc = 5 * d$ and $L_c = 1 * d$ in a Horizontal Pipe at $V_{av} = 1m/sec$	83
Figure 4.35. (a) Variations in C_p for Two Cylindrical Capsules of $k = 0.5$, $Sc = 5 * d$ and $L_c = 1 * d$ in a Horizontal Pipe at $V_{av} = 1m/sec$ (b) Variations in u/u_{max} for Two Cylindrical Capsules of $k = 0.5$, $Sc = 5 * d$ and $L_c = 1 * d$ in a Horizontal Pipe at $V_{av} = 1m/sec$	84
Figure 4.36. Variations in Normalised Pressure Drop for a Single Equi-Density Cylindrical Capsule of $L_c = 1 * d$ in a Horizontal Pipe	84
Figure 4.37. Variations in Normalised Pressure Drop for a Single Equi-Density Cylindrical Capsule of $k = 0.7$ in a Horizontal Pipe	85
Figure 4.38. Variations in Normalised Pressure Drop for Two Equi-Density Cylindrical Capsules of $L_c = 1 * d$ and $Sc = 1 * d$ in a Horizontal Pipe	86
Figure 4.39. Variations in Normalised Pressure Drop for Two Equi-Density Cylindrical Capsules of $L_c = 1 * d$ and $k = 0.7$ in a Horizontal Pipe	86
Figure 4.40. Variations in (a) Pressure and (b) Velocity, for a Single Spherical Capsule of $k = 0.5$ in a Horizontal Pipe at $V_{av} = 1m/sec$	87
Figure 4.41. (a) Variations in C_p for a Single Spherical Capsule of $k = 0.5$ in a Horizontal Pipe at $V_{av} = 1m/sec$ (b) Variations in u/u_{max} for a Single Spherical Capsule of $k = 0.5$ in a Horizontal Pipe at $V_{av} = 1m/sec$	88

Figure 4.42. Variations in the Cross-Sectional Velocity Profiles for a Single Spherical Capsule of $k = 0.5$ in a Horizontal Pipe at $V_{av} = 1\text{m/sec}$ at (a) Upstream and (b) Downstream of the Capsule	89
Figure 4.43. Development of Velocity Profile in the Presence of a Single Spherical Capsule in a Horizontal Pipe having Density Greater than Water	89
Figure 4.44. Variations in (a) Pressure and (b) Velocity, for a Single Spherical Capsule of $k = 0.5$ in a Horizontal Pipe at $V_{av} = 4\text{m/sec}$	90
Figure 4.45. (a) Variations in C_p for a Single Spherical Capsule of $k = 0.5$ in a Horizontal Pipe at $V_{av} = 4\text{m/sec}$ (b) Variations in u/u_{max} for a Single Spherical Capsule of $k = 0.5$ in a Horizontal Pipe at $V_{av} = 4\text{m/sec}$	91
Figure 4.46. Variations in (a) Pressure and (b) Velocity, for a Single Spherical Capsule of $k = 0.9$ in a Horizontal Pipe at $V_{av} = 1\text{m/sec}$	91
Figure 4.47. (a) Variations in C_p for a Single Spherical Capsule of $k = 0.5$ in a Horizontal Pipe at $V_{av} = 1\text{m/sec}$ (b) Variations in u/u_{max} for a Single Spherical Capsule of $k = 0.5$ in a Horizontal Pipe at $V_{av} = 1\text{m/sec}$	92
Figure 4.48. Variations in (a) Pressure and (b) Velocity, for Three Spherical Capsules of $k = 0.5$ and $Sc = 1 * d$ in a Horizontal Pipe at $V_{av} = 1\text{m/sec}$	93
Figure 4.49. (a) Variations in C_p for Three Spherical Capsules of $k = 0.5$ and $Sc = 1 * d$ in a Horizontal Pipe at $V_{av} = 1\text{m/sec}$ (b) Variations in u/u_{max} for Three Spherical Capsules of $k = 0.5$ and $Sc = 1 * d$ in a Horizontal Pipe at $V_{av} = 1\text{m/sec}$	93
Figure 4.50. Variations in (a) Pressure and (b) Velocity, for Three Spherical Capsules of $k = 0.5$ and $Sc = 5 * d$ in a Horizontal Pipe at $V_{av} = 1\text{m/sec}$	94
Figure 4.51. (a) Variations in C_p for Three Spherical Capsules of $k = 0.5$ and $Sc = 5 * d$ in a Horizontal Pipe at $V_{av} = 1\text{m/sec}$ (b) Variations in u/u_{max} for Three Spherical Capsules of $k = 0.5$ and $Sc = 5 * d$ in a Horizontal Pipe at $V_{av} = 1\text{m/sec}$	94
Figure 4.52. Variations in Normalised Pressure Drop for Three Heavy-Density Spherical Capsules in a Horizontal Pipe	95
Figure 4.53. Variations in Normalised Pressure Drop for Two Spherical Capsules of $k = 0.7$ in a Horizontal Pipe	96
Figure 4.54. Variations in (a) Pressure and (b) Velocity, for a Cylindrical Capsule of $k = 0.5$ and $L_c = 1 * d$ in a Horizontal Pipe at $V_{av} = 1\text{m/sec}$	97
Figure 4.55. (a) Variations in C_p for a Cylindrical Capsule of $k = 0.5$ and $L_c = 1 * d$ in a Horizontal Pipe at $V_{av} = 1\text{m/sec}$ (b) Variations in u/u_{max} for a Cylindrical Capsule of $k = 0.5$ and $L_c = 1 * d$ in a Horizontal Pipe at $V_{av} = 1\text{m/sec}$	97
Figure 4.56. Variations in the Cross-Sectional Velocity Profiles for a Single Cylindrical Capsule of $k = 0.5$ and $L_c = 1 * d$ in a Horizontal Pipe at $V_{av} = 1\text{m/sec}$ at (a) Upstream and (b) Downstream of the Capsule	98

Figure 4.57. Development of Velocity Profile in the Presence of a Single Cylindrical Capsule in a Horizontal Pipe having Density Equal to Water	98
Figure 4.58. Variations in (a) Pressure and (b) Velocity, for a Cylindrical Capsule of $k = 0.5$ and $L_c = 1 * d$ in a Horizontal Pipe at $V_{av} = 4m/sec$	99
Figure 4.59. (a) Variations in C_p for a Cylindrical Capsule of $k = 0.5$ and $L_c = 1 * d$ in a Horizontal Pipe at $V_{av} = 4m/sec$ (b) Variations in u/u_{max} for a Cylindrical Capsule of $k = 0.5$ and $L_c = 1 * d$ in a Horizontal Pipe at $V_{av} = 4m/sec$	100
Figure 4.60. Variations in (a) Pressure and (b) Velocity, for a Single Cylindrical Capsule of $k = 0.5$ and $L_c = 5 * d$ in a Horizontal Pipe at $V_{av} = 1m/sec$	100
Figure 4.61. (a) Variations in C_p for a Single Cylindrical Capsule of $k = 0.5$ and $L_c = 5 * d$ in a Horizontal Pipe at $V_{av} = 1m/sec$ (b) Variations in u/u_{max} for a Single Cylindrical Capsule of $k = 0.5$ and $L_c = 5 * d$ in a Horizontal Pipe at $V_{av} = 1m/sec$	101
Figure 4.62. (a) Variations in Pressure for a Single Cylindrical Capsule of $k = 0.9$ and $L_c = 5 * d$ in a Horizontal Pipe at $V_{av} = 1m/sec$ (b) Variations in C_p for a Single Cylindrical Capsule of $k = 0.9$ and $L_c = 5 * d$ in a Horizontal Pipe at $V_{av} = 1m/sec$	102
Figure 4.63. Variations in (a) Pressure and (b) Velocity, for Two Cylindrical Capsules of $k = 0.5$, Sc and $L_c = 1 * d$ in a Horizontal Pipe at $V_{av} = 1m/sec$	102
Figure 4.64. (a) Variations in C_p for Two Cylindrical Capsules of $k = 0.5$, Sc and $L_c = 1 * d$ in a Horizontal Pipe at $V_{av} = 1m/sec$ (b) Variations in u/u_{max} for Two Cylindrical Capsules of $k = 0.5$, Sc and $L_c = 1 * d$ in a Horizontal Pipe at $V_{av} = 1m/sec$	103
Figure 4.65. Variations in (a) Pressure and (b) Velocity, for Two Cylindrical Capsules of $k = 0.5$, $Sc = 5 * d$ and $L_c = 1 * d$ in a Horizontal Pipe at $V_{av} = 1m/sec$	104
Figure 4.66. (a) Variations in C_p for Two Cylindrical Capsules of $k = 0.5$, $Sc = 5 * d$ and $L_c = 1 * d$ in a Horizontal Pipe at $V_{av} = 1m/sec$ (b) Variations in u/u_{max} for Two Cylindrical Capsules of $k = 0.5$, $Sc = 5 * d$ and $L_c = 1 * d$ in a Horizontal Pipe at $V_{av} = 1m/sec$	104
Figure 4.67. Variations in Normalised Pressure Drop for a Single Heavy-Density Cylindrical Capsule of $L_c = 1 * d$ in a Horizontal Pipe	105
Figure 4.68. Variations in Normalised Pressure Drop for Two Heavy-Density Cylindrical Capsules of $L_c = 1 * d$ and $Sc = 1 * d$ in a Horizontal Pipe	106
Figure 4.69. Variations in Normalised Pressure Drop for Two Heavy-Density Cylindrical Capsules of $k = 0.7$ and $Sc = 1 * d$ in a Horizontal Pipe	106
Figure 4.70. Variations in Normalised Pressure Drop for Two Heavy-Density Cylindrical Capsules of $k = 0.7$ and $L_c = 1 * d$ in a Horizontal Pipe	107
Figure 4.71. f_c for Equi-Density Spherical Capsules	109

Figure 4.72. f_c for Heavy-Density Cylindrical Capsules	110
Figure 5.1. Pressure variations for Water Flow in a Vertical Pipe	113
Figure 5.2. Variations in C_p for Water Flow in a Vertical Pipe	114
Figure 5.3. Velocity distribution for Water Flow in a Vertical Pipe	115
Figure 5.4. Velocity Profile for Water Flow in a Vertical Pipe	115
Figure 5.5. Variations in (a) Pressure and (b) Velocity, for a Single Spherical Capsule of $k = 0.5$ in a Vertical Pipe at $V_{av} = 1\text{m/sec}$	116
Figure 5.6. (a) Variations in C_p for a Single Spherical Capsule of $k = 0.5$ in a Vertical Pipe at $V_{av} = 1\text{m/sec}$ (b) Variations in u/u_{max} for a Single Spherical Capsule of $k = 0.5$ in a Vertical Pipe at $V_{av} = 1\text{m/sec}$	117
Figure 5.7. Variations in the Cross-Sectional Velocity Profiles for a Single Spherical Capsule of $k = 0.5$ in a Vertical Pipe at $V_{av} = 1\text{m/sec}$ at (a) Upstream and (b) Downstream of the Capsule	118
Figure 5.8. Development of Velocity Profile in the Presence of a Single Spherical Capsule in a Vertical Pipe having Density Equal to Water	118
Figure 5.9. Variations in (a) Pressure and (b) Velocity, for a Single Spherical Capsule of $k = 0.5$ in a Vertical Pipe at $V_{av} = 4\text{m/sec}$	119
Figure 5.10. (a) Variations in C_p for a Single Spherical Capsule of $k = 0.5$ in a Vertical Pipe at $V_{av} = 4\text{m/sec}$ (b) Variations in u/u_{max} for a Single Spherical Capsule of $k = 0.5$ in a Vertical Pipe at $V_{av} = 4\text{m/sec}$	120
Figure 5.11. Variations in (a) Pressure and (b) Velocity, for a Single Spherical Capsule of $k = 0.9$ in a Vertical Pipe at $V_{av} = 1\text{m/sec}$	120
Figure 5.12. (a) Variations in C_p for a Single Spherical Capsule of $k = 0.5$ in a Vertical Pipe at $V_{av} = 1\text{m/sec}$ (b) Variations in u/u_{max} for a Single Spherical Capsule of $k = 0.5$ in a Vertical Pipe at $V_{av} = 1\text{m/sec}$	121
Figure 5.13. Variations in (a) Pressure and (b) Velocity, for Three Spherical Capsules of $k = 0.5$ and $Sc = 1 * d$ in a Vertical Pipe at $V_{av} = 1\text{m/sec}$	122
Figure 5.14. (a) Variations in C_p for Three Spherical Capsules of $k = 0.5$ and $Sc = 1 * d$ in a Vertical Pipe at $V_{av} = 1\text{m/sec}$ (b) Variations in u/u_{max} for Three Spherical Capsules of $k = 0.5$ and $Sc = 1 * d$ in a Vertical Pipe at $V_{av} = 1\text{m/sec}$	122
Figure 5.15. Variations in (a) Pressure and (b) Velocity, for Three Spherical Capsules of $k = 0.5$ and $Sc = 5 * d$ in a Vertical Pipe at $V_{av} = 1\text{m/sec}$	123
Figure 5.16. (a) Variations in C_p for Three Spherical Capsules of $k = 0.5$ and $Sc = 5 * d$ in a Vertical Pipe at $V_{av} = 1\text{m/sec}$ (b) Variations in u/u_{max} for Three Spherical Capsules of $k = 0.5$ and $Sc = 5 * d$ in a Vertical Pipe at $V_{av} = 1\text{m/sec}$	123

Figure 5.17. Variations in Normalised Pressure Drop for a Single Equi-Density Spherical Capsule in a Vertical Pipe	124
Figure 5.18. Variations in Normalised Pressure Drop for Three Equi-Density Spherical Capsules in a Vertical Pipe	125
Figure 5.19. Variations in Normalised Pressure Drop for Three Spherical Capsules of $k = 0.7$ in a Vertical Pipe	125
Figure 5.20. Variations in (a) Pressure and (b) Velocity, for a Cylindrical Capsule of $k = 0.5$ and $L_c = 1 * d$ in a Vertical Pipe at $V_{av} = 1\text{m/sec}$	126
Figure 5.21. (a) Variations in C_p for a Cylindrical Capsule of $k = 0.5$ and $L_c = 1 * d$ in a Vertical Pipe at $V_{av} = 1\text{m/sec}$ (b) Variations in u/u_{max} for a Cylindrical Capsule of $k = 0.5$ and $L_c = 1 * d$ in a Vertical Pipe at $V_{av} = 1\text{m/sec}$	127
Figure 5.22. Variations in the Cross-Sectional Velocity Profiles for a Single Cylindrical Capsule of $k = 0.5$ and $L_c = 1 * d$ in a Vertical Pipe at $V_{av} = 1\text{m/sec}$ at (a) Upstream and (b) Downstream of the Capsule	127
Figure 5.23. Development of Velocity Profile in the Presence of a Single Cylindrical Capsule in a Vertical Pipe having Density Equal to Water	128
Figure 5.24. Variations in (a) Pressure and (b) Velocity, for a Cylindrical Capsule of $k = 0.5$ and $L_c = 1 * d$ in a Vertical Pipe at $V_{av} = 4\text{m/sec}$	129
Figure 5.25. (a) Variations in C_p for a Cylindrical Capsule of $k = 0.5$ and $L_c = 1 * d$ in a Vertical Pipe at $V_{av} = 4\text{m/sec}$ (b) Variations in u/u_{max} for a Cylindrical Capsule of $k = 0.5$ and $L_c = 1 * d$ in a Vertical Pipe at $V_{av} = 4\text{m/sec}$	129
Figure 5.26. Variations in (a) Pressure and (b) Velocity, for a Single Cylindrical Capsule of $k = 0.5$ and $L_c = 5 * d$ in a Vertical Pipe at $V_{av} = 1\text{m/sec}$	130
Figure 5.27. (a) Variations in C_p for a Single Cylindrical Capsule of $k = 0.5$ and $L_c = 5 * d$ in a Vertical Pipe at $V_{av} = 1\text{m/sec}$ (b) Variations in u/u_{max} for a Single Cylindrical Capsule of $k = 0.5$ and $L_c = 5 * d$ in a Vertical Pipe at $V_{av} = 1\text{m/sec}$	130
Figure 5.28. (a) Variations in Pressure for a Single Cylindrical Capsule of $k = 0.9$ and $L_c = 5 * d$ in a Vertical Pipe at $V_{av} = 1\text{m/sec}$ (b) Variations in C_p for a Single Cylindrical Capsule of $k = 0.9$ and $L_c = 5 * d$ in a Vertical Pipe at $V_{av} = 1\text{m/sec}$	131
Figure 5.29. Variations in (a) Pressure and (b) Velocity, for Two Cylindrical Capsules of $k = 0.5$, Sc and $L_c = 1 * d$ in a Vertical Pipe at $V_{av} = 1\text{m/sec}$	132
Figure 5.30. (a) Variations in C_p for Two Cylindrical Capsules of $k = 0.5$, Sc and $L_c = 1 * d$ in a Vertical Pipe at $V_{av} = 1\text{m/sec}$ (b) Variations in u/u_{max} for Two Cylindrical Capsules of $k = 0.5$, Sc and $L_c = 1 * d$ in a Vertical Pipe at $V_{av} = 1\text{m/sec}$	132
Figure 5.31. Variations in (a) Pressure and (b) Velocity, for Two Cylindrical Capsules of $k = 0.5$, $Sc = 5 * d$ and $L_c = 5 * d$ in a Vertical Pipe at $V_{av} = 1\text{m/sec}$	133

Figure 5.32. (a) Variations in C_p for Two Cylindrical Capsules of $k = 0.5$, $Sc = 5 * d$ and $L_c = 5 * d$ in a Vertical Pipe at $V_{av} = 1\text{m/sec}$ (b) Variations in u/u_{max} for Two Cylindrical Capsules of $k = 0.5$, $Sc = 5 * d$ and $L_c = 5 * d$ in a Vertical Pipe at $V_{av} = 1\text{m/sec}$	133
Figure 5.33. Variations in Normalised Pressure Drop for a Single Equi-Density Cylindrical Capsule of $L_c = 1 * d$ in a Vertical Pipe	134
Figure 5.34. Variations in Normalised Pressure Drop for a Single Equi-Density Cylindrical Capsule of $k = 0.7$ in a Vertical Pipe	135
Figure 5.35. Variations in Normalised Pressure Drop for Two Equi-Density Cylindrical Capsules of $L_c = 1 * d$ and $Sc = 1 * d$ in a Vertical Pipe	135
Figure 5.36. Variations in Normalised Pressure Drop for Two Equi-Density Cylindrical Capsules of $L_c = 1 * d$ and $k = 0.7$ in a Vertical Pipe	136
Figure 5.37. Variations in (a) Pressure and (b) Velocity, for a Single Spherical Capsule of $k = 0.5$ in a Vertical Pipe at $V_{av} = 2\text{m/sec}$	137
Figure 5.38. (a) Variations in C_p for a Single Spherical Capsule of $k = 0.5$ in a Vertical Pipe at $V_{av} = 2\text{m/sec}$ (b) Variations in u/u_{max} for a Single Spherical Capsule of $k = 0.5$ in a Vertical Pipe at $V_{av} = 2\text{m/sec}$	138
Figure 5.39. Variations in the Cross-Sectional Velocity Profiles for a Single Spherical Capsule of $k = 0.5$ in a Vertical Pipe at $V_{av} = 2\text{m/sec}$ at (a) Upstream and (b) Downstream of the Capsule	139
Figure 5.40. Development of Velocity Profile in the Presence of a Single Spherical Capsule in a Vertical Pipe having Density Greater than Water	139
Figure 5.41. Variations in (a) Pressure and (b) Velocity, for a Single Spherical Capsule of $k = 0.5$ in a Vertical Pipe at $V_{av} = 4\text{m/sec}$	140
Figure 5.42. (a) Variations in C_p for a Single Spherical Capsule of $k = 0.5$ in a Vertical Pipe at $V_{av} = 4\text{m/sec}$ (b) Variations in u/u_{max} for a Single Spherical Capsule of $k = 0.5$ in a Vertical Pipe at $V_{av} = 4\text{m/sec}$	141
Figure 5.43. (a) Variations in Pressure for a Single Spherical Capsule of $k = 0.9$ in a Vertical Pipe at $V_{av} = 1\text{m/sec}$ (b) Variations in C_p for a Single Spherical Capsule of $k = 0.9$ in a Vertical Pipe at $V_{av} = 1\text{m/sec}$	141
Figure 5.44. (a) Variations in C_p for a Single Spherical Capsule of $k = 0.5$ in a Vertical Pipe at $V_{av} = 1\text{m/sec}$ (b) Variations in u/u_{max} for a Single Spherical Capsule of $k = 0.5$ in a Vertical Pipe at $V_{av} = 1\text{m/sec}$	142
Figure 5.45. Variations in (a) Pressure and (b) Velocity, for Three Spherical Capsules of $k = 0.5$ and $Sc = 1 * d$ in a Vertical Pipe at $V_{av} = 2\text{m/sec}$	143
Figure 5.46. (a) Variations in C_p for Three Spherical Capsules of $k = 0.5$ and $Sc = 1 * d$ in a Vertical Pipe at $V_{av} = 2\text{m/sec}$ (b) Variations in u/u_{max} for Three Spherical Capsules of $k = 0.5$ and $Sc = 1 * d$ in a Vertical Pipe at $V_{av} = 2\text{m/sec}$	143
Figure 5.47. Variations in (a) Pressure and (b) Velocity, for Three Spherical Capsules of $k = 0.5$ and $Sc = 5 * d$ in a Vertical Pipe at $V_{av} = 2\text{m/sec}$	144

Figure 5.48. (a) Variations in C_p for Three Spherical Capsules of $k = 0.5$ and $Sc = 5 * d$ in a Vertical Pipe at $V_{av} = 2m/sec$ (b) Variations in u/u_{max} for Three Spherical Capsules of $k = 0.5$ and $Sc = 5 * d$ in a Vertical Pipe at $V_{av} = 2m/sec$	144
Figure 5.49. Variations in Normalised Pressure Drop for a Heavy-Density Spherical Capsule in a Vertical Pipe	145
Figure 5.50. Variations in Normalised Pressure Drop for Three Spherical Capsules of $Sc = 1 * d$ in a Vertical Pipe	146
Figure 5.51. Variations in (a) Pressure and (b) Velocity, for a Cylindrical Capsule of $k = 0.5$ and $L_c = 1 * d$ in a Vertical Pipe at $V_{av} = 2m/sec$	147
Figure 5.52. (a) Variations in C_p for a Cylindrical Capsule of $k = 0.5$ and $L_c = 1 * d$ in a Vertical Pipe at $V_{av} = 2m/sec$ (b) Variations in u/u_{max} for a Cylindrical Capsule of $k = 0.5$ and $L_c = 1 * d$ in a Vertical Pipe at $V_{av} = 2m/sec$	147
Figure 5.53. Variations in the Cross-Sectional Velocity Profiles for a Single Cylindrical Capsule of $k = 0.5$ and $L_c = 1 * d$ in a Vertical Pipe at $V_{av} = 2m/sec$ at (a) Upstream and (b) Downstream of the Capsule	148
Figure 5.54. Development of Velocity Profile in the Presence of a Single Cylindrical Capsule in a Vertical Pipe having Density Equal to Water	149
Figure 5.55. Variations in (a) Pressure and (b) Velocity, for a Cylindrical Capsule of $k = 0.5$ and $L_c = 1 * d$ in a Vertical Pipe at $V_{av} = 4m/sec$	150
Figure 5.56. (a) Variations in C_p for a Cylindrical Capsule of $k = 0.5$ and $L_c = 1 * d$ in a Vertical Pipe at $V_{av} = 4m/sec$ (b) Variations in u/u_{max} for a Cylindrical Capsule of $k = 0.5$ and $L_c = 1 * d$ in a Vertical Pipe at $V_{av} = 4m/sec$	150
Figure 5.57. Variations in (a) Pressure and (b) Velocity, for a Single Cylindrical Capsule of $k = 0.5$ and $L_c = 5 * d$ in a Vertical Pipe at $V_{av} = 3m/sec$	151
Figure 5.58. (a) Variations in C_p for a Single Cylindrical Capsule of $k = 0.5$ and $L_c = 5 * d$ in a Vertical Pipe at $V_{av} = 2m/sec$ (b) Variations in u/u_{max} for a Single Cylindrical Capsule of $k = 0.5$ and $L_c = 5 * d$ in a Vertical Pipe at $V_{av} = 3m/sec$	152
Figure 5.59. Variations in Pressure for a Single Cylindrical Capsule of $k = 0.9$ and $L_c = 5 * d$ in a Vertical Pipe at $V_{av} = 1m/sec$ (b) Variations in C_p for a Single Cylindrical Capsule of $k = 0.9$ and $L_c = 5 * d$ in a Vertical Pipe at $V_{av} = 1m/sec$	152
Figure 5.60. Variations in (a) Pressure and (b) Velocity, for Two Cylindrical Capsules of $k = 0.5$, Sc and $L_c = 1 * d$ in a Vertical Pipe at $V_{av} = 2m/sec$	153
Figure 5.61. (a) Variations in C_p for Two Cylindrical Capsules of $k = 0.5$, Sc and $L_c = 1 * d$ in a Vertical Pipe at $V_{av} = 2m/sec$ (b) Variations in u/u_{max} for Two Cylindrical Capsules of $k = 0.5$, Sc and $L_c = 1 * d$ in a Vertical Pipe at $V_{av} = 2m/sec$	153

Figure 5.62. Variations in (a) Pressure and (b) Velocity, for Two Cylindrical Capsules of $k = 0.5$, $Sc = 5 * d$ and $Lc = 1 * d$ in a Vertical Pipe at $V_{av} = 4m/sec$	154
Figure 5.63. (a) Variations in C_p for Two Cylindrical Capsules of $k = 0.5$, $Sc = 5 * d$ and $Lc = 1 * d$ in a Vertical Pipe at $V_{av} = 2m/sec$ (b) Variations in u/u_{max} for Two Cylindrical Capsules of $k = 0.5$, $Sc = 5 * d$ and $Lc = 1 * d$ in a Vertical Pipe at $V_{av} = 4m/sec$	154
Figure 5.64. Variations in Normalised Pressure Drop for a Single Heavy-Density Cylindrical Capsule of $Lc = 1 * d$ in a Vertical Pipe	155
Figure 5.65. Variations in Normalised Pressure Drop for Two Heavy-Density Cylindrical Capsules of $Lc = 1 * d$ and $Sc = 1 * d$ in a Vertical Pipe	156
Figure 5.66. Variations in Normalised Pressure Drop for Two Heavy-Density Cylindrical Capsules of $k = 0.7$ and $Sc = 1 * d$ in a Vertical Pipe	156
Figure 5.67. Variations in Normalised Pressure Drop for Two Heavy-Density Cylindrical Capsules of $k = 0.7$ and $Lc = 1 * d$ in a Vertical Pipe	157
Figure 5.68. f_c for Equi-Density Spherical Capsules	159
Figure 5.69. f_c for Heavy-Density Cylindrical Capsules	159
Figure 6.1. Variations in (a) Pressure and (b) Velocity, for a Single Phase Flow in a Horizontal Bend of $r/R = 4$ at $V_{av} = 1m/sec$	162
Figure 6.2. Variations in (a) Pressure and (b) Velocity, for a Single Phase Flow in a Horizontal Bend of $r/R = 4$ at $V_{av} = 4m/sec$	163
Figure 6.3. Variations in (a) Pressure and (b) Velocity, for a Single Phase Flow in a Horizontal Bend of $r/R = 8$ at $V_{av} = 1m/sec$	163
Figure 6.4. Variations in (a) Pressure and (b) Velocity, for a Single Equi-Density Spherical Capsule of $k = 0.5$ at $V_{av} = 1m/sec$ in a Horizontal Bend of $r/R = 4$	164
Figure 6.5. Variations in (a) Pressure and (b) Velocity, for a Single Equi-Density Spherical Capsule of $k = 0.5$ at $V_{av} = 4m/sec$ in a Horizontal Bend of $r/R = 4$	165
Figure 6.6. Variations in (a) Pressure and (b) Velocity, for a Single Equi-Density Spherical Capsule of $k = 0.7$ at $V_{av} = 1m/sec$ in a Horizontal Bend of $r/R = 4$	165
Figure 6.7. Variations in (a) Pressure and (b) Velocity, for Two Equi-Density Spherical Capsules of $k = 0.7$ and $Sc = 1 * d$ at $V_{av} = 1m/sec$ in a Horizontal Bend of $r/R = 4$	166
Figure 6.8. Variations in (a) Pressure and (b) Velocity, for Two Equi-Density Spherical Capsules of $k = 0.7$ and $Sc = 3 * d$ at $V_{av} = 1m/sec$ in a Horizontal Bend of $r/R = 4$	167
Figure 6.9. Variations in (a) Pressure and (b) Velocity, for Two Equi-Density Spherical Capsules of $k = 0.7$ and $Sc = 3 * d$ at $V_{av} = 1m/sec$ in a Horizontal Bend of $r/R = 8$	167

Figure 6.10. Variations in (a) Pressure and (b) Velocity, for Two Equi-Density Cylindrical Capsules of $k = 0.7$, $Sc = 1 * d$ and $Lc = 1 * d$ at $V_{av} = 1\text{m/sec}$ in a Horizontal Bend of $r/R = 4$	168
Figure 6.11. Variations in (a) Pressure and (b) Velocity, for Two Equi-Density Cylindrical Capsules of $k = 0.7$, $Sc = 1 * d$ and $Lc = 2 * d$ at $V_{av} = 1\text{m/sec}$ in a Horizontal Bend of $r/R = 4$	169
Figure 6.12. Variations in (a) Pressure and (b) Velocity, for a Single Heavy-Density Spherical Capsule of $k = 0.5$ at $V_{av} = 1\text{m/sec}$ in a Horizontal Bend of $r/R = 4$	170
Figure 6.13. Variations in (a) Pressure and (b) Velocity, for a Single Heavy-Density Spherical Capsule of $k = 0.5$ at $V_{av} = 4\text{m/sec}$ in a Horizontal Bend of $r/R = 4$	170
Figure 6.14. Variations in (a) Pressure and (b) Velocity, for a Single Heavy-Density Spherical Capsule of $k = 0.7$ at $V_{av} = 1\text{m/sec}$ in a Horizontal Bend of $r/R = 4$	171
Figure 6.15. Variations in (a) Pressure and (b) Velocity, for Two Heavy-Density Spherical Capsules of $k = 0.7$ and $Sc = 1 * d$ at $V_{av} = 1\text{m/sec}$ in a Horizontal Bend of $r/R = 4$	172
Figure 6.16. Variations in (a) Pressure and (b) Velocity, for Two Heavy-Density Spherical Capsules of $k = 0.7$ and $Sc = 3 * d$ at $V_{av} = 1\text{m/sec}$ in a Horizontal Bend of $r/R = 4$	172
Figure 6.17. Variations in (a) Pressure and (b) Velocity, for Two Heavy-Density Spherical Capsules of $k = 0.7$ and $Sc = 3 * d$ at $V_{av} = 1\text{m/sec}$ in a Horizontal Bend of $r/R = 8$	173
Figure 6.18. Variations in (a) Pressure and (b) Velocity, for Two Heavy-Density Cylindrical Capsules of $k = 0.7$, $Sc = 1 * d$ and $Lc = 1 * d$ at $V_{av} = 1\text{m/sec}$ in a Horizontal Bend of $r/R = 4$	174
Figure 6.19. Variations in (a) Pressure and (b) Velocity, for Two Heavy-Density Cylindrical Capsules of $k = 0.7$, $Sc = 1 * d$ and $Lc = 2 * d$ at $V_{av} = 1\text{m/sec}$ in a Horizontal Bend of $r/R = 4$	174
Figure 6.20. Variations in (a) Pressure and (b) Velocity, for a Single Phase Flow in a Vertical Bend of $r/R = 4$ at $V_{av} = 1\text{m/sec}$	175
Figure 6.21. Variations in (a) Pressure and (b) Velocity, for a Single Phase Flow in a Vertical Bend of $r/R = 4$ at $V_{av} = 4\text{m/sec}$	176
Figure 6.22. Variations in (a) Pressure and (b) Velocity, for a Single Phase Flow in a Vertical Bend of $r/R = 8$ at $V_{av} = 1\text{m/sec}$	177
Figure 6.23. Variations in (a) Pressure and (b) Velocity, for a Single Equi-Density Spherical Capsule of $k = 0.5$ at $V_{av} = 1\text{m/sec}$ in a Vertical Bend of $r/R = 4$	177
Figure 6.24. Variations in (a) Pressure and (b) Velocity, for a Single Equi-Density Spherical Capsule of $k = 0.5$ at $V_{av} = 4\text{m/sec}$ in a Vertical Bend of $r/R = 4$	178
Figure 6.25. Variations in (a) Pressure and (b) Velocity, for a Single Equi-Density Spherical Capsule of $k = 0.7$ at $V_{av} = 1\text{m/sec}$ in a Vertical Bend of $r/R = 4$	179

Figure 6.26. Variations in (a) Pressure and (b) Velocity, for Two Equi-Density Spherical Capsules of $k = 0.7$ and $Sc = 1 * d$ at $V_{av} = 1\text{m/sec}$ in a Vertical Bend of $r/R = 4$	179
Figure 6.27. Variations in (a) Pressure and (b) Velocity, for Two Equi-Density Spherical Capsules of $k = 0.7$ and $Sc = 3 * d$ at $V_{av} = 1\text{m/sec}$ in a Vertical Bend of $r/R = 4$	180
Figure 6.28. Variations in (a) Pressure and (b) Velocity, for Two Equi-Density Spherical Capsules of $k = 0.7$ and $Sc = 3 * d$ at $V_{av} = 1\text{m/sec}$ in a Vertical Bend of $r/R = 8$	181
Figure 6.29. Variations in (a) Pressure and (b) Velocity, for Two Equi-Density Cylindrical Capsules of $k = 0.7$, $Sc = 1 * d$ and $L_c = 1 * d$ at $V_{av} = 1\text{m/sec}$ in a Vertical Bend of $r/R = 4$	181
Figure 6.30. Variations in (a) Pressure and (b) Velocity, for Two Equi-Density Cylindrical Capsules of $k = 0.7$, $Sc = 1 * d$ and $L_c = 2 * d$ at $V_{av} = 1\text{m/sec}$ in a Vertical Bend of $r/R = 4$	182
Figure 6.31. Variations in (a) Pressure and (b) Velocity, for a Single Heavy-Density Spherical Capsule of $k = 0.5$ at $V_{av} = 1\text{m/sec}$ in a Vertical Bend of $r/R = 4$	183
Figure 6.32. Variations in (a) Pressure and (b) Velocity, for a Single Heavy-Density Spherical Capsule of $k = 0.5$ at $V_{av} = 4\text{m/sec}$ in a Vertical Bend of $r/R = 4$	183
Figure 6.33. Variations in (a) Pressure and (b) Velocity, for a Single Heavy-Density Spherical Capsule of $k = 0.7$ at $V_{av} = 1\text{m/sec}$ in a Vertical Bend of $r/R = 4$	184
Figure 6.34. Variations in (a) Pressure and (b) Velocity, for Two Heavy-Density Spherical Capsules of $k = 0.7$ and $Sc = 1 * d$ at $V_{av} = 1\text{m/sec}$ in a Vertical Bend of $r/R = 4$	185
Figure 6.35. Variations in (a) Pressure and (b) Velocity, for Two Heavy-Density Spherical Capsules of $k = 0.7$ and $Sc = 3 * d$ at $V_{av} = 1\text{m/sec}$ in a Vertical Bend of $r/R = 4$	185
Figure 6.36. Variations in (a) Pressure and (b) Velocity, for Two Heavy-Density Spherical Capsules of $k = 0.7$ and $Sc = 3 * d$ at $V_{av} = 1\text{m/sec}$ in a Vertical Bend of $r/R = 8$	186
Figure 6.37. Variations in (a) Pressure and (b) Velocity, for Two Heavy-Density Cylindrical Capsules of $k = 0.7$, $Sc = 1 * d$ and $L_c = 1 * d$ at $V_{av} = 1\text{m/sec}$ in a Vertical Bend of $r/R = 4$	187
Figure 6.38. Variations in (a) Pressure and (b) Velocity, for Two Heavy-Density Cylindrical Capsules of $k = 0.7$, $Sc = 1 * d$ and $L_c = 2 * d$ at $V_{av} = 1\text{m/sec}$ in a Vertical Bend of $r/R = 4$	187
Figure 6.39. K_{lc} for Equi-Density Spherical Capsules in a Horizontal Bend	190
Figure 6.40. K_{lc} for Heavy-Density Cylindrical Capsules in a Vertical Bend	191
Figure 7.1. Flow Chart of the Optimisation Methodology	200
Figure 7.2. Variations in Operating and Operating Costs w.r.t. Pipeline Diameter	202
Figure 7.3. Variations in Total Cost and Pumping Power Required at Various Pipeline Diameters	203

Figure 7.4. Variations in Capsule Velocity and Total Pressure Drop w.r.t. Pipeline Diameter	204
Figure 7.5. Variations in Optimal Diameter and Pumping Power w.r.t. the Solid Throughput	205
Figure 7.6. Comparison of Various Costs of the Pipeline for Spherical and Cylindrical Capsules	208
Figure 7.7. Variations in Capsule Velocity and Total Pressure Drop w.r.t. Pipeline Diameter for Spherical and Cylindrical Capsules	209
Figure 7.8. Variations in Optimal Diameter w.r.t. the Solid Throughput for Spherical and Cylindrical Capsules	210
Figure 7.9. Comparison of Various Costs of the Pipeline for Equi-Density and Heavy-Density Spherical Capsules	212
Figure 7.10. Variations in Total Pressure Drop w.r.t. Pipeline Diameter for Equi-Density and Heavy-Density Spherical Capsules	213
Figure 7.11. Variations in Optimal Diameter w.r.t. the Solid Throughput for Equi-Density and Heavy-Density Spherical Capsules	214
Figure 7.12. Variations in Operating and Operating Costs w.r.t. Pipeline Diameter	216
Figure 7.13. Variations in Total Cost and Pumping Power Required at Various Pipeline Diameters	216
Figure 7.14. Variations in Capsule Velocity and Total Pressure Drop w.r.t. Pipeline Diameter	218
Figure 7.15. Variations in Optimal Diameter and Pumping Power w.r.t. the Solid Throughput	219
Figure 7.16. Variations in Total Pressure Drop w.r.t. Pipeline Diameter for Spherical and Cylindrical Capsules	221
Figure 7.17. Variations in Optimal Diameter w.r.t. the Solid Throughput for Spherical and Cylindrical Capsules	222
Figure 7.18. Comparison of Various Costs of the Pipeline for Equi-Density and Heavy-Density Spherical Capsules	224
Figure 7.19. Variations in Total Pressure Drop w.r.t. Pipeline Diameter for Equi-Density and Heavy-Density Spherical Capsules	225

LIST OF TABLES

Table 3.1. Boundary Types	47
Table 4.1. Pressure Drops in a Horizontal Pipe for the Flow of Water	59
Table 4.2. Entrance Length Requirements for a Horizontal Hydraulic Pipeline	62
Table 4.3. Mesh Independence Results	64
Table 4.4. Validation Tests.....	64
Table 4.5. Friction Factors for Capsules being transported in Horizontal Pipelines	108
Table 5.1. Pressure Drops for Water Flow in a Vertical Pipe	114
Table 5.2. Friction Factors for Capsules being transported in Vertical Pipelines	158
Table 6.1. Loss Coefficient of Bends for Capsule Flow	188
Table 7.1. Variations in Pumping Power and Various Costs w.r.t. Pipeline Diameter	201
Table 7.2. Variations in Capsule Velocity and Pressure Drops	203
Table 7.3. Variations in Optimal Diameter, Capsule Velocity and Pumping Power for Various Solid Throughputs	204
Table 7.4. Variations in Pumping Power and Total Cost from Agarwal et. al.'s Optimisation Model	206
Table 7.5. Variations in Pumping Power and Various Costs w.r.t. Pipeline Diameter	207
Table 7.6. Variations in Capsule Velocity and Pressure Drops	208
Table 7.7. Variations in Optimal Diameter, Capsule Velocity and Pumping Power for Various Solid Throughputs	209
Table 7.8. Comparison between Spherical and Cylindrical Capsules	210
Table 7.9. Variations in Pumping Power and Various Costs w.r.t. Pipeline Diameter	211
Table 7.10. Variations in Capsule Velocity and Pressure Drops	212
Table 7.11. Variations in Optimal Diameter, Capsule Velocity and Pumping Power for Various Solid Throughputs	213
Table 7.12. Comparison between Equi-Density and Heavy-Density Spherical Capsules	214

Table 7.13. Variations in Pumping Power and Various Costs w.r.t. Pipeline Diameter	215
Table 7.14. Variations in Capsule Velocity and Pressure Drop	217
Table 7.15. Variations in Optimal Diameter, Capsule Velocity and Pumping Power for Various Solid Throughputs	218
Table 7.16. Variations in Pumping Power and Various Costs w.r.t. Pipeline Diameter	219
Table 7.17. Variations in Capsule Velocity and Pressure Drops	220
Table 7.18. Variations in Optimal Diameter, Capsule Velocity and Pumping Power for Various Solid Throughputs	221
Table 7.19. Comparison between Spherical and Cylindrical Capsules	222
Table 7.20. Variations in Pumping Power and Various Costs w.r.t. Pipeline Diameter	223
Table 7.21. Variations in Capsule Velocity and Pressure Drops	224
Table 7.22. Variations in Optimal Diameter, Capsule Velocity and Pumping Power for Various Solid Throughputs	225
Table 7.23. Comparison between Equi-Density and Heavy-Density Spherical Capsules	226

NOMENCLATURE

A	Cross-sectional Area of the Pipe (m^2)
C_1	Cost of Power consumption per unit Watt (£/W)
C_2	Cost of Pipe per unit Weight of Pipe material (£/N)
C_3	Cost of Capsules per unit Weight of the Capsule Material (£/N)
C_c	Constant of Proportionality
C_p	Coefficient of Pressure
c	Concentration of Solid Phase
d	Diameter of Capsule (m)
D	Diameter of Pipe (m)
f	Darcy Friction Factor
Fr	Froude Number
g	Acceleration due to gravity (m/sec^2)
h	Elevation (m)
h_l	Head loss (m)
H	Holdup
k	Capsule to Pipe diameter ratio
K_l	Loss Coefficient of Bends
L	Length (m)
n	Number of Bends
N	Number of Capsules
ΔP	Pressure Drop (Pa)
Q	Flow Rate (m^3/sec)

r	Radius of Curvature of Pipe Bend (m)
R	Radius of Pipe Bend (m)
Re	Reynolds Number
s	Specific Gravity
Sc	Spacing between the Capsules (m)
u	Local Flow Velocity in X direction (m/sec)
V	Flow Velocity (m/sec)
x	Axial Distance (m)
y	Radial Distance (m)
Z	Coordinates of Capsule

SYMBOLS

α	Function of Reynolds Number
ρ	Density (Kg/m ³)
μ	Dynamic Viscosity (Pa-sec)
Υ	Specific Weight (N/m ³)
η	Efficiency of the Pump (%)
ε	Roughness Height of the Pipe (m)
θ	Angular Position (°)
π	Pi
i	Specific Internal Energy (J/Kg)
ψ	Shape Factor
σ	Normal Stress (Pa)
τ	Shear Stress (Pa)
ζ	Loss Coefficient of Abrupt Contraction

SUBSCRIPTS

av	Average
b	Bulk
c	Capsule
cn	Centreline
e	Entrance
h	Horizontal
m	Mixture
p	Pipe
v	Vertical
w	Water
∞	Free Stream

CHAPTER 1

INTRODUCTION

Pipelines are an integral part of various industries. Pipes used for on-shore applications largely consist of horizontal pipes. The third generation of horizontal pipes consist of pipes, transporting capsules. In order to effectively analyse the underlying complex flow phenomena occurring in hydraulic pipelines transporting capsules it is essential to first understand the flow structure within a hydraulic pipeline. The pressure drop co-relations for a hydraulic pipeline can be extended to incorporate the effects of the presence of solid phase in the pipelines. Hence, this chapter provides an introductory discussion regarding water flow and capsule flow in pipelines. Furthermore, this chapter provides with the details of the capsule pipeline components and design requirements.

1.1. Pipeline Transport

Pipeline transport is the transportation of goods through a pipe. Pipelines have long been used as a medium of transport. The history of pipeline transport can be divided into three generations. The first generation of pipelines comprises transport of a single phase within these pipelines. The single phase usually consists of a fluid; either a liquid or a gas. The history of first generation of pipelines dates back to 189 AD when a court of Han Dynasty ordered an engineer to construct a series of square-pallet chain pumps outside the capital city. Around the same time, Romans made use of large aqueducts to transport water from a higher elevation to a lower elevation. These aqueducts were quite famous throughout the Europe [1].

The second generation of pipelines consists of the transport of multiple phases in the pipelines. These multiple phases make use of the combination of solids, liquids and gases such as liquid-liquid (e.g. Oil in water etc.), liquid-gas (e.g. bubbly flow etc.), liquid-solid (e.g. slurry flow etc.) or even liquid-gas-solid flow. The slurry pipeline, in specific, has gained a lot of importance due to it being economically viable to the industries throughout the world for the transportation of solid materials. The solid medium usually consists of solid particles with diameter ranging from a few microns to a few millimetres. It is an effective medium of transport of solids such as coal, sand etc.

The third generation of pipelines comprises of the transportation of Capsules. These capsules are hollow containers filled with minerals, ores, radioactive materials or even goods such as mail, jewellery etc. In some cases, the material that needs to be transported is itself given the shape of the capsule. This technique is very famous in the transportation of coal, and such pipelines are termed as Coal-Log Pipelines (CLP) [2]. The shape of the capsule is normally cylindrical or spherical where wheels are usually attached to the cylindrical capsules to overcome the enormous static friction between the capsules and the pipe wall because of a larger contact area as compared to spherical capsules. The economic surveys that have been conducted by some companies and universities, have shown that the capsule transportation is more economical than conventional methods of transporting goods such as trucks, rails etc. [3]. Furthermore, the pipelines transporting capsules provide additional benefits such as [4]:

- The capsule transporting phenomena is quiet and hence is environment friendly as compared to conventional transporting methods
- There are no accidents or delays due to traffic reasons, and hence it is faster and safer for the goods being transported
- There is no man power required for the transporting phenomenon except at the injection and evacuation of the capsules from the pipeline
- Except CLP, the solid medium remains intact as there is no direct contact between the goods being transported and the transporting medium
- Tremendous economy of scale (operating costs are significantly reduced as the volume of transportation increases)
- Relative immunity to escalation of prices

- High degree of efficiency and reliability
- Simplicity of installation
- Can be readily automated

1.2. Pressure Drop Considerations in Hydraulic Pipelines

Pipeline flows have always been a topic of research throughout the world. Daniel Bernoulli (1700 – 1782 AD), a Swiss mathematician and physicist, while working on the principles of conservation of energy, realised that a moving fluid exchanges its kinetic energy with pressure. In his famous publication ‘Hydrodynamica’, Bernoulli states that “for an inviscid fluid flow, an increase in the fluid velocity results in a decrease in its pressure”. This is known as Bernoulli’s principle and can be mathematically written as [5]:

$$P + \frac{1}{2} \rho u^2 = \text{constant} \quad (1.1)$$

where P represents the static pressure of the fluid, ρ is the density of the fluid and u is the velocity of the fluid. The second term on the left-hand side of the equation represents the dynamic pressure. A more general form of this law, in which the effects of the elevation and the head loss in the pipeline has also been considered, is:

$$P_1 + \frac{1}{2} \rho_1 u_1^2 + \rho_1 g_1 h_1 = P_2 + \frac{1}{2} \rho_2 u_2^2 + \rho_2 g_2 h_2 + \rho_2 g_2 h_l \quad (1.2)$$

where g is the gravitational acceleration, h is the vertical elevation and h_l is the head loss experienced by the fluid. Subscripts 1 and 2 represent station 1 and 2 respectively as shown in figure 1.1.

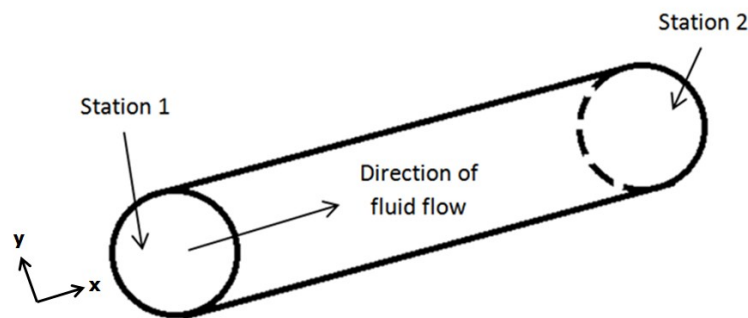


Figure 1.1. Flow in a Horizontal Pipe

The first term on the left-hand side in equation (1.2) is termed as static head, second term as dynamic head and the third term as potential head. For fluids flowing at very high velocities (typically $Ma > 0.7$) the compressibility effects are quite appreciable. For general purpose hydraulic pipelines, the typical flow velocity ranges from 0.5m/sec to 3m/sec which corresponds to $Ma \ll 0.1$. Hence, the fluid is typically considered incompressible in pipe flows. Similarly, the variation of gravitational acceleration between two points depends on the difference of elevation between the points. For an elevation

difference of 100m, the variation in gravitational acceleration is $\ll 1\text{m/sec}^2$. Hence, the gravitational acceleration can be considered constant for general-purpose pipelines.

1.2.1. Horizontal Pipelines

Considering incompressible flow and constant gravitational acceleration in a horizontal pipeline, equation (1.2) becomes:

$$P_1 + \frac{1}{2}\rho u_1^2 = P_2 + \frac{1}{2}\rho u_2^2 + \rho g h_l \quad (1.3)$$

$$\rho g h_l = (P_1 - P_2) + \frac{1}{2}\rho(u_1^2 - u_2^2) \quad (1.4)$$

The flow rate in a pipe can be represented by:

$$Q = V A \quad (1.5)$$

where Q is the flow rate of the fluid, V is the velocity of the fluid and A is the cross-sectional area of the pipe. The pipe considered in figure 1 has a constant diameter throughout its length, which further suggests that the cross-sectional area of the pipe remains constant. Furthermore, to satisfy the equilibrium condition, the flow rate at station 1 should be equal to flow rate at station 2.

$$Q_1 = Q_2 \quad (1.6)$$

$$V_1 A_1 = V_2 A_2 \quad (1.7)$$

Now, as $A_1 = A_2$ this implies that the velocity at station 1 should be equal to velocity at station 2.

$$V_1 = V_2 \quad (1.8)$$

For such a case, equation (1.4) becomes:

$$\rho g h_l = (P_1 - P_2) \quad (1.9)$$

or,

$$\Delta P = \rho g h_l \quad (1.10)$$

where ΔP is the pressure drop in the fluid between the two stations. Darcy-Weisbach equation, named after Henry Darcy (1803 – 1858 AD) and Julius Weisbach (1806 – 1871 AD), relates the head loss to the velocity of the fluid, and can be mathematically represented as [6]:

$$h_l = f \frac{L_p}{D} \frac{V^2}{2g} \quad (1.11)$$

where f is the Darcy Friction Factor, L_p is the length and D is the diameter of the pipe. Putting equation (1.11) into equation (1.10):

$$\Delta P = f \frac{L_p}{D} \frac{\rho V^2}{2} \quad (1.12)$$

The Darcy friction factor can be computed from Moody's chart; developed by Lewis Ferry Moody in 1944 AD. It is a function of the relative pipe roughness (ϵ/D) and the Reynolds number of the fluid, where ϵ is the absolute pipe roughness in meters. The Reynolds number can be represented by [7]:

$$Re = \frac{\rho V D}{\mu} \quad (1.13)$$

where μ is the dynamic viscosity of the fluid. Its value is 0.001003 Pa-sec for water at 20°C and 1 bar atmospheric pressure.

1.2.2. Vertical Pipelines

Considering incompressible flow and constant gravitational acceleration in a vertical pipeline, equation (1.2) becomes:

$$P_1 + \frac{1}{2} \rho u_1^2 + \rho g h_1 = P_2 + \frac{1}{2} \rho u_2^2 + \rho g h_2 + \rho g h_l \quad (1.14)$$

$$\rho g h_l = (P_1 - P_2) + \frac{1}{2} \rho (u_1^2 - u_2^2) + \rho g (h_1 - h_2) \quad (1.15)$$

For a constant diameter pipe, equation (1.15) becomes:

$$\rho g h_l = (P_1 - P_2) + \rho g (h_1 - h_2) \quad (1.16)$$

$$\Delta P = \rho g h_l + \rho g \Delta h \quad (1.17)$$

$$\Delta P = f \frac{L_p}{D} \frac{\rho V^2}{2} + \rho g \Delta h \quad (1.18)$$

Hence, the pressure drop in a vertical pipeline is equal to the pressure drop in a horizontal pipeline of the same length and diameter, plus $\rho g \Delta h$ where Δh represents the change in elevation between the two stations.

1.2.3. Pipeline Bends

The pressure drop occurring within horizontal pipeline bends is represented in terms of the loss coefficient of the bends as [8]:

$$\Delta P = K_l \frac{1}{2} n \rho V^2 \quad (1.19)$$

and the pressure drop occurring within vertical pipeline bends is represented in terms of the loss coefficient of the bends as:

$$\Delta P = K_l \frac{1}{2} n \rho V^2 + \rho g \Delta h \quad (1.20)$$

1.3. Transport of Capsules in Pipelines

Capsule pipelines are used to transport solid materials using water or any other liquid as a carrier fluid. This mode of transportation is suited for long distance haulage of bulk materials like mineral ore to processing plants, coal to thermal power plants, disposal of waste material, like fly ash, from processing plant to the disposal sites. Various industries have accepted capsule pipelines as an attractive mode of transport of solids because of its low maintenance and around the year availability. This mode of transportation is extremely safe besides being eco-friendly. Mole Solutions Ltd. [9] in their economic analysis has shown by comparison of different modes of transportation systems that long distance capsule pipelines are economically attractive. Technically, there are no limitations for adapting the capsule transportation system in a big way. However, to-date it has not gained high popularity because of some basic limitations, which are highlighted below:

- The initial capital cost is relatively high
- The pipeline transportation system requires water or other fluids as the carrier fluid in large volume, which may not be easily available at all places and at all times
- The blockage in the pipeline due to capsules can cause very long delays
- Quality control has to be very stringent for the efficient operation of the pipeline

The attractive features of the capsule transportation system offer wide scope for future applications for transporting material from inaccessible areas such as mountains across water bodies and deep-sea recovery of the minerals. Hence, there is a need to carry out extensive research in order to generate enough database which enables to develop optimum design methodologies.

The pipelines transporting capsules mainly consist of two types. The first type of pipelines transporting capsules is termed as Pneumatic Capsule Pipelines (PCP). In PCPs, the medium of transportation usually consists of a gas (normally air). The PCPs follow conventional fluid mechanic's principles i.e.

the two ends of the pipelines are kept at different pressures such that the capsules are propagated from the high-pressure end to the low-pressure end. Due to lesser kinematic viscosity of air (14.5 times less than water), the pressure difference between the ends of the pipelines is usually insufficient to transport a train of capsules continuously. Booster pumps are installed at regular intervals in the pipeline to increase the pressure difference for continuous supply of capsules at the capsule evacuation end of the pipeline.

The second type of pipelines transporting capsules is termed as Hydraulic Capsule Pipelines (HCP). In HCPs, the medium of transportation is water. The pressure difference between the two ends of the pipeline forces the capsules to become waterborne and hence the capsules are being propagated to the capsule evacuation end of the pipeline. The other types of pipelines transporting capsules include magnetic capsule transport where the capsules move under the influence of the magnetic field.

1.4. History of Hydraulic Capsule Pipelines

The concept of using capsules to transport freight has been around for 200 years [10]. The earliest proposal for moving goods in pipelines was given by George Medhurst in 1810 AD. A practical application was created by Latimer Clark in 1856 with a pneumatic tube connecting the central station of the Electric Telegraph Company to the London Stock Exchange. This simple technology continues to be used worldwide to move small objects over short distances, such as moving cash between tills and the central office in a supermarket. The first wheeled capsules made their appearance in 1861 AD with a 30-inch pipeline constructed by the London Pneumatic Dispatch Company. The technology was found to be too expensive to operate, and the system closed in 1874 AD. A new era of wheeled capsules began in 1970s with the construction of two large diameter pipeline systems with wheeled capsules. In the United States of America, Tubexpress Systems Inc. built and tested a 1400ft long x 36in diameter pipe with 7ft long capsules, powered by compressed air [11].

In the Republic of Georgia, the Lilo-1 system (figure 1.2) could transport 25 tonnes of sand and gravel at a time. The system used a 2.1km long pipeline of 1.02m diameter within which six capsules formed a capsule train. Speeds of up to 50km/hr were reported. A later system, Lilo-2, used an 8km pipeline of 1.27m diameter to move 8 million tonnes of sand and gravel per year. Both systems were powered by compressed air, but have now been closed [12]. A test system constructed by BHRA at Cranfield in the 1970s comprised a 550m loop using a 600mm diameter pipe. A report published by the British Technology Group, which examined why the technology had not been taken up, concluded that while many industries were prepared to consider pneumatic capsule pipelines, fears about the mechanical reliability of the system and unknown financial implications deterred companies from implementing a pneumatic capsule pipeline system without first seeing a real working example.



Figure 1.2. The Lilo-1 system [12]

The most successful application of the technology has been in Japan. Sumitomo Metal Industries, shown in figure 1.3, built a 3.2km pipe of 1m diameter in 1980 AD to transport limestone to a cement plant [13]. The system transports over 2 million tonnes of limestone each year and has reportedly achieved an operation rate in excess of 95%. This system is still in operation today. In 1997 AD, the Florida Institute of Phosphate Research commissioned a demonstration project from Magplane Technology Inc. for a capsule pipeline system using linear synchronous motors for propulsion, as shown in figure 1.4. The demonstration pipe was 275m in length and 610mm in diameter; each capsule could carry 300kg and achieved a peak speed of 18m/s. The final report, published by Magplane Technology in March 2001 AD, claimed that preliminary economic studies had shown a satisfactory return on capital [14]. However, in its conclusions, the Florida Institute of Phosphate Research stated that much more testing was required before the system could be considered as a candidate for commercial operation.

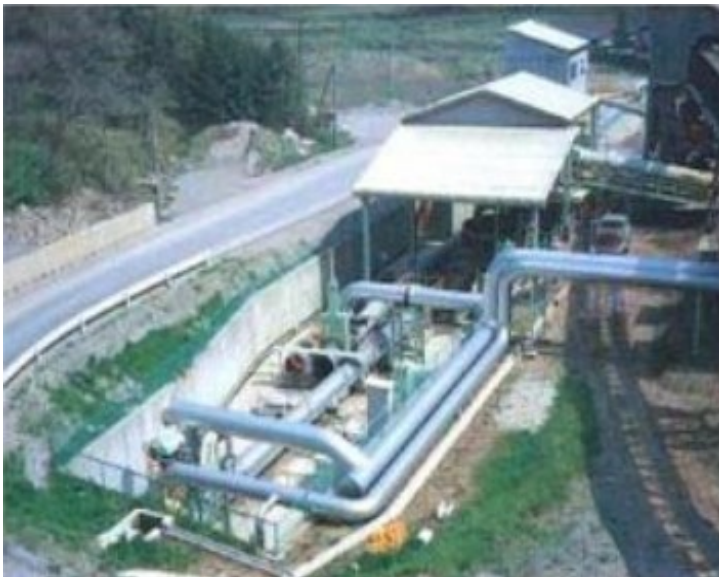


Figure 1.3. Sumitomo Metal Industries [13]



Figure 1.4. Magplane Technology [15]

1.5. Components of a Hydraulic Capsule Pipeline

The following are the main components of any HCP:

1. Pump
2. Capsules
3. Capsule Injection System
4. Capsule Evacuation System

1.5.1. Pump

The pump used for capsule transportation purposes is commonly known as Pump Bypass. It has gained widespread commercial acceptability in the recent years. The basic system (figure 1.5) includes two long parallel pipes, having a length sufficiently long to hold an entire train of capsules in each pipe. The two pipes are connected to a booster pump and a set of eight valves. By alternately opening and closing two sets of valves, capsule trains bypass the booster pump without affecting the pump's ability to put energy into water, which in turn carries the capsules through the booster station. The design of the pump-bypass is complicated by the unsteady flow and water hammer generated by rapid switching of the valves. This requires careful and sophisticated analysis and optimization by using the method of characteristics, modified to incorporate capsules in the flow. It also involves the use and analysis of surge tanks or air chambers to minimize water hammer [16].

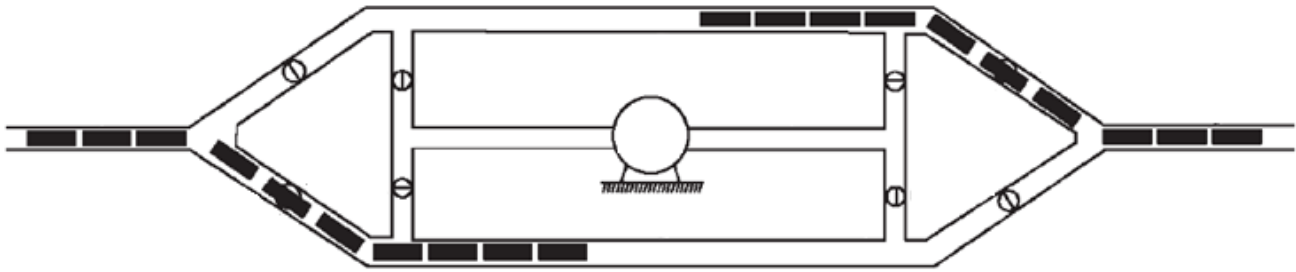


Figure 1.5. Top View of Pump for Pipelines transporting Capsules [16]

1.5.2. Capsules

Capsules are either hollow containers, filled with goods to be transported, or the goods themselves, being shaped into the form of a sphere or cylinder as in case of CLPs (Coal Log Pipelines). The shape of the capsules considerably affects the design process of an HCP in terms of energy requirements for the system [17]. The physical properties of capsules, such as density and specific gravity, play a vital role in the determination of the path followed by capsules in the pipeline. Furthermore, in a train of capsules, the geometric properties of the train are significant for the HCP design process.

1.5.3. Capsule Injection System

The capsule injection system commonly used is the Multi-Lock type system. This system uses a set of parallel launching tubes (locks) to receive capsules from conveyor belts, and to launch capsules into a common pipeline (figure 1.6). The locks are horizontal lines with their downstream ends connected to the main pipeline through a set of Y joints. The upstream end of each lock is connected to a common water reservoir. Capsules are first loaded on a set of conveyor belts, each of which is connected to the inlet of a lock, to bring the capsules into the lock. Connection between the conveyors and the locks requires that each conveyor be tilted at a slope of about 30° , with the end part of the conveyor in the reservoir underwater. An auxiliary pump has its suction side connected to the downstream ends of the locks and its discharge side connected to the reservoir. By opening the valve connected to a given lock, the auxiliary pump draws capsules from the corresponding conveyor belt into the lock. The main pump has its discharge side connected to the upstream ends (entrance) of the locks, and its suction side connected to the reservoir. By opening the discharge valve connected to any given lock this pump drives the capsules out of the lock and into the main pipeline downstream. During normal mode of operation, both pumps are on continuously, but valves are frequently switched. By alternately opening and closing valves, capsules can be drawn into the locks and then driven into the main pipeline one train at a time.

Each train of capsules entering the main pipeline consists of the capsules drawn into the lock at an earlier time. There will be some spacing between any two neighbouring trains in the pipeline but there will be little spacing between individual capsules in a train. Having multiple parallel locks reduces the speed needed for the feeding capsules by conveyors. A special advantage of this injection system is that

the capsules never go through the pumps. However, careful design of the system, including proper sizing of the diameter and the length of the locks to avoid cavitation, proper design of the Y diverters to avoid excessive abrasion, and proper design of the automatic control system to open and close valves alternatively, is a must for trouble-free operation [18].

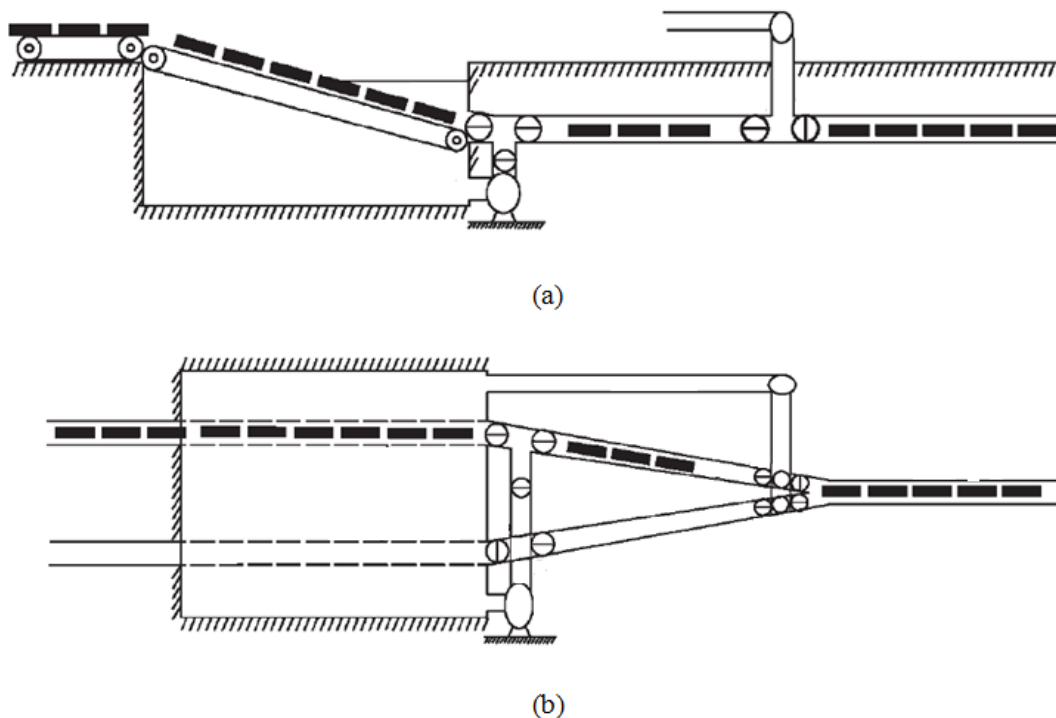


Figure 1.6. Capsule Injection System (a) Side View (b) Top View [18]

1.5.4. Capsule Ejection System

Ejection of capsules at any pipeline outlet station can be achieved in a reverse manner as injection, except that no pumps are needed and only one conveyor is required. The discussion of injection and ejection systems presented here is applicable to all types of HCPs. The only restriction is that the capsule's specific gravity must be greater than 1 so that the capsules will stay on the conveyor by gravity. A different design of the conveyors in the reservoirs is required if the capsule specific gravity is less than 1, such as by using an upside-down conveyor belt for the part where the capsules are underwater [18].

1.6. Mechanics of Transportation of Solids in Pipelines

In capsule transportation, the carrier fluid imparts energy to the capsules in order to move them along the flow. The motive force for the transportation of capsules along the flow is the fluid drag, which is a function of flow velocity, density, size and shape of the capsules. The effects of these parameters on the flow of capsules in pipelines, having fully developed turbulent flow, are listed below:

- Increasing the flow velocity increases the velocity of the capsules in the pipeline
- Capsules having density equal to that of their carrier fluid propagates along the centreline of the pipe, whereas the heavy-density capsules travel along the bottom wall of the pipeline
- Heavy-density capsules in a vertical pipeline travel along the centreline of the pipe
- Increase in the size of equi-density capsules decreases their velocity because of increased drag force acting on them
- Increase in the size of heavy-density capsules in a horizontal pipeline increases the velocity of the capsules. This is due to the fact that more area of the capsule is exposed to the high-velocity gradients in the pipeline
- The flow of capsules in pipe fittings such as bends is extremely complex

Concluding the aforementioned points, the flow of capsules in a pipeline is a heterogeneous phenomenon, where, there is a difference between capsule and flow velocities. This difference in the velocities of the capsules and the flow is often termed as Slip. Slip is shown to be a function of various parameters under different flow conditions [21, 25, 30, 35, 38, and 44]. Furthermore, for the flow of heavy-density capsules, if the flow velocity decreases to a very low value, the capsules might stop propagating along the flow. The minimum flow velocity to keep the capsules moving in the pipeline is termed as Incipient Velocity. Incipient velocity for the capsules is a function of many factors like shape, size and density of the capsules etc. The incipient velocity for the flow of capsules in a vertical pipeline is considerably higher than in horizontal pipelines.

1.6.1. Design Considerations for Pipelines Transporting Capsules

The first step in the design of capsule pipelines is to select the various process parameters. Subsequently, one would carry out a detailed engineering design based on the design parameters selected. The various design parameters that are required to be established for the design of pipeline are classified under the following three categories:

- Hydraulic parameters of the capsule pipelines
- Parameters dictating the mechanical design of the capsule pipelines
- Parameters affecting the operational stability of the capsule pipelines

The individual parameters to be selected for each category are:

Hydraulic Parameters of the Capsule Pipelines

- Selection of the carrier fluid
- Optimum capsules size
- Optimum concentration of the capsules in the pipeline
- Pipeline diameter
- Pressure drop in the pipeline
- Additives required for reducing pressure drop in the pipeline

Parameters Dictating the Mechanical Design of the Capsule Pipelines

- Pipeline life
- Selection of the pump
- Capsule injection system
- Capsules ejection system
- Metal allowance
- Abrasion of the pump
- Wear and tear in the pipeline

Parameters Affecting the Operational Stability of the Capsule Pipelines

- Shut-down start-up requirements
- Maximum allowable slope

It is apparent from the aforementioned lists that the design of a pipeline transporting capsules is very complex due to the involvement of a large number of parameters. Furthermore, at present, universal correlations are not available to predict the flow behaviour within pipelines transporting capsules. This is particularly true for pipe fittings such as bends etc. Thus, the design has to be largely based on the data obtained from various tests as well as on the accumulated experience. Normally, the data required for the selection of the design parameters is obtained from the following sources [19]:

- Pilot plant test loops
- Bench/accelerated tests
- Semi-empirical correlations

The preliminary data required by a capsule pipeline designer includes various properties of the capsules to be transported like density, diameter, length, solubility/physical-chemical stability, hardness etc. The present study is concerned with the optimal designing of a pipeline transporting capsules based on the hydraulic parameters, excluding the effects of the additives required for reducing pressure drop in the pipeline.

(a) Selection of the Carrier Fluid

The choice of the carrier fluid is primarily dictated by the availability, and thus water is generally used. This study presents a detailed analysis of the hydraulic pipelines (HCPs), transporting capsules. Depending on the end use of the capsules, other carrier fluids can also be used.

(b) Optimum Capsule Size

The pressure drop in a pipeline transporting capsules is dependent on the capsule velocities, which are a function of the size and shape of the capsules. Hence, optimum capsule size is carefully decided according to the pressure drop and end use requirements. This study presents detailed investigations on the effects of the capsule size on the design of a pipeline transporting capsules.

(c) Optimum Concentration of the Capsules in the Pipeline

The concentration of the solid phase in a pipeline transporting capsules is often controlled by the annual throughput requirements from the system. However, for long distance pipelines, it will be generally economical to transport the capsules at the optimum concentration level for a specific size of the pipeline. This avoids wasteful expenditure of energy for the transportation of the carrier fluid. The upper limit of the concentration in a pipeline transporting capsules is governed by the fact that at high concentrations, the pressure drop in the pipeline increases sharply. Generally, the optimum concentration for hydraulic transport of capsules is selected on the basis of the lowest specific energy consumption, i.e. energy spent per ton of the capsule material. This study presents detailed investigations on the effects of the capsule concentration on the optimal design of the pipeline.

(d) Pipe Diameter

The pipeline diameter should be sufficient enough to transport the required throughput of the solid material within the pipeline at reasonably practical concentration and capsule velocities. In practice, the concentration, pipe diameter and the capsule velocities are interdependent, and it becomes necessary for a designer to optimise all of these parameters simultaneously, subject to constraints on the energy consumption. This study presents an optimisation methodology for pipelines transporting capsules which results into the optimal diameter of the pipeline.

(e) Pressure Drop in the Pipeline

Pressure drop, or head loss, in a pipeline transporting capsules is the primary parameter which dictates the design methodology for optimum capsule transport pipeline selection. The data for the pressure drop in a pipeline transporting capsules is obtained from the numerical simulations performed in the present study under various geometric and flow conditions. These simulations are based on the results obtained from iterative solution of the equation governing fluid flow in pipelines transporting capsules. The pressure variations and velocity distribution within a pipeline transporting capsules can be quantified in order to gain more insight into the complex flow phenomena occurring within the pipelines transporting capsules. Pressure and velocity profiles can be drawn wherever necessary to explain the nature of the flow within the pipe. Using the pressure drop data, semi-empirical relationships can be developed to predict the pressure drop in the pipeline.

1.7. Pressure Drop Considerations in Hydraulic Capsule Pipelines

Similar to the pressure drop considerations in a hydraulic pipeline, the pressure drop considerations for HCPs have been presented in this section.

1.7.1. Horizontal Pipelines

Equation (1.12) can be re-written for multiphase flow applications as [20]:

$$\Delta P_m = f_m \frac{L_p}{D} \frac{\rho_m V_m^2}{2} \quad (1.21)$$

where ΔP_m is the pressure drop in the mixture, ρ_m is the mixture density and V_m is the mixture velocity. Equation (1.20) can be written to differentiate between the effects of water and the capsules on the pressure drop as:

$$\Delta P_m = \Delta P_w + \Delta P_c \quad (1.22)$$

where ΔP_c is the pressure drop due to the presence of the solid phase, i.e. capsules, in the pipe. Equation (1.21) can be expanded as:

$$\Delta P_m = k_1 f_w \frac{L_p}{D} \frac{k_2 \rho_w (1-c) k_3 V_{av}^2}{2} + k_4 f_c \frac{L_p}{D} \frac{k_5 \rho_w c k_6 V_{av}^2}{2} \quad (1.23)$$

where c represents the concentration of the solid phase in the mixture, V_{av} is the average flow velocity and the constants $k_1, k_2, k_3, k_4, k_5, k_6$ are the coefficients which relate the friction factor, density and the velocity of both the water and the capsules respectively to that of the mixture. If the effect of the concentration of the solid phase c and the constants $k_1, k_2, k_3, k_4, k_5, k_6$ are represented in f_w and f_c then equation (1.22) can be simplified as:

$$f_w = f(c, k_1, k_2, k_3) \quad (1.24)$$

$$f_c = f(c, k_4, k_5, k_6) \quad (1.25)$$

Hence, the pressure drop in an HCP can be represented by:

$$\Delta P_m = f_w \frac{L_p}{D} \frac{\rho_w V_{av}^2}{2} + f_c \frac{L_p}{D} \frac{\rho_w V_{av}^2}{2} \quad (1.26)$$

1.7.2. Vertical Pipelines

Equation (1.18) can be re-written for multiphase flow applications as:

$$\Delta P_m = f_m \frac{L_p}{D} \frac{\rho_m V_m^2}{2} + \rho_m g \Delta h \quad (1.27)$$

$$\Delta P_m = (\Delta P_w + \Delta P_c) + \rho_m g \Delta h \quad (1.28)$$

$$\Delta P_m = \left(k_7 f_w \frac{L_p}{D} \frac{k_8 \rho_w (1-c) k_9 V_{av}^2}{2} + k_{10} f_c \frac{L_p}{D} \frac{k_{11} \rho_w c k_{12} V_{av}^2}{2} \right) + k_{13} \rho_w g \Delta h \quad (1.29)$$

Where:

$$f_w = f(c, k_7, k_8, k_9) \quad (1.30)$$

$$f_c = f(c, k_{10}, k_{11}, k_{12}, k_{13}) \quad (1.31)$$

Hence, the pressure drop in a vertical HCP can be represented by:

$$\Delta P_m = f_w \frac{L_p}{D} \frac{\rho_w V_{av}^2}{2} + f_c \frac{L_p}{D} \frac{\rho_w V_{av}^2}{2} + \rho_w g \Delta h \quad (1.32)$$

1.7.3. Pipeline Bends

Equation (1.19) can be re-written for multiphase flow applications as:

$$\Delta P_m = K_{lm} \frac{1}{2} n \rho_m V_m^2 \quad (1.33)$$

For horizontal pipeline bends, equation (1.32) can be written in the form:

$$\Delta P_m = k_{14} K_{lw} \frac{n k_{15} \rho_w k_{16} V_{av}^2}{2} + k_{17} K_{lc} \frac{n k_{18} \rho_w k_{19} V_{av}^2}{2} \quad (1.34)$$

Where:

$$K_{lw} = f(k_{14}, k_{15}, k_{16}) \quad (1.35)$$

$$K_{lc} = f(k_{17}, k_{18}, k_{19}) \quad (1.36)$$

Hence:

$$\Delta P_m = K_{lw} \frac{n \rho_w V_{av}^2}{2} + K_{lc} \frac{n \rho_w V_{av}^2}{2} \quad (1.37)$$

Similarly, for vertical pipeline bends, equation (1.32) can be written in the form:

$$\Delta P_m = k_{20}K_{lw} \frac{n k_{21} \rho_w k_{22} V_{av}^2}{2} + k_{23}K_{lc} \frac{n k_{24} \rho_w k_{25} V_{av}^2}{2} + k_{26} \rho_w g \Delta h \quad (1.38)$$

Where:

$$K_{lw} = f(k_{20}, k_{21}, k_{22}) \quad (1.39)$$

$$K_{lc} = f(k_{23}, k_{24}, k_{25}, k_{26}) \quad (1.40)$$

Hence:

$$\Delta P_m = K_{lw} \frac{n \rho_w V_{av}^2}{2} + K_{lc} \frac{n \rho_w V_{av}^2}{2} + \rho_w g \Delta h \quad (1.41)$$

1.8. Motivation

Flow parameters required for the design of pipelines transporting capsules are too many and are interdependent. Therefore, it is an uphill task to optimally design a pipeline transporting capsules unless the exact interdependence of these parameters is known. This fact is especially true for pipe bends. This has motivated the author of the present study to conduct detailed research studies on a few important aspects of the flow of capsules in a pipeline.

Majority of the on-shore pipelines installed throughout the globe consist of horizontal pipes. It is therefore essential to analyse the flow field in a horizontal HCP. The flow field diagnostics of HCPs commonly refers to head loss occurring in the HCP due to the presence of the solid medium. The head loss occurring in an HCP is directly related to the pressure drop and hence pressure drop becomes one of the primary flow field diagnostics parameter. Furthermore, the flow field analysis encompasses the understanding of other flow variables such as velocities within an HCP. The flow field variables, together with geometric variables, give rise to the formulation of the prediction models for pressure drop in an HCP. These prediction models can then be directly used for the optimal designing of HCPs.

The off-shore pipelines consist primarily of vertical pipes. As the energy requirements for vertical pipelines are much more stringent as compared to horizontal pipelines, the design process is severely affected by the additional pressure drop in the pipe due to the change in the elevation of the pipe. Hence, necessary modifications in terms of the friction factor and the pressure drop considerations need to be made in order to accurately design a vertical HCP with reasonable accuracy. Furthermore, it has become very important to analyse the flow structure within vertical HCPs as it substantially differs from horizontal HCPs due to the fact that the capsule velocities are significantly different in vertical pipelines. Hence, a thorough understanding of the pressure distribution and velocity variations within a vertical HCP is essential.

Bends are an integral part of pipeline network. It is almost impossible to neglect the effect of the bends on the energy requirements of an HCP. Hence, a detailed flow diagnostics of bends, transporting capsules, is essential towards optimal HCP designing. The complex flow field phenomena, such as centrifugal forces acting on the capsules, within HCP bends remarkably alters the pressure and velocity distributions in the vicinity of the capsules, and hence new relationships are required for optimal HCP designing, accounting for the effects of the bends. Furthermore, due to severely limited studies conducted on bends, transporting capsules, the author is particularly interested in understanding the flow structure within such bends.

For commercial viability of HCPs, it is quite evident that these pipelines need to be designed optimally for widespread acceptability. The designers are in need of a design methodology which accounts for the hydraulic and mechanical design of a pipeline transporting capsules. Hence, an optimisation model needs to be developed, which should be robust and user-friendly. The optimisation model should be based on the fact that the total cost involved in the design of a pipeline transporting capsules is kept to a minimum.

1.9. Research Aims

The specific research aims formulated for this research study are described in this section whereas the objectives for this study will be discussed after carrying out an extensive literature review in the next chapter. Based on the motivation of this study, the research aims have been broken down into the following:

1. CFD Based Flow Diagnostics and Design of Horizontal Pipelines Transporting Capsules
2. CFD Based Flow Diagnostics and Design of Vertical Pipelines Transporting Capsules
3. CFD Based Flow Diagnostics and Design of Bends Transporting Capsules
4. Development of an Analytical Model for the Optimum Design of Pipelines Transporting Capsules

These research aims will cover most of the practical problems encountered in the real world as far as capsule transporting pipelines are concerned and hence can be considered satisfactory for this study. Detailed literature review is presented in the next chapter which focuses on the aforementioned research aims in order to find knowledge gaps in the existing literature.

1.10. Organization of Thesis

Based on the discussions presented in the previous sections, this thesis presents the body of work, which has been carried out for the current research study.

Chapter 1 provides an overview of the transportation mechanism in pipelines. The correlations for the transport of capsules in an HCP are presented in their raw form. From this overview, the motivation for carrying out this research is described, which identifies key areas to be reviewed in Chapter 2.

Chapter 2 consists of a detailed review of the research that has been carried out in the area of capsule transport in pipelines. It includes the review of published literature regarding the horizontal and vertical HCPs. Furthermore, a review of the literature available for HCP bends has also been included. It comprises of the literature review being carried out on the optimisation techniques that have been incorporated for HCPs. Details of the scope of research are provided in the form of specific research aims and objectives.

Chapter 3 documents the fundamental principles of Computational Fluid Dynamics. It includes the CFD modelling of the capsule pipelines; including the solver settings and the appropriate boundary conditions that have been specified to solve the flow domain. The meshing technique that has been used for the flow domain has been discussed. Furthermore, a detailed discussion on the velocity of the capsules, obtained from experimental data available in literature, is the highlight of the chapter.

Chapter 4 sheds light on the flow structure in horizontal pipelines transporting capsules for on-shore applications. The pressure and the velocity fields have been analysed in detail to formulate the effects of the presence of the solid medium within these pipelines on the pressure drop. Both, the flow of spherical and cylindrical capsules of various geometric variables and specific gravities has been analysed under various flow conditions. Semi-empirical models for the prediction of pressure drop in horizontal HCPs have been developed to facilitate the optimal design process.

Chapter 5 consists of detailed studies on the flow of capsule in vertical pipelines for off-shore applications. The range of parameters is similar to the one presented in Chapter 4. However, due to additional energy requirements because of elevation effects, and different capsule velocities, the flow structure is significantly different from the one observed in horizontal HCP. Furthermore, the effect of the density of the capsules on the pressure drop is the highlight of the chapter. Semi-empirical models for the prediction of pressure drop in vertical HCPs have been developed to facilitate the optimal design process.

Chapter 6 sheds light on the complex flow structure within HCP bends. The flow of both, the spherical and cylindrical capsules of various sizes and densities, has been numerically simulated to capture the complex flow structure within HCP bends. Semi-empirical models for the prediction of pressure drop in both horizontal and vertical HCP bends have been developed to facilitate the optimal design process.

Chapter 7 presents an optimisation model for HCPs based on Least-Cost Principle. The optimisation model is robust and user friendly. The input of the model is the solid throughput required from the

HCP, whereas, the outputs of the model are the optimal pipeline diameter and the pumping requirements. The optimisation model is quite straightforward and can be used at commercial scale.

Chapter 8 concludes the findings of this study, clearly mentioning the goals achieved and additions to the existing knowledge about HCPs in terms of both the design process and the flow mapping within these pipelines. Recommendations for future work have also been included.

CHAPTER 2

LITERATURE REVIEW

After getting detailed information regarding the parameter affecting the design of capsule transporting pipelines in the previous chapter, a detailed literature review has been presented in this chapter which will highlight the knowledge gaps in the existing literature. It includes the published works regarding horizontal pipes, vertical pipes, pipe bends and optimisation methodologies for the designing of pipelines transporting capsules. Based on the knowledge gaps found in the literature review, scope of research has been defined and research objectives of this study have been formulated.

2.1. Horizontal HCPs

Ellis [21] carried out experimental studies on the flow of an equi-density spherical capsule in a horizontal hydraulic pipe. From dimensional analysis, it was found out that the velocity of the capsule depends on the diameter ratio of capsule to pipe, k ($k = \frac{d}{D}$), and the average flow velocity, V_{av} . The range of investigations was $k = 0.39$ to 0.89 , $V_{av} = 1$ to 3.7 m/sec and number of capsules $N = 1$. The discussion on the results, obtained for the capsule's velocity, has been limited to the effects of k and V_{av} on capsule velocity, V_c . No expression for the velocity of the capsule has been developed. The analysis of the pressure drop, and the flow structure within the pipe, has not been included in the study.

Mathur et. al. [22] conducted experimental investigations on the transport of equi-density spherical capsules in a horizontal hydraulic pipe. Dimensional analysis identified that the capsule's velocity is a function of k , the Reynolds number of the capsules (Rec) and the densiometric froud number (Fr_c) of the capsules, where Rec and Fr_c have been expressed as:

$$Rec = \frac{\rho_c V_c d}{\mu} \quad (2.1)$$

$$Fr_c = \frac{g d \Delta\gamma_c}{V_c^2 \gamma_w} \quad (2.2)$$

Experiments were conducted for a range of $k = 0.47$ to 0.67 , and an average flow velocity V_{av} of 0.2 to 2.2 m/sec. The capsule's velocities were noted down and regression analysis was used to develop equations representing holdup velocities H ($H = \frac{V_c}{V_{av}}$). The study is purely based on the calculation of the capsule velocities and no information regarding the flow distribution within the pipe has been presented, such as the pressure distributions or the velocity profiles within the pipe.

Mishra et. al [23] conducted experiments on the flow of a train of spherical capsules, having density equal to water, in a hydraulic pipe. No spacing was being provided between the capsules in the train. The range of experimental investigations was $k = 0.44$ to 0.67 and $V_{av} = 1$ to 2.2 m/sec. Using multiple regression analysis, an expression for the prediction of the holdup velocities has been developed, but no analysis has been carried out on the flow variables within the pipe. Furthermore, the pressure drop within the pipeline has not been calculated.

Mishra et. al [24] carried out experimental studies on equi-density spherical capsule's flow in a hydraulic pipe of diameter $D = 103.4$ mm. The dimensional analysis showed the same dependencies as observed by Mathur et. al. [22]. Experiments were being carried out for a range of $k = 0.47$ to 0.67 and average flow velocity V_{av} of 1.1 to 2.2 m/sec. The capsule velocities were noted down and regression analysis was used to develop equations representing holdup velocities (figure 2.1). The figure shows that as the diameter of the capsule increases, or as the density of the capsule decreases, the velocity of the capsule increases. Furthermore, the gravitational forces reduce the velocity of the capsules. The study provides no information regarding the flow fields within the pipe such as pressure and velocity fields.

Ulusarslan et. al. [25] carried out a series of experiments on the flow of spherical capsules, with density equal to water, in a hydraulic pipe. The investigation was limited to $k = 0.8$ and $V_{av} = 0.2$ to 1.6 m/sec.

The results presented in the study show the effects of the bulk velocity on the capsule velocity and the spacing between the capsules. The pressure drop within the pipe has not been computed.

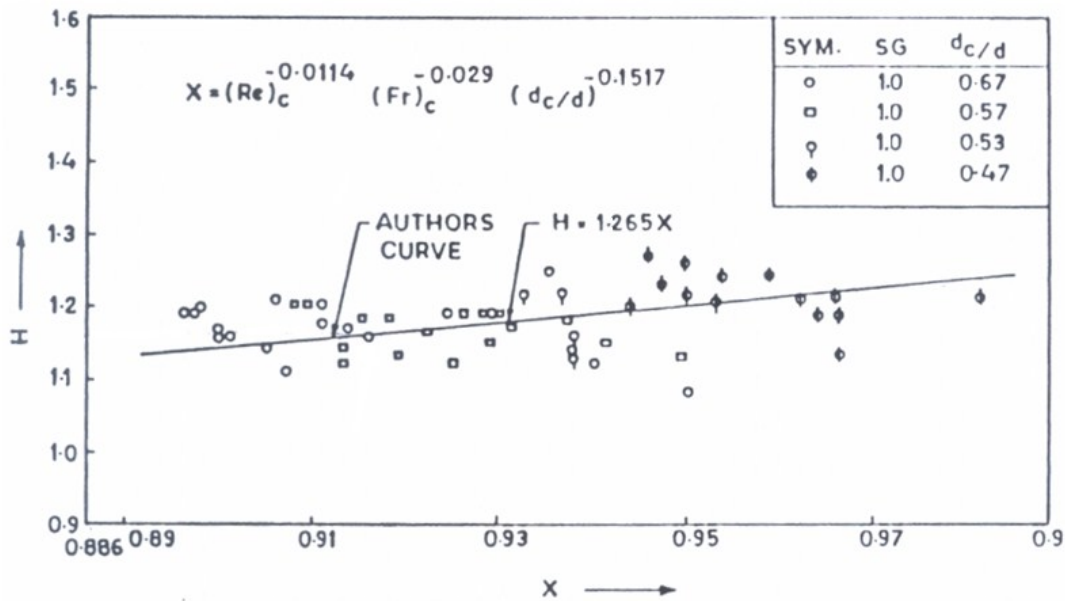


Figure 2.1. Prediction of Holdup in Equi-Density Spherical Capsules [24]

Ulusarlan [26] conducted experimental investigations on the flow of spherical capsules train having density equal to that of water. The range of investigations was limited to $k = 0.8$ and $V_{av} = 0.2$ to 1.6 m/sec. The results show the effects of the bulk velocity on the pressure drop in the pipe (figure 2.2). It can be seen from the figure that as the concentration of the solid phase in the pipeline increase, the pressure drop also increases. Furthermore, increase in the bulk velocity increases the pressure drop within the pipeline. However, no analysis on the flow variations within the pipe has been presented. Furthermore, the effect of the spacing between the capsules has not been investigated.

Charles [27] conducted a theoretical study on the flow of a cylindrical capsule with density equal to that of its carrier fluid. A theoretical expression for the velocity of the capsule, and for the pressure drop in the pipeline, has been presented. The velocity of the capsule and the pressure drop has been assumed to be a function of k only. Hence, the range of investigations is severely limited to a single cylindrical capsule without considering the effect of the length of the capsule on the velocity of the capsule and the pressure drop. Furthermore, no analysis on the flow field within the pipeline has been included in the study.

Ellis [21] carried out experimental studies on the flow of an equi-density cylindrical capsule in a hydraulic pipe. From dimensional analysis, it was found out that the velocity of the capsule depends on the diameter ratio of capsule to pipe and the average flow velocity. The range of investigations was $k = 0.39$ to 0.89 , $V_{av} = 1$ to 3.7 m/sec and $N = 1$. The discussion on the results, obtained for the capsule's velocity, has been limited to the effects of k and V_{av} on capsule's velocity, V_c . No expression for the velocity of the capsule has been developed. The analysis of the pressure drop, and the flow structure within the pipe, has not been included in the study.

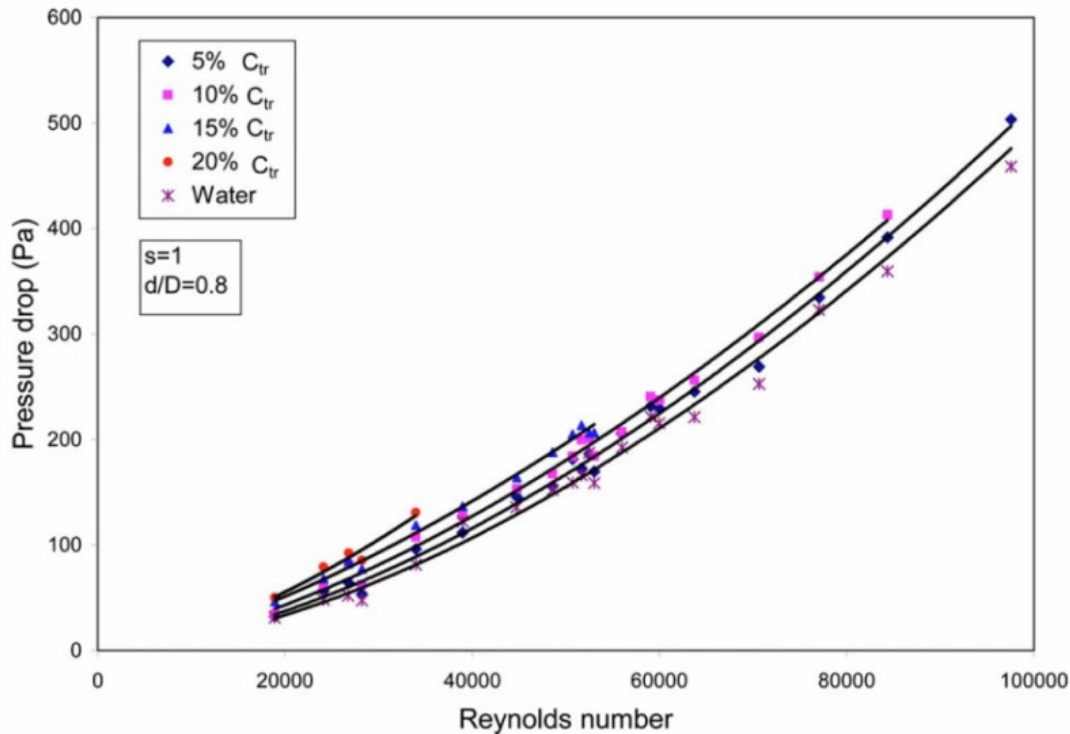


Figure 2.2. Relation between ΔP and Re of Mixture based on Experiments [26]

Newton et. al. [28] conducted perhaps the first numerical investigation on the flow of a cylindrical capsule in a pipeline. The range of investigations has been kept the same as for Ellis [15] with a difference that the capsule length to diameter ratio has been varied from 1 to 20. The results presented are focused on the capsule velocity and the pressure drop within the pipe. However, the flow has been considered to be laminar, which severely limits the practical application of the study conducted. Furthermore, no analysis of the flow field within the pipe has been presented in the study. The study focuses on the flow of a single cylindrical capsule only.

Kroonenberg [29] developed a mathematical model for the prediction of a cylindrical capsule's velocity and the pressure drop within the pipeline. The velocity field within the pipe has also been investigated in this study (equation (2.3)). However, the actual velocity profiles in the pipe, and in the region between the capsule and the pipe wall, have been neglected, and only mean velocities have been taken into account. This assumption, let alone the other assumptions that have been considered in this study, makes it more of a theoretical analysis rather than a practical study. This is because the velocity profiles in the pipe, and in the annulus region between the capsule and the pipe wall, have a great impact on the flow behaviour in pipelines transporting capsules. The acceleration of the flow in the annulus, and the presence of a wake region downstream of a cylindrical capsule, has significant impacts on the calculation of capsule velocities and pressure drops within the pipeline. The pressure distribution within the pipeline has been investigated (equation (2.4)); however, the effect of the length and the number of capsules has not been included in the study.

$$V_c = V_b \left[\frac{\left(1 - \frac{f_w}{f_c} k^3\right) + (1-k^2) \sqrt{\frac{f_w k}{f_c}}}{1 - \frac{f_w}{f_c} k^5} \right] \quad (2.3)$$

$$\Delta P = \frac{f L_p}{D} \frac{1}{2} \rho V_b^2 \left[\frac{1}{\left(1 + k^2 \sqrt{\frac{f_w k}{f_c}}\right)^2} \right] \quad (2.4)$$

Tomita et. al. [30] carried out numerical analysis of the flow of a single cylindrical capsule in a hydraulic pipeline. The study focuses on the velocity and the trajectory of the capsule in the pipe. The capsule has been considered as a point mass in this study. A limited discussion on the velocity and pressure distribution in the vicinity of the capsule has been included, but no analysis on a train of cylindrical capsules has been carried out. Wheels have been assumed to be attached to the capsule in order to keep the capsule in the centre of the pipeline, and hence, no analysis of a freely flowing cylindrical capsule has been conducted. Furthermore, the effect of the length of the capsule has not been considered in this study.

Tomita et. al [31] extended their own work [30] by taking into account the flow of a train of cylindrical capsules, where the spacing between the capsules has been kept variable. Again, the study has been limited to the discussion of the capsule's trajectories and the velocity of the capsules. A point mass approach has been used to numerically analyse the flow of the cylindrical capsules in the pipeline, assuming a fully developed co-axial flow in the annulus between the capsule and the pipe wall.

Lenau et. al. [32] extended Tomita et. al. [31] works to develop a numerical model in which the cylindrical capsule has been considered as an elastic and rigid body respectively (figure 2.3). The capsule velocity and the capsule trajectory have been found out at various nodes (e.g. C_1 , C_2 , C_3 etc.). Some discussion on the pressure and velocity distributions has been included. However, the study is limited to the flow of a single cylindrical capsule. The study lacks in-depth analysis of the flow distribution within the pipeline.

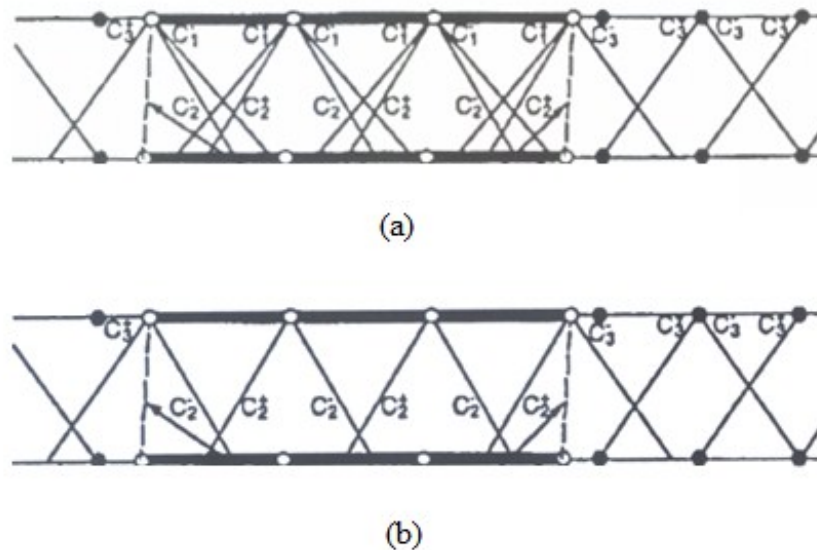


Figure 2.3. Characteristics near Capsule for (a) Elastic and (b) Rigid Capsule Models [32]

Khalil et. al [33] carried out numerical analysis on the flow of a single cylindrical capsule in a pipeline. The range of investigations has been limited to $k = 0.8$ to 0.9 . A comparison of various turbulence models has been presented. Velocity profiles and pressure drop calculations have been analysed in detail. However, the length of the capsule has been taken to be the same for all the cases in the investigation. A limited analysis of the flow field within the pipeline has been presented.

Ellis et. al. [34] carried out experimental investigations on the flow of a heavy density spherical capsule in a hydraulic pipeline. The range of investigations was $k = 0.4$ to 0.9 , $V_{av} = 1$ to 3.5 m/sec and $N = 1$. The discussion on the results, obtained for the capsule's velocity, has been limited to the effects of k and V_{av} on capsule velocity, V_c . No expression for the velocity of the capsule has been developed. The analysis on the pressure drop, and the flow variations within the pipe, has not been included in the study.

Round et. al. [35] carried out experimental investigations on the flow of heavy density spherical capsules. From dimensional analysis, it was found out that the velocity of the capsule depends on the diameter ratio of capsule to pipe and the average flow velocity, V_{av} . The range of investigations was $k = 0.39$ to 0.89 , $V_{av} = 1$ to 3.7 m/sec and $N = 1$. The discussion on the results, obtained for the capsule's velocities, has been limited to the effects of k and V_{av} on V_c . No expression for the velocity of the capsule has been developed. The analysis of the pressure drop, and the flow distribution within the pipe, has not been included in the study.

Ellis et. al. [36] carried out experimental investigations on the flow of heavy density spherical capsules in a hydraulic pipeline. The range of investigations was $k = 0.7$ to 0.9 and $V_{av} = 1$ to 3.5 m/sec. The discussion on the results, obtained for the pressure drop, has been limited to the effects of k and V_{av} . No discussion of the velocity of the capsule has been presented.

Ellis et. al. [37] carried out experimental investigations on the flow of heavy density cylindrical capsules. The study primarily focuses on the pressure drop calculations and power requirements for the pipeline transporting capsules. The study does not present any insight into the flow structure within the pipe, or the variations in the velocity of the capsules.

Jan et. al. [38] carried out experimental investigations on the flow of heavy density cylindrical capsules in a hydraulic pipeline. The range of investigations was $k = 0.7$ to 0.95 and $V_c = 0$ to 0.8 m/sec. The discussion on the results obtained for the holdup has been limited to the effects of k (figure 2.4). It can be seen in the figure that as the capsules become smaller in size, i.e. reducing k values, the holdup also decreases. The study does not present any insight into the flow field within the pipe.

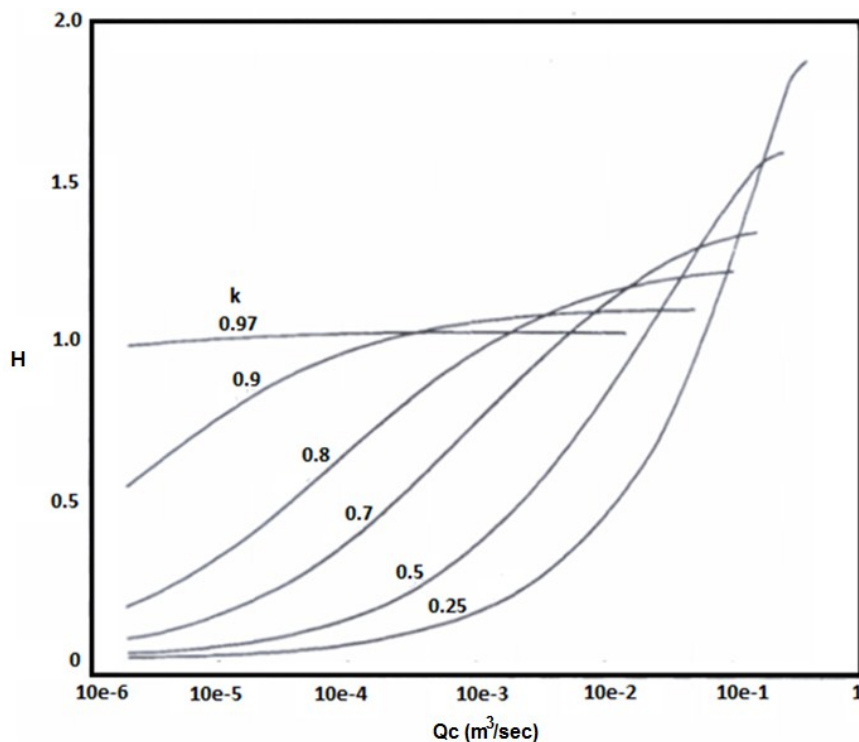


Figure 2.4. The Predicted Effect of k on the Holdup at various Solid Throughputs [38]

Ellis et. al. [39] carried out experimental investigations on the flow of heavy density cylindrical capsules in a hydraulic pipeline. The range of investigations was $k = 0.39$ to 0.89 and $V_{av} = 1$ to 3.5 m/sec. The discussion on the results, obtained for the capsule velocities, has been limited to the effects of k and V_{av} on capsule velocity, V_c . No expression for the velocity of the capsule has been developed. The analysis on the pressure drop, and the flow structure within the pipe, has not been included in the study.

Kyuyer et. al. [40] carried out analytical analysis on the flow of heavy-density cylindrical capsules in a laminar flow of water. Detailed analysis, for the capsule velocity and the pressure drop, has been presented. The model has been extended to cover turbulent flow problems as well. However, the discussion does not include any information regarding the flow variables within the pipe.

Tomita et. al [41] carried out analytical studies on the flow of heavy-density cylindrical capsules in a horizontal pipeline. The focus of the study is towards the trajectory and the velocity of the capsules in the pipeline (equation (2.5)) based on such variables as p_f , p_r , V_r and Z which represents the fluid pressures acting on the front and rear faces of the capsule, the capsule velocity in the radial direction (V_r) and the coordinates of the capsule (Z). The analysis makes use of the loss coefficient of an abrupt

contraction within the pipeline, i.e. ζ . No information regarding the pressure drop or the flow distributions within the pipe has been included.

Agarwal [42] carried out experimental investigations on the flow of heavy density cylindrical capsules in a hydraulic pipeline. The range of investigations was $k = 0.5$ to 0.9 and $V_{av} = 1.4$ to 2.96 m/sec. The discussion focuses on the velocity ratio. The detailed analysis of the flow structure in the pipe has not been reported. Furthermore, the pressure drop in the pipeline has not been reported.

$$V_b = \frac{D^2}{32\mu L} \left(1 + k^2 + \left(\frac{1-k^2}{\ln(k)} \right) \right) \left[p_r - p_f - \left(\frac{\zeta + k^4}{(1-k^2)^2} \right) \frac{1}{2} \rho (V_r - Z)^2 \right] - \frac{Z}{1-k^2} - \frac{Z}{2 \ln(k)} \quad (2.5)$$

2.1.1. Summary of Literature regarding Horizontal HCPs

Based on the literature review presented above, for the transport of capsules in horizontal pipelines, it can be summarised that the published literature is severely limited in terms of the range of flow velocities, capsule diameters, concentration of the capsules in the horizontal pipeline, pressure drop considerations and detailed analysis of the flow parameters within these pipelines, such as the pressure variations and the velocity distributions. Based on the results summarised here, a generic horizontal pipeline transporting capsules cannot be accurately designed for practical purposes. Hence, there is a need of better understanding of the flow structure within horizontal pipelines transporting capsules. Furthermore, a wider range of investigations are required in order to built-up an adequate database for accurate analysis of horizontal pipelines transporting capsules.

2.2. Vertical HCPs

Chow [43] carried out extensive investigations on the flow of equi-density spherical and cylindrical capsules in a vertical pipeline. The range of investigations are $k = 0.5$ to 0.9 $V_{av} = 1$ to 4 m/sec and $L_c = 1$ to 14 times the diameter of the capsule. A detailed analysis has been presented regarding the velocity of the capsules and the pressure drop calculations in the pipeline. Semi-empirical expressions for the said have been developed. However, no information regarding the flow structure within the pipeline has been reported.

Hwang et. al [44] carried out both analytical and experimental investigations on the flow of heavy-density cylindrical capsules in a vertical pipeline. The range of investigations is $k = 0.5$ to 0.9 . The primary focus of the study is to find the overall efficiency of the capsule transporting system, in terms of energy loss or pressure drop. It has been reported that the best value of k , which corresponds to the maximum efficiency of the system, is $2/3$ or 0.66 . Furthermore, it has been reported that the length of the capsule has little influence on the efficiency of the system. However, the flow structure within the pipeline has not been analysed in the study.

Latto et. al [45] carried out experimental studies on the flow of heavy-density spherical and cylindrical capsules in a vertical pipe. The range of investigations is $k = 0.5$ to 0.9 , $V_{av} = 1$ to 4m/sec and $L_c = 1$ to 14 times the diameter of the capsule. A detailed analysis of the capsule velocities and the pressure drop within the pipeline has been presented. However, no information regarding the flow structure within the pipeline has been recorded.

Motoyoshi [46] conducted experimental studies on the flow of heavy-density cylindrical capsules in inclined and vertical pipelines. The range of investigations is $k = 0.5$ to 0.9 and $L_c/d = 2$ to 10 . The study focuses on the energy loss in the systems (figure 2.5). It can be seen that capsules with lower L_c/d have lower energy loss associated with them. Furthermore, the variations in energy loss are non-linear w.r.t. the angle of inclination of the pipeline. No information regarding the flow structure within the pipelines has been presented.

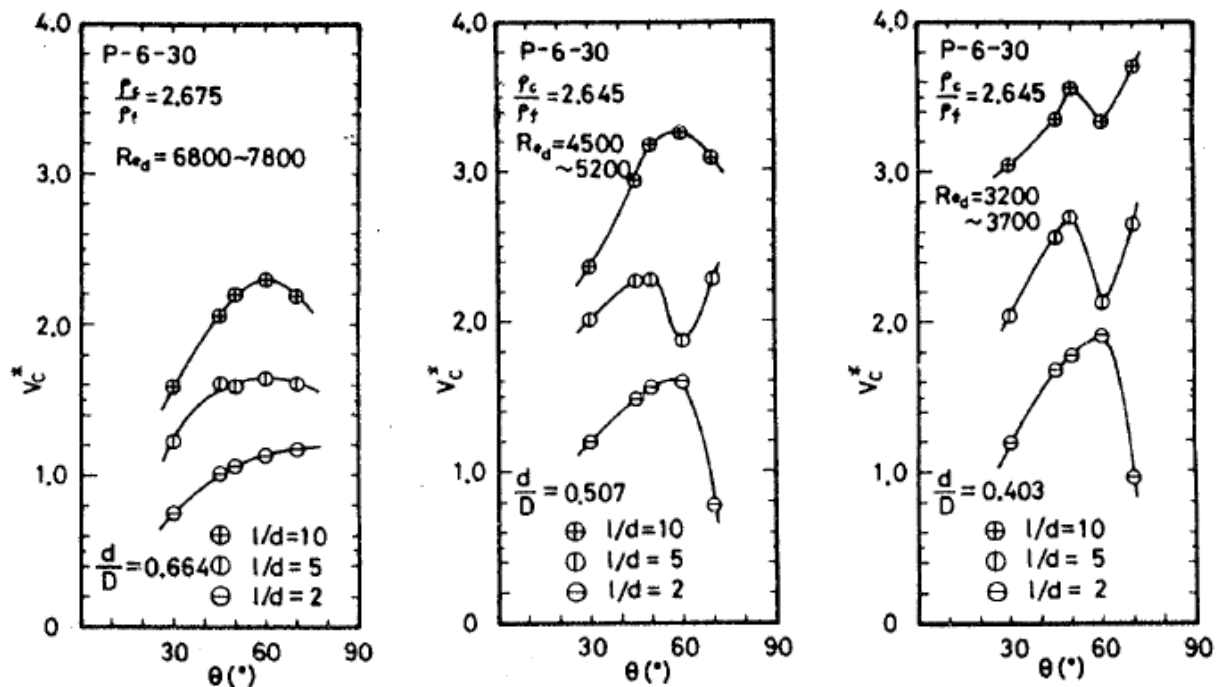


Figure 2.5. The Relation between the Balance Velocity and the Inclination Angle (a) $k = 0.664$ (b) $k = 0.507$ (c) $k = 0.403$ [46]

Yutaka et. al [47] conducted experimental investigations on stationary capsules in a vertical pipe. Detailed investigations on the flow structure regarding the wake region downstream of the capsules, and its effect on the trailing capsules in the train, has been reported in terms of the drag coefficient of the capsules (figure 2.6). The figure shows that how the presence of the capsules in the pipeline affects the velocity profile at different cross sections of the pipe. However, the study is severely limited by the fact that the capsules are stationary in the pipeline.

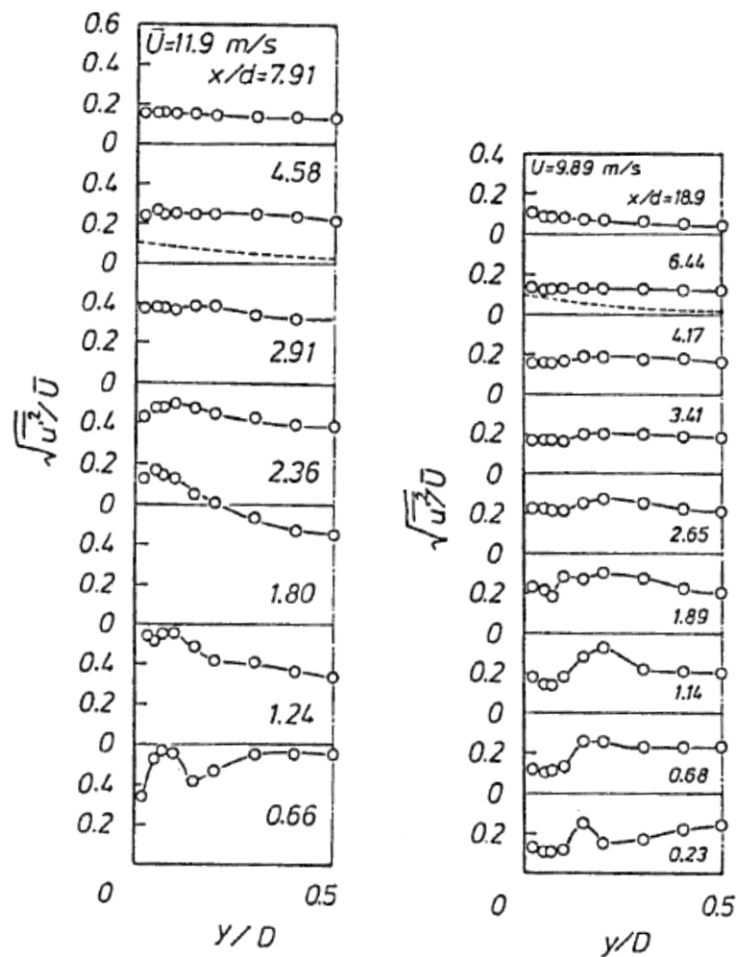


Figure 2.6. Distributions of Turbulent Intensity (a) $k = 0.9$ (b) $k = 0.67$ [47]

Akira et. al [48] conducted both analytical and experimental studies on the flow of cylindrical capsules in a vertical pipeline. The range of investigations is $k = 0.78$ to 0.96 , $s = 1.39$ to 7.84 and $Lc/d = 1.5$ to 5 . A model for the prediction of the pressure drop (ΔP) in the pipeline, as a function of the froud number of the capsules (Fr), has been presented (figure 2.7). The figure shows that the pressure drop within a pipeline has an inverse relationship with the froud number (Fr) of the capsules. No information regarding the flow structure within the pipeline has been reported.

Bartosik et. al [49] carried out numerical studies on the flow of solid-water mixtures in vertical pipelines. The results that have been reported are focused on the analysis of the velocity field and the effects of the concentration of the solid phase in the pipeline on the pressure drop. However, no information regarding the pressure distribution and pressure drop in the pipeline has been reported.

Katsuya et. al [50] conducted analytical and experimental investigations on the flow of cylindrical capsules in a vertical pipeline. A detailed discussion on the flow development in such pipelines has been presented. Furthermore, the drag coefficient of the capsules under varying geometric and flow conditions has been reported. However, the pressure drop calculations have not been made in the pipeline.

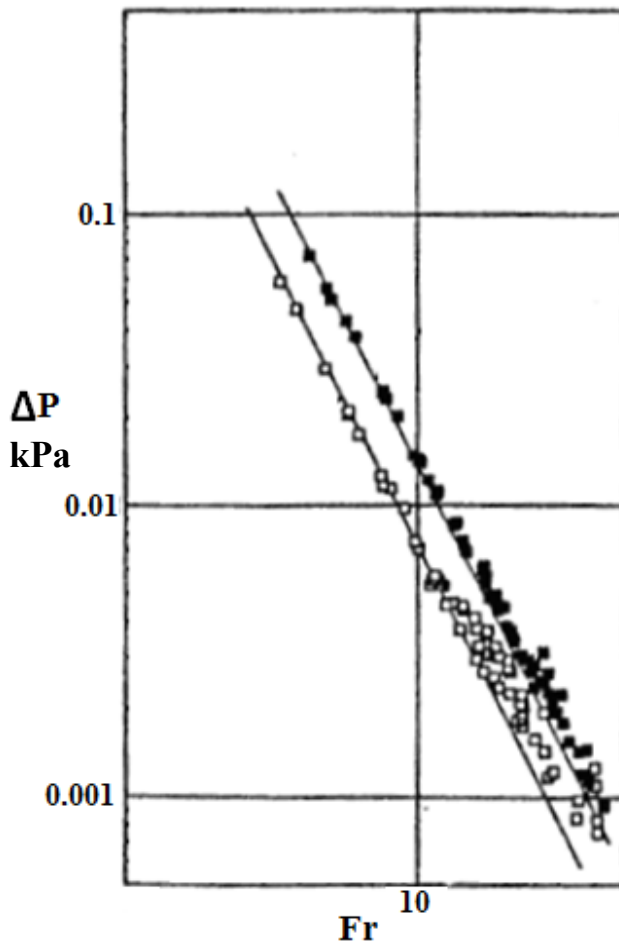


Figure 2.7. Pneumatic, Steadily Moving Capsule [48]

Prabhata et. al [51] conducted design studies on the flow of cylindrical capsules of various densities (both equal and heavy) in a vertical pipeline. However, the study is severely limited because no information on the flow structure within the pipeline has been provided.

2.2.1. Summary of Literature regarding Vertical HCPs

Based on the literature review presented above, for the transport of capsules in vertical pipelines, it can be summarised that the published literature is severely limited in terms of the range of flow velocities, capsule diameters, concentration of the capsules in the vertical pipeline, pressure drop considerations and detailed analysis of the flow parameters within these pipelines, such as the pressure variations and the velocity distributions. Based on the results summarised here, a generic vertical pipeline transporting capsules cannot be accurately designed for practical purposes. Hence, there is a need of better understanding of the flow structure within vertical pipelines transporting capsules. Furthermore, a wider range of investigations are required in order to built-up an adequate database for accurate analysis of vertical pipelines transporting capsules.

2.3. HCP Bends

Published literature regarding the flow of capsules in pipe bends is severely limited. Vlasak et. al. [52] conducted experimental studies on the flow of heavy-density cylindrical capsules in both horizontal and vertical bends of various radii of curvature. The results presented for the velocity ratio and pressure gradient indicated that the pressure drop in vertical bends is significantly higher as compared to horizontal pipe bends. Furthermore, it has been reported that the radius of curvature of the bend has an insignificant effect on the velocity ratio of the capsules. However, no information regarding the flow structure within the pipe bends has been reported.

Pavel et. al. [53] conducted experimental studies on the flow of heavy-density cylindrical capsules in vertical bends of $r/R = 2$ and $Lc/d = 5$. The results for the velocity ratio, where V_0 is the same as average velocity V_{av} considered in the present study, and the pressure gradient have been presented (figure 2.8). It can be seen from the figure that as the average flow velocity increases within a pipe bend, the holdup also increases. However, no information regarding the flow structure within the pipe bends has been reported.

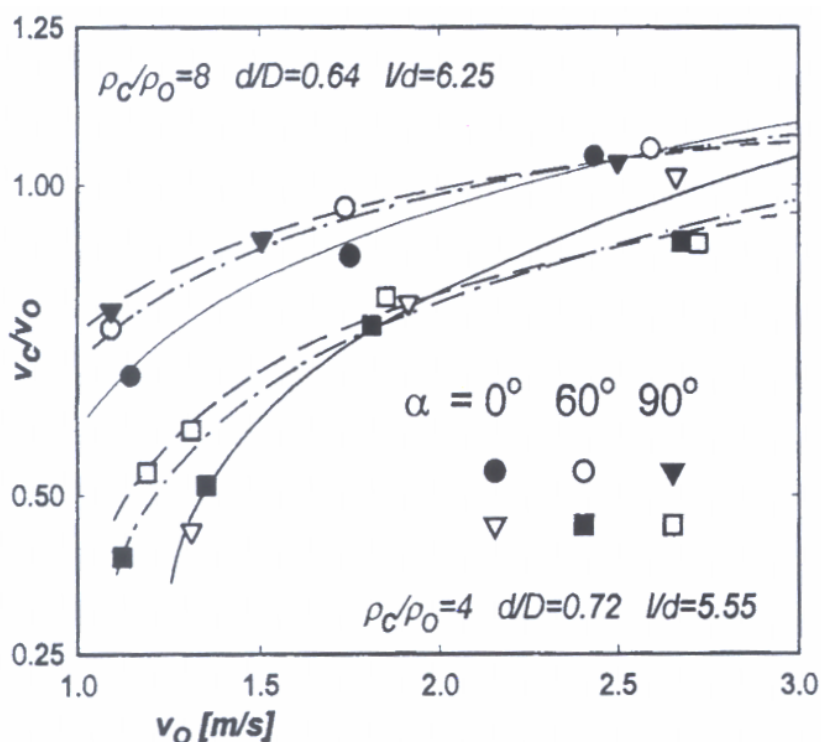


Figure 2.8. Effect of Bend Central Angle on Velocity Ratio of Capsule in Bend [53]

Azzi et. al [54] conducted numerical studies on the two-phase flow in vertical pipe bends. Detailed analysis on the pressure and velocity distributions within the bend has been presented; however, the study is severely limited to the flow in pipe bends. Deniz [55] conducted experimental investigations on the flow of low-density spherical capsules in 45° and 90° pipe bends with $k = 0.8$ and $V_{av} = 0.2$ to 1.4 m/sec. A semi-empirical model for the prediction of pressure drop has been developed (equation (2.6)). However, no information regarding the flow structure with the pipe bend has been reported. Furthermore, only horizontal pipe bends have been used for analysis.

$$n K_c \frac{V_b^2}{2g} = \frac{\Delta P_{total}}{\gamma} - \left(\lambda \frac{L}{D} \frac{V_b^2}{2g} \right) \quad (2.6)$$

Motamedian et. al [56] conducted numerical investigations on two-phase flow in horizontal pipe bends. The study is primarily concerned with the pressure drop calculations in the pipe bend. The study is severely limited to capsule flow in pipe bends. Spedding et. al. [57] conducted experimental investigations on three-phase flow in horizontal pipe bends. The study is primarily concerned with the pressure drop ($\Delta P/\Delta L$) calculations in the pipe bend and the effect of the friction factor of capsules (f_c) on the pressure drop (figure 2.9). The study is limited to capsule flow in pipe bends.

Silva et. al [58] conducted experimental studies on two-phase flow in horizontal pipe bends. The study is primarily concerned with the pressure drop calculations in the pipe bend. The study is severely limited to the flow in pipe bends. Ulusarslan [59] conducted experimental investigations on the flow of low-density spherical capsules in 45° and 90° pipe bends with $k = 0.7$ to 0.9 and $V_{av} = 0.2$ to 1.4 m/sec. A semi-empirical model for the prediction of pressure drop has been developed. However, no information regarding the flow structure with the pipe bend has been reported. Furthermore, only horizontal pipe bends have been used for analysis.

Mazumder et. al. [60] conducted numerical studies on the effect of bend's radius on the multi-phase flow in vertical pipe bends. Detailed analysis of the pressure and velocity distributions within the bend has been presented; however, the study is severely limited to capsule flow in pipe bends.

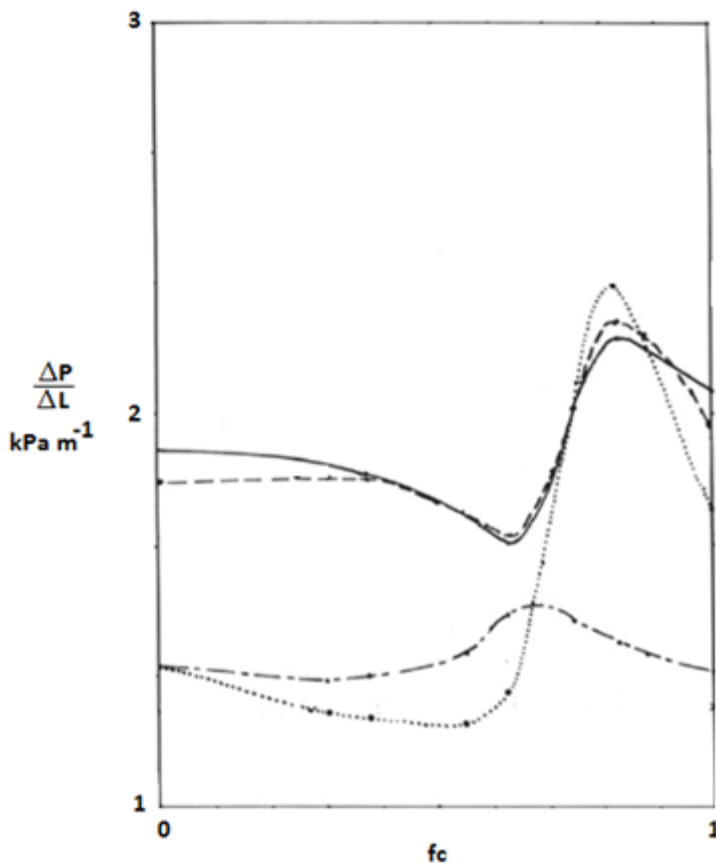


Figure 2.9. Pressure Losses through Various Regions in a Horizontal Bend [57]

Quamrul [61] conducted numerical studies on multi-phase flow in vertical pipe bends. Detailed analysis of the pressure and velocity distributions within the bend has been presented (figure 2.10); however, the study is severely limited to the flow in pipe bends.

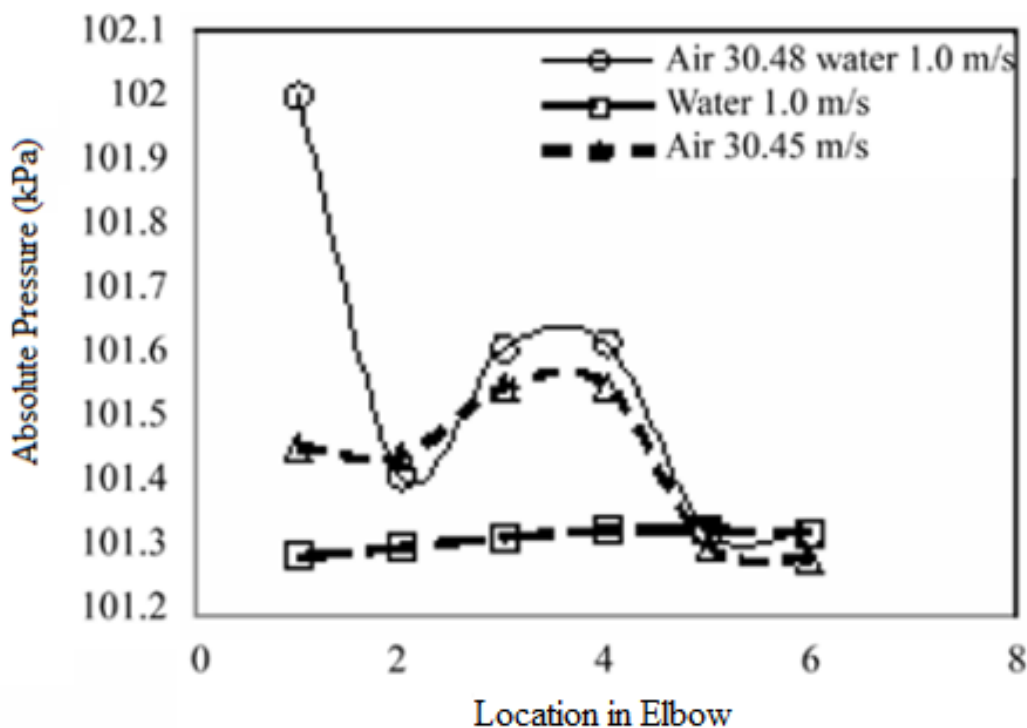


Figure 2.10. Single and Multiphase Pressure Drop [61]

2.3.1. Summary of Literature regarding HCP Bends

Based on the literature review presented above, for the transport of capsules in pipe bends, it can be summarised that the published literature is severely limited in terms of the range of flow velocities, capsule diameters, concentration of the capsules in the bends, pressure drop considerations and detailed analysis of the flow parameters within these bends, such as the pressure variations and the velocity distributions. Based on the results summarised here, a generic pipeline transporting capsules cannot be accurately designed for practical purposes. Hence, there is a need of better understanding of the flow structure within pipe bends, transporting capsules. Furthermore, a wider range of investigations are required in order to built-up an adequate database for accurate analysis of pipe bends, transporting capsules.

2.4. HCP's Optimisation

Polderman [62] reports design rules for hydraulic capsule systems for both on-shore and off-shore applications. The design rules are based on such variables as the pressure drop in the pipeline, Reynolds Number of capsules etc. A general indication towards parameters that might be used for an optimisation model has been given. However, no such optimisation model has been developed, which can be used for a pipeline transporting capsules.

Morteza et. al. [63] developed an optimisation model for pipelines transporting capsules based on maximum pumping efficiency (figure 2.11). The costs involved in the design of such pipelines are, however, not included.

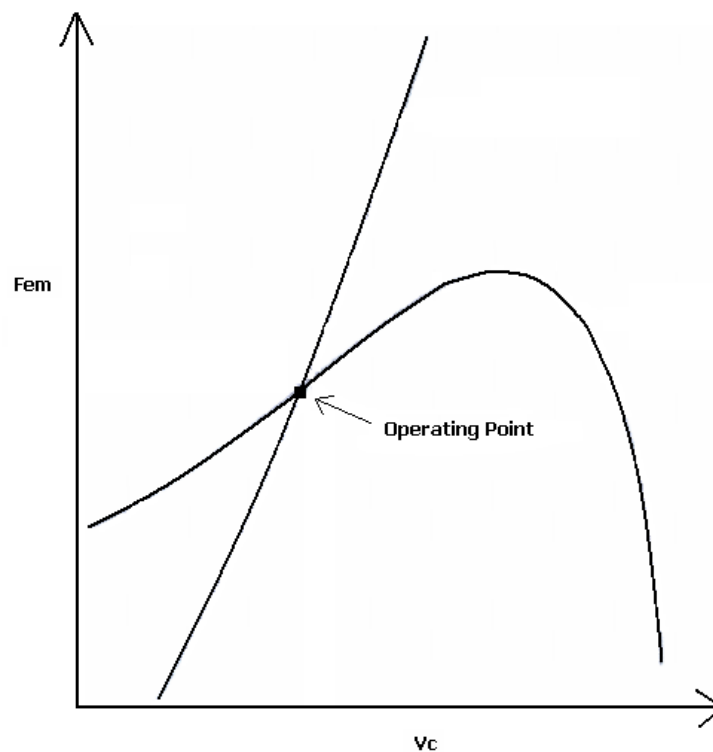


Figure 2.11. Operation of TLIM Capsule Pump [63]

Prabhata [64] has developed an optimisation model for sediment transport pipelines based on the least-cost principle. The model assumes the value of the friction factor as the input to the model, strictly limiting its usefulness for commercial applications. Swamee [65] has developed a model for the optimisation of equi-density cylindrical capsules in a hydraulic pipeline (figure 2.12). The model is based on least-cost principle. The input to the model is the solid throughput required from the system. The friction factors considered, however, are not representative of the capsule flow in the pipeline, and hence severely limit the practicality of the model.

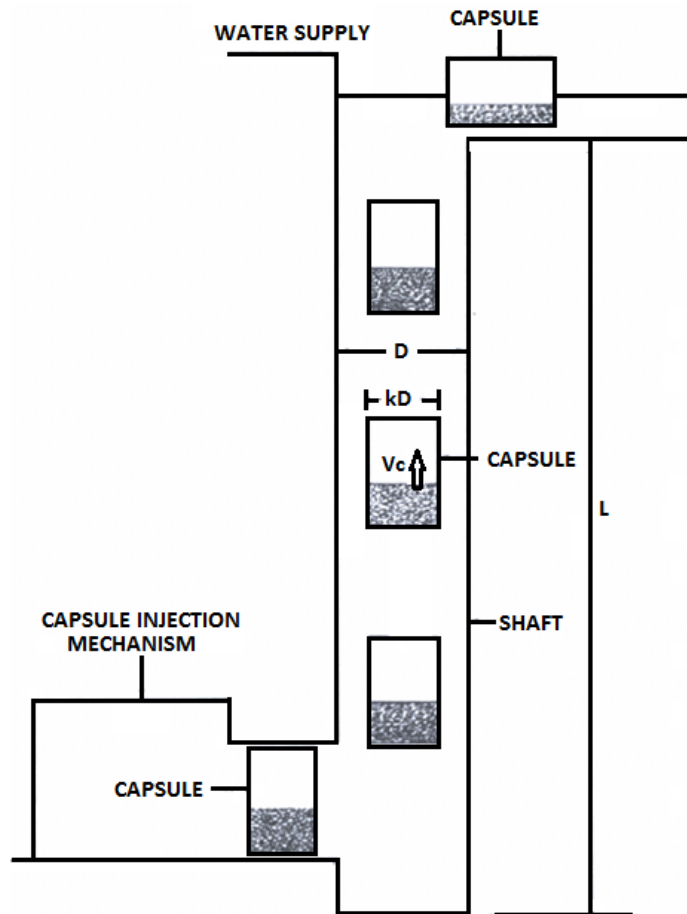


Figure 2.12. Hoist Description [65]

The model is based on the iterative process. The model has a severe limitation in terms of the friction factor assumption and hence cannot be used for pipelines transporting capsules.

Agarwal et. al. [66] has developed an optimisation model for multi-stage pipelines transporting capsules. The model is based on the principle of least-cost and uses the solid throughput as the input to the model. The model developed is applicable for contacting spherical capsules only, occupying the complete length of the pipeline. Furthermore, this optimisation model has the following limitations:

- Limited parameters for the analysis of pipelines transporting capsules
- Homogeneous model for pressure drop prediction

The friction factor used for the model is an approximation of the Colebrook – White's equation for friction factor in a hydraulic pipeline [67], severely limiting the utility of the model in terms of accurate representation of the pressure drop in the pipeline transporting capsules. Yongbai [68] has developed an optimisation model for hydraulic pipelines based on saving energy sources. The model, however, cannot be used for multi-phase flows.

2.4.1. Summary of Literature regarding Optimisation of HCPs

The optimisation methodologies presented in the literature review above mainly comprises of estimated prediction models, or even in some cases, the prediction models used for the flow of water in pipelines, which is an immense knowledge gap in the existing literature. Based on the literature review presented above, for the optimisation of pipelines transporting capsules it can be summarised that fairly accurate prediction models, for the pressure drop calculations in a pipeline transporting capsules are required in order to design and optimise such pipelines. The results for the pressure drop calculations from the transport of capsules in horizontal and vertical pipelines, including bends, can be used to develop semi-empirical relationships for the transport of capsules in pipelines.

2.5. Scope of Research

At present, the knowledge regarding the complex flow structure within pipelines transporting capsules is severely limited. It is due to the fact that most of the research being carried out based on experimental findings where it becomes very difficult to monitor and analyse the flow variables while capsules are being propagated within the pipelines. With the advent of modern computational tools and sophisticated software to model and simulate fluid flow in pipelines, it has now become possible to study the complex flow structure within pipelines transporting capsules.

Based on the review of published literature, key areas of research for capsule transport mechanism have been found. The first main area of the present study is the flow diagnostics of capsule flow for on-shore applications. As most of the on-shore pipelines constitute of horizontal pipes, hence capsule flow in horizontal pipelines needs to be analysed in great detail. Furthermore, the effect of geometric and flow parameters, discussed in chapter 1, on the flow of capsules in horizontal pipes need to be analysed.

The second key area of research for this study is the flow diagnostics of capsule flow for off-shore applications. Off-shore pipeline networks largely constitute of vertical pipes, hence capsule flow in vertical pipelines needs to be analysed in great detail. Furthermore, the effect of geometric and flow parameters, discussed in Chapter 1, on the flow of capsules in horizontal pipes need to be analysed.

The third key area of research for this study is the analysis of capsule flow in pipe fittings such as bends. Bends are an integral part of any pipeline design, hence capsule flow in pipe bends (both horizontal and vertical) needs to be analysed in great detail. Furthermore, the effect of geometric and flow parameters, discussed in Chapter 1, on the flow of capsules in horizontal pipes need to be analysed.

The fourth key area of research for this study is the optimisation of the pipelines transporting capsules based on the findings of the first three key areas of research mentioned above. The optimisation is essential as far as the commercial viability of these pipelines is concerned.

2.6. Specific Research Objectives

Based on the research aims presented in the previous chapter, and after conducting a detailed literature review, the following objectives have been formulated which will aid the research aims and address the issues in the existing knowledge:

1. To determine the effect of the shape of the capsule on the flow structure and the pressure drop within the pipelines.
2. To analyse the effect of the density of the capsules on the flow distribution and the pressure drop within the pipes.
3. To establish the effect of the concentration of the capsules on the flow variations and the pressure drop within the capsule pipelines.
4. To formulate the effect of the length of the cylindrical capsules on the flow distribution and the pressure drop within the pipes.
5. To determine the effect of the spacing between the capsules in a train on the flow variations and the pressure drop within the capsule pipelines.
6. To establish the effect of the diameter of the capsules on the flow structure and the pressure drop within the pipelines.
7. To formulate the effect of the average flow velocity on the flow variations and the pressure drop within the capsule pipelines.
8. Development of semi-empirical relations for the friction factor and pressure drop in pipelines transporting.
9. Development of a robust optimisation model based on the least-cost principle.

In order to satisfactorily achieve the aforementioned research objectives, this study uses Computational Fluid Dynamics tools to numerically simulate the flow within capsule pipelines. The next chapter presents the numerical modelling techniques being incorporated in this study.

CHAPTER 3

CFD MODELLING OF HYDRAULIC CAPSULE PIPELINES

Based on the research objectives of this study that have been identified in the previous chapter, advanced CFD techniques have been used in order to computationally simulate and solve the flow of capsules in a pipeline. The use of these techniques, along-with a novel methodology for the prediction of trajectory, velocity, position and orientation of the capsules in the pipeline has been presented in this chapter. Appropriate solver settings and the boundary conditions prescribed in the present study, have been mentioned. Furthermore, using the holdup data from literature review carried out in Chapter 2, correlations have been developed for the velocity of the capsules under various geometric and flow conditions. The numerical experiments conducted for this research study have been identified.

The equations governing flow of fluids in a continuum forms the basis of Computational Fluid Dynamics. These equations can be found in any CFD related book and hence have not been included in the main text of the present study. However, for the completeness of this study, and for naive readers, the basics of CFD have been included in Appendix A-1. For reader's interest, some good books regarding CFD are recommended here [69 – 74]. The following sections provide details of the numerical modelling that has been used in the present study. The CFD package that has been used to achieve this is known as Ansys [75]. At the time when this study was carried out, version 13.0.0 was the latest version of this package and hence has been used for simulations/analysis in this thesis.

3.1. Pre-Processing

The pre-processing in CFD is subdivided into two main categories, i.e. creation of the geometry and the meshing of the flow domain. This section provides details of the geometric modelling and the meshing of the hydraulic capsule pipelines.

3.1.1. Pipe and Bend Geometries

The geometry of the pipe has been created using the Design Modeller facility in Ansys 13. The geometry of the pipe has been created in three separate steps. The first section is named as Inlet pipe, the second as Test section and the third as Outlet pipe. This has been purposely done because of the way how the boundary conditions are being applied in the solver. The length of the Inlet pipe is 5m. The detailed discussion on the length of the Inlet pipe is provided in next chapter. According to Munson et. al [76], it takes about $50 * D$ length of the pipe for the flow to become fully developed. As the pipe diameter is 0.1m, therefore, the Inlet pipe of 5m length has been used for analysis.

The test section that has been used for the flow diagnostics of capsule transport is 1m long. The test section used in this study has the same properties as that of Ulusarslan et. al. [77] i.e. 1m length, 100mm diameter and the pipe is hydrodynamically smooth, which means that the absolute roughness constant ϵ of the pipe is zero. The Outlet pipe has a length ranging of 1m and is shown in figure 3.1. This numerical test setup has been used throughout this study for the analysis of HCPs.

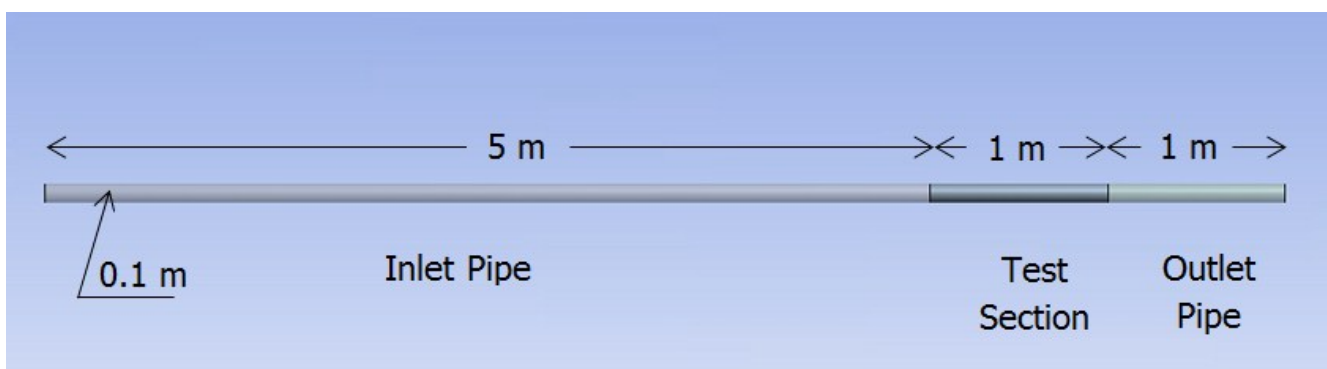


Figure 3.1. Geometry of the Pipe

Two different practical pipe bend configurations, having r/R equal to 4 and 8, have been used for the flow diagnostics of capsule transport in pipe bends. The geometric details of the bends have been taken from industrial standards [78]. The angle of the bends under investigation is $\theta = 90^\circ$. Figure 3.2 shows the different configurations of the bends being investigated for the flow of capsules in them.

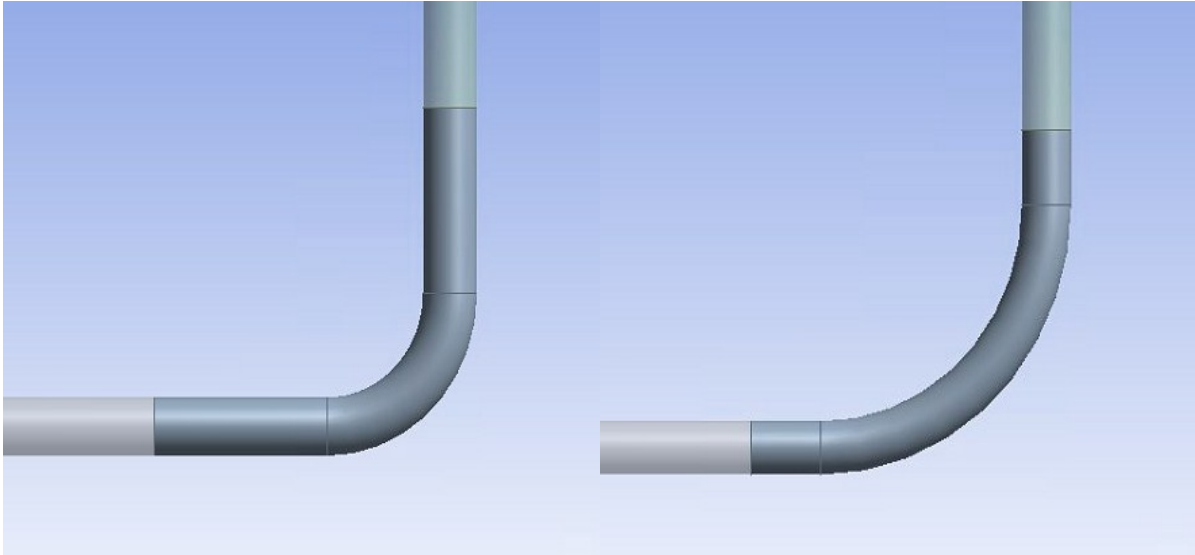


Figure 3.2. Geometry of the Bends

It is noteworthy here to mention the fact that the analyses presented in this study are based on the pressure drop considerations per unit length of the pipeline. In case of straight pipes, this is quite straightforward and is achieved by modelling the test section having a length of 1m. For pipe bends, the volume of the bend has been calculated and compared against the volume of 1m of a straight pipe. Additional straight pipe lengths have been added to the pipe bends in order to match the volume of the two. In figure 3.2, it can be clearly seen that additional straight pipe lengths have been added, equally on both sides of the standard bend configurations, so that the pressure drop across the complete bend geometry corresponds to per unit length of the pipeline.

Another important point to note at this stage is that the Inlet and Outlet pipes have been created in a different way as compared to the test section of the pipes or the bends. This has been purposefully done in order to control the quality and quantity of the control volumes (mesh) in the pipeline. Further discussion on the meshing techniques being used in the present study will follow the next section.

3.1.2. Capsule Geometries

The capsules have been introduced into the Test section of the pipe. Various sizes, shapes and number of capsules have been used for the analysis. Figure 3.3 shows the Test section of the pipe having three spherical capsules of $k = 0.5$ with a spacing of $3 * d$ between them where d is the diameter of the capsules. The capsules shown in figure 3.3 have the same density as that of water.

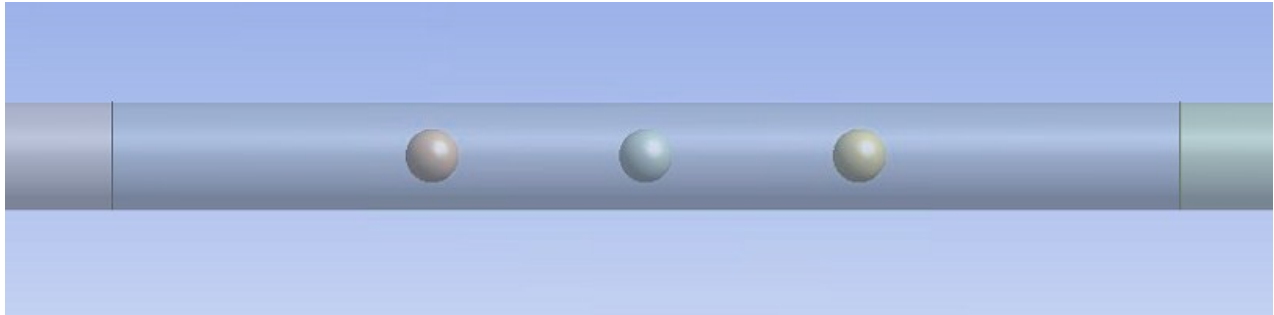


Figure 3.3. Geometry of Equi-Density Spherical Capsules

Modifications in the modelling of the capsules in a pipeline have been made when the density of the capsules becomes greater than that of water, and the capsules travel along the bottom pipe wall. Figure 3.4 shows the presence of a capsule train consisting of two aluminium cylinders with a spacing of $3 * d$ between them.

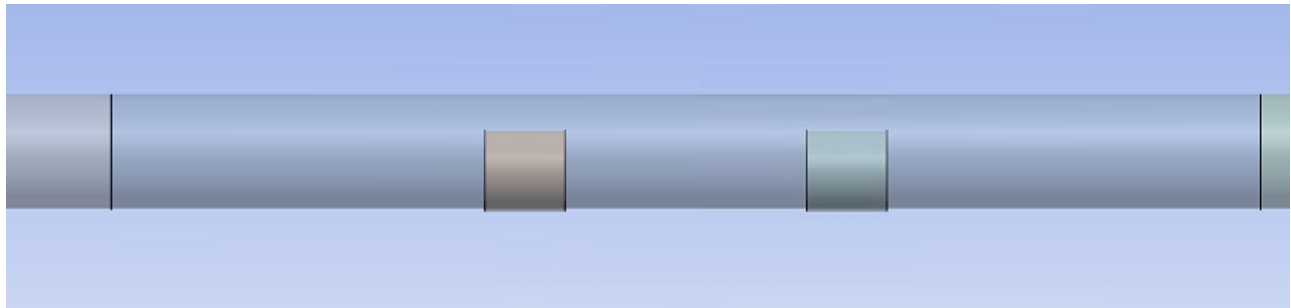


Figure 3.4. Geometry of Heavy-Density Cylindrical Capsules

The flow of capsules in a pipe bend is quite complicated to model as the trajectory of the capsules keep on changing while passing through the bend. A novel modelling technique has been used in the present study to accommodate these effects. A detailed discussion on this method has been presented here.

Using Discrete Phase Model (DPM), which is used for tracking the trajectory of particles in the flow domain, a particle having the same diameter and density as that of the capsule is injected at the inlet boundary of the pipeline [79]. The history of the particle's trajectory and velocity in space has been monitored and recorded. Figure 3.5 shows the trajectory and velocity of a spherical particle having a density equal to that of aluminium and $k = 0.7$ in a horizontal bend of $r/R = 4$ in which water is flowing at an average flow velocity of 4m/sec. From the trajectory of the particle, it was noted that the capsule travelled along the bottom wall of the pipe as shown in figure 3.5. Further details about DPM are included in section 3.2.6.

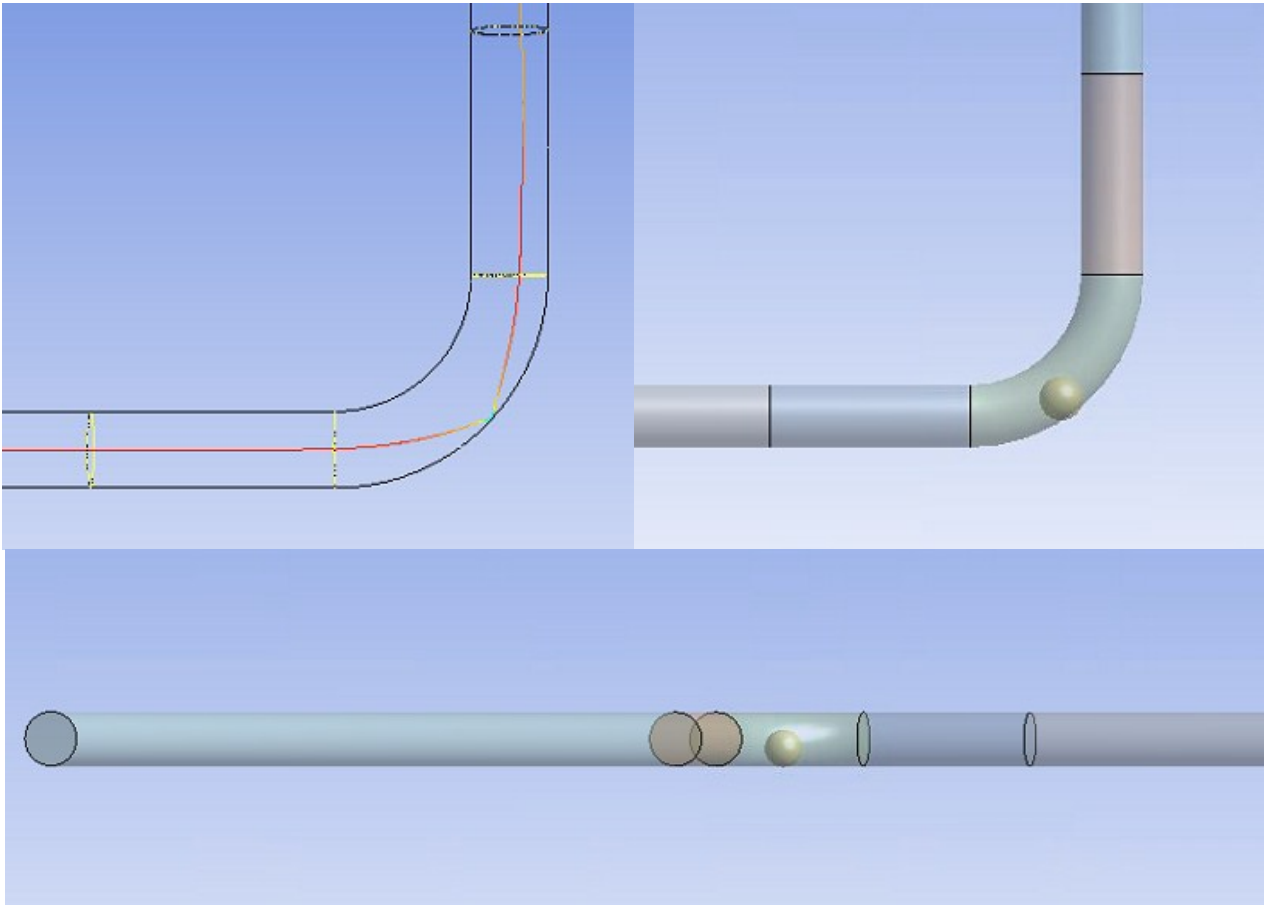


Figure 3.5. Trajectory of Heavy-Density Spherical Capsules in HCP Bends

Similarly, an example of a different scenario has been included here. Figure 3.6 shows the trajectory and the velocity of a cylindrical capsule of density equal to that of water, having $k = 0.5$ and $L_c = 1 * d$, flowing in a vertical pipe bend of $r/R = 8$ within which water is flowing at an average velocity of 1m/sec. A cylindrical particle is being generated using the shape factor which can be defined as [80]:

$$\psi = \left(\frac{\text{Volume of Capsule}}{\text{Volume of Circumscribing Sphere}} \right)^{\frac{1}{3}} \quad (3.1)$$

It can be seen that the capsule is travelling concentric to the central axis of the pipe due to its density being equal to that of water.

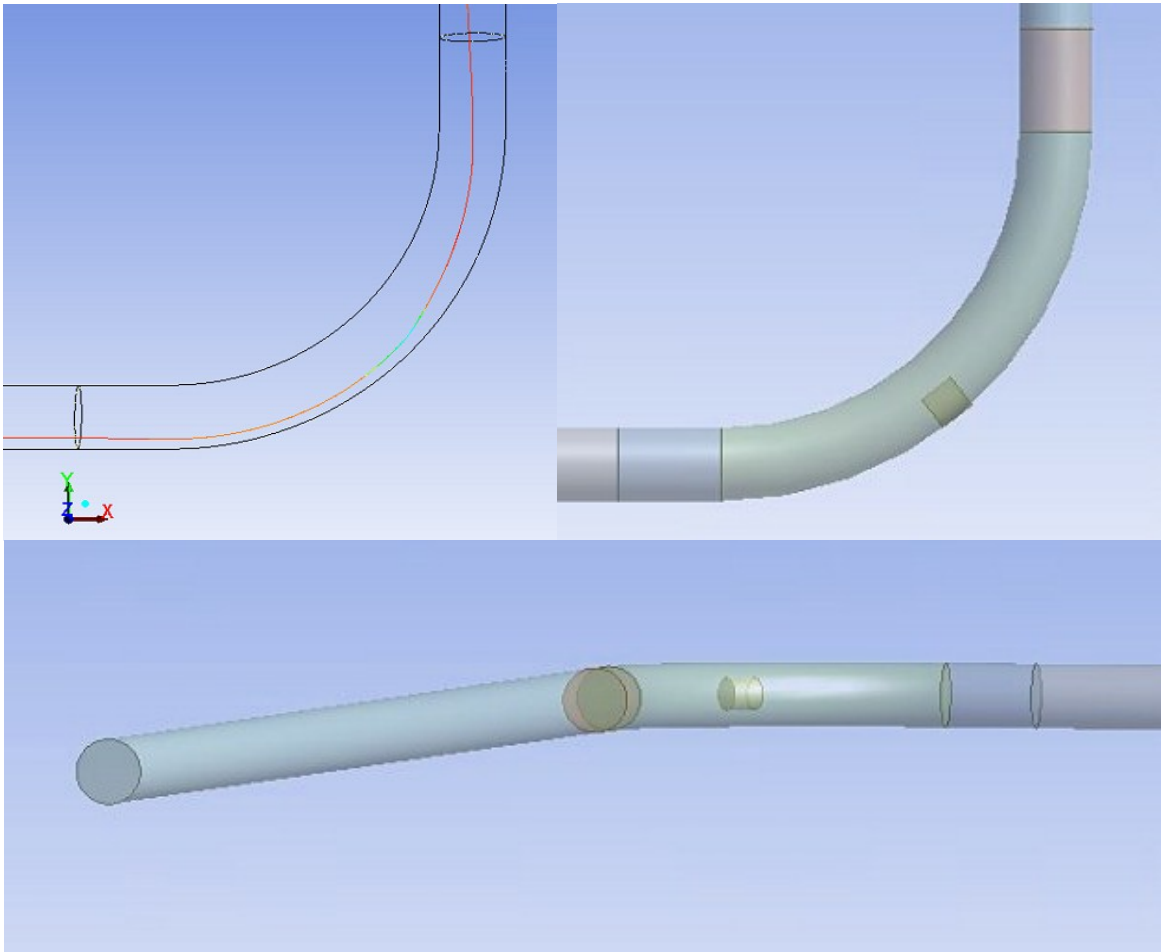


Figure 3.6. Trajectory of Equi-Density Cylindrical Capsules in HCP Bends

It is noteworthy that the trajectory data obtained from the DPM can be directly applied to spherical capsules only because of their axisymmetric shape. As far as the cylindrical capsules are concerned, trajectory data at a specific point does not lead towards the orientation of the capsule at that point. An angular position is w.r.t. a reference axis is required in order to accurately model a cylindrical capsule. This has been achieved by considering the data of the particle trajectory at some neighbouring points as well. This gives the co-ordinates of two points in space on which simple trigonometric operations can be carried out to find the angle subtended between those two points w.r.t. X axis for the current modelling scenario. The cylindrical capsule is then given that angular orientation.

3.1.3. Meshing of the Flow Domain

The concept of hybrid meshing has been incorporated for the meshing of the flow domain. It means that two different meshes have been created in the domain. The Inlet and the Outlet pipes have been meshed using hexahedral elements whereas the Test section has been meshed with tetrahedral elements. The reasons behind the use of hexahedral mesh elements for the Inlet and the Outlet pipes are:

- The structure of these pipes is simple and hence hexahedral mesh elements, with a very low skewness, can be generated in these pipes.
- Hexahedral mesh elements give more accurate results due to lower numerical diffusion.

In the test section, due to the presence of capsules, the hexahedral mesh elements are very difficult to create and that too with a very high skewness. Hence, tetrahedral elements were chosen for meshing of the Test section. Figure 3.7 shows both the meshes and the interface between them.

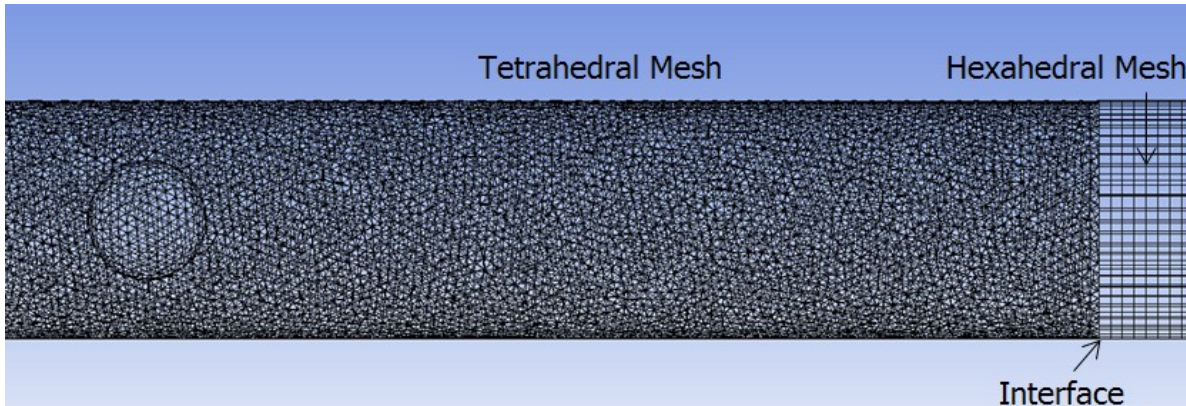


Figure 3.7. Meshing of the Flow Domain

Two meshes were chosen for Mesh Independence Test. The first mesh had 1 million mesh elements whereas the second mesh had 2 million mesh elements. The results for the Mesh Independence testing are discussed in the next chapter.

3.2. Solver Execution

The solver used in the present study is called Fluent, which is an integral part of CFD package Ansys 13. The details of the solver settings used in the present study have been presented in the following sections.

3.2.1. Selection of the Physical Models

As discussed in Chapter 1, the velocity of the flow within hydraulic pipelines is such that the compressibility effects can be neglected in such pipelines. Therefore, a pressure based solver has been nominated for the flow diagnostics of the pipelines transporting capsules. In this model, the density of the fluid remains constant and the primary fluid flow parameter that is being solved iteratively is the pressure within the flow domain.

The pipelines transporting capsules which are currently in operation are designed such that they can deliver a constant solid throughput. Hence, for a given pumping power and for a constant solid throughput, the flow in pipelines transporting capsules can be considered as steady. Therefore, a steady state solver has been used in the present study for the flow diagnostics of pipelines transporting capsules.

In addition to the aforementioned settings, there is a need to model the turbulence in the flow as well. This is because the investigations carried out in the present study focuses on the turbulent flow in the pipelines. The criteria for internal flows (such as pipeline flows) to be turbulent is that the Reynolds number of the flow should be higher than 4000. Furthermore, in practical applications of pipelines transporting capsules the velocity of the flow normally ranges from 0.5m/sec to 4m/sec. These velocities correspond to Reynolds number of 50,000 to 400,000 for the pipeline under consideration. Hence, the flow is turbulent in the pipeline transporting capsules and a turbulence model is required to predict the parameters of turbulence in the pipeline with reasonable accuracy.

There are many turbulence models available in the commercial CFD package that has been used in this study. Each one of these turbulence models has got their own advantages and disadvantages, which can be found out in any CFD text book. As far as the transport of capsules in a pipeline is concerned, due to the formation of a wake region downstream of the capsule because of flow separation, $k-\omega$ model has been chosen for the modelling of turbulence in such pipelines. The primary reason behind choosing $k-\omega$ model is its superiority in accurately modelling the wake regions and extreme pressure gradients, which are expected to occur between the capsule/s and the pipe wall, i.e. the annulus region. Khalil et. al. [81] has also shown that $k-\omega$ turbulence model predicts the changes in the flow parameters in HCPs with reasonable accuracy.

The $k-\omega$ is a two equation model that is further divided into two types. The first type is called Standard $k-\omega$ model whereas the second type is called Shear-Stress Transport (SST) $k-\omega$ model. In the present study, SST $k-\omega$ model has been chosen because it includes the following refinements [82]:

- The standard $k-\omega$ model and the transformed $k-\epsilon$ model are both multiplied by a blending function, and both models are added together. The blending function is designed to be one in the near-wall region, which activates the standard $k-\omega$ model, and zero away from the surface, which activates the transformed $k-\epsilon$ model.
- The definition of the turbulent viscosity is modified to account for the transport of the turbulent shear stress.

These features make the SST $k-\omega$ model more accurate and reliable for a wider class of flows (e.g., adverse pressure gradient flows, aerofoils, transonic shock waves) than the standard $k-\omega$ model. Other modifications include the addition of a cross-diffusion term in the ω equation and a blending function to ensure that the model equations behave appropriately in both the near-wall and far-field zones. Further details of SST $k-\omega$ model can be found in any turbulence modelling text book and hence have not been included here.

3.2.2. Defining Material Properties and Operating Conditions

In the present study, the investigations have been carried out in a hydraulic pipeline transporting capsules where the capsules have variable densities. The fluid medium within the pipe has been defined as liquid-water with a density of 998.2Kg/m^3 and dynamic viscosity of 0.001003Kg/m-sec . The capsules that have been used in the current study consist of two separate solid materials. One set of investigations have been carried out on capsules made of Polypropylene with a density equal to that of the carrier fluid, i.e. 998.2Kg/m^3 , whereas, the second set of investigations have been conducted on the capsules made of Aluminium having a density of 2695Kg/m^3 such that the heavier capsules (Aluminium capsules) have a specific gravity of 2.7.

The operating conditions being given to the solver are the operating pressure of 101325Pa (i.e. atmospheric pressure) and turning the gravitational acceleration of 9.81m/sec^2 on for the investigations carried out in a vertical pipeline transporting capsules.

3.2.3. Boundary Conditions

The boundary types that have been specified are listed in table 3.1:

Table 3.1. Boundary Types

Boundary Name	Boundary Type
Inlet to the Pipe	Velocity Inlet
Outlet of the Pipe	Pressure Outlet
Wall of the Pipe	Stationary Wall
Capsules	Translating Walls in the direction of the flow

The pipeline inlet velocity that has been used in the current study ranges from 1m/sec to 4m/sec , in increments of 1m/sec . The reason for choosing these velocities is that these flow velocities represent the practical flow velocities in such pipelines. The pressure at the outlet of the pipe has been kept at atmospheric pressure, i.e. 0Pa gauge. As discussed earlier, the pipe has been considered to be hydrodynamically smooth, having a wall roughness constant of zero.

Capsules have been modelled as translating walls where the capsule velocities depend on many factors such as shape of the capsule, diameter of the capsule, density of the capsule etc. Experimental data for the velocities of the capsules has been provided by many researchers in various publications. The available experimental data has been collected and analysed to develop models for the prediction of capsule velocities using multiple regression analysis. The next section is devoted to the calculation of capsule velocities for different geometric and flow variables considered in the present study.

3.2.4. Capsule Velocities in Horizontal HCPs

This section deals with the computation of the capsule velocities in horizontal HCPs. Based on the aims and objectives of the present study, the cases to be numerically investigated using CFD tools have been identified. Capsule velocities have been computed for individual cases. The listed cases have been chosen such that they cover a wide range of analysis and provide with a clearer picture of the flow variations under different geometric and flow scenarios in a HCP. The details of cases to be investigated are presented in Appendix A-2.

➤ Flow of Spherical Capsules with Density Equal to Water

Ellis [21] conducted experimental investigations on the transport of a spherical capsule with density equal to that of water. It was observed that as the average flow velocity V_{av} increases, the capsule holdup H decreases, where the capsule holdup can be expressed as:

$$H = \frac{V_c}{V_{av}} \quad (3.2)$$

The collected data for the holdup, ranging between average flow velocity of 0.5m/sec to 3.5m/sec, is shown in figure 3.8. The experimental data has been analysed using multiple variable regression, and the following coefficients are determined:

$$\text{Intercept} = 1.22$$

$$k = -0.145$$

showing that as the diameter of the capsule increases, the holdup for the capsule decreases. Using the coefficients obtained from multiple variable regression analysis, the following expression for the velocity of the capsule has been obtained:

$$V_c = (1.22 * V_{av}) - (0.15 * k * V_{av}) \quad (3.3)$$

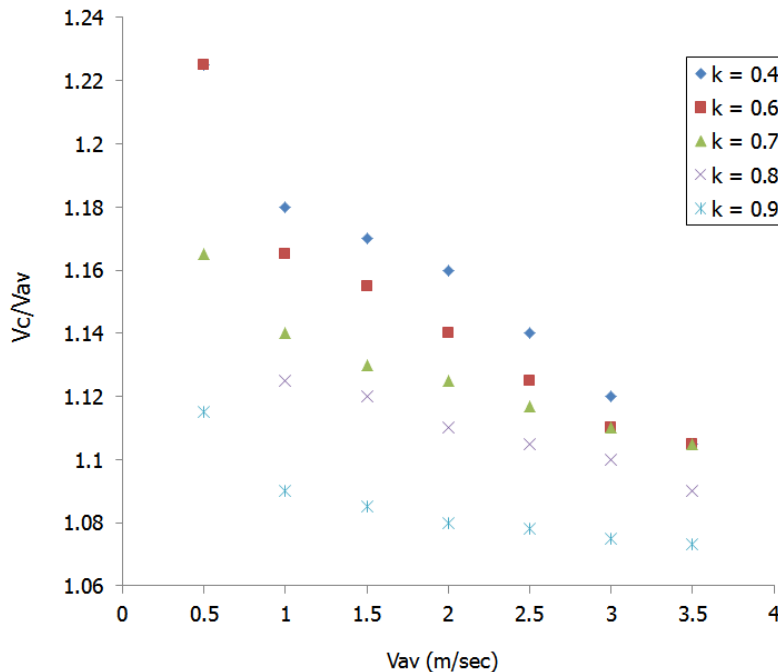


Figure 3.8. Experimental data for Equi-Density Spherical Capsule in a Horizontal Pipeline

The velocities of the capsule calculated using equation (3.3) and obtained from the experimental data have been plotted. It can be clearly seen in figure 3.9 that the calculated velocities of the capsule are in good agreement with the experimental data and more than 90% of the data lies within $\pm 5\%$ error bound of the equation above.

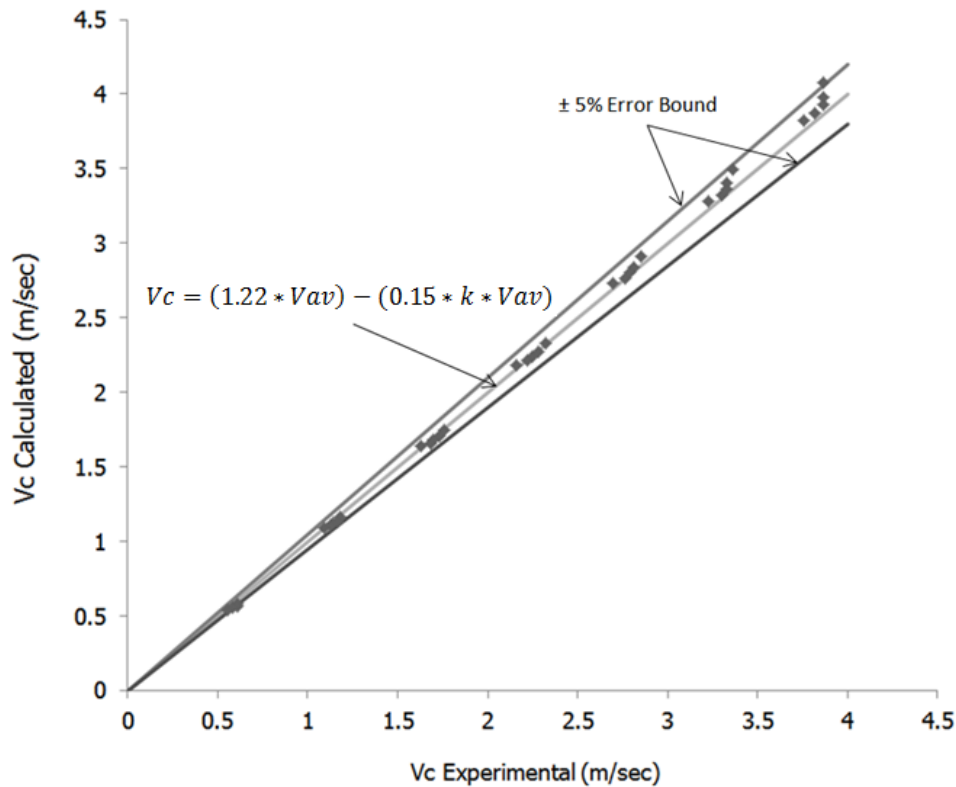


Figure 3.9. Curve fitting on the experimental data for Equi-Density Spherical Capsule in a Horizontal Pipeline

For the various cases identified, regarding the flow of spherical capsules in horizontal pipelines with the density of the capsules equal to that of water, the capsule velocities have been computed using equation (3.3). Table A-2.1 in Appendix A-2 lists all the cases and the capsule velocities where N is the number of capsules in the Test section of the pipe, k is the capsule to pipe diameter ratio ($k = d/D$) and Sc is the spacing between two consecutive capsules in meters. The spacing between the capsules has been specified in terms of the capsule diameter, and the investigations have been carried out on the spacing of one, three and five diameters of the capsules.

➤ Flow of Cylindrical Capsules with Density Equal to Water

Charles [27] presented a theoretical analysis of the concentric flow of a cylindrical capsule with density of the capsule equal to that of water. The model developed for the prediction of the capsule's velocity in the turbulent flow within a horizontal pipeline, shows that the holdup for the capsule depends on the capsule to pipe diameter ratio k . The velocity of the capsule has been represented by the following expression:

$$Vc = \left[\frac{1}{\left\{ \frac{7}{4} k (1-k) + \frac{49}{60} (1-k^2) + k^2 \right\}} \right] * Vav \quad (3.4)$$

Using equation (3.4), the velocity of the capsules, for different cases under investigation, has been calculated. Table A-2.2 in Appendix A-2 lists the various geometric and flow variables under investigation.

➤ Flow of Spherical Capsules with Density Greater than Water

Ellis [34] conducted experimental investigations on the transport of a spherical capsule with density greater than water. The collected data for the holdup, ranging between average flow velocity of 0.5m/sec to 3.5m/sec, is shown in figure 3.10.

The experimental data has been analysed using multiple variable regression and the following coefficients are determined:

$$\text{Intercept} = 1.067$$

$$s = -0.0196$$

$$k = 0.042$$

showing that as the diameter of the capsule increases, the holdup for the capsule increases and as the specific gravity of the capsule increases, the holdup for the capsule decreases.

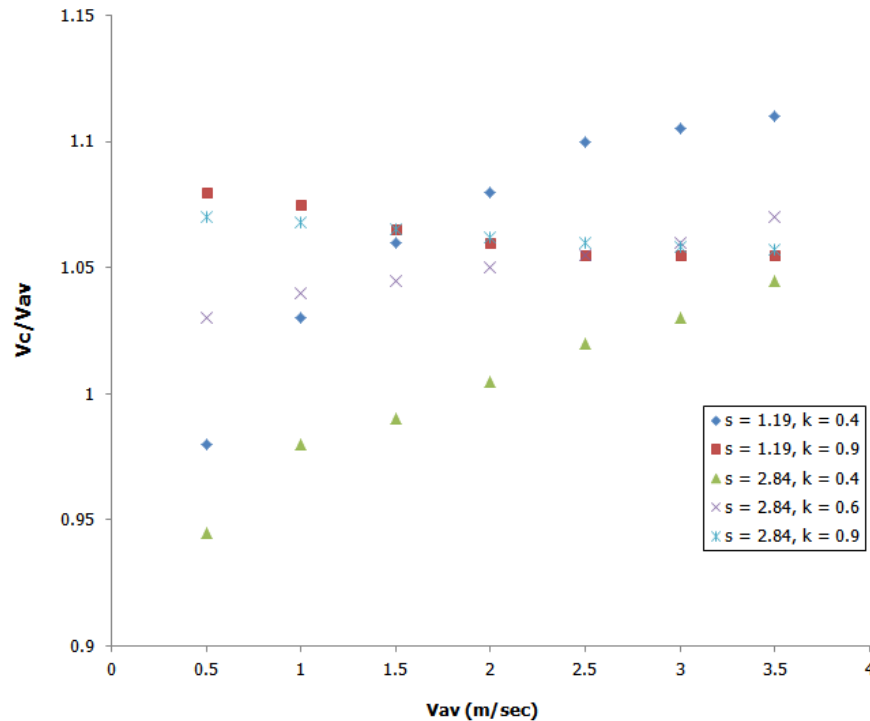


Figure 3.10. Experimental data for Heavy-Density Spherical Capsule in a Horizontal Pipeline

Using the coefficients obtained from multiple variable regression analysis, the following expression for the velocity of the capsule has been obtained:

$$V_c = (1.067 * V_{av}) - (0.0196 * s * V_{av}) + (0.042 * k * V_{av}) \quad (3.5)$$

The velocities of the capsule calculated using the equation above and obtained from the experimental data have been plotted. It can be clearly seen in figure 3.11 that the calculated velocities of the capsules are in good agreement with the experimental data and more than 90% of the data lies within $\pm 5\%$ error bound of the equation above.

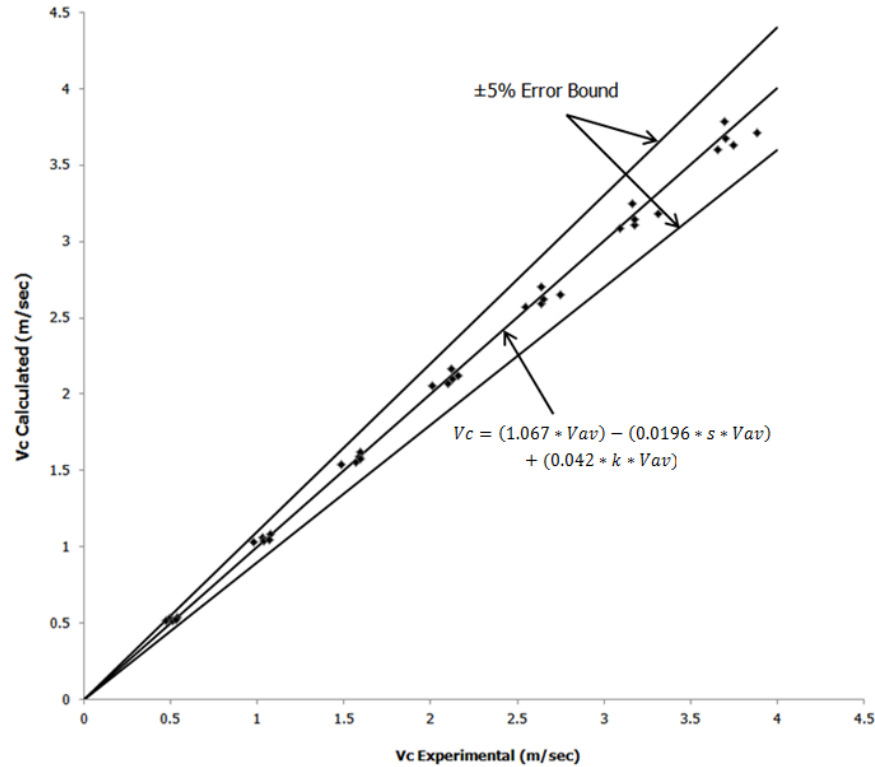


Figure 3.11. Curve fitting for Heavy-Density Spherical Capsule in a Horizontal Pipeline

For the various cases identified regarding the flow of spherical capsules in horizontal pipelines with the density of the capsules greater than water, the capsule velocities have been computed using equation (3.5). Table A-2.3 in Appendix A-2 lists all the cases and the capsule velocities.

➤ Flow of Cylindrical Capsules with Density Greater than Water

Ellis [37] conducted experimental investigations on the transport of a cylindrical capsule made of aluminium with a specific gravity of 2.7. The collected data for the holdup, ranging between average flow velocity of 0.5m/sec to 4m/sec, is shown in figure 3.12.

The experimental data has been analysed using multiple variable regression and the following coefficients are determined:

$$\text{Intercept} = 0.77$$

$$\frac{Lc}{d} = -0.008$$

$$k = 0.302$$

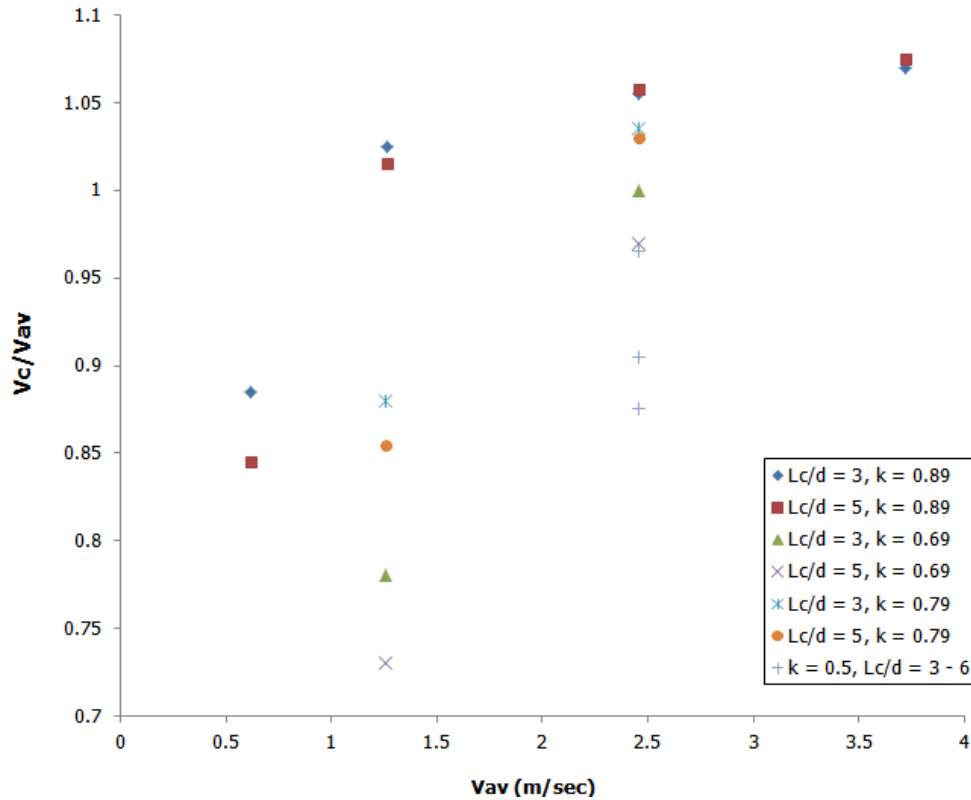


Figure 3.12. Experimental data for Heavy-Density Cylindrical Capsule in a Horizontal Pipeline

showing that as the diameter of the capsule increases, the holdup for the capsule increases and as the length to diameter ratio of the capsule increases, the holdup for the capsule decreases. Using the coefficients obtained from multiple variable regression analysis, the following expression for the velocity of the capsule has been obtained:

$$Vc = (0.77 * Vav) - \left(0.008 * \frac{Lc}{d} * Vav\right) + (0.302 * k * Vav) \quad (3.6)$$

The velocities of the capsule calculated using the equation above and obtained from the experimental data have been plotted. It can be clearly seen in figure 3.13 that the calculated velocities of the capsules are in good agreement with the experimental data and more than 80% of the data lies within $\pm 5\%$ error bound of the equation above.

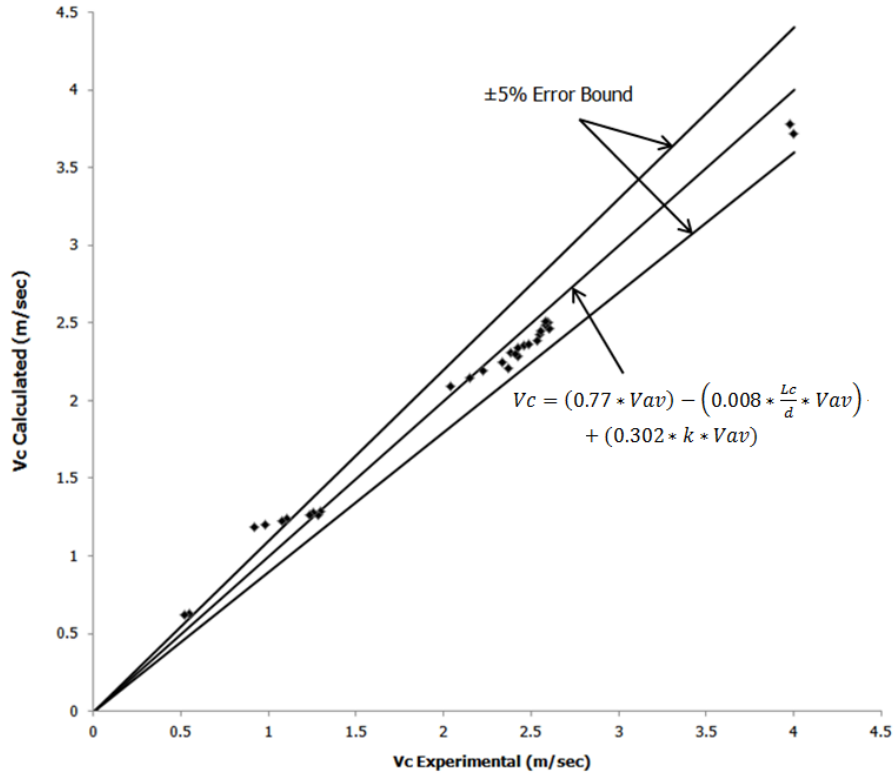


Figure 3.13. Curve fitting for Heavy-Density Cylindrical Capsule in a Horizontal Pipeline

For the various cases identified regarding the flow of cylindrical capsules in horizontal pipelines with the density of the capsules greater than water, the capsule velocities have been computed using equation (3.6). Table A-2.4 in Appendix A-2 lists all the cases and the capsule velocities.

3.2.5. Capsule Velocities in Vertical HCPs

This section deals with the computation of the capsule velocities in vertical HCPs, for various cases identified based on the literature survey.

➤ Flow of Spherical Capsules with Density Equal to Water

Chow [43] conducted a series of experiments on the flow of capsules in a vertical pipeline. The velocity of the spherical capsules with density equal to that of water has been represented by the following expression:

$$Vc = \frac{Vav}{k^{0.34}} \quad (3.7)$$

Using the above equation, the velocity of the capsules, for different cases under investigation, has been calculated. Table A-2.5 lists the various geometric and flow variables identified.

➤ **Flow of Cylindrical Capsules with Density Equal to Water**

Latto [45] reports the velocity of the cylindrical capsules with density equal to that of water as:

$$V_C = \frac{V_{av}}{k^{0.128}} * \left(\frac{Lc}{d}\right)^{0.128} \quad (3.8)$$

Using the above equation, the velocity of the capsules, for different cases under investigation, has been calculated. Table A-2.6 lists the various geometric and flow variables identified.

➤ **Flow of Spherical Capsules with Density Greater than Water**

Chow [43] reports the velocity of the spherical capsules with density greater than that of water as:

$$V_C = \frac{V_{av}}{k^{0.34}} - \frac{\left(\sqrt{\frac{\left(\frac{4}{3}gD(s-1)\right)}{k}}(1-k^2)\left(1-\frac{1}{s}\right)^{0.05}\right)}{k^{0.34}} \quad (3.9)$$

Using the above equation, the velocity of the capsules, for different cases under investigation, has been calculated. Table A-2.7 lists the various geometric and flow variables identified.

➤ **Flow of Cylindrical Capsules with Density Greater than Water**

Latto [45] reports the velocity of the cylindrical capsules with density greater than that of water as:

$$V_C = \frac{V_{av}}{k^{0.128}} \left(\frac{Lc}{d}\right)^{0.128} - \frac{\left(\sqrt{2gD\left(\frac{Lc}{d}\right)(s-1)}(1-k^2)\left(1-\frac{1}{s}\right)^{0.05}\right)}{k^{0.128}} \quad (3.10)$$

Using the above equation, the velocity of the capsules, for different cases under investigation, has been calculated. Table A-2.8 lists the various geometric and flow variables identified.

3.2.6. Capsule Velocities in Bends

As mentioned earlier, to model the flow of capsules in pipe bends, Discrete Phase Modelling (DPM) has been used to obtain the capsule's trajectories and velocities along the path followed by the capsules in the bend. DPM solves transport equations for the continuous phase, i.e. water in case of hydraulic capsule bends. It also allows simulating a discrete second phase in a Lagrangian frame of reference. This second phase consists of spherical or cylindrical particles (which may be taken to represent capsules) dispersed in the continuous phase. DPM computes the trajectories of these discrete phase entities. The coupling between the phases and its impact on both the discrete phase velocities and

trajectories, and the continuous phase flow has been included in the present study. Calculation of the discrete phase velocity and trajectory using a Lagrangian formulation includes the discrete phase inertia, hydrodynamic drag and the force of gravity. DPM also predicts the effects of turbulence on the dispersion of capsules due to turbulent eddies present in the continuous phase. The discrete phase in the DPM is defined by defining the initial position and size of the capsules. These initial conditions, along with the inputs defining the physical properties of the discrete phase (water), are used to initiate trajectory and velocity calculations. The trajectory and velocity calculations are based on the force balance on the capsules, using the local continuous phase conditions as the capsules moves through the flow.

The procedure for setting up and solving capsule flow in pipe bends include enabling the discrete phase modelling in CFD, choosing a steady treatment of capsules, specifying tracking parameters and selection of a drag law. In the present study, Stokes Drag Law has been used because of its better accuracy for large sized particles, i.e. capsules. Further steps include specifying the capsules size and position in the injections, defining the material properties for the capsules, turning the gravity on, initializing the flow field and solving the coupled flow.

The velocity of a capsule in a bend depends on the angular position of the capsule in the bend. Hence, the analysis of the flow of capsules in a pipe bend has been carried out at six equally spaced angular positions of 0° , 18° , 36° , 54° , 72° and 90° to cover a wide range of analysis. After conducting some preliminary investigations on the flow of capsules in pipe bends, it has been observed that the pressure drop in a pipe bend transporting capsules is independent of the angular position of the capsule, where the density of the capsules is equal to that of water. However, the pressure drop is different at different locations in case of the flow of heavy density capsules in pipe bends. Hence, an average pressure drop has been considered for the analysis of the flow of heavy-density capsules in pipe bends. Further discussions on this topic have been presented in Chapter 6. The cases that have been investigated in this study, along with the velocity of the capsules, are listed in table A-2.9 in Appendix A-2, where V_{cx} and V_{cy} represent the capsule velocity in X and Y directions respectively. It is noteworthy that the capsules of $k = 0.9$ have been excluded from the analysis in pipe bends. The reason is presented in chapters 4 and 5.

3.2.7. Solver Settings

Application based solver settings are required to accurately predict the fluid flow behaviour in the flow domain. These settings comprise:

- Pressure – Velocity Coupling
- Gradient
- Spatial Discretisation

The Navier-Stokes equations are solved in discretised form. This refers to linear dependency of velocity on pressure and vice versa. Hence, a pressure – velocity is required to predict the pressure distribution in the flow domain with reasonable accuracy. In the present study, SIMPLE algorithm for pressure – velocity coupling has been incorporated because it converges the solution faster and is often quite accurate for flows in and around simple geometries such as spheres, cylinders etc [83]. In

SIMPLE algorithm, approximation of the velocity field is obtained by solving the momentum equation. The pressure gradient term is calculated using the pressure distribution from the previous iteration or an initial guess. The pressure equation is formulated and solved in order to obtain the new pressure distribution. Velocities are corrected and a new set of conservative fluxes is calculated.

Gradients are needed for constructing values of a scalar at the cell faces, for computing secondary diffusion terms and velocity derivatives. Green – Gauss Node – based gradient evaluation has been used in the present study [84]. This scheme reconstructs exact values of a linear function at a node from surrounding cell – centred values on arbitrary unstructured meshes by solving a constrained minimization problem, preserving a second-order spatial accuracy.

The CFD solver stores discrete values of the scalars at the cell centres. However, face values are required for the convection terms and must be interpolated from the cell centre values. This is accomplished using an upwind spatial discretisation scheme. Upwinding means that the face value is derived from quantities in the cell upstream, or upwind relative to the direction of the normal velocity. In the present study, 2nd order upwind schemes have been chosen for pressure, momentum, turbulent kinetic energy and turbulent dissipation rate. The use of 2nd order upwind scheme results in increased accuracy of the results obtained [85].

3.2.8. Convergence Criteria

Getting to a converged solution is often necessary. A converged solution indicates that the solution has reached a stable state and the variations in the flow parameters, w.r.t. the iterative process of the solver, have died out. Hence, only a converged solution can be treated as one which predicts the solution of the flow problem with reasonable accuracy [86].

The default convergence criterion for the continuity, velocities in three dimensions and the turbulence parameters in Ansys 13 is 0.001. This means that when the change in the continuity, velocities and turbulence parameters drops down to the fourth place after decimal, the solution is treated as a converged solution. However, in many practical applications, the default criterion does not necessarily indicate that the changes in the solution parameters have died out. Hence, it is often better to monitor the convergence rather than relying on the default convergence criteria.

In the present study, static pressure on the inlet and outlet faces of the Test section has been monitored throughout the iterative process. The solution has been considered converged once the static pressure at both these faces has become stable. Here a stable solution can be either one in which the pressure fluctuations have died out completely or have become cyclic having same amplitude in each cycle.

After numerically simulating the flow of capsules in hydraulic pipelines, various results have been gathered from CFD. Detailed discussions on these results are presented in the proceeding chapters, where the next chapter deals with the flow of capsules in horizontal pipes.

CHAPTER 4

ANALYSIS OF HORIZONTAL PIPELINES TRANSPORTING CAPSULES

The results obtained after performing CFD simulations for the cases discussed in the previous chapter, regarding the transport of capsules in a horizontal pipeline, have been presented here. A detailed qualitative and quantitative analysis of the results obtained has been carried out in order to understand the complex flow structure in horizontal pipelines transporting capsules. The effect of various geometric and flow-related parameters on the pressure drop in a capsule transporting horizontal pipeline has been investigated. Furthermore, semi-empirical relationships, for the flow of capsules in a horizontal pipeline, have been developed.

4.1. Analysis of Single Phase Flow in a Horizontal Pipe

Before moving on to the analysis of the flow of capsules in horizontal pipes, the flow structure of a single phase in the pipe needs to be understood and validated with CFD model created in the previous chapter. The pressure distribution within the test section of the pipe at an average flow velocity of 1m/sec is shown in figure 4.1. The pressure of water has dropped from 178Pa to 97Pa, as shown in the figure, along the pipe length which corresponds to 45% decrease in the pressure. Using Moody's chart for a hydrodynamically smooth pipe, the friction factor at an average flow velocity of 1m/sec in a 0.1m diameter pipe has been found out to be 0.0185. Putting this value of friction factor in equation (1.12):

$$\Delta P = 92\text{Pa}$$

and the pressure drop predicted by Computational Fluid Dynamics between the inlet and the outlet of the pipe is:

$$\Delta P = 184 - 92 = 92\text{Pa}$$

It can be thus concluded that Computational Fluid Dynamics predict the pressure drop in a single phase flow within pipelines with reasonable accuracy.

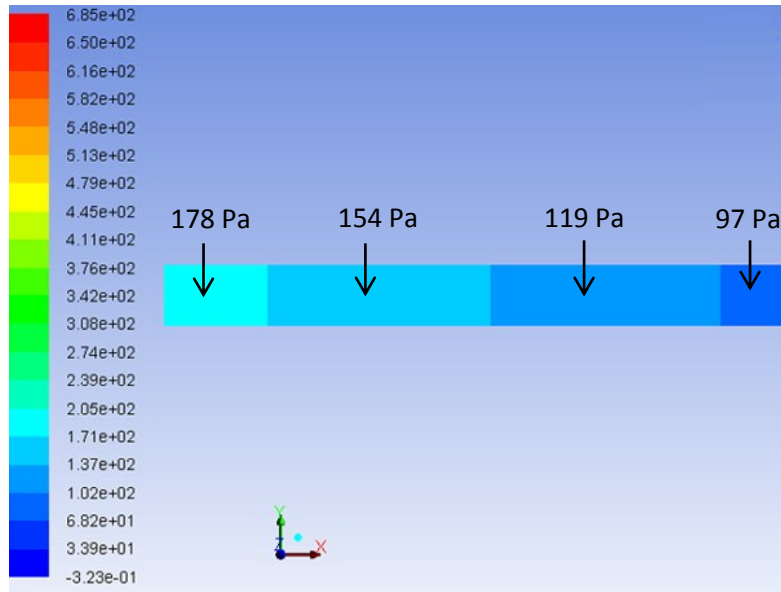


Figure 4.1. Pressure Variations for Water Flow in a Horizontal Pipe

Figure 4.2 shows the variations in pressure coefficient w.r.t. the axial location within the pipe. The pressure coefficient can be represented as [87]:

$$C_p = \frac{P - P_\infty}{0.5 \rho_\infty V_\infty^2} \quad (4.1)$$

where P is the pressure at a point, P_∞ is the free stream pressure, ρ_∞ is the density of the fluid at the free stream location and V_∞ is the velocity of the fluid at the free stream location. C_p represents the pressure at a given location in the flow field, with respect to an undisturbed point in the flow domain, in dimensionless form. C_p is normally used to represent the pressure distributions around a bluff body. The flow parameters, in the vicinity of the capsules, are strongly dependent on the shape and size of the capsules; hence, C_p has been used to analyse the flow near the capsules.

It can be seen in figure 4.2 that the pressure within the pipe drops linearly. This trend is consistent with equation (1.12) which, for a given pipe diameter and fluid flow velocity, can be written as:

$$\frac{\Delta P}{L_p} = \text{constant} \tag{4.2}$$

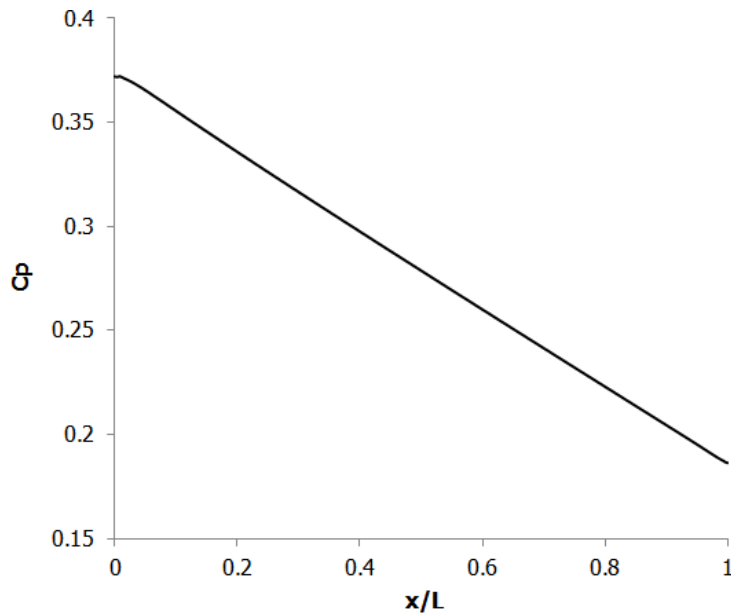


Figure 4.2. Variations in C_p for Water Flow in a Horizontal Pipe

Table 4.1 shows a comparison between the pressure drop predictions, from both equation (1.12) and Computational Fluid Dynamics, for different flow velocities in a horizontal pipeline.

Table 4.1. Pressure Drops in a Horizontal Pipe for the Flow of Water

Vav	$\Delta P_{wh}/L_p$ (Equation (1.12))	$\Delta P_{wh}/L_p$ (CFD)	Difference
(m/sec)	(Pa/m)	(Pa/m)	(%)
1	92	92	0
2	317	317	0
3	657	658	0.15
4	1102	1104	0.18

In order to analyse the velocity field within a hydraulic pipeline, it needs to be estimated whether the flow within the pipe is laminar or turbulent. Equation (1.13), for the case considered in figure 4.1, results into:

$$Re = 99521$$

The criterion for internal flows to be turbulent is that the Reynolds number should be above 4000. As it can be clearly seen that the Reynolds number under consideration is $\gg 4000$, it can be safely concluded that the flow inside the pipe under discussion is turbulent. The velocity profile for a turbulent flow is given by Power-Law velocity profile as [88]:

$$\frac{u}{V_{cn}} = \left(1 - \frac{y}{R}\right)^{\frac{1}{\alpha}} \quad (4.3)$$

where u is the local flow velocity in the x direction, V_{cn} is the centreline velocity, r is the distance from the origin to the point where local velocity needs to be computed, R is the radius of the pipe and n is a function of Reynolds number. Furthermore, the flow rate can be written as:

$$Q = A V = V_{cn} \int_{y=0}^{y=R} \left(1 - \frac{y}{R}\right)^{\frac{1}{\alpha}} (2\pi r) dr \quad (4.4)$$

Upon integration, the flow rate becomes:

$$Q = 2\pi R^2 V_{cn} \frac{\alpha^2}{(\alpha+1)(2\alpha+1)} \quad (4.5)$$

As $Q = \pi R^2 V$, equation (4.3) becomes:

$$V_{cn} = \frac{(\alpha+1)(2\alpha+1)}{2\alpha^2} V \quad (4.6)$$

For the Reynolds number of 99521, $\alpha = 7$. Furthermore, for an average flow velocity of 1m/sec, the centreline velocity will be:

$$V_{cn} = 1.22\text{m/sec}$$

Figure 4.3 depicts the velocity field within the pipe. It can be seen that the flow velocity at the walls of the pipe is zero due to the no-slip boundary condition whereas it is higher in the centre of the pipe. It is noteworthy that in a fully developed turbulent flow, the velocity at the centre of the pipe is higher than the average flow velocity. In this case, the velocity of the fully developed flow at the centre of the pipe is 1.2m/sec and the average velocity of the flow V_{av} is 1m/sec. Computational Fluid Dynamics thus predicts the velocity distribution within a hydraulic pipeline with 98% accuracy.

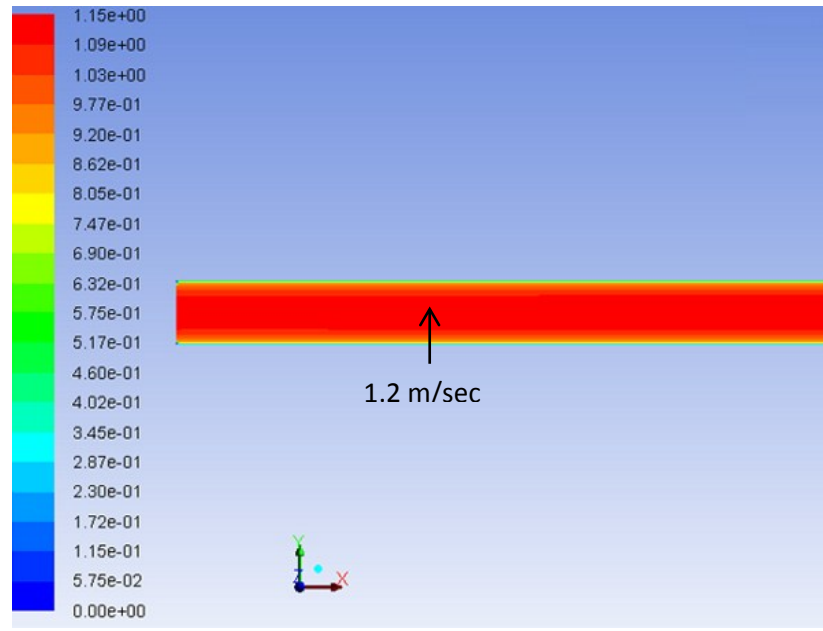


Figure 4.3. Velocity Distribution for Water Flow in a Horizontal Pipe

Figure 4.4 further shows the velocity profile in the cross-section of the pipe and u is the local flow velocity along the pipe. Due to no-slip boundary condition at the walls of the pipe, and as the walls of the pipe have been kept stationary, the flow velocity at the pipe walls is zero. The velocity in the vicinity of the pipe wall, also known as the boundary layer, increases sharply while the flow velocity at the centre of the pipe, where the shear forces acting on the fluid are minimum, is highest.

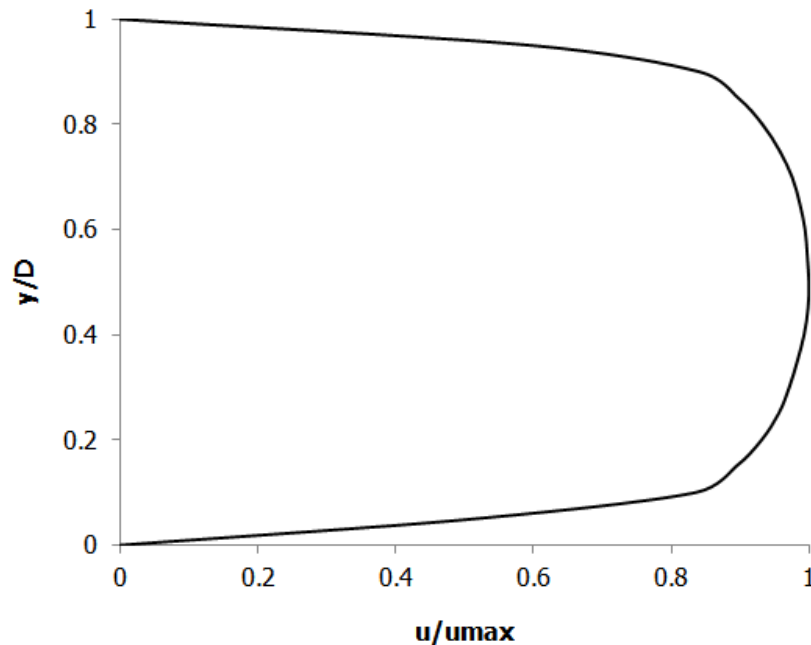


Figure 4.4. Velocity Profile for Water Flow in a Horizontal Pipe

It will be prudent to show that the approximation taken in the previous chapter regarding the entrance length effect is indeed practical. The entrance length effects on lower flow velocities will be lesser as compared to highest flow velocities because the entrance length depends on the Reynolds number of the fluid flowing in the pipe. The entrance length for turbulent flow is given by:

$$\frac{L_e}{D} = 4.4 Re^{\frac{1}{6}} \quad (4.7)$$

Table 4.2 shows the requirements for the entrance length for a 0.1m diameter pipe at various flow velocities. The results show that an entrance length of 3.77m is required for $V_{av} = 4\text{m/sec}$.

Table 4.2. Entrance Length Requirements for a Horizontal Hydraulic Pipeline

V_{av}	L_e
(m/sec)	(m)
1	2.99
2	3.36
3	3.59
4	3.77

Figure 4.5 shows the axial velocity profile along the pipe for an average flow velocity of 4m/sec.

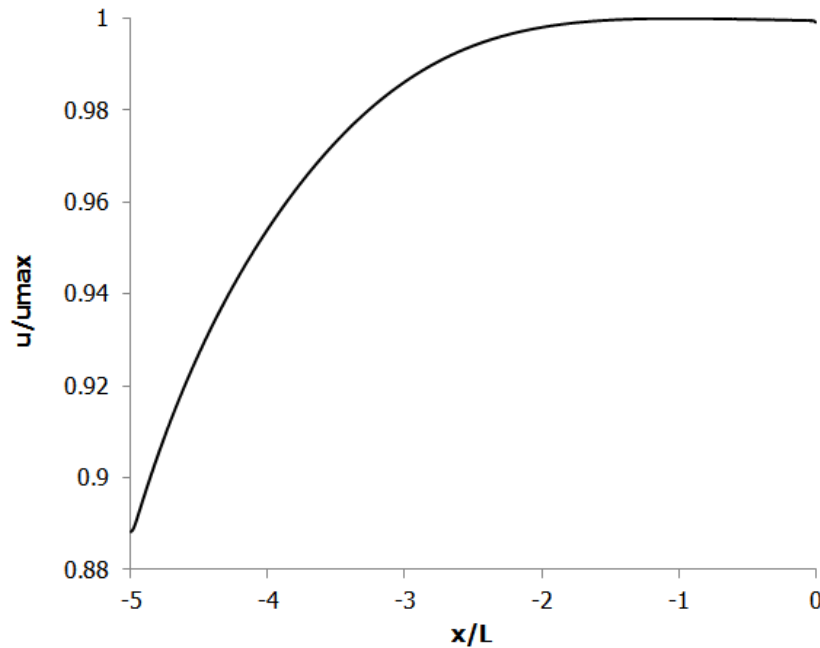


Figure 4.5. Entrance Length Effects for Water Flow in a Horizontal Pipe

It can be clearly seen that the entrance length effects die out in the initial 3 – 4 m of the pipe (-5 to -1 m in figure 4.5), and there is no appreciable change in the axial velocity profile afterwards. Hence, the entrance length of 5m taken in this study is enough for the flow development prior to entering the test section of the pipe.

4.2. Analysis of Horizontal Pipelines Transporting Capsules

The results for various cases mentioned in the previous chapter have been presented here. Both qualitative and quantitative analysis has been included to understand the complex fluid flow phenomena occurring within a horizontal HCP. In order to understand the complex flow structure in the vicinity of the capsules, coefficient of pressure (C_p) and normalised local flow velocity (u/u_{max}) have been chosen to analyse the pressure and velocity fields within the horizontal HCP. It is noteworthy that these graphs have been plotted along a straight line passing throughout the test section of the pipe. Furthermore, this line passes exactly between the capsule/s and the pipe wall as shown in figure 4.6. This line has been named as Analysis Line and will be used throughout this document.

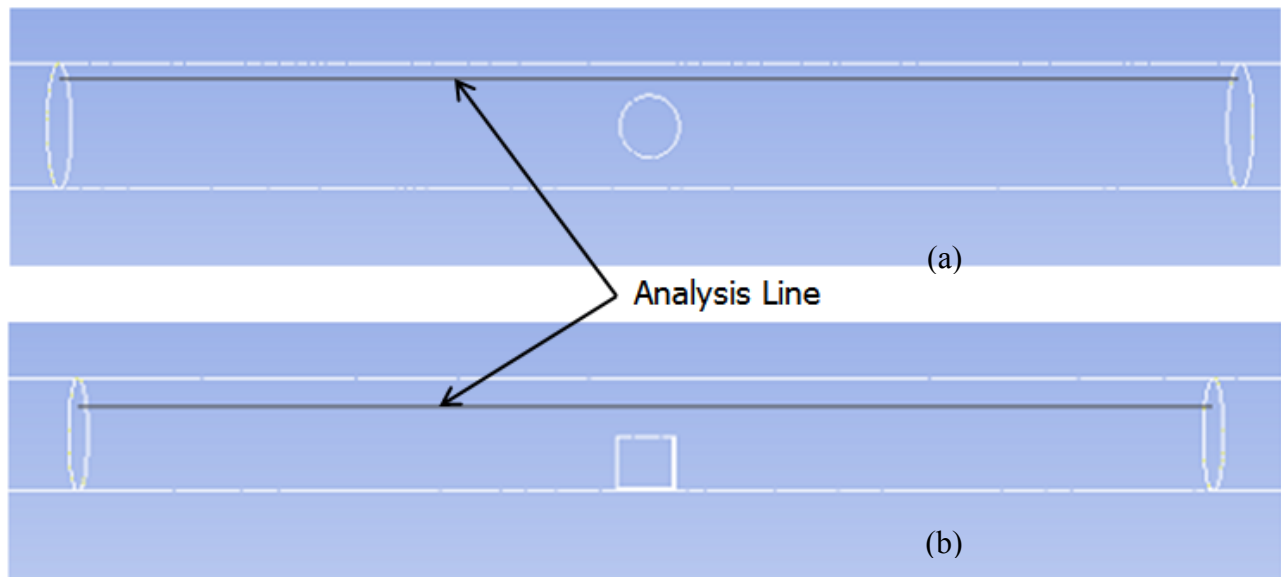


Figure 4.6. Analysis Line for the flow of (a) An Equi-Density Spherical Capsule (b) A Heavy-Density Cylindrical Capsule, in a Horizontal Pipe

4.3. Mesh Independence Tests

As discussed in Chapter 3, two different meshes with one million and 2 million mesh elements were chosen for mesh independence testing. The results obtained, shown in table 4.3, depicts that the difference in the pressure drop is less than 1% between the two meshes under consideration. It can therefore be concluded that the mesh with one million elements is capable of accurately predicting the flow features and hence has been chosen for further analysis of pipelines transporting capsules.

Table 4.3. Mesh Independence Results

Mesh	Pressure at Inlet	Pressure at Outlet	Pressure Drop per unit Length	Difference in Pressure Drops
	(Pa)	(Pa)	(Pa/m)	(%)
1 million	11163	401	10762	0.75
2 million	11265	584	10681	

4.4. Benchmark Tests

One of the most important steps while conducting numerical studies is the benchmarking of the results. This means that some of the results obtained from the numerical simulations are compared against experimental findings to confidently authorise that the numerical model represents the physical model of the real world. Hence, all the geometric, flow and solver-related parameters/variables become important in benchmarking studies.

For the present study, the numerical model has been validated against the experimental findings for the pressure drop in the pipeline given by Uluarslan [26]. The numerical model has been set for the conditions listed in table 4.4, in addition to the one already discussed in Chapter 3 regarding the geometry of the pipe which is in accordance with the test apparatus of Uluarslan [25]:

Table 4.4. Validation Tests

Name / Property	Value / Range / Comment	Units
Specific Gravity	1	N/A
k	0.8	N/A
Vav	0.2 – 1	(m/sec)
Capsule Shape	Spherical	N/A
Number of Capsules	1 – 4 (depending on concentration)	N/A

Further to the aforementioned discussion, and after numerically solving the cases discussed in table 4.4, figure 4.7 depicts the variations in the pressure drop within the pipeline, from both CFD and experiments, at various flow velocities, for the flow of equi-density spherical capsules in a horizontal pipeline. It can be seen that the CFD results are in close agreement with the experimental results, with an average variation of less than 5%. It can be thus concluded that the numerical model considered in the present study does represent the physical model of a pipeline transporting capsules. The same model has been used for simulating the various cases discussed in Chapter 3 regarding the flow of capsules in both vertical pipelines and bends as well.

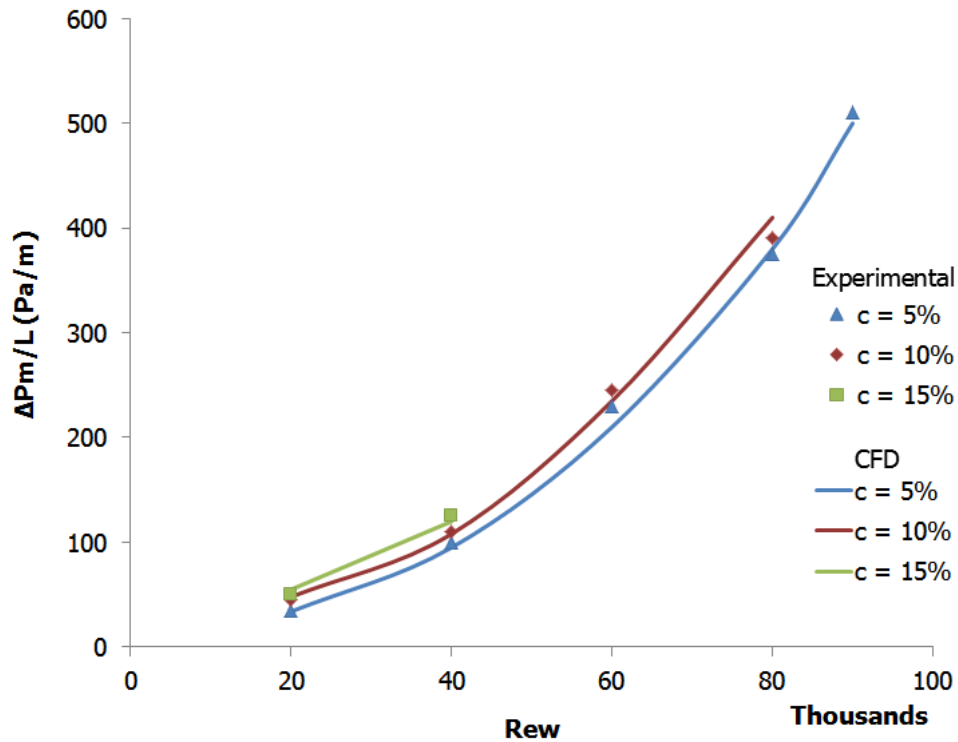


Figure 4.7. Validation of the CFD results w.r.t. the Experimental results, for the Pressure Drop in a Horizontal Pipe, Transporting Equi-Density Spherical Capsules, at Various Flow Velocities

4.5. Analysis of the Flow of Equi-Density Spherical Capsules in a Horizontal HCP

Spherical capsules offer many advantages over cylindrical capsules. Some of the advantages are:

- Spherical capsules don't tilt in the pipeline irrespective of their location
- Spherical capsules can easily pass through pipe bends and other pipe fittings such as bends

- The onset of turbulence is delayed in case of spherical capsules due to their curvaceous shape.

Conversely, the limited size the spherical capsules offer is the biggest disadvantage of such shapes. Figure 4.8 depicts the variations in the pressure and velocity distribution within the test section of the pipe transporting a single spherical capsule of $k = 0.5$ at $V_{av} = 1\text{m/sec}$. It can be seen that the presence of a capsule changes the pressure distribution inside a horizontal pipe altogether as compared to single phase flow shown in figure 4.1. The pressure gradients in the vicinity of the capsule are severely large as can be seen at upstream and downstream of the capsule. At upstream, the pressure of water increases from 181Pa to 738Pa as it approaches the capsule. This happens due to the additional resistance offered by the capsule to the flow within the pipe. The flow then passes through the annulus between the pipe wall and the capsule. As the cross sectional area decreases the pressure of water decreases to -137Pa. Once the flow exits the annulus, due to the increase in the cross-sectional area, the static pressure of water recovers to some extent. It can be seen in the figure that the pressure downstream has been recovered to 130Pa as compared to 181Pa at upstream location.

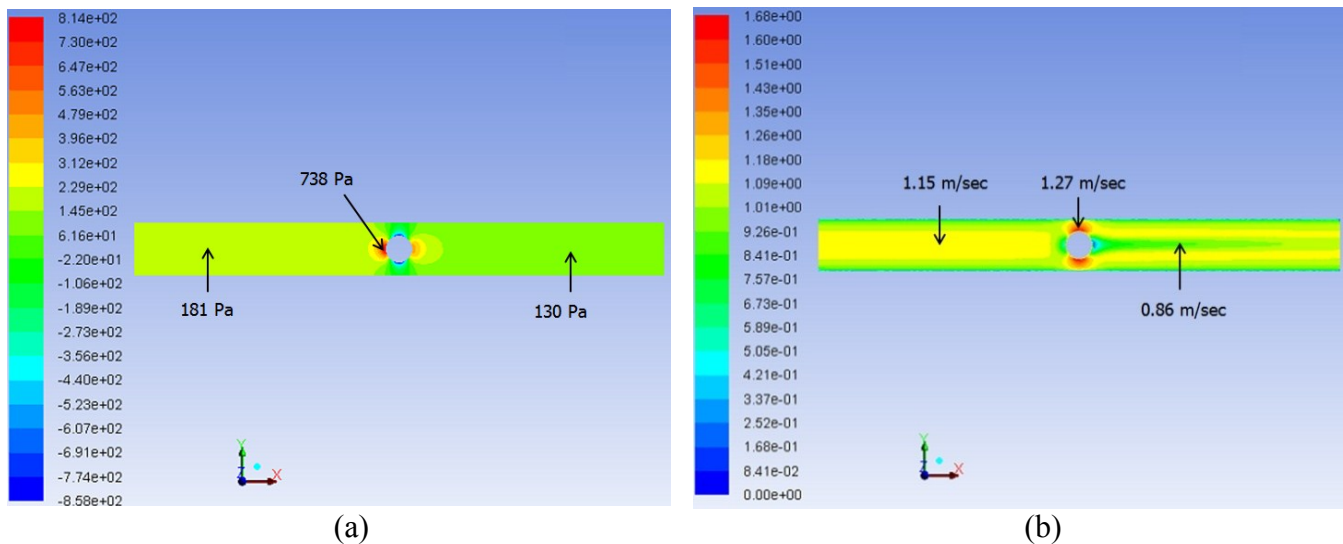


Figure 4.8. Variations in (a) Pressure and (b) Velocity, for a Single Spherical Capsule of $k = 0.5$ in a Horizontal Pipe at $V_{av} = 1\text{m/sec}$

Figure 4.8 (b) depicts that the flow slows down from 1.15m/sec to 0.518m/sec as it reaches the capsule. Once the flow passes through the annulus between the capsule and the pipe wall, the flow velocity increases to 1.27m/sec due to reduction in the cross-sectional area of the flow and then drops again to 0.86m/sec in the centre of the pipe as the flow exits the annulus. The extreme velocity gradients present in the annulus regions (both up and down of the capsule) gives rise to shear forces acting on the capsule. As the capsule is perfectly aligned with the central axis of the pipe, these opposite and equal shearing forces cancel out each other's effects and hence the capsule propagates along the centreline of the pipe.

Figure 4.9 shows the variations in C_p and u/u_{max} along the analysis line for the case under consideration. The results depict that the pressure drop in a capsule transporting pipe is higher than the

pressure drop in a hydraulic pipe. The pressure at the downstream location for both types of flows is the same because pressure boundary condition has been set at the outlet of the pipe. In real world, the pressure boundary condition is actually set at the inlet boundary of the pipe due to the presence of pump at the inlet side. Hence, the pressure would be the same at the upstream locations for both the types of flows whereas the pressure for capsule flow would be higher than the pressure for single phase flow at the downstream locations. It is also worth noticing that the pressure drops sharply in the annulus between the capsule and the pipe wall and then recovers to some extent as the flow exits the annulus region. The difference in the pressure between the upstream and the downstream locations is due to the fact that some part of the kinetic energy of water has been converted into the work being done on the capsule. The total pressure drop for the present case is 124Pa.

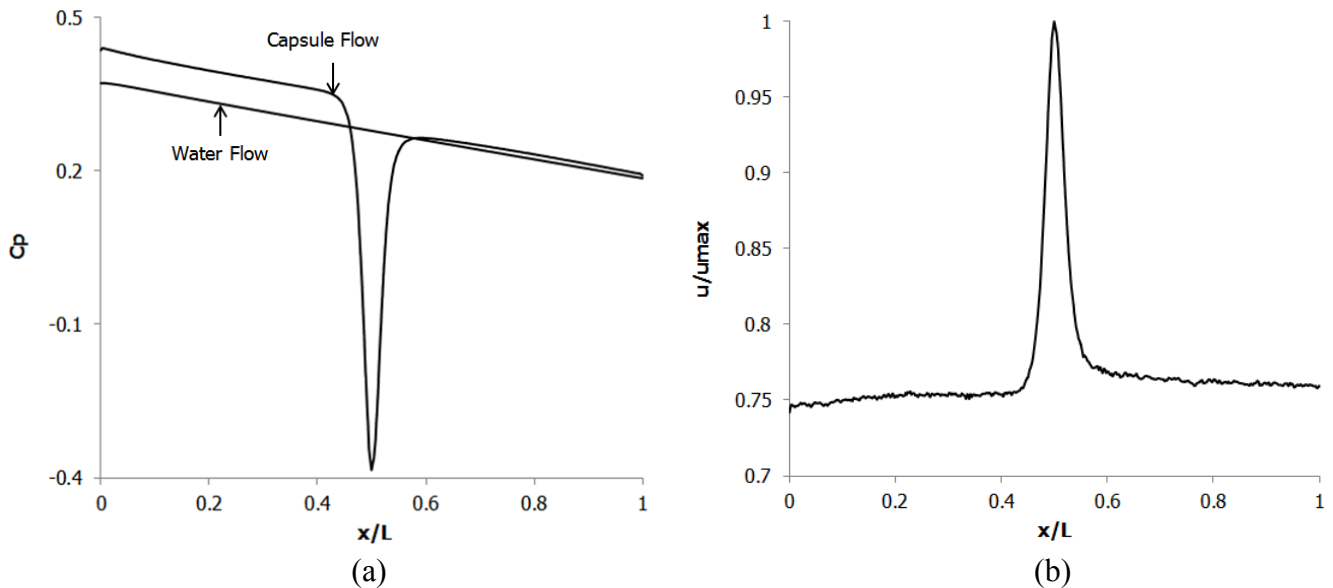


Figure 4.9. (a) Variations in C_p for a Single Spherical Capsule of $k = 0.5$ in a Horizontal Pipe at $V_{av} = 1\text{m/sec}$ (b) Variations in u/u_{max} for a Single Spherical Capsule of $k = 0.5$ in a Horizontal Pipe at $V_{av} = 1\text{m/sec}$

Figure 4.9 (b) depicts that the flow velocity increases sharply as it passes through the annulus and then decreases as it exits the annulus. The variations in the cross-sectional area of the flow in the annulus are responsible for such a sharp rise and drop in the local flow velocity. To further investigate the velocity distribution within the capsule transporting pipe, velocity profiles have been drawn across the cross-section of the pipe at both 0.1m upstream and downstream locations from the centre of the capsule as shown in figure 4.10. It can be seen that the velocity profile is undisturbed at the upstream location and the presence of the capsule has not affected the velocity profile at this location. However, at the downstream location, the presence of the capsule in the pipe has distorted the velocity profile.

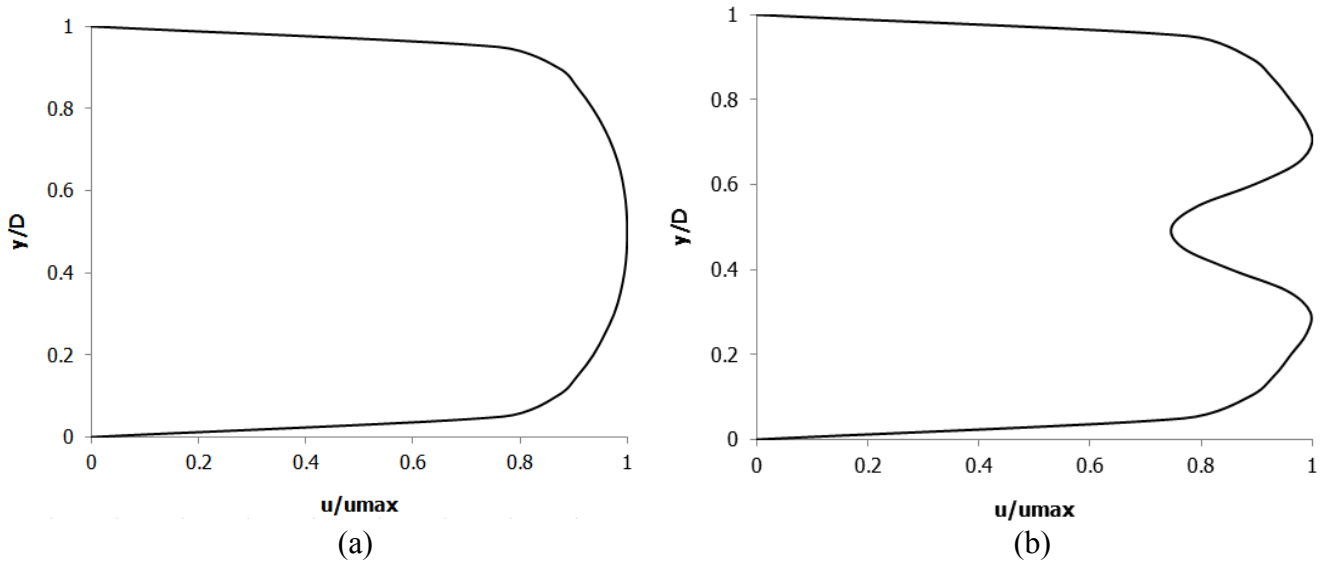


Figure 4.10. Variations in the Cross-Sectional Velocity Profiles for a Single Spherical Capsule of $k = 0.5$ in a Horizontal Pipe at $V_{av} = 1\text{m/sec}$ at (a) Upstream and (b) Downstream of the Capsule

Figure 4.11 depicts the variations in the velocity profiles at various locations within the capsule transporting pipe under consideration at an average flow velocity of 1m/sec.

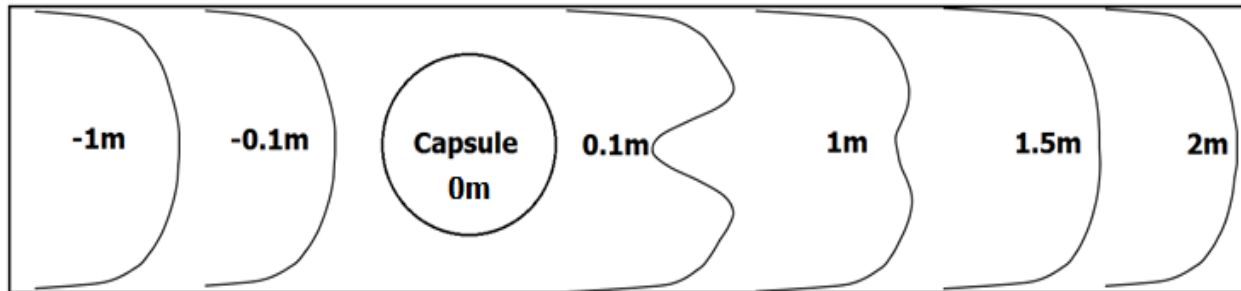


Figure 4.11. Development of Velocity Profile in the Presence of a Single Spherical Capsule in a Horizontal Pipe having Density Equal to Water

4.5.1. Average Flow Velocity Effects

To investigate the effect of the average flow velocity on the flow structure within the pipe, an average velocity of 4m/sec for a spherical capsule of $k = 0.5$ has been chosen for flow diagnostics. Figure 4.12 depicts the pressure and velocity variations in the capsule transporting pipe for an average flow velocity of 4m/sec, keeping $k = 0.5$. The trend of pressure distribution is the same as observed for $V_{av} = 1\text{m/sec}$ i.e. a high pressure of 2414Pa at the upstream location, a very low pressure of -2632Pa in the annulus region, a relatively low pressure of 1379Pa at downstream location as compared to upstream location and a very high pressure of 10047Pa at the location where the flow strikes the capsule. There is an average increase of 92% in the pressure at the upstream, downstream and the point of highest pressure as compared to $V_{av} = 1\text{m/sec}$. Furthermore, there is a decrease of 95% in the pressure in the annulus region. The pressure drop between the inlet and the outlet of the pipe is 1533Pa, which is 92% higher than the pressure drop for $V_{av} = 1\text{m/sec}$. It can be concluded that increase in the average

velocity of the flow increases the pressure drop but does not affect the overall pressure distribution in a capsule transporting pipe. The same trend has been observed by Deniz [89]. Furthermore, it can be seen in figure 4.12 (b) that the velocity field resembles the one observed in case of $V_{av} = 1$ m/sec i.e. higher velocity in the annulus.

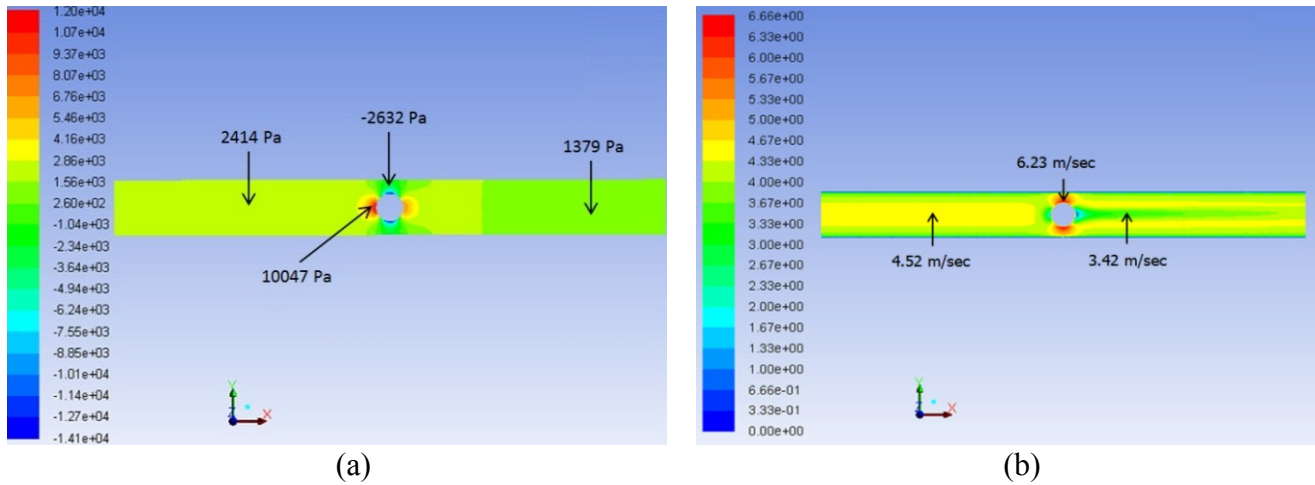


Figure 4.12. Variations in (a) Pressure and (b) Velocity, for a Single Spherical Capsule of $k = 0.5$ in a Horizontal Pipe at $V_{av} = 4\text{m/sec}$

Figure 4.13 shows the variations in C_p and u/u_{max} along the analysis line for the case under consideration. The results depict that the pressure drop for $V_{av} = 4\text{m/sec}$ is higher than for 1m/sec . However, the pressure distribution in the pipeline is similar for both the cases. Furthermore, the velocity distribution for both $V_{av} = 4\text{m/sec}$ and 1m/sec are exactly similar indicating that the change in the velocity within the pipe is proportional to the average flow velocity. More detailed results have been presented in table A-3.1.

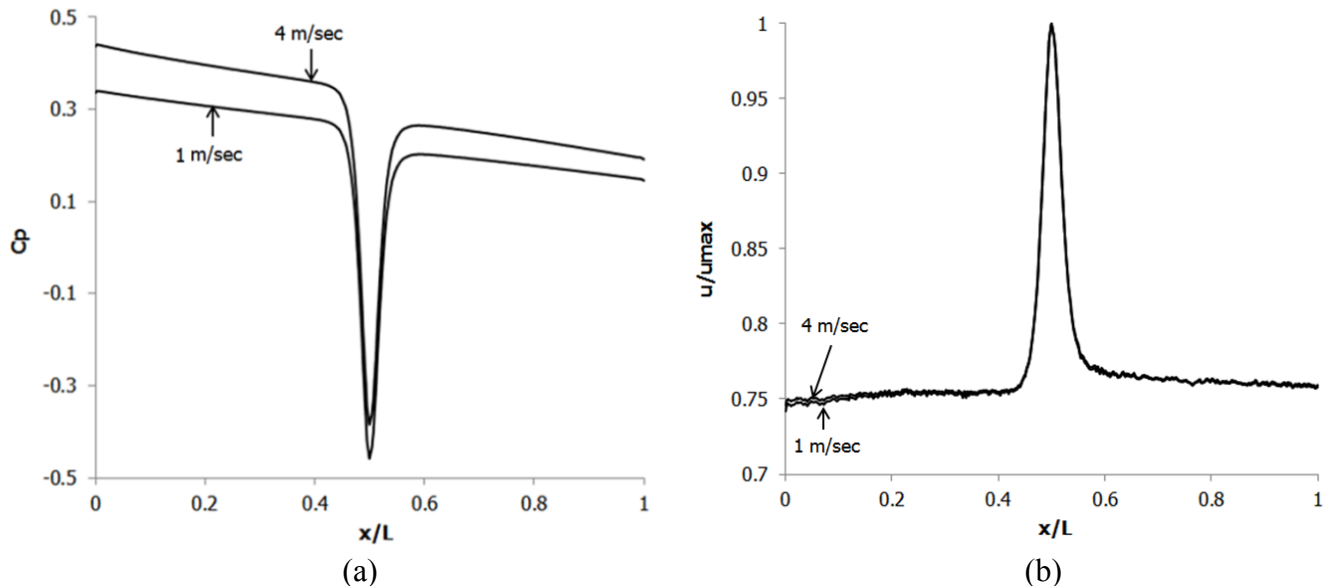


Figure 4.13. (a) Variations in C_p for a Single Spherical Capsule of $k = 0.5$ in a Horizontal Pipe at $V_{av} = 4\text{m/sec}$ (b) Variations in u/u_{max} for a Single Spherical Capsule of $k = 0.5$ in a Horizontal Pipe at $V_{av} = 4\text{m/sec}$

4.5.2. Capsule Diameter Effects

Figure 4.14 shows the pressure and velocity distributions in a spherical capsule transporting horizontal pipe for $k = 0.9$ and $V_{av} = 1\text{m/sec}$. It can be seen that although the overall pressure distribution seems to be the same as compared with the pressure field for $k = 0.5$ at the same average flow velocity, but the pressure at upstream location has increased by 88% and the pressure at downstream location has decreased by 116% which suggests that the overall pressure drop in the pipe has increased sharply. The pressure drop between the inlet and the outlet of the pipe is 1450Pa, which is 91.5% higher than the pressure drop for $k = 0.5$. Furthermore, the pressure in the annulus region has decreased by 99% and the pressure at the immediate upstream location of the capsule has increased by 58%. Such a sharp decrease in the pressure in the annulus region is due to the fact that the cross-sectional area of the flow has reduced by 80%. Furthermore, it can be seen in figure 4.14 (b) that velocity of the flow in the annulus region has increased tremendously while a large wake region exists downstream of the capsule where the flow velocity is very low.

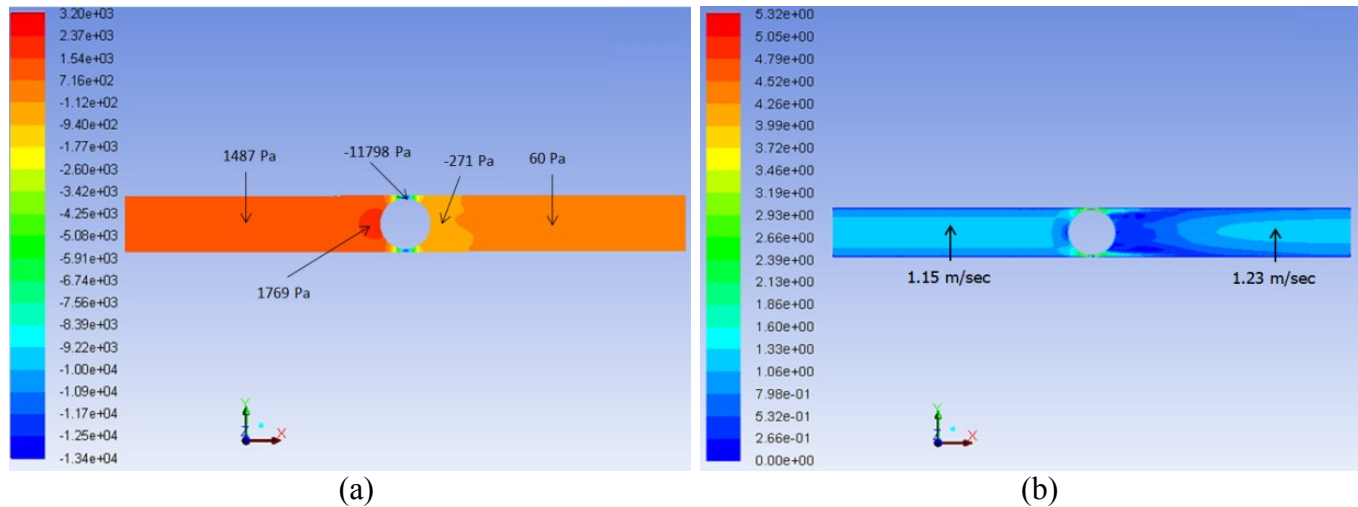


Figure 4.14. Variations in (a) Pressure and (b) Velocity, for a Single Spherical Capsule of $k = 0.9$ in a Horizontal Pipe at $V_{av} = 1\text{m/sec}$

Figure 4.15 shows the variations in C_p and u/u_{max} along the analysis line for the case under consideration. The results depict that the pressure drop for $k = 0.9$ is considerably higher than for 0.5. That's why the pressure coefficient for $k = 0.5$ has been plotted on the secondary Y axis of the graph as the scale is considerably different for both the cases. However, the pressure distribution in the pipeline is similar for both the cases. Furthermore, the velocity distribution for both $k = 0.9$ and 0.5 are similar though the magnitude of the velocity differs appreciably between the two cases, i.e. an extremely high flow velocity in the annulus region. More detailed results have been presented in table A-3.1.

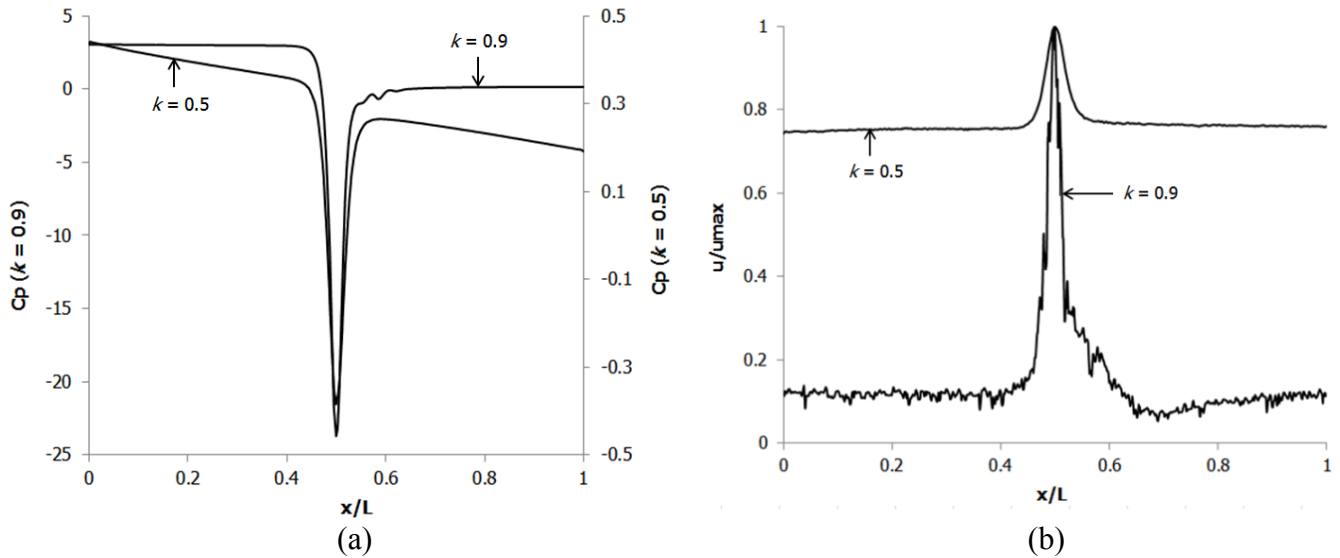


Figure 4.15. (a) Variations in C_p for a Single Spherical Capsule of $k = 0.5$ in a Horizontal Pipe at $V_{av} = 1\text{m/sec}$ (b) Variations in u/u_{max} for a Single Spherical Capsule of $k = 0.5$ in a Horizontal Pipe at $V_{av} = 1\text{m/sec}$

4.5.3. Capsule Concentration Effects

Figure 4.16 depicts the pressure and velocity variations in a hydraulic pipe carrying three spherical capsules of $k = 0.5$ and $V_{av} = 1\text{m/sec}$. The spacing between the capsules is equal to one diameter of the capsule. The trend of the pressure distribution is the same as observed for a single spherical capsule. The pressure at upstream location has increased to 248Pa (27%) while it has decreased to 117Pa (11%) downstream as compared to a single spherical capsule. Hence, an overall pressure drop increase of 16% has been observed for $N = 3$ as compared to $N = 1$. Furthermore, as compared to a single spherical capsule, it can be seen that although the flow velocity upstream of the capsules is the same (i.e. 1.15m/sec), but the velocity downstream of the capsules has reduced by 17.5% to 0.71m/sec. Hence, increased concentration of the solid phase in the pipe offers more resistance to the flow; increasing the pressure drop and decreasing the average flow velocity.

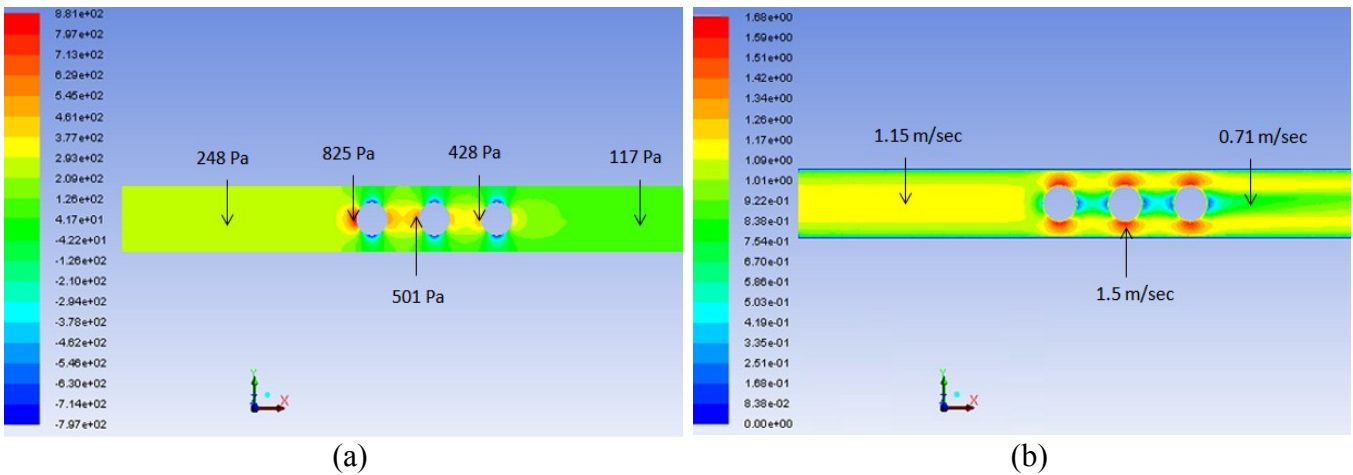


Figure 4.16. Variations in (a) Pressure and (b) Velocity, for Three Spherical Capsules of $k = 0.5$ and $Sc = 1 * d$ in a Horizontal Pipe at $V_{av} = 1\text{m/sec}$

Figure 4.17 represents the variations in C_p and u/u_{max} for the case under consideration. It can be clearly seen that the pressure drop for three spherical capsules is higher than the pressure drop for a single spherical capsule. This is because the concentration of the solid medium within the pipe is more in case of $N = 3$ as compared to $N = 1$. The same trend has been observed by Ulusarslan [90]. The three peaks in the curve representing $N = 3$ indicates the presence of the three capsules in the pipe. The velocity profile is quite similar for both the cases. More detailed results have been presented in table A-3.1.

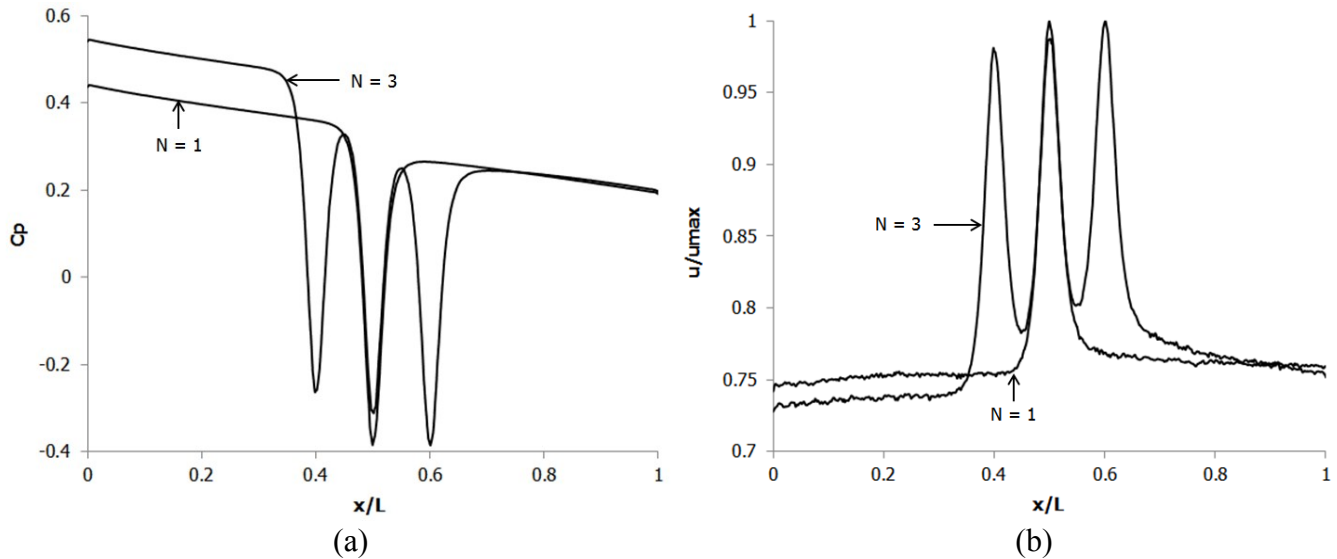


Figure 4.17. (a) Variations in C_p for Three Spherical Capsules of $k = 0.5$ and $Sc = 1 * d$ in a Horizontal Pipe at $V_{av} = 1\text{m/sec}$ (b) Variations in u/u_{max} for Three Spherical Capsules of $k = 0.5$ and $Sc = 1 * d$ in a Horizontal Pipe at $V_{av} = 1\text{m/sec}$

4.5.4. Effects of Spacing between the Capsules

Figure 4.18 depicts the pressure and velocity variations in a hydraulic pipe carrying three spherical capsules of $k = 0.5$ and $V_{av} = 1\text{m/sec}$. The spacing between the capsules is equal to five diameters of the capsule. The trend of the pressure distribution is the same as observed for $Sc = 1 * d$. The pressure at upstream location has increased by 7% while it has decreased 14% as compared to $Sc = 1 * d$ case. Hence, an overall pressure drop increase of 2% has been observed for $Sc = 5 * d$ as compared to $1 * d$. Furthermore, as compared to $Sc = 1 * d$, it can be seen that the pressures at upstream locations of each capsule have increased by 7% on average. The flow velocity upstream of the capsules is the same (i.e. 1.15m/sec), but the velocity downstream of the capsules has increased by 15% to 0.82m/sec . Hence, increased spacing between the capsules leads to a marginally higher pressure drop within the pipe in comparison with other parameters.

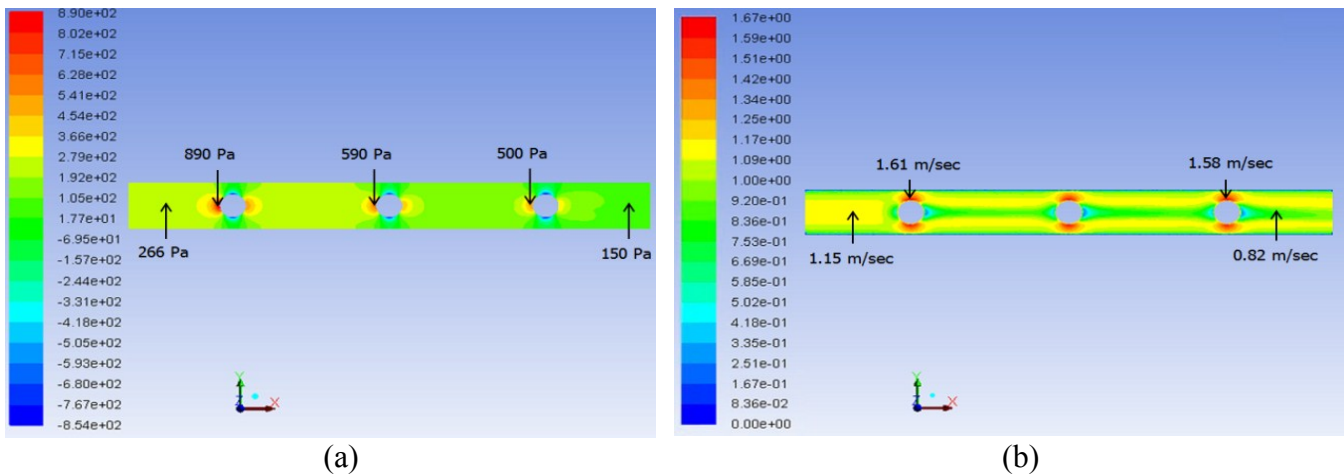


Figure 4.18. Variations in (a) Pressure and (b) Velocity, for Three Spherical Capsules of $k = 0.5$ and $Sc = 5 * d$ in a Horizontal Pipe at $V_{av} = 1\text{m/sec}$

Figure 4.19 represents the variations in C_p and u/u_{max} for the case under consideration. It can be seen that the pressure drop for $Sc = 5 * d$ is marginally higher than the pressure drop for $Sc = 1 * d$ in comparison with other parameters. Furthermore, the velocity distribution remains quite the same for both the cases. More detailed results have been presented in table A-3.1.

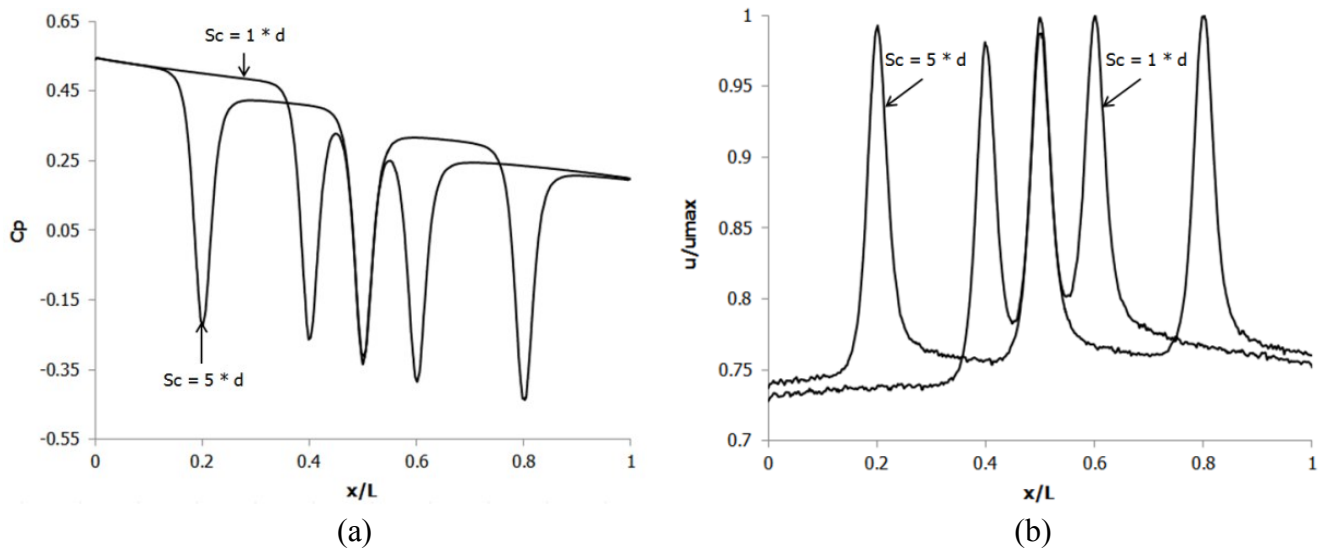


Figure 4.19. (a) Variations in C_p for Three Spherical Capsules of $k = 0.5$ and $Sc = 5 * d$ in a Horizontal Pipe at $V_{av} = 1\text{m/sec}$ (b) Variations in u/u_{max} for Three Spherical Capsules of $k = 0.5$ and $Sc = 5 * d$ in a Horizontal Pipe at $V_{av} = 1\text{m/sec}$

Table A-3.1 in Appendix A-3 summarises the results for various Computational Fluid Dynamics based investigations being carried out on the flow of spherical capsules in a horizontal pipe with density equal to that of water.

Further analysing the results obtained, figure 4.20 depicts the variations in the normalised pressure drop in the test section of the pipe for a single spherical capsule at various flow velocities. The pressure drop for the mixture flow has been non-dimensionalised with the pressure drop for water flow, and the flow velocity has been represented in terms of the Reynolds Number of water. The curves in the figure are for different k values ranges between 0.5 and 0.9. The results show that as the velocity of the flow increases, the pressure drop in the pipe increases. Furthermore, as the diameter of the capsule increases, the pressure drop increases. This trend was also noticed by Uluarslan [91]. The reason for the increase in pressure drop with an increase in the capsule diameter is due to the fact that a capsule of bigger size offers more resistance to the flow. From table A-3.1, it can be seen that the pressure drop increases by 52% on average for $k = 0.7$ and by 11 times for $k = 0.9$ w.r.t. $k = 0.5$ for a single spherical capsule. Figure 4.20 further suggests that $k = 0.7$ is the best option in terms of pressure drop in the pipeline.

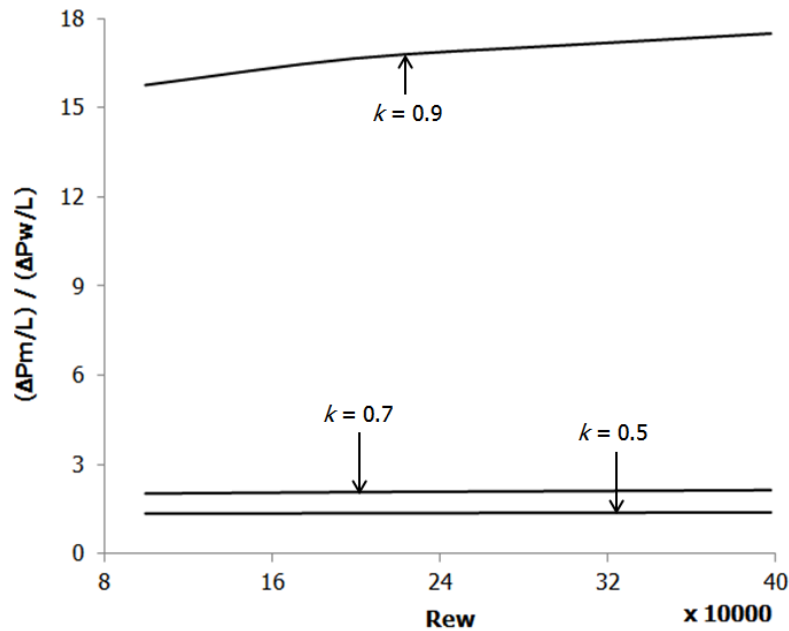


Figure 4.20. Variations in Normalised Pressure Drop for a Single Equi-Density Spherical Capsule in a Horizontal Pipe

Figure 4.21 depicts the variation in the normalised pressure drops in the test section of the pipe for a train of three spherical capsules having a spacing of $1 * d$ between the consecutive capsules respectively. The results show that as the flow velocity increases, the pressure drop in the test section of the pipe increases. Furthermore, as the size of the capsule increases, the pressure drop further increases. It is evident that equi-density spherical capsules of diameter equal to 90% of the pipeline diameter offer substantial pressure drop and hence are not recommended for practical applications. The pressure drop for $k = 0.9$ and 0.7 are 21 times and 122% higher on average respectively than capsules of $k = 0.5$ at the same average flow velocity and the same spacing between the capsules in the train. Comparing figures 4.20 and 4.21 reveals that an increase in the concentration of the capsules in the pipe increases the pressure drop.

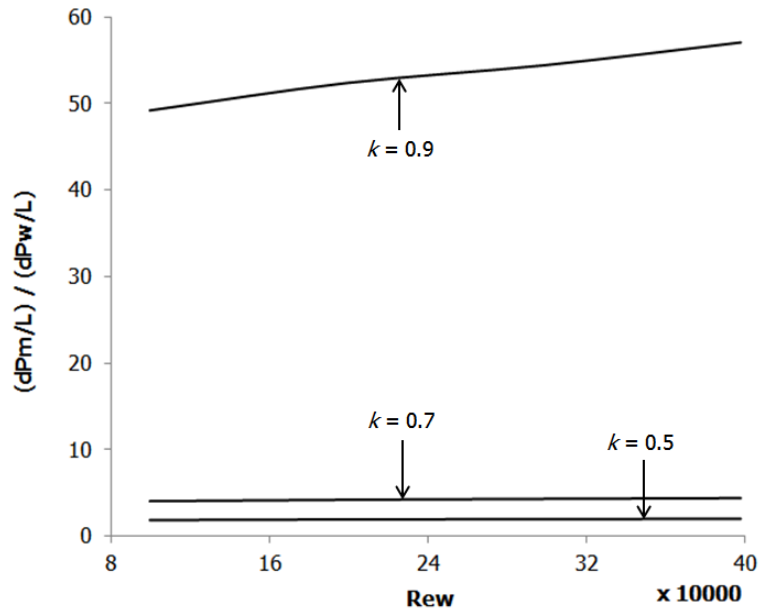


Figure 4.21. Variations in Normalised Pressure Drop for Three Equi-Density Spherical Capsules in a Horizontal Pipe

Figure 4.22 depicts the variations in the normalised pressure drop for a spherical capsule train consisting of three capsules of $k = 0.7$ and having different spacing between them. It can be clearly seen that as the spacing between the capsules increases, the normalised pressure drop in the pipe increases. This trend is similar at all average flow velocities under consideration. Furthermore, the increase in the normalised pressure drop shows a linearly increasing trend w.r.t. the spacing between the capsules.

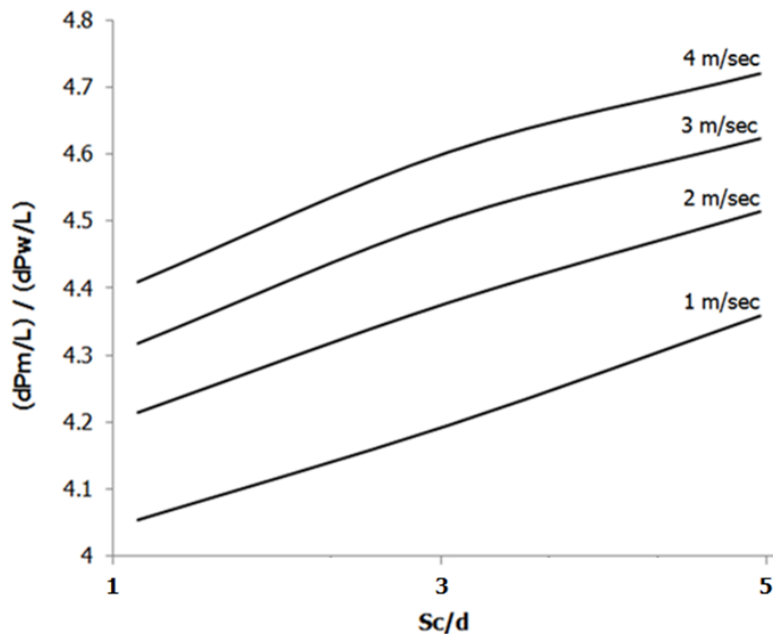


Figure 4.22. Variations in Normalised Pressure Drop for Three Spherical Capsules of $k = 0.7$ in a Horizontal Pipe

The information provided in this section, regarding the flow of equi-density spherical capsules in horizontal pipes, has a huge impact on the design process of HCPs, which is presented in Chapter 7. Similar kind of analysis that has been carried out in this section is also presented in the next chapter for the flow of equi-density spherical capsules in vertical pipes.

4.6. Analysis of the Flow of Equi-Density Cylindrical Capsules in a Horizontal HCP

Figure 4.23 depicts the pressure and velocity variations around a single cylindrical capsule of $k = 0.5$ at an average flow velocity of 1m/sec for a capsule length $L_c = 1 * d$. The pressure field around a cylindrical capsule resembles the pressure field around a spherical capsule. At upstream, the pressure of water increases from 497Pa to 1057Pa as it approaches the capsule. This happens due to the additional resistance offered by the capsule to the flow within the pipe. The flow then passes through the annulus between the pipe wall and the capsule. As the cross-sectional area decreases, the pressure of water also decreases. Once the flow exits the annulus, due to increase in the cross-sectional area, the pressure of water recovers to some extent. It can be seen that the pressure downstream has been recovered to 124Pa. Furthermore, the trend of the velocity distribution is the same as seen in case of a single spherical capsule. The velocity upstream of the capsule remains the same, i.e. 1.15m/sec. In the annulus region, the flow accelerates to 1.78m/sec due to the reduction in the cross-sectional area which is 39% higher than a spherical capsule. Behind a capsule, a large wake region has been observed in case of a cylindrical capsule where the flow velocity reduces to 0.038m/sec. This wake region shows that separation takes place in the flow for a cylindrical capsule due to its flat ends. This wake region delays the development of the velocity profile downstream of the capsule. The velocity further downstream of the capsule, as indicated in the figure 4.23 (b), is 0.72m/sec which is 16% less than for a spherical capsule.

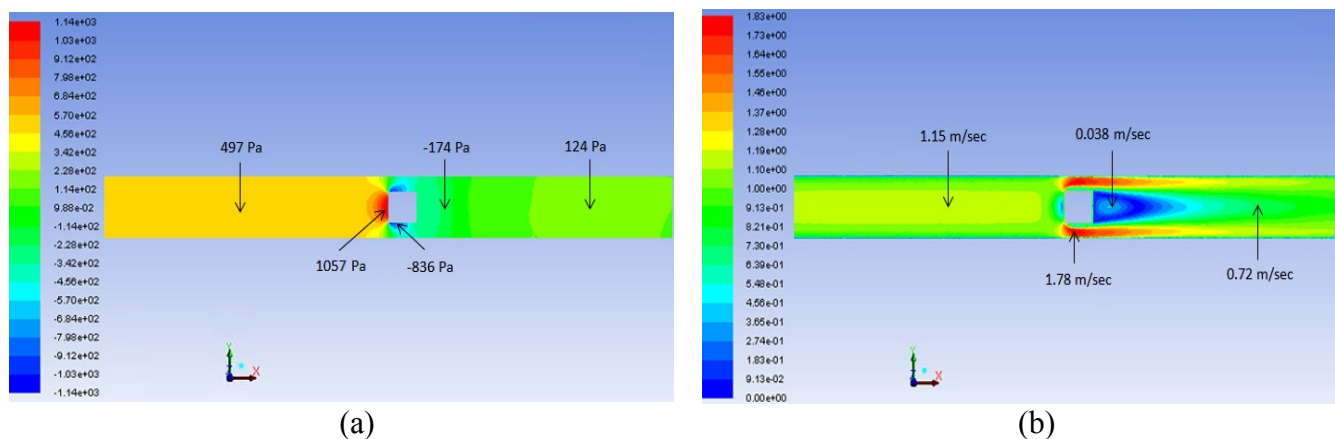


Figure 4.23. Variations in (a) Pressure and (b) Velocity, for a Cylindrical Capsule of $k = 0.5$ and $L_c = 1 * d$ in a Horizontal Pipe at $V_{av} = 1\text{m/sec}$

Figure 4.24 shows the variations in C_p and u/u_{max} for the case under consideration, where C_p represents the coefficient of pressure and u is the local flow velocity along the pipe. The profiles for a single spherical capsule flow have also been included for comparison. It can be clearly seen that the pressure drop in case of a cylindrical capsule is higher than the pressure drop for a spherical capsule. It is worth noticing that the pressure drops sharply in the annulus between the cylindrical capsule and the pipe wall and then recovers to some extent as the flow exits the annulus region. The difference in the pressure between the upstream and the downstream locations is due to the fact that some part of the kinetic energy of water has been converted into the work done on the capsule. The total pressure drop in case of a cylindrical capsule is 414 Pa, which is 233% higher than for a single spherical capsule and 350% higher than for a single phase water flow.

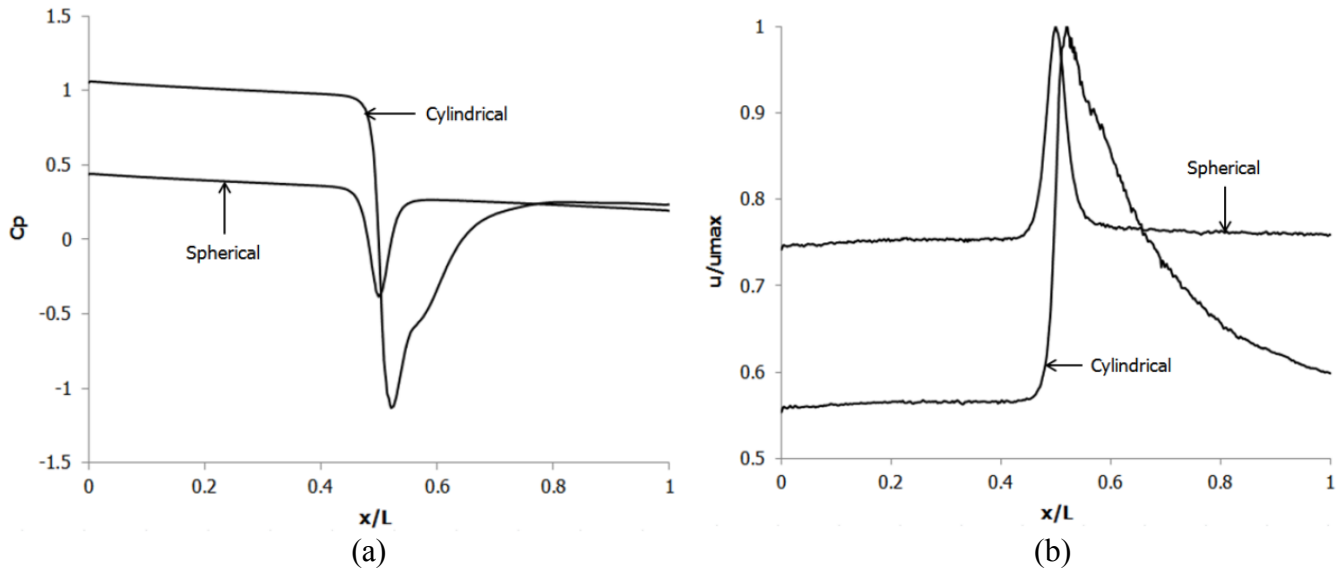


Figure 4.24. (a) Variations in C_p for a Cylindrical Capsule of $k = 0.5$ and $L_c = 1 * d$ in a Horizontal Pipe at $V_{av} = 1\text{m/sec}$ (b) Variations in u/u_{max} for a Cylindrical Capsule of $k = 0.5$ and $L_c = 1 * d$ in a Horizontal Pipe at $V_{av} = 1\text{m/sec}$

Furthermore, figure 4.24 (b) shows a sudden rise in flow velocity in the annulus region. This suggests that the flow velocity at both the upstream and downstream locations for a cylindrical capsule is lower as compared to a spherical capsule, although the clearance between the capsule and the pipe wall is the same for both the cases. The reason behind this is the fact that flow separates at the front edge of the cylindrical capsule, resulting into a further decrease of the effective cross-sectional area for the flow of water. This trend has also been observed by Fujiwara [92].

To further investigate the velocity distribution within the capsule transporting pipe, velocity profiles have been drawn across the cross-section of the pipe at both 0.1m upstream and downstream locations from the centre of the capsule as shown in figure 4.25. It can be seen that the velocity profile is undisturbed at the upstream location, and the presence of the capsule has not affected the velocity profile at this location. However, at the downstream location, the presence of the capsule in the pipe has distorted the velocity profile.

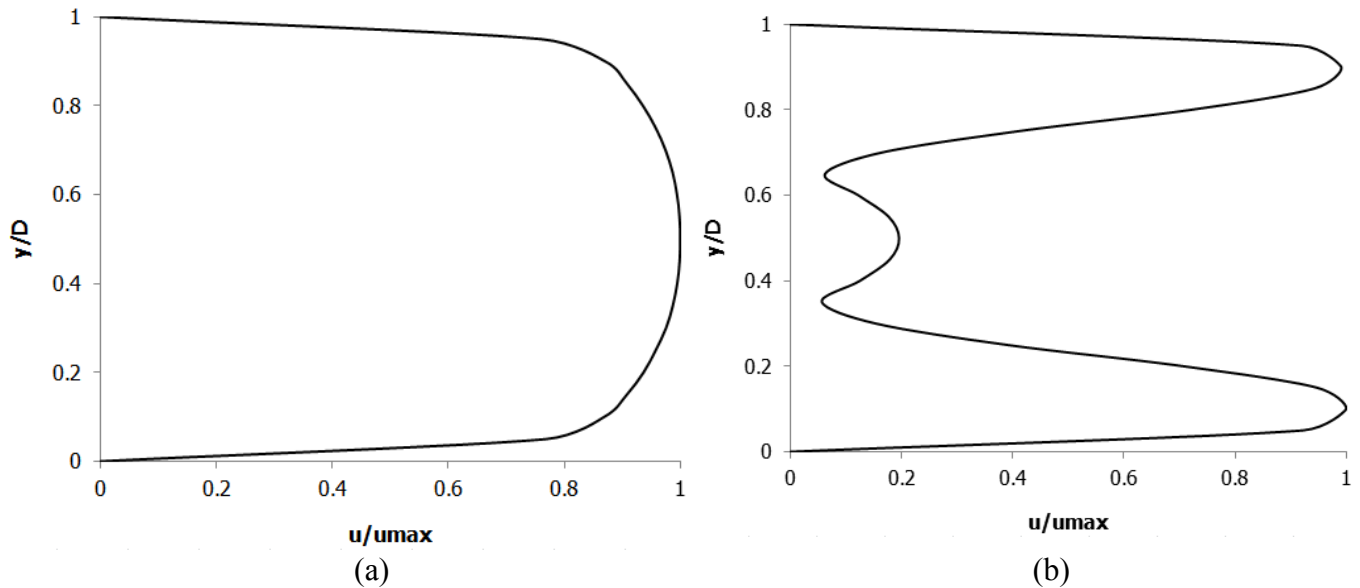


Figure 4.25. Variations in the Cross-Sectional Velocity Profiles for a Single Cylindrical Capsule of $k = 0.5$ and $L_c = 1 * d$ in a Horizontal Pipe at $V_{av} = 1\text{m/sec}$ at (a) Upstream and (b) Downstream of the Capsule

Figure 4.26 depicts the variations in the velocity profiles at various locations within the cylindrical capsule transporting pipe under consideration at an average flow velocity of 1m/sec .

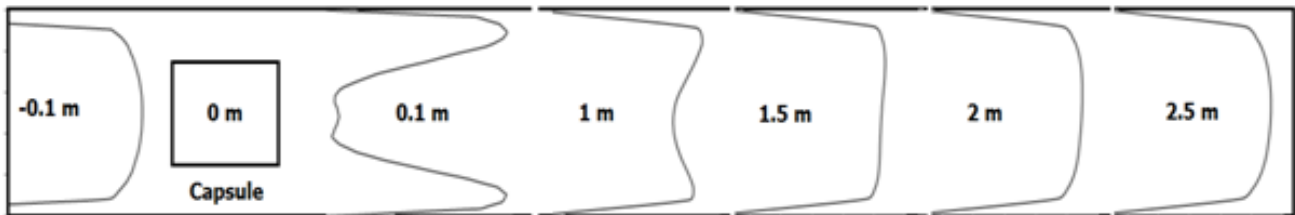


Figure 4.26. Development of Velocity Profile in the Presence of a Single Cylindrical Capsule in a Horizontal Pipe having Density Equal to Water

4.6.1. Average Flow Velocity Effects

Figure 4.27 depicts the pressure and velocity variations within the test section of the pipe carrying a cylindrical capsule of $k = 0.5$ at an average flow velocity of 4m/sec . The length of the capsule $L_c = 1 * d$. It can be seen that both the pressure and velocity fields are identical to the one observed for $V_{av} = 1\text{m/sec}$. The pressure upstream of the capsule is 202% higher and downstream of the capsule is 5% higher as compared to $V_{av} = 1\text{m/sec}$.

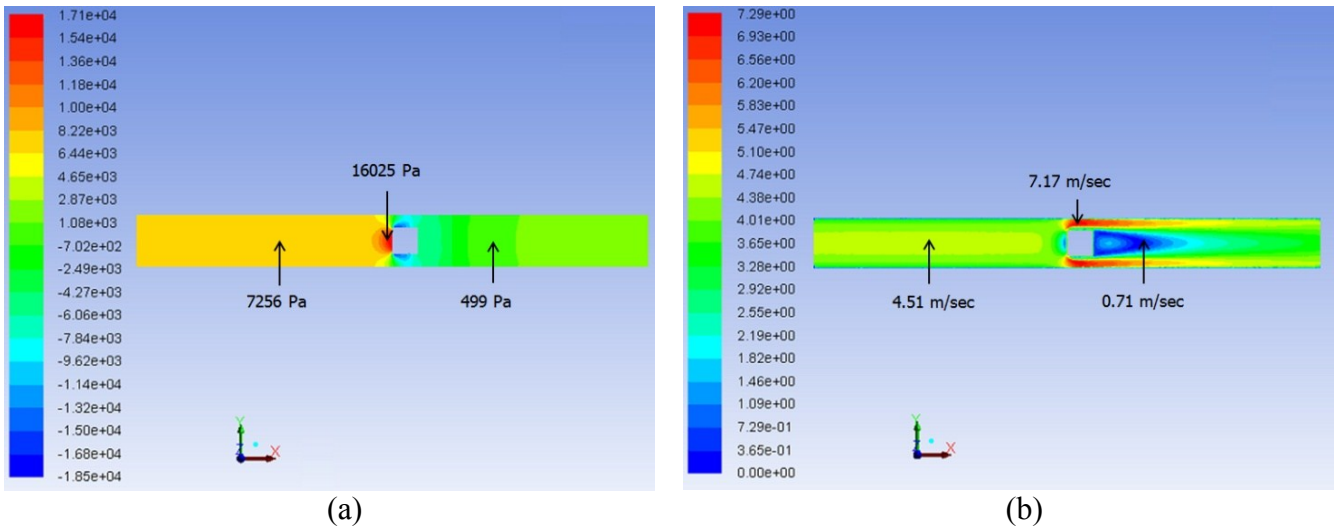


Figure 4.27. Variations in (a) Pressure and (b) Velocity, for a Cylindrical Capsule of $k = 0.5$ and $L_c = 1 * d$ in a Horizontal Pipe at $V_{av} = 4m/sec$

Figure 4.28 shows the variations in C_p and u/u_{max} for the case under consideration. The profiles for a single cylindrical capsule flow at $V_{av} = 1m/sec$ have also been included for comparison. It can be seen that the pressure drop for $V_{av} = 4m/sec$ is higher than for $V_{av} = 1m/sec$. Furthermore, the velocity distribution for both $V_{av} = 4m/sec$ and $1m/sec$ are identical indicating that the change in the velocity within the pipe is proportional to the average flow velocity. More detailed results have been presented in table A-3.2.

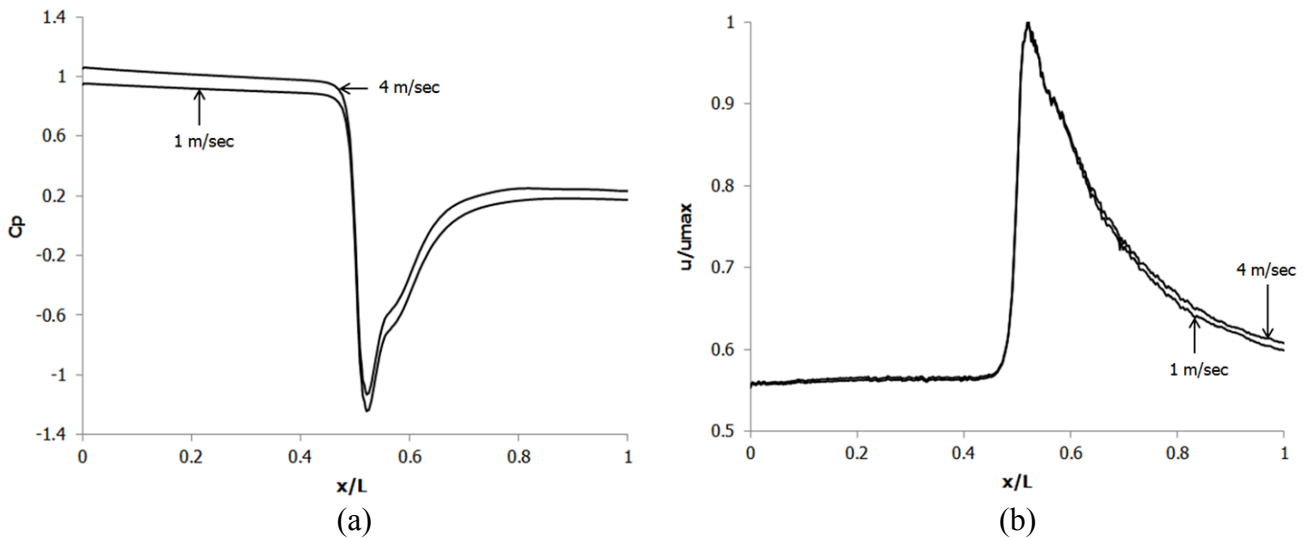


Figure 4.28. (a) Variations in C_p for a Cylindrical Capsule of $k = 0.5$ and $L_c = 1 * d$ in a Horizontal Pipe at $V_{av} = 4m/sec$ (b) Variations in u/u_{max} for a Cylindrical Capsule of $k = 0.5$ and $L_c = 1 * d$ in a Horizontal Pipe at $V_{av} = 4m/sec$

4.6.2. Length of the Capsule Effects

Figure 4.29 shows the pressure and velocity distributions in a cylindrical capsule transporting horizontal pipe for $k = 0.5$, $L_c = 5 * d$ and $V_{av} = 1\text{m/sec}$. It can be seen that the overall pressure and velocity distributions seem to be the same as compared with $L_c = 1 * d$ at the same average flow velocity and capsule diameter.

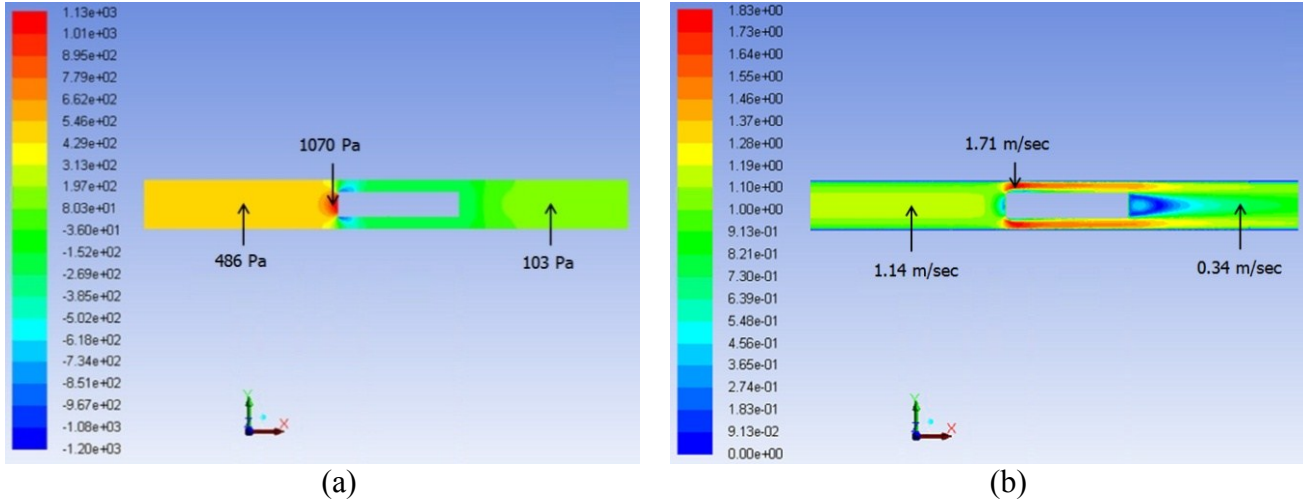


Figure 4.29. Variations in (a) Pressure and (b) Velocity, for a Single Cylindrical Capsule of $k = 0.5$ and $L_c = 5 * d$ in a Horizontal Pipe at $V_{av} = 1\text{m/sec}$

Figure 4.30 shows the variations in C_p and u/u_{max} along the analysis line for the case under consideration. The results depict that the both the pressure and velocity variations for a longer cylindrical capsule are identical to a shorter capsule. The difference in the pressure and velocity variations is marginal for the range of lengths considered in the present study. More detailed results have been presented in table A-3.2.

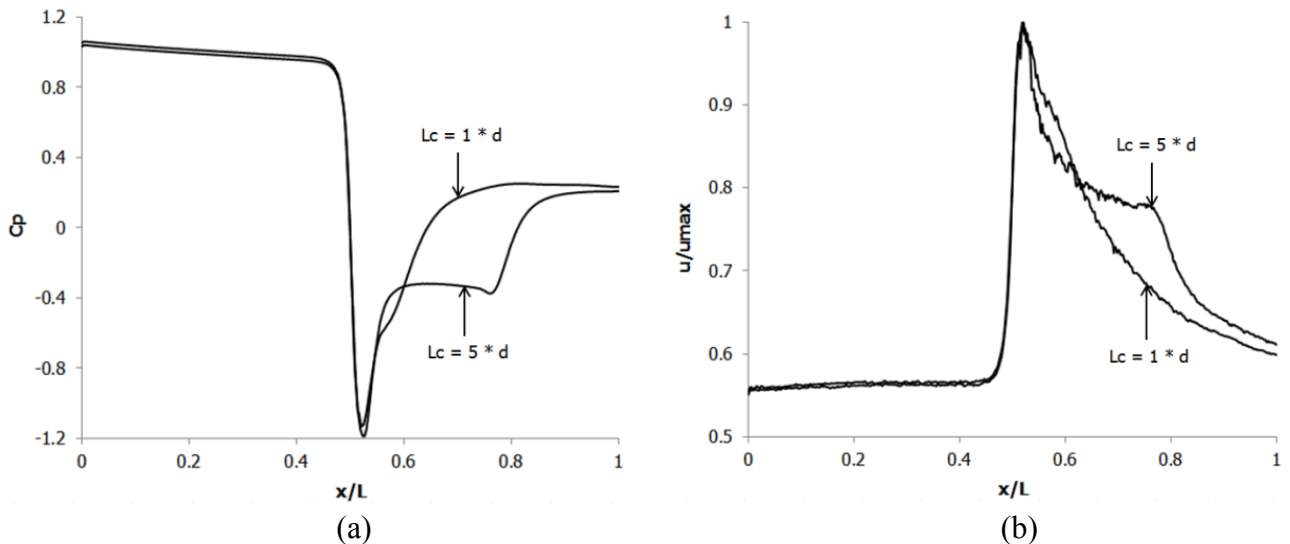


Figure 4.30. (a) Variations in C_p for a Single Cylindrical Capsule of $k = 0.5$ and $L_c = 5 * d$ in a Horizontal Pipe at $V_{av} = 1\text{m/sec}$ (b) Variations in u/u_{max} for a Single Cylindrical Capsule of $k = 0.5$ and $L_c = 5 * d$ in a Horizontal Pipe at $V_{av} = 1\text{m/sec}$

4.6.3. Capsule Diameter Effects

Figure 4.31 depicts the variations in the pressure field and C_p for an equi-density cylindrical capsule of $L_c = 5 * d$, $k = 0.9$ at $V_{av} = 1\text{m/sec}$ in a horizontal pipe. The trend of the pressure distribution is the same as observed for $k = 0.5$ at same average flow velocity and for the same length of the capsule. The pressure at upstream and downstream locations from the capsule has increased by 62 times and 49 times respectively. Moreover, the pressure at the front face of the capsule has increased by 36 times as compared to $k = 0.5$ for the same length of the capsule and at same average flow velocity. An overall pressure drop increase by 68 times has been observed in the present case compared with $k = 0.5$, $L_c = 5 * d$ and $V_{av} = 1\text{m/sec}$. This increase in the pressure drop is evident from figure 4.31 (b) as well. It can be clearly seen in figure 4.31 (b) that the pressure drop for $k = 0.9$ is remarkably higher than for $k = 0.5$. More detailed results have been presented in table A-3.2.

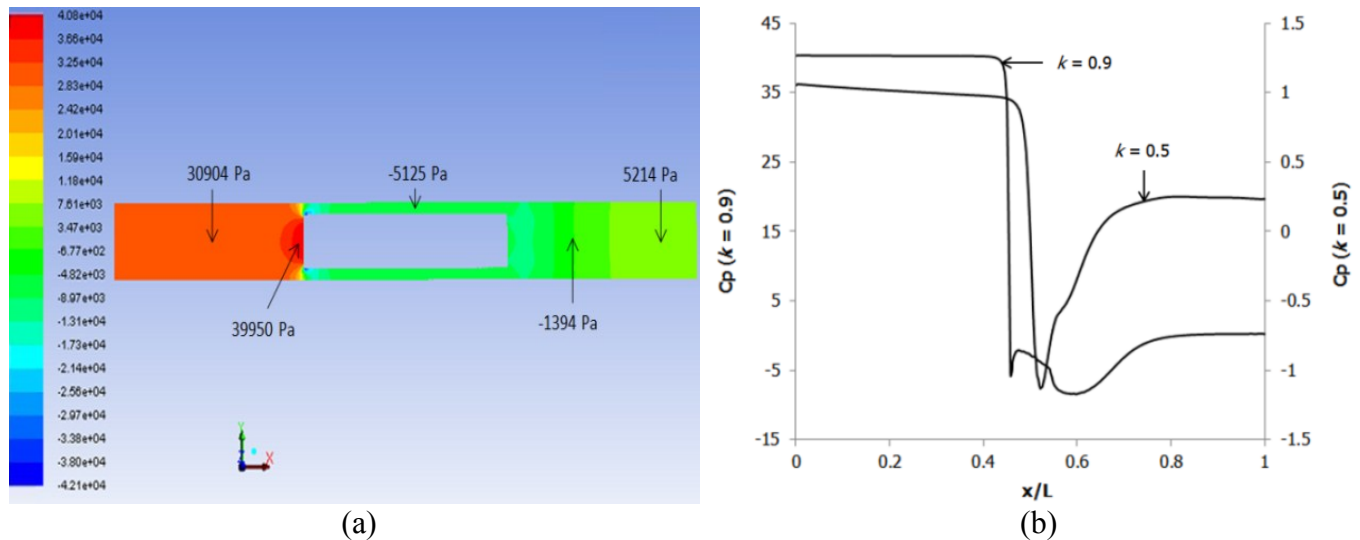
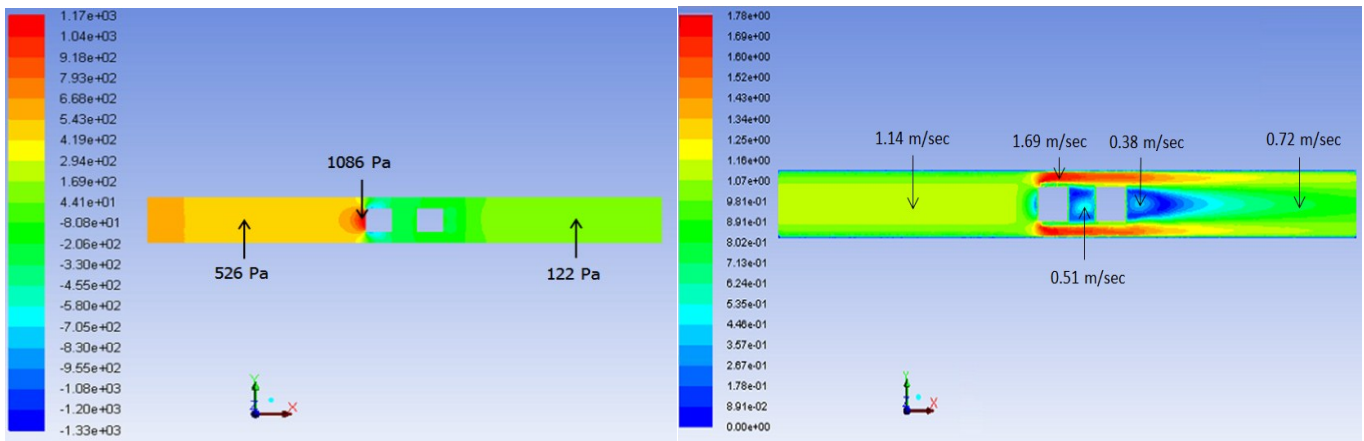


Figure 4.31. (a) Variations in Pressure for a Single Cylindrical Capsule of $k = 0.9$ and $L_c = 5 * d$ in a Horizontal Pipe at $V_{av} = 1\text{m/sec}$ (b) Variations in C_p for a Single Cylindrical Capsule of $k = 0.9$ and $L_c = 5 * d$ in a Horizontal Pipe at $V_{av} = 1\text{m/sec}$

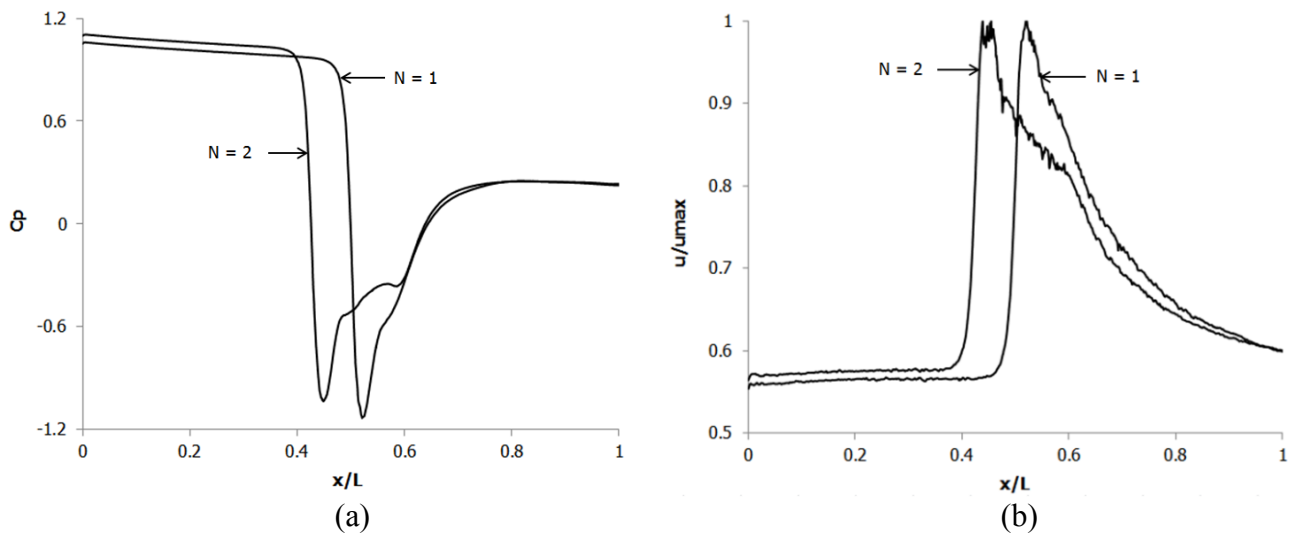
4.6.4. Capsule Concentration Effects

Figure 4.32 depicts the pressure and velocity variations in a horizontal hydraulic pipe carrying two cylindrical capsules of $k = 0.5$, $L_c = 1 * d$, $Sc = 1 * d$ and density equal to that of water. The trend of the pressure distribution is the same as observed for a single cylindrical capsule. The pressure at upstream and downstream locations has increased by 6% and 1.6% respectively as compared to a single cylindrical capsule. An overall pressure drop increase of 6% has been observed for $N = 2$ as compared to $N = 1$ at $V_{av} = 1\text{ m/sec}$. Furthermore, the velocity field is identical to $N = 1$, i.e. a high flow velocity in the annulus and a large wake region downstream of the capsules.



(a) (b)
 Figure 4.32. Variations in (a) Pressure and (b) Velocity, for Two Cylindrical Capsules of $k = 0.5$, Sc and $Lc = 1 * d$ in a Horizontal Pipe at $V_{av} = 1\text{m/sec}$

Figure 4.33 shows the variations in C_p and u/u_{max} along the analysis line for the case under consideration. The results depict that the pressure drop for two cylindrical capsules is marginally higher than for a single capsule in comparison with other parameters. Furthermore, the velocity profiles along the analysis line are identical for both $N = 1$ and 2 . More detailed results have been presented in table A-3.2.



(a) (b)
 Figure 4.33. (a) Variations in C_p for Two Cylindrical Capsules of $k = 0.5$, Sc and $Lc = 1 * d$ in a Horizontal Pipe at $V_{av} = 1\text{m/sec}$ (b) Variations in u/u_{max} for Two Cylindrical Capsules of $k = 0.5$, Sc and $Lc = 1 * d$ in a Horizontal Pipe at $V_{av} = 1\text{m/sec}$

4.6.5. Effects of Spacing between the Capsules

Figure 4.34 depicts the effect of spacing between the capsules on the pressure and velocity distribution within the pipe. In comparison with figure 66 it can be seen that the pressure upstream of the capsules having $Sc = 5 * d$ is 33% higher than for $Sc = 1 * d$ whereas it is the same at the downstream location. Furthermore, the pressure at the front face of the first capsule is 20% higher than the pressure at the front face of the first capsule in the train for $Sc = 1 * d$. The overall increase in the pressure drop within the test section of the pipe is 37% for $Sc = 5 * d$ as compared to $Sc = 1 * d$ for the same average flow velocity, diameter of the capsule and the length of the capsule. The velocity field is similar for both the cases. Table A-3.2 in Appendix A-3 summarises the results for various Computational Fluid Dynamics based investigations being carried out on the flow of cylindrical capsules in a horizontal pipe with density equal to that of water.

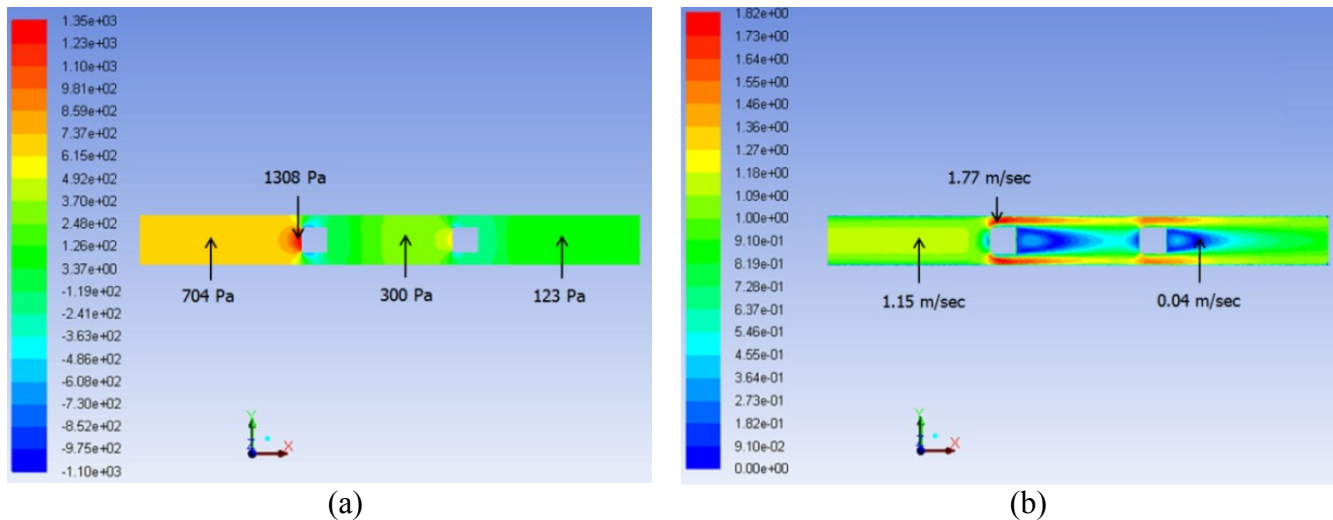


Figure 4.34. Variations in (a) Pressure and (b) Velocity, for Two Cylindrical Capsules of $k = 0.5$, $Sc = 5 * d$ and $Lc = 1 * d$ in a Horizontal Pipe at $V_{av} = 1\text{m/sec}$

Figure 4.35 shows the variations in C_p and u/u_{max} along the analysis line for the case under consideration. The results depict that the pressure drop is higher for more spacing between the capsules. Moreover, the velocity distribution is similar for different spacing between the capsules. More detailed results have been presented in table A-3.2.

Further analysing the results obtained in the table above, figure 4.36 depicts the variation in the normalised pressure drop in the test section of the pipe for a single cylindrical capsule having $Lc = 1 * d$. The results show that as the flow velocity increases, the pressure drop in the test section of the pipe increases. Furthermore, as the size of the capsule increases, the pressure drop further increases.

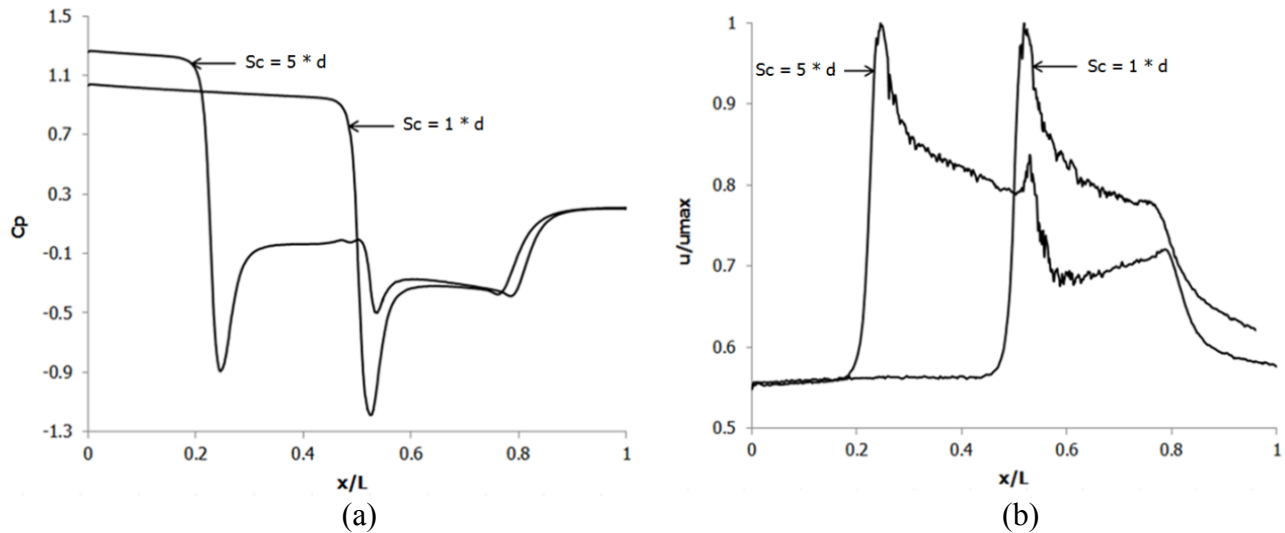


Figure 4.35. (a) Variations in C_p for Two Cylindrical Capsules of $k = 0.5$, $Sc = 5 * d$ and $L_c = 1 * d$ in a Horizontal Pipe at $V_{av} = 1 \text{ m/sec}$ (b) Variations in u/u_{max} for Two Cylindrical Capsules of $k = 0.5$, $Sc = 5 * d$ and $L_c = 1 * d$ in a Horizontal Pipe at $V_{av} = 1 \text{ m/sec}$

It is evident from table A-3.2 and figure 4.36 that equi-density cylindrical capsules of diameter equal to 90% of the pipeline offer substantial pressure drop and hence are not recommended for practical applications. The pressure drop for $k = 0.9$ is 58 times higher on average than capsules of $k = 0.5$ at the same average flow velocity and the same capsule length. Whereas, the pressure drop for $k = 0.7$ is 320% higher on average than capsules of $k = 0.5$ at the same average flow velocities and the same length of the capsule. Furthermore, in comparison with a single spherical capsule, the pressure drop for a single cylindrical capsule of $L_c = 1 * d$ is 275%, 8 times and 14 times higher for $k = 0.5$, 0.7 and 0.9 respectively for same average flow velocities.

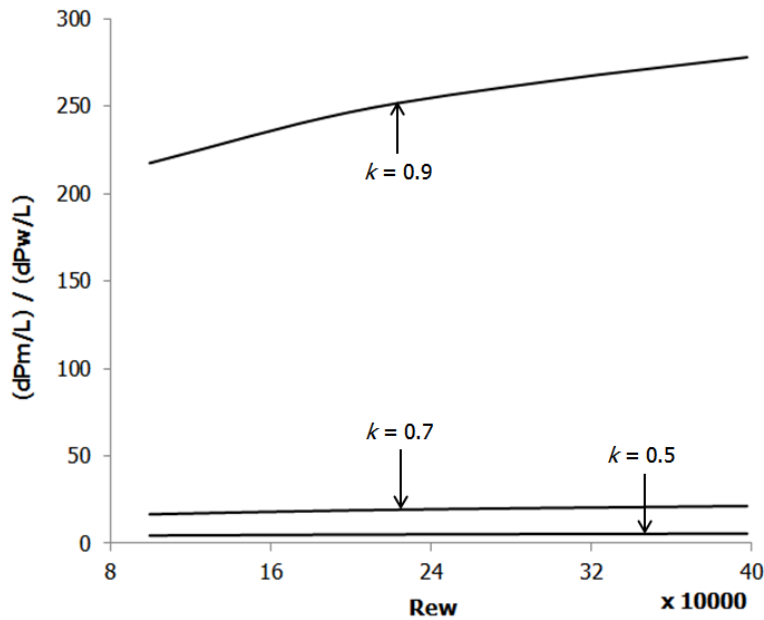


Figure 4.36. Variations in Normalised Pressure Drop for a Single Equi-Density Cylindrical Capsule of $L_c = 1 * d$ in a Horizontal Pipe

The results presented in figure 4.37 depicts the normalised pressure drop for a cylindrical capsule of $k = 0.7$ having various lengths. It can be seen that as the length of the capsule increases, the normalised pressure drop increases where this increase is shown to be non-uniform as the difference between $L_c = 1 * d$ and $3 * d$ is smaller than between $L_c = 3 * d$ and $5 * d$.

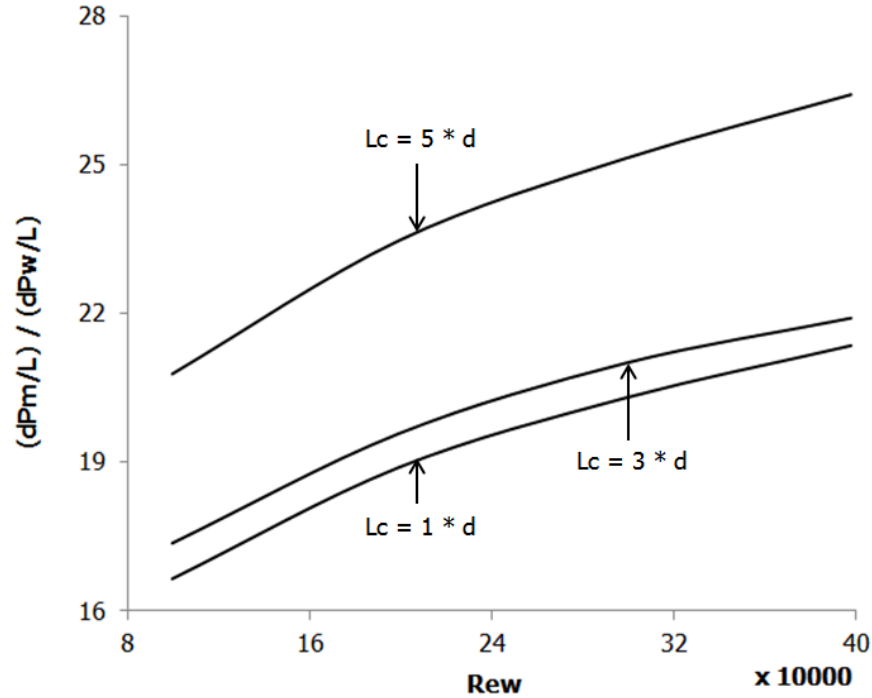


Figure 4.37. Variations in Normalised Pressure Drop for a Single Equi-Density Cylindrical Capsule of $k = 0.7$ in a Horizontal Pipe

Figure 4.38 depicts the variations in the normalised pressure drop for two cylindrical capsules of $L_c = 1 * d$ and $Sc = 1 * d$. It is again noted here that the pressure drop for $k = 0.9$ is significantly higher than for $k = 0.5$ and 0.7 and hence the capsules of diameter equal to 90% diameter of the pipeline are not recommended for practical applications. Moreover, in comparison with figure 4.37, it is clear that an increase in the concentration of the capsule increases the pressure drop within the pipeline.

Figure 4.39 depicts the variations in the normalised pressure drop to analyse the effects of the spacing between the capsules. It can be seen that as the spacing between the capsules increases, the normalised pressure drop increases. This trend is similar to the ones observed earlier for the effect of the length of the cylindrical capsules on the normalised pressure drop within the pipeline (figure 4.37).

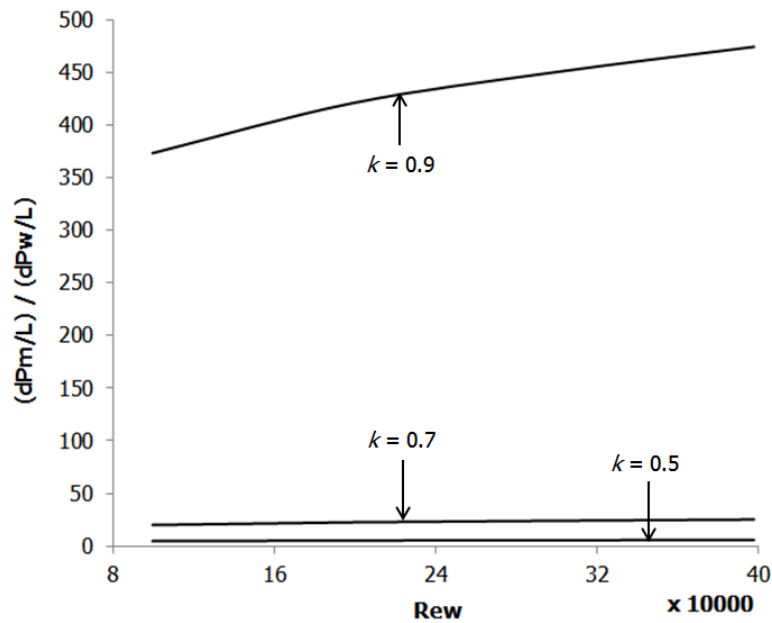


Figure 4.38. Variations in Normalised Pressure Drop for Two Equi-Density Cylindrical Capsules of $L_c = 1 * d$ and $Sc = 1 * d$ in a Horizontal Pipe

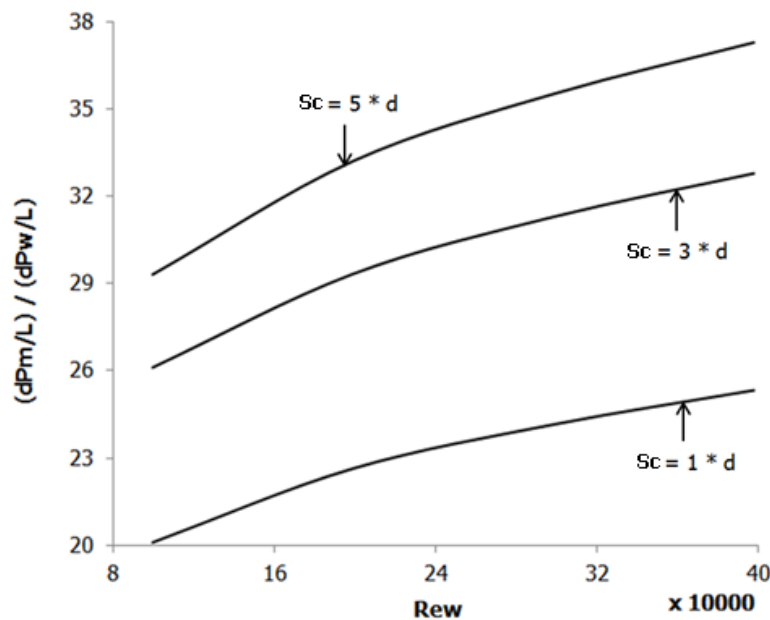


Figure 4.39. Variations in Normalised Pressure Drop for Two Equi-Density Cylindrical Capsules of $L_c = 1 * d$ and $k = 0.7$ in a Horizontal Pipe

The information provided in this section, regarding the flow of equi-density cylindrical capsules in horizontal pipes, has a huge impact on the design process of HCPs, which is presented in Chapter 7. Similar kind of analysis that has been carried out in this section is also presented in the next chapter for the flow of equi-density cylindrical capsules in vertical pipes.

4.7. Analysis of the Flow of Heavy-Density Spherical Capsules in a Horizontal HCP

The flow of heavy density capsules in a horizontal pipe is different from the flow of equi-density capsules. The reason being the weight of the capsules becomes higher than the buoyant force acting on the capsules. Thus, the capsules no longer remain concentric to the pipeline and settle down on the bottom wall of the pipe. A greater force is required to transport the capsules and hence the pressure drop in the pipeline increases.

As far as the flow of heavy-density spherical capsules in a horizontal pipeline is concerned, Teke [87] has reported that in addition to the translational motion, a rolling movement of the capsules has also been observed. This happens because of un-equal pressure gradients acting on the upstream face of the capsules. The capsules, under the action of higher pressure towards their top, attempt to roll in a clockwise manner. In the present study, however, the rolling motion of the capsules is neglected because the pressure drop imparted by this motion of the capsules is very small as compared to that generated by the translational motion [93].

Figure 4.40 depicts the variations in the pressure and velocity distribution within the test section of the pipe transporting a single spherical capsule of $k = 0.5$ at $V_{av} = 1\text{m/sec}$. It can be seen that the presence of a heavy-density spherical capsule within the pipe changes the pressure distribution altogether as compared to an equi-density spherical capsule shown in figure 4.8. The pressure gradients in the vicinity of the capsule are severely large as can be seen at upstream and downstream of the capsule. At upstream, the pressure of water increases from 290Pa to 669Pa as it approaches the capsule. This happens due to the additional resistance offered by the capsule to the flow within the pipe. The flow then passes through the annulus between the pipe wall and the capsule. As the cross-sectional area decreases, the pressure of water decreases to 45Pa. Once the flow exits the annulus, due to the increase in the cross-sectional area, the pressure of water recovers to some extent. It can be seen in figure 4.40 (a) that the pressure downstream has been recovered to 117Pa as compared to 290Pa at upstream location.

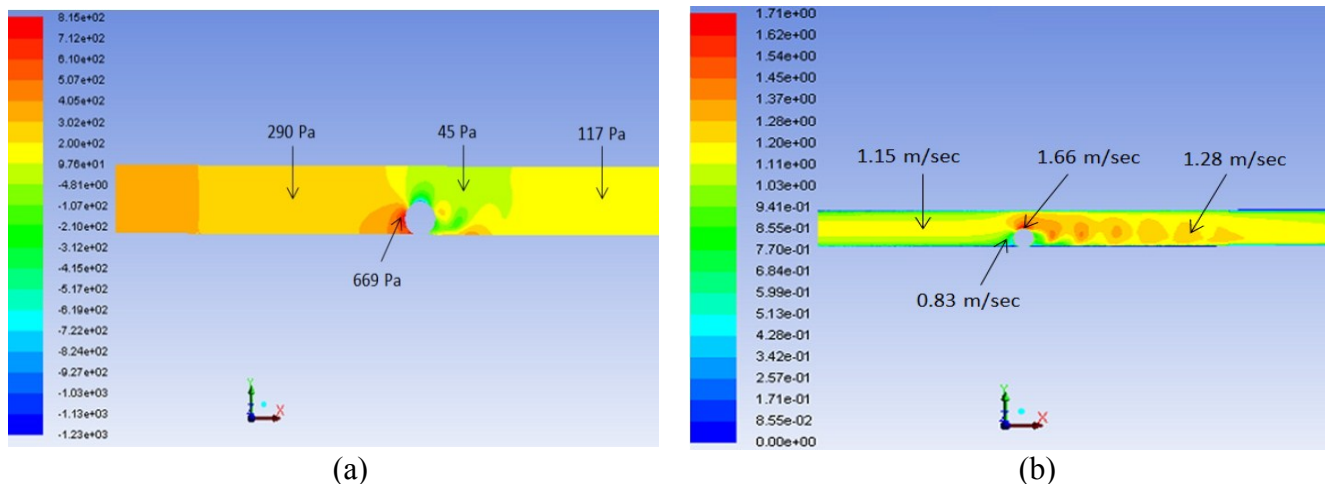


Figure 4.40. Variations in (a) Pressure and (b) Velocity, for a Single Spherical Capsule of $k = 0.5$ in a Horizontal Pipe at $V_{av} = 1\text{m/sec}$

Figure 4.40 (b) depicts that the flow slows down from 1.15m/sec to 0.83m/sec as it reaches the capsule. Once the flow passes through the annulus between the capsule and the pipe wall, flow velocity increases to 1.66m/sec due to reduction in the cross-sectional area of the flow. Due to the blockage effect, the velocity of the flow at the rear face of the capsule reduces to a very low value. As the flow exits the annulus region, it is encountered with adverse velocity gradients. In order to establish equilibrium, the flow curls in a clockwise manner and then separates itself from the top face of the capsule. This leads towards the formation of packets of spinning/swirling flow downstream of the capsules. Due to higher flow velocities in the upper half of the pipeline, these packets of spinning fluid is forced towards the bottom wall of the pipe, where after striking against the wall of the pipe, these packets lose their identity and become a part of the potential flow.

The discussion presented above reveals that the flow structure within heavy-density capsule pipelines is completely different from the one observed in the pipelines carrying equi-density capsules. Hence, the flow of heavy-density capsules has been discussed in separate sections in this chapter. The advent of Computational Fluid Dynamics based sophisticated software has led to carry out detailed flow diagnostics within pipelines transporting heavy-density capsules.

Figure 4.41 shows the variations in C_p and u/u_{max} along the analysis line for the case under consideration, where C_p represents the coefficient of pressure and u is the local flow velocity along the pipe. The results depict that the pressure drop for heavy-density capsules is higher than for equi-density capsules. The pressure at the downstream location for both types of flows is the same because pressure boundary condition has been set at the outlet of the pipe. It is also worth noticing that the pressure recovery in case of a heavy-density spherical capsule takes more space than for an equi-density spherical capsule. The difference in the pressure between the upstream and the downstream locations is due to the fact that some part of the kinetic energy of water has been converted into the work being done on the capsule. The total pressure drop for the present case is 226Pa.

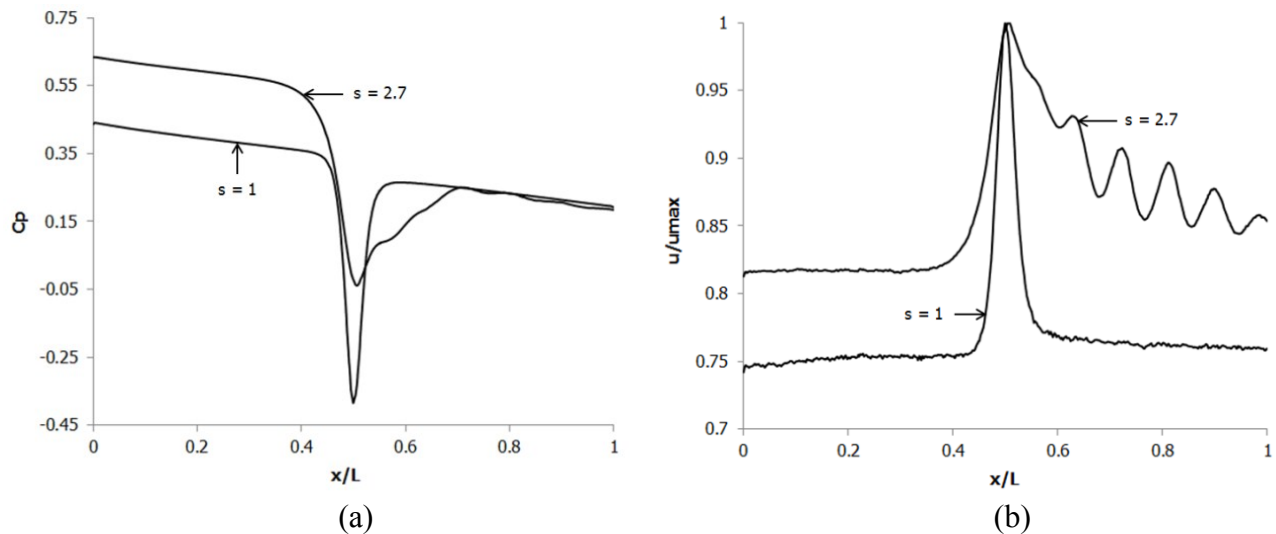


Figure 4.41. (a) Variations in C_p for a Single Spherical Capsule of $k = 0.5$ in a Horizontal Pipe at $V_{av} = 1\text{m/sec}$ (b) Variations in u/u_{max} for a Single Spherical Capsule of $k = 0.5$ in a Horizontal Pipe at $V_{av} = 1\text{m/sec}$

Figure 4.41 (b) depicts that the flow velocity at both upstream and downstream locations from the capsule is higher for heavy-density capsule as compared to an equi-density capsule. This is due to the eccentric orientation of the capsule within the pipe. There is more space available for the flow of those layers of water which have higher velocity, i.e. in the centre of the pipe. Furthermore, the presence of the swirling flow packets can be clearly seen downstream the heavy-density spherical capsule. The dynamics of these packets reveals that the maximum flow velocity is in the centre of the packets. The flow velocity reduces radially in these packets.

To further investigate the velocity distribution within the heavy-density spherical capsule transporting horizontal pipe, velocity profiles have been drawn across the cross-section of the pipe at both 0.1m upstream and downstream locations from the centre of the capsule as shown in figure 4.42. It can be seen that the velocity profile is undisturbed at the upstream location, and the presence of the capsule has not affected the velocity profile at this location. However, at the downstream location, the presence of the capsule in the pipe has distorted the velocity profile.

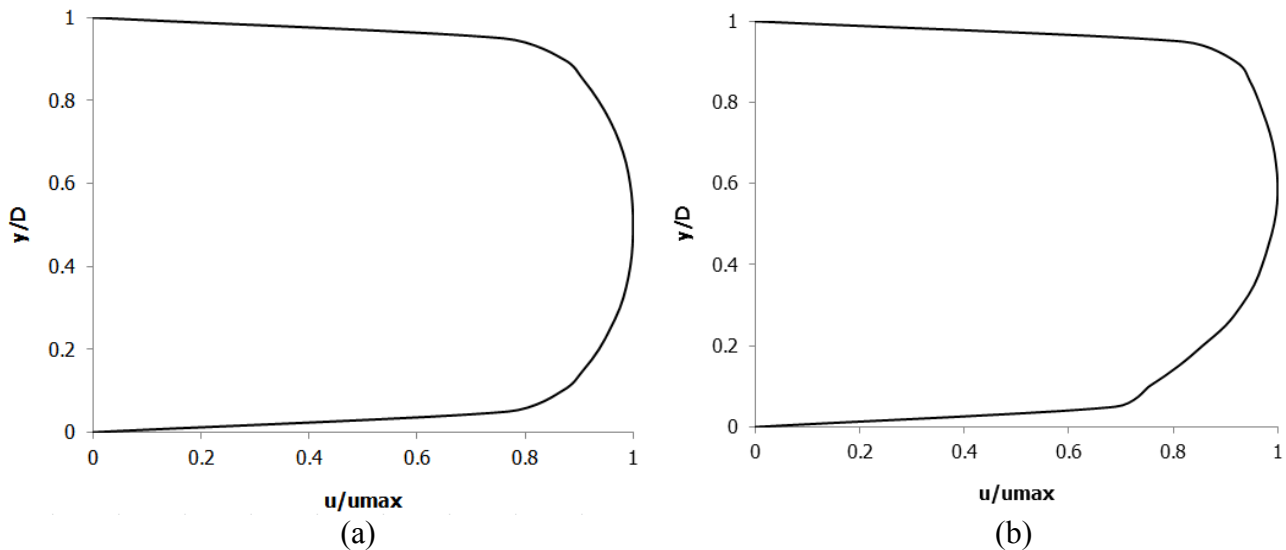


Figure 4.42. Variations in the Cross-Sectional Velocity Profiles for a Single Spherical Capsule of $k = 0.5$ in a Horizontal Pipe at $V_{av} = 1\text{m/sec}$ at (a) Upstream and (b) Downstream of the Capsule

Figure 4.43 depicts the variations in the velocity profiles at various locations within the capsule transporting pipe under consideration at an average flow velocity of 1m/sec.

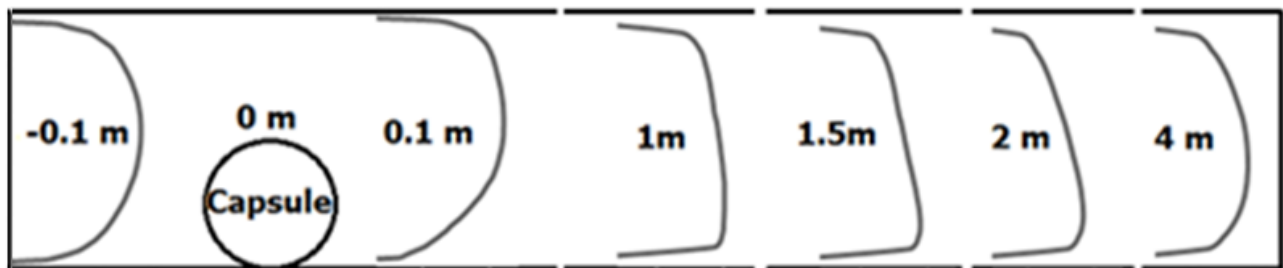


Figure 4.43. Development of Velocity Profile in the Presence of a Single Spherical Capsule in a Horizontal Pipe having Density Greater than Water

4.7.1. Average Flow Velocity Effects

To investigate the effect of the average flow velocity on the flow structure within the pipe, an average velocity of 4m/sec for a heavy-density spherical capsule of $k = 0.5$ has been chosen for flow diagnostics. Figure 4.44 depicts the pressure and velocity variations in the capsule transporting pipe for an average flow velocity of 4m/sec, keeping $k = 0.5$. The trend of pressure distribution is the same as observed for $V_{av} = 1\text{m/sec}$, i.e. a high pressure of 8884Pa at the upstream location, a low pressure of 4824Pa in the annulus region, a relatively low pressure of 6079Pa at downstream location as compared to upstream location and a very high pressure of 15501Pa at the location where the flow strikes the capsule. There is an average increase by 14 times in the pressure at the upstream, downstream and the point of highest pressure as compared to $V_{av} = 1\text{m/sec}$. The pressure drop between the inlet and the outlet of the pipe is 3412Pa, which is 14 times higher than the pressure drop for $V_{av} = 1\text{m/sec}$. It can be concluded that increase in the average velocity of the flow increases the pressure drop. Furthermore, it can be seen in figure 4.44 (b) that the velocity field resembles the one observed in case of $V_{av} = 1\text{m/sec}$, i.e. higher velocity in the annulus and the formation of swirling flow packets.

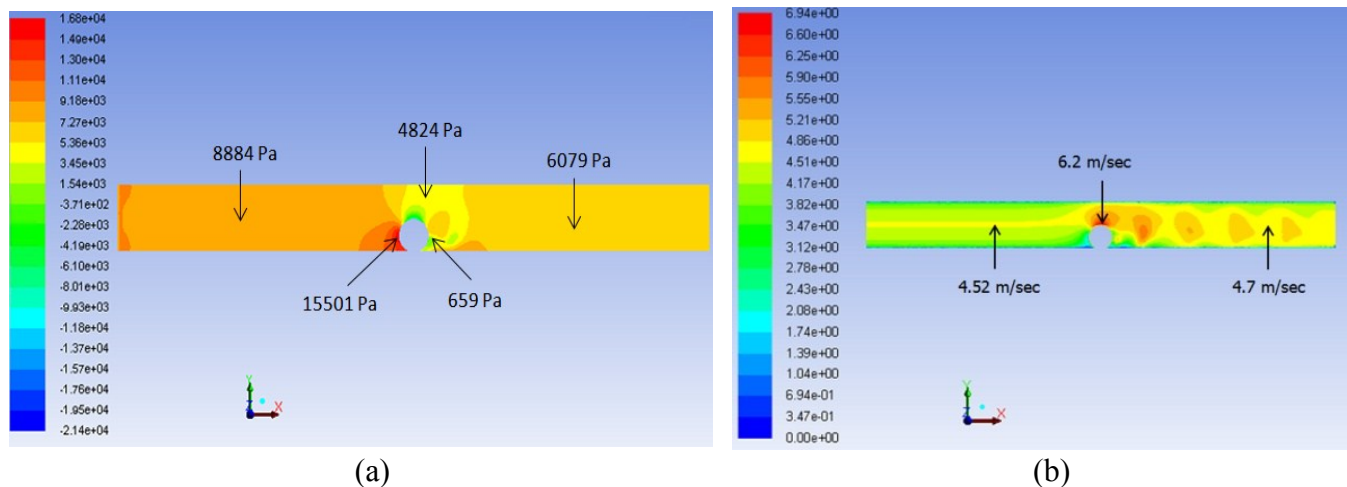


Figure 4.44. Variations in (a) Pressure and (b) Velocity, for a Single Spherical Capsule of $k = 0.5$ in a Horizontal Pipe at $V_{av} = 4\text{m/sec}$

Figure 4.45 shows the variations in C_p and u/u_{max} along the analysis line for the case under consideration. The results depict that the pressure drop for $s = 2.7$ is higher than for $s = 1$. The recovery of pressure downstream of the capsule covers a longer axial distance along the pipe. Furthermore, the velocity distribution for $V_{av} = 4\text{m/sec}$ resembles that of $V_{av} = 1\text{m/sec}$ but there is a significant change w.r.t. $s = 1$ because of the formation of swirling flow packets. More detailed results have been presented in table A-3.3.

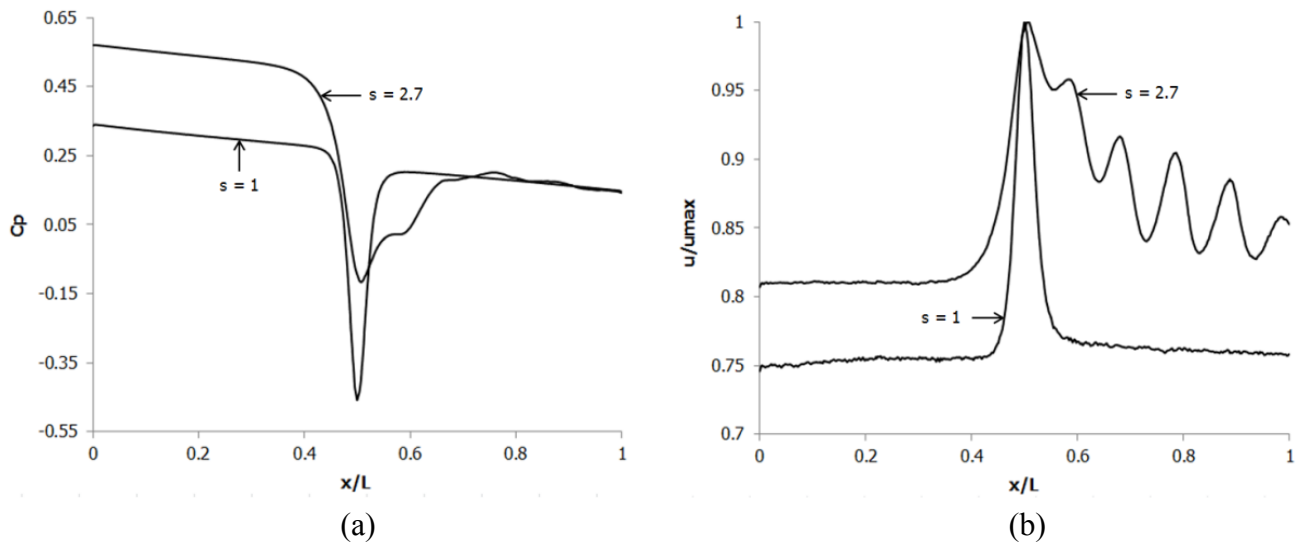


Figure 4.45. (a) Variations in C_p for a Single Spherical Capsule of $k = 0.5$ in a Horizontal Pipe at $V_{av} = 4\text{m/sec}$ (b) Variations in u/u_{max} for a Single Spherical Capsule of $k = 0.5$ in a Horizontal Pipe at $V_{av} = 4\text{m/sec}$

4.7.2. Capsule Diameter Effects

Figure 4.46 shows the pressure and velocity distributions in a heavy-density spherical capsule transporting horizontal pipe for $k = 0.9$ and $V_{av} = 1\text{m/sec}$. It can be seen that although the overall pressure distribution seems to be the same as compared with the pressure field for $k = 0.5$ at the same average flow velocity, but the pressure at upstream location has increased by 277 times and the static pressure at downstream location has increased by 39 times, which suggests that the overall pressure drop in the pipe has increased. The pressure drop between the inlet and the outlet of the pipe is 4854Pa, which is 20 times higher than the pressure drop for $k = 0.5$. Furthermore, it can be seen in figure 4.46 (b) that velocity of the flow in the annulus region has increased while a large wake region exists downstream of the capsule where the flow velocity is relatively low.

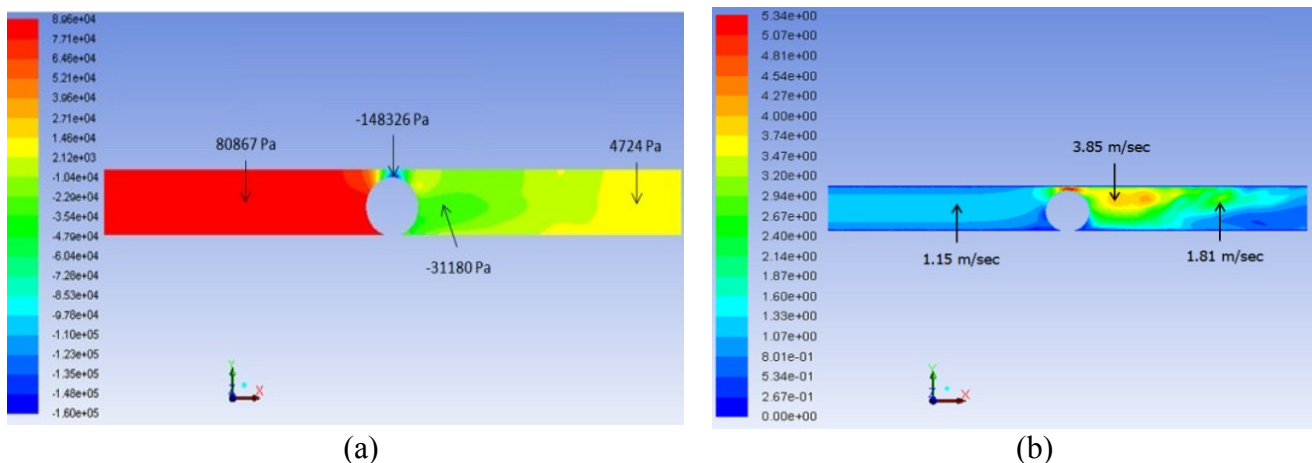


Figure 4.46. Variations in (a) Pressure and (b) Velocity, for a Single Spherical Capsule of $k = 0.9$ in a Horizontal Pipe at $V_{av} = 1\text{m/sec}$

Figure 4.47 shows the variations in C_p and u/u_{max} along the analysis line for the case under consideration. The results depict that the pressure drop for $s = 2.7$ is considerably higher than for $s = 1$. Furthermore, the velocity distribution for both $s = 2.7$ and 1 have been plotted in figure 4.47 (b) for comparison. It can be seen that the velocity profiles are quite similar upstream of the capsule. However, due to the swirling flow downstream of the capsule in case of $s = 2.7$, the velocity profile is different from one observed in case of $s = 1$. More detailed results have been presented in table A-3.3.

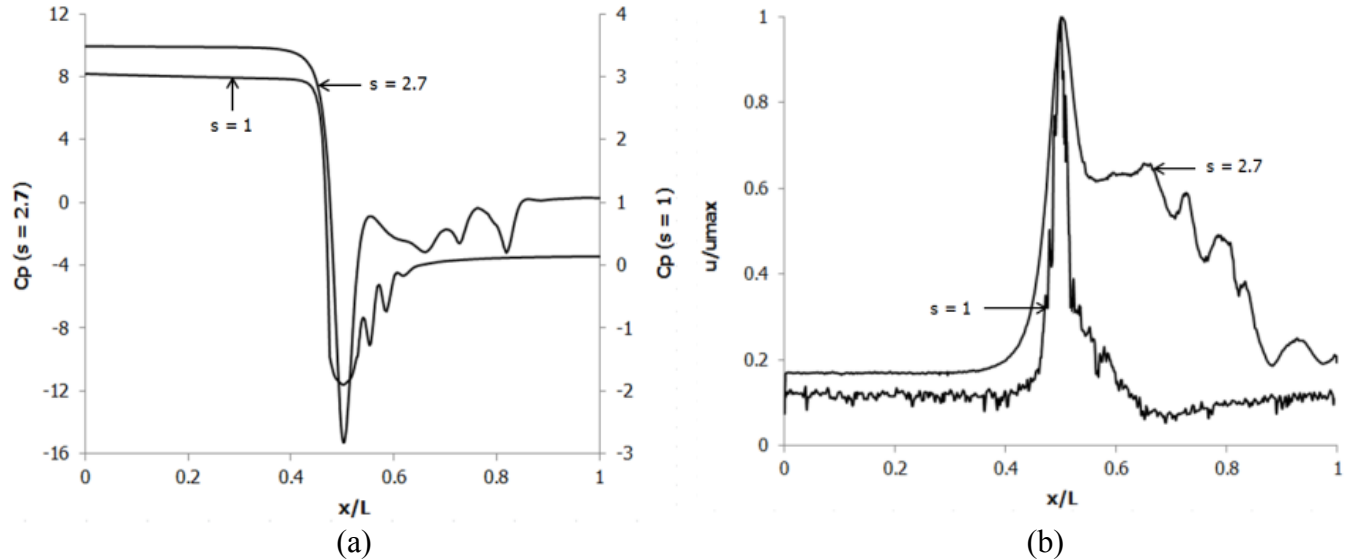


Figure 4.47. (a) Variations in C_p for a Single Spherical Capsule of $k = 0.5$ in a Horizontal Pipe at $V_{av} = 1\text{m/sec}$ (b) Variations in u/u_{max} for a Single Spherical Capsule of $k = 0.5$ in a Horizontal Pipe at $V_{av} = 1\text{m/sec}$

4.7.3. Capsule Concentration Effects

Figure 4.48 depicts the pressure and velocity variations in a hydraulic pipe carrying three heavy-density spherical capsules of $k = 0.5$, $Sc = 1 * d$ and $V_{av} = 1\text{m/sec}$. The trend of the pressure distribution is the same as observed for a single heavy-density spherical capsule. The pressure at upstream location has increased by 109%. An overall pressure drop increase of 137% has been observed for $N = 3$ as compared to $N = 1$. Furthermore, as compared to a single heavy-density spherical capsule, it can be seen that although the velocity field for $N = 3$ is different in terms of the formation of swirling flow packets. Rather than swirls, a continuous stream of high velocity flow is observed downstream of the capsule train, originating from the top faces of the individual capsules in the train. However, the trajectory of the trailing stream is identical to the one observed for a single heavy-density spherical capsule, i.e. the flow is subjected to a downward force, until it strikes with the bottom wall of the pipe and then merges into the main stream flow.

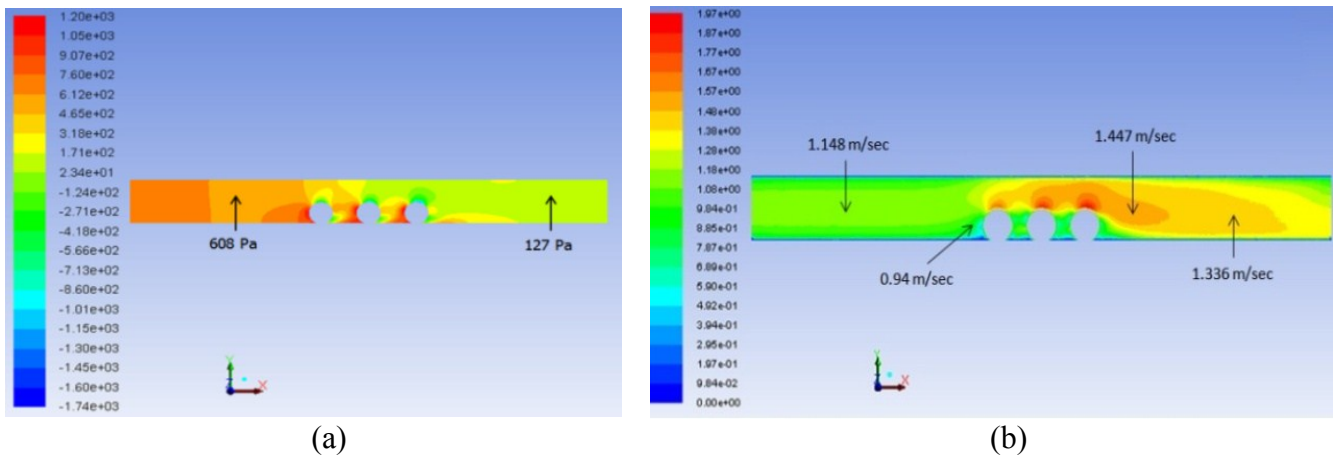


Figure 4.48. Variations in (a) Pressure and (b) Velocity, for Three Spherical Capsules of $k = 0.5$ and $Sc = 1 * d$ in a Horizontal Pipe at $V_{av} = 1\text{m/sec}$

Figure 4.49 represents the variations in C_p and u/u_{max} for the case under consideration. It can be clearly seen that the pressure drop for heavy-density spherical capsules is considerably higher than for equi-density spherical capsules for the same k , V_{av} and Sc . Furthermore, the velocity profile is completely different for both the cases, where $s = 2.7$ represents a more uniform stream of water flow within the pipe as compared to $s = 1$. More detailed results have been presented in table A-3.3.

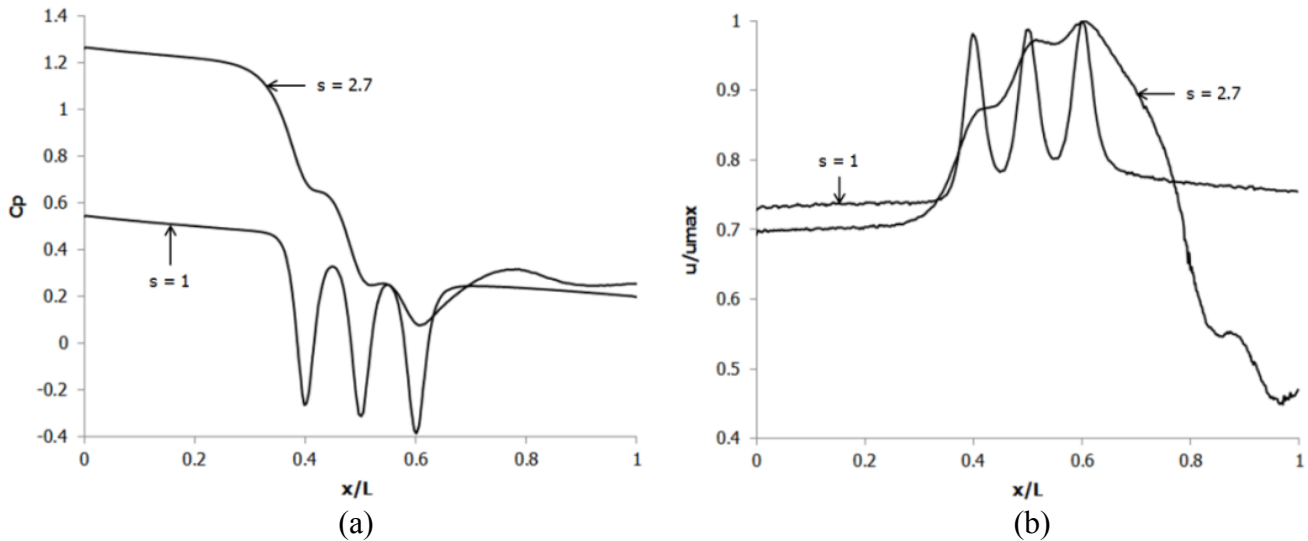


Figure 4.49. (a) Variations in C_p for Three Spherical Capsules of $k = 0.5$ and $Sc = 1 * d$ in a Horizontal Pipe at $V_{av} = 1\text{m/sec}$ (b) Variations in u/u_{max} for Three Spherical Capsules of $k = 0.5$ and $Sc = 1 * d$ in a Horizontal Pipe at $V_{av} = 1\text{m/sec}$

4.7.4. Effects of Spacing between the Capsules

Figure 4.50 depicts the pressure and velocity variations in a hydraulic pipe carrying three heavy-density spherical capsules of $k = 0.5$, $Sc = 5 * d$ and $V_{av} = 1\text{m/sec}$. The pressure distribution is the same as observed for $Sc = 1 * d$. The pressure at both upstream and downstream locations has decreased by 4%

and 8% respectively as compared to $Sc = 1 * d$. A marginal pressure drop decrease (10%) has been observed for $Sc = 5 * d$ as compared to $1 * d$. Furthermore, the velocity field in the vicinity of each capsule resembles the one observed for a single heavy-density spherical capsule, i.e. generation of swirling flow packets.

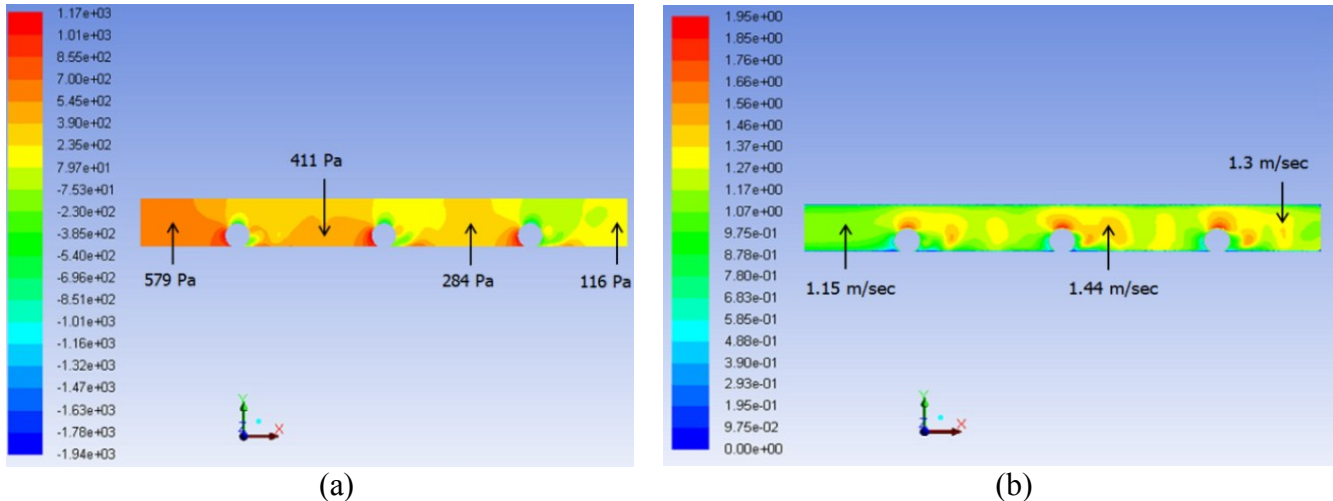


Figure 4.50. Variations in (a) Pressure and (b) Velocity, for Three Spherical Capsules of $k = 0.5$ and $Sc = 5 * d$ in a Horizontal Pipe at $V_{av} = 1\text{m/sec}$

Figure 4.51 represents the variations in C_p and u/u_{max} for the case under consideration. It can be seen that the pressure drop for heavy-density spherical capsules is considerably higher than the pressure drop for equi-density spherical capsules of same k , Sc and V_{av} . Furthermore, the velocity distribution for $Sc = 5 * d$ is different from $Sc = 1 * d$. For $Sc = 5 * d$, the velocity gradually rises along the length of the pipe. More detailed results have been presented in table A-3.3.

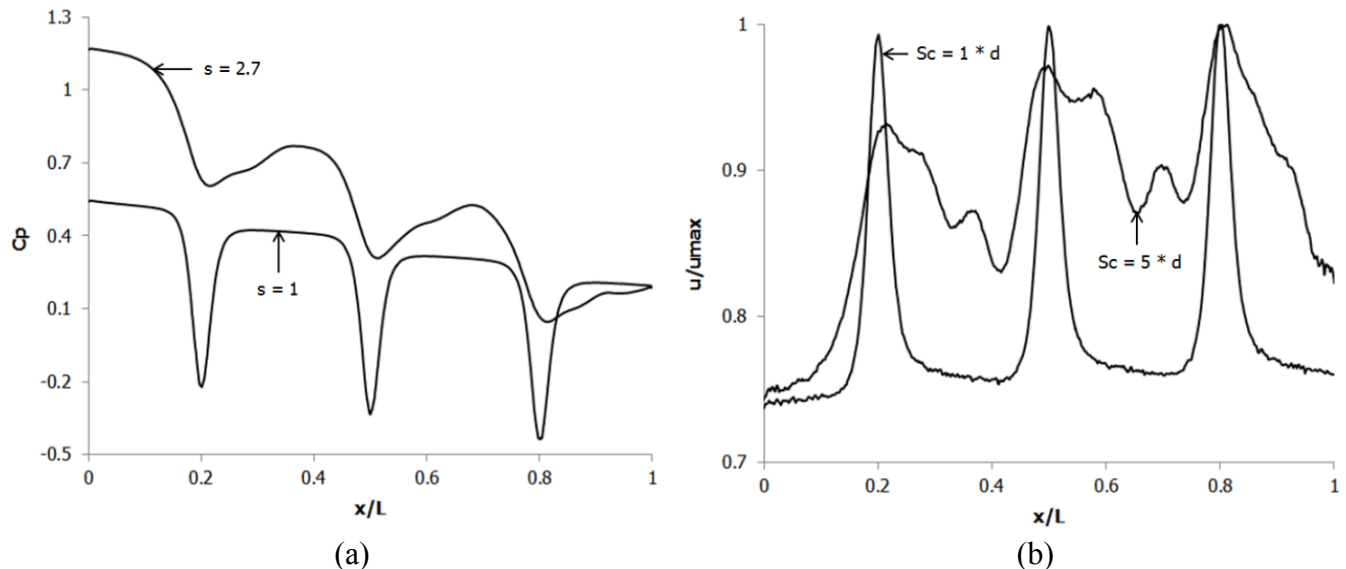


Figure 4.51. (a) Variations in C_p for Three Spherical Capsules of $k = 0.5$ and $Sc = 5 * d$ in a Horizontal Pipe at $V_{av} = 1\text{m/sec}$ (b) Variations in u/u_{max} for Three Spherical Capsules of $k = 0.5$ and $Sc = 5 * d$ in a Horizontal Pipe at $V_{av} = 1\text{m/sec}$

Table A-3.3 in Appendix A-3 summarises the results for various CFD based investigations being carried out on the flow of heavy-density spherical capsules in a horizontal pipe.

Figure 4.52 depicts the variation in the normalised pressure drops in the test section of the pipe for a train three heavy-density spherical capsules having a spacing of $1 * d$ between the consecutive capsules respectively. The results show that as the flow velocity increases, the pressure drop in the test section of the pipe increases. Furthermore, as the size of the capsule increases, the pressure drop further increases. It is evident that heavy-density spherical capsules of diameter equal to 90% of the pipeline offer substantial pressure drop and hence are not recommended for practical applications.

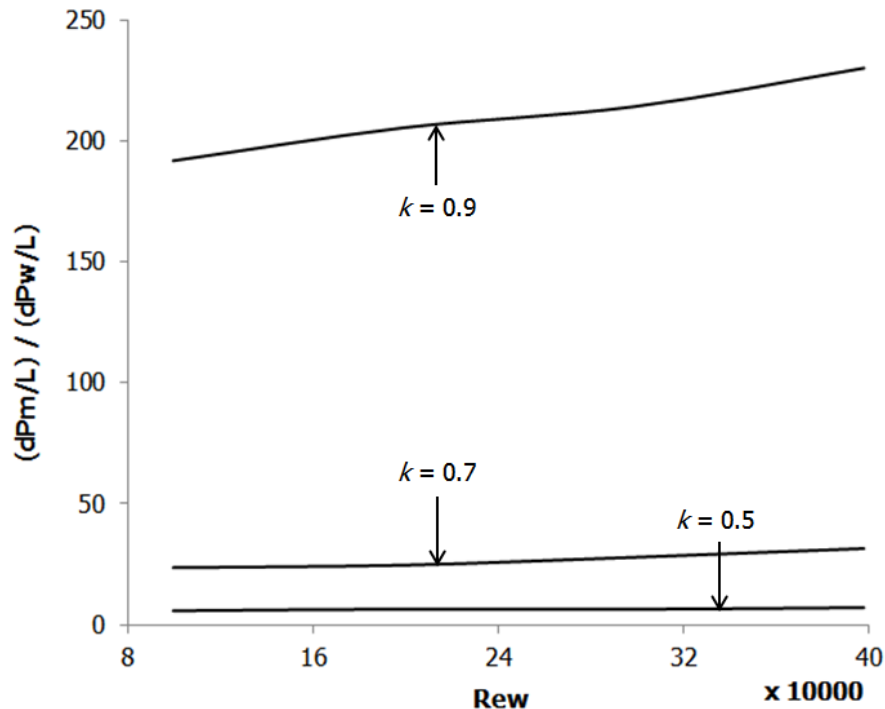


Figure 4.52. Variations in Normalised Pressure Drop for Three Heavy-Density Spherical Capsules in a Horizontal Pipe

Figure 4.53 depicts the variations in the normalised pressure drop for a heavy-density spherical capsule train consisting of two capsules of $k = 0.7$ and having different spacing between them. It can be clearly seen that as the spacing between the capsules increases, the normalised pressure drop in the pipe decreases. This trend is similar at all average flow velocities under consideration.

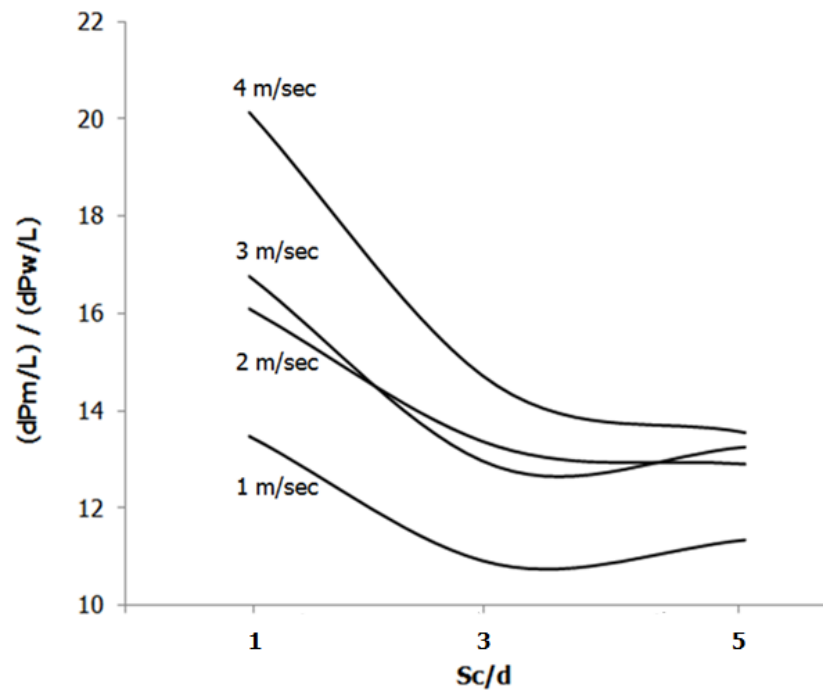


Figure 4.53. Variations in Normalised Pressure Drop for Two Spherical Capsules of $k = 0.7$ in a Horizontal Pipe

The information provided in this section, regarding the flow of heavy-density spherical capsules in horizontal pipes, has a huge impact on the design process of HCPs, which is presented in Chapter 7. Similar kind of analysis that has been carried out in this section is also presented in the next chapter for the flow of heavy-density spherical capsules in vertical pipes.

4.8. Analysis of the Flow of Heavy-Density Cylindrical Capsules in a Horizontal HCP

Figure 4.54 depicts the pressure and velocity variations around a single heavy-density cylindrical capsule of $k = 0.5$ at an average flow velocity of 1m/sec for a capsule length of $L_c = 1 * d$. The pressure field around a cylindrical capsule resembles the pressure field around a heavy-density spherical capsule. At upstream, the pressure of water increases from 459Pa to 946Pa as it approaches the capsule. Furthermore, it can be seen that the pressure downstream is 30Pa. The velocity distribution within the pipe is different from the velocity field for a heavy-density spherical capsule. In case of a cylindrical capsule, the swirling flow effect is considerably reduced because of the blunt shape of the cylindrical capsule as compared to curvaceous shape of a spherical capsule.

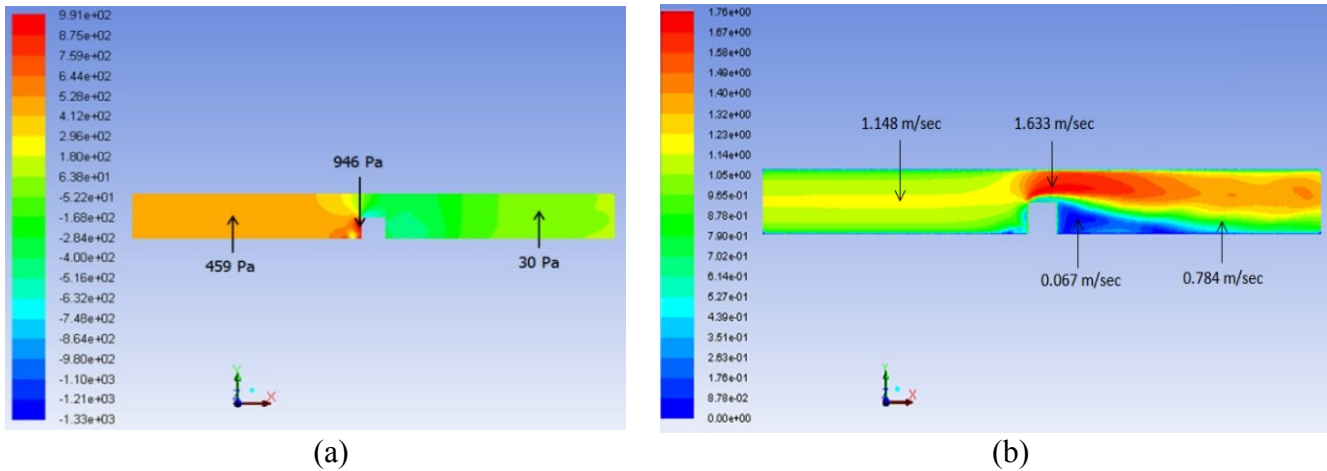


Figure 4.54. Variations in (a) Pressure and (b) Velocity, for a Cylindrical Capsule of $k = 0.5$ and $L_c = 1 * d$ in a Horizontal Pipe at $V_{av} = 1\text{m/sec}$

Figure 4.55 shows the variations in C_p and u/u_{max} for the case under consideration, where C_p represents the coefficient of pressure and u is the local flow velocity along the pipe. The profiles for a single equi-density cylindrical capsule flow have also been included for comparison. It can be clearly seen that the pressure drop in case of a heavy-density cylindrical capsule is marginally higher than the pressure drop for an equi-density cylindrical capsule in comparison with other parameters. The total pressure drop in case of $s = 2.7$ is 430Pa, which is 3.8% higher than for $s = 1$.

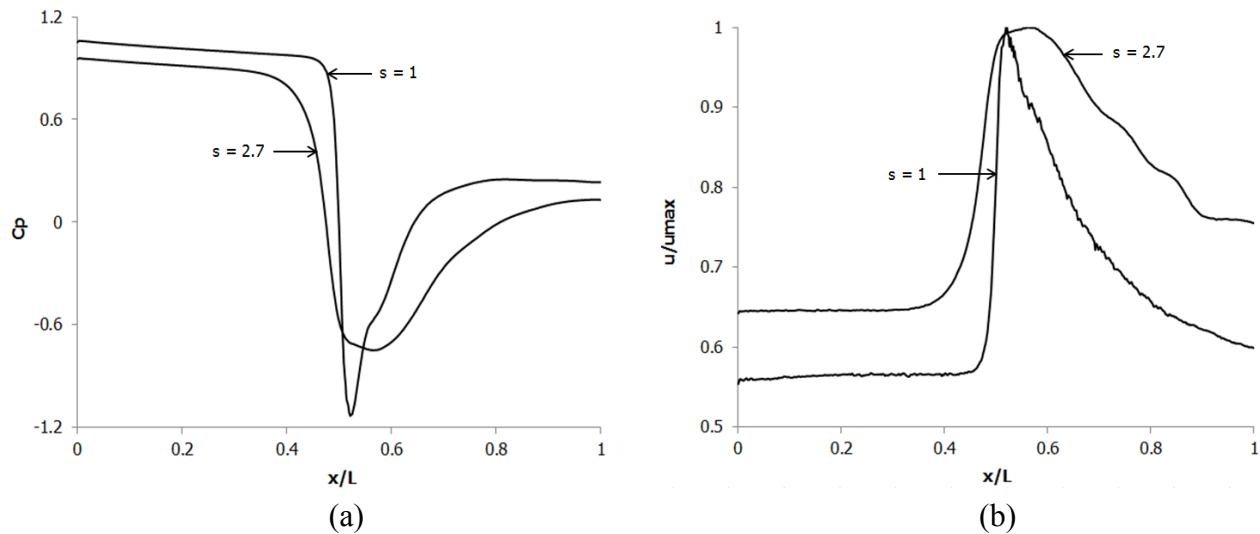


Figure 4.55. (a) Variations in C_p for a Cylindrical Capsule of $k = 0.5$ and $L_c = 1 * d$ in a Horizontal Pipe at $V_{av} = 1\text{m/sec}$ (b) Variations in u/u_{max} for a Cylindrical Capsule of $k = 0.5$ and $L_c = 1 * d$ in a Horizontal Pipe at $V_{av} = 1\text{m/sec}$

Figure 4.55 (b) depicts that the velocity magnitude of the flow for the case under consideration is higher, both at upstream and downstream locations, for the flow of a heavy-density cylindrical capsule

as compared to the flow of equi-density cylindrical capsule. Furthermore, it can be seen that the formation of swirling flow packets is negligibly small in case of a heavy-density cylindrical capsule.

To further investigate the velocity distribution within the capsule transporting pipe, velocity profiles have been drawn across the cross-section of the pipe at both 0.1m upstream and downstream locations from the centre of the heavy-density cylindrical capsule as shown in figure 4.56. It can be seen that the velocity profile is undisturbed at the upstream location, and the presence of the capsule has not affected the velocity profile at this location. However, at the downstream location, the presence of the capsule in the pipe has distorted the velocity profile.

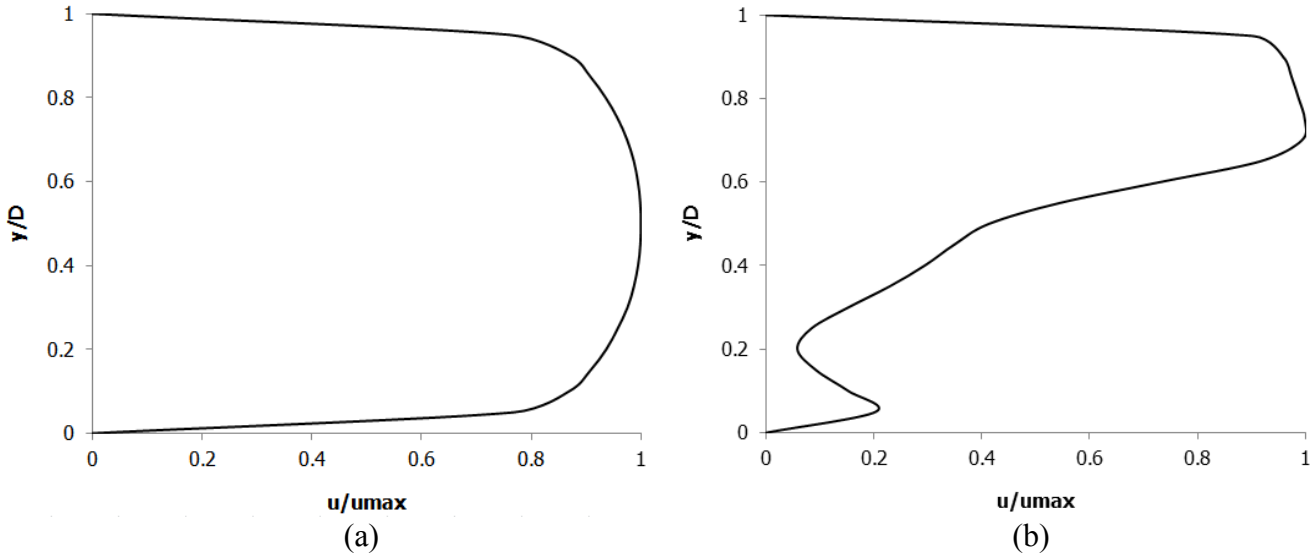


Figure 4.56. Variations in the Cross-Sectional Velocity Profiles for a Single Cylindrical Capsule of $k = 0.5$ and $L_c = 1 * d$ in a Horizontal Pipe at $V_{av} = 1\text{m/sec}$ at (a) Upstream and (b) Downstream of the Capsule

Figure 4.57 depicts the variations in the velocity profiles at various locations within the heavy-density cylindrical capsule transporting pipe under consideration at an average flow velocity of 1m/sec.



Figure 4.57. Development of Velocity Profile in the Presence of a Single Cylindrical Capsule in a Horizontal Pipe having Density Equal to Water

4.8.1. Average Flow Velocity Effects

Figure 4.58 depicts the pressure and velocity variations within the test section of the pipe carrying a heavy-density cylindrical capsule of $k = 0.5$ at an average flow velocity of 4m/sec. The length of the capsule $L_c = 1 * d$. It can be seen that both the pressure and velocity fields are identical to the one observed for $V_{av} = 1\text{m/sec}$. The pressure upstream of the capsule is 13 times higher and downstream of the capsule is 6 times lower as compared to $V_{av} = 1\text{m/sec}$. Hence, the pressure drop within the pipeline increases by 12 times. Furthermore, the velocity distribution resembles the one observed for $V_{av} = 1\text{m/sec}$.

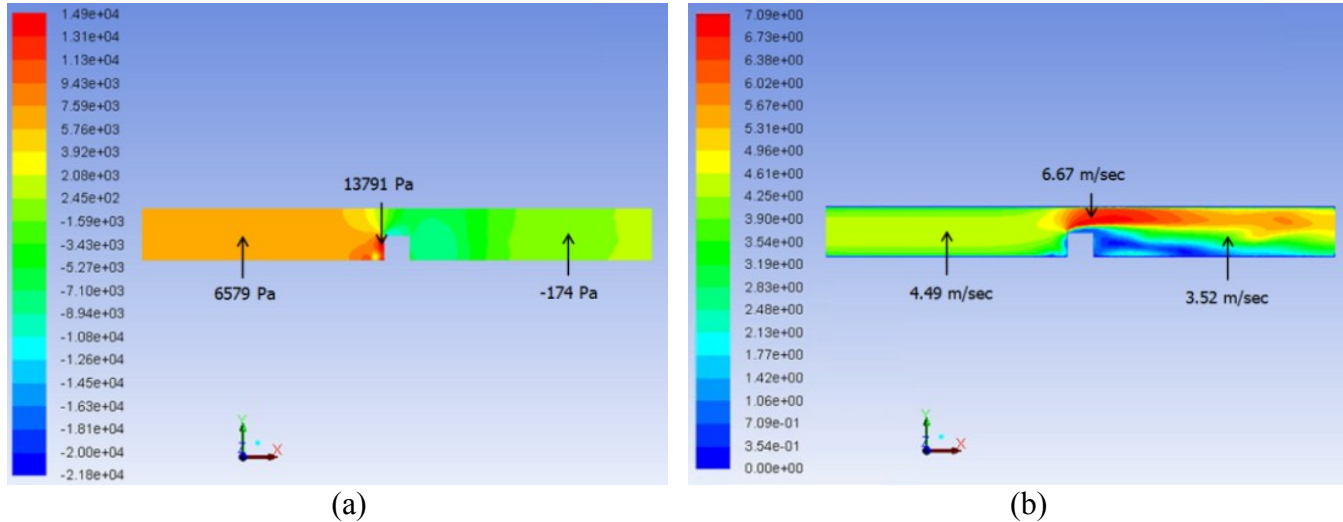


Figure 4.58. Variations in (a) Pressure and (b) Velocity, for a Cylindrical Capsule of $k = 0.5$ and $L_c = 1 * d$ in a Horizontal Pipe at $V_{av} = 4\text{m/sec}$

Figure 4.59 shows the variations in C_p and u/u_{max} for the case under consideration. The profiles for $s = 1$ at $V_{av} = 1\text{m/sec}$ have also been included for comparison. It can be seen that the pressure drop for $s = 2.7$ is marginally less than for $s = 1$ in comparison with other parameters. As the difference in the pressure drop is very small, it could be an effect of the numerical diffusion within the solver. It will be shown in table 4.8 that the overall trend of the pressure drop is similar to the one observed for heavy-density capsules, i.e. as the flow velocity increases, the pressure drop increases. Furthermore, the velocity distribution for a heavy-density cylindrical capsule flow is different from the flow of equi-density cylindrical capsule. For $s = 2.7$, there is some hint of the generation of swirling flow condition. More detailed results have been presented in table A-3.4.

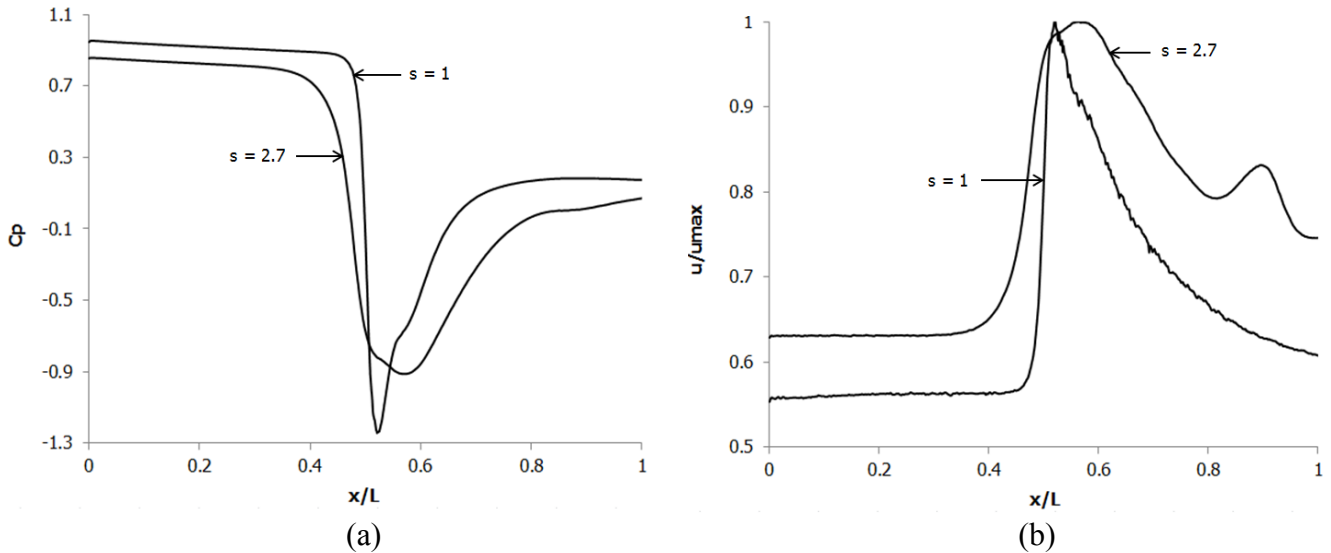


Figure 4.59. (a) Variations in C_p for a Cylindrical Capsule of $k = 0.5$ and $L_c = 1 * d$ in a Horizontal Pipe at $V_{av} = 4\text{m/sec}$ (b) Variations in u/u_{max} for a Cylindrical Capsule of $k = 0.5$ and $L_c = 1 * d$ in a Horizontal Pipe at $V_{av} = 4\text{m/sec}$

4.8.2. Length of the Capsule Effects

Figure 4.60 shows the pressure and velocity distributions in a heavy-density cylindrical capsule transporting horizontal pipe for $k = 0.5$, $L_c = 5 * d$ and $V_{av} = 1\text{m/sec}$. It can be seen that the overall pressure and velocity distributions seem to be the same as compared with $L_c = 1 * d$ at the same average flow velocity and capsule diameter. However, the upstream and downstream pressures, as compared to $L_c = 1 * d$, are 8% lower and 70% higher respectively.

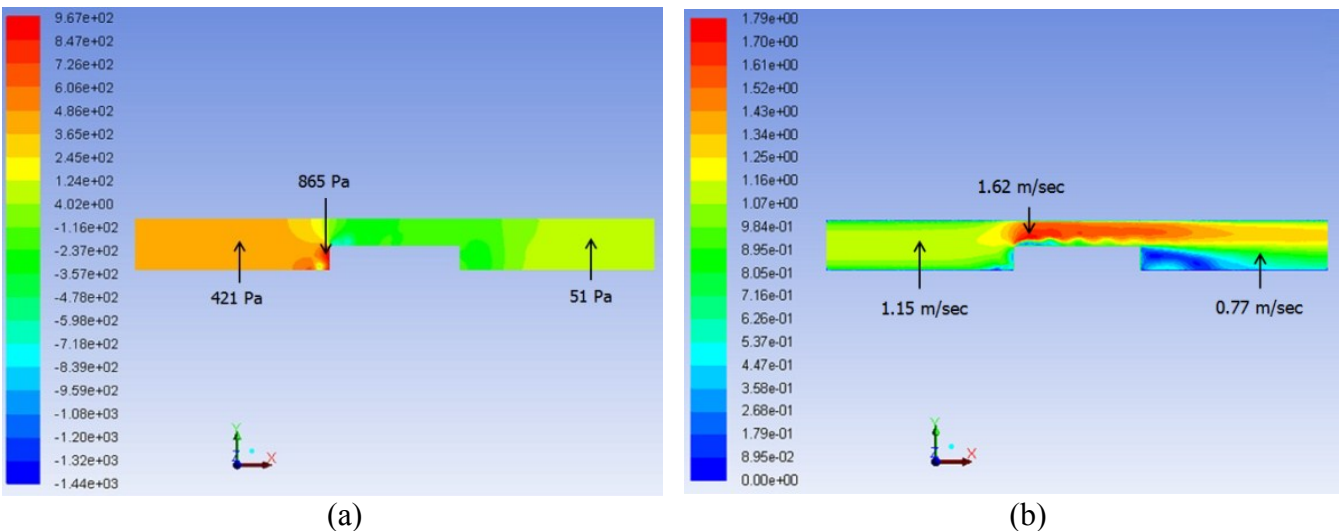


Figure 4.60. Variations in (a) Pressure and (b) Velocity, for a Single Cylindrical Capsule of $k = 0.5$ and $L_c = 5 * d$ in a Horizontal Pipe at $V_{av} = 1\text{m/sec}$

Figure 4.61 shows the variations in C_p and u/u_{max} along the analysis line for the case under consideration. Here again, the pressure distribution is suggesting that the pressure drop for equi-density cylindrical capsule is higher than for heavy-density cylindrical capsule. However, this is not the general trend and can be associated to the numerical diffusion in the solution. Furthermore, it can be seen in figure 4.61 (b) that the velocity profile for a heavy-density cylindrical capsule is different from equi-density cylindrical capsule as both the upstream and downstream velocities of the flow are considerably higher in case of a heavy-density cylindrical capsule. More detailed results have been presented in table A-3.4.

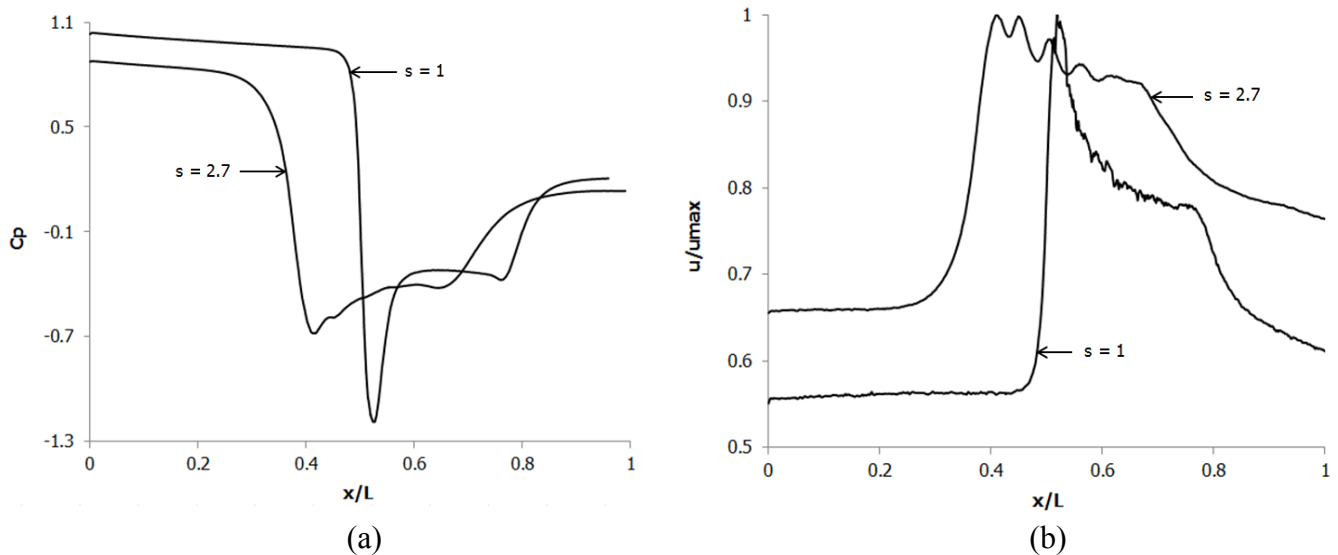


Figure 4.61. (a) Variations in C_p for a Single Cylindrical Capsule of $k = 0.5$ and $L_c = 5 * d$ in a Horizontal Pipe at $V_{av} = 1\text{m/sec}$ (b) Variations in u/u_{max} for a Single Cylindrical Capsule of $k = 0.5$ and $L_c = 5 * d$ in a Horizontal Pipe at $V_{av} = 1\text{m/sec}$

4.8.3. Capsule Diameter Effects

Figure 4.62 depicts the variations in the pressure field and C_p for a heavy-density cylindrical capsule of $L_c = 5 * d$, $k = 0.9$ at $V_{av} = 1\text{m/sec}$ in a horizontal pipe. The trend of the pressure distribution is the same as observed for $k = 0.5$ at same average flow velocity and for the same length of the capsule. The pressure at upstream and downstream locations from the capsule has increased by 742 times and 211 times respectively. An overall pressure drop increase by 63 times has been observed in the present case compared with $k = 0.5$, $L_c = 5 * d$ and $V_{av} = 1\text{m/sec}$. Figure 4.62 (b) presents a comparison of the case under consideration with that of an equi-density cylindrical capsule of the same length, diameter and at same average flow velocity. More detailed results have been presented in table A-3.4.

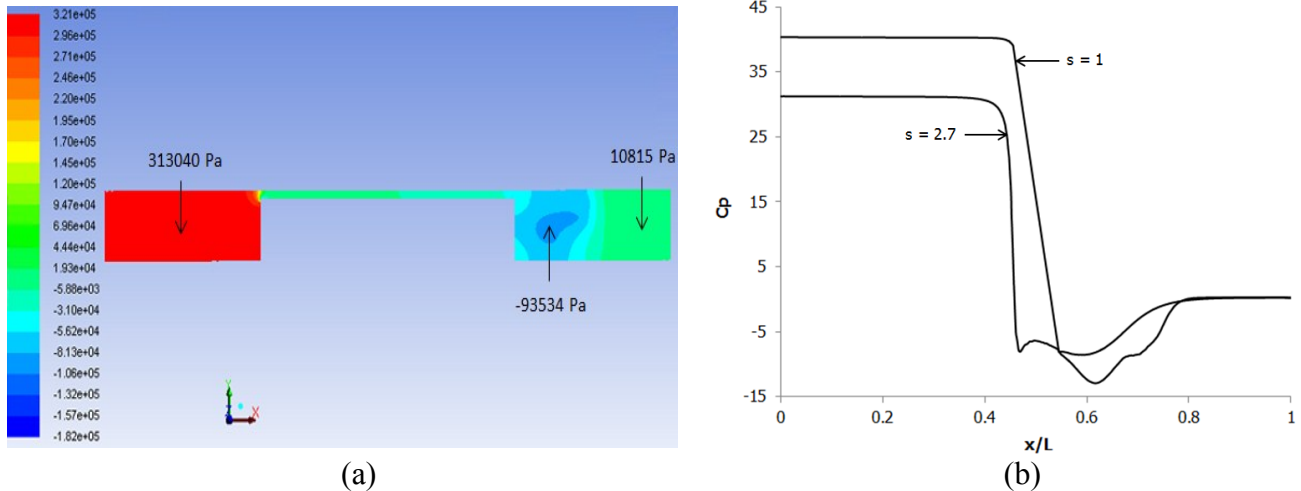


Figure 4.62. (a) Variations in Pressure for a Single Cylindrical Capsule of $k = 0.9$ and $L_c = 5 * d$ in a Horizontal Pipe at $V_{av} = 1\text{m/sec}$ (b) Variations in C_p for a Single Cylindrical Capsule of $k = 0.9$ and $L_c = 5 * d$ in a Horizontal Pipe at $V_{av} = 1\text{m/sec}$

4.8.4. Capsule Concentration Effects

Figure 4.63 depicts the pressure and velocity variations in a horizontal hydraulic pipe carrying two heavy-density cylindrical capsules of $k = 0.5$, $L_c = 1 * d$, $Sc = 1 * d$. The trend of the pressure distribution is the same as observed for a single heavy-density cylindrical capsule. The pressure at upstream location has decreased by 0.6%; whereas at downstream location, it has increased by 26% as compared to a single heavy-density cylindrical capsule. Furthermore, the velocity field is identical to $N = 1$, i.e. a high flow velocity in the annulus and a large wake region downstream of the capsules. It can be seen that there is a large wake region downstream of the capsule train and also in-between the individual capsules in the train.

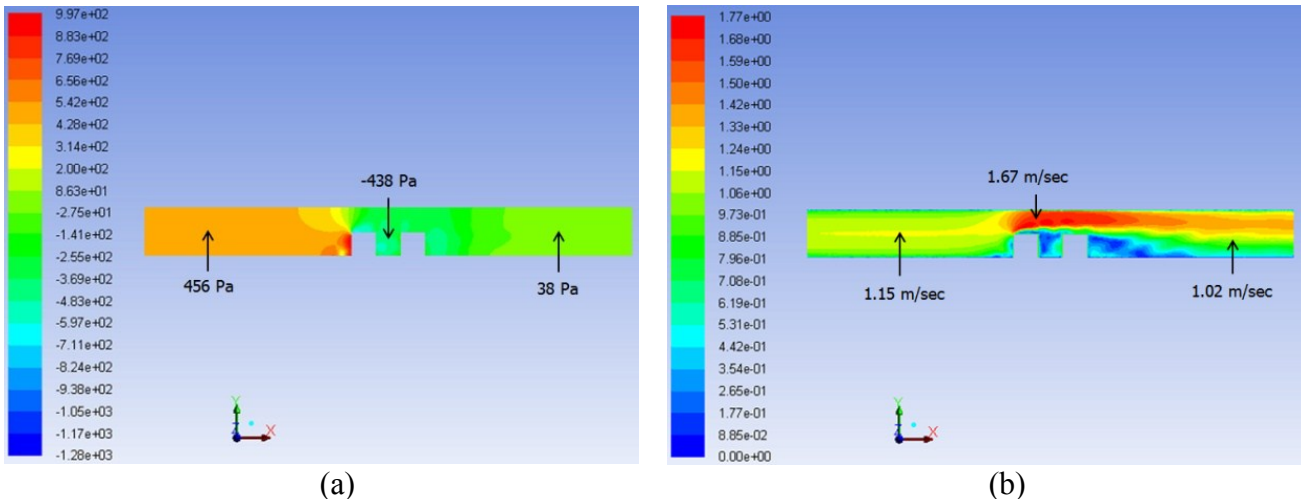


Figure 4.63. Variations in (a) Pressure and (b) Velocity, for Two Cylindrical Capsules of $k = 0.5$, Sc and $L_c = 1 * d$ in a Horizontal Pipe at $V_{av} = 1\text{m/sec}$

Figure 4.64 shows the variations in C_p and u/u_{max} along the analysis line for the case under consideration. The results depict that the pressure drop for $s = 2.7$ is marginally lower than for $s = 1$ in comparison with other parameters. Furthermore, the velocity profiles along the analysis line are similar for both $s = 2.7$ and 1. More detailed results have been presented in table A-3.4.

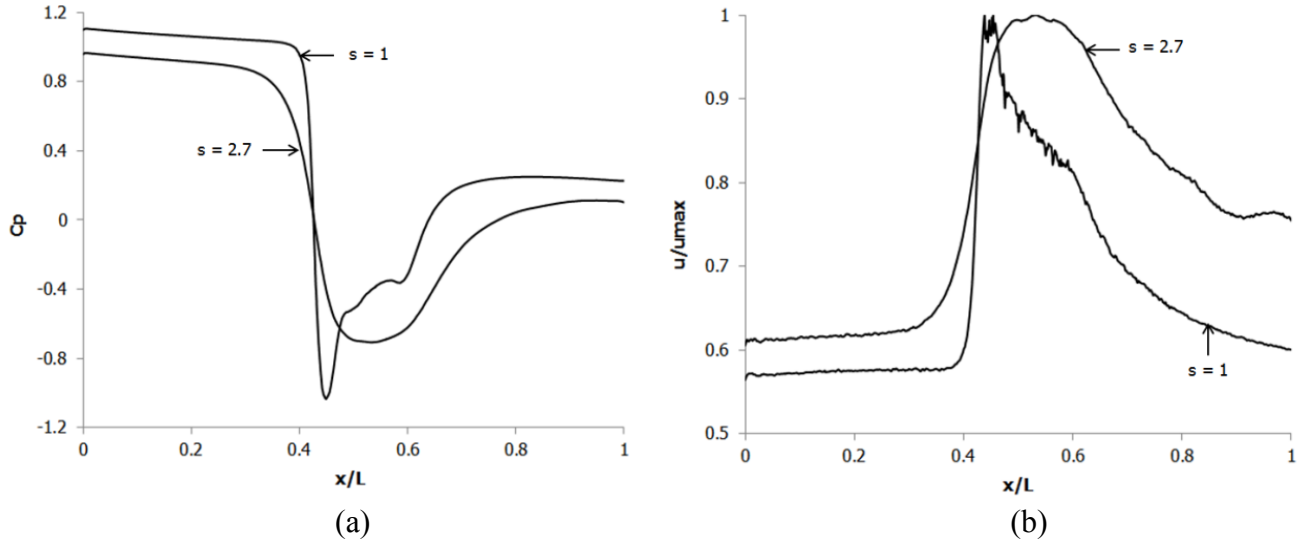


Figure 4.64. (a) Variations in C_p for Two Cylindrical Capsules of $k = 0.5$, Sc and $L_c = 1 * d$ in a Horizontal Pipe at $V_{av} = 1\text{m/sec}$ (b) Variations in u/u_{max} for Two Cylindrical Capsules of $k = 0.5$, Sc and $L_c = 1 * d$ in a Horizontal Pipe at $V_{av} = 1\text{m/sec}$

4.8.5. Effects of Spacing between the Capsules

Figure 4.65 depicts the effect of spacing between the capsules on the pressure and velocity distribution within the pipe. In comparison with figure 97 it can be seen that the pressure upstream of the capsules having $Sc = 5 * d$ is 38% higher than for $Sc = 1 * d$ whereas it has decreased by 131% at the downstream location. The overall increase in the pressure drop within the test section of the pipe is 48% higher for $Sc = 5 * d$ as compared to $Sc = 1 * d$ for the same average flow velocity, diameter of the capsule and the length of the capsule. The velocity field is similar for both the cases.

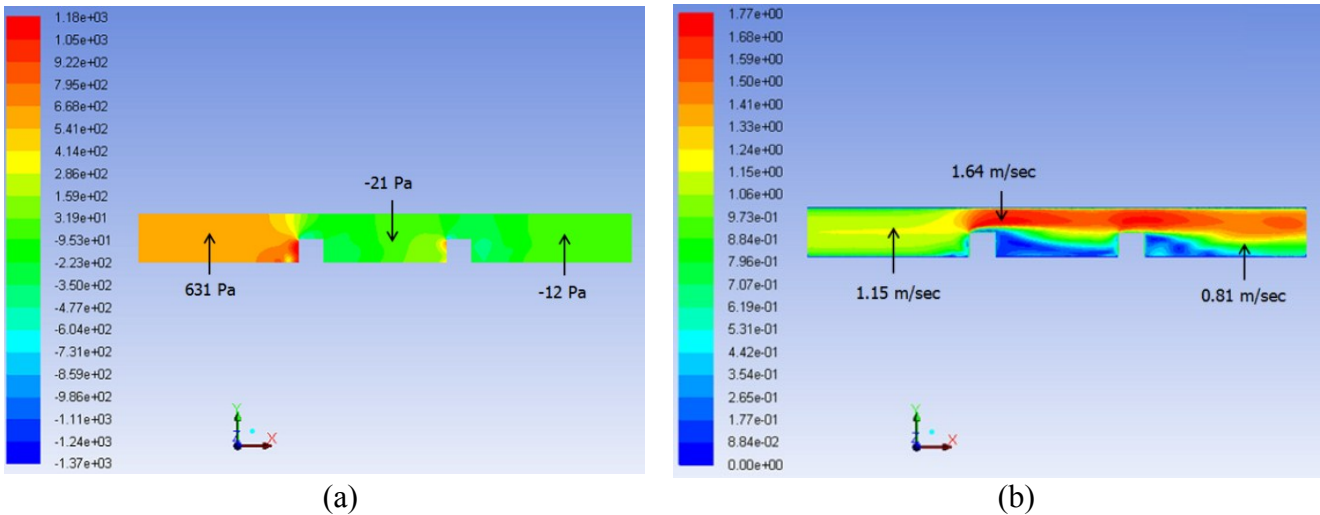


Figure 4.65. Variations in (a) Pressure and (b) Velocity, for Two Cylindrical Capsules of $k = 0.5$, $Sc = 5 * d$ and $Lc = 1 * d$ in a Horizontal Pipe at $V_{av} = 1\text{m/sec}$

Figure 4.66 shows the variations in C_p and u/u_{max} along the analysis line for the case under consideration. The results depict that for heavy-density cylindrical capsule, the velocity magnitude of the flow upstream and downstream of the capsule is higher than for equi-density cylindrical capsule. Furthermore, the velocity of the flow in the region between the capsules is more uniform in case of a heavy-density cylindrical capsule as compared to equi-density cylindrical capsule. More detailed results have been presented in table A-3.4.

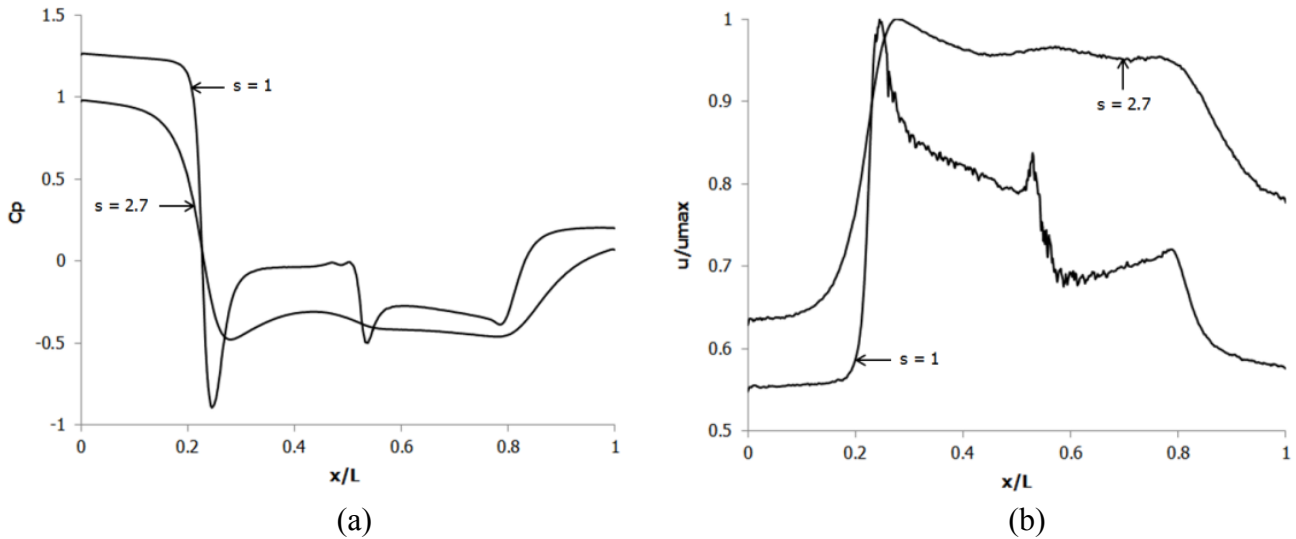


Figure 4.66. (a) Variations in C_p for Two Cylindrical Capsules of $k = 0.5$, $Sc = 5 * d$ and $Lc = 1 * d$ in a Horizontal Pipe at $V_{av} = 1\text{m/sec}$ (b) Variations in u/u_{max} for Two Cylindrical Capsules of $k = 0.5$, $Sc = 5 * d$ and $Lc = 1 * d$ in a Horizontal Pipe at $V_{av} = 1\text{m/sec}$

Table A-3.4 in Appendix A-3 summarises the results for various CFD based investigations being carried out on the flow of cylindrical capsules in a horizontal pipe with density greater than water.

Figure 4.67 depicts the variation in the normalised pressure drop in the test section of the pipe for a single cylindrical capsule having $L_c = 1 * d$. The results show that as the flow velocity increases, the pressure drop in the test section of the pipe increases. Furthermore, as the size of the capsule increases, the pressure drop further increases. It is evident from figure 4.67 that heavy-density cylindrical capsules of diameter equal to 90% of the pipeline offer substantial pressure drop and hence are not recommended for practical applications. In comparison with the results listed in table A-3.4, the pressure drop for $k = 0.9$ is 58 times higher on average than capsules of $k = 0.5$ at the same average flow velocity and the same capsule length. Whereas, the pressure drop for $k = 0.7$ is 320% higher on average than capsules of $k = 0.5$ at the same average flow velocities and the same length of the capsule. Furthermore, in comparison with a single heavy-density spherical capsule, the pressure drop for a single heavy-density cylindrical capsule of $L_c = 1 * d$ is 275%, 8 times and 14 times higher for $k = 0.5$, 0.7 and 0.9 respectively for same average flow velocities.

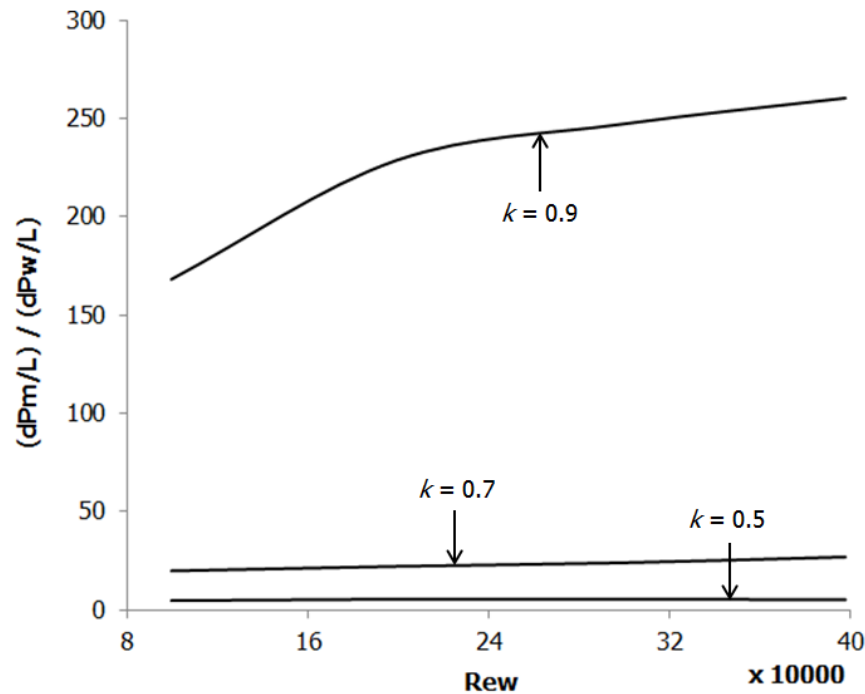


Figure 4.67. Variations in Normalised Pressure Drop for a Single Heavy-Density Cylindrical Capsule of $L_c = 1 * d$ in a Horizontal Pipe

Figure 4.68 depicts the variations in the normalised pressure drop for two heavy-density cylindrical capsules of $L_c = 1 * d$ and $Sc = 1 * d$. It is again noted here that the pressure drop for $k = 0.9$ is significantly higher than for $k = 0.5$ and 0.7 and hence the capsules of diameter equal to 90% diameter of the pipeline are not recommended for practical applications.

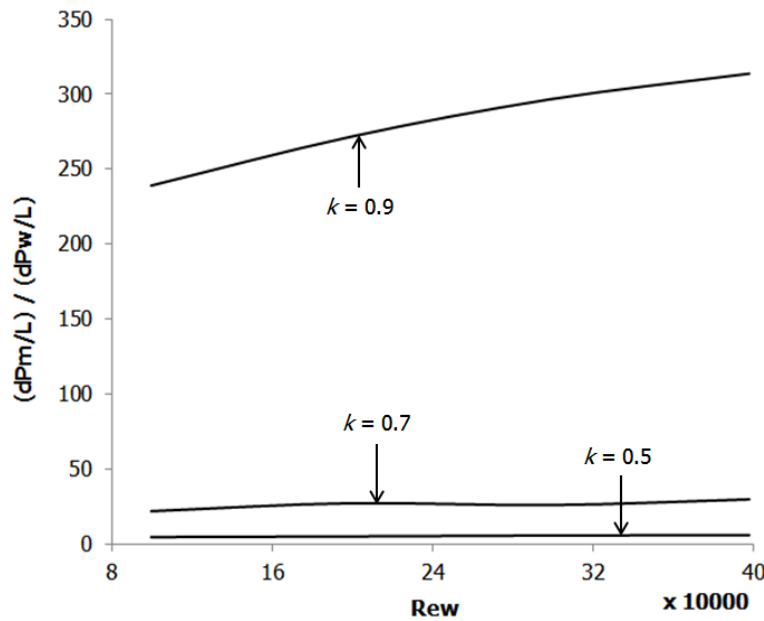


Figure 4.68. Variations in Normalised Pressure Drop for Two Heavy-Density Cylindrical Capsules of $L_c = 1 * d$ and $Sc = 1 * d$ in a Horizontal Pipe

Figures 4.69 and 4.70 depict the variations in the normalised pressure drop to analyse the effects of the length and the spacing between the capsules. It can be seen that as the length of the capsules increases, the normalised pressure drop increases. Similarly, as the spacing between the capsules increases, the normalised pressure drop increases.

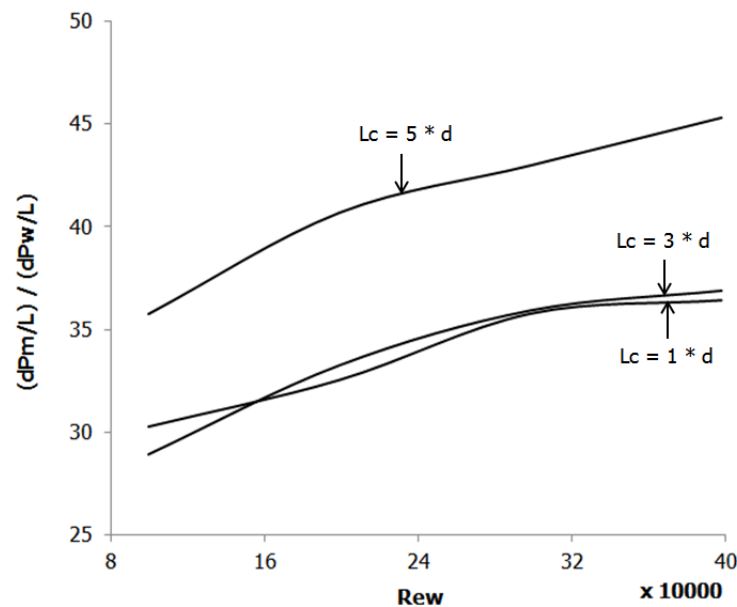


Figure 4.69. Variations in Normalised Pressure Drop for Two Heavy-Density Cylindrical Capsules of $k = 0.7$ and $Sc = 1 * d$ in a Horizontal Pipe

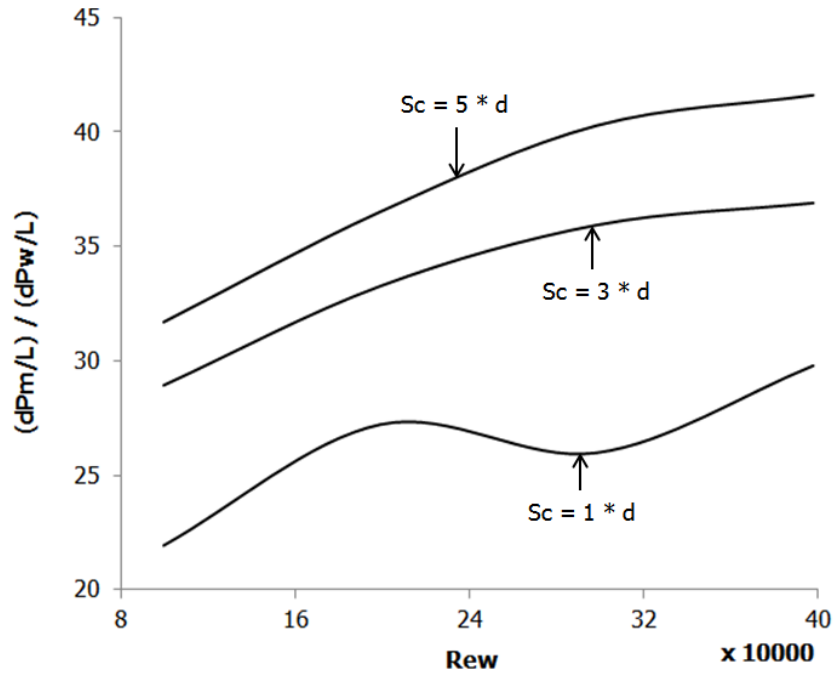


Figure 4.70. Variations in Normalised Pressure Drop for Two Heavy-Density Cylindrical Capsules of $k = 0.7$ and $L_c = 1 * d$ in a Horizontal Pipe

The information provided in this section, regarding the flow of heavy-density cylindrical capsules in horizontal pipes, has a huge impact on the design process of HCPs, which is presented in Chapter 7. Similar kind of analysis that has been carried out in this section is also presented in the next chapter for the flow of heavy-density cylindrical capsules in vertical pipes.

4.9. Prediction Models

Based on the results presented in this chapter, prediction models for the friction factor of capsules can be developed as discussed in Chapter 1. Capsules of $k = 0.9$ have been excluded from the formulation of prediction models based on the results which shows that $k = 0.9$ is not a practical option for horizontal pipelines transporting capsules as it leads to extensively large pressure drops in the pipeline.

The friction factors for water flow [7] and capsule flow separately can be calculated by the following expressions:

$$f_w = 0.0055 + \frac{0.55}{Re_w^{\frac{1}{3}}} \quad (4.8)$$

and:

$$f_c = 2D \frac{\left(\frac{\Delta P_m}{L_p} - \frac{\Delta P_w}{L_p}\right)}{\rho_w L_p V_{av}^2} \quad (4.9)$$

Using multiple variable regression analysis, semi-empirical correlations for the prediction of friction factor due to capsules, as a function of geometric and flow variables discussed in Chapter 3, have been developed. These prediction models are listed in table 4.5.

Table 4.5. Friction Factors for Capsules being transported in Horizontal Pipelines

Capsule Shape	Density of the Capsules	Friction Factor due to Capsules
Spherical	Equi-Density	$f_c = \frac{\left(2.63 \left(\frac{N}{L_p} * d\right)^{1.069} k^{2.56} \frac{Sc + Lp^{0.218}}{Lp}\right)}{Re_c^{0.116}}$
	Heavy-Density	$f_c = \frac{\left(5.5 \left(\frac{N}{L_p} * d\right)^{0.87} k^{4.12}\right)}{Re_c^{0.004} \frac{Sc + Lp^{0.089}}{Lp}}$
Cylindrical	Equi-Density	$f_c = \frac{\left(13.18 \left(\frac{N}{L_p} * Lc\right)^{0.178} k^{5.13} \frac{Lc^{0.1}}{d} \frac{Sc + Lp^{0.1}}{Lp}\right)}{Re_c^{0.117}}$
	Heavy-Density	$f_c = \frac{\left(3.38 \left(\frac{N}{L_p} * Lc\right)^{0.016} k^{5.24} \frac{Lc^{0.1}}{d} \frac{Sc + Lp^{0.1}}{Lp}\right)}{Re_c^{0.019}}$

Figures 4.71 and 4.72 show the difference between the friction factors, due to capsules within the pipeline, calculated using the expressions presented in table 4.9 and that obtained from the CFD results in this chapter to authorise the usefulness of these semi-empirical relationships. From figure 4.71, it can be clearly seen that more than 90% of the data lies within $\pm 10\%$ error bound of the semi-empirical

expression for equi-density spherical capsules. Similarly, it can be seen in figure 4.72 that more than 90% of the data lies within $\pm 10\%$ error bound of the semi-empirical relation for heavy-density cylindrical capsules within a horizontal pipeline. Hence, the prediction models developed here represent the friction factors due to the presence of the capsules in a horizontal pipeline with reasonable accuracy. The remaining two prediction models, i.e. for the flow of heavy-density spherical capsules and equi-density cylindrical capsules in a horizontal pipeline, have the same order of accuracy.

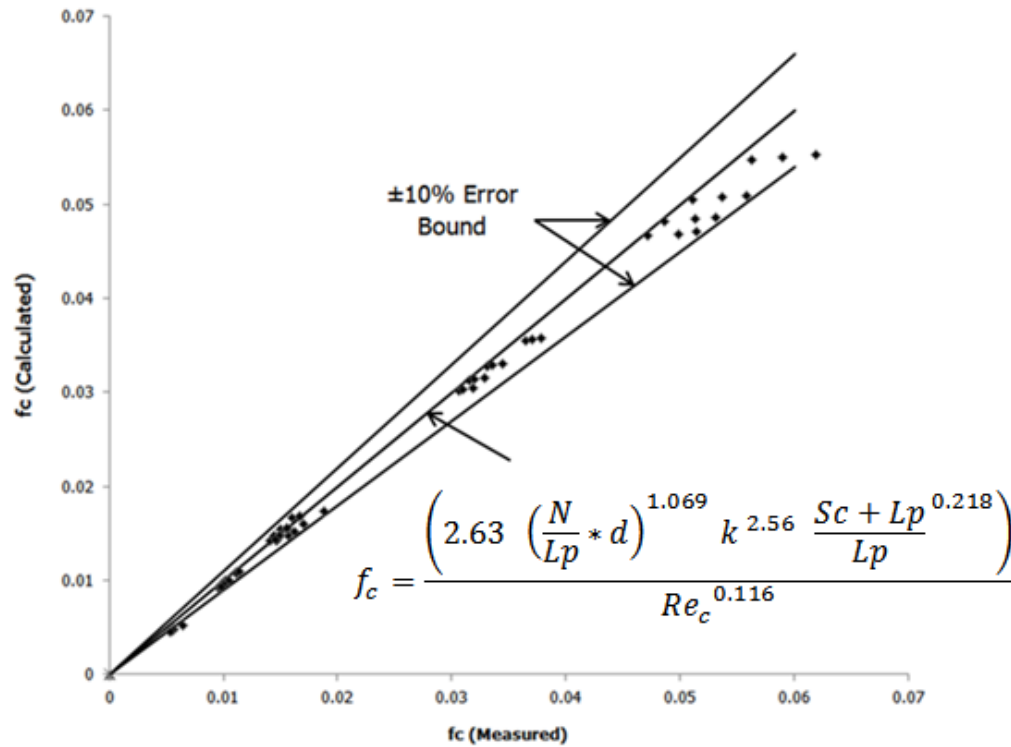


Figure 4.71. f_c for Equi-Density Spherical Capsules

From the prediction models, it can be seen that as the number of capsules, diameter of capsules, length of capsules or the velocity of the capsules becomes zero, i.e. no capsule in the pipeline; the value for f_c automatically goes to zero and the expression for the pressure drop in the pipeline is only left with the friction factor due to water in equation (1.26). Furthermore, as Sc becomes zero, i.e. contacting capsules in the pipeline, the prediction models will still be valid. In order to prove this, a separate case regarding the flow of contacting capsules has been simulated and the results show that the difference between f_c from CFD and f_c from the prediction models is within the error bounds of the prediction models, i.e. $\pm 10\%$. Hence, the prediction models presented in this chapter can be used for a variety of capsule flow conditions within horizontal pipelines. Furthermore, the prediction models developed here can be directly used in the design of HCPs (see Chapter 7 for further details).

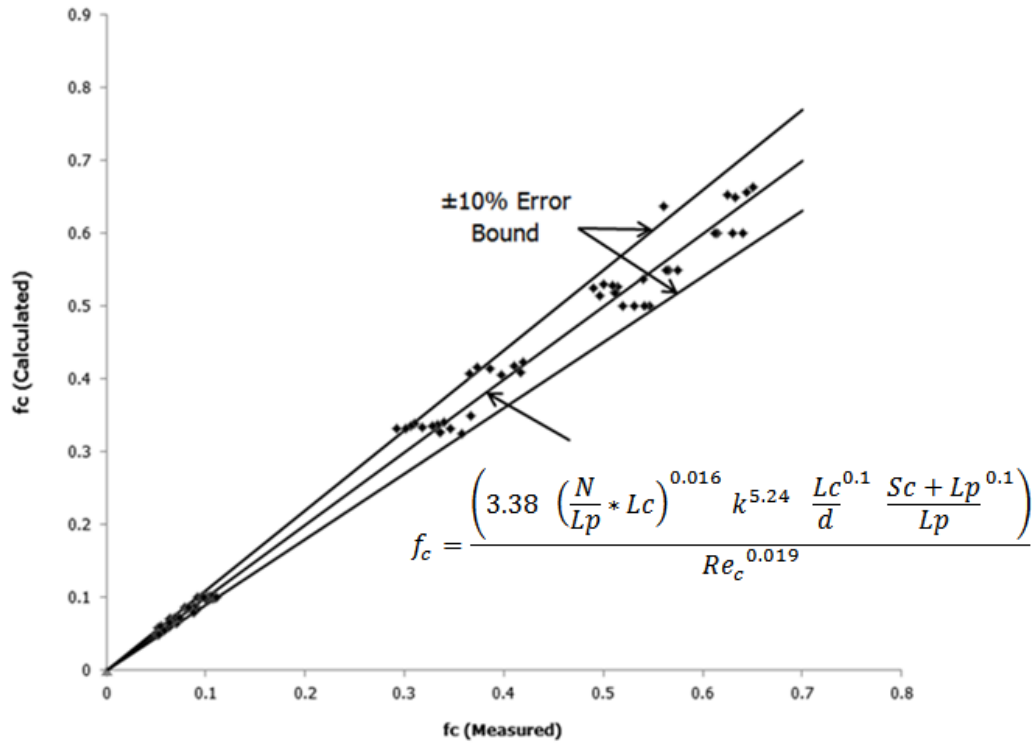


Figure 4.72. f_c for Heavy-Density Cylindrical Capsules

4.10. Summary of the Analysis of a Horizontal HCP

A detailed flow diagnostics of the capsule transporting horizontal pipes has revealed the following results:

- Increase in the average flow velocity increases the pressure drop in the pipeline (see sections 4.5.1, 4.6.1, 4.7.1 and 4.8.1 for reference)
- Increase in the capsules diameter increases the pressure drop in the pipeline (see sections 4.5.2, 4.6.3, 4.7.2 and 4.8.3 for reference)
-
- Increase in the length of the capsules increases the pressure drop in the pipeline (see sections 4.6.2, and 4.8.2 for reference)
- Increase in the spacing between the capsules marginally increases the pressure drop in the pipeline, in comparison with other parameters, except for the flow of heavy-density spherical capsules (see sections 4.5.4, 4.6.5, 4.7.4 and 4.8.5 for reference)

- Increase in the density of the capsules increases the pressure drop in the pipeline (see Appendix A-3 for reference)
- Cylindrical capsules result in an increased pressure drop in the pipeline as compared to the flow of spherical capsules (see Appendix A-3 for reference)
- Increase in the concentration of the capsules increases the pressure drop in the pipeline (see section 4.5.3, 4.6.4, 4.7.3 and 4.8.4 for reference)

The information provided in this chapter, regarding the flow of capsules in horizontal pipes, and the prediction models developed for the friction factor of capsules, dictates the design process of hydraulic capsule pipelines. Further details about the design of HCPs are presented in Chapter 7. For off-shore applications of HCPs, where the pipelines comprise primarily of vertical pipes, the next chapter provides details on the results obtained from CFD regarding the flow of capsules in such pipelines.

CHAPTER 5

ANALYSIS OF VERTICAL PIPELINES TRANSPORTING CAPSULES

The results obtained after performing CFD simulations for the cases discussed in Chapter 3, regarding the transport of capsules in a vertical pipeline, have been presented here. A detailed qualitative and quantitative analysis of the results obtained has been carried out in order to understand the complex flow structure in vertical pipelines transporting capsules. The effect of various geometric and flow-related parameters on the pressure drop in a capsule transporting vertical pipeline has been investigated. Furthermore, semi-empirical relationships, for the flow of capsules in a vertical pipeline, have been developed.

5.1. Analysis of Single Phase Flow in a Vertical Pipe

Before moving on to the flow of capsules in vertical pipes, the flow structure of a single phase in the pipe needs to be understood and validated with Computational Fluid Dynamics. The pressure distribution within the test section of the pipe at an average flow velocity of 1m/sec is shown in figure 5.1. The pressure of water has dropped from 18874Pa to 10118Pa along the pipe length, i.e. in +Y direction, which corresponds to 46% decrease in the pressure. Using Moody's chart for a hydrodynamically smooth pipe, the friction factor at an average flow velocity of 1m/sec in a 0.1m diameter pipe has been found to be 0.0185. Putting this value of friction factor in equation (1.18):

$$\Delta P = 9902\text{Pa}$$

and the pressure drop predicted by Computational Fluid Dynamics between the inlet and the outlet of the pipe is:

$$\Delta P = 9898\text{Pa}$$

It can thus be concluded that Computational Fluid Dynamics predict the pressure drop in a single phase flow within vertical pipelines with reasonable accuracy.

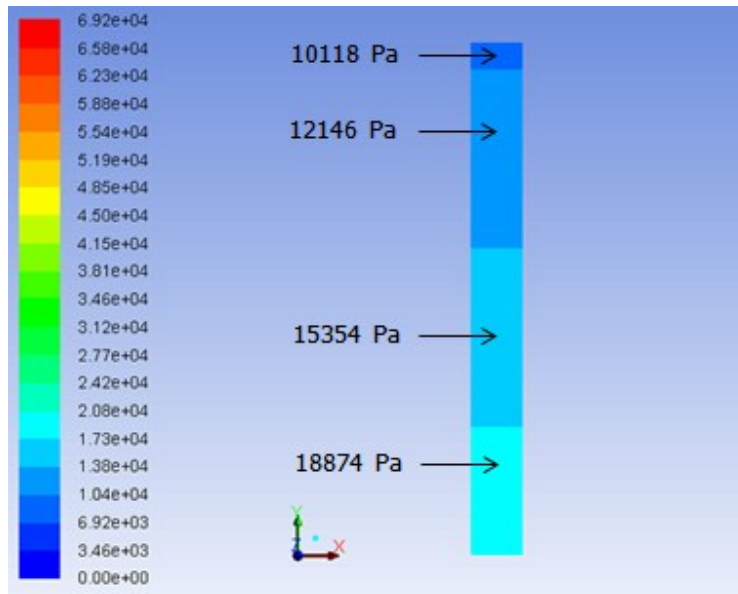


Figure 5.1. Pressure variations for Water Flow in a Vertical Pipe

Figure 5.2 shows the variations in pressure coefficient w.r.t. the axial location within the vertical pipe. C_p curve for the flow of water in a horizontal pipe has also been included for comparison, where C_p represents the coefficient of pressure. It can be seen that the pressure within the vertical pipe drops linearly as observed for horizontal pipe.

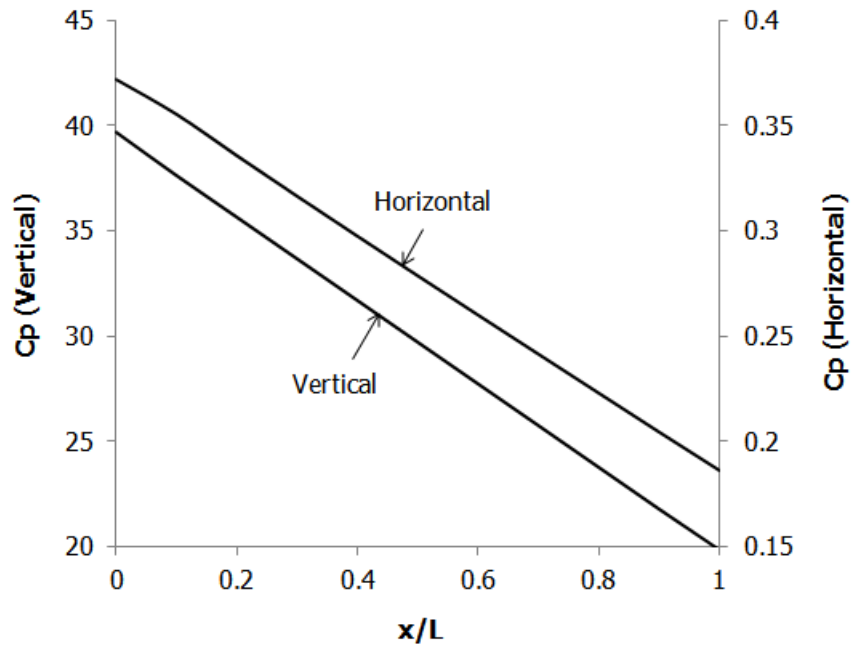


Figure 5.2. Variations in C_p for Water Flow in a Vertical Pipe

Table 5.1 shows a comparison between the pressure drop predictions, from both equation (1.18) and Computational Fluid Dynamics, for different flow velocities in the pipe considered above. It can be seen that the pressure drops uniformly in a vertical pipe, as seen in a horizontal pipe. Furthermore, the difference in the pressure drop between a horizontal and vertical pipe is $\rho g \Delta h$.

Table 5.1. Pressure Drops for Water Flow in a Vertical Pipe

V_{av}	$\Delta P_{w_h}/L_p$	$\Delta P_{w_v}/L_p$	$\Delta P_{w_v}/L_p - \Delta P_{w_h}/L_p$
(m/sec)	(Pa/m)	(Pa/m)	(Pa/m)
1	92	9898	9806
2	317	10123	9806
3	658	10463	9805
4	1104	10910	9806

Figure 5.3 depicts the velocity field within the pipe. It can be seen that the flow velocity at the walls of the pipe is zero due to the no-slip boundary condition whereas it is higher in the centre of the pipe. It is noteworthy that in a fully developed turbulent flow, the velocity at the centre of the pipe is higher than the average flow velocity. In this case the velocity of the fully developed flow at the centre of the pipe is 1.2m/sec and the average velocity of the flow V_{av} is 1m/sec.

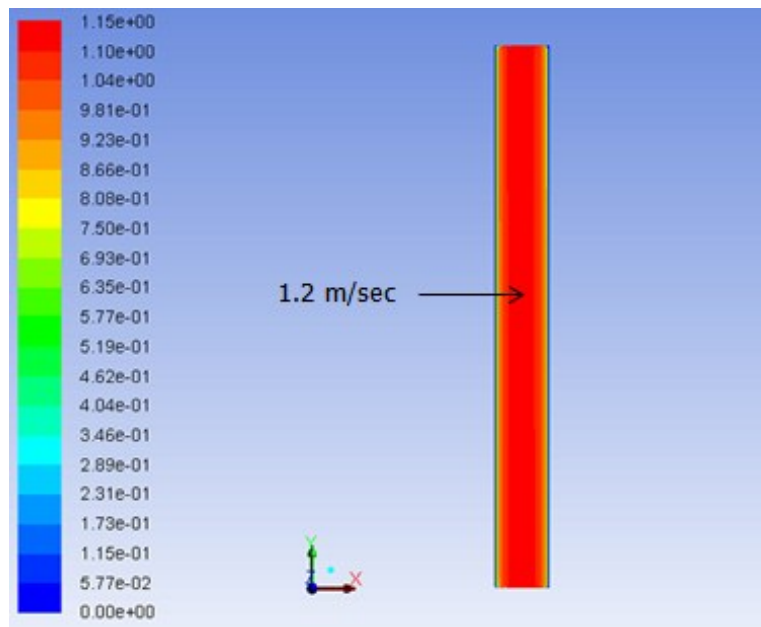


Figure 5.3. Velocity distribution for Water Flow in a Vertical Pipe

Figure 5.4 further shows the velocity profile in the cross-section of the pipe and u is the local flow velocity along the pipe. Due to no-slip boundary condition at the walls of the pipe, and as the walls of the pipe have been kept stationary, the flow velocity at the pipe walls is zero. The velocity in the vicinity of the pipe wall, also known as the boundary layer, increases sharply while the flow velocity at the centre of the pipe, where the shear forces acting on the fluid are minimum, is highest.

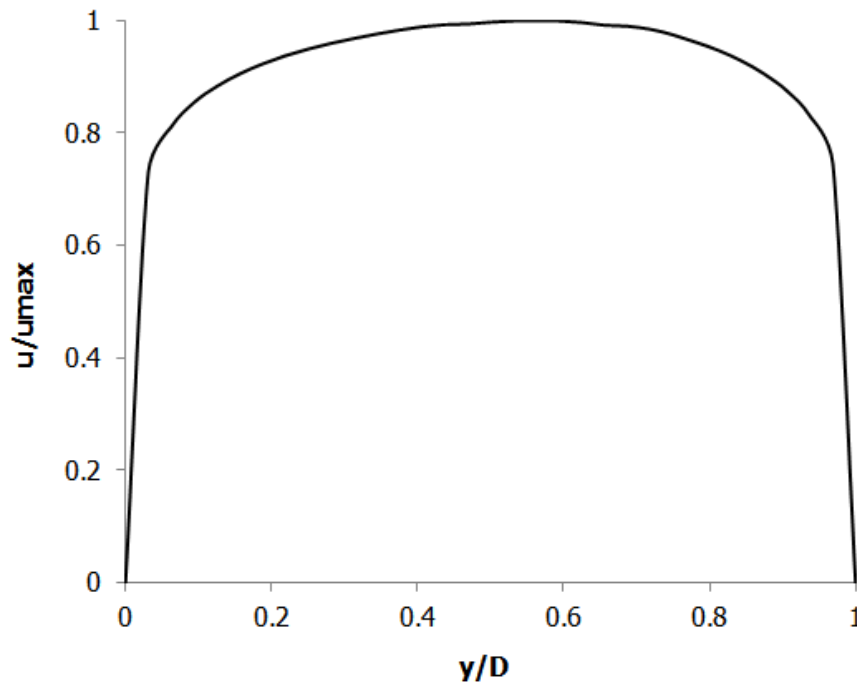


Figure 5.4. Velocity Profile for Water Flow in a Vertical Pipe

5.2. Analysis of the Flow of Equi-Density Spherical Capsules in a Vertical HCP

Figure 5.5 depicts the variations in the pressure and velocity distribution within the test section of the pipe transporting a single spherical capsule of $k = 0.5$ at $V_{av} = 1\text{m/sec}$. It can be seen that the presence of a capsule changes the pressure distribution inside a vertical pipe, as compared to single phase flow shown in figure 5.1. The pressure in the pipeline decreases continuously from the inlet to the outlet of the pipe. It can be seen that the pressure decreases by 15% upstream of the capsule and 28% downstream of the capsule. At such a low velocity of the capsule in a vertical pipe, the effect of the presence of the capsule on the pressure drop within the pipeline is dominated by the pressure drop due to the elevation of the pipe.

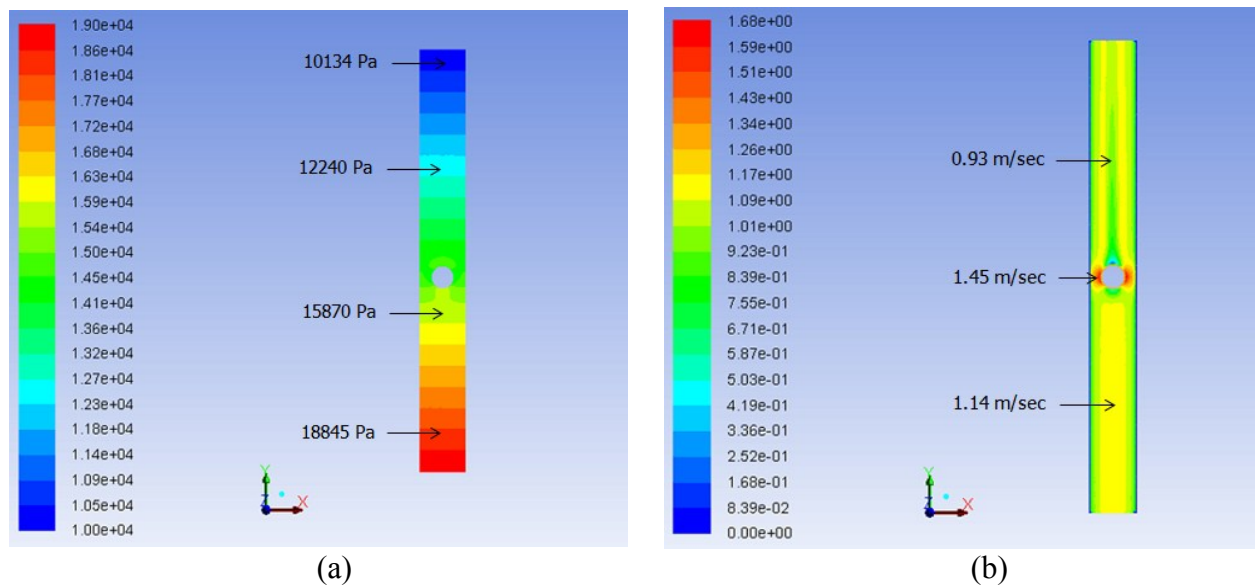


Figure 5.5. Variations in (a) Pressure and (b) Velocity, for a Single Spherical Capsule of $k = 0.5$ in a Vertical Pipe at $V_{av} = 1\text{m/sec}$

Figure 5.5 (b) depicts that the flow accelerates from 1.15m/sec to 1.45m/sec as it passes through the annulus region. This happens because of the reduction in the cross-sectional area of the flow. As the flow exits the annulus, it slows down to 0.94m/sec in the centre of the pipe due to increase in the cross-sectional area. The extreme velocity gradients present in the annulus regions (both up and down of the capsule) gives rise to shear forces acting on the capsule. As the capsule is perfectly aligned with the central axis of the pipe, these opposite and equal shearing forces cancel out each other's effects and hence the capsule propagates along the centreline of the pipe.

Figure 5.6 depicts the variations in C_p and u/u_{max} along the analysis line for the case under consideration. The results show that the pressure drop in capsule transporting vertical pipe is considerably higher than the pressure drop in a capsule transporting horizontal pipe. It can be seen that the pressure drops linearly within a vertical pipe, and the effect of the presence of a capsule in a vertical pipeline, as compared to a horizontal pipeline, is considerably less. The total pressure drop for the present case is 9929Pa . As compared to the pressure drop due to water flow only in a vertical pipeline, the increase in the pressure drop due to the presence of a capsule (in this case) is only 0.3% which

suggests that the pressure drop in the pipeline due to the elevation is dominating. Further analysing the figure reveals that the pressure recovery is negligibly small in a vertical pipeline. This is again due to the fact that the pressure recovery effect occurs only due to the capsule and as the presence of the capsule has a very little effect on the pressure drop within the pipeline, the pressure recovery is incomparable to the overall pressure drop within the pipe.

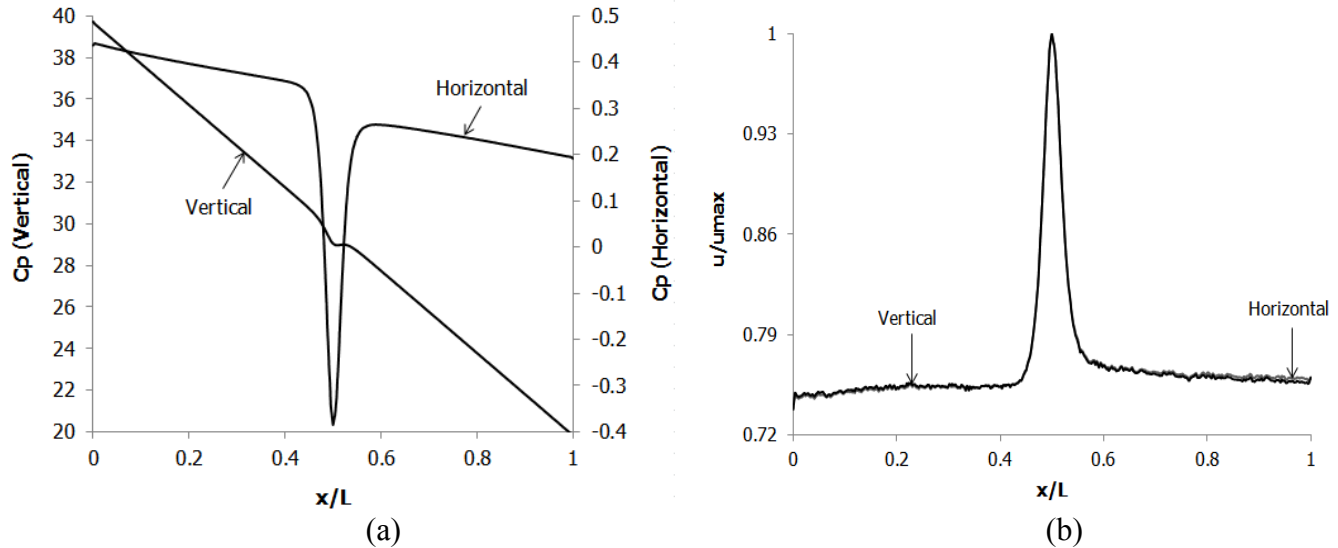


Figure 5.6. (a) Variations in C_p for a Single Spherical Capsule of $k = 0.5$ in a Vertical Pipe at $V_{av} = 1\text{m/sec}$ (b) Variations in u/u_{max} for a Single Spherical Capsule of $k = 0.5$ in a Vertical Pipe at $V_{av} = 1\text{m/sec}$

Figure 5.6 (b) depicts that the flow velocity increases sharply as it passes through the annulus and then decreases as it exits the annulus for both the horizontal and vertical pipelines. The trend, as well as the magnitude of these changes, are the same for both the pipelines, hence, the two curves in figure 5.6 (b) are superimposed on each other. Thus, the velocity distribution within a vertical pipeline transporting capsules is identical to the velocity distribution within a capsule transporting horizontal pipeline. To further investigate the velocity distribution within the capsule transporting vertical pipe, velocity profiles have been drawn across the cross-section of the pipe at both 0.1m upstream and downstream locations from the centre of the capsule as shown in figure 5.7. It can be seen that the velocity profile is undisturbed at the upstream location and the presence of the capsule has not affected the velocity profile at this location. However, at the downstream location, the presence of the capsule in the pipe has distorted the velocity profile. These profiles are similar to the one observed for the horizontal pipe in figure 4.10.

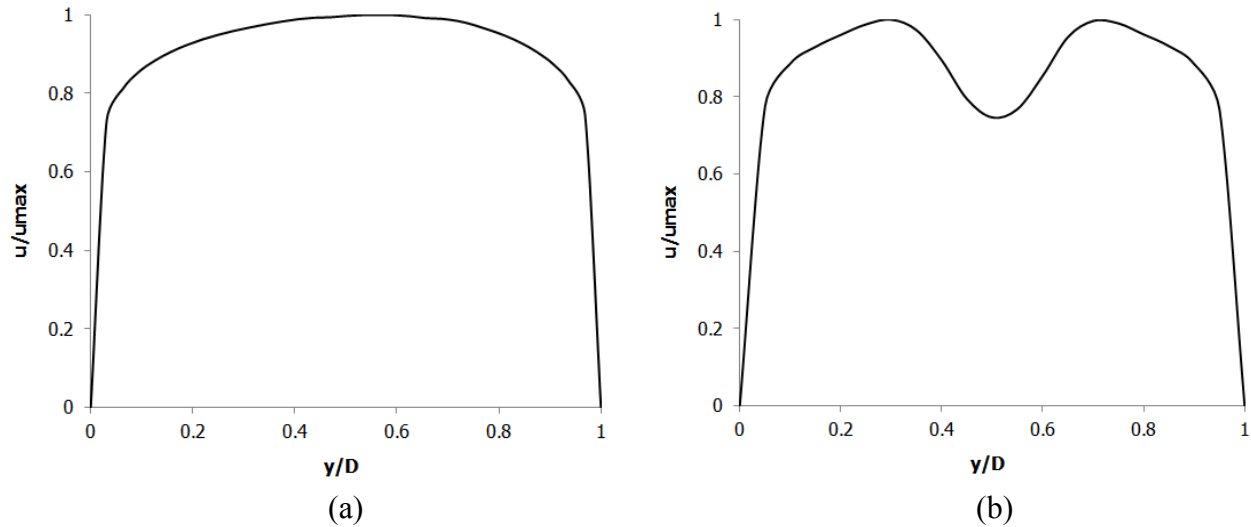


Figure 5.7. Variations in the Cross-Sectional Velocity Profiles for a Single Spherical Capsule of $k = 0.5$ in a Vertical Pipe at $V_{av} = 1\text{m/sec}$ at (a) Upstream and (b) Downstream of the Capsule

Figure 5.8 depicts the variations in the velocity profiles at various locations within the capsule transporting vertical pipe under consideration at an average flow velocity of 1m/sec .

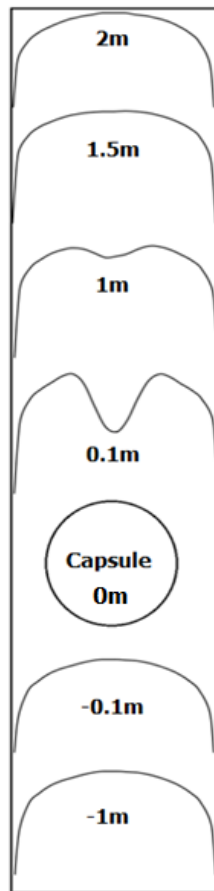


Figure 5.8. Development of Velocity Profile in the Presence of a Single Spherical Capsule in a Vertical Pipe having Density Equal to Water

5.2.1. Average Flow Velocity Effects

To investigate the effect of the average flow velocity on the flow structure within the pipe, an average velocity of 4m/sec for a spherical capsule of $k = 0.5$ has been chosen for flow diagnostics. Figure 5.9 depicts the pressure and velocity variations in the capsule transporting pipe for an average flow velocity of 4m/sec, keeping $k = 0.5$. The trend of pressure distribution is the same as observed in case of a horizontal pipeline transporting capsules i.e. a high pressure of 18251Pa at the upstream location, a low pressure of 10655Pa in the annulus region and a very high pressure of 22461Pa at the location where the flow strikes the capsule. The pressure drop between the inlet and the outlet of the pipe is 11335Pa, which is 151% higher than the pressure drop for $V_{av} = 1\text{m/sec}$. The pressure drop increases in case of a horizontal pipeline for the same conditions is 94%. It can be concluded that increase in the average velocity of the flow increases the pressure drop within the pipeline and for $V_{av} = 4\text{m/sec}$ in a vertical pipe, the effect of the presence of a capsule in the pipe is considerable on the pressure drop as compared to water flow. Furthermore, it can be seen in figure 5.9 (b) that the velocity field resembles the one observed in case of $V_{av} = 1\text{ m/sec}$, i.e. higher velocity in the annulus.

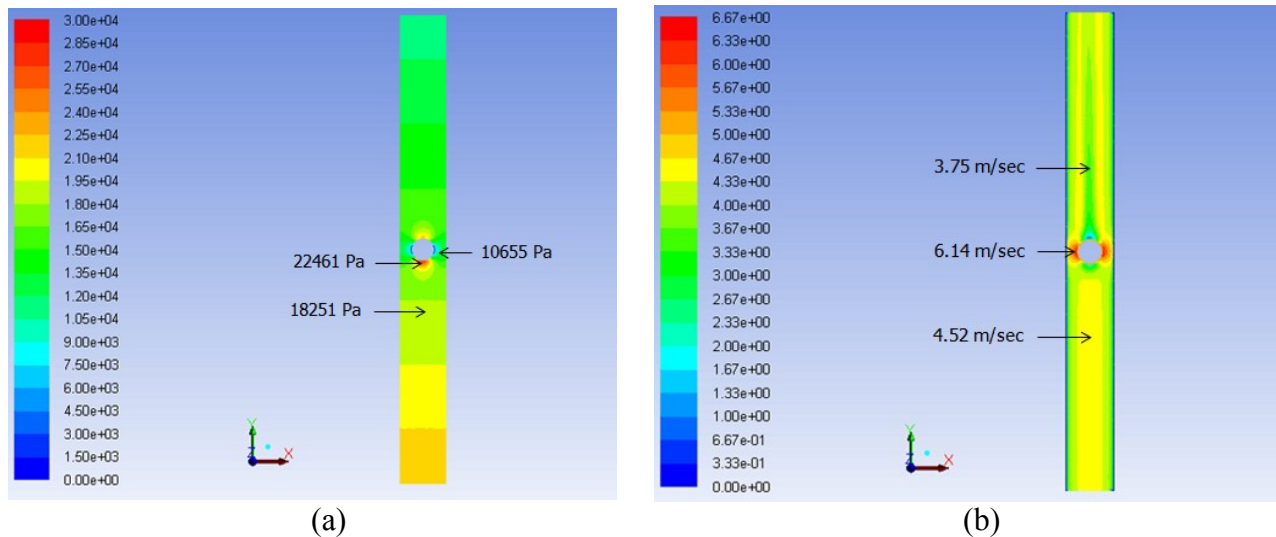


Figure 5.9. Variations in (a) Pressure and (b) Velocity, for a Single Spherical Capsule of $k = 0.5$ in a Vertical Pipe at $V_{av} = 4\text{m/sec}$

Figure 5.10 shows the variations in C_p and u/u_{max} along the analysis line for the case under consideration. The results depict that the pressure drop for a vertical capsule transporting pipe is considerably higher than for a horizontal pipe. Furthermore, the effect of the presence of the capsule in the pipe is no longer negligible, as observed in case of $V_{av} = 1\text{m/sec}$. The velocity distribution for both vertical and horizontal pipes, transporting capsules, is exactly similar. More detailed results have been presented in table A-4.1.

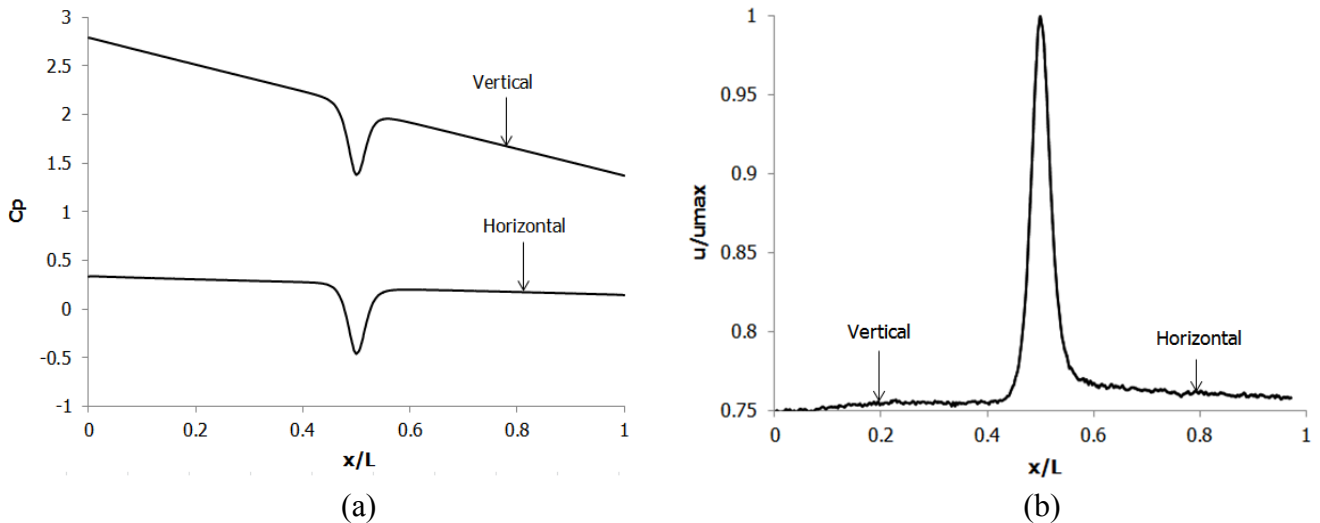


Figure 5.10. (a) Variations in C_p for a Single Spherical Capsule of $k = 0.5$ in a Vertical Pipe at $V_{av} = 4\text{m/sec}$ (b) Variations in u/u_{max} for a Single Spherical Capsule of $k = 0.5$ in a Vertical Pipe at $V_{av} = 4\text{m/sec}$

5.2.2. Capsule Diameter Effects

Figure 5.11 shows the pressure and velocity distributions in a spherical capsule transporting vertical pipe for $k = 0.9$ and $V_{av} = 1\text{m/sec}$. It can be seen that although the overall pressure distribution seems to be the same as compared with the pressure field for $k = 0.5$ at the same average flow velocity, but the pressure at upstream location has increased by 8% and the pressure at downstream location has increased by 11%. The pressure drop between the inlet and the outlet of the pipe is 11276Pa , which is 13% higher than the pressure drop for $k = 0.5$. Furthermore, the pressure in the annulus region has decreased by 78%. Such a sharp decrease in the pressure in the annulus region is due to the fact that the cross-sectional area of the flow has reduced by 80%. Furthermore, it can be seen in figure 5.11 (b) that velocity of the flow in the annulus region has increased to 4.62m/sec while a large wake region exists downstream of the capsule where the flow velocity is very low.

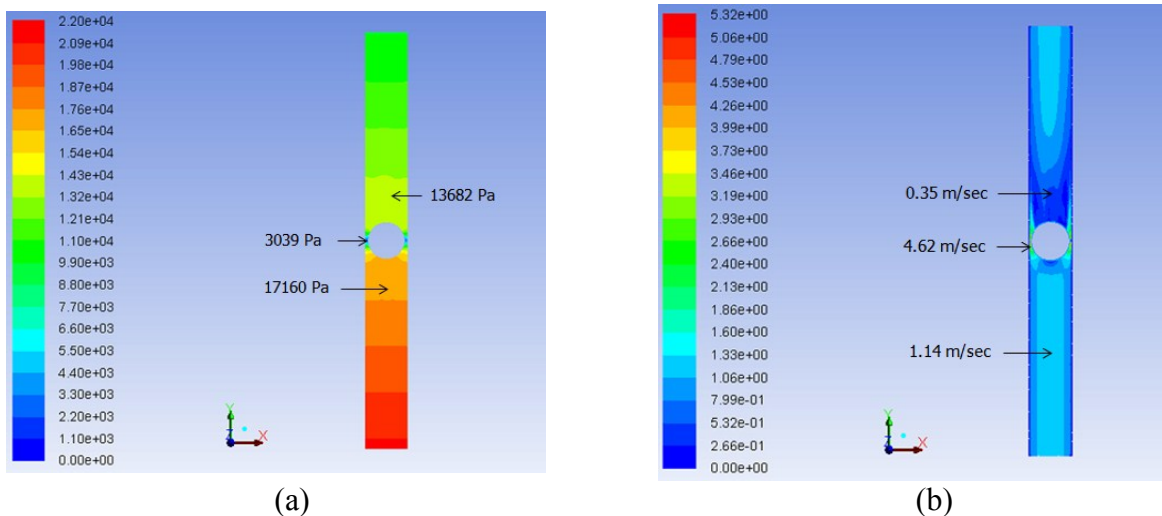


Figure 5.11. Variations in (a) Pressure and (b) Velocity, for a Single Spherical Capsule of $k = 0.9$ in a Vertical Pipe at $V_{av} = 1\text{m/sec}$

Figure 5.12 shows the variations in C_p and u/u_{max} along the analysis line for the case under consideration. The results depict that the pressure drop in case of a vertical pipeline transporting capsules is considerably higher than the pressure drop in a horizontal pipeline transporting capsules. That's why the pressure coefficient for horizontal capsule transporting pipe has been plotted on the secondary Y axis of the graph as the scale is considerably different for both the cases. Furthermore, it can be seen that the pressure recovery in case of a vertical pipeline is dominated by the elevation effects. Figure 5.12 (b) reveals that the velocity distribution within pipelines transporting capsules both horizontal and vertical is identical, i.e. the velocity of the flow increases sharply in the annulus region and then drops sharply as it exits from the annulus. It can be further seen that the velocity upstream and downstream of the capsule has the same magnitude. More detailed results have been presented in table A-4.1.

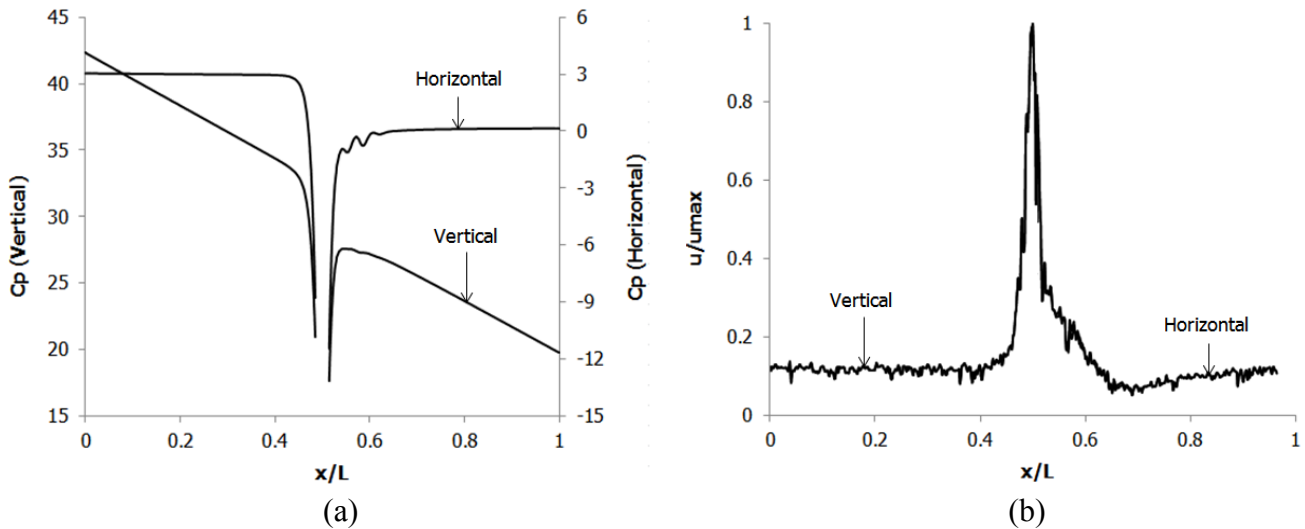


Figure 5.12. (a) Variations in C_p for a Single Spherical Capsule of $k = 0.5$ in a Vertical Pipe at $V_{av} = 1\text{m/sec}$ (b) Variations in u/u_{max} for a Single Spherical Capsule of $k = 0.5$ in a Vertical Pipe at $V_{av} = 1\text{m/sec}$

5.2.3. Capsule Concentration Effects

Figure 5.13 depicts the pressure and velocity variations in a vertical pipe carrying three spherical capsules of $k = 0.5$ and $V_{av} = 1\text{m/sec}$. The spacing between the capsules is equal to one diameter of the capsule. The trend of the pressure distribution is the same as observed for a single spherical capsule. The pressure at upstream location has increased to 17158Pa (8%) while it has decreased to 13257Pa (8%) downstream as compared to a single spherical capsule. Hence, an overall pressure drop increase of 0.5% has been observed for $N = 3$ as compared to $N = 1$. Furthermore, as compared to a single spherical capsule, it can be seen that although the flow velocity upstream of the capsules is the same (i.e. 1.14m/sec), but the velocity downstream of the capsules has reduced by 15% to 0.79m/sec . Hence, increased concentration of the solid phase in the pipe offers more resistance to the flow; increasing the pressure drop and decreasing the average flow velocity.

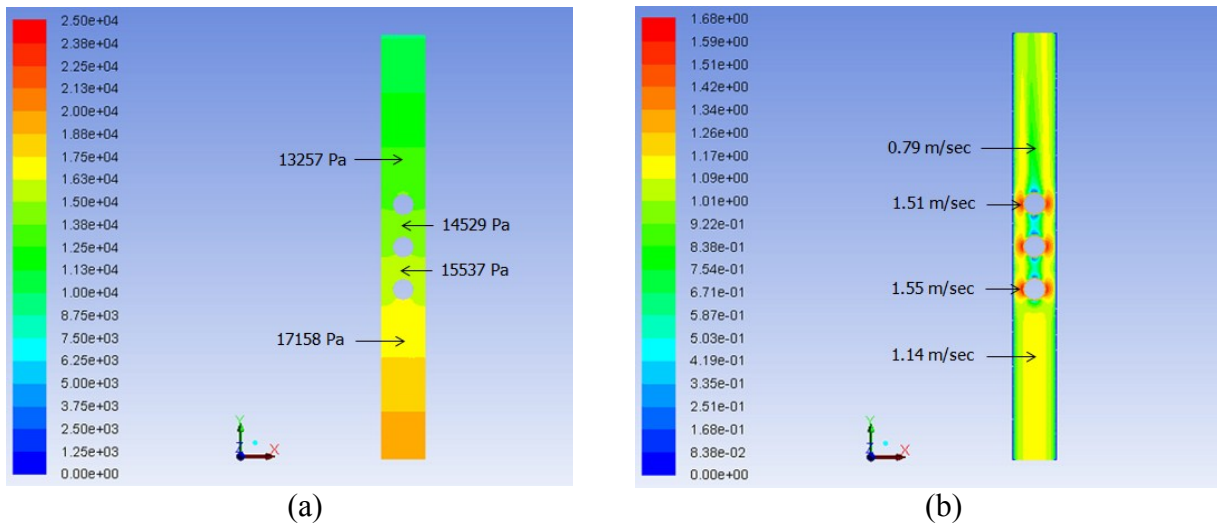


Figure 5.13. Variations in (a) Pressure and (b) Velocity, for Three Spherical Capsules of $k = 0.5$ and $Sc = 1 * d$ in a Vertical Pipe at $V_{av} = 1\text{m/sec}$

Figure 5.14 represents the variations in C_p and u/u_{max} for the case under consideration. It can be clearly seen that the pressure drop in a vertical capsule transporting pipe is higher than the pressure drop for a horizontal capsule transporting pipe. It can be seen that the effect of the presence of the capsule within the pipe on the pressure drop is being dominated by the elevation effects. More detailed results have been presented in table A-4.1.

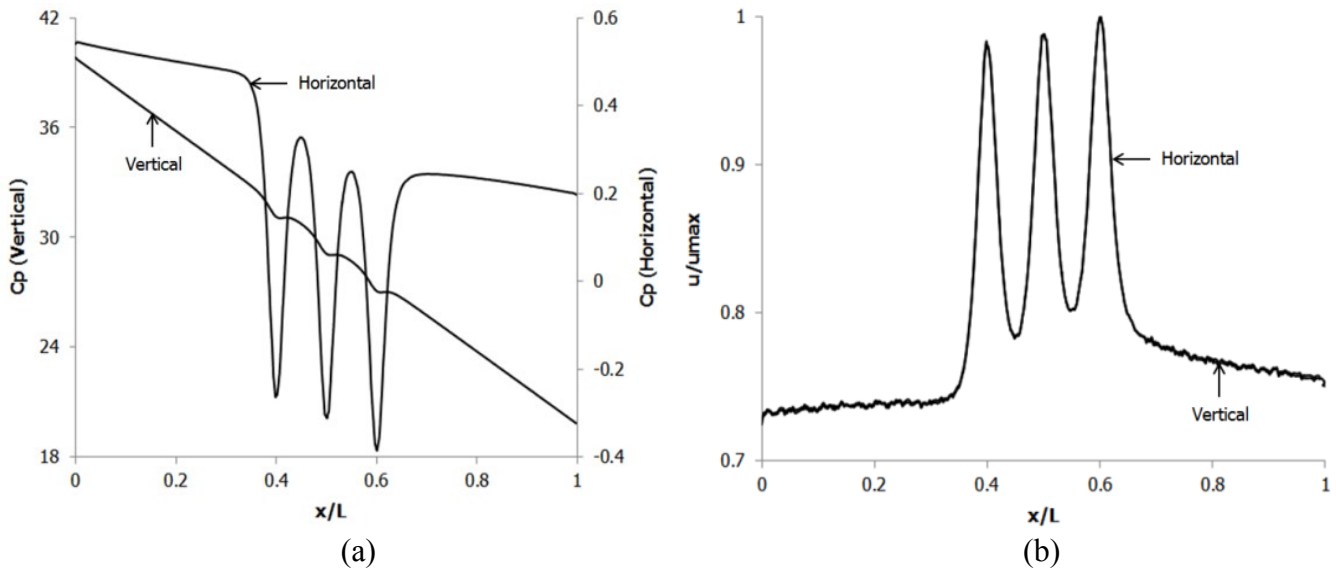


Figure 5.14. (a) Variations in C_p for Three Spherical Capsules of $k = 0.5$ and $Sc = 1 * d$ in a Vertical Pipe at $V_{av} = 1\text{m/sec}$ (b) Variations in u/u_{max} for Three Spherical Capsules of $k = 0.5$ and $Sc = 1 * d$ in a Vertical Pipe at $V_{av} = 1\text{m/sec}$

5.2.4. Effects of Spacing between the Capsules

Figure 5.15 depicts the pressure and velocity variations in a hydraulic pipe carrying three spherical capsules of $k = 0.5$ and $V_{av} = 1\text{m/sec}$. The spacing between the capsules is equal to five diameters of the capsule. The trend of the pressure distribution is the same as observed for $Sc = 1 * d$. The pressure at upstream location has increased by 8% while it has decreased 20% as compared to $Sc = 1 * d$ case. Furthermore, the flow velocity upstream of the capsules is the same (i.e. 1.15m/sec), but the velocity downstream of the capsules has increased by 3% to 0.82m/sec . Hence, increased spacing between the capsules leads to a marginally higher pressure drop within the pipe as compared to smaller spacing between the capsules.

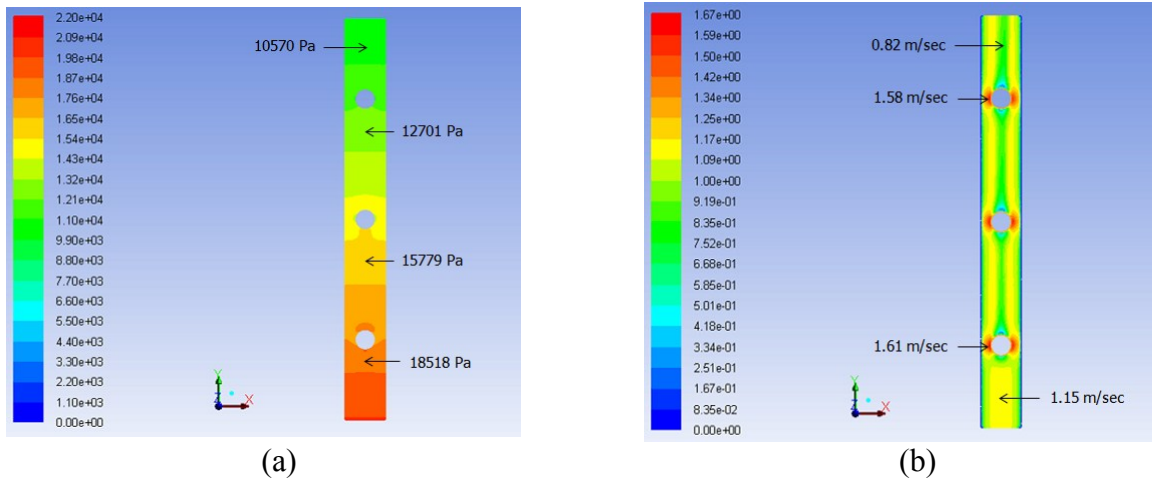


Figure 5.15. Variations in (a) Pressure and (b) Velocity, for Three Spherical Capsules of $k = 0.5$ and $Sc = 5 * d$ in a Vertical Pipe at $V_{av} = 1\text{m/sec}$

Figure 5.16 represents the variations in C_p and u/u_{max} for the case under consideration. It can be seen that the pressure drop for $Sc = 5 * d$ in a vertical pipe is considerably higher than a horizontal pipe. Furthermore, the velocity distribution remains identical for both the cases. More detailed results have been presented in table A-4.1.

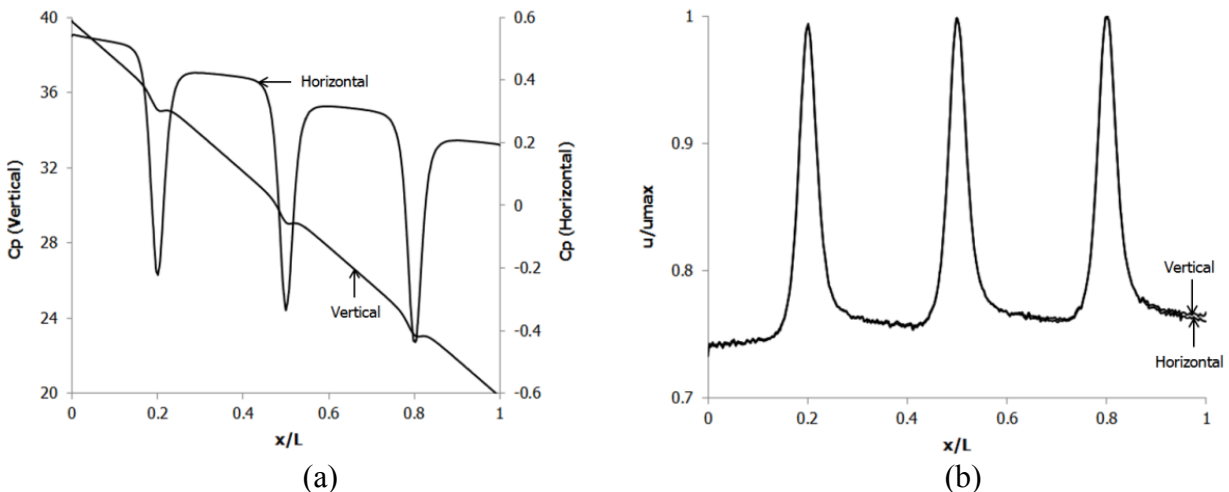


Figure 5.16. (a) Variations in C_p for Three Spherical Capsules of $k = 0.5$ and $Sc = 5 * d$ in a Vertical Pipe at $V_{av} = 1\text{m/sec}$ (b) Variations in u/u_{max} for Three Spherical Capsules of $k = 0.5$ and $Sc = 5 * d$ in a Vertical Pipe at $V_{av} = 1\text{m/sec}$

Table A-4.1 in Appendix A-4 summarises the results for various CFD based investigations being carried out on the flow of spherical capsules in a vertical pipe with density equal to that of water.

Further analysing the results obtained in the table above, figure 5.17 depicts the variations in the normalised pressure drop in the test section of the pipe for a single spherical capsule at various flow velocities. The pressure drop for the mixture flow has been non-dimensionalised with the pressure drop for water flow, and the flow velocity has been represented in terms of the Reynolds Number of water. The curves in the figure are for different k value ranges between 0.5 and 0.9. The results show that as the velocity of the flow increases, the pressure drop in the pipe increases. Furthermore, as the diameter of the capsule increases, the pressure drop increases. The reason for the increase in the pressure drop with an increase in the capsule diameter is due to the fact that a capsule of bigger size offers more resistance to the flow. From table A-4.1, it can be seen that the pressure drop increases by 3.6% on average for $k = 0.7$ and by 80% for $k = 0.9$ w.r.t. $k = 0.5$ for a single spherical capsule. Figure 5.17 further suggests that $k = 0.7$ is the best option in terms of pressure drop in the pipeline. These trends are similar to the one observed in case of a horizontal pipeline transporting capsules.

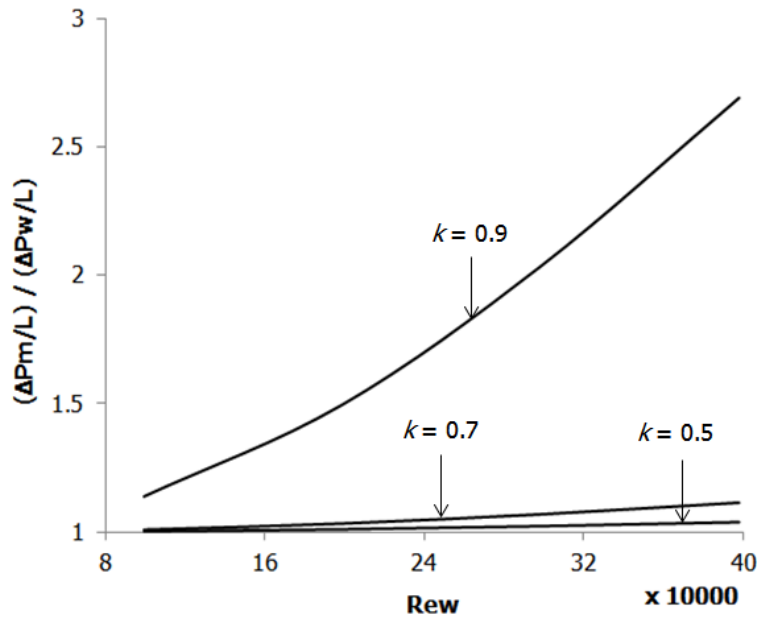


Figure 5.17. Variations in Normalised Pressure Drop for a Single Equi-Density Spherical Capsule in a Vertical Pipe

Figure 5.18 depicts the variation in the normalised pressure drops in the test section of the pipe for a train of three spherical capsules having a spacing of $1 * d$ between the consecutive capsules respectively. The results show that as the flow velocity increases, the pressure drop in the test section of the pipe increases. Furthermore, as the size of the capsule increases, the pressure drop further increases. It is evident that equi-density spherical capsules of diameter equal to 90% of the pipeline diameter offer substantial pressure drop and hence are not recommended for practical applications. The pressure drop for $k = 0.9$ and 0.7 are 12% and 247% higher on average respectively than capsules of $k = 0.5$ at the same average flow velocity and the same spacing between the capsules in the train. Comparing figures 5.18 and 5.17 reveals that an increase in the concentration of the capsules in the pipe increases the pressure drop.

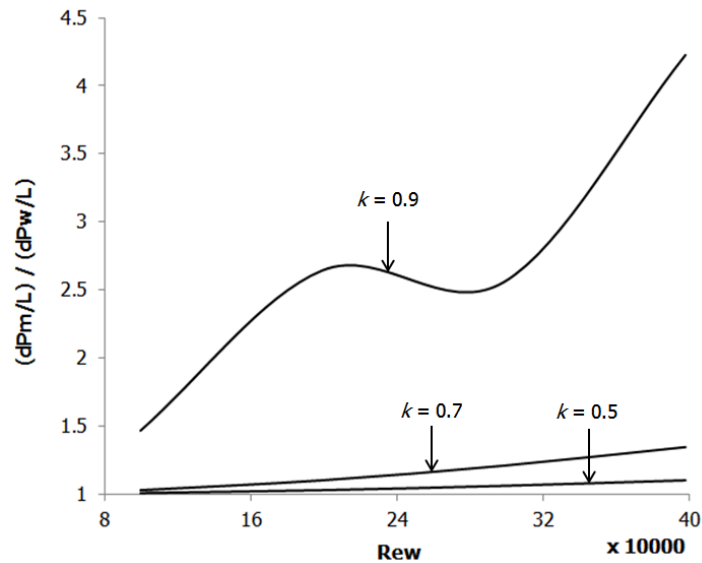


Figure 5.18. Variations in Normalised Pressure Drop for Three Equi-Density Spherical Capsules in a Vertical Pipe

Figure 5.19 depicts the variations in the normalised pressure drop for a spherical capsule train consisting of three capsules of $k = 0.7$ and having different spacing between them.

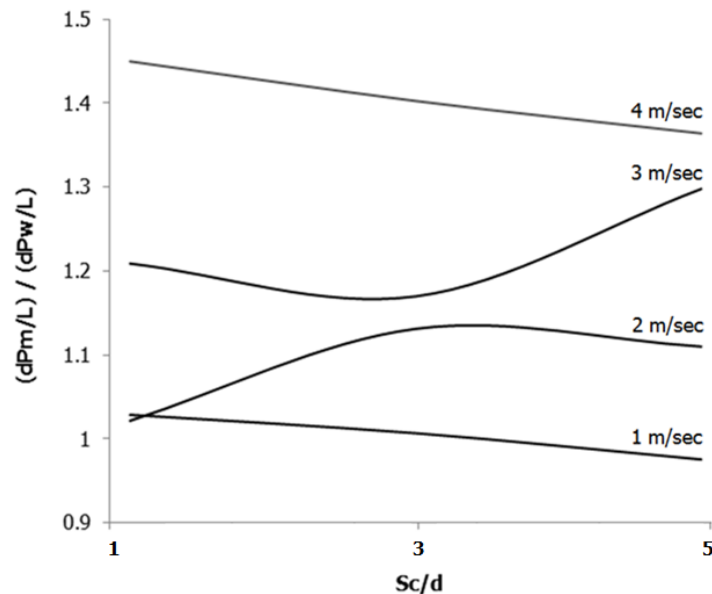


Figure 5.19. Variations in Normalised Pressure Drop for Three Spherical Capsules of $k = 0.7$ in a Vertical Pipe

The information provided in this section, regarding the flow of equi-density spherical capsules in vertical pipes, has a huge impact on the design process of HCPs, which is presented in Chapter 7. Similar kind of analysis that has been carried out in this section is also presented in the next chapter for the flow of equi-density spherical capsules in pipe bends.

5.3. Analysis of the Flow of Equi-Density Cylindrical Capsules in a Vertical HCP

Figure 5.20 depicts the pressure and velocity variations around a single cylindrical capsule of $k = 0.5$ at an average flow velocity of 1m/sec for a capsule length $L_c = 1 * d$. The pressure field around a cylindrical capsule resembles the pressure field around a spherical capsule. At upstream and downstream locations from the capsule, the pressure of water is 15727Pa and 13586Pa . The total pressure drop within the pipe is 10231Pa , which is 3% higher than a spherical capsule of same diameter and at same average flow velocity. Furthermore, it can be seen that the velocity profile is similar as observed in case of a horizontal pipe, i.e. higher velocity in the annulus region and the formation of a large wake region downstream of the capsule.

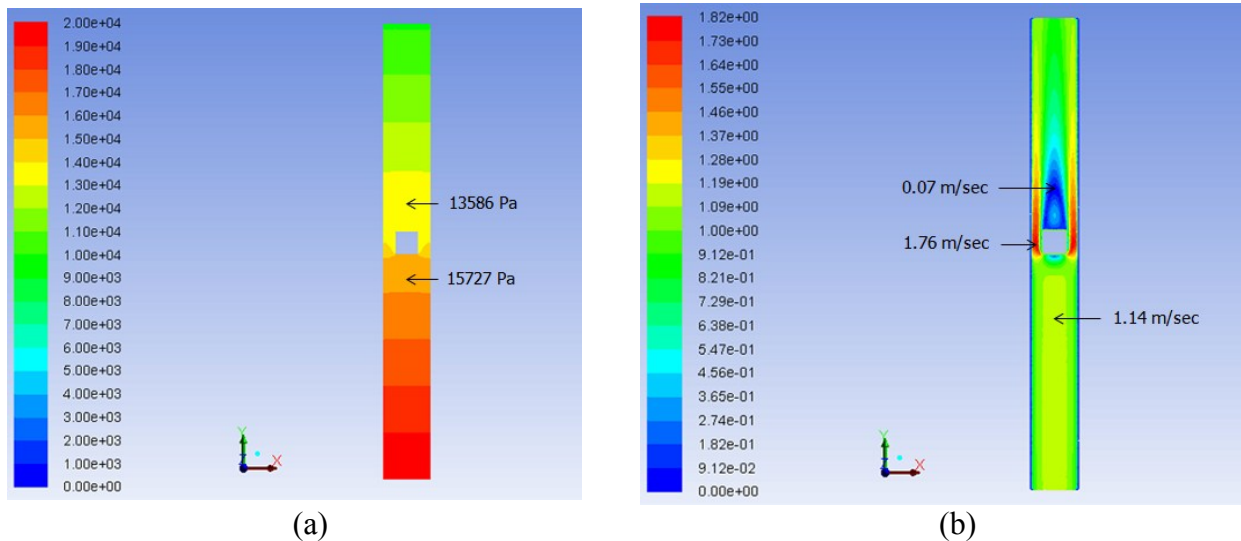


Figure 5.20. Variations in (a) Pressure and (b) Velocity, for a Cylindrical Capsule of $k = 0.5$ and $L_c = 1 * d$ in a Vertical Pipe at $V_{av} = 1\text{m/sec}$

Figure 5.21 shows the variations in C_p and u/u_{max} for the case under consideration, where C_p represents the coefficient of pressure and u is the local flow velocity along the pipe. It can be clearly seen that the pressure drop in case of a vertical pipe is considerably higher than the pressure drop in a horizontal pipe. Furthermore, the velocity profiles for both the vertical and horizontal pipelines transporting capsules are identical to each other suggesting the same velocity distribution within the pipeline.

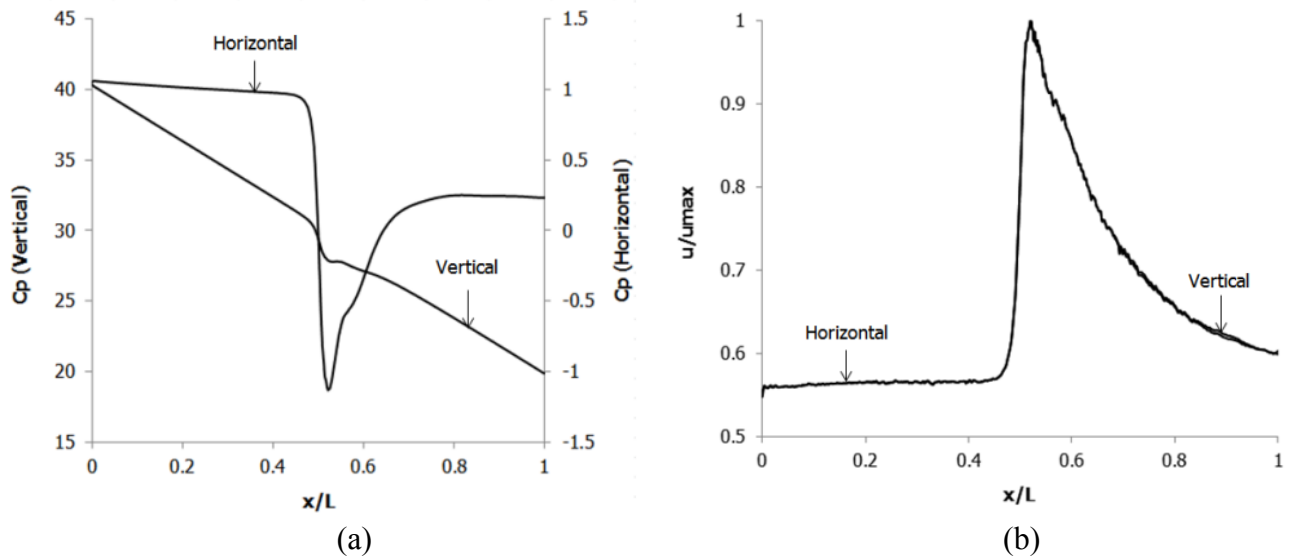


Figure 5.21. (a) Variations in C_p for a Cylindrical Capsule of $k = 0.5$ and $L_c = 1 * d$ in a Vertical Pipe at $V_{av} = 1\text{m/sec}$ (b) Variations in u/u_{max} for a Cylindrical Capsule of $k = 0.5$ and $L_c = 1 * d$ in a Vertical Pipe at $V_{av} = 1\text{m/sec}$

To further investigate the velocity distribution within the capsule transporting pipe, velocity profiles have been drawn across the cross-section of the pipe at both 0.1m upstream and downstream locations from the centre of the capsule as shown in figure 5.22. It can be seen that the velocity profile is undisturbed at the upstream location, and the presence of the capsule has not affected the velocity profile at this location. However, at the downstream location, the presence of the capsule in the pipe has distorted the velocity profile.

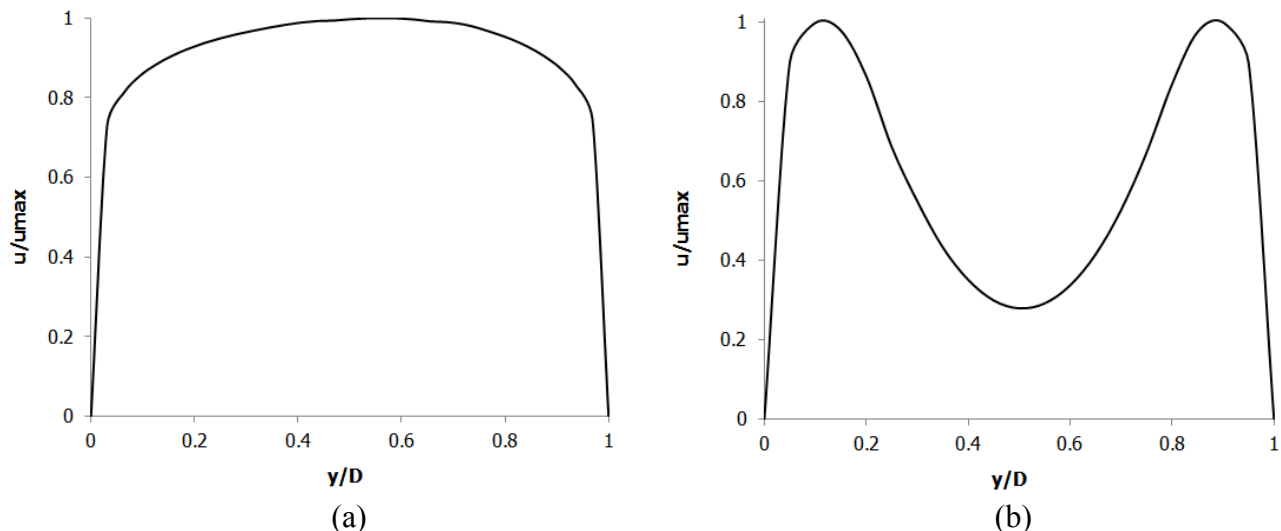


Figure 5.22. Variations in the Cross-Sectional Velocity Profiles for a Single Cylindrical Capsule of $k = 0.5$ and $L_c = 1 * d$ in a Vertical Pipe at $V_{av} = 1\text{m/sec}$ at (a) Upstream and (b) Downstream of the Capsule

Figure 5.23 depicts the variations in the velocity profiles at various locations within the cylindrical capsule transporting pipe under consideration at an average flow velocity of 1m/sec.

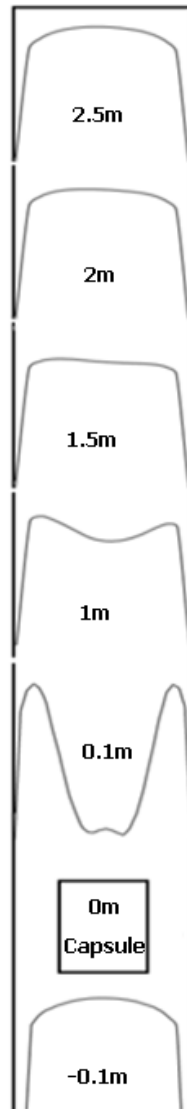


Figure 5.23. Development of Velocity Profile in the Presence of a Single Cylindrical Capsule in a Vertical Pipe having Density Equal to Water

5.3.1. Average Flow Velocity Effects

Figure 5.24 depicts the pressure and velocity variations within the test section of the pipe carrying a cylindrical capsule of $k = 0.5$ at an average flow velocity of 4m/sec. The length of the capsule $L_c = 1 * d$. It can be seen that both the pressure and velocity fields are identical to the one observed in case of a horizontal capsule transporting pipe. The pressure upstream of the capsule is 43% higher and downstream of the capsule is 37% lower as compared to $V_{av} = 1m/sec$.

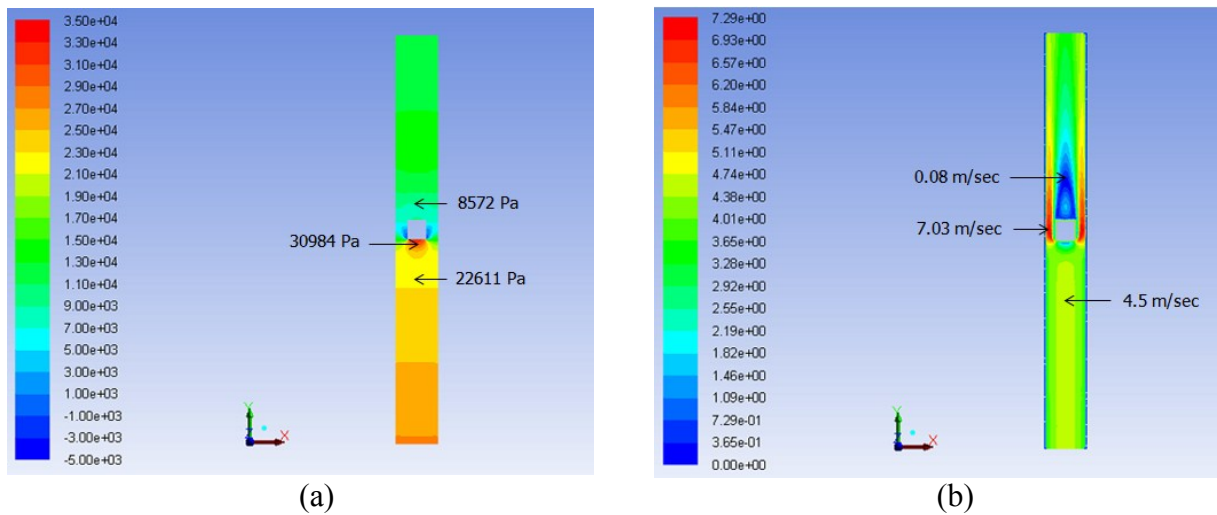


Figure 5.24. Variations in (a) Pressure and (b) Velocity, for a Cylindrical Capsule of $k = 0.5$ and $L_c = 1 * d$ in a Vertical Pipe at $V_{av} = 4\text{m/sec}$

Figure 5.25 shows the variations in C_p and u/u_{max} for the case under consideration. The profiles for an equi-density single cylindrical capsule flow in a horizontal pipe at $V_{av} = 4\text{m/sec}$ have also been included for comparison. It can be seen that the pressure drop in a vertical pipe is higher than the pressure drop in a horizontal pipe. Furthermore, the linear reduction in the pressure drop upstream and downstream of the capsule in a vertical pipe indicates the elevation effects. In figure 5.25 (b) the velocity distribution for both vertical and horizontal capsule transporting pipe at $V_{av} = 4\text{m/sec}$ have been plotted. It is clear from the figure that the velocity distribution in both the cases resembles each other indicating that the velocity variations are identical. More detailed results have been presented in table A-4.2.

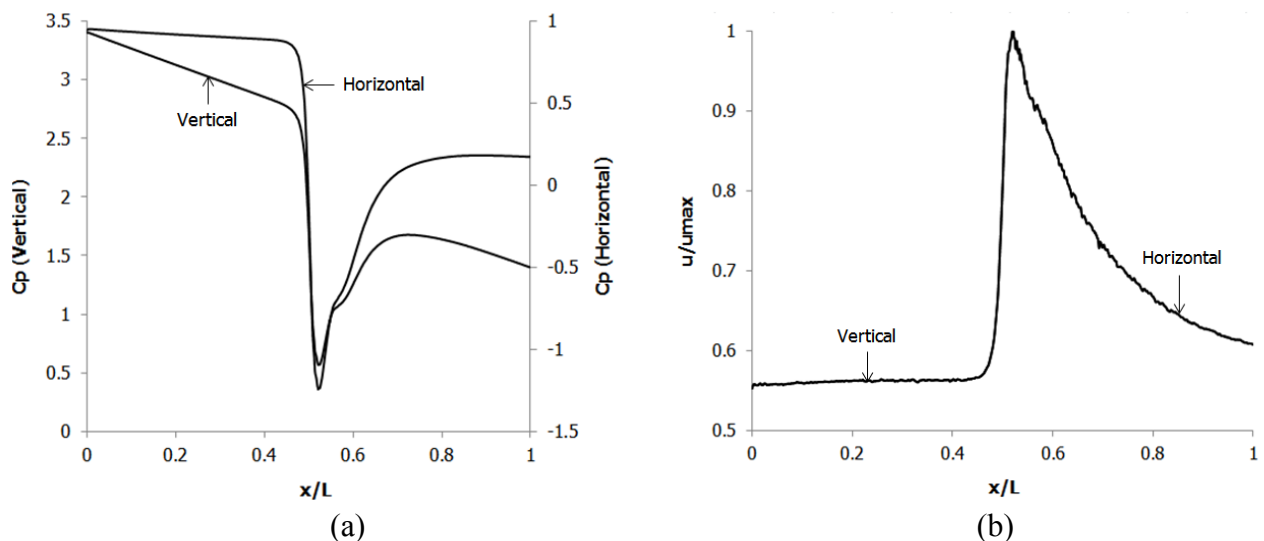


Figure 5.25. (a) Variations in C_p for a Cylindrical Capsule of $k = 0.5$ and $L_c = 1 * d$ in a Vertical Pipe at $V_{av} = 4\text{m/sec}$ (b) Variations in u/u_{max} for a Cylindrical Capsule of $k = 0.5$ and $L_c = 1 * d$ in a Vertical Pipe at $V_{av} = 4\text{m/sec}$

5.3.2. Length of the Capsule Effects

Figure 5.26 shows the pressure and velocity distributions in a cylindrical capsule transporting vertical pipe for $k = 0.5$, $L_c = 5 * d$ and $V_{av} = 1\text{m/sec}$. It can be seen that the overall pressure and velocity distributions seem to be the same as compared with $L_c = 1 * d$ at the same average flow velocity and capsule diameter. The pressure upstream of the capsule has increased by 0.44%, and the pressure downstream of the capsule has decreased by 16%. The pressure drop within the pipeline is 10219Pa which is 0.11% less than the pressure drop observed for $L_c = 1 * d$. Furthermore, the velocity field remains identical to one observed in $L_c = 1 * d$.

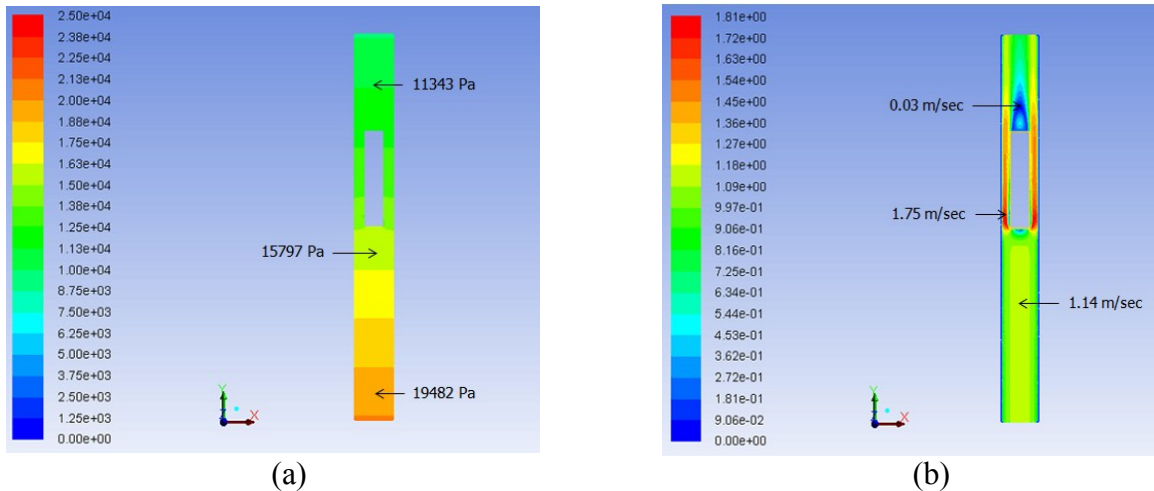


Figure 5.26. Variations in (a) Pressure and (b) Velocity, for a Single Cylindrical Capsule of $k = 0.5$ and $L_c = 5 * d$ in a Vertical Pipe at $V_{av} = 1\text{m/sec}$

Figure 5.27 shows the variations in C_p and u/u_{max} along the analysis line for the case under consideration. The results depict that both the pressure and velocity variations in a vertical pipe with a longer capsule, follow the same trend as observed in case of a shorter capsule. More detailed results have been presented in table A-4.2.

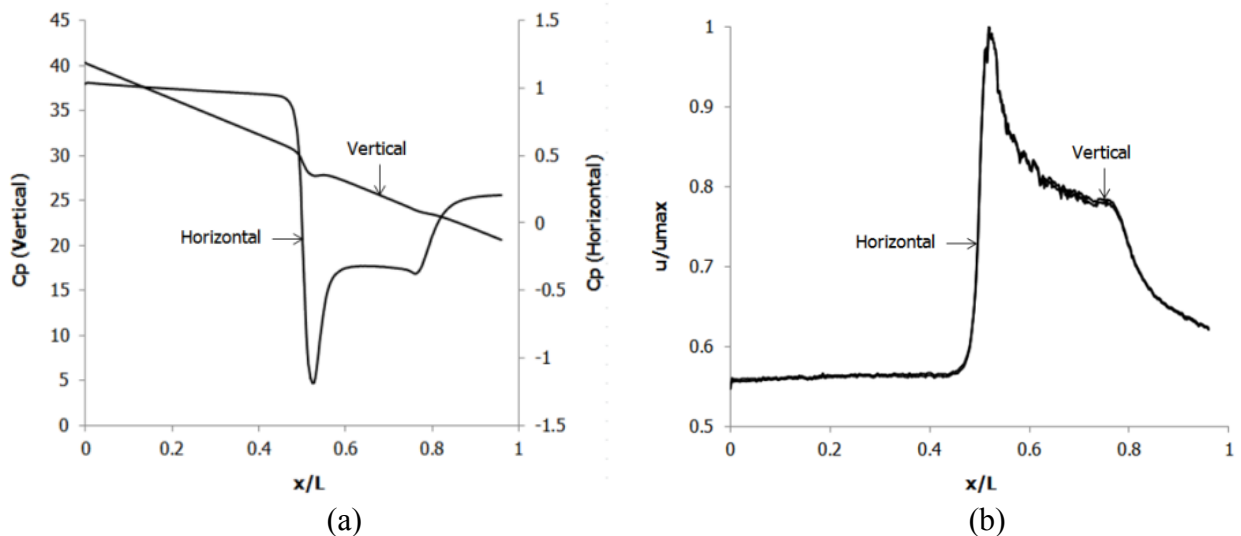


Figure 5.27. (a) Variations in C_p for a Single Cylindrical Capsule of $k = 0.5$ and $L_c = 5 * d$ in a Vertical Pipe at $V_{av} = 1\text{m/sec}$ (b) Variations in u/u_{max} for a Single Cylindrical Capsule of $k = 0.5$ and $L_c = 5 * d$ in a Vertical Pipe at $V_{av} = 1\text{m/sec}$

5.3.3. Capsule Diameter Effects

Figure 5.28 depicts the variations in the pressure field and C_p for an equi-density cylindrical capsule of $L_c = 5 * d$, $k = 0.9$ at $V_{av} = 1\text{m/sec}$ in a vertical pipe. The trend of the pressure distribution is the same as observed for $k = 0.5$ at same average flow velocity and for the same length of the capsule. The pressure at upstream and downstream locations from the capsule has increased by 132% and decreased by 29% respectively. An overall pressure drop increase of 191% has been observed in the present case compared with $k = 0.5$, $L_c = 1 * d$ and $V_{av} = 1\text{m/sec}$. Furthermore, in comparison with a horizontal pipeline carrying an equi-density cylindrical capsule of $k = 0.9$, the pressure drop in a vertical pipe is considerably higher. More detailed results have been presented in table A-4.2.

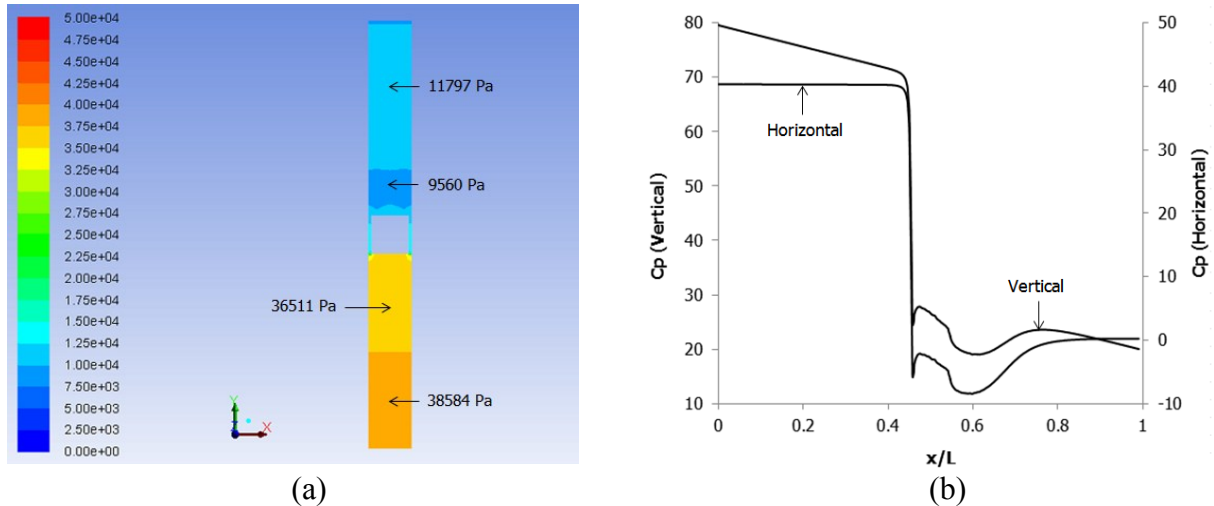


Figure 5.28. (a) Variations in Pressure for a Single Cylindrical Capsule of $k = 0.9$ and $L_c = 5 * d$ in a Vertical Pipe at $V_{av} = 1\text{m/sec}$ (b) Variations in C_p for a Single Cylindrical Capsule of $k = 0.9$ and $L_c = 5 * d$ in a Vertical Pipe at $V_{av} = 1\text{m/sec}$

5.3.4. Capsule Concentration Effects

Figure 5.29 depicts the pressure and velocity variations in a vertical hydraulic pipe carrying two cylindrical capsules of $k = 0.5$, $L_c = 1 * d$, $Sc = 1 * d$ and density equal to that of water. The trend of the pressure distribution is the same as observed for a single cylindrical capsule. The pressure at upstream and downstream locations has increased by 8.5% and decreased by 1.8% respectively as compared to a single cylindrical capsule. An overall pressure drop increase of 0.26% has been observed for $N = 2$ as compared to $N = 1$ at $V_{av} = 1\text{ m/sec}$. Furthermore, the velocity field is identical to $N = 1$, i.e. a high flow velocity in the annulus and a large wake region downstream of the capsules.

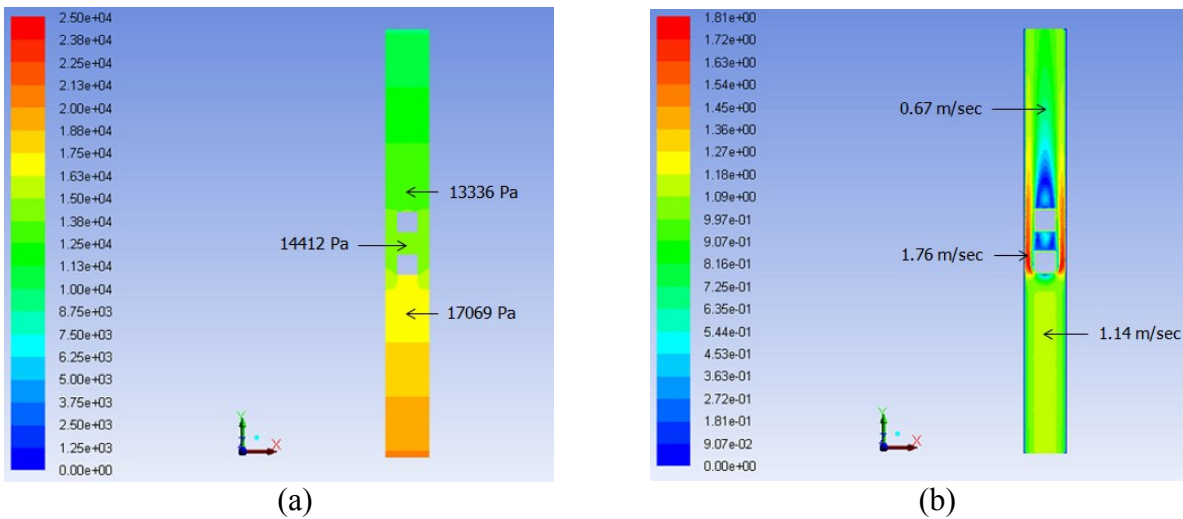


Figure 5.29. Variations in (a) Pressure and (b) Velocity, for Two Cylindrical Capsules of $k = 0.5$, Sc and $Lc = 1 * d$ in a Vertical Pipe at $V_{av} = 1\text{m/sec}$

Figure 5.30 shows the variations in C_p and u/u_{max} along the analysis line for the case under consideration. The results depict that the pressure drop for two cylindrical capsules in a vertical pipe is higher than for a horizontal pipe. Furthermore, the velocity profiles along the analysis line are identical for both the cases. More detailed results have been presented in table A-4.2.

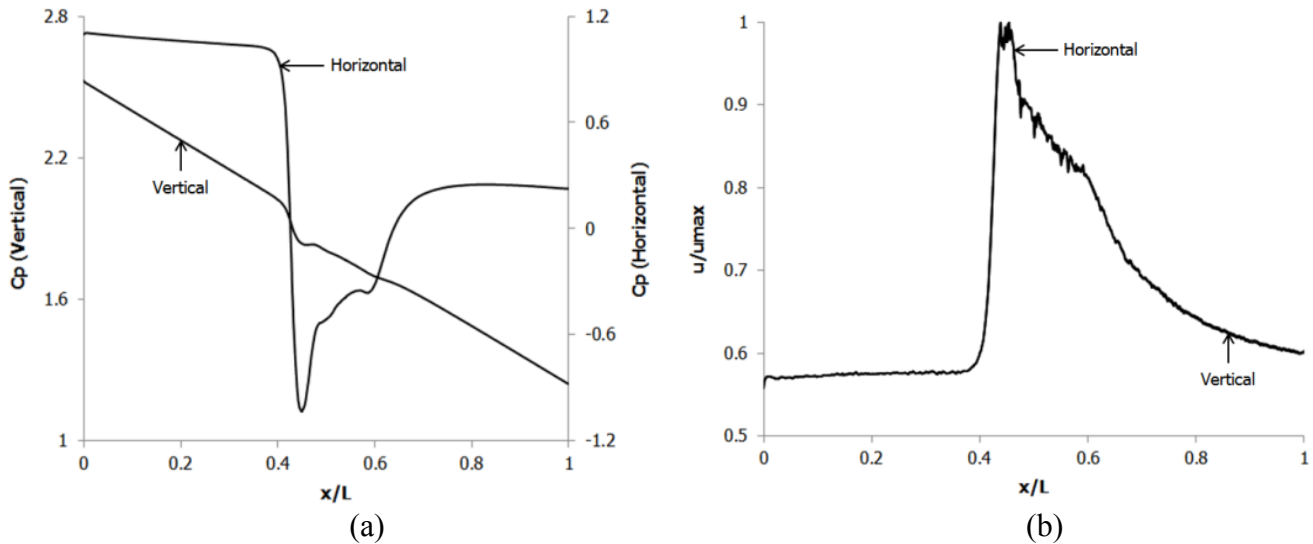


Figure 5.30. (a) Variations in C_p for Two Cylindrical Capsules of $k = 0.5$, Sc and $Lc = 1 * d$ in a Vertical Pipe at $V_{av} = 1\text{m/sec}$ (b) Variations in u/u_{max} for Two Cylindrical Capsules of $k = 0.5$, Sc and $Lc = 1 * d$ in a Vertical Pipe at $V_{av} = 1\text{m/sec}$

5.3.5. Effects of Spacing between the Capsules

Figure 5.31 depicts the effect of spacing between the capsules ($Sc = 5 * d$) on the pressure and velocity distribution within the pipe. It can be seen that both the pressure and velocity fields resemble the one observed in case of $Sc = 1 * d$ in figure 5.29. However, the pressure upstream of the capsule has

increased by 15% whereas the pressure downstream of the capsules has decreased by 2%. Hence, the pressure drop marginally increases in comparison with other parameters, and the overall pressure drop for the case under consideration is 10469Pa.

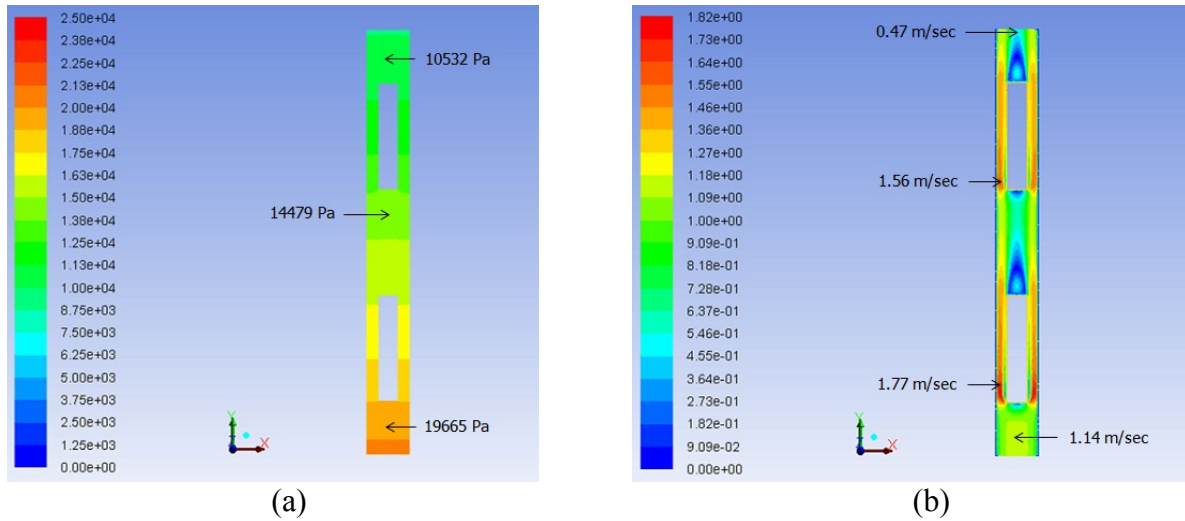


Figure 5.31. Variations in (a) Pressure and (b) Velocity, for Two Cylindrical Capsules of $k = 0.5$, $Sc = 5 * d$ and $Lc = 5 * d$ in a Vertical Pipe at $V_{av} = 1\text{m/sec}$

Figure 5.32 shows the variations in C_p and u/u_{max} along the analysis line for the case under consideration. The results depict that the pressure drop is higher for a vertical pipe in comparison with a horizontal pipe. Moreover, the velocity distribution is similar for both the pipes. More detailed results have been presented in table A-4.2.

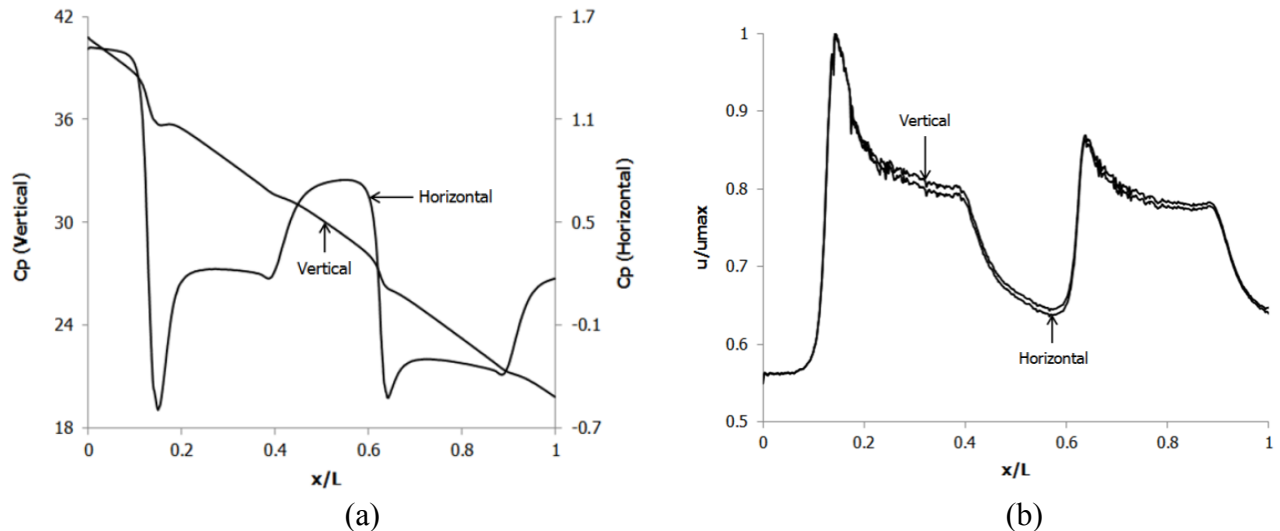


Figure 5.32. (a) Variations in C_p for Two Cylindrical Capsules of $k = 0.5$, $Sc = 5 * d$ and $Lc = 5 * d$ in a Vertical Pipe at $V_{av} = 1\text{m/sec}$ (b) Variations in u/u_{max} for Two Cylindrical Capsules of $k = 0.5$, $Sc = 5 * d$ and $Lc = 5 * d$ in a Vertical Pipe at $V_{av} = 1\text{m/sec}$

Table A-4.2 in Appendix A-4 summarises the results for various CFD based investigations being carried out on the flow of cylindrical capsules in a vertical pipe with density equal to that of water.

Further analysing the results obtained in the table above, figure 5.33 depicts the variation in the normalised pressure drop in the test section of the pipe for a single cylindrical capsule having $L_c = 1 * d$. The results show that as the flow velocity increases, the pressure drop in the test section of the pipe increases. Furthermore, as the size of the capsule increases, the pressure drop further increases. It is evident from table A-4.2 and Figure 5.33 that equi-density cylindrical capsules of diameter equal to 90% of the pipeline offer substantial pressure drop and hence are not recommended for practical applications. The pressure drop for $k = 0.9$ is 643% higher on average than capsules of $k = 0.5$ at the same average flow velocity and the same capsule length. Whereas, the pressure drop for $k = 0.7$ is 65% higher on average than capsules of $k = 0.5$ at the same average flow velocities and the same length of the capsule.

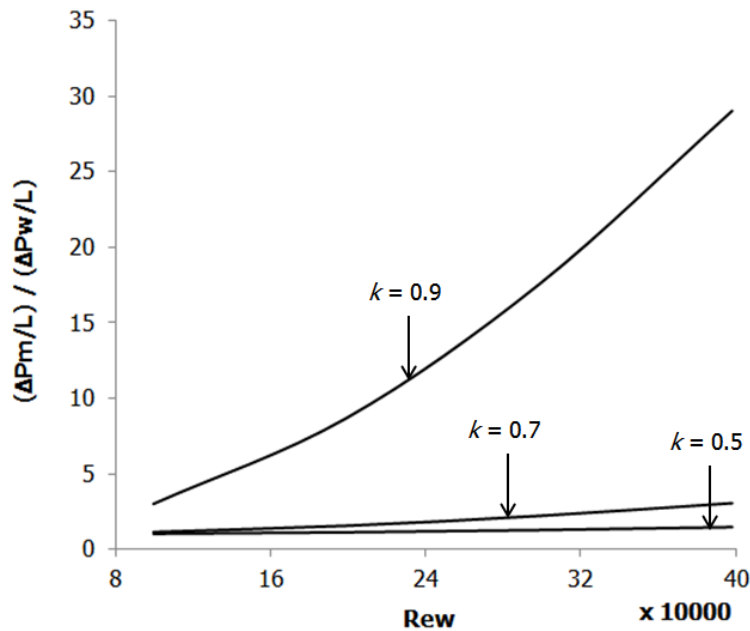


Figure 5.33. Variations in Normalised Pressure Drop for a Single Equi-Density Cylindrical Capsule of $L_c = 1 * d$ in a Vertical Pipe

The results presented in figure 5.34 depicts the normalised pressure drop for a cylindrical capsule of $k = 0.7$ having various lengths. It can be seen that as the length of the capsule increases, the normalised pressure drop increases. The same trend has been observed for equi-density cylindrical capsules in a horizontal pipeline (figure 4.37).

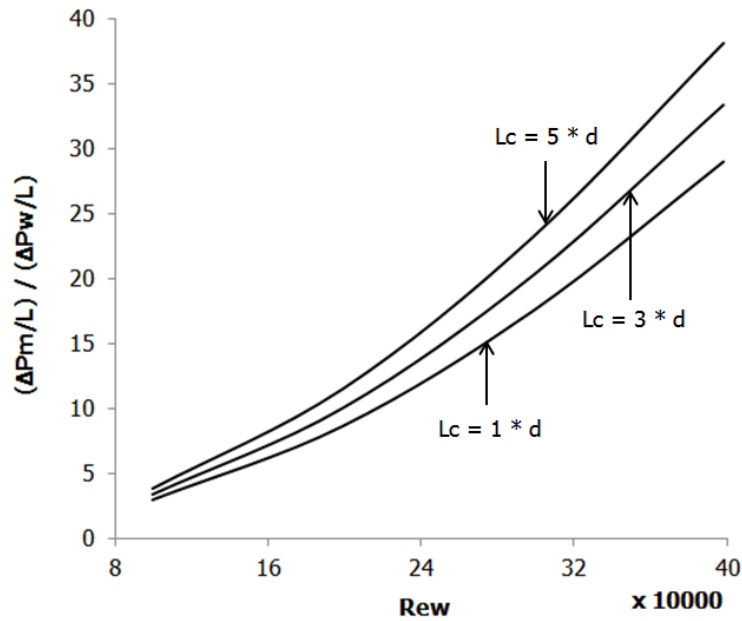


Figure 5.34. Variations in Normalised Pressure Drop for a Single Equi-Density Cylindrical Capsule of $k = 0.7$ in a Vertical Pipe

Figure 5.35 depicts the variations in the normalised pressure drop for two cylindrical capsules of $L_c = 1 * d$ and $Sc = 1 * d$. It is again noted here that the pressure drop for $k = 0.9$ is significantly higher than for $k = 0.5$ and 0.7 and hence the capsules of diameter equal to $0.9 * d$ are not recommended for practical applications. Moreover, in comparison with figure 5.33, it is clear that an increase in the concentration of the capsule increases the pressure drop within the vertical pipeline.

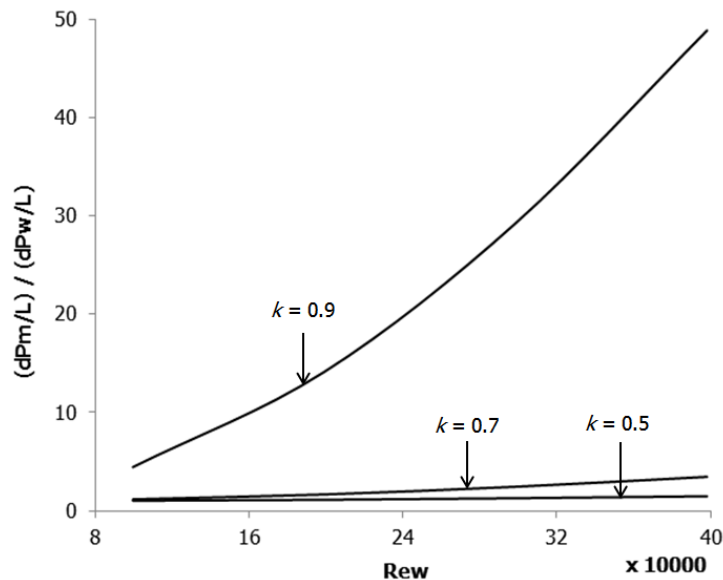


Figure 5.35. Variations in Normalised Pressure Drop for Two Equi-Density Cylindrical Capsules of $L_c = 1 * d$ and $Sc = 1 * d$ in a Vertical Pipe

Figure 5.36 depicts the variations in the normalised pressure drop to analyse the effects of the spacing between the capsules. It can be seen that as the spacing between the capsules increases, the normalised pressure drop increases. This trend is similar to the one observed in case of a horizontal pipeline (figure 4.39)

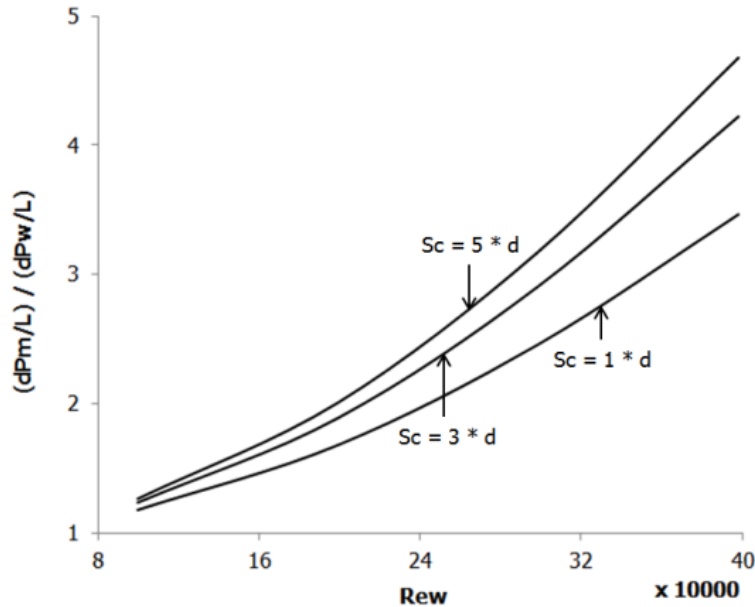


Figure 5.36. Variations in Normalised Pressure Drop for Two Equi-Density Cylindrical Capsules of $L_c = 1 * d$ and $k = 0.7$ in a Vertical Pipe

The information provided in this section, regarding the flow of equi-density cylindrical capsules in vertical pipes, has a huge impact on the design process of HCPs, which is presented in Chapter 7. Similar kind of analysis that has been carried out in this section is also presented in the next chapter for the flow of equi-density cylindrical capsules in pipe bends.

5.4. Analysis of the Flow of Heavy-Density Spherical Capsules in a Vertical HCP

The flow of heavy density capsules in a vertical pipe is different from the flow of heavy-density spherical capsules in a horizontal pipeline. The reason is the direction of the gravitational acceleration acting on the capsules in any pipeline. In contrast to the flow of heavy-density capsules on the bottom wall of a horizontal pipeline, the capsules in a vertical pipeline travel along the centreline of the pipe. As the weight of the capsules is directed towards the centre of the earth, in a vertical pipe, for both the equi-density and heavy-density capsules, the trajectory remains the same, i.e. propagation of the capsules along the centreline of the pipe. Hence, the flow structure within a vertical pipeline, carrying heavy-density spherical or cylindrical capsules, resembles the flow structure observed for the flow of equi-density capsules in a vertical pipeline. Thus, the motion of the capsules is dominated by the translational velocity in comparison with rotational velocity. Furthermore, due to the alignment of the capsules in the centre of the pipe, the complex flow structures, which were observed in case of a

horizontal pipeline carrying heavy-density capsules, are not expected to occur in a vertical pipeline transporting capsules.

Figure 5.37 depicts the variations in the pressure and velocity distribution within the test section of the pipe transporting a single spherical capsule of $k = 0.5$ at $V_{av} = 2\text{m/sec}$. Using the DPM model available in CFD, it can be shown that spherical capsules of $k = 0.5$ and density equal to aluminium (2695kg/m^3) cannot propagate along a vertical pipe if the average flow velocity is 1m/sec . Furthermore, equation (3.22), which has been used for the determination of heavy-density spherical capsule's velocities in a vertical pipeline, results in negative capsule velocity at $V_{av} = 1\text{m/sec}$. Hence, V_{av} of 2m/sec onwards has been considered in the present case. The figure depicts that both the pressure and velocity fields resemble the one observed in case of equi-density spherical capsule flow in a vertical pipe (figure 5.5). The total pressure drop in the pipe is 10255Pa .

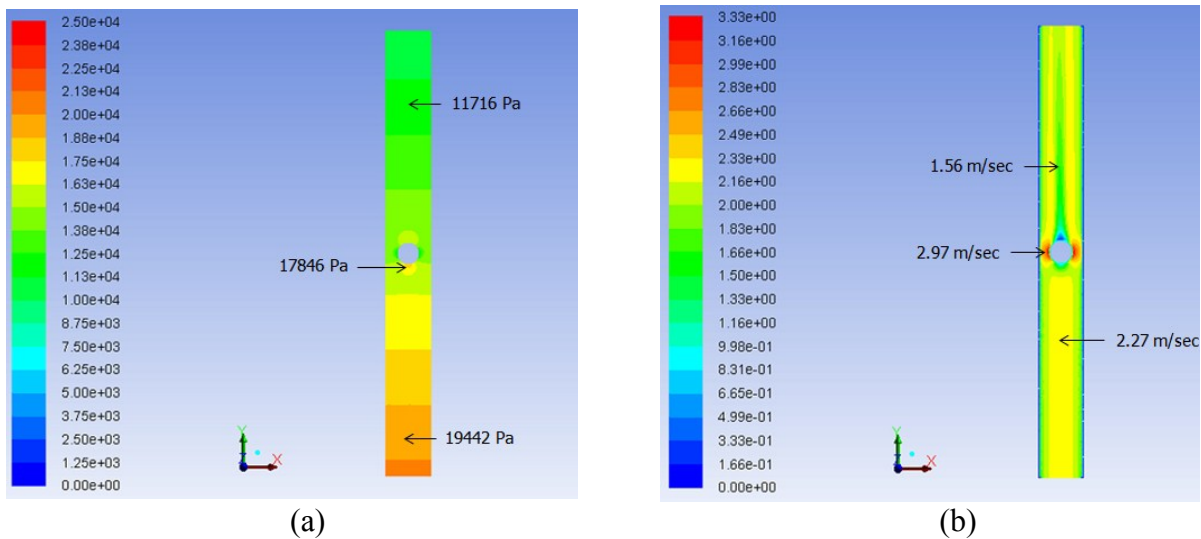


Figure 5.37. Variations in (a) Pressure and (b) Velocity, for a Single Spherical Capsule of $k = 0.5$ in a Vertical Pipe at $V_{av} = 2\text{m/sec}$

Figure 5.38 shows the variations in C_p and u/u_{max} along the analysis line for the case under consideration, where C_p represents the coefficient of pressure and u is the local flow velocity along the pipe. The results depict that the pressure drop for heavy-density capsules in a vertical pipe is higher than a horizontal pipe. This trend is consistent with the one observed in case of equi-density spherical capsule flow in a vertical pipe. Furthermore, the velocity distribution in figure 5.38 (b) reveals a marked difference between the velocity variations in the vertical and horizontal pipes. This is due to the fact that the heavy-density spherical capsules propagate along the bottom wall of the horizontal pipe whereas in case of a vertical pipe, the flow of heavy-density spherical capsules is along the centreline of the pipe.

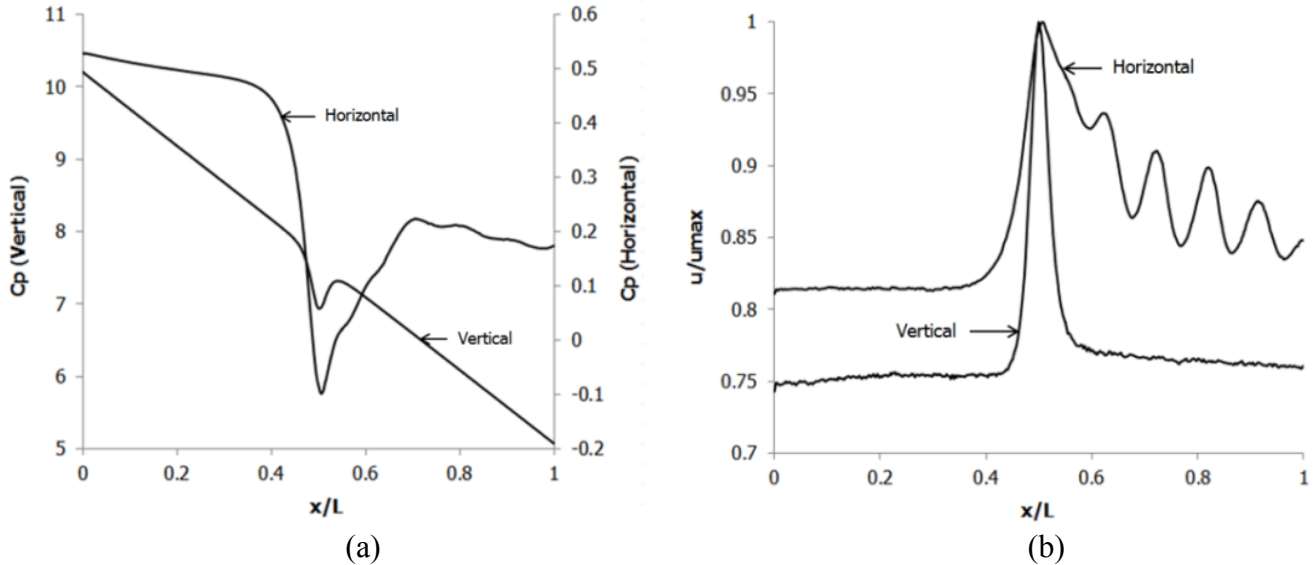


Figure 5.38. (a) Variations in C_p for a Single Spherical Capsule of $k = 0.5$ in a Vertical Pipe at $V_{av} = 2\text{m/sec}$ (b) Variations in u/u_{max} for a Single Spherical Capsule of $k = 0.5$ in a Vertical Pipe at $V_{av} = 2\text{m/sec}$

Figure 5.38 (b) depicts that the flow velocity at both upstream and downstream locations from the capsule is higher for heavy-density capsule as compared to an equi-density capsule. This is due to the eccentric orientation of the capsule within the pipe. There is more space available for the flow of those layers of water, which have higher velocity, i.e. in the centre of the pipe. Furthermore, the presence of the swirling flow packets can be clearly seen downstream the heavy-density spherical capsule. The dynamics of these packets reveals that the maximum flow velocity is in the centre of the packets. The flow velocity reduces radially in these packets.

To further investigate the velocity distribution within the heavy-density spherical capsule transporting vertical pipe, velocity profiles have been drawn across the cross-section of the pipe at both 0.1m upstream and downstream locations from the centre of the capsule as shown in figure 5.39. It can be seen that the velocity profile is undisturbed at the upstream location, and the presence of the capsule has not affected the velocity profile at this location. However, at the downstream location, the presence of the capsule in the pipe has distorted the velocity profile.

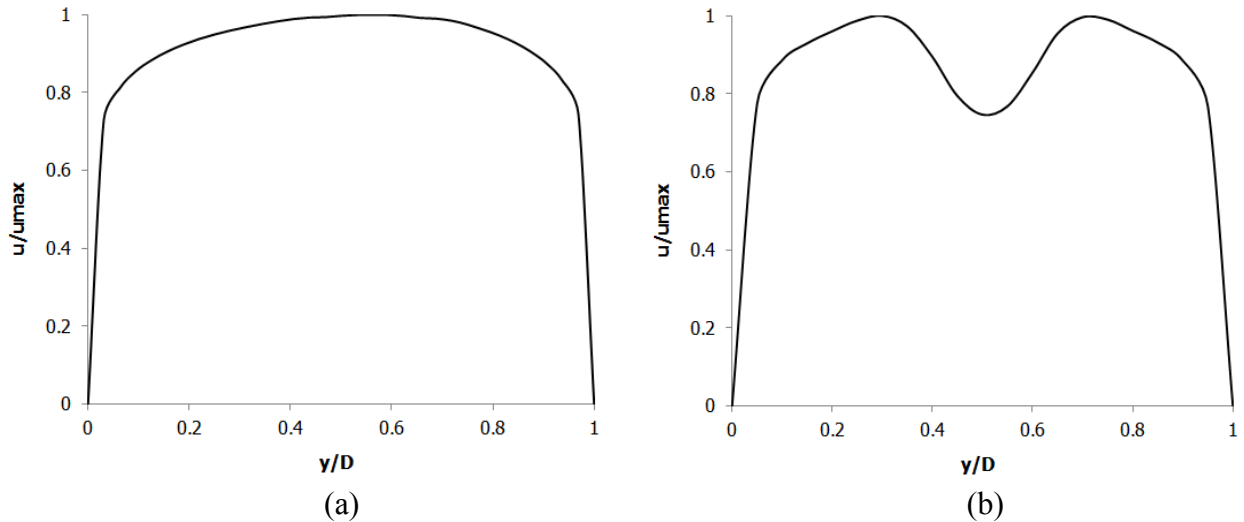


Figure 5.39. Variations in the Cross-Sectional Velocity Profiles for a Single Spherical Capsule of $k = 0.5$ in a Vertical Pipe at $V_{av} = 2\text{m/sec}$ at (a) Upstream and (b) Downstream of the Capsule

Figure 5.40 depicts the variations in the velocity profiles at various locations within the capsule transporting pipe under consideration at an average flow velocity of 1m/sec .

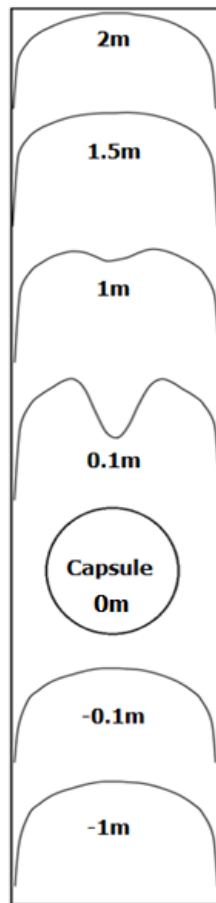


Figure 5.40. Development of Velocity Profile in the Presence of a Single Spherical Capsule in a Vertical Pipe having Density Greater than Water

5.4.1. Average Flow Velocity Effects

To investigate the effect of the average flow velocity on the flow structure within the pipe, an average velocity of 4m/sec for a heavy-density spherical capsule of $k = 0.5$ has been chosen for flow diagnostics. Figure 5.41 depicts the pressure and velocity variations in the capsule transporting pipe for an average flow velocity of 4m/sec, keeping $k = 0.5$. The trend of pressure distribution is the same as observed for $V_{av} = 2\text{m/sec}$. The pressure upstream and downstream of the capsule has increased by 4.5% and 23% respectively. The pressure drop between the inlet and the outlet of the pipe is 11361Pa, which is 10% higher than the pressure drop for $V_{av} = 2\text{m/sec}$. It can be concluded that increase in the average velocity of the flow increases the pressure drop. Furthermore, it can be seen in figure 5.41 (b) that the velocity field resembles the one observed in case of $V_{av} = 2\text{m/sec}$.

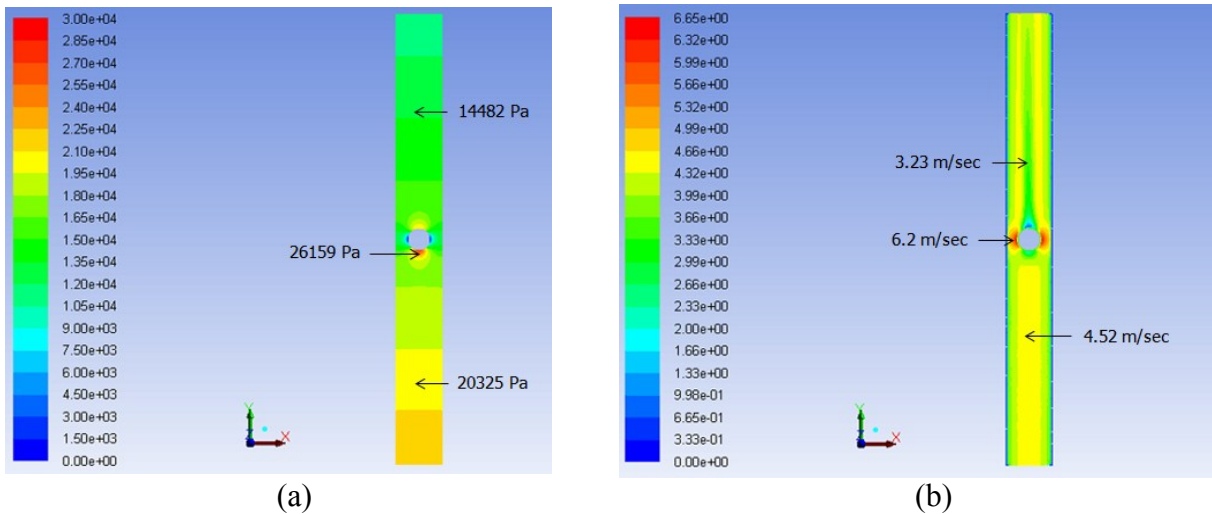


Figure 5.41. Variations in (a) Pressure and (b) Velocity, for a Single Spherical Capsule of $k = 0.5$ in a Vertical Pipe at $V_{av} = 4\text{m/sec}$

Figure 5.42 shows the variations in C_p and u/u_{max} along the analysis line for the case under consideration. The results depict that the pressure drop for heavy-density spherical capsule in a vertical pipe is higher as compared to the pressure drop in a horizontal pipe. Furthermore, the velocity distribution for the vertical pipe resembles the one observed for $V_{av} = 2\text{m/sec}$. More detailed results have been presented in table A-4.3.

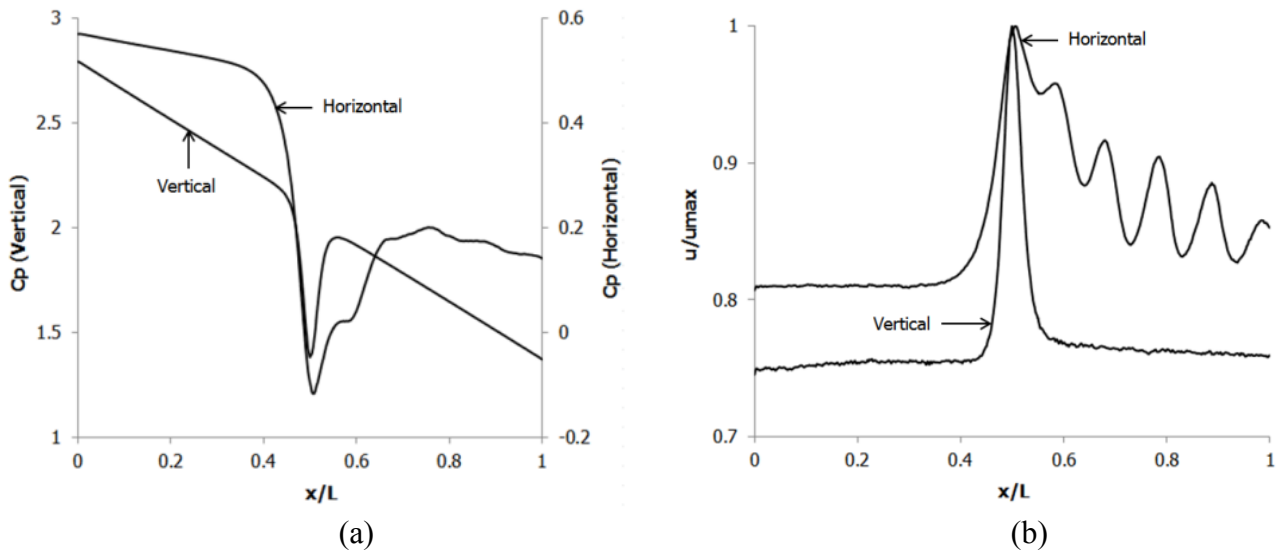


Figure 5.42. (a) Variations in C_p for a Single Spherical Capsule of $k = 0.5$ in a Vertical Pipe at $V_{av} = 4\text{m/sec}$ (b) Variations in u/u_{max} for a Single Spherical Capsule of $k = 0.5$ in a Vertical Pipe at $V_{av} = 4\text{m/sec}$

5.4.2. Capsule Diameter Effects

Figure 5.43 shows the pressure and velocity distributions in a heavy-density spherical capsule transporting vertical pipe for $k = 0.9$ and $V_{av} = 1\text{m/sec}$. As the capsule size becomes bigger (in the present case), the area of the capsule in the centre of the pipe increases; increasing the effective area of the capsule meeting with the high velocity gradients of the flow. This increases the force being exerted on the capsule and hence the capsule is propagated along the pipe. This is the reason that $k = 0.9$ capsule can travel along a vertical pipe at $V_{av} = 1\text{m/sec}$.

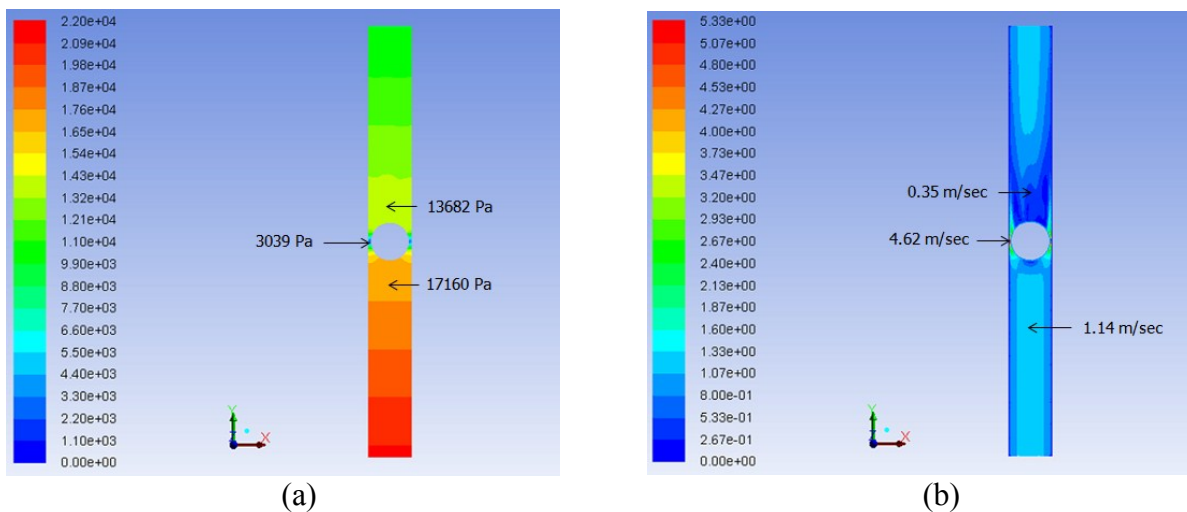


Figure 5.43. (a) Variations in Pressure for a Single Spherical Capsule of $k = 0.9$ in a Vertical Pipe at $V_{av} = 1\text{m/sec}$ (b) Variations in C_p for a Single Spherical Capsule of $k = 0.9$ in a Vertical Pipe at $V_{av} = 1\text{m/sec}$

Figure 5.44 shows the variations in C_p and u/u_{max} along the analysis line for the case under consideration. The results depict that the pressure drop in case of a vertical pipe is higher than a horizontal pipe. It is noteworthy here that the effect of the presence of the capsule in the pipe is more pronounced as compared to the flow of equi-density spherical capsule in a vertical pipe. This is due to the fact that the capsule velocity is considerably lower but the trajectory is the same, hence, increasing the resistance to the flow of water within the pipe by blocking the area for the flow. This imparts additional pressure drop in the pipeline. More detailed results have been presented in table A-4.3.

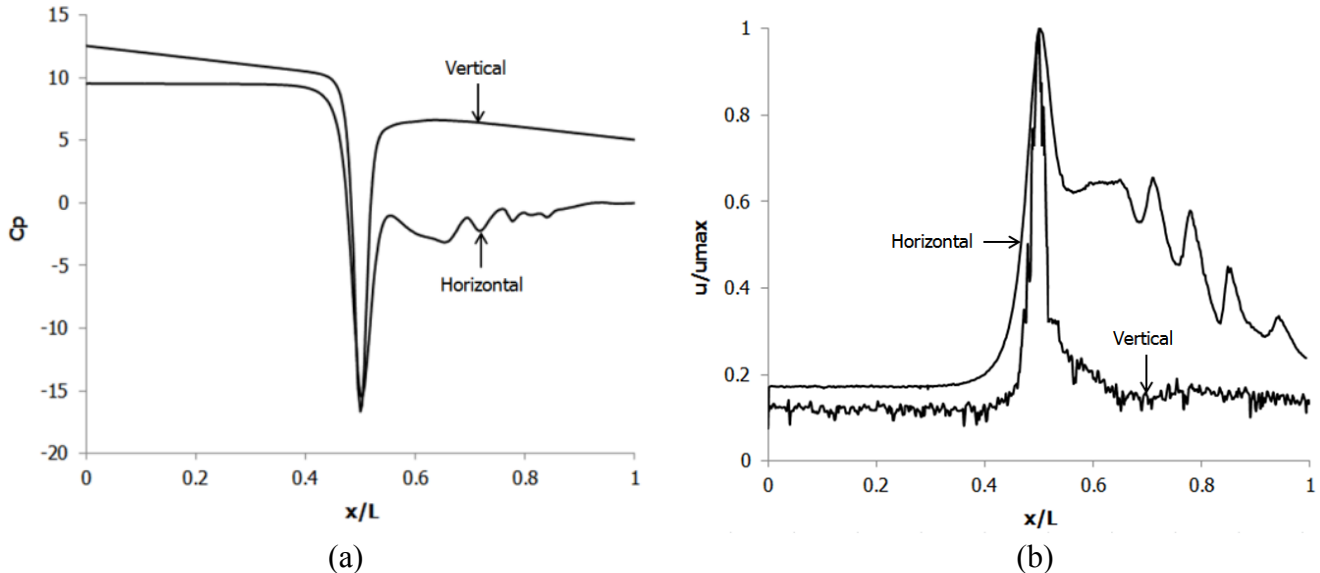


Figure 5.44. (a) Variations in C_p for a Single Spherical Capsule of $k = 0.5$ in a Vertical Pipe at $V_{av} = 1\text{m/sec}$ (b) Variations in u/u_{max} for a Single Spherical Capsule of $k = 0.5$ in a Vertical Pipe at $V_{av} = 1\text{m/sec}$

5.4.3. Capsule Concentration Effects

Figure 5.45 depicts the pressure and velocity variations in a vertical pipe carrying three heavy-density spherical capsules of $k = 0.5$, $Sc = 1 * d$ and $V_{av} = 2\text{m/sec}$. The trend of the pressure distribution is the same as observed for a single heavy-density spherical capsule. The pressure at upstream location has decreased by 6%. An overall pressure drop increase of 2.9% has been observed for $N = 3$ as compared to $N = 1$. Furthermore, as compared to a single heavy-density spherical capsule, it can be seen that the velocity field is similar.

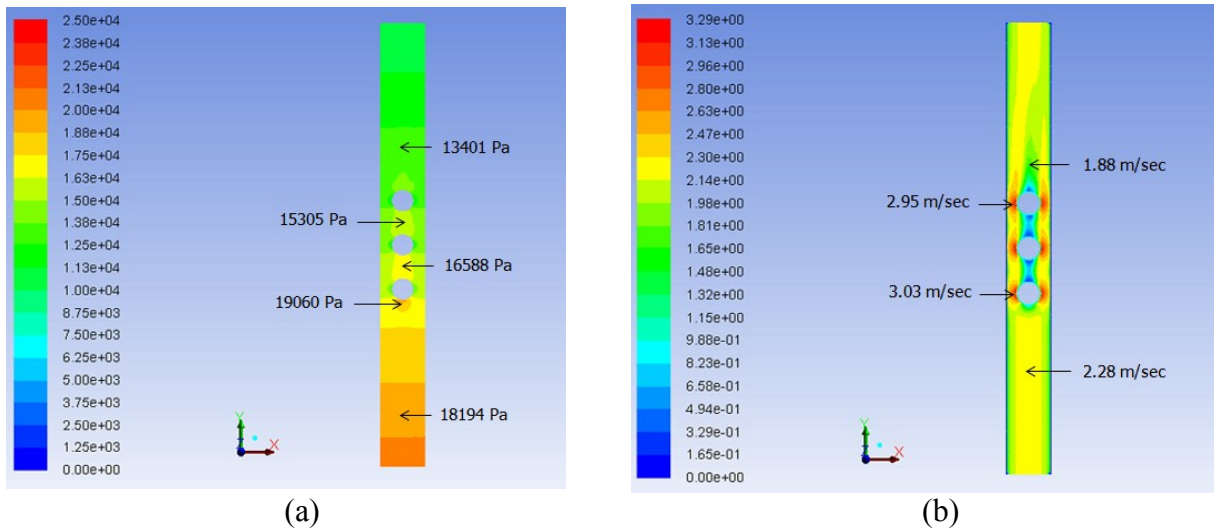


Figure 5.45. Variations in (a) Pressure and (b) Velocity, for Three Spherical Capsules of $k = 0.5$ and $Sc = 1 * d$ in a Vertical Pipe at $V_{av} = 2\text{m/sec}$

Figure 5.46 represents the variations in C_p and u/u_{max} for the case under consideration. It can be clearly seen that the pressure drop for heavy-density spherical capsules in a vertical pipe is considerably higher than a horizontal pipe. Furthermore, the velocity profile is completely different for both the cases. More detailed results have been presented in table A-4.3.

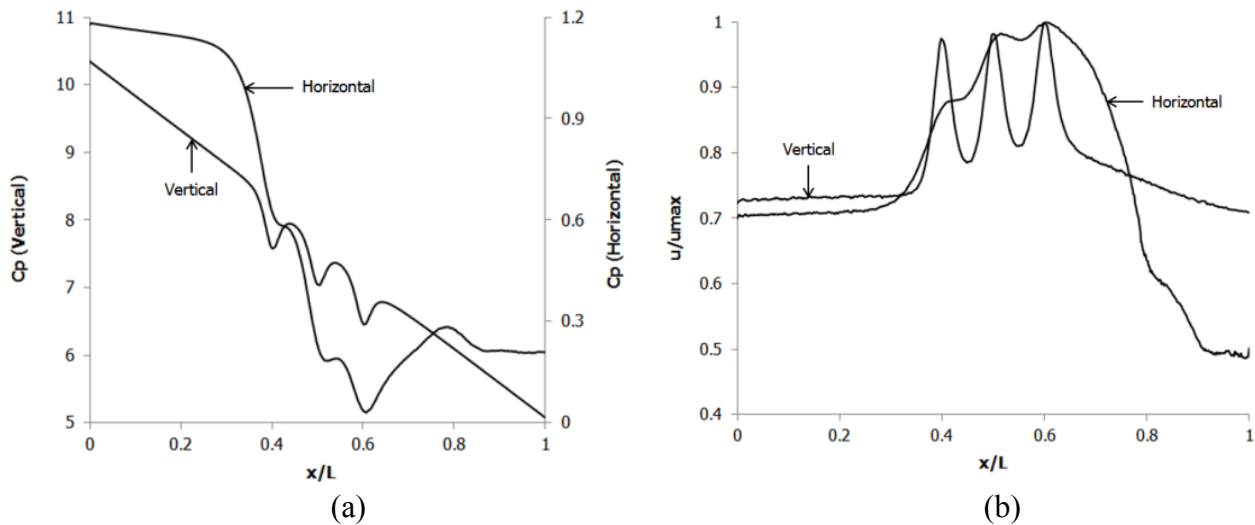


Figure 5.46. (a) Variations in C_p for Three Spherical Capsules of $k = 0.5$ and $Sc = 1 * d$ in a Vertical Pipe at $V_{av} = 2\text{m/sec}$ (b) Variations in u/u_{max} for Three Spherical Capsules of $k = 0.5$ and $Sc = 1 * d$ in a Vertical Pipe at $V_{av} = 2\text{m/sec}$

5.4.4. Effects of Spacing between the Capsules

Figure 5.47 depicts the pressure and velocity variations in a hydraulic pipe carrying three heavy-density spherical capsules of $k = 0.5$, $Sc = 5 * d$ and $V_{av} = 2\text{m/sec}$. The pressure distribution is the same as observed for $Sc = 1 * d$. The pressure at upstream and downstream locations has increased by 8% and decreased by 17% respectively as compared to $Sc = 1 * d$. A marginal pressure drop decrease (0.44%) has been observed for $Sc = 5 * d$ as compared to $1 * d$. Furthermore, the velocity field in the vicinity of each capsule resembles the one observed for a single heavy-density spherical capsule.

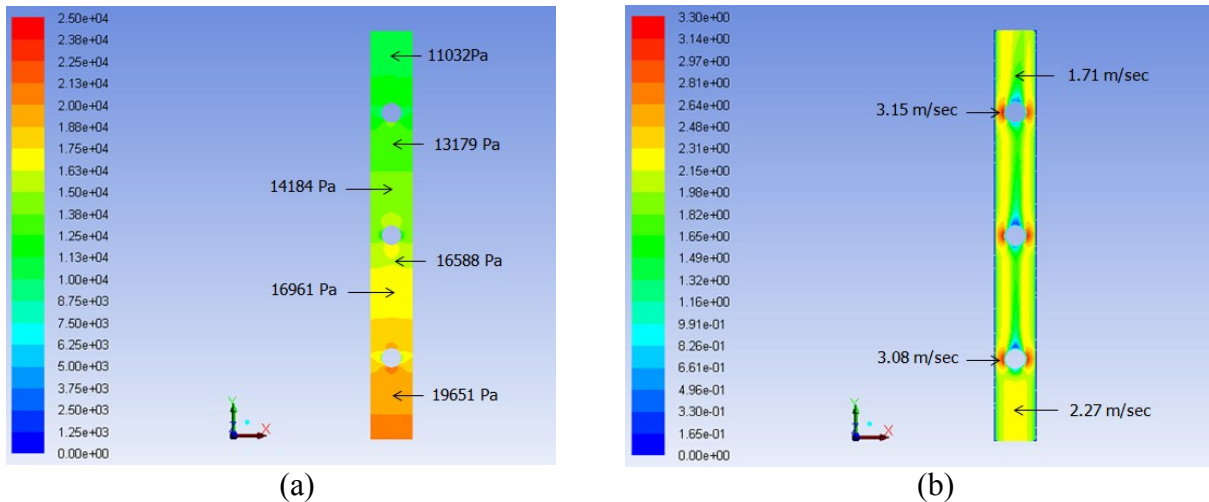


Figure 5.47. Variations in (a) Pressure and (b) Velocity, for Three Spherical Capsules of $k = 0.5$ and $Sc = 5 * d$ in a Vertical Pipe at $V_{av} = 2\text{m/sec}$

Figure 5.48 represents the variations in C_p and u/u_{max} for the case under consideration. It can be seen that the pressure drop for heavy-density spherical capsules in a vertical pipe is considerably higher than a horizontal pipe. Furthermore, the velocity distribution in a vertical pipe is completely different from the one observed in a horizontal pipe. More detailed results have been presented in table A-4.3.

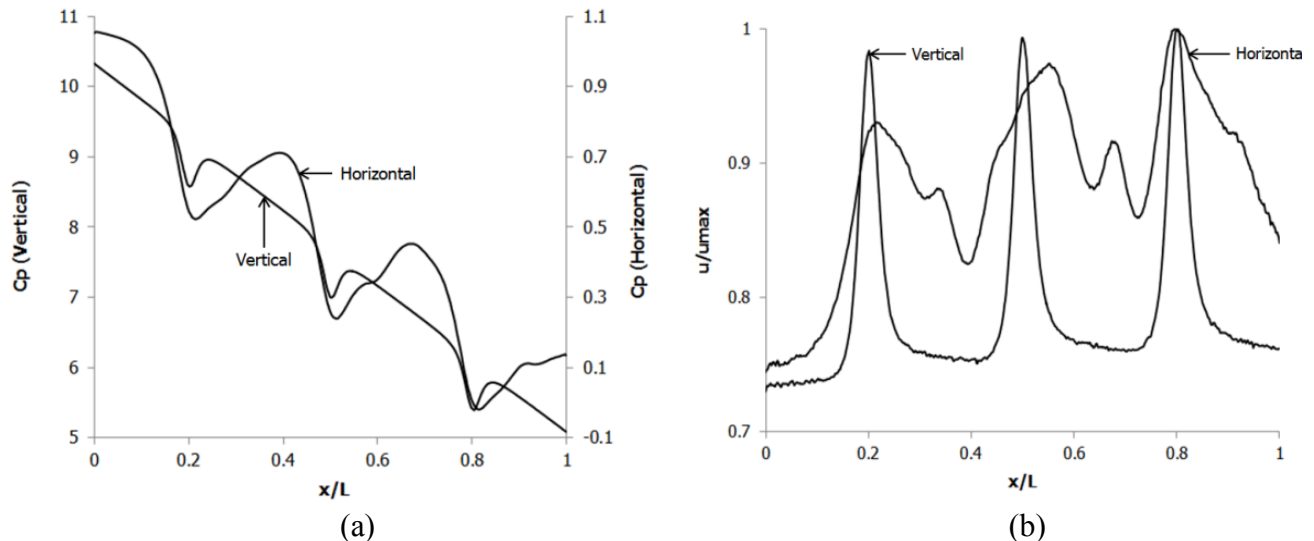


Figure 5.48. (a) Variations in C_p for Three Spherical Capsules of $k = 0.5$ and $Sc = 5 * d$ in a Vertical Pipe at $V_{av} = 2\text{m/sec}$ (b) Variations in u/u_{max} for Three Spherical Capsules of $k = 0.5$ and $Sc = 5 * d$ in a Vertical Pipe at $V_{av} = 2\text{m/sec}$

Table A-4.3 in Appendix A-4 summarises the results for various CFD based investigations being carried out on the flow of heavy-density spherical capsules in a vertical pipe.

Figure 5.49 depicts the variation in the normalised pressure drops in the test section of the pipe for a train three heavy-density spherical capsules having a spacing of $1 * d$ between the consecutive capsules respectively. The results show that as the flow velocity increases, the pressure drop in the test section of the pipe increases. Furthermore, as the size of the capsule increases, the pressure drop further increases. It is evident that heavy-density spherical capsules of diameter equal to 90% of the pipeline offer substantial pressure drop and hence are not recommended for practical applications.

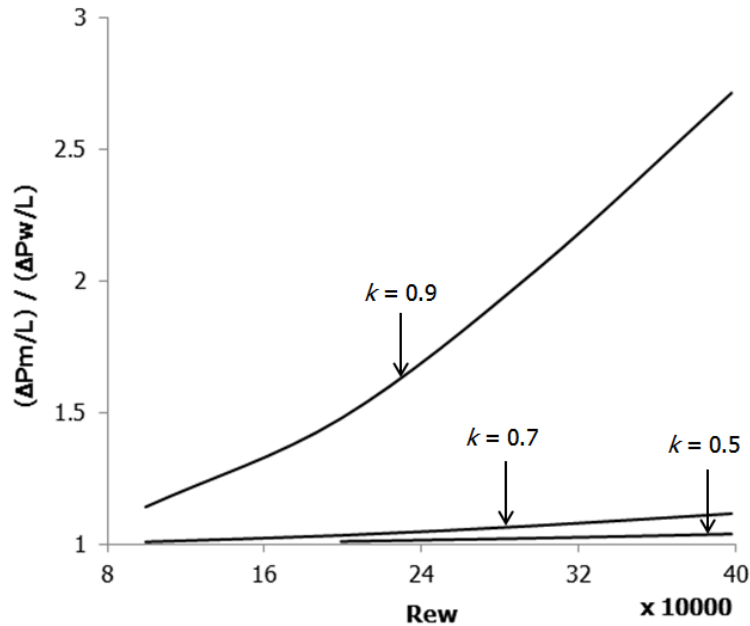


Figure 5.49. Variations in Normalised Pressure Drop for a Heavy-Density Spherical Capsule in a Vertical Pipe

Figure 5.50 depicts the variations in the normalised pressure drop for a heavy-density spherical capsule train consisting of three capsules having $Sc = 1 * d$. It can be seen that as the concentration of the capsules increases (as compared to figure 5.49), the normalised pressure drop in the pipe decreases. The slight decrease in the pressure drop for $k = 0.9$ at $Re_w = 30 \times 10000$ can be attributed to the numerical diffusion in the solver.

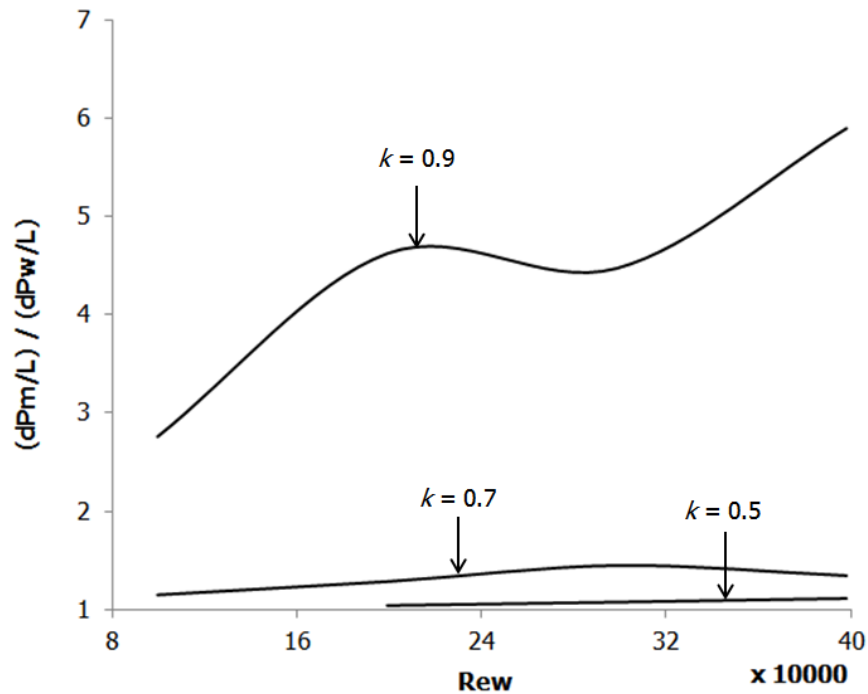


Figure 5.50. Variations in Normalised Pressure Drop for Three Spherical Capsules of $Sc = 1 * d$ in a Vertical Pipe

The information provided in this section, regarding the flow of heavy-density spherical capsules in vertical pipes, has a huge impact on the design process of HCPs, which is presented in Chapter 7. Similar kind of analysis that has been carried out in this section is also presented in the next chapter for the flow of heavy-density spherical capsules in pipe bends.

5.5. Analysis of the Flow of Heavy-Density Cylindrical Capsules in a Vertical HCP

Similar to the flow of heavy-density spherical capsules in a vertical pipe, heavy-density cylindrical capsules also propagate along the centreline of a vertical pipe. Figure 5.51 depicts the pressure and velocity variations around a single heavy-density cylindrical capsule of $k = 0.5$ at an average flow velocity of 2m/sec for a capsule length of $L_c = 1 * d$. The pressure field around a cylindrical capsule resembles the pressure field around a heavy-density spherical capsule. At upstream, the pressure of water increases from 170019Pa to 19037Pa as it approaches the capsule. Furthermore, it can be seen that the pressure downstream is 13150Pa. The velocity distribution within the pipe is similar to the velocity field for a heavy-density spherical capsule.

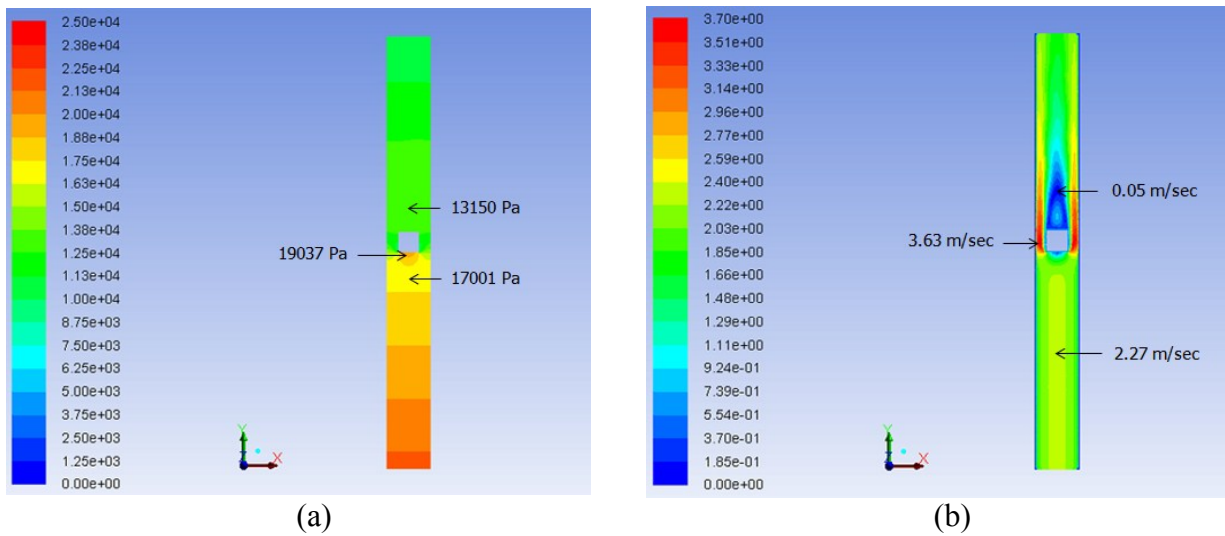


Figure 5.51. Variations in (a) Pressure and (b) Velocity, for a Cylindrical Capsule of $k = 0.5$ and $L_c = 1 * d$ in a Vertical Pipe at $V_{av} = 2\text{m/sec}$

Figure 5.52 shows the variations in C_p and u/u_{max} for the case under consideration, where C_p represents the coefficient of pressure and u is the local flow velocity along the pipe. It can be clearly seen that the pressure drop in case of a heavy-density cylindrical capsule in a vertical pipe is considerably higher than the pressure drop in a horizontal pipe. The total pressure drop in case of a vertical pipe is 11456 Pa which is 5.7 times higher than for a horizontal pipe.

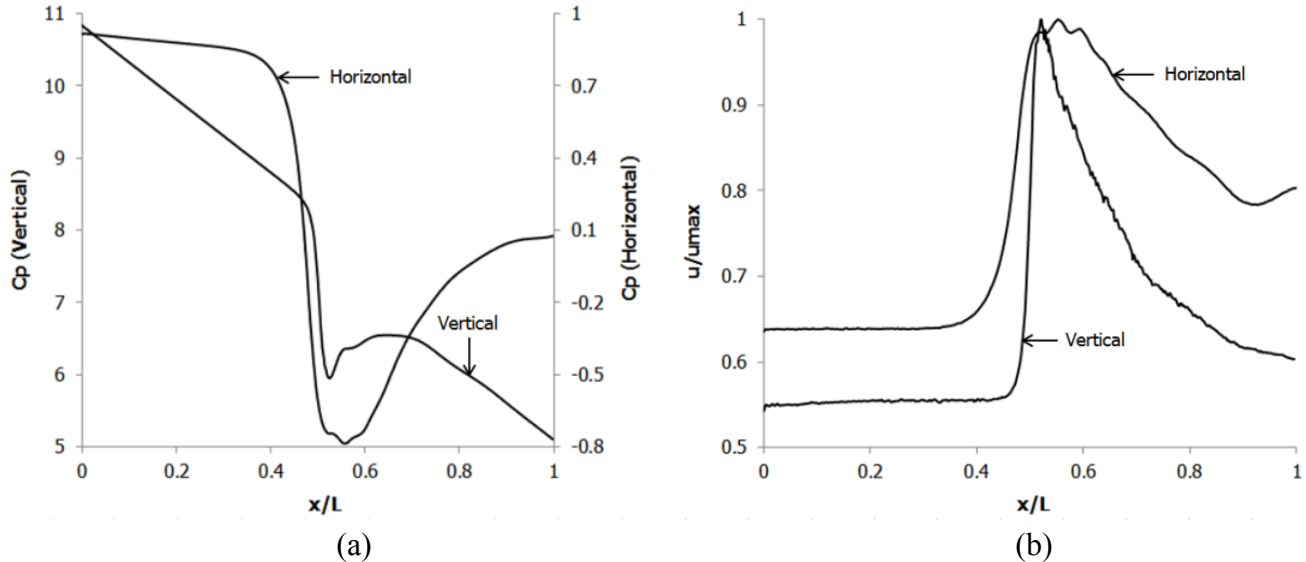


Figure 5.52. (a) Variations in C_p for a Cylindrical Capsule of $k = 0.5$ and $L_c = 1 * d$ in a Vertical Pipe at $V_{av} = 2\text{m/sec}$ (b) Variations in u/u_{max} for a Cylindrical Capsule of $k = 0.5$ and $L_c = 1 * d$ in a Vertical Pipe at $V_{av} = 2\text{m/sec}$

Figure 5.52 (b) depicts that the velocity magnitude of the flow for the case under consideration is lower, both at upstream and downstream locations, for the flow of a heavy-density cylindrical capsule

in a vertical pipe as compared to the flow in a horizontal pipe due to the alignment of the capsule along the centreline of the pipe.

To further investigate the velocity distribution within the capsule transporting pipe, velocity profiles have been drawn across the cross-section of the pipe at both 0.1m upstream and downstream locations from the centre of the heavy-density cylindrical capsule as shown in figure 5.53. It can be seen that the velocity profile is undisturbed at the upstream location, and the presence of the capsule has not affected the velocity profile at this location. However, at the downstream location, the presence of the capsule in the pipe has distorted the velocity profile.

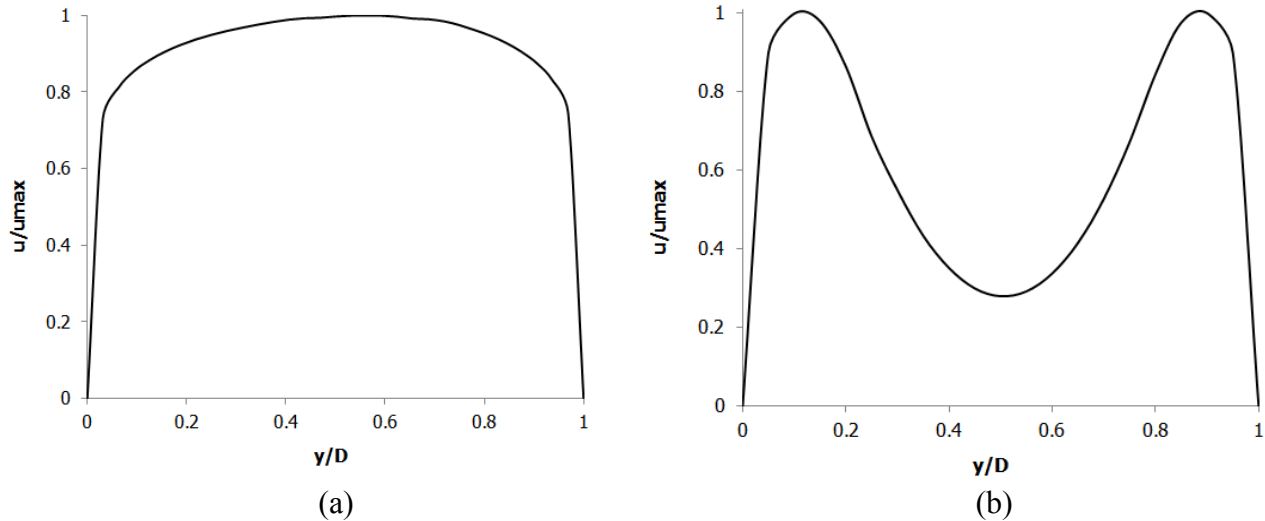


Figure 5.53. Variations in the Cross-Sectional Velocity Profiles for a Single Cylindrical Capsule of $k = 0.5$ and $L_c = 1 * d$ in a Vertical Pipe at $V_{av} = 2\text{m/sec}$ at (a) Upstream and (b) Downstream of the Capsule

Figure 5.54 depicts the variations in the velocity profiles at various locations within the heavy-density cylindrical capsule transporting pipe under consideration at an average flow velocity of 1m/sec.

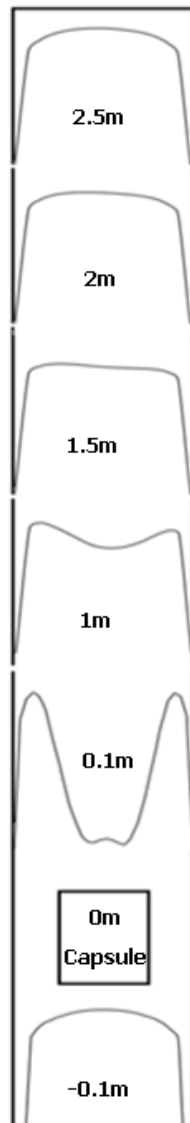


Figure 5.54. Development of Velocity Profile in the Presence of a Single Cylindrical Capsule in a Vertical Pipe having Density Equal to Water

5.5.1. Average Flow Velocity Effects

Figure 5.55 depicts the pressure and velocity variations within the test section of the pipe carrying a heavy-density cylindrical capsule of $k = 0.5$ at an average flow velocity of 4m/sec. The length of the capsule $L_c = 1 * d$. It can be seen that both the pressure and velocity fields are identical to the one observed in case of a heavy-density spherical capsule. The pressure upstream of the capsule is 39% higher and downstream of the capsule is 9% lower as compared to $V_{av} = 1\text{m/sec}$. Hence, the pressure drop within the pipeline increases by 40%. Furthermore, the velocity distribution resembles the one observed for $V_{av} = 1\text{m/sec}$.

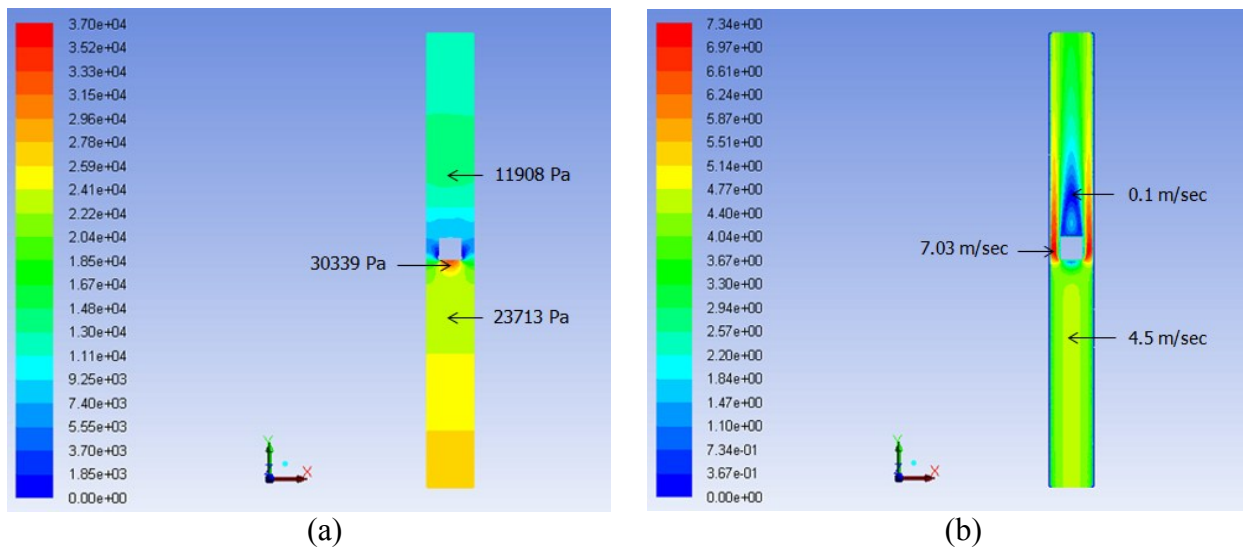


Figure 5.55. Variations in (a) Pressure and (b) Velocity, for a Cylindrical Capsule of $k = 0.5$ and $L_c = 1 * d$ in a Vertical Pipe at $V_{av} = 4\text{m/sec}$

Figure 5.56 shows the variations in C_p and u/u_{max} for the case under consideration. It can be seen that the pressure drop in a vertical pipe is higher as compared to a horizontal pipe. Furthermore, the pressure recovery in a vertical pipe is quicker in space as compared to a horizontal pipe. This is due to the fact that the pressure drop due to the elevation effects plays a major role in dictating the pressure distribution within a vertical pipeline. It can also be seen that the velocity distribution within a vertical pipe is more uniform as compared to a horizontal pipe. More detailed results have been presented in table A-4.4.

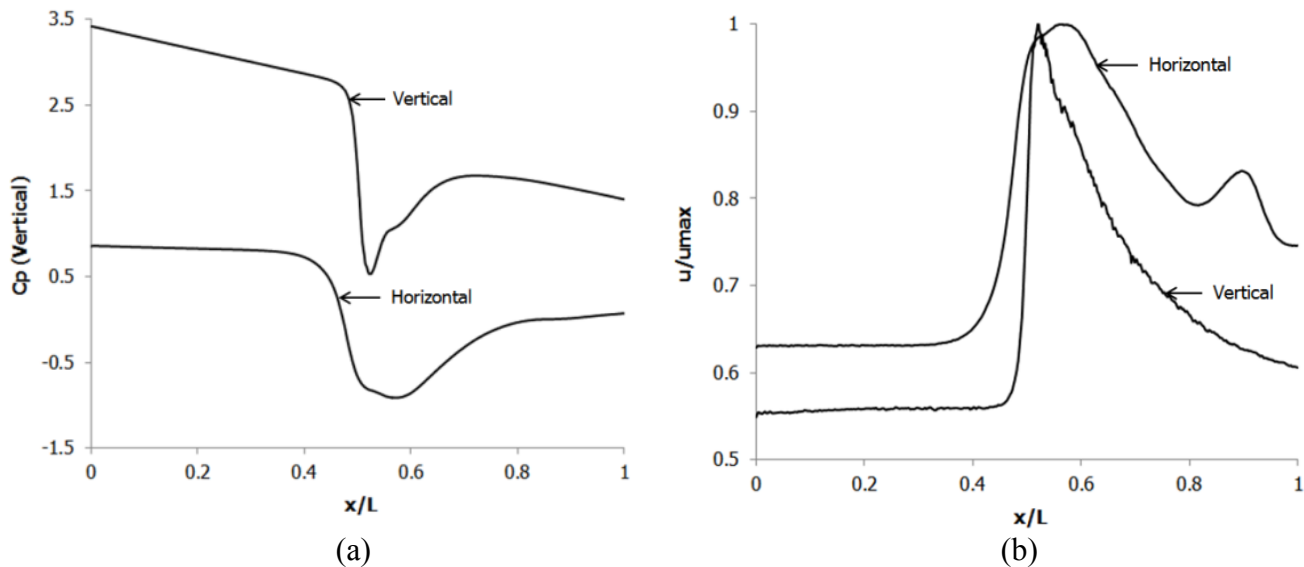


Figure 5.56. (a) Variations in C_p for a Cylindrical Capsule of $k = 0.5$ and $L_c = 1 * d$ in a Vertical Pipe at $V_{av} = 4\text{m/sec}$ (b) Variations in u/u_{max} for a Cylindrical Capsule of $k = 0.5$ and $L_c = 1 * d$ in a Vertical Pipe at $V_{av} = 4\text{m/sec}$

5.5.2. Length of the Capsule Effects

Figure 5.57 shows the pressure and velocity distributions in a heavy-density cylindrical capsule transporting vertical pipe for $k = 0.5$, $L_c = 5 * d$ and $V_{av} = 3\text{m/sec}$. It can be seen that the overall pressure and velocity distributions seem to be the same as compared with $L_c = 1 * d$ at the same average flow velocity and capsule diameter. However, the upstream and downstream pressures, as compared to $L_c = 1 * d$, are 20% higher and 12% lower respectively.

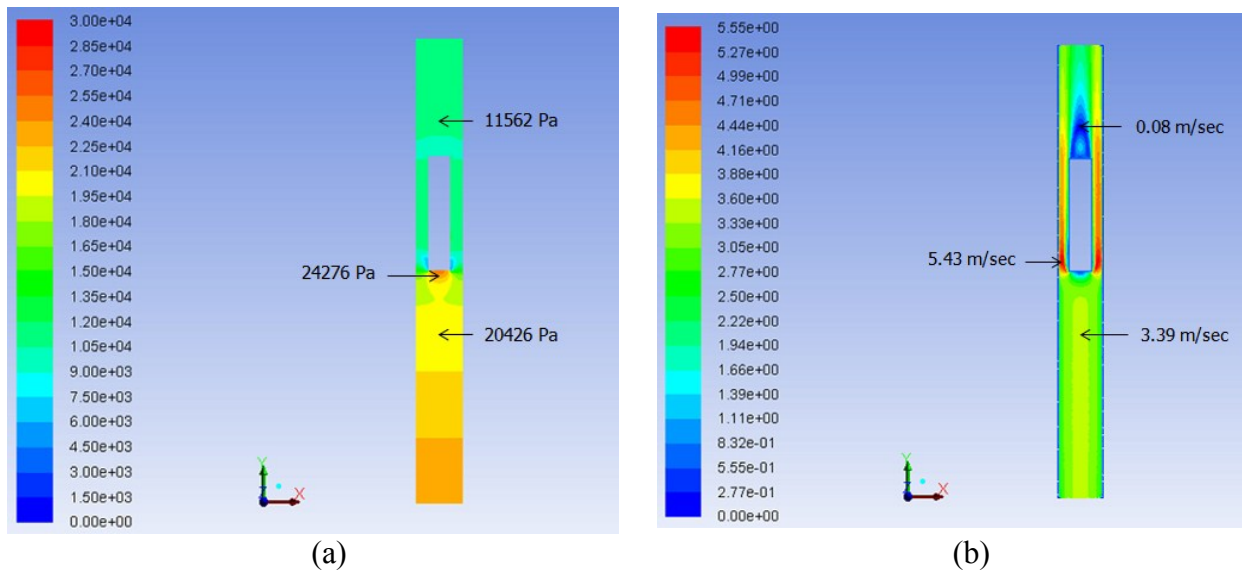


Figure 5.57. Variations in (a) Pressure and (b) Velocity, for a Single Cylindrical Capsule of $k = 0.5$ and $L_c = 5 * d$ in a Vertical Pipe at $V_{av} = 3\text{m/sec}$

Figure 5.58 shows the variations in C_p and u/u_{max} along the analysis line for the case under consideration. Here again, the pressure distribution indicates that the pressure drop in a vertical pipe is considerably higher than a horizontal pipe carrying heavy-density cylindrical capsule. Furthermore, it can be seen in figure 5.58 (b) that the velocity profile for heavy-density cylindrical capsule in a vertical pipe resembles the velocity profile observed in case of equi-density cylindrical capsule in a vertical pipe (figure 5.27 (b)). More detailed results have been presented in table A-4.4.

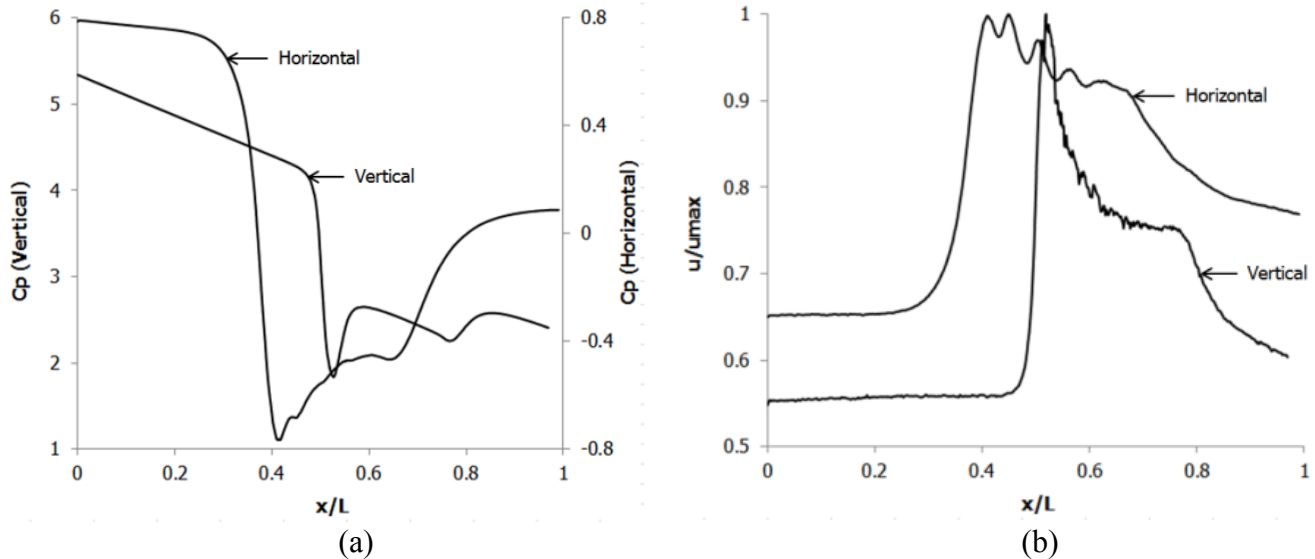


Figure 5.58. (a) Variations in C_p for a Single Cylindrical Capsule of $k = 0.5$ and $L_c = 5 * d$ in a Vertical Pipe at $V_{av} = 2\text{m/sec}$ (b) Variations in u/u_{max} for a Single Cylindrical Capsule of $k = 0.5$ and $L_c = 5 * d$ in a Vertical Pipe at $V_{av} = 3\text{m/sec}$

5.5.3. Capsule Diameter Effects

Figure 5.59 depicts the variations in the pressure field and C_p for a heavy-density cylindrical capsule of $L_c = 5 * d$, $k = 0.9$ at $V_{av} = 1\text{m/sec}$ in a vertical pipe. The trend of the pressure distribution is the same as observed for $k = 0.5$ (figure 5.51 (a)). Furthermore, it can be seen in figure 5.59 (b) that the pressure drop in a vertical pipe is higher than a horizontal pipe carrying heavy-density cylindrical capsules of the same length, diameter and at same average flow velocity. More detailed results have been presented in table A-4.4.

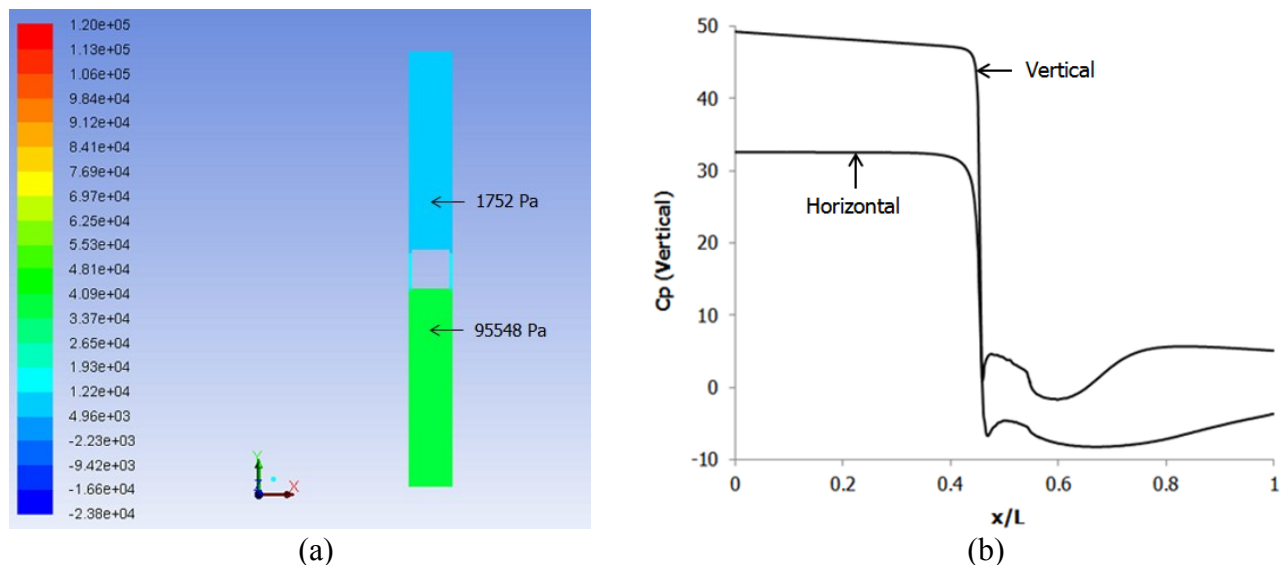


Figure 5.59. Variations in Pressure for a Single Cylindrical Capsule of $k = 0.9$ and $L_c = 5 * d$ in a Vertical Pipe at $V_{av} = 1\text{m/sec}$ (b) Variations in C_p for a Single Cylindrical Capsule of $k = 0.9$ and $L_c = 5 * d$ in a Vertical Pipe at $V_{av} = 1\text{m/sec}$

5.5.4. Capsule Concentration Effects

Figure 5.60 depicts the pressure and velocity variations in a vertical pipe carrying two heavy-density cylindrical capsules of $k = 0.5$, $L_c = 1 * d$, $Sc = 1 * d$. The trend of the pressure distribution is the same as observed for a single heavy-density cylindrical capsule. The pressure at upstream location has increased by 8%. The overall pressure drop in the pipe is 11566Pa, which is 0.9% higher than $N = 1$. Furthermore, the velocity field is identical to $N = 1$, i.e. a high flow velocity in the annulus and a large wake region downstream of the capsules.

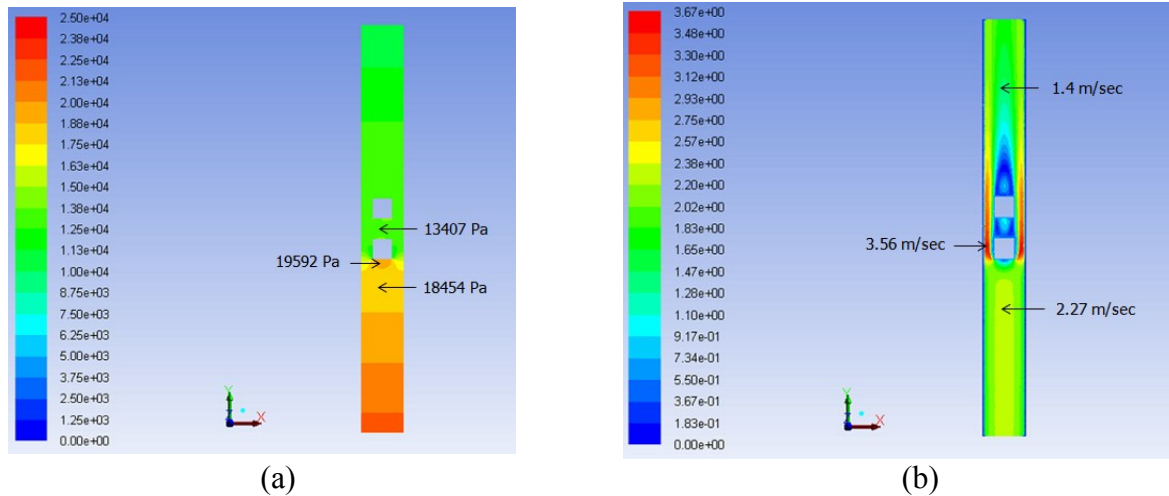


Figure 5.60. Variations in (a) Pressure and (b) Velocity, for Two Cylindrical Capsules of $k = 0.5$, Sc and $L_c = 1 * d$ in a Vertical Pipe at $V_{av} = 2\text{m/sec}$

Figure 5.61 shows the variations in C_p and u/u_{max} along the analysis line for the case under consideration. The results depict that the pressure drop in a vertical pipe is considerably higher than a horizontal. Furthermore, the velocity distribution in both these cases is quite different where the velocity field within a vertical pipe resembles that of a horizontal pipe carrying equi-density cylindrical capsules. More detailed results have been presented in table A-4.4.

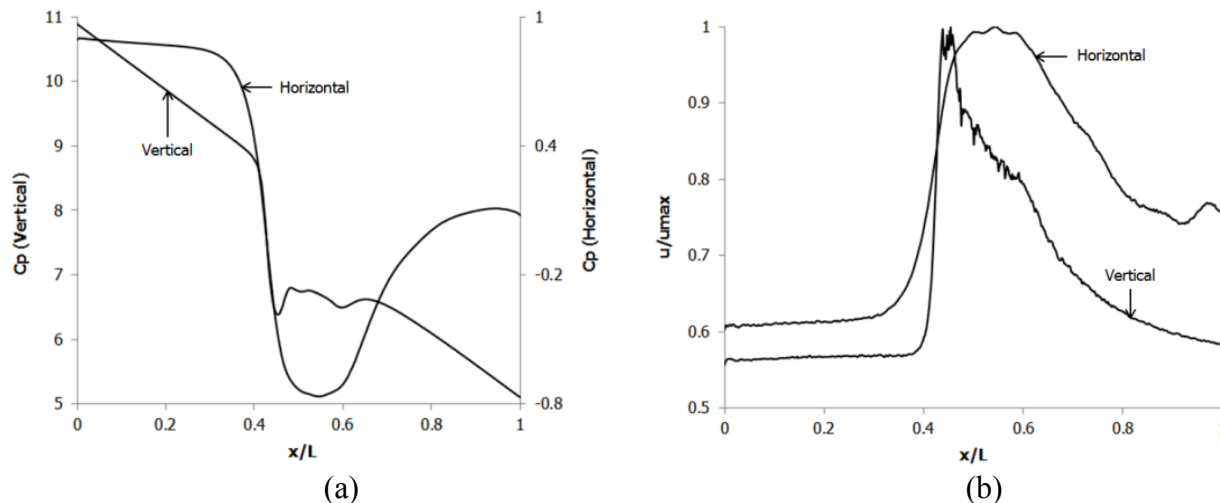


Figure 5.61. (a) Variations in C_p for Two Cylindrical Capsules of $k = 0.5$, Sc and $L_c = 1 * d$ in a Vertical Pipe at $V_{av} = 2\text{m/sec}$ (b) Variations in u/u_{max} for Two Cylindrical Capsules of $k = 0.5$, Sc and $L_c = 1 * d$ in a Vertical Pipe at $V_{av} = 2\text{m/sec}$

5.5.5. Effects of Spacing between the Capsules

Figure 5.62 depicts the effect of spacing between the capsules on the pressure and velocity distribution within the pipe. It can be seen that although both the pressure and the velocity fields resemble the velocity fields for $Sc = 1 * d$, the pressure drop for $Sc = 5 * d$ is marginally higher as compared to $Sc = 1 * d$.

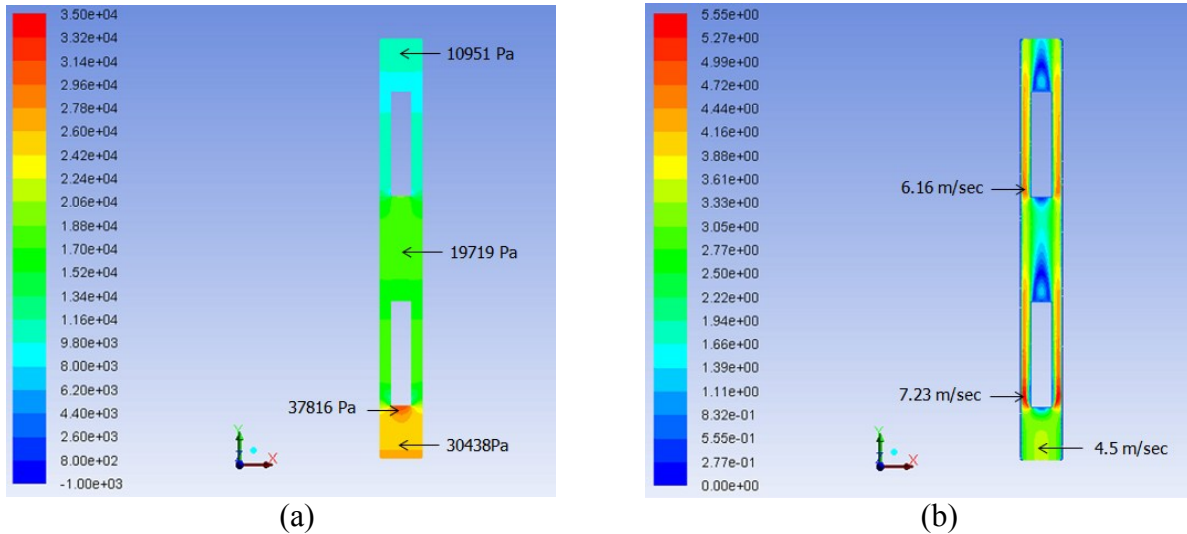


Figure 5.62. Variations in (a) Pressure and (b) Velocity, for Two Cylindrical Capsules of $k = 0.5$, $Sc = 5 * d$ and $Lc = 1 * d$ in a Vertical Pipe at $V_{av} = 4\text{m/sec}$

Figure 5.63 shows the variations in C_p and u/u_{max} along the analysis line for the case under consideration. The results depict that the pressure drop in a vertical pipe is considerably higher than a horizontal pipe transporting heavy-density cylindrical capsules. More detailed results have been presented in table A-4.4.

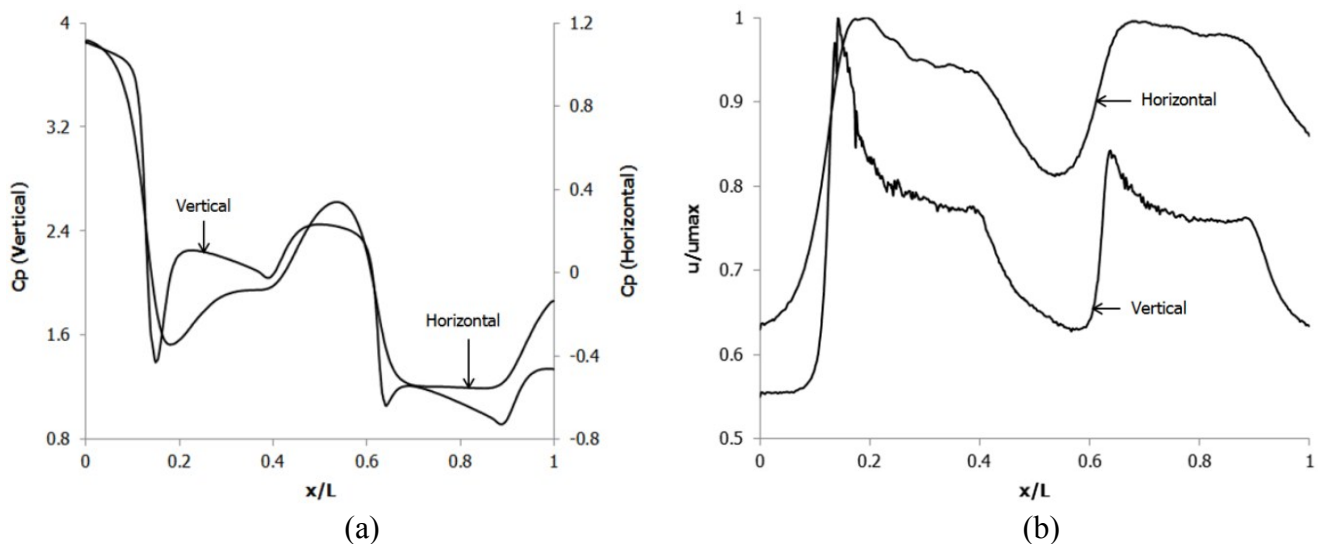


Figure 5.63. (a) Variations in C_p for Two Cylindrical Capsules of $k = 0.5$, $Sc = 5 * d$ and $Lc = 1 * d$ in a Vertical Pipe at $V_{av} = 2\text{m/sec}$ (b) Variations in u/u_{max} for Two Cylindrical Capsules of $k = 0.5$, $Sc = 5 * d$ and $Lc = 1 * d$ in a Vertical Pipe at $V_{av} = 4\text{m/sec}$

Table A-4.4 in Appendix A-4 summarises the results for various CFD based investigations being carried out on the flow of cylindrical capsules in a vertical pipe with density greater than water.

Figure 5.64 depicts the variation in the normalised pressure drop in the test section of the pipe for a single cylindrical capsule having $L_c = 1 * d$. The results show that as the flow velocity increases, the pressure drop in the test section of the pipe increases. Furthermore, as the size of the capsule increases, the pressure drop further increases. It is evident from figure 5.64 that heavy-density cylindrical capsules of diameter equal to 90% of the pipeline offer substantial pressure drop and hence are not recommended for practical applications. From the results listed in table A-4.4, the pressure drop for $k = 0.9$ is 16 times higher on average than capsules of $k = 0.5$ at the same average flow velocity and the same capsule length. Whereas, the pressure drop for $k = 0.7$ is 94% higher on average than capsules of $k = 0.5$.

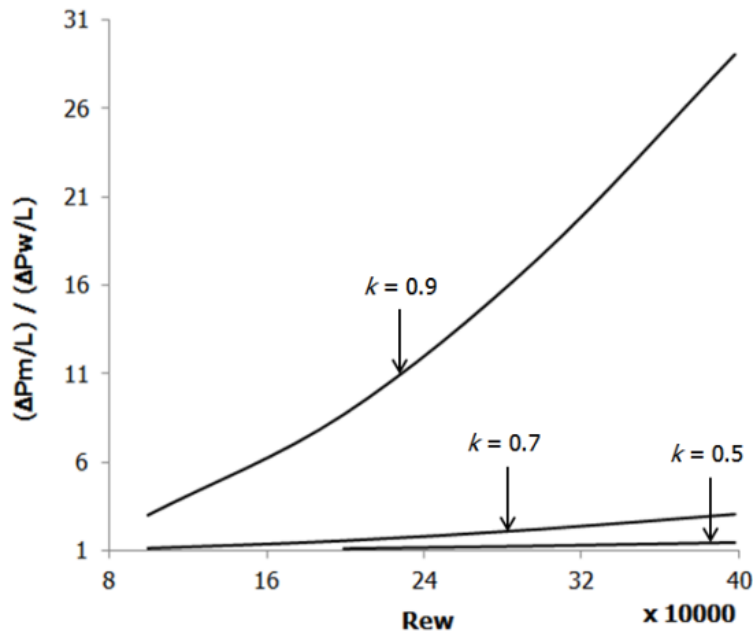


Figure 5.64. Variations in Normalised Pressure Drop for a Single Heavy-Density Cylindrical Capsule of $L_c = 1 * d$ in a Vertical Pipe

Figure 5.65 depicts the variations in the normalised pressure drop for two heavy-density cylindrical capsules of $L_c = 1 * d$ and $Sc = 1 * d$. It is again noted here that the pressure drop for $k = 0.9$ is significantly higher than for $k = 0.5$ and 0.7 and hence the capsules of diameter equal to $0.9 * d$ of the pipeline are not recommended for practical applications.

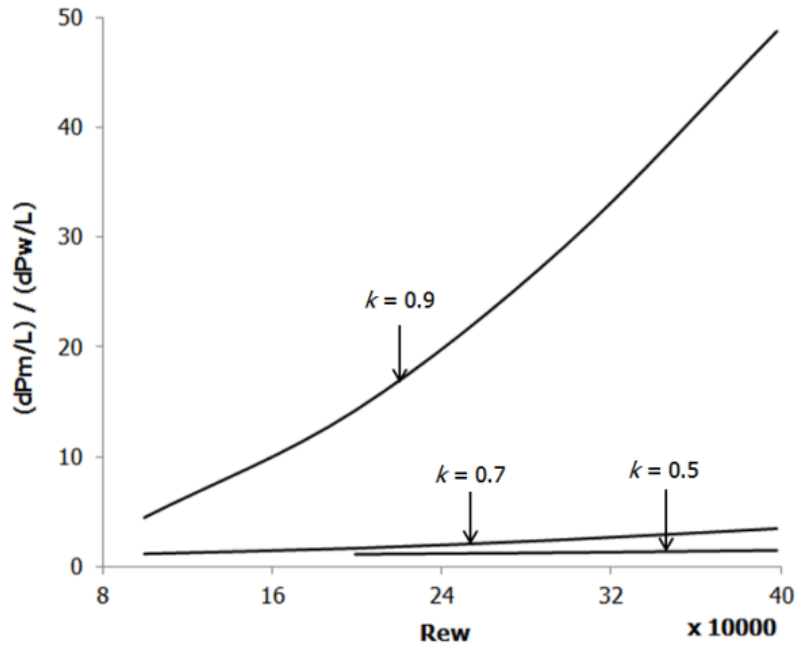


Figure 5.65. Variations in Normalised Pressure Drop for Two Heavy-Density Cylindrical Capsules of $L_c = 1 * d$ and $Sc = 1 * d$ in a Vertical Pipe

Figures 5.66 and 5.67 depict the variations in the normalised pressure drop to analyse the effects of the length and the spacing between the capsules. It can be seen that as the length of the capsules increases, the normalised pressure drop increases. Similarly, as the spacing between the capsules increases, the normalised pressure drop increases. This trend is similar as observed in previous such cases.

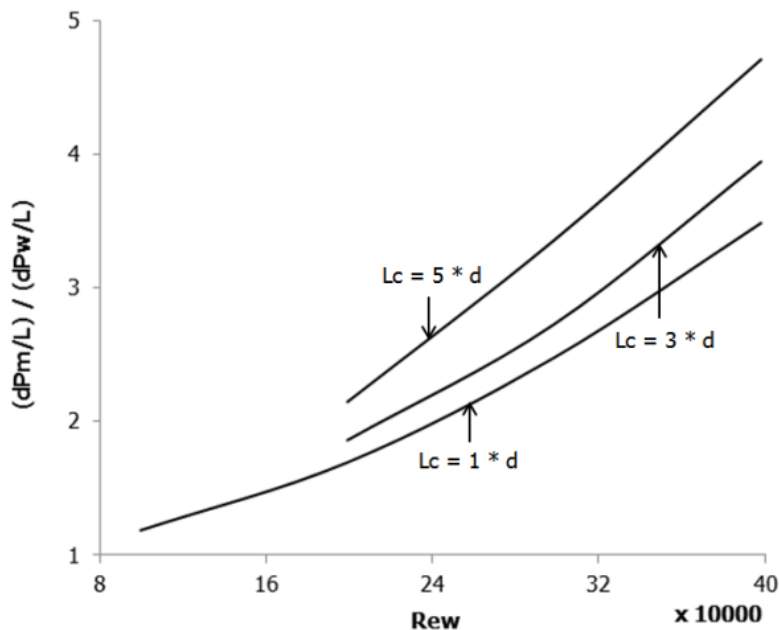


Figure 5.66. Variations in Normalised Pressure Drop for Two Heavy-Density Cylindrical Capsules of $k = 0.7$ and $Sc = 1 * d$ in a Vertical Pipe

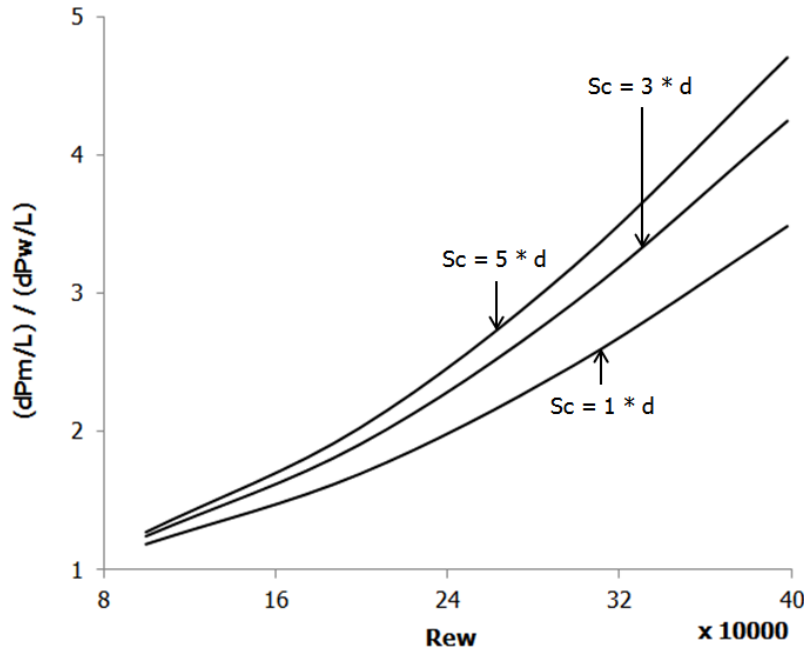


Figure 5.67. Variations in Normalised Pressure Drop for Two Heavy-Density Cylindrical Capsules of $k = 0.7$ and $L_c = 1 * d$ in a Vertical Pipe

The information provided in this section, regarding the flow of heavy-density cylindrical capsules in vertical pipes, has a huge impact on the design process of HCPs, which is presented in Chapter 7. Similar kind of analysis that has been carried out in this section is also presented in the next chapter for the flow of heavy-density cylindrical capsules in pipe bends.

5.6. Prediction Models

Based on the results presented in this chapter, prediction models for the friction factor of capsules can be developed as discussed in Chapter 1. Capsules of $k = 0.9$ have been excluded from the formulation of prediction models based on the results which shows that $k = 0.9$ is not a practical option for vertical pipelines transporting capsules as it leads to extensively large pressure drops in the pipeline.

The friction factors for water flow [7] and capsule flow separately can be calculated by the following expressions:

$$f_w = 0.0055 + \frac{0.55}{Re_w^3} \quad (5.1)$$

and:

$$f_c = 2D \frac{\left(\frac{\Delta P_m}{L_p} - \frac{\Delta P_w}{L_p} \right)}{\rho_w L_p V_{av}^2} \quad (5.2)$$

Using multiple variable regression analysis, semi-empirical correlations for the prediction of friction factor due to capsules, as a function of geometric and flow variables discussed in Chapter 3, have been developed. These prediction models are listed in table 5.2.

Table 5.2. Friction Factors for Capsules being transported in Vertical Pipelines

Capsule Shape	Density of the Capsules	Friction Factor due to Capsules
Spherical	Equi-Density	$f_c = \frac{\left(2.75 \left(\frac{N}{Lp} * d\right)^{1.058} k^{2.59} \frac{Sc + Lp^{0.2}}{Lp}\right)}{Re_c^{0.12}}$
	Heavy-Density	$f_c = \frac{\left(5.58 \left(\frac{N}{Lp} * d\right)^{1.12} k^{2.64} \frac{Sc + Lp^{0.074}}{Lp}\right)}{Re_c^{0.146}}$
Cylindrical	Equi-Density	$f_c = \frac{\left(6.3 \left(\frac{N}{Lp} * Lc\right)^{0.13} k^{4.96} \frac{Lc^{0.1}}{d} \frac{Sc + Lp^{0.1}}{Lp}\right)}{Re_c^{0.07}}$
	Heavy-Density	$f_c = \frac{\left(4.16 \left(\frac{N}{Lp} * Lc\right)^{0.14} k^{4.8} \frac{Lc^{0.1}}{d} \frac{Sc + Lp^{0.1}}{Lp}\right)}{Re_c^{0.035}}$

Figures 5.68 and 5.69 show the difference between the friction factors, due to capsules within the pipeline, calculated using the expressions presented in table 26 and that obtained from the CFD results in this chapter to authorise the usefulness of these semi-empirical relationships. From figure 5.68, it can be clearly seen that more than 90% of the data lies within $\pm 10\%$ error bound of the semi-empirical expression for equi-density spherical capsules. Similarly, it can be seen in figure 5.69 that more than 90% of the data lies within $\pm 10\%$ error bound of the semi-empirical relation for heavy-density cylindrical capsules within a vertical pipeline. Hence, the prediction models developed here represent the friction factors due to the presence of the capsules in a vertical pipeline with reasonable accuracy. The remaining two prediction models, i.e. for the flow of heavy-density spherical capsules and equi-density cylindrical capsules in a horizontal pipeline, have the same order of accuracy.

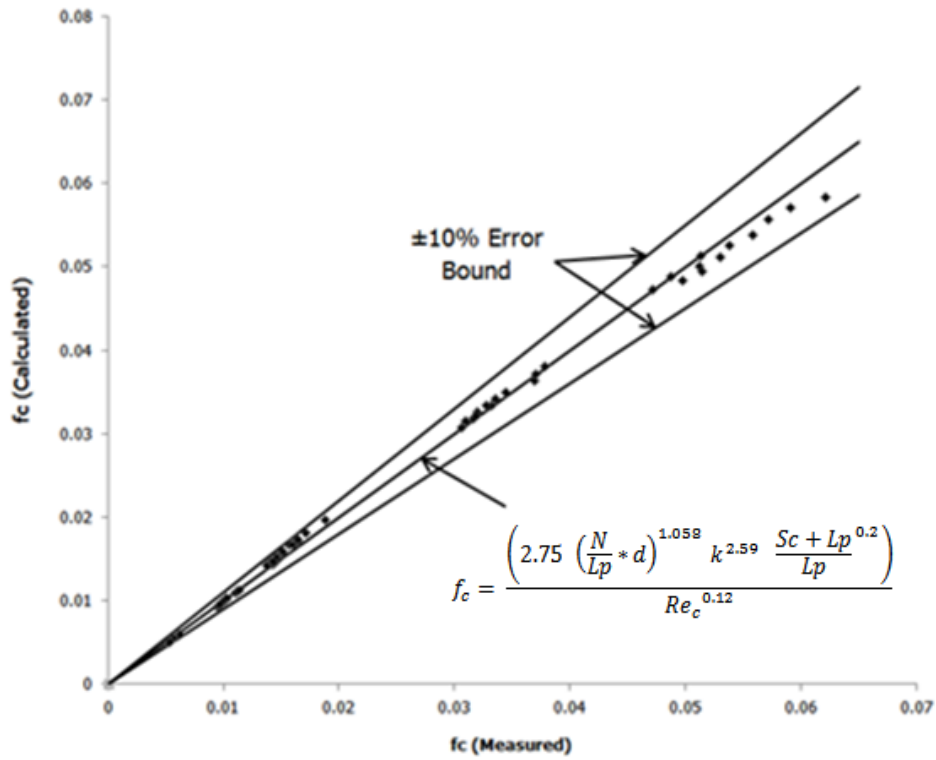


Figure 5.68. f_c for Equi-Density Spherical Capsules

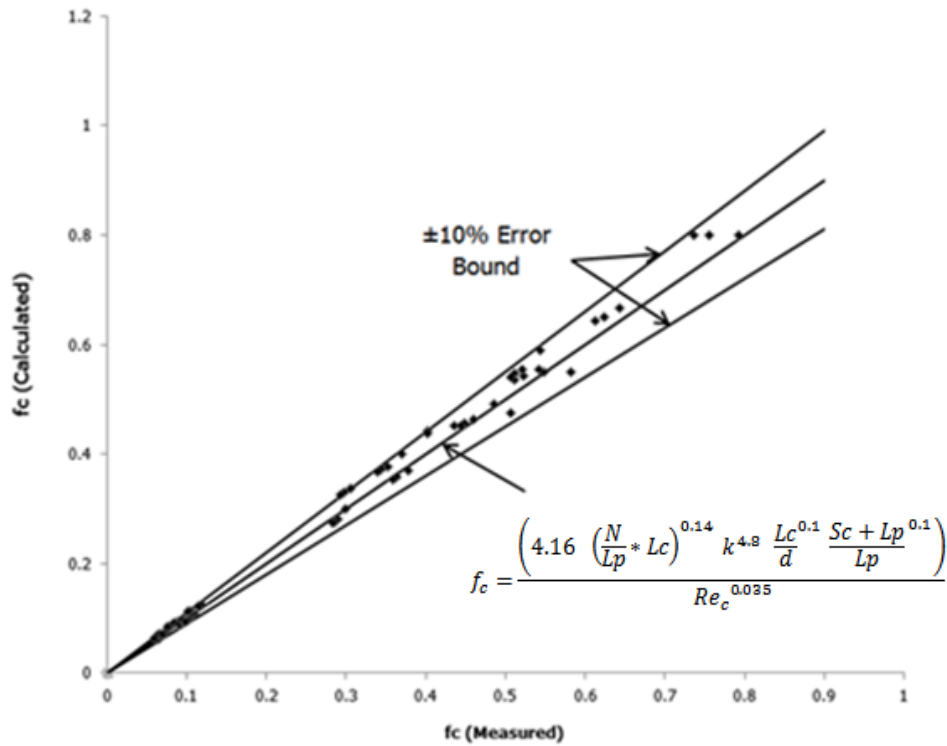


Figure 5.69. f_c for Heavy-Density Cylindrical Capsules

From the prediction models, it can be seen that as the number of capsules, diameter of capsules, length of capsules or the velocity of the capsules becomes zero, i.e. no capsule in the pipeline, the value for f_c automatically goes to zero and the expression for the pressure drop in the pipeline is only left with the friction factor due to water in equation (1.32). Furthermore, as Sc becomes zero, i.e. contacting capsules in the pipeline, the prediction models will still be valid. In order to prove this, a separate case regarding the flow of contacting capsules has been simulated and the results show that the difference between f_c from CFD and f_c from the prediction models is within the error bounds of the prediction models, i.e. $\pm 10\%$. Hence, the prediction models presented in this chapter can be used for a variety of capsule flow conditions within vertical pipelines. Furthermore, the prediction models developed here can be directly used in the design of HCPs (see Chapter 7 for further details).

5.7. Summary of the Analysis of a Vertical HCP

A detailed flow diagnostics of the capsule transporting vertical pipes has revealed the following results:

- Increase in the average flow velocity increases the pressure drop in the pipeline (see section 5.2.1, 5.3.1, 5.4.1 and 5.5.1 for reference)
- Increase in the capsules diameter increases the pressure drop in the pipeline (see section 5.2.2, 5.3.3, 5.4.2 and 5.5.3 for reference)
- Increase in the length of the capsules increases the pressure drop in the pipeline (see section 5.3.2 and 5.5.2 for reference)
- Increase in the spacing between the capsules marginally increases the pressure drop in the pipeline as compared to other parameters (see section 5.2.4, 5.3.5, 5.4.4 and 5.5.5 for reference)
- Increase in the density of the capsules increases the pressure drop in the pipeline (see Appendix A-4 for reference)
- Cylindrical capsules results in an increased pressure drop in the pipeline as compared to the flow of spherical capsules (see Appendix A-4 for reference)
- Increase in the concentration of the capsules increases the pressure drop in the pipeline (see section 5.2.3, 5.3.4, 5.4.3 and 5.5.4 for reference)

The information provided in this chapter, regarding the flow of capsules in vertical pipes, and the prediction models developed for the friction factor of capsules, has a huge impact on the design process of hydraulic capsule pipelines. Further details about the design of HCPs are presented in Chapter 7. For complete analysis of HCPs, pipe bends need to be considered within the framework of analysis and development of semi-empirical relationships, as presented in the current and the previous chapter. Thus, the next chapter provides details on the results obtained from CFD regarding the flow of capsules in pipe bends.

CHAPTER 6

ANALYSIS OF BENDS TRANSPORTING CAPSULES

Bends are an integral part of any pipeline network. The bends contribute towards the minor losses in the pipelines. For practical designing of any pipeline, it is mandatory to accommodate the effects (commonly in terms of pressure drop or head loss) of the pipe bends for a realistic pipeline design. The focus of this chapter is towards the flow diagnostics within bends, transporting capsules in comparison with bends transporting only a single phase, i.e. water. A detailed qualitative and quantitative analysis of the results obtained has been carried out in order to understand the complex flow structure in bends, transporting capsules. The effect of various geometric and flow-related parameters on the pressure drop in bends, transporting capsules has been investigated. Furthermore, semi-empirical relationships, for the flow of capsules in pipe bends, have been developed.

6.1. Analysis of Single Phase Flow in Horizontal Bends

Before moving on to the flow of capsules in pipe bends, the flow structure of a single phase in within bends needs to be understood and validated with Computational Fluid Dynamics. The pressure and velocity distributions within a pipe bend of radius of curvature $r/R = 4$ at an average flow velocity of 1m/sec are shown in figure 6.1. It is observed that the pressure on the outer wall of the bend is higher (747Pa) as compared to the inner wall (403Pa). This happens due to the centrifugal force acting on water as it passes through the bend. Furthermore, the velocity distribution is quite symmetric along the bend except for the exit of the bend where the velocity distribution shows that the velocity at the outer wall as higher than the inner wall of the bend. Munson [70] has provided with the loss coefficient values for various pipe fittings, including bends. For a hydrodynamically smooth pipe bend, the loss coefficient for $r/R = 4$ is 0.26. Putting this value of the loss coefficient in equation (1.19):

$$\Delta P = 130\text{Pa}$$

and the pressure drop predicted by Computational Fluid Dynamics between the inlet and the outlet of the pipe is:

$$\Delta P = 132\text{Pa}$$

It can be thus concluded that Computational Fluid Dynamics predict the pressure drop in a single phase flow within horizontal pipe bends with reasonable accuracy.

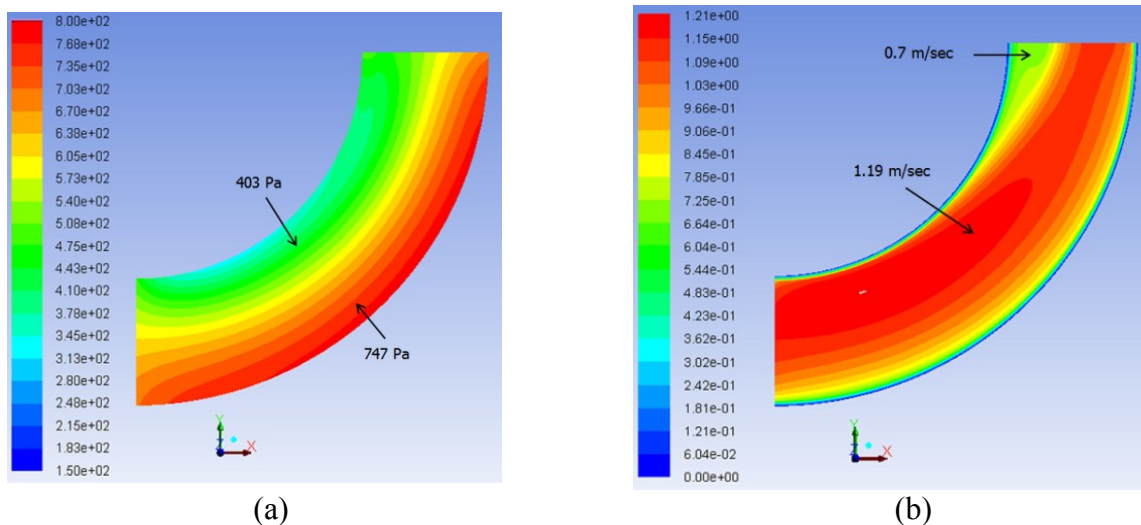


Figure 6.1. Variations in (a) Pressure and (b) Velocity, for a Single Phase Flow in a Horizontal Bend of $r/R = 4$ at $V_{av} = 1\text{m/sec}$

6.1.1. Average Flow Velocity Effects

Figure 6.2 depicts the pressure and velocity distributions in a horizontal bend of $r/R = 4$ at $V_{av} = 4\text{m/sec}$. It can be seen that the pressure and velocity variations are similar to the one observed in case of $V_{av} = 1\text{m/sec}$, i.e. higher pressure on the outer wall and lower pressure on the inner wall of the

bend. It can be seen that the pressure on the outer wall has increased by 12 times and on the inner wall by 9 times. The total pressure drop for the case under consideration is 1644Pa, which is 11 times higher than for $V_{av} = 1\text{m/sec}$. Thus, increase in average flow velocity increases the pressure drop in a horizontal bend.

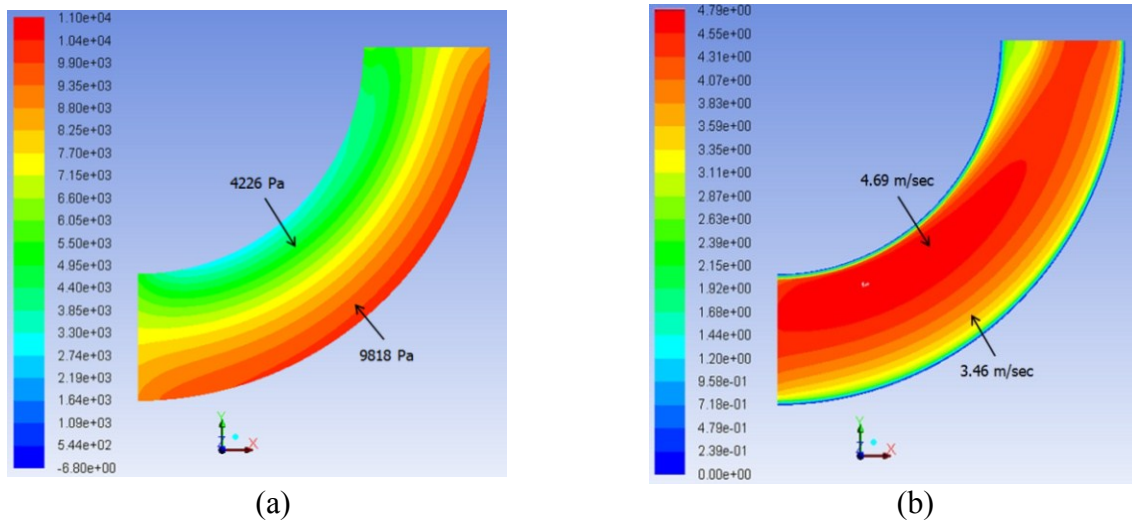


Figure 6.2. Variations in (a) Pressure and (b) Velocity, for a Single Phase Flow in a Horizontal Bend of $r/R = 4$ at $V_{av} = 4\text{m/sec}$

6.1.2. Effects of Radius of Curvature

Figure 6.3 depicts the pressure and velocity distributions in a horizontal bend of $r/R = 8$ at $V_{av} = 1\text{m/sec}$. It can be seen that the pressure and velocity variations are similar to the one observed in case of $r/R = 4$. Pressure on the outer wall has decreased by 11% and has increased by 20% on the inner wall of the bend. The total pressure drop for the case under consideration is 117Pa which is 11% lower than for $r/R = 4$. Hence, an increase in the radius of curvature of the bend decreases the pressure drop due to reduced secondary flows.

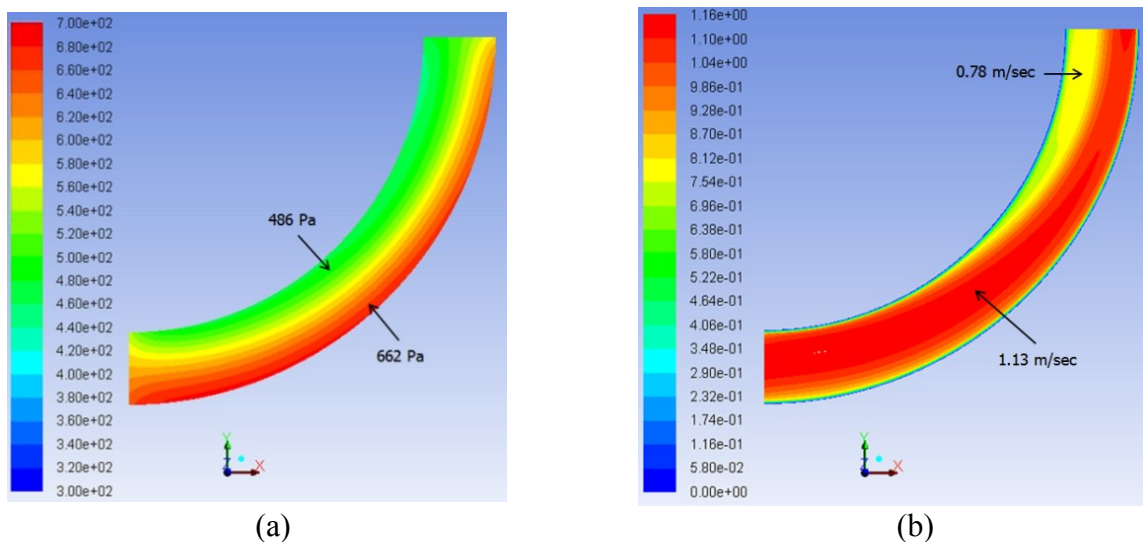


Figure 6.3. Variations in (a) Pressure and (b) Velocity, for a Single Phase Flow in a Horizontal Bend of $r/R = 8$ at $V_{av} = 1\text{m/sec}$

6.2. Analysis of the Flow of Equi-Density Capsules in Horizontal Bends

Figure 6.4 depicts the pressure and velocity distributions in a horizontal bend of $r/R = 4$ carrying a single spherical capsule of $k = 0.5$ and having density equal to water, being transported at $V_{av} = 1\text{m/sec}$. The results depict that the trends are similar to the one observed in a horizontal pipe, i.e. the flow pressure is higher at the upstream locations of the capsule while the velocity is low. Furthermore, the pressure is less and the velocity is higher in the annulus region due to the area reduction for the flow. The pressure and velocity are recovered to some extent downstream of the capsule. The total pressure drop in this case is 169Pa , which is 28% higher as compared to the flow of water in the same bend at same average flow velocity.

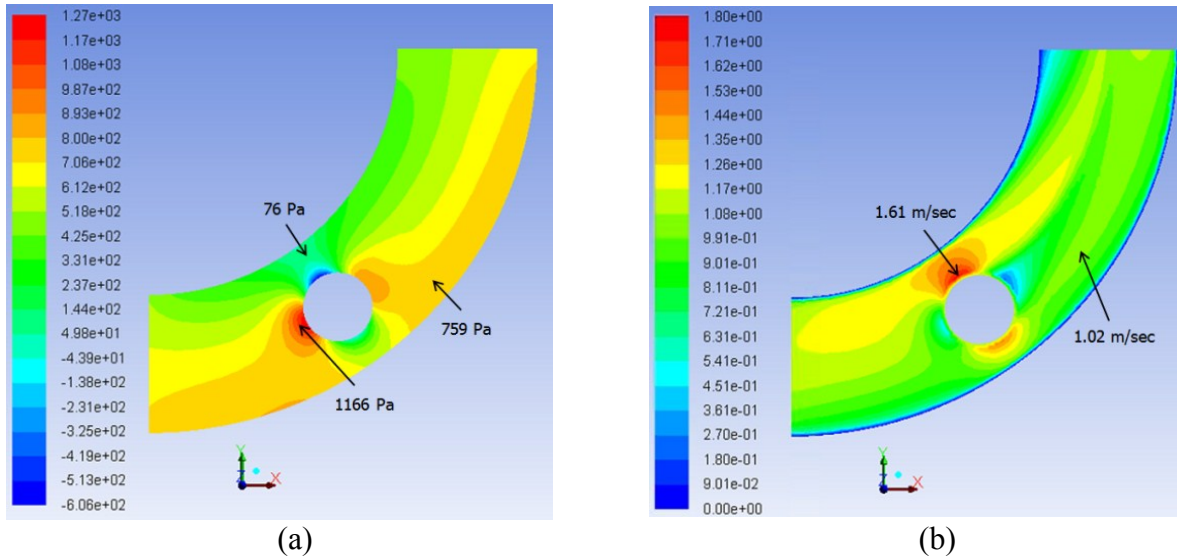


Figure 6.4. Variations in (a) Pressure and (b) Velocity, for a Single Equi-Density Spherical Capsule of $k = 0.5$ at $V_{av} = 1\text{m/sec}$ in a Horizontal Bend of $r/R = 4$

6.2.1. Average Flow Velocity Effects

Figure 6.5 depicts the pressure and velocity distributions in a horizontal bend of $r/R = 4$ carrying a single equi-density spherical capsule of $k = 0.5$ at $V_{av} = 4\text{m/sec}$. The results depict that the trends are similar to the one observed in case of $V_{av} = 1\text{m/sec}$. The pressure at the front face of the capsule has increased by 12 times while the pressure has decreased by 27 times in the annulus region. The total pressure drop in this case is 2010Pa , which is 10 times higher as compared to the flow of an equi-density spherical capsule of $k = 0.5$ at $V_{av} = 1\text{m/sec}$ in a horizontal pipe bend of $r/R = 4$. Hence, increase in the average flow velocity within a pipe bend, transporting capsules, increases the pressure drop. This trend is similar to the one observed in case of single phase flow in the previous section. More detailed results have been presented in table A-5.1.

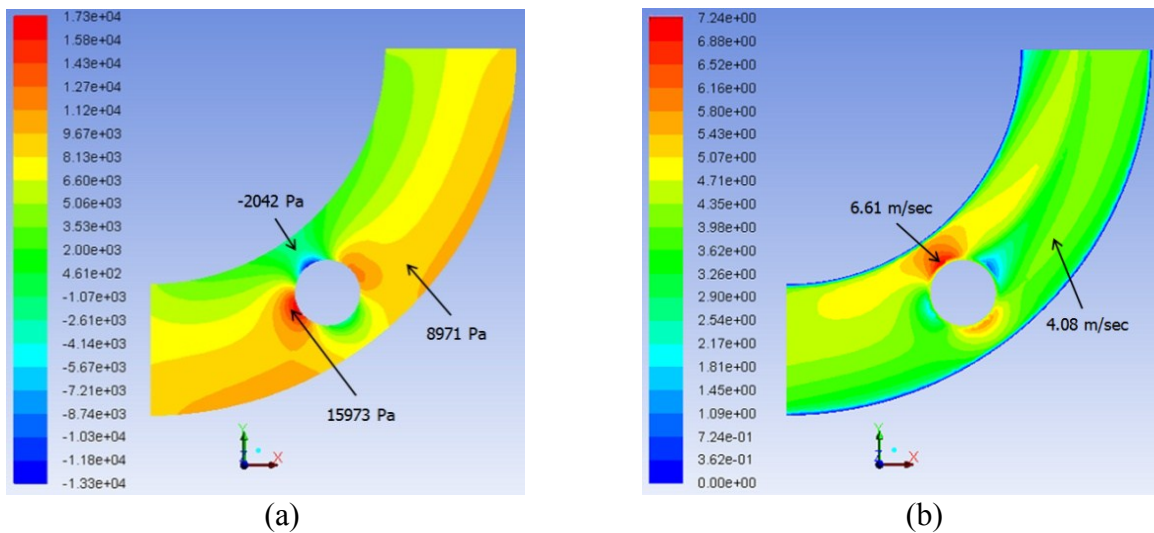


Figure 6.5. Variations in (a) Pressure and (b) Velocity, for a Single Equi-Density Spherical Capsule of $k = 0.5$ at $V_{av} = 4\text{m/sec}$ in a Horizontal Bend of $r/R = 4$

6.2.2. Capsule Diameter Effects

Figure 6.6 depicts the pressure and velocity distributions in a horizontal bend of $r/R = 4$ carrying a single equi-density spherical capsule of $k = 0.7$ at $V_{av} = 1\text{m/sec}$. The pressure at the front face of the capsule has increased by 6% while the pressure has decreased by 14 times in the annulus region as compared to $k = 0.5$. The total pressure drop in this case is 244Pa , which is 44% higher as compared to the flow of an equi-density spherical capsule of $k = 0.5$ at $V_{av} = 1\text{m/sec}$ in a horizontal pipe bend of $r/R = 4$. Hence, increase in the capsule diameter within a pipe bend, transporting capsules, increases the pressure drop. This trend is similar to the one observed in case of capsule transporting straight pipelines. More detailed results have been presented in table A-5.1.

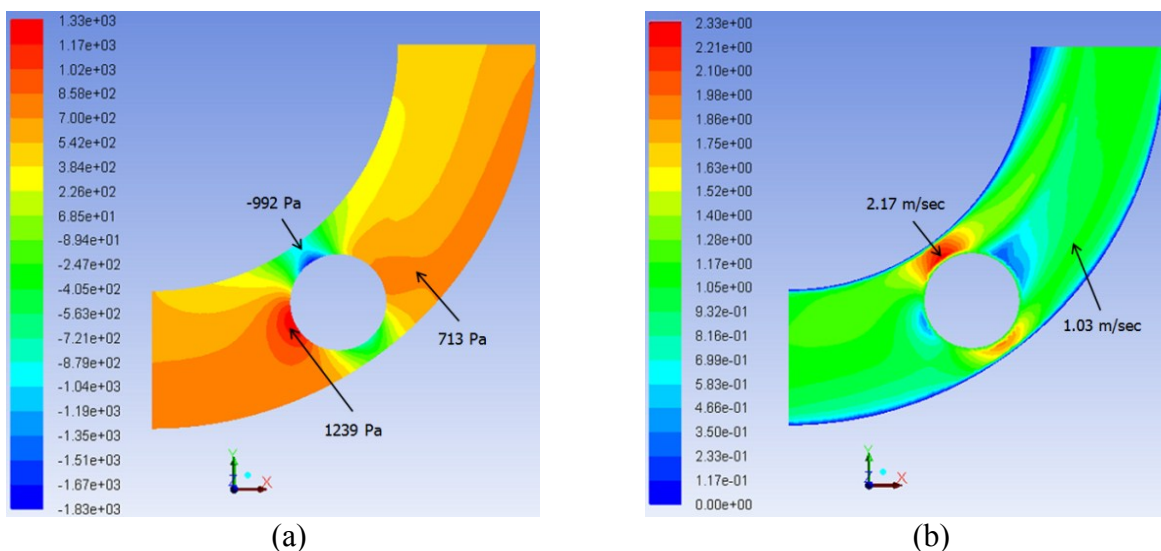


Figure 6.6. Variations in (a) Pressure and (b) Velocity, for a Single Equi-Density Spherical Capsule of $k = 0.7$ at $V_{av} = 1\text{m/sec}$ in a Horizontal Bend of $r/R = 4$

6.2.3. Capsule Concentration Effects

Figure 6.7 depicts the pressure and velocity distributions in a horizontal bend of $r/R = 4$ carrying two equi-density spherical capsules of $k = 0.7$ and $Sc = 1 * d$ at $V_{av} = 1\text{m/sec}$. The total pressure drop in this case is 378Pa, which is 55% higher as compared to the flow of an equi-density spherical capsule of $k = 0.7$ at $V_{av} = 1\text{m/sec}$ in a horizontal pipe bend of $r/R = 4$. Hence, increase in the concentration of the capsules within a pipe bend, transporting capsules, increases the pressure drop. This trend is similar to the one observed in case of capsule transporting straight pipelines. More detailed results have been presented in table A-5.1.

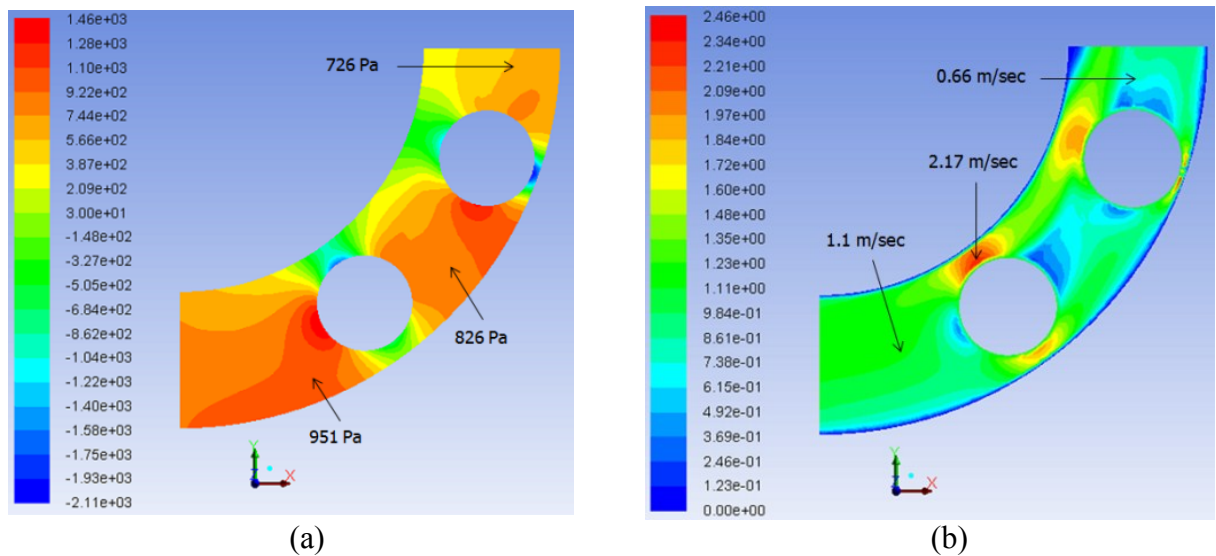


Figure 6.7. Variations in (a) Pressure and (b) Velocity, for Two Equi-Density Spherical Capsules of $k = 0.7$ and $Sc = 1 * d$ at $V_{av} = 1\text{m/sec}$ in a Horizontal Bend of $r/R = 4$

6.2.4. Effects of Spacing between the Capsules

Figure 6.8 depicts the pressure and velocity distributions in a horizontal bend of $r/R = 4$ carrying two equi-density spherical capsules of $k = 0.7$ and $Sc = 3 * d$ at $V_{av} = 1\text{m/sec}$. The total pressure drop in this case is 602Pa which is 59% higher as compared to $Sc = 1 * d$. Hence, increase in the spacing between the capsules marginally increases the pressure drop within the bend in comparison with other parameters. More detailed results have been presented in table A-5.1.

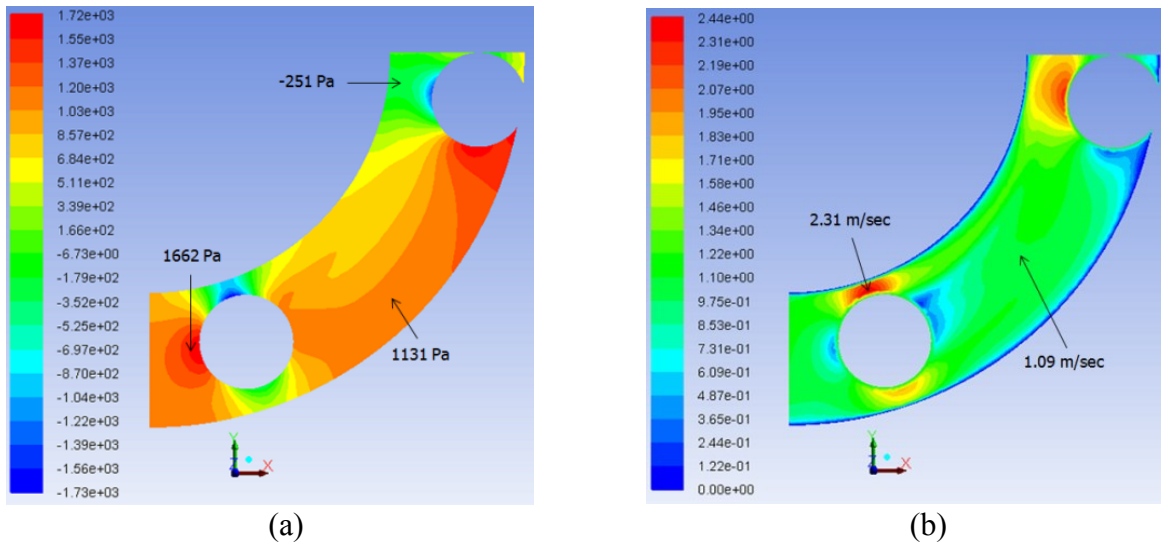


Figure 6.8. Variations in (a) Pressure and (b) Velocity, for Two Equi-Density Spherical Capsules of $k = 0.7$ and $Sc = 3 * d$ at $V_{av} = 1$ m/sec in a Horizontal Bend of $r/R = 4$

6.2.5. Effects of Radius of Curvature of the Bend

Figure 6.9 depicts the pressure and velocity distributions in a horizontal bend of $r/R = 8$ carrying two equi-density spherical capsules of $k = 0.7$ and $Sc = 3 * d$ at $V_{av} = 1$ m/sec. The total pressure drop in this case is 654 Pa, which is 0.6% lower as compared to $r/R = 4$. Hence, increase in the radius of curvature of the bend decreases the pressure drop due to reduced secondary flows within the bend (detailed discussion is available in section 6.4.2). More detailed results have been presented in table A-5.1.

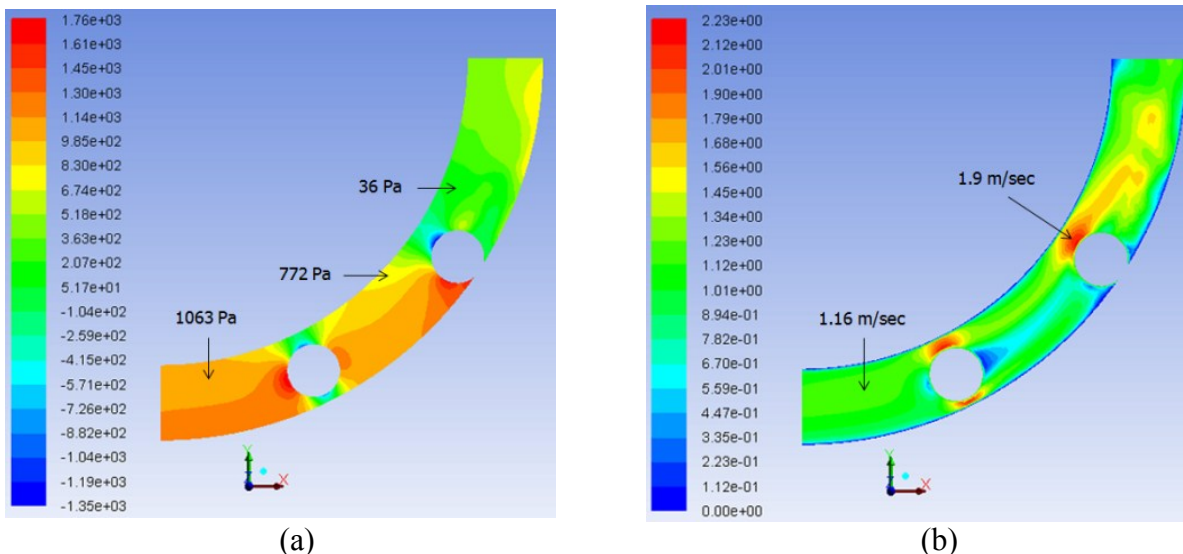


Figure 6.9. Variations in (a) Pressure and (b) Velocity, for Two Equi-Density Spherical Capsules of $k = 0.7$ and $Sc = 3 * d$ at $V_{av} = 1$ m/sec in a Horizontal Bend of $r/R = 8$

6.2.6. Capsule Shape Effects

Figure 6.10 depicts the pressure and velocity distributions in a horizontal bend of $r/R = 4$ carrying two equi-density cylindrical capsules of $k = 0.7$, $Sc = 1 * d$ and $Lc = 1 * d$ at $V_{av} = 1\text{m/sec}$. The total pressure drop in this case is 3101Pa which is 7 times higher as compared to two equi-density spherical capsules of same diameter, spacing and average flow velocity (figure 6.7). Hence, cylindrical capsules offer substantially more resistance to the flow and thus increase the pressure drop within the bend. More detailed results have been presented in table A-5.1.

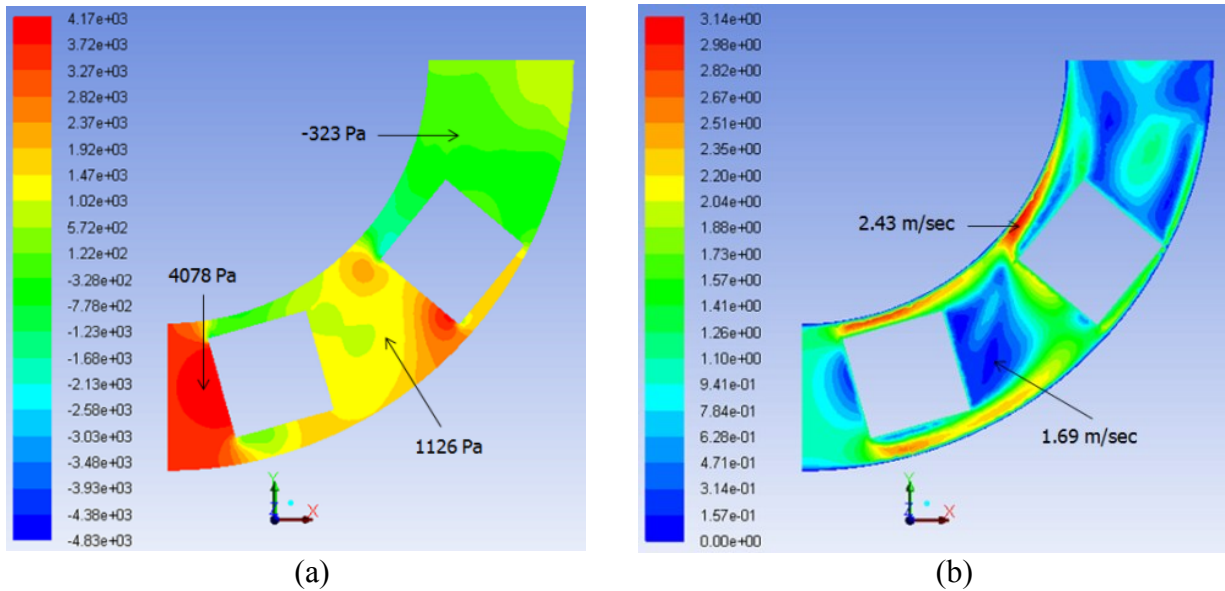


Figure 6.10. Variations in (a) Pressure and (b) Velocity, for Two Equi-Density Cylindrical Capsules of $k = 0.7$, $Sc = 1 * d$ and $Lc = 1 * d$ at $V_{av} = 1\text{m/sec}$ in a Horizontal Bend of $r/R = 4$

6.2.7. Length of the Capsule Effects

Figure 6.11 depicts the pressure and velocity distributions in a horizontal bend of $r/R = 4$ carrying two equi-density cylindrical capsules of $k = 0.7$, $Sc = 1 * d$ and $Lc = 2 * d$ at $V_{av} = 1\text{m/sec}$. The total pressure drop in this case is 2761Pa which is 11% lower as compared to $Lc = 1 * d$. Hence, longer cylindrical capsules offer less resistance to the flow and thus decrease the pressure drop within the bend. This is because longer capsules reduce the secondary flows within the bends by offering more solid area to the flow to remain attached. More detailed results have been presented in table A-5.1.

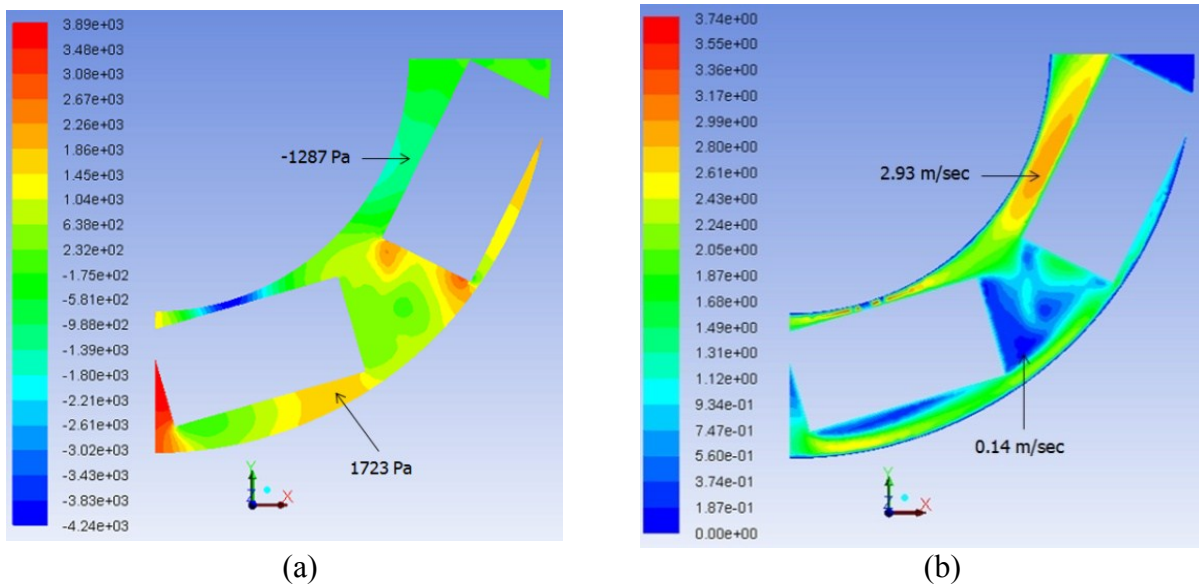


Figure 6.11. Variations in (a) Pressure and (b) Velocity, for Two Equi-Density Cylindrical Capsules of $k = 0.7$, $Sc = 1 * d$ and $Lc = 2 * d$ at $V_{av} = 1\text{m/sec}$ in a Horizontal Bend of $r/R = 4$

Table A-5.1 in Appendix A-5 summarises the results for various CFD based investigations being carried out on the flow of equi-density capsules in horizontal bends. The information provided in this section, regarding the flow of equi-density capsules in horizontal pipe bends, has a huge impact on the design process of HCPs, which is presented in Chapter 7. Similar kind of analysis that has been carried out in this section is also presented in the section 6.5 for the flow of equi-density capsules in vertical pipe bends.

6.3. Analysis of the Flow of Heavy-Density Capsules in Horizontal Bends

Figure 6.12 depicts the pressure and velocity distributions in a horizontal bend of $r/R = 4$ carrying a single spherical capsule of $k = 0.5$ and having density greater than water, being transported at $V_{av} = 1\text{m/sec}$. The results depict that the trends are similar to the one observed in a horizontal pipe, i.e. the flow pressure is higher at the upstream locations of the capsule while the velocity is low. Furthermore, the pressure is less and the velocity is higher in the annulus region due to the area reduction for the flow. The pressure and velocity are recovered to some extent downstream of the capsule. There is some hint for the generation of swirling flow packets in figure 6.12 (b). It can also be seen that due to the density of the capsule and the centrifugal force being exerted on the capsule in the bend, the capsule is being transported along the outer wall of the bend. The total pressure drop in this case is 246Pa, which is 136% higher as compared to the flow of equi-density spherical capsule of the same diameter and same average flow velocity.

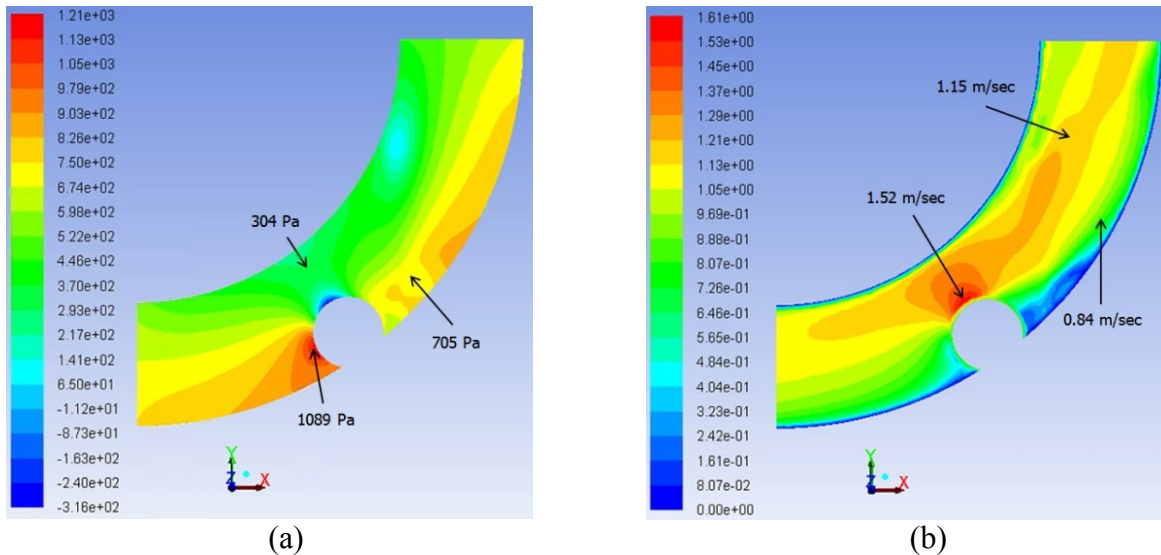


Figure 6.12. Variations in (a) Pressure and (b) Velocity, for a Single Heavy-Density Spherical Capsule of $k = 0.5$ at $V_{av} = 1\text{m/sec}$ in a Horizontal Bend of $r/R = 4$

6.3.1. Average Flow Velocity Effects

Figure 6.13 depicts the pressure and velocity distributions in a horizontal bend of $r/R = 4$ carrying a single heavy-density spherical capsule of $k = 0.5$ at $V_{av} = 4\text{m/sec}$. The results depict that the trends are similar to the one observed in case of $V_{av} = 1\text{m/sec}$. The pressure at the front face of the capsule has increased by 13 times. The total pressure drop in this case is 2899Pa , which is 44% higher as compared to the flow of an equi-density spherical capsule of $k = 0.5$ at $V_{av} = 1\text{m/sec}$ in a horizontal pipe bend of $r/R = 4$. Hence, increase in the average flow velocity within a pipe bend, transporting capsules, increases the pressure drop. This trend is similar to the one observed in case of equi-density capsule flow within horizontal bends. More detailed results have been presented in table A-5.2.

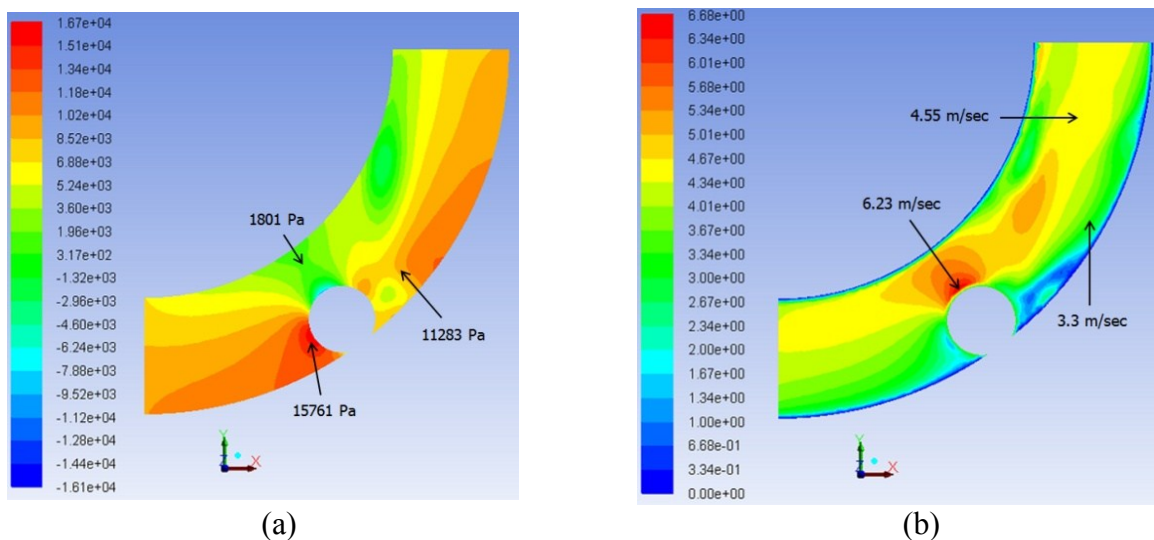


Figure 6.13. Variations in (a) Pressure and (b) Velocity, for a Single Heavy-Density Spherical Capsule of $k = 0.5$ at $V_{av} = 4\text{m/sec}$ in a Horizontal Bend of $r/R = 4$

6.3.2. Capsule Diameter Effects

Figure 6.14 depicts the pressure and velocity distributions in a horizontal bend of $r/R = 4$ carrying a single heavy-density spherical capsule of $k = 0.7$ at $V_{av} = 1\text{m/sec}$. The pressure at the front face of the capsule has increased by 27% while the pressure has decreased by 396% in the annulus region as compared to $k = 0.5$. The total pressure drop in this case is 581Pa, which is 138% higher as compared to the flow of an equi-density spherical capsule of $k = 0.5$ at $V_{av} = 1\text{m/sec}$ in a horizontal pipe bend of $r/R = 4$. Hence, increase in the capsule diameter within a pipe bend, transporting capsules, increases the pressure drop. This trend is similar to the one observed in case of equi-density capsule flow within horizontal bends. More detailed results have been presented in table A-5.2.

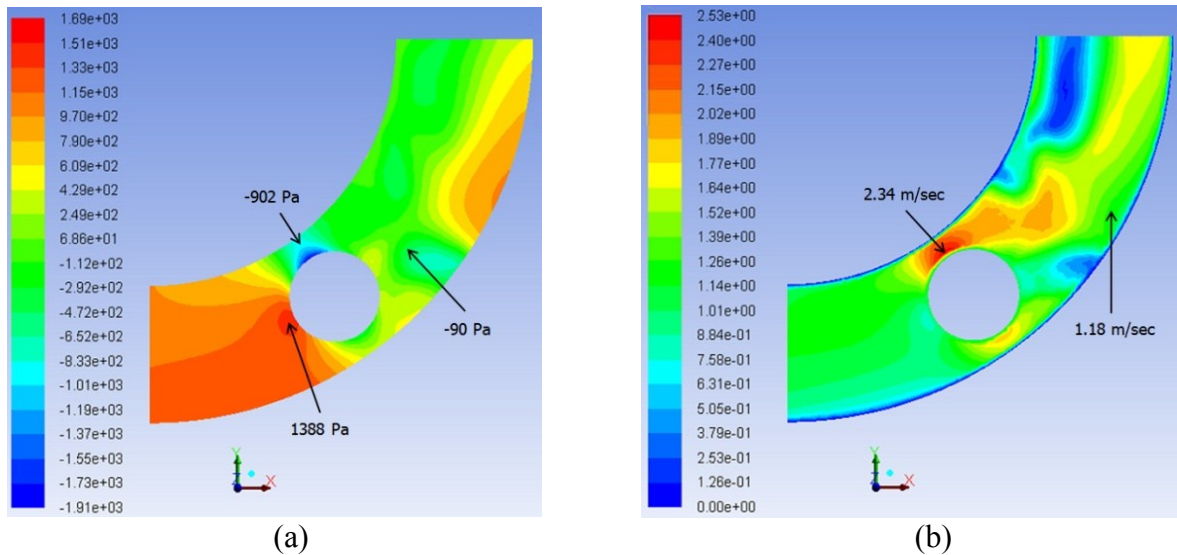


Figure 6.14. Variations in (a) Pressure and (b) Velocity, for a Single Heavy-Density Spherical Capsule of $k = 0.7$ at $V_{av} = 1\text{m/sec}$ in a Horizontal Bend of $r/R = 4$

6.3.3. Capsule Concentration Effects

Figure 6.15 depicts the pressure and velocity distributions in a horizontal bend of $r/R = 4$ carrying two heavy-density spherical capsules of $k = 0.7$ and $Sc = 1 * d$ at $V_{av} = 1\text{m/sec}$. The total pressure drop in this case is 2365Pa, which is 5 times higher as compared to the flow of equi-density spherical capsules of $k = 0.7$ at $V_{av} = 1\text{m/sec}$ in a horizontal pipe bend of $r/R = 4$. Hence, increase in the concentration of the capsules within a pipe bend, transporting capsules, increases the pressure drop. This trend is similar to the one observed in case of equi-density capsule flow within horizontal bends. More detailed results have been presented in table A-5.2.

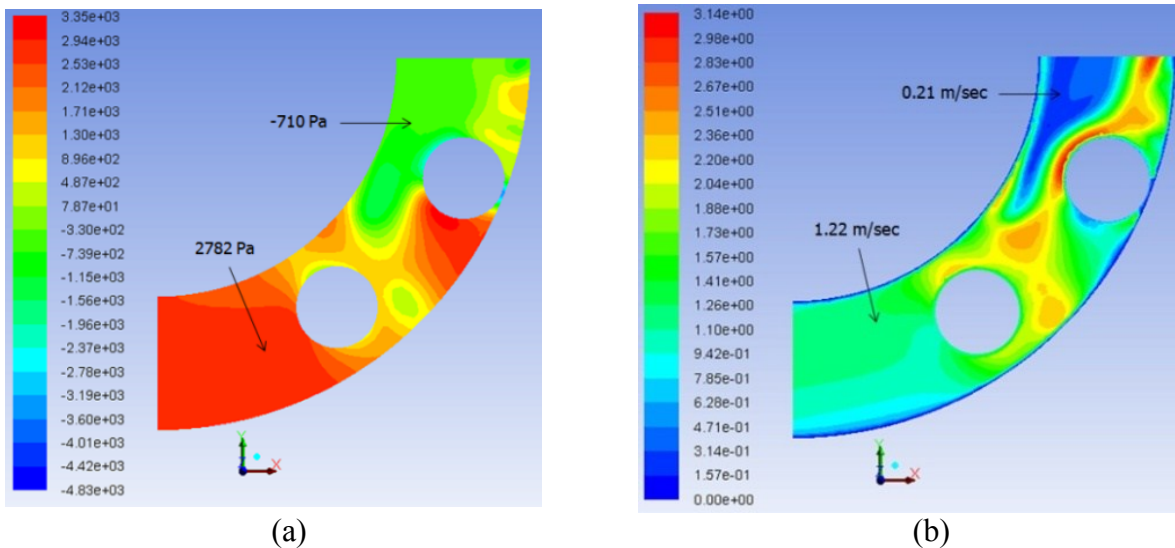


Figure 6.15. Variations in (a) Pressure and (b) Velocity, for Two Heavy-Density Spherical Capsules of $k = 0.7$ and $Sc = 1 * d$ at $V_{av} = 1 \text{ m/sec}$ in a Horizontal Bend of $r/R = 4$

6.3.4. Effects of Spacing between the Capsules

Figure 6.16 depicts the pressure and velocity distributions in a horizontal bend of $r/R = 4$ carrying two heavy-density spherical capsules of $k = 0.7$ and $Sc = 3 * d$ at $V_{av} = 1 \text{ m/sec}$. The total pressure drop in this case is 1203 Pa , which is 99% higher as compared to the flow of equi-density spherical capsules. Hence, increase in the spacing between the capsules marginally decreases the pressure drop within the bend in comparison with other parameters. More detailed results have been presented in table A-5.2.

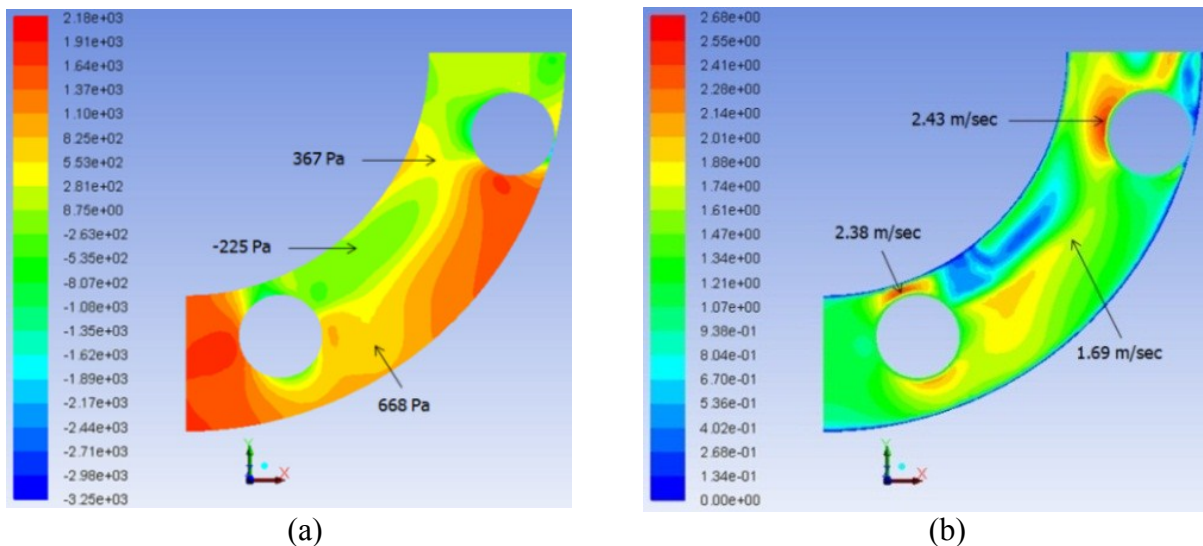


Figure 6.16. Variations in (a) Pressure and (b) Velocity, for Two Heavy-Density Spherical Capsules of $k = 0.7$ and $Sc = 3 * d$ at $V_{av} = 1 \text{ m/sec}$ in a Horizontal Bend of $r/R = 4$

6.3.5. Effects of Radius of Curvature of the Bend

Figure 6.17 depicts the pressure and velocity distributions in a horizontal bend of $r/R = 8$ carrying two heavy-density spherical capsules of $k = 0.7$ and $Sc = 3 * d$ at $V_{av} = 1\text{m/sec}$. The total pressure drop in this case is 1148Pa , which is 75% higher as compared to the flow of equi-density spherical capsules. Hence, increase in the radius of curvature of the bend decreases the pressure drop due to reduced secondary flows within the bend. More detailed results have been presented in table A-5.2.

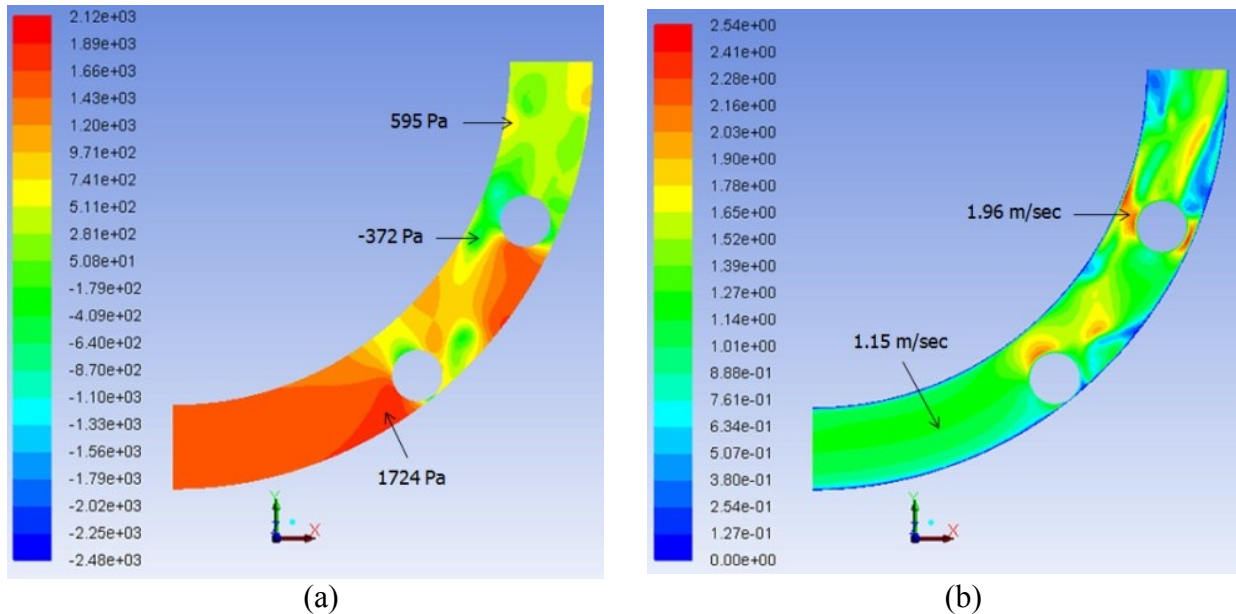


Figure 6.17. Variations in (a) Pressure and (b) Velocity, for Two Heavy-Density Spherical Capsules of $k = 0.7$ and $Sc = 3 * d$ at $V_{av} = 1\text{m/sec}$ in a Horizontal Bend of $r/R = 8$

6.3.6. Capsule Shape Effects

Figure 6.18 depicts the pressure and velocity distributions in a horizontal bend of $r/R = 4$ carrying two heavy-density cylindrical capsules of $k = 0.7$, $Sc = 1 * d$ and $L_c = 1 * d$ at $V_{av} = 1\text{m/sec}$. The total pressure drop in this case is 6654Pa , which is 114% higher as compared to the flow of equi-density cylindrical capsules. Hence, cylindrical capsules offer substantially more resistance to the flow and thus increase the pressure drop within the bend. More detailed results have been presented in table A-5.2.

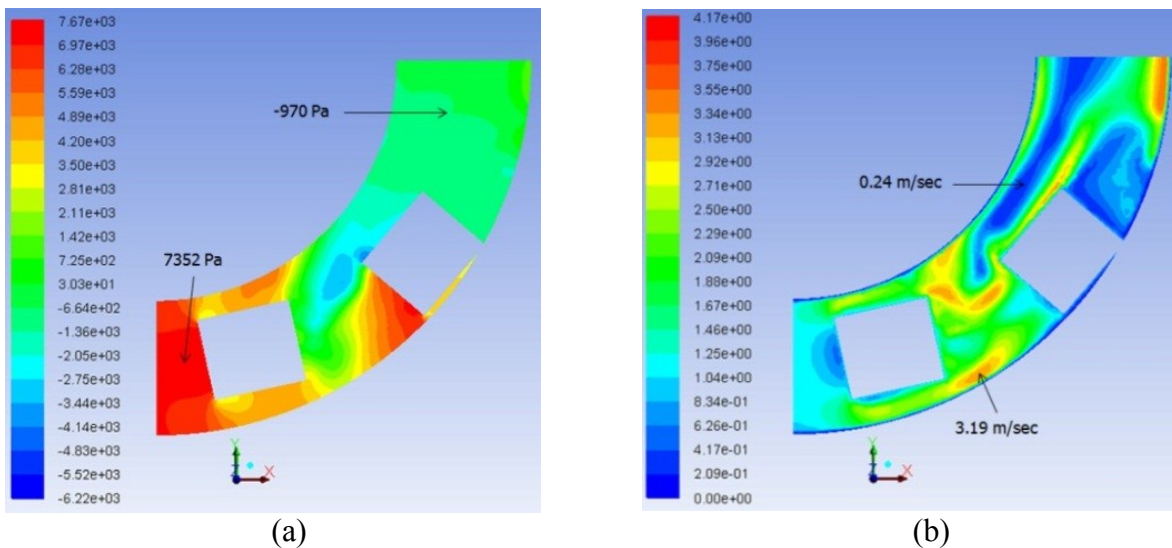


Figure 6.18. Variations in (a) Pressure and (b) Velocity, for Two Heavy-Density Cylindrical Capsules of $k = 0.7$, $Sc = 1 * d$ and $Lc = 1 * d$ at $V_{av} = 1\text{m/sec}$ in a Horizontal Bend of $r/R = 4$

6.3.7. Length of the Capsule Effects

Figure 6.19 depicts the pressure and velocity distributions in a horizontal bend of $r/R = 4$ carrying two heavy-density cylindrical capsules of $k = 0.7$, $Sc = 1 * d$ and $Lc = 2 * d$ at $V_{av} = 1\text{m/sec}$. The total pressure drop in this case is 3868Pa , which is 40% higher as compared to the flow of equi-density cylindrical capsules. Hence, increase in the length of the cylindrical capsules decreases the pressure drop within horizontal bends. Furthermore, from the aforementioned discussions, the pressure drop in horizontal bends carrying heavy-density capsules is considerably higher as compared to the flow of equi-density capsules in horizontal bends. More detailed results have been presented in table A-5.2.

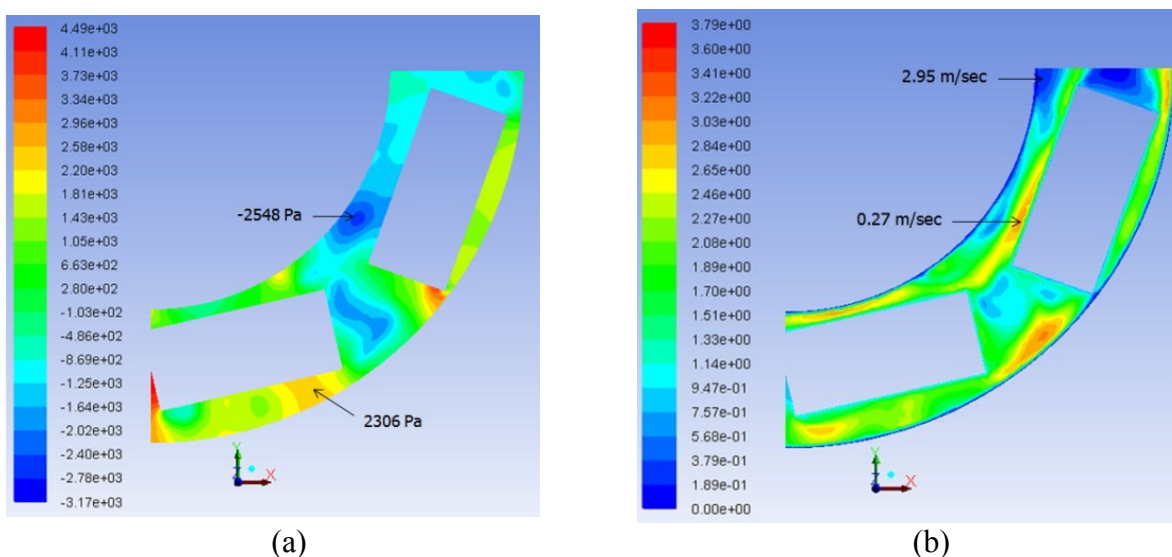


Figure 6.19. Variations in (a) Pressure and (b) Velocity, for Two Heavy-Density Cylindrical Capsules of $k = 0.7$, $Sc = 1 * d$ and $Lc = 2 * d$ at $V_{av} = 1\text{m/sec}$ in a Horizontal Bend of $r/R = 4$

Table A-5.2 in Appendix A-5 summarises the results for various CFD based investigations being carried out on the flow of heavy-density capsules in horizontal bends. The information provided in this section, regarding the flow of heavy-density capsules in horizontal pipe bends, has a huge impact on the design process of HCPs, which is presented in Chapter 7. Similar kind of analysis that has been carried out in this section is also presented in the section 6.6 for the flow of heavy-density capsules in vertical pipe bends.

6.4. Analysis of Single Phase Flow in Vertical Bends

Figure 6.20 depicts the variations in the pressure and velocity distribution within a vertical bend of $r/R = 4$ at an average flow velocity of 1m/sec. The pressure on the outer wall is 1000Pa higher than the inner wall of the bend due to the action of the centrifugal force. The velocity distribution reveals that the velocity of the flow is higher near the inner wall of the bend as compared to the outer wall. The overall pressure drop observed in this case is 5547Pa, which is 41 times higher as compared to a horizontal bend of same r/R and at same average flow velocity.

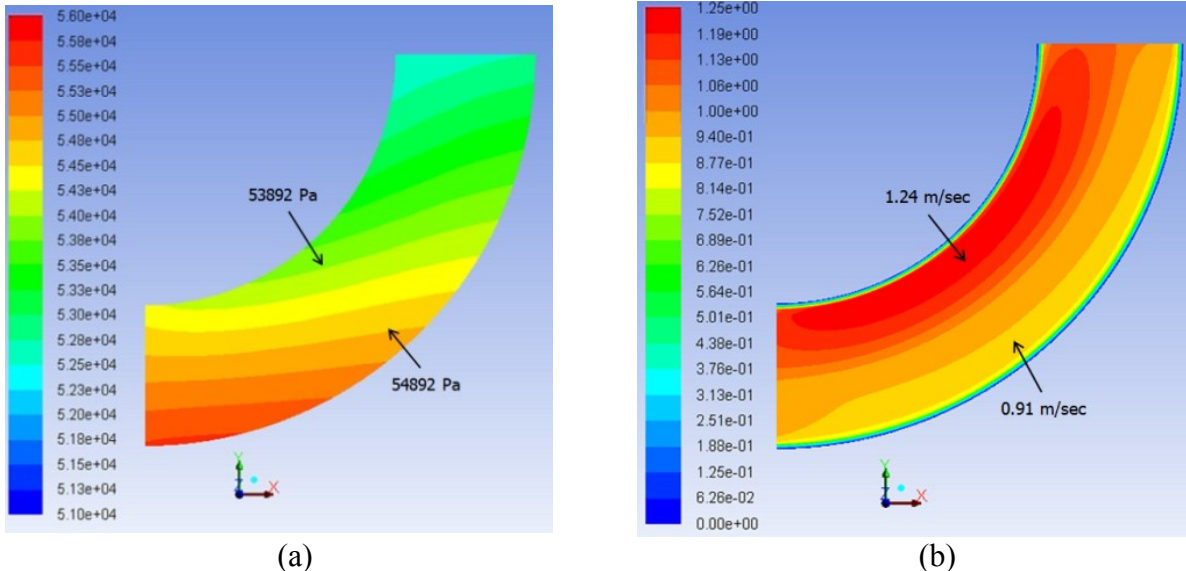


Figure 6.20. Variations in (a) Pressure and (b) Velocity, for a Single Phase Flow in a Vertical Bend of $r/R = 4$ at $V_{av} = 1\text{m/sec}$

6.4.1. Average Flow Velocity Effects

Figure 6.21 depicts the pressure and velocity distributions in a vertical bend of $r/R = 4$ at $V_{av} = 4\text{m/sec}$. It can be seen that high pressure is more uniformly distributed along the outer wall of the bend while the velocity is more evenly distributed throughout the bend. The total pressure drop in the case under consideration is 7021Pa, which is 26% higher as compared to $V_{av} = 1\text{m/sec}$. Thus, increase in average flow velocity increases the pressure drop in a vertical bend. This trend is similar to the one observed in case of horizontal pipe bends.

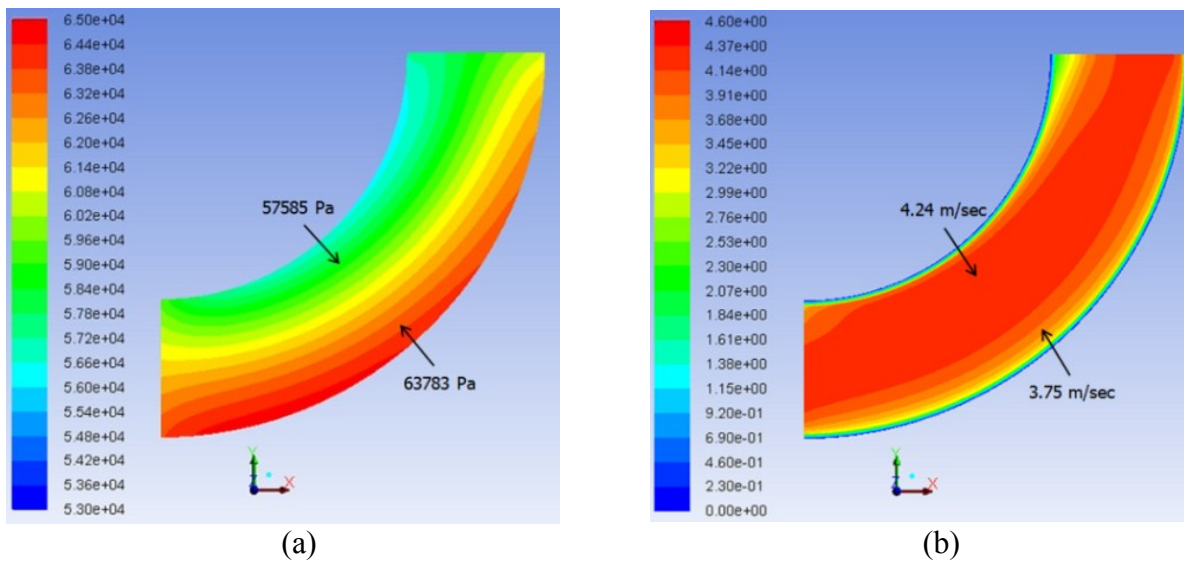


Figure 6.21. Variations in (a) Pressure and (b) Velocity, for a Single Phase Flow in a Vertical Bend of $r/R = 4$ at $V_{av} = 4\text{m/sec}$

6.4.2. Effects of Radius of Curvature

Figure 6.22 depicts the pressure and velocity distributions in a vertical bend of $r/R = 8$ at $V_{av} = 1\text{m/sec}$. It can be seen that the pressure and velocity variations are similar to the one observed in case of $r/R = 4$. Pressure on the outer wall has decreased by 13% on the outer wall of the bend. The total pressure drop for the case under consideration is 5998Pa, which is 8% higher than for $r/R = 4$ at the same average flow velocity. Although it seems that the pressure drop increases as r/R increases in vertical bends, which is opposite to the trend observed in case of horizontal bends, but actually, it is the difference in the elevation of the two bends, i.e. $r/R = 4$ and 8, which is responsible for this increase in the pressure drop. The height for $r/R = 4$ is 0.54906m and for $r/R = 8$ is 0.59810m. Hence, $r/R = 8$ is 0.04904m higher in elevation than $r/R = 4$. This corresponds to 480Pa due to elevation alone. Now, the difference between the pressure drops for $r/R = 4$ and 8 is equal to 451Pa. Hence, $r/R = 8$ bend has actually reduced the pressure drop in the bend by $480 - 451 = 29\text{Pa}$. It is therefore concluded that the pressure drop decreases as r/R increases in vertical bends, which is a similar trend as observed in case of horizontal bends.

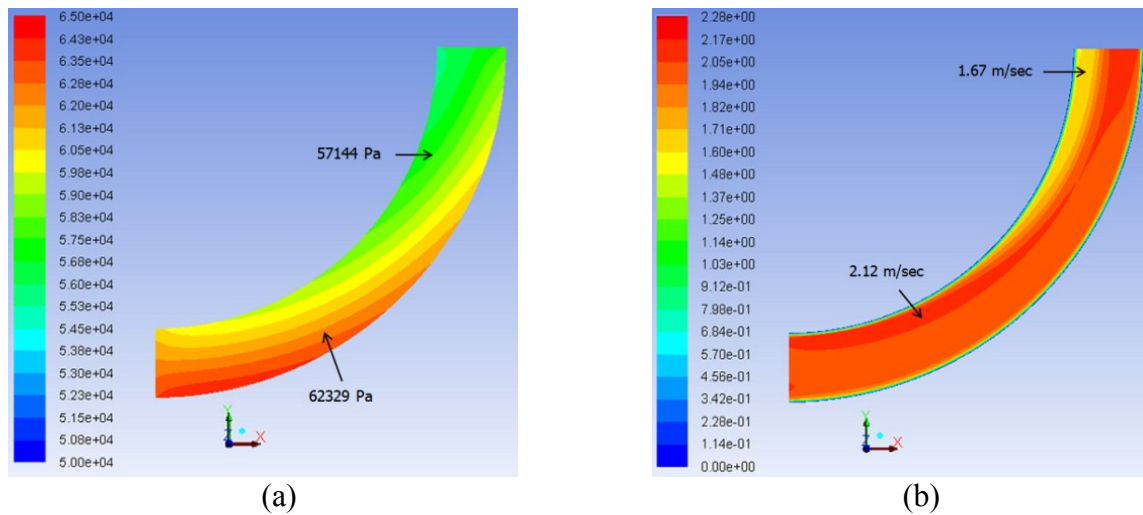


Figure 6.22. Variations in (a) Pressure and (b) Velocity, for a Single Phase Flow in a Vertical Bend of $r/R = 8$ at $V_{av} = 1\text{m/sec}$

6.5. Analysis of the Flow of Equi-Density Capsules in Vertical Bends

Figure 6.23 depicts the pressure and velocity distributions in a vertical bend of $r/R = 4$ carrying a single spherical capsule of $k = 0.5$ and having density equal to water, being transported at $V_{av} = 1\text{m/sec}$. The results depict that the trends are similar to the one observed in a vertical pipe, i.e. the flow pressure is higher at the upstream locations of the capsule while the velocity is low. Furthermore, the pressure is less and the velocity is higher in the annulus region due to the area reduction for the flow. The pressure and velocity are recovered to some extent downstream of the capsule. The total pressure drop in this case is 5995Pa , which is 34 times higher as compared to the flow of an equi-density spherical capsule of $k = 0.5$ in a horizontal bend of $r/R = 4$ at $V_{av} = 1\text{m/sec}$.

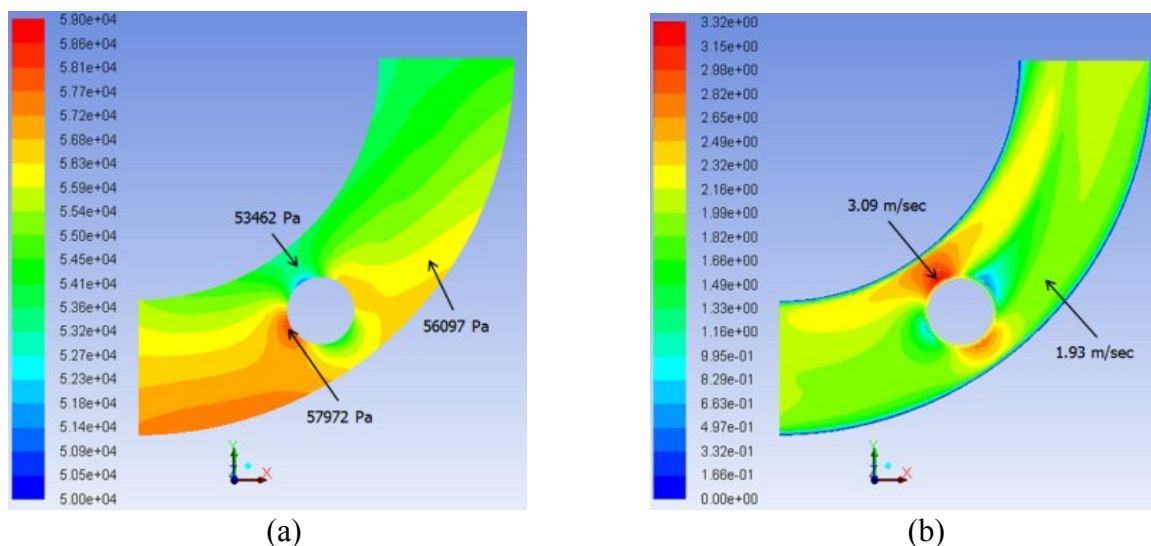


Figure 6.23. Variations in (a) Pressure and (b) Velocity, for a Single Equi-Density Spherical Capsule of $k = 0.5$ at $V_{av} = 1\text{m/sec}$ in a Vertical Bend of $r/R = 4$

6.5.1. Average Flow Velocity Effects

Figure 6.24 depicts the pressure and velocity distributions in a vertical bend of $r/R = 4$ carrying a single equi-density spherical capsule of $k = 0.5$ at $V_{av} = 4\text{m/sec}$. Due to higher centrifugal force acting on the capsule in this case (because of higher velocity of the flow), the capsule is forced to propagate along the outer wall of the bend. Hence, the pressure and velocity distribution is somewhat different to the one observed in case of $V_{av} = 1\text{m/sec}$. The total pressure drop in this case is 8612Pa , which is 328% higher as compared to the flow of an equi-density spherical capsule of $k = 0.5$ at $V_{av} = 4\text{m/sec}$ in a horizontal pipe bend of $r/R = 4$. Hence, increase in the average flow velocity within a pipe bend, transporting capsules, increases the pressure drop. This trend is similar to the one observed in case of horizontal bends, transporting capsules. More detailed results have been presented in table A-5.3.

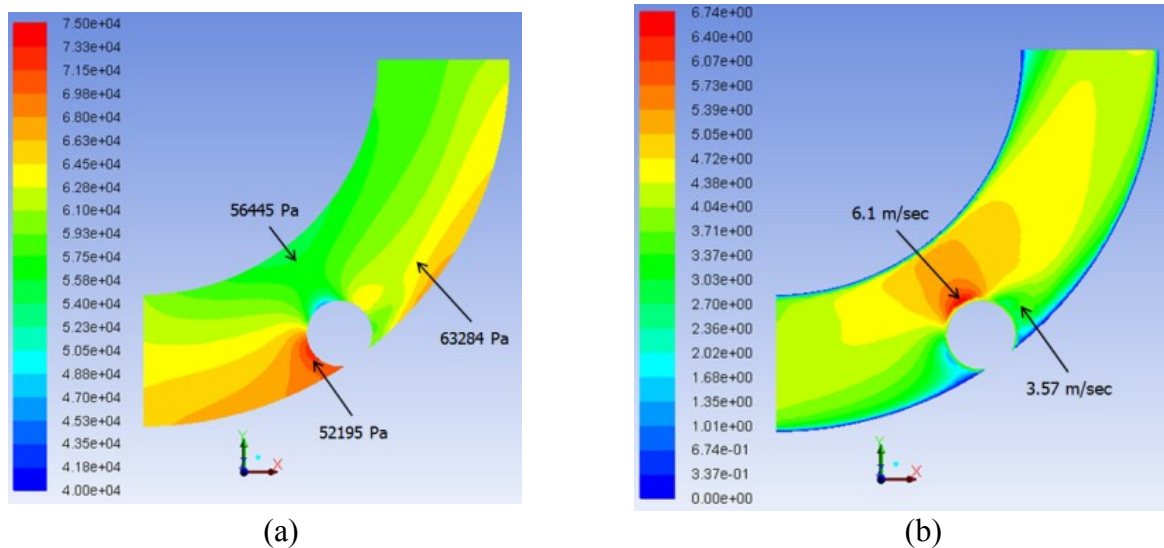


Figure 6.24. Variations in (a) Pressure and (b) Velocity, for a Single Equi-Density Spherical Capsule of $k = 0.5$ at $V_{av} = 4\text{m/sec}$ in a Vertical Bend of $r/R = 4$

6.5.2. Capsule Diameter Effects

Figure 6.25 depicts the pressure and velocity distributions in a vertical bend of $r/R = 4$ carrying a single equi-density spherical capsule of $k = 0.7$ at $V_{av} = 1\text{m/sec}$. The total pressure drop in this case is 6280Pa , which is 24 times higher as compared to the flow of an equi-density spherical capsule of $k = 0.7$ at $V_{av} = 1\text{m/sec}$ in a horizontal pipe bend of $r/R = 4$. Hence, increase in the capsule diameter within a pipe bend, transporting capsules, increases the pressure drop. This trend is similar to the one observed in case of capsule transporting horizontal bends. More detailed results have been presented in table A-5.3.

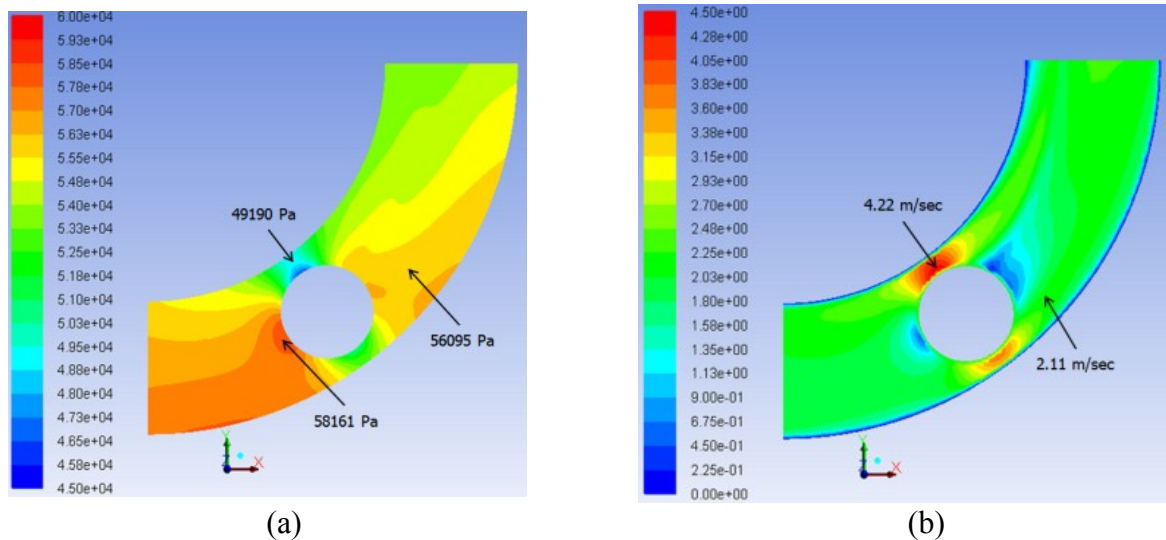


Figure 6.25. Variations in (a) Pressure and (b) Velocity, for a Single Equi-Density Spherical Capsule of $k = 0.7$ at $V_{av} = 1\text{ m/sec}$ in a Vertical Bend of $r/R = 4$

6.5.3. Capsule Concentration Effects

Figure 6.26 depicts the pressure and velocity distributions in a vertical bend of $r/R = 4$ carrying two equi-density spherical capsules of $k = 0.7$ and $Sc = 1 * d$ at $V_{av} = 1\text{ m/sec}$. The total pressure drop in this case is 6735 Pa , which is 16 times higher as compared to the flow of equi-density spherical capsules of $k = 0.7$ at $V_{av} = 1\text{ m/sec}$ in a horizontal pipe bend of $r/R = 4$. Hence, increase in the concentration of the capsules within a pipe bend, transporting capsules, increases the pressure drop. This trend is similar to the one observed in case of capsule transporting horizontal bends. More detailed results have been presented in table A-5.3.

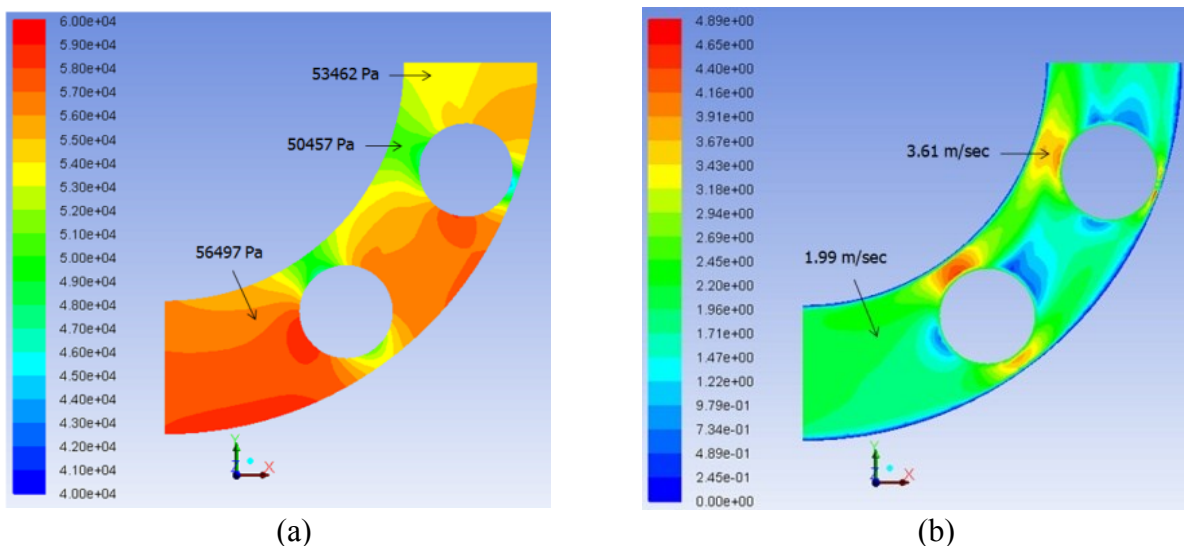


Figure 6.26. Variations in (a) Pressure and (b) Velocity, for Two Equi-Density Spherical Capsules of $k = 0.7$ and $Sc = 1 * d$ at $V_{av} = 1\text{ m/sec}$ in a Vertical Bend of $r/R = 4$

6.5.4. Effects of Spacing between the Capsules

Figure 6.27 depicts the pressure and velocity distributions in a vertical bend of $r/R = 4$ carrying two equi-density spherical capsules of $k = 0.7$ and $Sc = 3 * d$ at $V_{av} = 1\text{m/sec}$. The total pressure drop in this case is 7328Pa , which is 11 times higher as compared to horizontal bend. Hence, increase in the spacing between the capsules marginally increases the pressure drop within capsule transporting vertical bends in comparison with other parameters. More detailed results have been presented in table A-5.3.

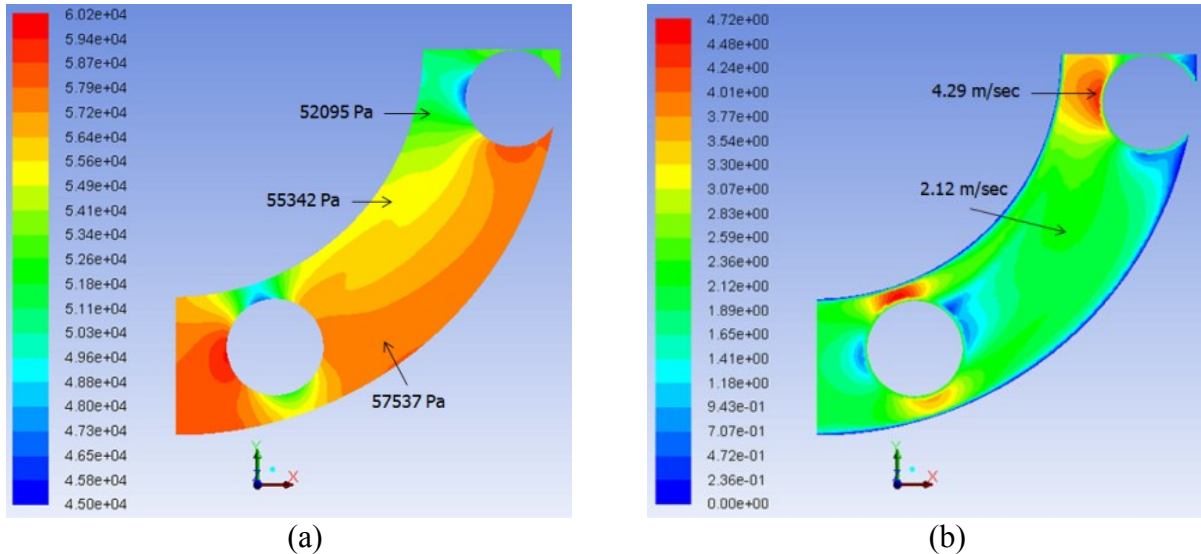


Figure 6.27. Variations in (a) Pressure and (b) Velocity, for Two Equi-Density Spherical Capsules of $k = 0.7$ and $Sc = 3 * d$ at $V_{av} = 1\text{m/sec}$ in a Vertical Bend of $r/R = 4$

6.5.5. Effects of Radius of Curvature of the Bend

Figure 6.28 depicts the pressure and velocity distributions in a vertical bend of $r/R = 8$ carrying two equi-density spherical capsules of $k = 0.7$ and $Sc = 3 * d$ at $V_{av} = 1\text{m/sec}$. The total pressure drop in this case is 10274Pa , which is 14 times higher as compared to horizontal bend for the same case. The reason for the increase in the pressure drop as compared to $r/R = 4$ of vertical bend is due to the elevation difference between the two vertical bends. It has already been explained in detail in section 6.4.2. More detailed results have been presented in table A-5.3.

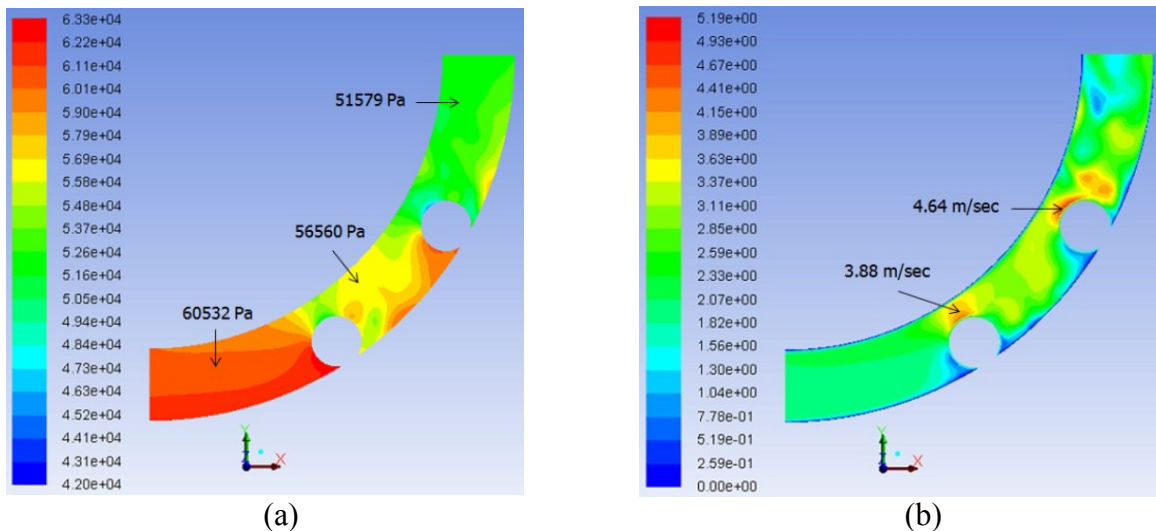


Figure 6.28. Variations in (a) Pressure and (b) Velocity, for Two Equi-Density Spherical Capsules of $k = 0.7$ and $Sc = 3 * d$ at $V_{av} = 1\text{m/sec}$ in a Vertical Bend of $r/R = 8$

6.5.6. Capsule Shape Effects

Figure 6.29 depicts the pressure and velocity distributions in a vertical bend of $r/R = 4$ carrying two equi-density cylindrical capsules of $k = 0.7$, $Sc = 1 * d$ and $L_c = 1 * d$ at $V_{av} = 1\text{m/sec}$. The total pressure drop in this case is 28533Pa, which is 8 times higher as compared to two equi-density cylindrical capsules of same diameter, spacing and average flow velocity in a horizontal bend of same r/R . Hence, cylindrical capsules offer substantially more resistance to the flow and thus increase the pressure drop within vertical bends. More detailed results have been presented in table A-5.3.

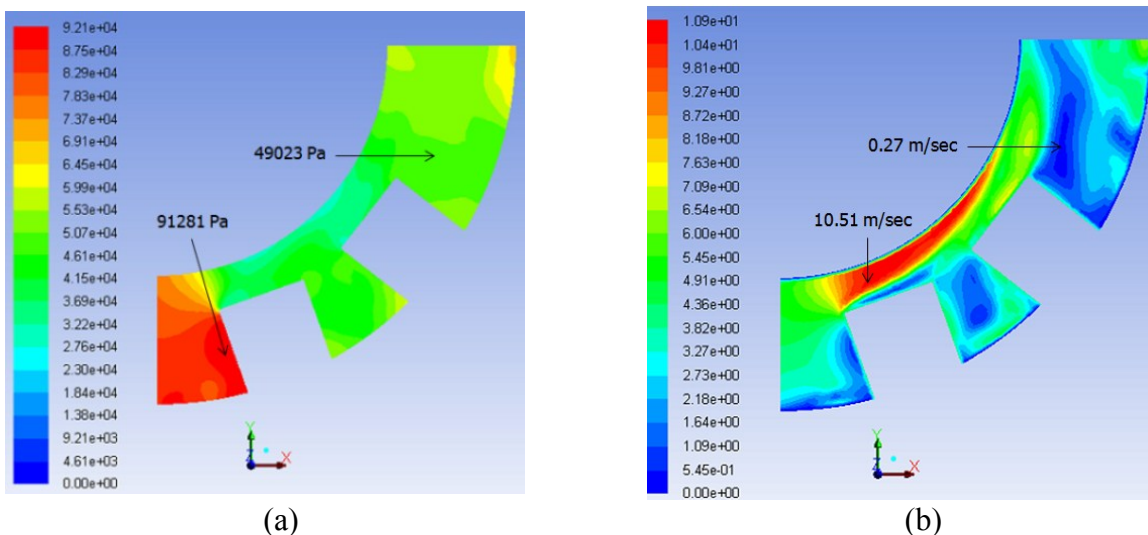


Figure 6.29. Variations in (a) Pressure and (b) Velocity, for Two Equi-Density Cylindrical Capsules of $k = 0.7$, $Sc = 1 * d$ and $L_c = 1 * d$ at $V_{av} = 1\text{m/sec}$ in a Vertical Bend of $r/R = 4$

6.5.7. Length of the Capsule Effects

Figure 6.30 depicts the pressure and velocity distributions in a vertical bend of $r/R = 4$ carrying two equi-density cylindrical capsules of $k = 0.7$, $Sc = 1 * d$ and $Lc = 2 * d$ at $V_{av} = 1\text{m/sec}$. The total pressure drop in this case is 20315Pa, which is 6 times higher as compared to horizontal bends. Hence, longer cylindrical capsules offer less resistance to the flow and thus decrease the pressure drop within the bend. More detailed results have been presented in table A-5.3.

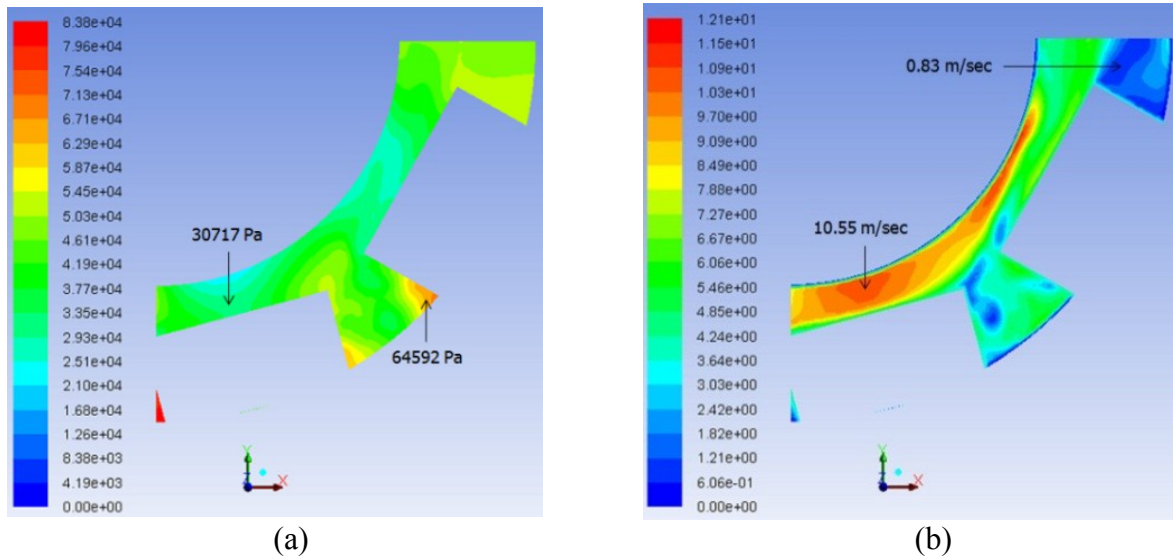


Figure 6.30. Variations in (a) Pressure and (b) Velocity, for Two Equi-Density Cylindrical Capsules of $k = 0.7$, $Sc = 1 * d$ and $Lc = 2 * d$ at $V_{av} = 1\text{m/sec}$ in a Vertical Bend of $r/R = 4$

Table A-5.3 in Appendix A-5 summarises the results for various CFD based investigations being carried out on the flow of equi-density capsules in vertical bends. The information provided in this section, regarding the flow of equi-density capsules in vertical pipe bends, has a huge impact on the design process of HCPs, which is presented in Chapter 7.

6.6. Analysis of the Flow of Heavy-Density Capsules in Vertical Bends

Figure 6.31 depicts the pressure and velocity distributions in a vertical bend of $r/R = 4$ carrying a single spherical capsule of $k = 0.5$ and having density greater than water, being transported at $V_{av} = 1\text{m/sec}$. The trend of pressure and velocity variations resembles the one observed in the case of a heavy-density spherical capsule in a horizontal bend. It can be seen that due to the density of the capsule, and the centrifugal force being exerted on the capsule in the bend, the capsule is being transported along the outer wall of the bend. The total pressure drop in this case is 6312Pa, which is 24 times higher as compared to the flow of a heavy-density spherical capsule of the same diameter and same average flow velocity in a horizontal bend of $r/R = 4$.

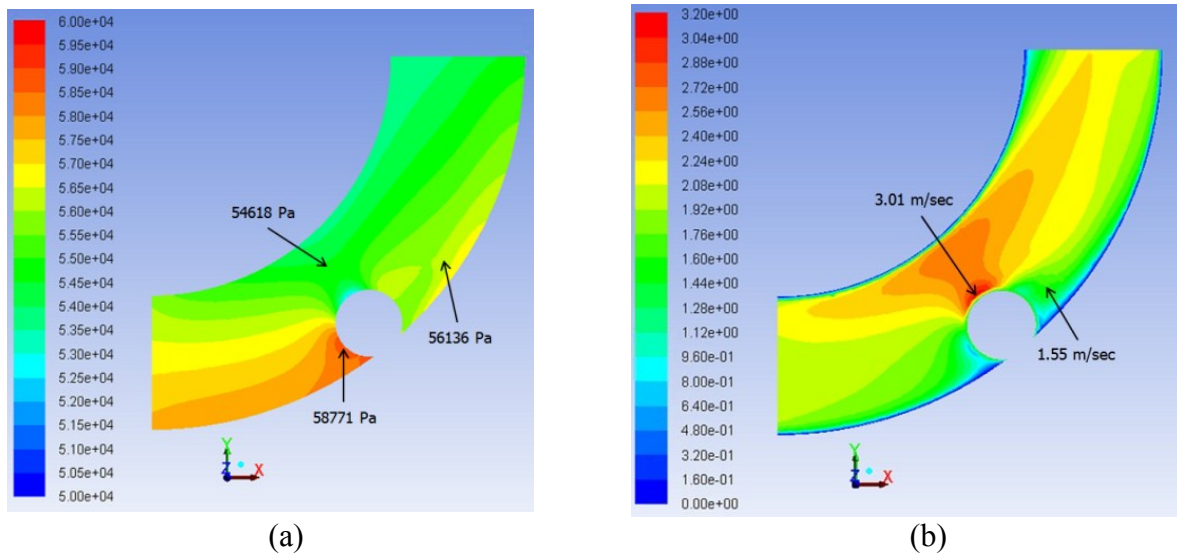


Figure 6.31. Variations in (a) Pressure and (b) Velocity, for a Single Heavy-Density Spherical Capsule of $k = 0.5$ at $V_{av} = 1\text{m/sec}$ in a Vertical Bend of $r/R = 4$

6.6.1. Average Flow Velocity Effects

Figure 6.32 depicts the pressure and velocity distributions in a vertical bend of $r/R = 4$ carrying a single heavy-density spherical capsule of $k = 0.5$ at $V_{av} = 4\text{m/sec}$. The total pressure drop in this case is 8562Pa , which is 195% higher as compared to the flow of a heavy-density spherical capsule of $k = 0.5$ at $V_{av} = 1\text{m/sec}$ in a horizontal pipe bend of $r/R = 4$. Hence, increase in the average flow velocity within a vertical pipe bend, transporting capsules, increases the pressure drop. This trend is similar to the one observed in case of horizontal bends. More detailed results have been presented in table A-5.4.

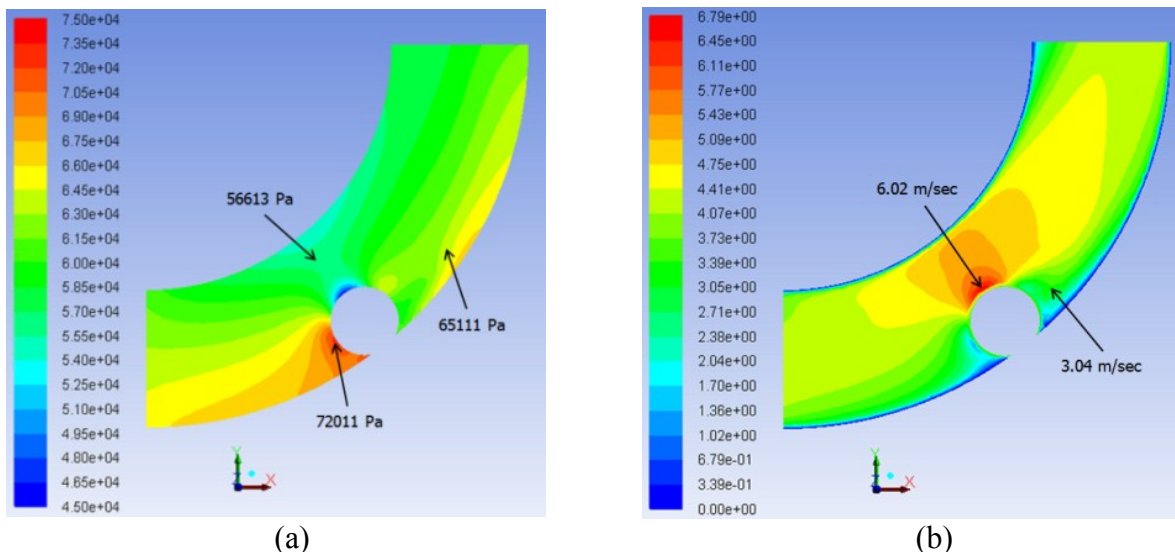


Figure 6.32. Variations in (a) Pressure and (b) Velocity, for a Single Heavy-Density Spherical Capsule of $k = 0.5$ at $V_{av} = 4\text{m/sec}$ in a Vertical Bend of $r/R = 4$

6.6.2. Capsule Diameter Effects

Figure 6.33 depicts the pressure and velocity distributions in a vertical bend of $r/R = 4$ carrying a single heavy-density spherical capsule of $k = 0.7$ at $V_{av} = 1\text{m/sec}$. The total pressure drop in this case is 7370Pa , which is 11 times higher as compared to the flow of a heavy-density spherical capsule of $k = 0.5$ at $V_{av} = 1\text{m/sec}$ in a horizontal pipe bend of $r/R = 4$. Hence, increase in the capsule diameter within a vertical pipe bend increases the pressure drop. More detailed results have been presented in table A-5.4.

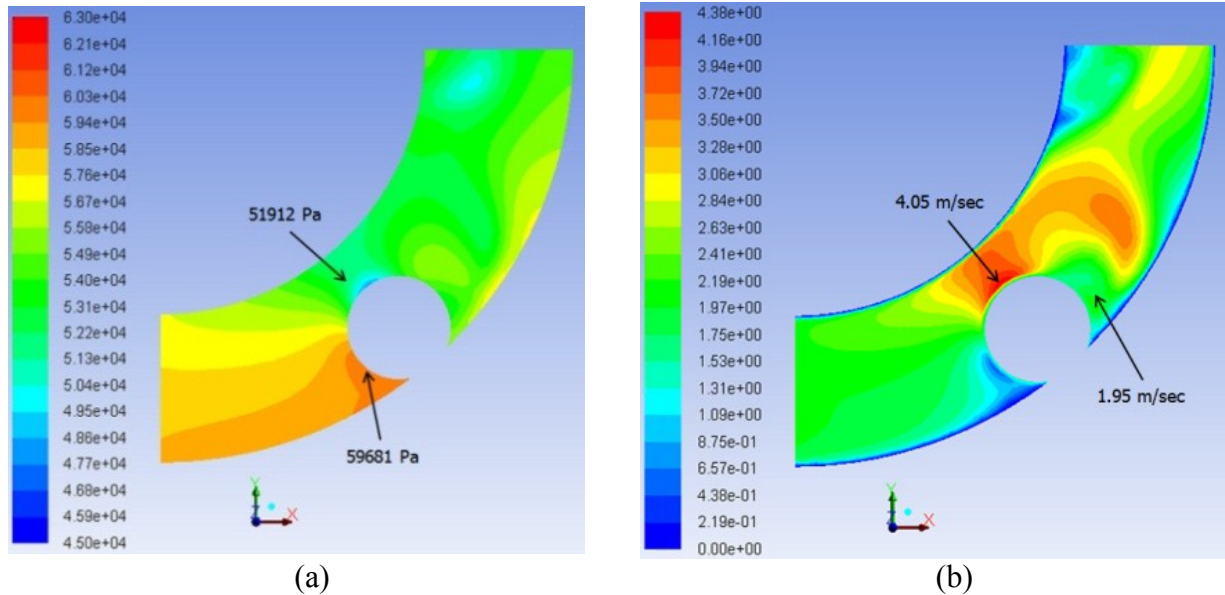


Figure 6.33. Variations in (a) Pressure and (b) Velocity, for a Single Heavy-Density Spherical Capsule of $k = 0.7$ at $V_{av} = 1\text{m/sec}$ in a Vertical Bend of $r/R = 4$

6.6.3. Capsule Concentration Effects

Figure 6.34 depicts the pressure and velocity distributions in a vertical bend of $r/R = 4$ carrying two heavy-density spherical capsules of $k = 0.7$ and $Sc = 1 * d$ at $V_{av} = 1\text{m/sec}$. The total pressure drop in this case is 10453Pa , which is 342% higher as compared to the flow of heavy-density spherical capsules of $k = 0.7$ at $V_{av} = 1\text{m/sec}$ in a horizontal pipe bend of $r/R = 4$. Hence, increase in the concentration of the capsules within a vertical pipe bend increases the pressure drop. This trend is similar to the one observed in case of heavy-density capsule flow within horizontal bends. More detailed results have been presented in table A-5.4.

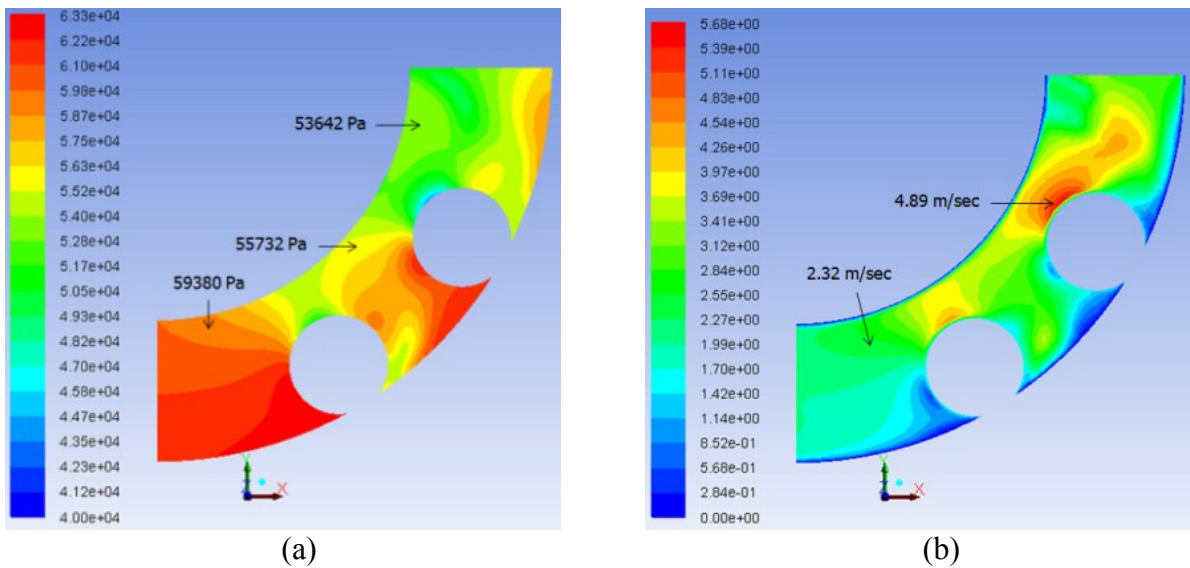


Figure 6.34. Variations in (a) Pressure and (b) Velocity, for Two Heavy-Density Spherical Capsules of $k = 0.7$ and $Sc = 1 * d$ at $V_{av} = 1\text{m/sec}$ in a Vertical Bend of $r/R = 4$

6.6.4. Effects of Spacing between the Capsules

Figure 6.35 depicts the pressure and velocity distributions in a vertical bend of $r/R = 4$ carrying two heavy-density spherical capsules of $k = 0.7$ and $Sc = 3 * d$ at $V_{av} = 1\text{m/sec}$. The total pressure drop in this case is 10419Pa , which is 7 times higher as compared to the flow of heavy-density spherical capsules in horizontal bends. Hence, increase in the spacing between the capsules marginally increases the pressure drop within capsule transporting vertical bends in comparison with other parameters. More detailed results have been presented in table A-5.4.

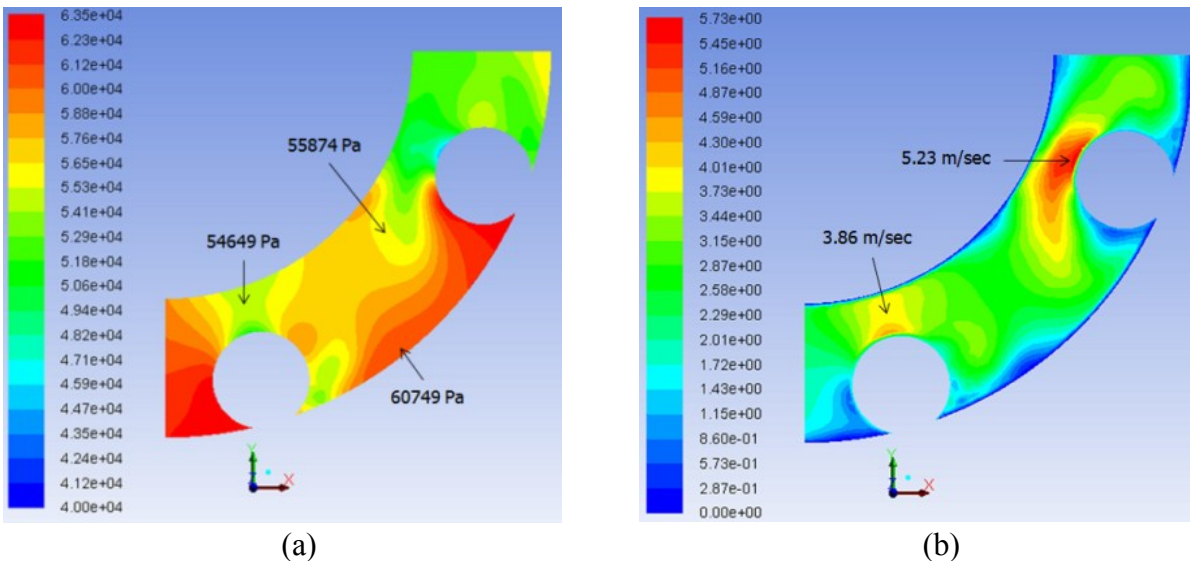


Figure 6.35. Variations in (a) Pressure and (b) Velocity, for Two Heavy-Density Spherical Capsules of $k = 0.7$ and $Sc = 3 * d$ at $V_{av} = 1\text{m/sec}$ in a Vertical Bend of $r/R = 4$

6.6.5. Effects of Radius of Curvature of the Bend

Figure 6.36 depicts the pressure and velocity distributions in a vertical bend of $r/R = 8$ carrying two heavy-density spherical capsules of $k = 0.7$ and $Sc = 3 * d$ at $V_{av} = 1\text{m/sec}$. The total pressure drop in this case is 8520Pa , which is 6 times higher as compared to the flow of heavy-density spherical capsules in a vertical bend of $r/R = 4$. Hence, increase in the radius of curvature of the bend decreases the pressure drop due to reduced secondary flows within the bend. More detailed results have been presented in table A-5.4.

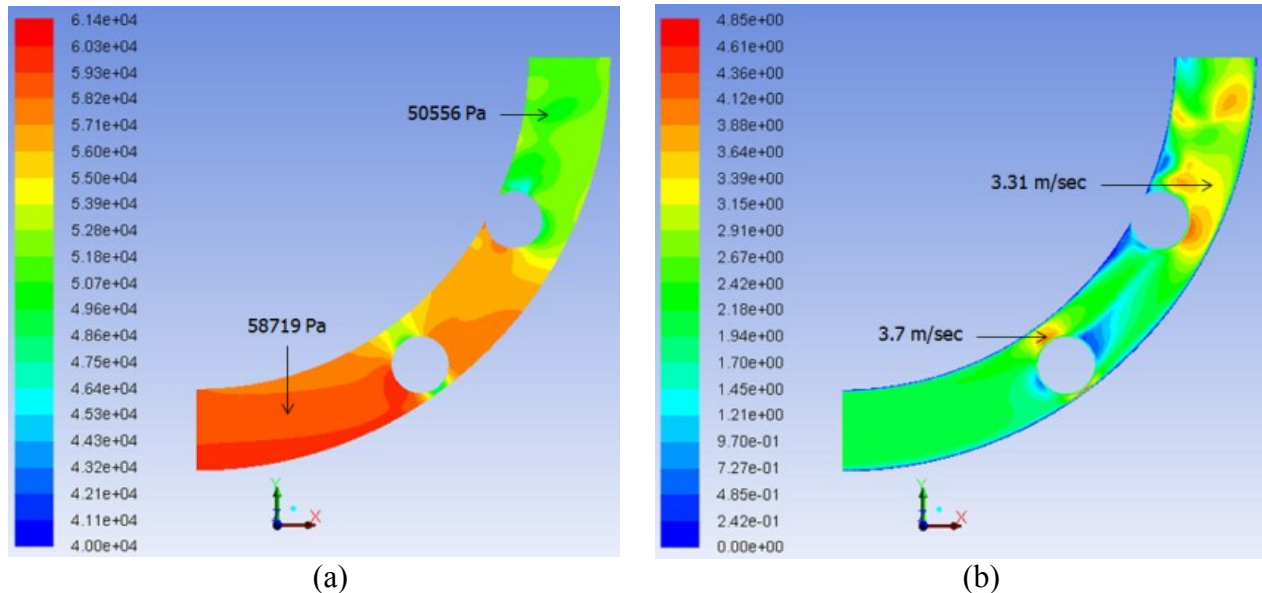


Figure 6.36. Variations in (a) Pressure and (b) Velocity, for Two Heavy-Density Spherical Capsules of $k = 0.7$ and $Sc = 3 * d$ at $V_{av} = 1\text{m/sec}$ in a Vertical Bend of $r/R = 8$

6.6.6. Capsule Shape Effects

Figure 6.37 depicts the pressure and velocity distributions in a vertical bend of $r/R = 4$ carrying two heavy-density cylindrical capsules of $k = 0.7$, $Sc = 1 * d$ and $L_c = 1 * d$ at $V_{av} = 1\text{m/sec}$. The total pressure drop in this case is 29058Pa , which is 336% higher as compared to the flow of heavy-density cylindrical capsules in a horizontal bend of $r/R = 4$. Hence, cylindrical capsules offer substantially more resistance to the flow and thus increase the pressure drop within the bend. More detailed results have been presented in table A-5.4.

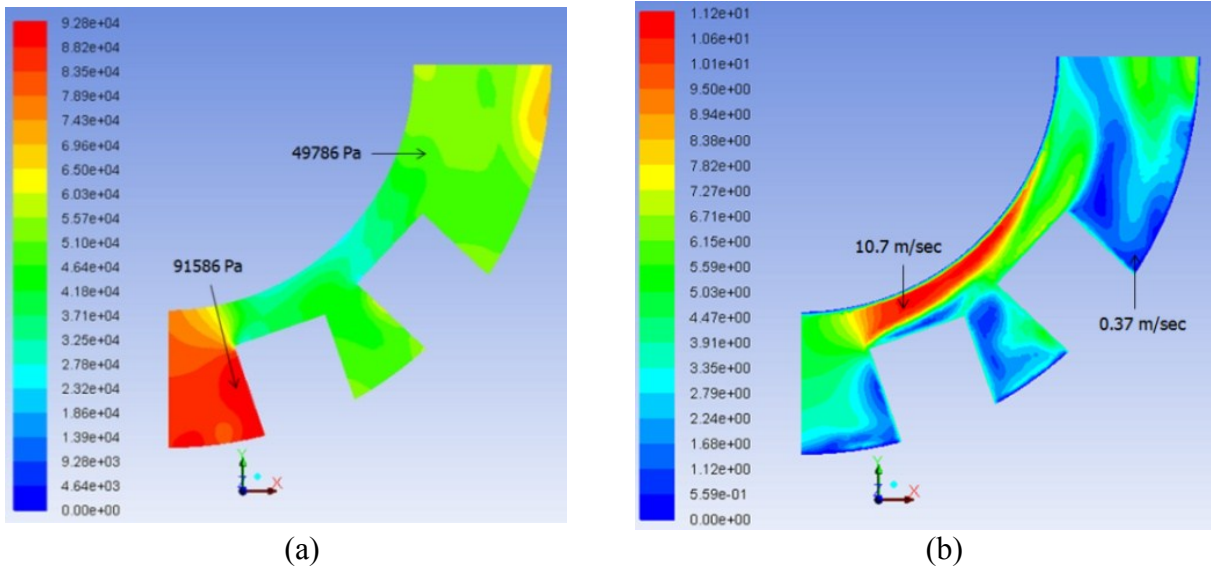


Figure 6.37. Variations in (a) Pressure and (b) Velocity, for Two Heavy-Density Cylindrical Capsules of $k = 0.7$, $Sc = 1 * d$ and $Lc = 1 * d$ at $V_{av} = 1\text{m/sec}$ in a Vertical Bend of $r/R = 4$

6.6.7. Length of the Capsule Effects

Figure 6.38 depicts the pressure and velocity distributions in a vertical bend of $r/R = 4$ carrying two heavy-density cylindrical capsules of $k = 0.7$, $Sc = 1 * d$ and $Lc = 2 * d$ at $V_{av} = 1\text{m/sec}$. The total pressure drop in this case is 23476Pa, which is 5 times higher as compared to the flow of heavy-density cylindrical capsules in a horizontal bend of $r/R = 4$. Hence, increase in the length of the cylindrical capsules decreases the pressure drop within vertical bends. Furthermore, from the aforementioned discussions, the pressure drop in vertical bends carrying heavy-density capsules is considerably higher as compared to the flow of equi-density capsules in vertical bends. More detailed results have been presented in table A-5.4.

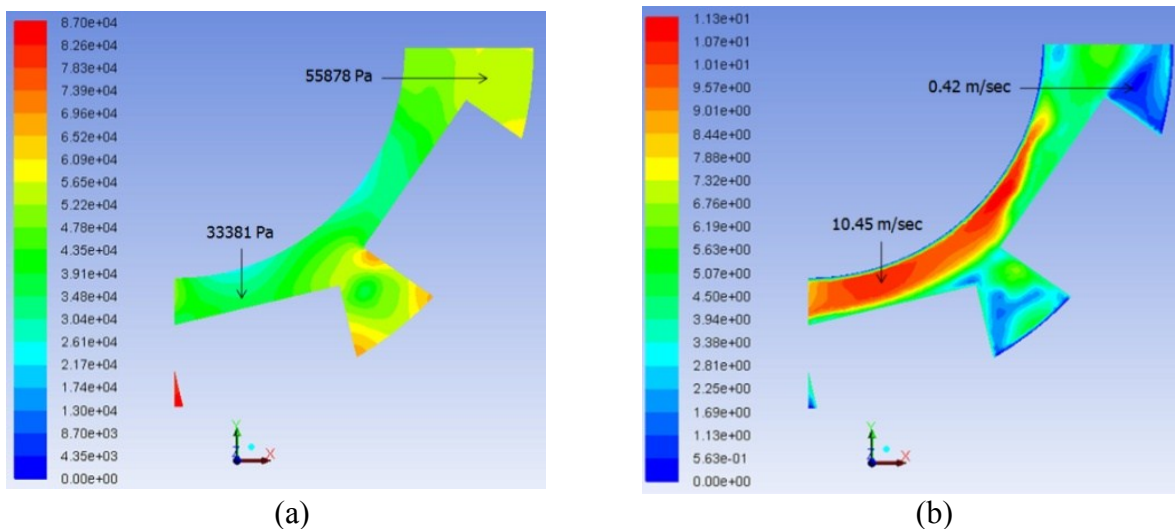


Figure 6.38. Variations in (a) Pressure and (b) Velocity, for Two Heavy-Density Cylindrical Capsules of $k = 0.7$, $Sc = 1 * d$ and $Lc = 2 * d$ at $V_{av} = 1\text{m/sec}$ in a Vertical Bend of $r/R = 4$

Table A-5.4 in Appendix A-5 summarises the results for various CFD based investigations being carried out on the flow of heavy-density capsules in vertical bends. The information provided in this section, regarding the flow of heavy-density capsules in vertical pipe bends, has a huge impact on the design process of HCPs, which is presented in Chapter 7.

6.7. Prediction Models

Based on the results presented in this chapter, prediction models for the loss coefficient of bends, due to the presence of capsules in the bends, can be developed as discussed in Chapter 1. The loss coefficient of bends for can be calculated by the following expressions:

$$K_{lc} = 2 \frac{\left(\frac{\Delta P_m}{L_p} - \frac{\Delta P_w}{L_p} \right)}{n \rho_w V_{av}^2} \quad (6.1)$$

Using multiple variable regression analysis, semi-empirical correlations for the prediction of loss coefficient of bends due to water and capsule flow, as a function of geometric and flow variables discussed in Chapter 3, have been developed. The loss coefficient of bends due to water flow can be computed as:

$$K_{lw} = \frac{\left(3.05 - 0.0875 \frac{r}{R} \right)}{Re_w^{\frac{1}{5}}} \quad (6.2)$$

The prediction models for the loss coefficient of bends due to capsules are listed in table 6.5.

Table 6.5. Loss Coefficient of Bends for Capsule Flow

Bend Type	Capsule Shape	Density of the Capsules	Loss Coefficient due to Capsules
Horizontal	Spherical	Equi-Density	$K_{lc} = \frac{\left(22387 \left(\frac{N}{L_p} * d \right)^{2.26} k^{3.5} \frac{Sc + Lp^{1.5}}{Lp} \right)}{Re_c^{0.38} \frac{r^{0.2}}{R}}$

		Heavy-Density	$K_{lc} = \frac{\left(138 \left(\frac{N}{Lp} * d\right)^{0.66} k^{3.5}\right)}{Re_c^{0.077} \frac{r}{R} \frac{Sc + Lp}{Lp}^{1.17}}$
	Cylindrical	Equi-Density	$K_{lc} = \frac{\left(691 \left(\frac{N}{Lp} * Lc\right)^{1.63} k^{2.92} \frac{Sc + Lp}{Lp}^{1.05}\right)}{Re_c^{0.026} \frac{r}{R} \frac{Lc}{d}^{1.88}}$
		Heavy-Density	$K_{lc} = \frac{\left(549 \left(\frac{N}{Lp} * Lc\right)^{0.5} k^{3.92}\right)}{Re_c^{0.14} \frac{Lc}{d}^{0.43} \frac{r}{R} \frac{Sc + Lp}{Lp}^{0.45}}$
Vertical	Spherical	Equi-Density	$K_{lc} = \frac{\left(33884 \left(\frac{N}{Lp} * d\right)^{1.19} k^{3.24} \frac{Sc + Lp}{Lp}^{1.39}\right)}{Re_c^{0.55} \frac{r}{R}^{0.2}}$
		Heavy-Density	$K_{lc} = \frac{\left(10^{5.6} \left(\frac{N}{Lp} * d\right)^{0.044} k^{4.33} \frac{Sc + Lp}{Lp}^{0.036}\right)}{Re_c^{0.83} \frac{r}{R}^{0.2}}$
	Cylindrical	Equi-Density	$K_{lc} = \frac{\left(10^{6.8} \left(\frac{N}{Lp} * Lc\right)^{1.22} k^{4.5} \frac{Sc + Lp}{Lp}^{1.35}\right)}{Re_c^{0.81} \frac{r}{R} \frac{Lc}{d}^{1.5}}$
		Heavy-Density	$K_{lc} = \frac{\left(10^8 \left(\frac{N}{Lp} * Lc\right)^{1.33} k^{4.5} \frac{Sc + Lp}{Lp}^{1.35}\right)}{Re_c^{0.96} \frac{r}{R} \frac{Lc}{d}^{1.58}}$

Figures 6.39 and 6.40 show the difference between the loss coefficients of bends, due to capsules within the pipeline, calculated using the expressions presented in table 31 and that obtained from the CFD results in this chapter to authorise the usefulness of these semi-empirical relationships. From figure 6.39, it can be clearly seen that more than 90% of the data lies within $\pm 10\%$ error bound of the semi-empirical expression for equi-density spherical capsules in a horizontal bend. Similarly, it can be seen in figure 6.40 that more than 90% of the data lies within $\pm 10\%$ error bound of the semi-empirical relation for heavy-density cylindrical capsules within a vertical bend. Hence, the prediction models developed here represent the loss coefficient of bends due to the presence of the capsules with reasonable accuracy. The remaining prediction models have the same order of accuracy.

From the prediction models, it can be seen that as the number of capsules, diameter of capsules, length of capsules or the velocity of the capsules becomes zero, i.e. no capsule in the pipeline, the value for K_{lc} automatically goes to zero and the expression for the pressure drop in the pipeline is only left with the loss coefficient due to water in equation (1.41). Furthermore, as Sc becomes zero, i.e. contacting capsules in the bend, the prediction models will still be valid. In order to prove this, a separate case regarding the flow of contacting capsules has been simulated and the results show that the difference between K_{lc} from CFD and K_{lc} from the prediction models is within the error bounds of the prediction models, i.e. $\pm 10\%$. Hence, the prediction models presented in this chapter can be used for a variety of capsule flow conditions within vertical pipelines. Furthermore, the prediction models developed here can be directly used in the design of HCPs (see Chapter 7 for further details).

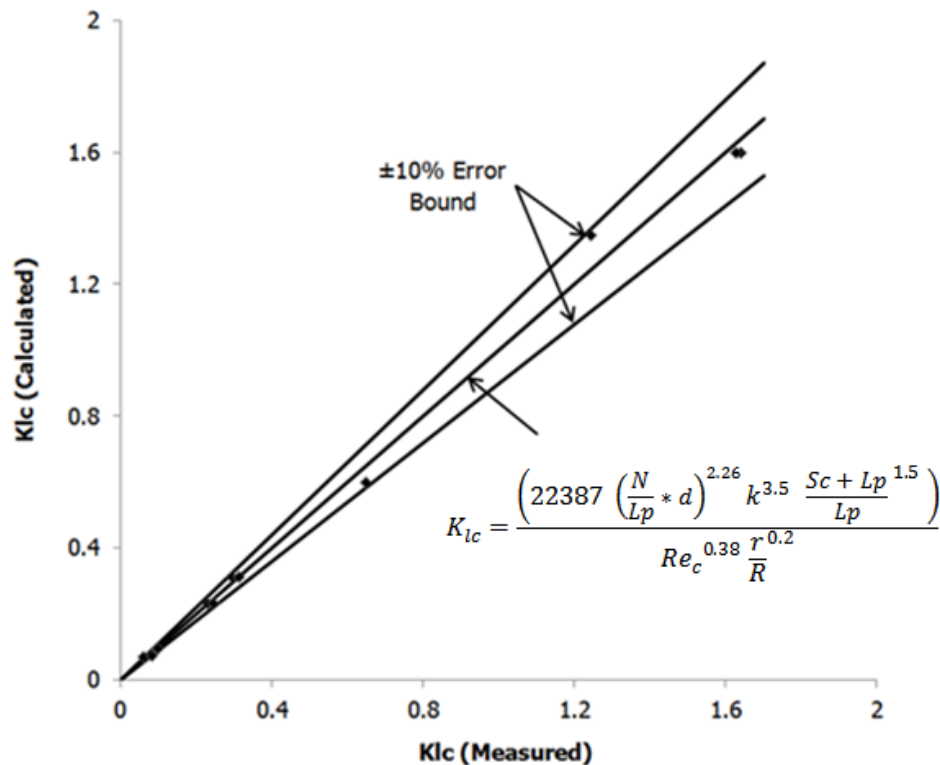


Figure 6.39. K_{lc} for Equi-Density Spherical Capsules in a Horizontal Bend

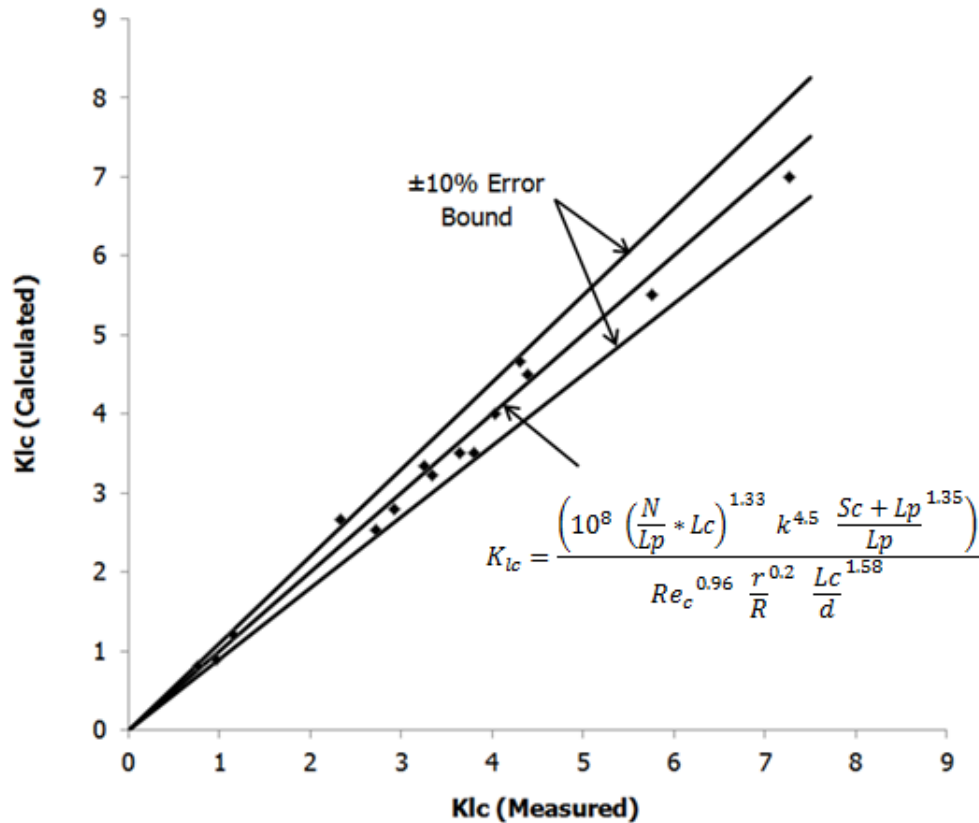


Figure 6.40. K_{lc} for Heavy-Density Cylindrical Capsules in a Vertical Bend

6.8. Summary of the Analysis of a HCP Bends

A detailed flow diagnostics of the pipe bends, transporting capsules has revealed the following results:

- Increase in the average flow velocity increases the pressure drop in the bend (see section 6.2.1, 6.3.1, 6.5.1 and 6.6.1 for reference)
- Increase in the capsules diameter increases the pressure drop in the bend (see section 6.2.2, 6.3.2, 6.5.2 and 6.6.2 for reference)
- Increase in the length of the capsules decreases the pressure drop in the bend (see section 6.2.7, 6.3.7, 6.5.7 and 6.6.7 for reference)
- Increase in the spacing between the capsules marginally increases the pressure drop in the bend, in comparison with other parameters, except for the flow of heavy-density capsules in horizontal bends (see section 6.2.4, 6.3.4, 6.5.4 and 6.6.4 for reference)
- Increase in the density of the capsules increases the pressure drop in the bend (see Appendix A-5 for reference)

- Cylindrical capsules result in an increased pressure drop in the bend as compared to the flow of spherical capsules (see section 6.2.6, 6.3.6, 6.5.6 and 6.6.6 for reference)
- Increase in the radius of curvature of a bend decreases the pressure drop in the bend (see section 6.1.2, 6.2.5, 6.3.5, 6.4.2, 6.5.5 and 6.6.5 for reference)
- Increase in the concentration of the capsules increases the pressure drop in the bend (see section 6.2.3, 6.3.3, 6.5.3 and 6.6.3 for reference)

The information provided in this chapter, regarding the flow of capsules in pipe bends, and the prediction models developed for the friction factor of capsules, has a huge implication on the design process of hydraulic capsule pipelines. Further details about the design of HCPs are presented in Chapter 7. Once the complete analysis of HCPs has been carried out, in the current and the previous chapters, the next stage is the design of HCPs. The next chapter includes the details regarding the optimal design of such pipelines.

CHAPTER 7

OPTIMISATION OF HCPs

Optimisation of HCPs is essential as far as the commercial viability of the HCPs is concerned. Based on the results obtained from Chapters 4, 5 and 6 regarding the flow of capsules in HCPs, an optimisation methodology has been developed in this chapter for various geometric and flow conditions. The optimisation model presented in this study is based on the least-cost principle. The correlations developed for the friction factors and the loss coefficients in the previous chapters, for pipelines transporting capsules and bends, have been used to develop a methodology to find out the optimal HCP design. The optimisation model presented is both robust and user-friendly.

7.1. Introduction

The literature review presented in Chapter 2 sheds light on some of the existing design and optimisation models available. The bases of the models presented are different; while some models optimise HCPs on the basis of mechanical design while others optimise the design of HCPs on the basis of hydraulic design. As mentioned in Chapter 1 that this study is based on the hydraulic parameters affecting the design of HCPs, hence, the optimisation model developed is also based on the hydraulic design of HCPs.

In order to validate the results of the optimisation model presented in this chapter with the existing optimisation models, only those parameters have been considered which forms the basis of the existing models. These parameters include the manufacturing cost and the operating cost of an HCP. Other costs involved in the design of HCPs, such as installation cost, maintenance cost etc. have not been included in the existing models. However, these costs can be included for better understanding of all the costs involved in the optimal design of an HCP. Hence, HCP designers are cautioned here to use this model with carefulness as this model is based on the hydraulic design of HCPs only.

Furthermore, the existing optimisation models, which are based on the hydraulic design of HCPs, makes use of the Least-Cost Principle which states that the optimal design of any HCP is such that the total cost of the pipeline is at minimum, where the total cost refers to the sum of the operating and the manufacturing costs only. This principle has been used in the present study as well in order to validate the model presented here with the existing optimisation models.

7.2. Optimisation of HCPs

Optimisation of any pipeline is essential for its commercial viability. Presented here is an optimisation model which can be used for pipelines transporting capsules. The model is based on the least-cost principle, i.e. the pipeline transporting capsules is designed such that the total cost of the pipeline is minimum.

As stated above, the least-cost principle refers to the minimum total cost of the pipeline. The total cost of a pipeline transporting capsules consists of the manufacturing cost of the pipeline and the capsules plus the operating cost of the system.

$$C_{Total} = C_{Manufacturing} + C_{Operating} \quad (7.1)$$

The manufacturing cost can be further divided into the cost of the pipeline and the cost of the capsules. The operating cost refers to the cost of the power being consumed.

$$C_{Total} = C_{Pipe} + C_{Capsule} + C_{Power} \quad (7.2)$$

7.3. Cost of Pipes

The cost of pipe per unit weight of the pipe material is given by [94]:

$$C_{pipe} = \pi D t Y_p C_2 L_p \quad (7.3)$$

where t is the thickness of the pipe wall. According to Davis and Sorenson [95] and Russel [96], the pipe wall thickness can be expressed as:

$$t = C_c D \quad (7.4)$$

where C_c is a constant of proportionality dependent on expected pressure and diameter ranges of the pipeline. Hence, the cost of the pipe becomes:

$$C_{pipe} = \pi D^2 Y_p C_2 C_c L_p \quad (7.5)$$

7.4. Cost of Capsules

The cost of spherical capsules per unit weight of the capsule material can be calculated as:

$$C_{Spherical\ Capsules} = \pi k^2 D^2 t_c N Y_{cap} C_3 \quad (7.6)$$

where t_c is the thickness of the capsule, N is the total number of capsules in the pipeline and Y_{cap} is the specific weight of the capsule material. The cost of cylindrical capsules per unit weight of the capsule material can be calculated as:

$$C_{Cylindrical\ Capsules} = \pi k D L_c t_c N Y_{cap} C_3 \quad (7.7)$$

where L_c is the length of the cylindrical capsules in the pipeline.

7.5. Cost of Power

The cost of power consumption per unit watt is given by:

$$C_{power} = C_1 P \quad (7.8)$$

where P is the power requirement of the pipeline transporting capsules. It is the power that dictates the selection of the pumping unit to be installed. The power can be expressed as:

$$P = \frac{Q_m \times \Delta P_{Total}}{\eta} \quad (7.9)$$

where Q_m is the flow rate of the mixture, ΔP_{Total} is the total pressure drop in the pipeline transporting capsules and η is the efficiency of the pumping unit. Generally the efficiency of industrial pumping unit ranges between 60 to 75%. The total pressure drop can be calculated from the friction factor relations developed in the previous chapters whereas the mixture flow rate has been computed from the cases that have been investigated in this study.

7.6. Mixture Flow Rate

Liu [13] reports the expression to find the mixture flow rate as:

$$Q_m = \frac{\pi D^2}{4} V_{av} \quad (7.10)$$

for a circular pipe. V_{av} can be expressed in terms of the velocity of the capsule from the holdup data discussed in Chapter 3 and is listed in table A-6.1 in Appendix A-6.

7.7. Total Pressure Drop

The total pressure drop in a pipeline can be expressed as a sum of the major pressure drop and minor pressure drop resulting from pipeline and pipe fittings respectively.

$$\Delta P_{Total} = \Delta P_{Major} + \Delta P_{Minor} \quad (7.11)$$

The major pressure drop can be expressed as follows for horizontal pipes as:

$$\Delta P_{Major} = f_w \frac{L_p}{D} \frac{\rho_w V_{av}^2}{2} + f_c \frac{L_p}{D} \frac{\rho_w V_{av}^2}{2} \quad (7.12)$$

and for vertical pipes as:

$$\Delta P_{Major} = f_w \frac{L_p}{D} \frac{\rho_w V_{av}^2}{2} + f_c \frac{L_p}{D} \frac{\rho_w V_{av}^2}{2} + \rho_w g \Delta h \quad (7.13)$$

Similarly, the minor pressure drop can be expressed as follows for horizontal bends as:

$$\Delta P_{Minor} = K_{lw} \frac{n \rho_w V_{av}^2}{2} + K_{lc} \frac{n \rho_w V_{av}^2}{2} \quad (7.14)$$

and for vertical bends as:

$$\Delta P_{Minor} = K_{lw} \frac{n\rho_w V_{av}^2}{2} + K_{lc} \frac{n\rho_w V_{av}^2}{2} + \rho_w g \Delta h \quad (7.15)$$

where n is the number of bends in the pipeline. Here, f_w can be found by the Moody's approximation [7] as:

$$f_w = 0.0055 + \frac{0.55}{Re_w^{1/3}} \quad (7.16)$$

K_{lw} has been found out to be:

$$K_{lw} = \frac{(3.05 - 0.0875 \frac{r}{R})}{Re_w^{1/5}} \quad (7.17)$$

Expressions to calculate f_c and K_{lc} have been developed in the previous chapters and are listed in table A-6.2 in Appendix A-6.

7.8. Solid Throughput

The solid throughput in m^3/sec is the input to the model. One important point to note over here is that the pipeline designer has no information regarding the velocities in the pipeline, whether it is the average flow velocity or the velocity of the capsules. In order to replace the velocities mentioned in the above equations, the solid throughput has been used to as:

Solid Throughput = Amount of substance flowing per unit time

$Q_c = \text{Volume of a capsule} \times \text{Time taken by the capsules to travel unit length}$

For spherical capsules:

$$Q_c = \frac{\pi d^3}{6} \times \frac{\text{Number of capsules in the train}}{\text{Time taken to travel unit length}} \quad (7.18)$$

The number of capsules in the train can be calculated as follows:

$$L_p = NL_c + (N - 1)S_c \quad (7.19)$$

Hence:

$$N = \frac{L_p + S_c}{L_c + S_c} \quad (7.20)$$

where $L_c = d$ for spherical capsules. Length of the capsules and the spacing between them should be chosen such that N is an integer. The time taken to travel unit distance will be:

$$\text{Time taken to cover 1m distance} = \frac{L_p}{V_c}$$

Hence:

$$Q_c = \frac{\pi d^3}{6} \times \frac{L_p + S_c}{L_c + S_c} \times \frac{V_c}{L_p}$$

$$Q_c = \frac{\pi d^3 V_c}{6 L_p} \times \frac{L_p + S_c}{L_c + S_c} \quad (7.21)$$

Similarly, for cylindrical capsules:

$$Q_c = \frac{\pi d^2 L_c V_c}{4 L_p} \times \frac{L_p + S_c}{L_c + S_c} \quad (7.22)$$

V_c can be represented in terms of Q_c . Furthermore, V_{av} can be expressed in terms of V_c using holdup expressions. Hence, there will be no velocity expression that will be explicitly required in the optimisation model.

7.9. Working of the Optimisation Model

The following steps should be followed to run the optimisation model. The input to the model is the solid throughput.

1. Assume a value of D
2. The length of the pipeline is already known from the information of the capsules injection and evacuations sites
3. Calculate the cost of pipes and capsules based on the information regarding the materials of the pipe and the capsules, and the market price of these materials
4. Fix the value of k (this study suggests a value of 0.7 as optimum)
5. Assume the value of the efficiency of the pumping unit (0.6 – 0.75) and then keep it fixed
6. Calculate V_{av} , V_c , Re_w and Re_c

7. Calculate friction factors and pressure drop (both major and minor)
8. Calculate Q_m
9. Find out the power requirement for the system
10. Calculate the total cost of the pipeline based on the cost of per unit of electricity
11. Repeat steps 1 to 10 for various values of D until that value is reached at which the total cost of the pipeline is minimum

Figure 7.1 presents a flow chart for the optimisation methodology presented here.

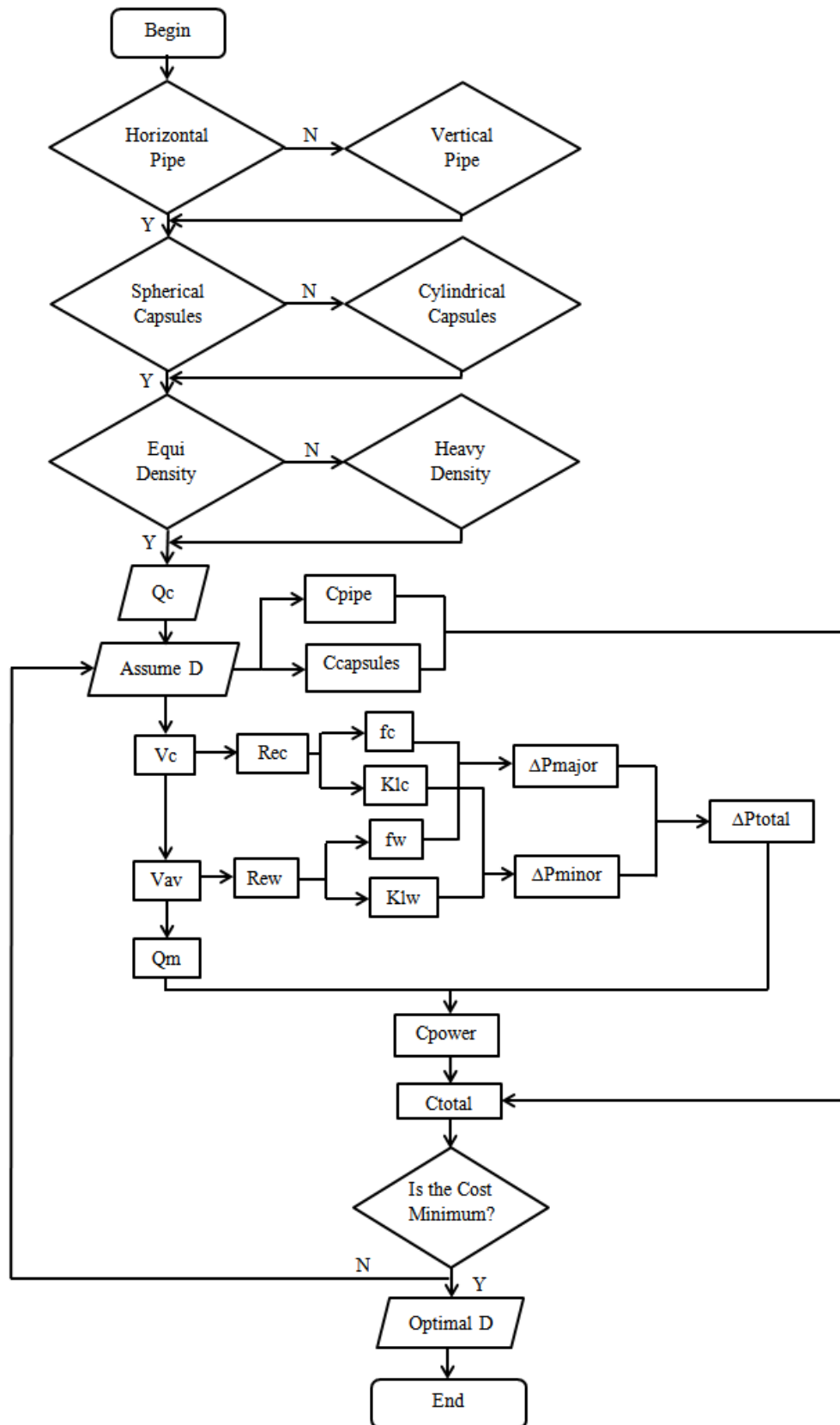


Figure 7.1. Flow Chart of the Optimisation Methodology

7.10. Limitations of the Optimisation Model

As mentioned in section 7.1, the basis of the model presented in this study is the hydraulic design of HCPs. This marks the biggest limitation of this optimisation model. Further to this limitation, listed below are some of the other assumptions/limitations of the model presented here:

- The value of the pumping unit's efficiency has been assumed in the present optimisation model
- The prediction models developed for the friction factor of capsules flowing in pipe bends have not been validated/testing against experimental data and hence can lead to inaccuracies in the design process
- This model is applicable only in a certain range of parameters such as average flow velocity of 1m/sec to 4m/sec, capsule diameter equals 50 to 70% of the pipeline diameter etc.

Further studies are required, both numerical and experimental, to increase the range of operation of the optimisation model presented in this study, in order to design an HCP with more accuracy.

7.11. Design Example for On-Shore Applications

Polypropylene needs to be transferred from the processing plant to the storage area of the factory half kilometre away in the form of spherical capsules of $k = 0.7$. The spacing between the capsules should be $3 * d$. The required throughput of polypropylene is $0.001\text{m}^3/\text{sec}$. Find the optimal size of the pipeline and the pumping power required for this purpose.

Solution: According to the current market, the values of different constants involved in the optimisation process are:

$$C_1 = 1.4$$

$$C_3 = 1.1$$

$$C_2 = 0.95$$

Polypropylene has a density equal to that of water. Assuming the efficiency of the pumping unit $\eta = 60\%$ and following the steps described in the working of the optimisation model, the following results (table 7.1) are obtained.

Table 7.1. Variations in Pumping Power and Various Costs w.r.t. Pipeline Diameter

D	P	C_{Manufacturing}	C_{Power}	C_{Total}
(m)	(kW)	(£)	(£)	(£)
0.08	20.87	9129	29218	38347
0.09	11.77	11468	16487	27955
0.10	7.06	14073	9883	23956

0.11	4.44	16944	6222	23166
0.12	2.91	20081	4079	24160
0.13	1.97	23485	2766	26251
0.14	1.38	27154	1930	29084

The results presented in table 7.1 depicts that a pipeline of diameter = 110 cm is optimum for the problem under consideration because the total cost for the pipeline is minimum at $D = 0.11\text{m}$. The power of the pumping unit required, corresponding to the optimal diameter of the pipeline, is 4.44 kW. Further analysing the results presented in table 7.1, figure 7.2 depicts the variations in the manufacturing and operating costs for various pipeline diameters. It can be seen that as the pipeline diameter increases, the manufacturing cost increases. This is due to the fact that pipes of larger diameters are more expensive than pipes of relatively smaller diameters. Furthermore, as the pipeline diameter increases, the operating cost decreases. This is due to the fact that, for the same solid throughput, increasing the pipeline diameter decreases the velocity of the flow within the pipeline. The operating cost has a proportional relationship with the velocity of the flow; hence, increase in the pipeline diameter decreases the operating cost of the pipeline.

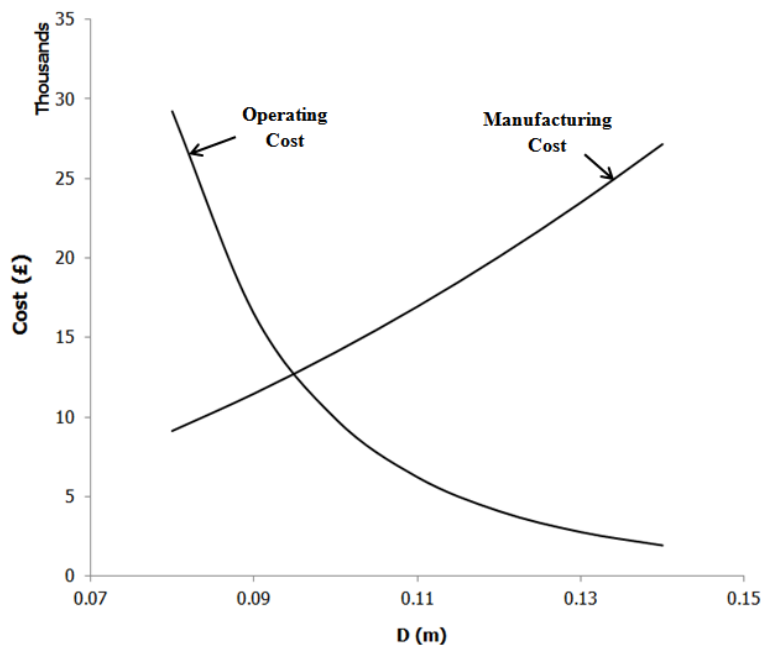


Figure 7.2. Variations in Operating and Operating Costs w.r.t. Pipeline Diameter

Figure 7.3 depicts the variations in the total cost and the pumping power required at various pipeline diameters. It can be seen that as the pipeline diameter increases, the required pumping power decreases. Furthermore, as the pipeline diameter increases, the total cost of the pipeline first decreases and then increases. As the total cost of the pipeline is a sum of the manufacturing and operating costs, which have opposite trends w.r.t. the pipeline diameter, hence, the combination of these costs give rise to the total cost curve. The pipeline diameter, which corresponds to the minimum total cost of the pipeline, is the optimal pipeline diameter.

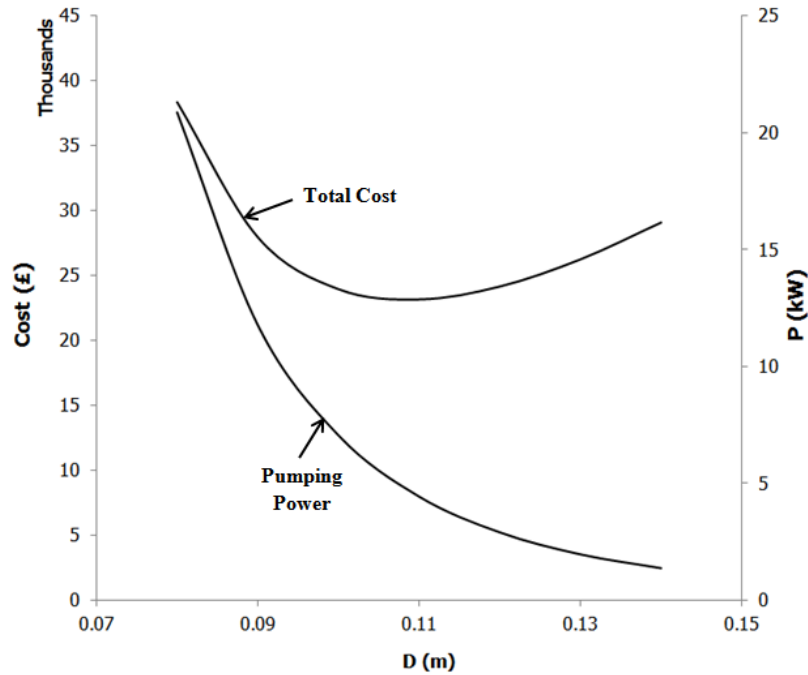


Figure 7.3. Variations in Total Cost and Pumping Power Required at Various Pipeline Diameters

Table 7.2 summarises the variations in the capsule velocity and the various pressure drops in the pipeline at different pipeline diameters. It can be seen that the capsule velocity and the total pressure drop that corresponds to the optimal pipeline diameter are 1.28m/sec and 242.93kPa respectively.

Table 7.2. Variations in Capsule Velocity and Pressure Drops

D	V_c	ΔP_{Minor}	ΔP_{Major}	ΔP_{Total}
(m)	(m/sec)	(kPa)	(kPa)	(kPa)
0.08	2.43	5.43	1135.20	1140.63
0.09	1.92	3.54	640.12	643.66
0.10	1.55	2.41	383.46	385.87
0.11	1.28	1.70	241.23	242.93
0.12	1.08	1.24	158.01	159.25
0.13	0.92	0.93	107.08	108.01
0.14	0.79	0.71	74.68	75.39

Figure 7.4 depicts the variations in the capsule velocity and the total pressure drop in the pipeline for various pipeline diameters. It is evident from the figure that as the pipeline diameter increases, the velocity of the capsules decreases. This supports the aforementioned statement regarding the variations in the flow velocity for increasing pipeline diameters. Furthermore, as the pipeline diameter increases, the total pressure drop decreases. This statement is again supporting the results presented above for the variations in pumping power required for the pipeline. Hence, all the results presented here are in agreement with the design methodology presented in this chapter for the flow of capsules in a pipeline.

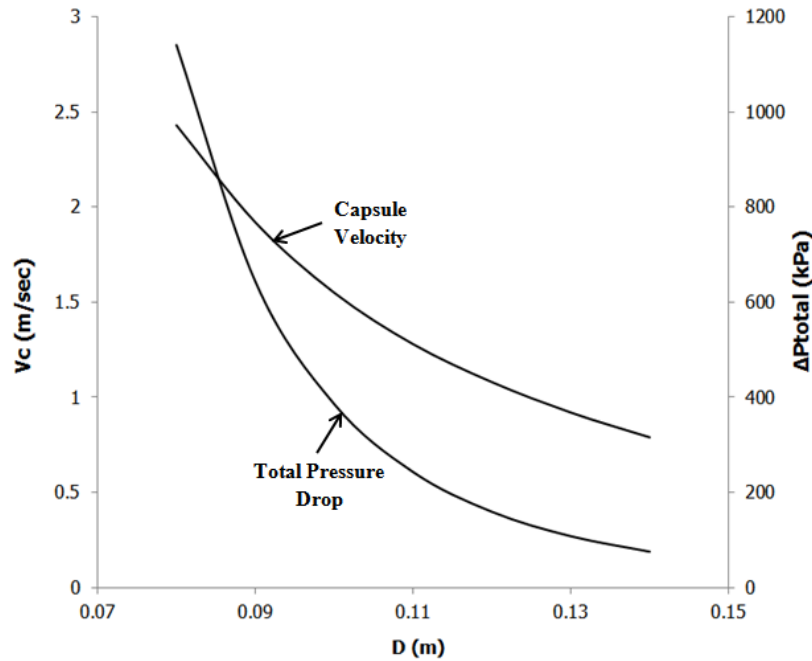


Figure 7.4. Variations in Capsule Velocity and Total Pressure Drop w.r.t. Pipeline Diameter

Table 7.3 presents the variations in the capsule velocity, pumping power and the optimal diameter of the pipeline for various solid throughputs. Hence, table 7.3 can be used as a design chart for the problem under consideration.

Table 7.3. Variations in Optimal Diameter, Capsule Velocity and Pumping Power for Various Solid Throughputs

Qc	Vc	P	D
(m ³ /sec)	(m/sec)	(kW)	(m)
0.001	1.28	4.44	0.11
0.002	1.38	7.16	0.15
0.005	1.76	19.30	0.21
0.008	1.84	26.31	0.26
0.010	1.98	34.81	0.28

Figure 7.5 depicts the variations in the optimal diameter of the pipeline and the required pumping power at various solid throughputs. It can be seen that as the solid throughput increases, the optimal pipeline diameter increases. Furthermore, as the solid throughput increases, the required pumping power also increases.

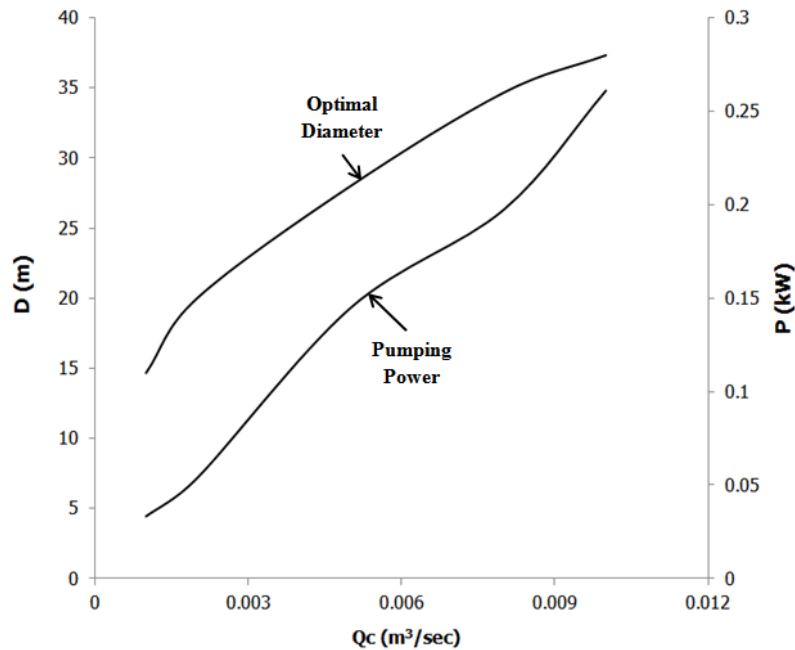


Figure 7.5. Variations in Optimal Diameter and Pumping Power w.r.t. the Solid Throughput

7.11.1. Comparison of the Optimisation Model w.r.t. Agarwal et. al.'s [66] Optimisation Model

It will be prudent at this point to validate the results predicted by this model with the results from an existing optimisation model for validation purposes. Comparison between the optimisation models developed in this study (Asim's Optimisation Model) and the optimisation model of Agarwal et. al [66] is presented here for a solid throughput of $0.001m^3/sec$ along 500m length of a horizontal pipeline. Agarwal et. al.'s optimisation model is limited for contacting capsules only. Hence, Asim's optimisation model has been specified with $Sc = 0$ for the flow of equi-density spherical capsules within the pipeline. Table 7.4 shows the variations in the pumping power and the total cost of the pipeline for the problem under consideration from both optimisation models. It can be seen that the optimal pipeline diameter, required pumping power and the total cost of the pipeline predicted by Agarwal et. al.'s optimisation model are 60cm, 6.54kW and £ = 15800 respectively. Whereas, the results from Asim's optimisation model for these parameters are 50cm, 6.15kW and £ = 13470.

Agawal et. al.'s optimisation model gives 20% higher optimal pipeline diameter. At respective optimal pipeline diameters from both the models, the pumping power from Agarwal et. al.'s optimisation model is 6.34% higher in comparison with Asim's optimisation model. The differences in results from both the optimisation models are due to the reasons pointed out in the literature review. Agarwal et. al.'s optimisation model has the following limitations:

- Limited parameters for the analysis of pipelines transporting capsules
- Homogeneous model for pressure drop prediction

The aforementioned points severely limit the utility of the model in terms of accurate representation of the pressure drop, pumping power and the total cost of the pipeline transporting capsules.

Table 7.4. Variations in Pumping Power and Total Cost from Agarwal et. al.'s Optimisation Model

Pipeline Diameter	Agarwal. et. al.'s Optimisation Model		Asim's Optimisation Model	
	P	C _{Total}	P	C _{Total}
(m)	(kW)	(£)	(kW)	(£)
0.03	15.53	23866	10.92	17413
0.04	10.84	18538	7.90	14422
0.05	8.21	16360	6.15	13470
0.06	6.54	15800	5.01	13646
0.07	5.40	16241	4.21	14567
0.08	4.58	17390	3.62	16048
0.09	3.96	19088	3.17	17987
0.10	3.47	21246	2.82	20326

7.11.2. Capsule Shape Effects

Pipeline designers are always in search for the best options, in terms of the combination of various parameters, to design the pipeline for a specified throughput. Hence, the example considered above is solved again using cylindrical capsules and keeping all other parameters the same. Table 7.5 presents the results for the modified pipeline design.

Table 7.5. Variations in Pumping Power and Various Costs w.r.t. Pipeline Diameter

D	P	C_{Manufacturing}	C_{Power}	C_{Total}
(m)	(kW)	(£)	(£)	(£)
0.08	24.55	9129	34383	43512
0.09	13.83	11468	19362	30830
0.10	8.27	14073	11585	25658
0.11	5.20	16944	7280	24224
0.12	3.40	20081	4763	24844
0.13	2.30	23485	3225	26710
0.14	1.60	27154	2247	29401

From the results presented in table 7.5 it can be seen that the optimal pipeline diameter for the flow of cylindrical capsules is 0.11m or 110cm, which is the same as for the flow of spherical capsules in the pipeline. Furthermore, the pumping power required at the optimal pipeline diameter is 5.2kW, which was 4.44kW for the spherical capsules. Hence, by introducing the cylindrical capsules in the pipeline, both the pumping power and the optimal pipeline diameter increases. This is because cylindrical capsules offer more resistance to the flow within a pipeline (according to the results from Chapter 4, 5 and 6) and hence the pressure drop in the pipeline is considerably higher for the flow of cylindrical capsules in comparison with the flow of spherical capsules in the pipeline. This not only increases the pumping power required to transport the same throughput of the solids in the pipeline but also increases the optimal pipeline diameter.

Figure 7.6 depicts the variations in the total cost and the operating cost of the pipeline for the flow of both the spherical and the cylindrical capsules. It is evident from the figure that the total cost of the pipeline for the flow of spherical capsules is lower than for the flow of cylindrical capsules. Furthermore, the operating cost for the flow of cylindrical capsules is higher as compared to the flow of spherical capsules in the pipeline. The reasons for all the trends are the same as mentioned above, i.e. cylindrical capsules results in a higher pressure drop in the pipeline.

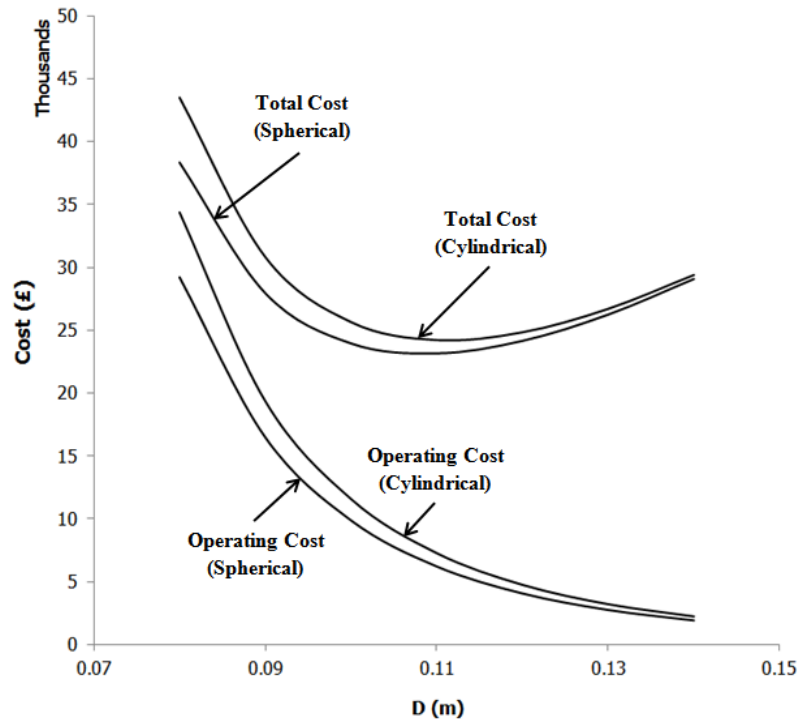


Figure 7.6. Comparison of Various Costs of the Pipeline for Spherical and Cylindrical Capsules

The variations in the capsule velocity and the various pressure drops in the pipeline, for the flow of cylindrical capsules, are shown in table 7.6. The results presented show that the total pressure drop for the optimal pipeline diameter, i.e. $D = 0.11\text{m}$, is 487.13kPa .

Table 7.6. Variations in Capsule Velocity and Pressure Drops

D	V_c	ΔP_{Minor}	ΔP_{Major}	ΔP_{Total}
(m)	(m/sec)	(kPa)	(kPa)	(kPa)
0.08	1.62	10.31	2290.10	2300.41
0.09	1.28	6.46	1289.04	1295.50
0.10	1.04	4.25	770.92	775.17
0.11	0.85	2.91	484.22	487.13
0.12	0.72	2.06	316.72	318.78
0.13	0.61	1.50	214.32	215.82
0.14	0.53	1.11	149.29	150.40

Figure 7.7 depicts the variations in the capsule velocity and the total pressure drop within the pipeline, for the flow of both the spherical and cylindrical shaped capsules. It can be seen that the total pressure drop is considerably higher for the flow of cylindrical capsules in the pipeline. Furthermore, it is evident that the velocity of the cylindrical capsules is lower as compared to the velocity of the spherical capsules in the pipeline.

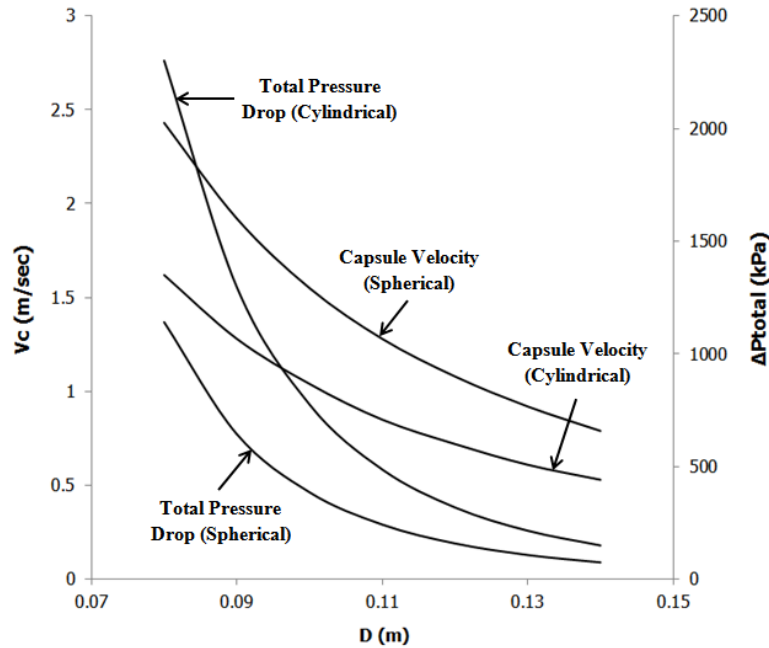


Figure 7.7. Variations in Capsule Velocity and Total Pressure Drop w.r.t. Pipeline Diameter for Spherical and Cylindrical Capsules

As shown in case of the spherical capsules, table 7.7 presents the variations in the optimal pipeline diameter, capsule velocity and required pumping power for various solid throughputs. It can be seen that as the solid throughput increases, the optimal pipeline diameter also increases.

Table 7.7. Variations in Optimal Diameter, Capsule Velocity and Pumping Power for Various Solid Throughputs

Qc	Vc	P	D
(m ³ /sec)	(m/sec)	(kW)	(m)
0.001	0.85	5.20	0.11
0.002	0.92	8.43	0.15
0.005	1.07	18.28	0.22
0.008	1.14	26.13	0.27
0.010	1.23	32.10	0.29

A comparison of the optimal diameter of the pipeline, for the flow of both the spherical and cylindrical capsules within the pipeline, w.r.t. the solid throughput is shown in figure 7.8. It can be seen that the optimal diameter of the pipeline, for the flow of cylindrical capsules, is higher as compared to the flow of spherical capsules, at higher solid throughput.

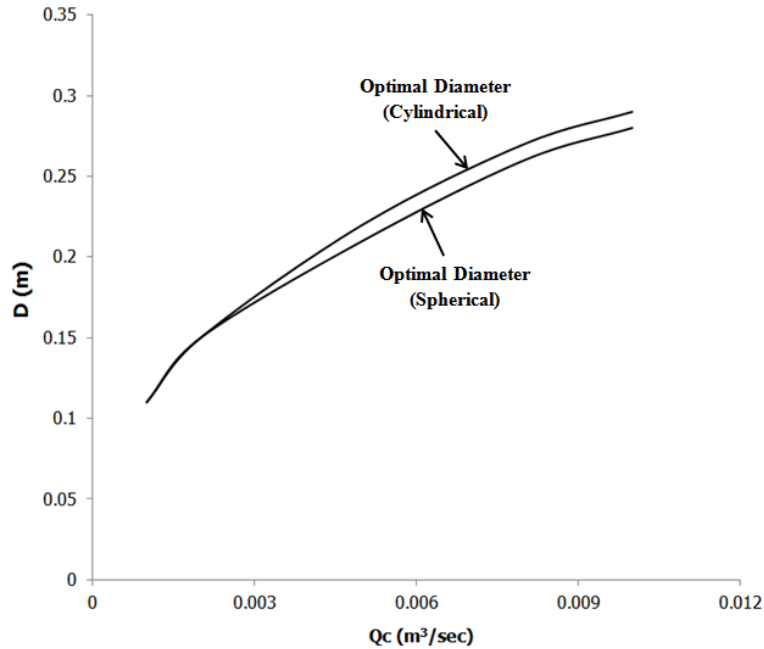


Figure 7.8. Variations in Optimal Diameter w.r.t. the Solid Throughput for Spherical and Cylindrical Capsules

Comparison between the flow of spherical and cylindrical capsules in a pipeline is further highlighted in table 7.8 which shows the percentage increase in the optimal pipeline diameter, for the flow of cylindrical capsules, as compared to the flow of spherical capsules at various solid throughputs.

Table 7.8. Comparison between Spherical and Cylindrical Capsules

Qc	% Increase in Optimal D for Cylindrical Capsules w.r.t. Spherical Capsules
(m³/sec)	(%)
0.001	0.00
0.002	0.00
0.005	4.76
0.008	3.85
0.010	3.57

7.11.3. Effects of the Density of the Capsules

In order to analyse the effects of the density of the capsules on the optimal pipeline design, the example under consideration has been solved for heavy-density spherical capsules made of aluminium. The results for the variations in the pumping power and the various costs of the pipeline w.r.t. the pipeline diameter are presented in table 7.9.

Table 7.9. Variations in Pumping Power and Various Costs w.r.t. Pipeline Diameter

D	P	C_{Manufacturing}	C_{Power}	C_{Total}
(m)	(kW)	(£)	(£)	(£)
0.11	25.51	18384	35715	54099
0.12	16.53	21652	23146	44798
0.13	11.09	25186	15531	40717
0.14	7.66	28986	10735	39721
0.15	5.43	33053	7611	40664
0.16	3.94	37386	5518	42904
0.17	2.91	41984	4079	46063

From the results presented in table 7.9 it can be seen that the optimal pipeline diameter for the flow of heavy-density spherical capsules is 0.14m or 140cm, which is 30cm higher than for the flow of equi-density spherical capsules in the pipeline. Furthermore, the pumping power required at optimal pipeline diameter is 7.66kW. Hence, by introducing heavy-density capsules in the pipeline, both the pumping power and the optimal pipeline diameter increases. This is because heavy-density capsules offer more resistance to the flow within a pipeline (according to the results from Chapter 4, 5 and 6) and hence the pressure drop in the pipeline is considerably higher for the flow of heavy-density spherical capsules in comparison with the flow of equi-density spherical capsules in the pipeline. This not only increases the pumping power required to transport the same throughput of the solids in the pipeline but also increases the optimal pipeline diameter.

Figure 7.9 depicts the variations in the total cost and the operating cost for the flow of both the equi-density and heavy-density spherical capsules in the pipeline. It is evident from the figure that the total cost of the pipeline for the flow of heavy-density spherical capsules is considerably higher than for the flow of equi-density spherical capsules. The same trend is shown in the optimal pipeline diameter. Furthermore, the operating cost for the flow of heavy-density spherical capsules is higher as compared to the flow of equi-density spherical capsules in the pipeline. The reasons for all the trends are the same as mentioned above, i.e. heavy-density capsules results in a higher pressure drop in the pipeline.

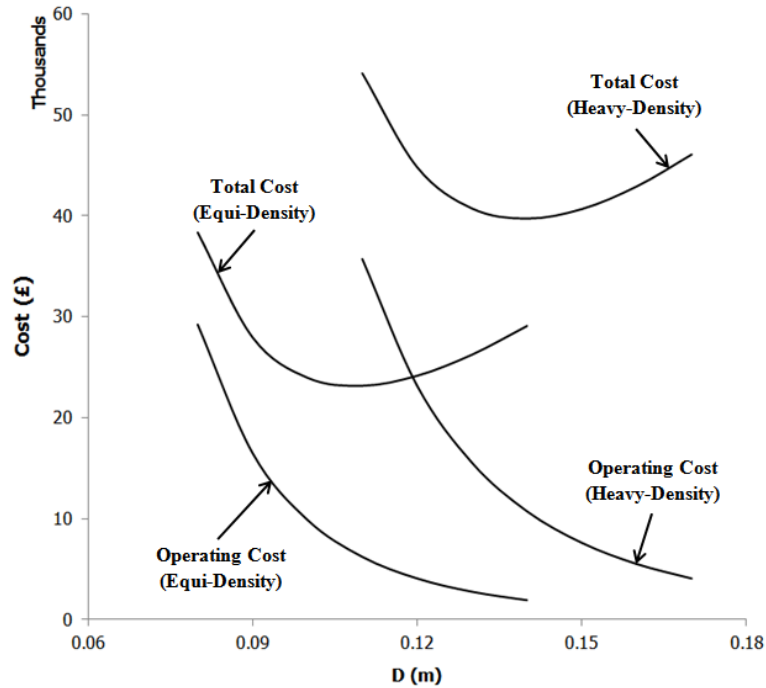


Figure 7.9. Comparison of Various Costs of the Pipeline for Equi-Density and Heavy-Density Spherical Capsules

The variations in the capsule velocity and the various pressure drops in the pipeline, for the flow of heavy-density spherical capsules, are shown in table 7.10. The results presented show that the total pressure drop for the optimal pipeline diameter, i.e. $D = 0.14\text{m}$, is 392.29kPa .

Table 7.10. Variations in Capsule Velocity and Pressure Drops

D	V_c	ΔP_{Minor}	ΔP_{Major}	ΔP_{Total}
(m)	(m/sec)	(kPa)	(kPa)	(kPa)
0.11	1.28	3.20	1301.79	1304.99
0.12	1.08	2.28	843.50	845.78
0.13	0.92	1.66	565.88	567.54
0.14	0.79	1.24	391.05	392.29
0.15	0.69	0.95	277.21	278.16
0.16	0.60	0.74	200.93	201.67
0.17	0.54	0.58	148.51	149.09

Figure 7.10 depicts the variations in the total pressure drop within the pipeline, for the flow of both the equi-density and heavy-density spherical capsules. It can be seen that the total pressure drop is considerably higher for the flow of heavy-density spherical capsules in the pipeline.

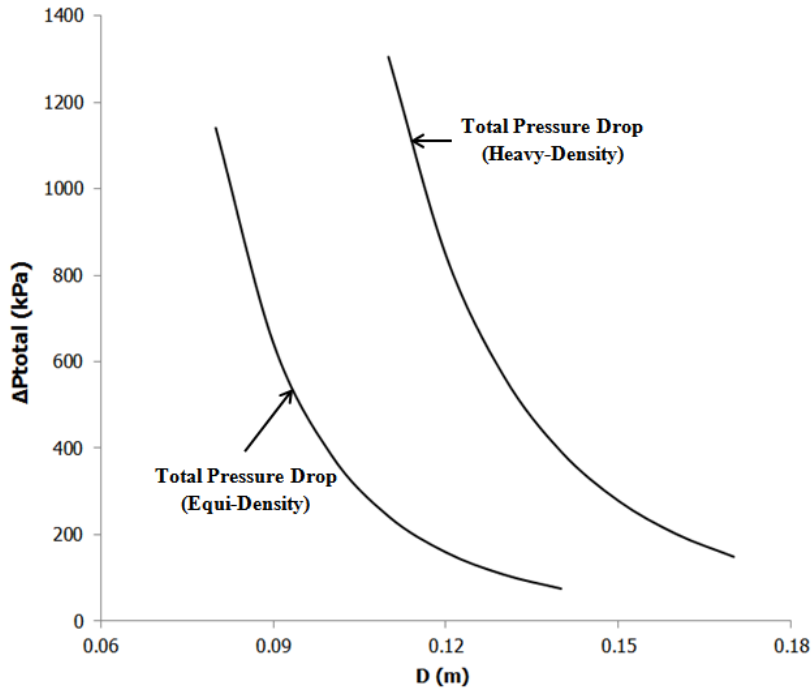


Figure 7.10. Variations in Total Pressure Drop w.r.t. Pipeline Diameter for Equi-Density and Heavy-Density Spherical Capsules

As shown in case of equi-density spherical capsules, table 7.11 presents the variations in the optimal pipeline diameter, capsule velocity and pumping power for various solid throughputs. It can be seen that as the solid throughput increases, the optimal pipeline diameter also increases.

Table 7.11. Variations in Optimal Diameter, Capsule Velocity and Pumping Power for Various Solid Throughputs

Q_c	V_c	P	D
(m ³ /sec)	(m/sec)	(kW)	(m)
0.001	0.79	7.66	0.14
0.002	0.86	13.26	0.19
0.005	0.99	29.64	0.28
0.008	1.07	45.88	0.34
0.010	1.08	51.34	0.38

A comparison of the optimal diameter of the pipeline, for the flow of both the equi-density and heavy-density spherical capsules within the pipeline, w.r.t. the solid throughput is shown in figure 7.11. It can be seen that the optimal diameter of the pipeline, for the flow of heavy-density spherical capsules, is higher as compared to the flow of equi-density spherical capsules, at any solid throughput.

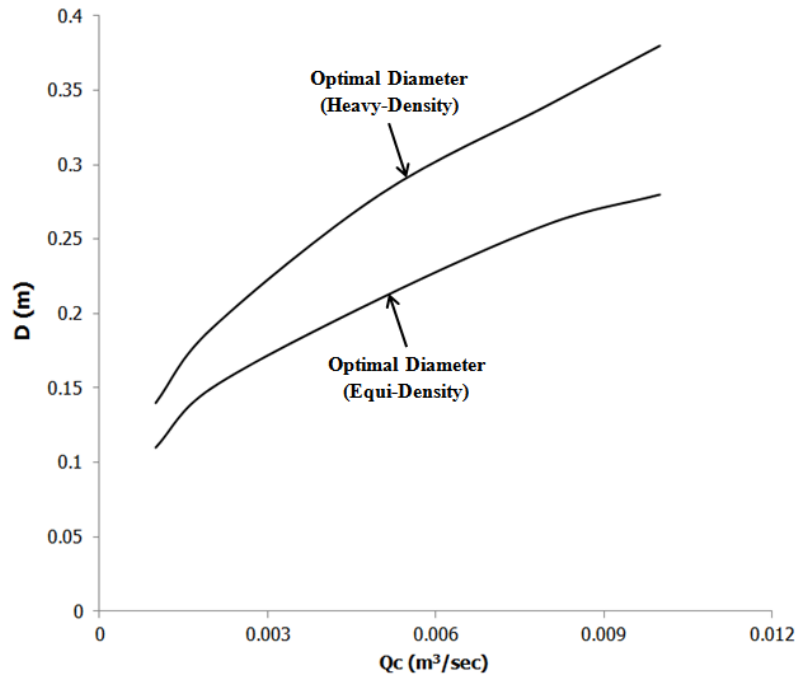


Figure 7.11. Variations in Optimal Diameter w.r.t. the Solid Throughput for Equi-Density and Heavy-Density Spherical Capsules

Comparison between the flow of equi-density and heavy-density spherical capsules in a pipeline is further highlighted in table 7.12 which shows the percentage increase in the optimal pipeline diameter, for the flow of heavy-density spherical capsules, as compared to the flow of equi-density spherical capsules at various solid throughputs.

Table 7.12. Comparison between Equi-Density and Heavy-Density Spherical Capsules

Qc	% Increase in Optimal D for Equi-Density Spherical Capsules w.r.t. Heavy-Density Spherical Capsules
(m ³ /sec)	(%)
0.001	27.27
0.002	26.67
0.005	33.33
0.008	30.77
0.010	35.71

7.12. Design Example for Off-Shore Applications

Polypropylene needs to be transferred from the sea bed to the upper deck, 100m up, in the form of spherical capsules of $k = 0.7$. The spacing between the capsules should be $3 * d$. The required throughput is $0.003\text{m}^3/\text{sec}$. Find the optimal size of the pipeline and the pumping power required for this purpose.

Solution: According to the current market, the values of different constants are:

$$C_1 = 1.4$$

$$C_3 = 1.1$$

$$C_2 = 0.95$$

Furthermore, polypropylene has a density equal to that of water. Assuming the efficiency of the pumping unit $\eta = 60\%$ and following the steps described in the working of the optimisation model, the following results (table 7.13) have been obtained.

Table 7.13. Variations in Pumping Power and Various Costs w.r.t. Pipeline Diameter

D	P	C_{Manufacturing}	C_{Power}	C_{Total}
(m)	(kW)	(£)	(£)	(£)
0.17	72.23	8039	101130	109169
0.18	70.77	8992	99082	108074
0.19	69.71	9997	97596	107593
0.20	68.92	11055	96498	107553
0.21	68.33	12167	95673	107840
0.22	67.88	13332	95043	108375
0.23	67.54	14550	94555	109105

The results presented here suggests that a pipeline of diameter = 200 cm is optimum for the problem under consideration. The power of the pumping unit required, corresponding to the optimal pipeline diameter, is 68.92kW. Further analysing the results presented in table 7.13, figure 7.12 depicts the variations in the manufacturing and operating costs for various pipeline diameters. It can be seen that as the pipeline diameter increases, the manufacturing cost increases. This is due to the fact that pipes of larger diameters are more expensive than pipes of relatively smaller diameters. Furthermore, as the pipeline diameter increases, the operating cost decreases. This is due to the fact that, for the same solid throughput, increasing the pipeline diameter decreases the velocity of the flow within the pipeline. The operating cost has a proportional relationship with the velocity of the flow; hence, increase in the pipeline diameter decreases the operating cost of the pipeline.

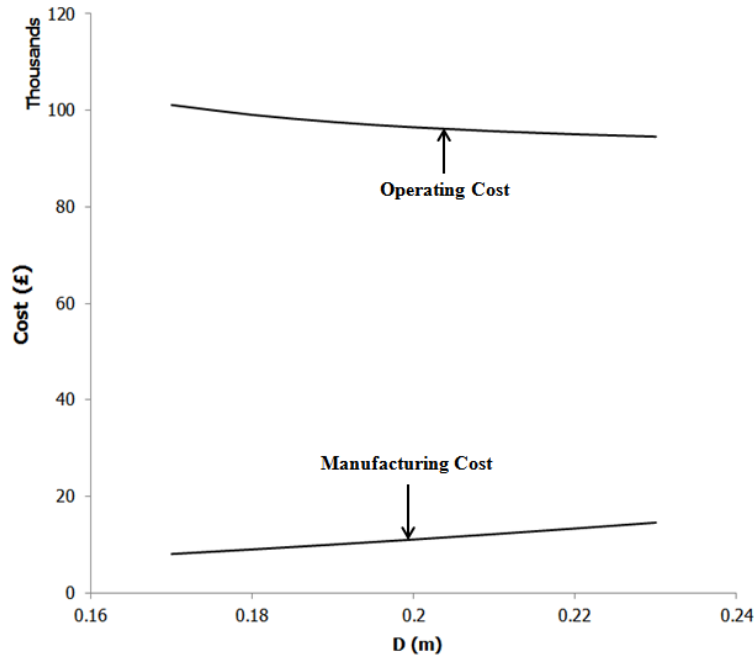


Figure 7.12. Variations in Operating and Operating Costs w.r.t. Pipeline Diameter

Figure 7.13 depicts the variations in the total cost and the pumping power required at various pipeline diameters. It can be seen that as the pipeline diameter increases, the required pumping power decreases. Furthermore, as the pipeline diameter increases, the total cost of the pipeline first decreases and then increases. As the total cost of the pipeline is a sum of the manufacturing and operating costs, which have opposite trends w.r.t. the pipeline diameter, hence, the combination of these costs give rise to the total cost curve. The pipeline diameter, which corresponds to the minimum total cost of the pipeline, is the optimal pipeline diameter.

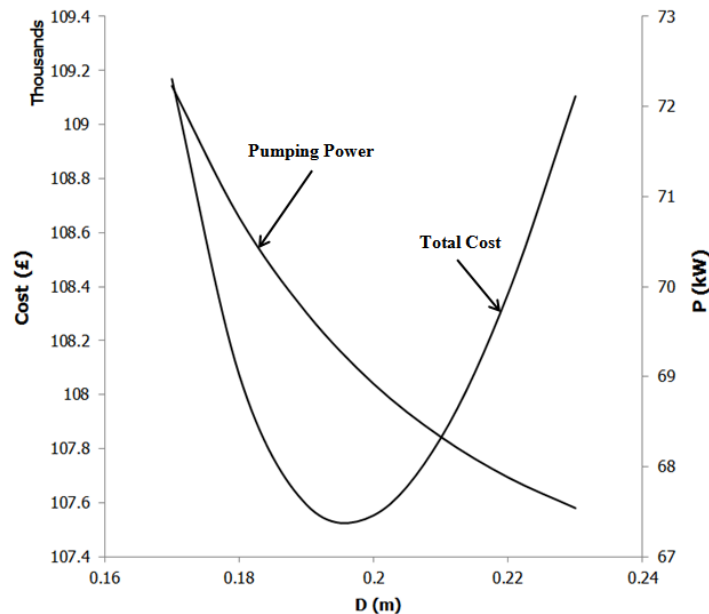


Figure 7.13. Variations in Total Cost and Pumping Power Required at Various Pipeline Diameters

Table 7.14 presents the variations in the capsule velocity and the various pressure drops in the pipeline at different pipeline diameters. It can be seen that the capsule velocity and the total pressure drop that corresponds to the optimal pipeline diameter are 1.45m/sec and 1021.03kPa respectively.

Table 7.14. Variations in Capsule Velocity and Pressure Drop

D	V_c	ΔP_{Minor}	ΔP_{Major}	ΔP_{Total}
(m)	(m/sec)	(kPa)	(kPa)	(kPa)
0.17	2.01	4.68	1064.74	1069.42
0.18	1.79	3.98	1043.96	1047.94
0.19	1.61	3.47	1028.97	1032.44
0.20	1.45	3.06	1017.97	1021.03
0.21	1.32	2.74	1009.78	1012.52
0.22	1.20	2.47	1003.59	1006.06
0.23	1.10	2.26	998.84	1001.14

Figure 7.14 depicts the variations in the capsule velocity and the total pressure drop in the pipeline for various pipeline diameters. It is evident from the figure that as the pipeline diameter increases, the velocity of the capsules decreases. This supports the aforementioned statement regarding the variations in the flow velocity for increasing pipeline diameters. Furthermore, as the pipeline diameter increases, the total pressure drop decreases. This statement is again supporting the results presented above for the variations in pumping power required for the pipeline. Hence, all the results presented here are in agreement with the design methodology presented in this chapter for the flow of capsules in a pipeline.

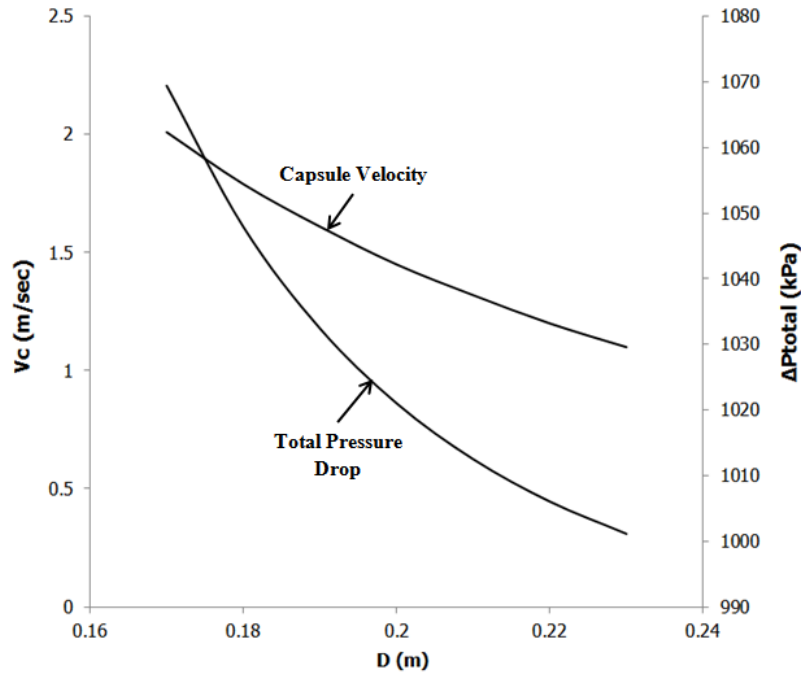


Figure 7.14. Variations in Capsule Velocity and Total Pressure Drop w.r.t. Pipeline Diameter

Table 7.15 presents the variations in the capsule velocity, pumping power and the optimal diameter of the pipeline for various solid throughputs. Hence, table 7.15 can be used as a design chart for the problem under consideration.

Table 7.15. Variations in Optimal Diameter, Capsule Velocity and Pumping Power for Various Solid Throughputs

Q_c	V_c	P	D
(m ³ /sec)	(m/sec)	(kW)	(m)
0.005	1.45	68.92	0.20
0.008	1.76	111.11	0.23
0.010	2.02	140.49	0.24
0.020	2.25	273.58	0.35

Figure 7.15 depicts the variations in the optimal diameter of the pipeline and the required pumping power at various solid throughputs. It can be seen that as the solid throughput increases, the optimal pipeline diameter increases. Furthermore, as the solid throughput increases, the required pumping power also increases.

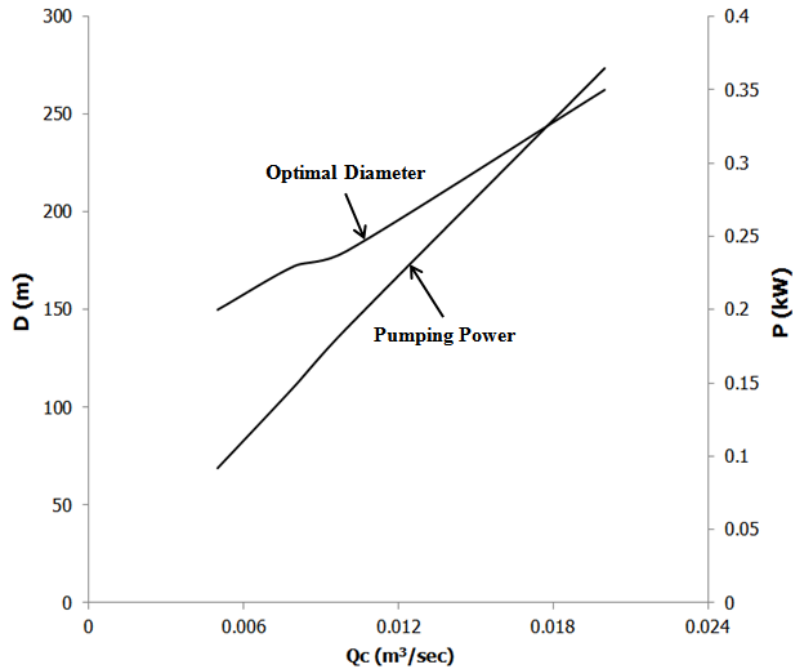


Figure 7.15. Variations in Optimal Diameter and Pumping Power w.r.t. the Solid Throughput

7.12.1. Capsule Shape Effects

In order to analyse the effect of the capsule shape on the pipeline design, the example considered above is solved for cylindrical capsules keeping all other parameters the same. Table 7.16 presents the results for the modified pipeline design.

Table 7.16. Variations in Pumping Power and Various Costs w.r.t. Pipeline Diameter

D	P	C_{Manufacturing}	C_{Power}	C_{Total}
(m)	(kW)	(£)	(£)	(£)
0.18	50.40	8992	70561	79553
0.19	48.95	9997	68531	78528
0.20	47.88	11055	67037	78092
0.21	47.08	12167	65920	78087
0.22	46.48	13332	65072	78404
0.23	46.01	14550	64418	78968
0.24	45.65	15822	63909	79731

From the results presented in table 7.16 it can be seen that the optimal pipeline diameter and the required pumping power for the flow of cylindrical capsules are 0.21m and 47.08kW. Hence, by introducing the cylindrical capsules in the pipeline, the optimal pipeline diameter increases. The variations in the capsule velocity and the various pressure drops in the pipeline, for the flow of cylindrical capsules, are shown in table 7.17. The results presented show that the total pressure drop for the optimal pipeline diameter is 1046.46kPa.

Table 7.17. Variations in Capsule Velocity and Pressure Drops

D	V_c	ΔP_{Minor}	ΔP_{Major}	ΔP_{Total}
(m)	(m/sec)	(kPa)	(kPa)	(kPa)
0.18	1.19	9.06	1110.37	1119.43
0.19	1.07	7.77	1079.68	1087.45
0.20	0.97	6.75	1057.23	1063.98
0.21	0.88	5.91	1040.55	1046.46
0.22	0.80	5.23	1027.97	1033.20
0.23	0.73	4.67	1018.38	1023.05
0.24	0.67	4.20	1010.96	1015.16

Figure 7.16 depicts the variations in the total pressure drop within the pipeline, for the flow of both the spherical and cylindrical shaped capsules. It can be seen that the total pressure drop is considerably higher for the flow of cylindrical capsules in the pipeline.

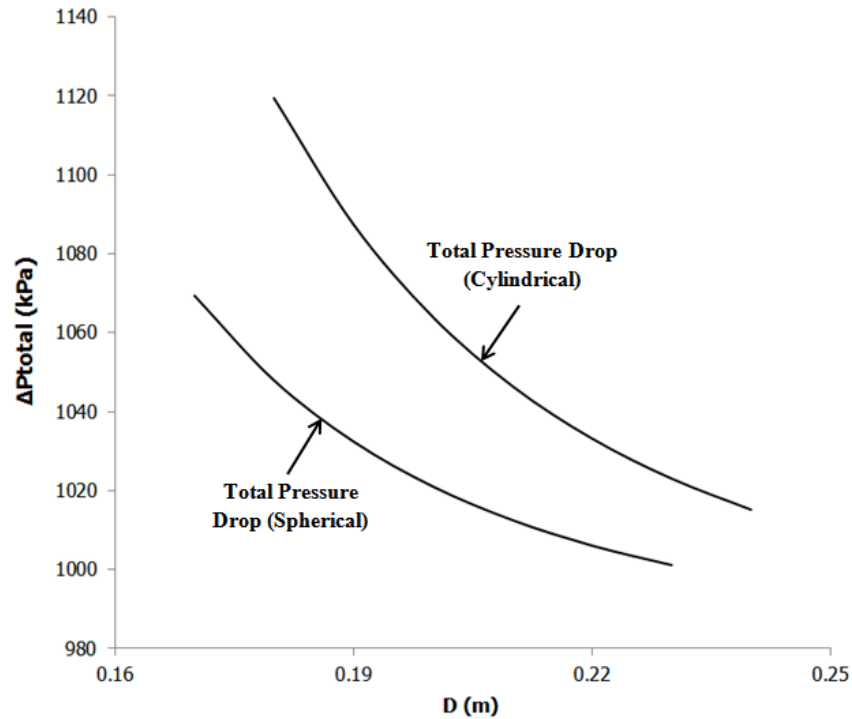


Figure 7.16. Variations in Total Pressure Drop w.r.t. Pipeline Diameter for Spherical and Cylindrical Capsules

As shown in case of the spherical capsules, table 7.18 presents the variations in the optimal pipeline diameter, capsule velocity and required pumping power for various solid throughputs. It can be seen that as the solid throughput increases, the optimal pipeline diameter also increases.

Table 7.18. Variations in Optimal Diameter, Capsule Velocity and Pumping Power for Various Solid Throughputs

Q_c	V_c	P	D
(m ³ /sec)	(m/sec)	(kW)	(m)
0.005	0.88	47.08	0.21
0.008	0.99	75.47	0.25
0.010	1.05	93.54	0.28
0.020	1.13	186.3	0.37

A comparison of the optimal diameter of the pipeline, for the flow of both the spherical and cylindrical capsules within the pipeline, w.r.t. the solid throughput is shown in figure 7.17. It can be seen that the

optimal diameter of the pipeline, for the flow of cylindrical capsules, is higher as compared to the flow of spherical capsules, at any solid throughput.

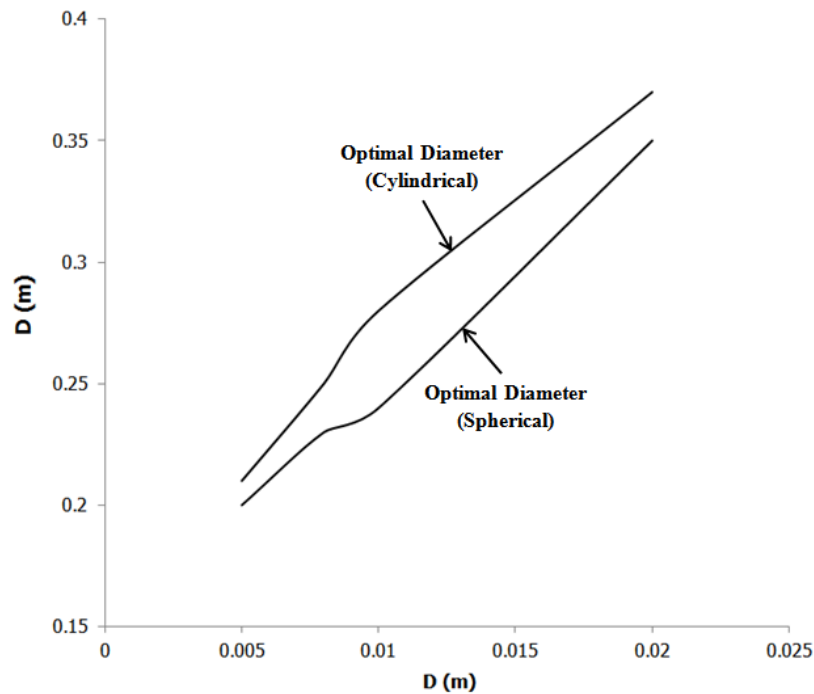


Figure 7.17. Variations in Optimal Diameter w.r.t. the Solid Throughput for Spherical and Cylindrical Capsules

Comparison between the flow of spherical and cylindrical capsules in a pipeline is further highlighted in table 7.19 which shows the percentage increase in the optimal pipeline diameter, for the flow of cylindrical capsules, as compared to the flow of spherical capsules at various solid throughputs.

Table 7.19. Comparison between Spherical and Cylindrical Capsules

Q_c	% Increase in Optimal D for Cylindrical Capsules w.r.t. Spherical Capsules
(m ³ /sec)	(%)
0.005	5.00
0.008	8.70
0.010	16.67
0.020	5.71

7.12.2. Effects of the Density of the Capsules

In order to analyse the effects of the density of the capsules on the optimal pipeline design, the example under consideration has been solved for heavy-density spherical capsules made of aluminium. The results for the variations in the pumping power and the various costs w.r.t. the pipeline diameter are presented in table 7.20.

Table 7.20. Variations in Pumping Power and Various Costs w.r.t. Pipeline Diameter

D	P	C_{Manufacturing}	C_{Power}	C_{Total}
(m)	(kW)	(£)	(£)	(£)
0.12	157.88	4497	221034	225531
0.13	145.56	5218	203793	209011
0.14	139.09	5992	194726	200718
0.15	136.47	6820	191069	197889
0.16	135.25	7701	190825	198526
0.17	134.67	8635	190705	199340
0.18	134.01	9622	189812	199434

From the results presented in table 7.20 it can be seen that the optimal pipeline diameter for the flow of heavy-density spherical capsules is 0.15m or 150cm. Furthermore, the pumping power required at optimal pipeline diameter is 136.47kW.

Figure 7.18 depicts the variations in the total cost and the operating cost for the flow of both the equi-density and heavy-density spherical capsules in the pipeline. It is evident from the figure that the total cost of the pipeline for the flow of heavy-density spherical capsules is considerably higher than for the flow of equi-density spherical capsules. Furthermore, the operating cost for the flow of heavy-density spherical capsules is higher as compared to the flow of equi-density spherical capsules in the pipeline. The reasons for these trends are the same as mentioned above, i.e. heavy-density capsules results in a higher pressure drop in the pipeline.

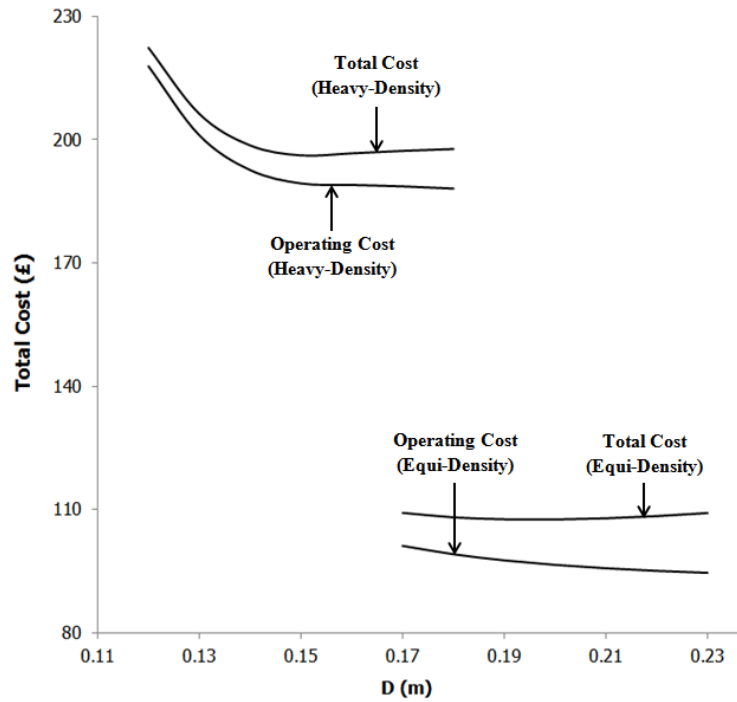


Figure 7.18. Comparison of Various Costs of the Pipeline for Equi-Density and Heavy-Density Spherical Capsules

The variations in the capsule velocity and the various pressure drops in the pipeline, for the flow of heavy-density spherical capsules, are shown in table 7.21. The results presented show that the total pressure drop for the optimal pipeline diameter, i.e. $D = 0.15\text{m}$, is 1370.59kPa .

Table 7.21. Variations in Capsule Velocity and Pressure Drops

D	V_c	ΔP_{Minor}	ΔP_{Major}	ΔP_{Total}
(m)	(m/sec)	(kPa)	(kPa)	(kPa)
0.12	4.05	8.95	1828.22	1837.17
0.13	3.45	7.68	1610.07	1617.75
0.14	2.97	6.76	1464.77	1471.53
0.15	2.59	6.08	1364.51	1370.59
0.16	2.27	5.57	1293.18	1298.75
0.17	2.01	5.19	1241.06	1246.25
0.18	1.79	4.89	1202.07	1206.96

Figure 7.19 depicts the variations in the total pressure drop within the pipeline, for the flow of both the equi-density and heavy-density spherical capsules. It can be seen that the total pressure drop is higher for the flow of heavy-density spherical capsules in the pipeline.

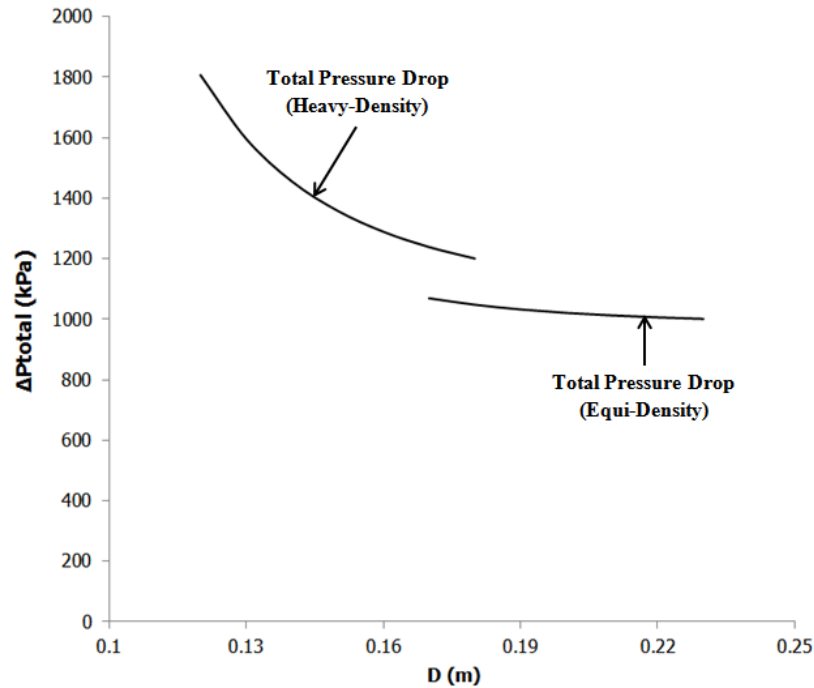


Figure 7.19. Variations in Total Pressure Drop w.r.t. Pipeline Diameter for Equi-Density and Heavy-Density Spherical Capsules

As shown in case of equi-density spherical capsules, table 7.22 presents the variations in the optimal pipeline diameter, capsule velocity and pumping power for various solid throughputs. It can be seen that as the solid throughput increases, the optimal pipeline diameter also increases.

Table 7.22. Variations in Optimal Diameter, Capsule Velocity and Pumping Power for Various Solid Throughputs

Q_c	V_c	P	D
(m ³ /sec)	(m/sec)	(kW)	(m)
0.005	2.59	136.47	0.15
0.008	2.87	215.83	0.18
0.010	2.91	267.93	0.20
0.020	3.44	527.18	0.26

Comparison between the flow of equi-density and heavy-density spherical capsules in a pipeline is further highlighted in table 7.23 which shows the percentage decrease in the optimal pipeline diameter, for the flow of heavy-density spherical capsules, as compared to the flow of equi-density spherical capsules at various solid throughputs.

Table 7.23. Comparison between Equi-Density and Heavy-Density Spherical Capsules

Q_c	% Decrease in Optimal D for Equi-Density Spherical Capsules w.r.t. Heavy-Density Spherical Capsules
(m ³ /sec)	(%)
0.005	25.00
0.008	21.74
0.010	16.67
0.020	25.71

The design examples presented in this chapter reveals that the optimisation methodology presented in this study is both user-friendly and robust. Furthermore, the optimisation model can be used for commercial applications with reasonable accuracy.

7.13. Summary of HCP's Optimisation

A detailed investigation of the various costs involved in a pipeline transporting capsules has revealed the following results for a fixed solid throughput:

- Increase in the pipeline diameter increases the manufacturing cost of the pipeline (see figures 7.2 and 7.12 for reference)
- Increase in the pipeline diameter decreases the operating cost of the pipeline (see figures 7.2 and 7.12 for reference)
- Increase in the pipeline diameter first decreases and then increases the total cost of the pipeline (see figures 7.3 and 7.13 for reference)
- Increase in the pipeline diameter decreases the pressure drops in the pipeline (see figures 7.4 and 7.14 for reference)

- Increase in the pipeline diameter decreases the capsule velocity (see figures 7.4 and 7.14 for reference)
- Increase in the pipeline diameter decreases the pumping power required for the pipeline
- Optimal pipeline diameter, for the flow of cylindrical capsules in the pipeline, is higher as compared to the flow of spherical capsules
- Optimal pipeline diameter, for the flow of heavy-density capsules in horizontal pipelines, is higher as compared to the flow of equi-density capsules. Furthermore, optimal pipeline diameter, for the flow of heavy-density capsules in vertical pipelines, is lower as compared to the flow of equi-density capsules.

Furthermore, as the solid throughput increases, the optimal pipeline diameter and the pumping power required increases. Hence, a complete design and optimisation methodology has been presented in this chapter, which is based on the results from Chapters 4, 5 and 6 regarding the CFD based analysis of the flow of capsules in pipelines, both for on-shore and off-shore applications.

CHAPTER 8

CONCLUSIONS

From the results obtained in the previous chapters regarding the flow of capsules in pipes, bends and the development of an optimisation model for such HCPs, detailed conclusions have been drawn in this chapter. The major achievements and contributions to the existing knowledge base are summarised and wherever possible referenced back to the initial aims of this study. Finally, the works carried out in this study are evaluated and requirements for future work in the area of capsule transportation through pipelines are defined.

8.1. Research Problem Synopsis

Transport of goods within hollow spherical or cylindrical containers through pipelines is a relatively new mode of freight transport, which is gaining more and more importance globally due to increase in the fuel prices and depletion of the fossil fuels. It has been reported in various studies [97, 98 and 99] that this mode of transport is economically more viable for commercial applications as compared to the conventional modes of transportation. However, the majority of research studies carried out in the area of capsule transport in pipelines is based on either experiments (both in laboratories and on-field) or analytical modelling which lacks a detailed investigation into the complex flow structure and behaviour within such pipelines. With the advent of powerful computing machines and sophisticated software to analyse the flow fields, it has now become possible to computationally model a pipeline transporting capsules and analyse map the flow within these pipelines under varying geometric and flow conditions.

From a comprehensive review of the published literature, a number of limitations have been found out which are concerned with the aforementioned points. In order to accurately predict the flow behaviour in pipelines transporting capsules a set of aims and objectives have been formulated which define the scope of this research study. A summary of the primary aims of the thesis is provided in the following sections of this chapter along with the major achievements and contributions. For reference, the detailed objectives within each of these aims are given in Chapter 2.

8.2. Research Aims and Major Achievements

The main aims of the thesis defined from an extensive literature review in this area are as follows:

Research Aim # 1: CFD Based Flow Diagnostics and Design of Horizontal Pipelines Transporting Capsules

Achievement # 1: This study provides a detailed CFD based investigation on the flow diagnostics of horizontal pipelines transporting capsules for on-shore applications and proposes pressure drop prediction models for such pipelines. A numerical study on the flow of spherical and cylindrical capsules, having density both equal to and greater than water, has been presented. The experimental data available in the published literature, on the velocity of the capsules in horizontal pipelines for various geometric and flow characteristics, has been processed using multiple variable regression analysis to develop explicit expressions for capsules velocities. This capsule velocity was then used as an input to the numerical model. In order to cover a wide range of operating conditions for a commercial HCP (only limited operating conditions are available in literature for which local flow fields have been analysed), flow of both equi-density and heavy-density spherical and cylindrical capsules in a horizontal pipeline has been numerically simulated for various (a) diameters of the capsules (b) lengths of the capsules (c) average flow velocities (d) concentration/number of the capsules and (e) spacing between the capsules.

Based on the detailed numerical investigation of the flow structure and behaviour, the pressure and velocity fields in a capsule transporting horizontal pipe have been critically analysed both qualitatively and quantitatively. Qualitative analysis makes use of the pressure and velocity contours in the capsule transporting pipe whereas, the quantitative analysis makes use of the coefficient of pressure and

normalised local flow velocity for the analysis of pressure and velocity distribution within the pipe respectively. The results presented give a clear picture of the flow behaviour within the pipe and the effect of the presence of the capsules on the flow structure and the pressure drop within the pipe. As the pipeline designers use the pressure drop (or head loss) considerations in a pipeline to design it, the present study made use of the pressure drop values for various cases under investigation in order to develop semi-empirical correlations, which predict the pressure drop in a capsule transporting horizontal pipeline for various flow and geometric configurations mentioned above. The development of such prediction models for the pressure drop which includes the effects of different geometric parameters of a pipeline, transporting capsules, is a major achievement of the present study. It has also been shown that these prediction models have a good accuracy.

Research Aim # 2: CFD Based Flow Diagnostics and Design of Vertical Pipelines Transporting Capsules

Achievement # 2: Extensive CFD based investigations have been carried out on the flow diagnostics of vertical pipelines transporting capsules for off-shore applications in this study, and pressure drop prediction models for such pipelines have been developed. A numerical study on the flow of spherical and cylindrical capsules, having density both equal to and greater than water, has been presented. The holdup data available in the literature, on the velocity of the capsules in vertical pipelines for various geometric and flow characteristics, has been processed using multiple variable regression analysis to develop explicit expressions for capsules velocities in vertical pipelines. The capsule velocity has been used as an input to the numerical model. Only limited operating conditions are available in literature for which local flow fields have been analysed. In order to cover a wide range of operating conditions for a commercial HCP, flow of both equi-density and heavy-density spherical and cylindrical capsules in a vertical pipeline has been numerically simulated for various (a) diameters of the capsules (b) lengths of the capsules (c) average flow velocities (d) concentration/number of the capsules and (e) spacing between the capsules.

Detailed numerical investigations of the flow structure and behaviour in a vertical pipeline transporting capsules have been carried out. Both qualitative and quantitative analysis of the pressure and velocity fields in a capsule transporting vertical pipe has been presented where these flow fields have been critically analysed. Qualitative analysis makes use of the pressure and velocity contours in the capsule transporting pipe whereas, the quantitative analysis makes use of the coefficient of pressure and normalised local flow velocity for the analysis of pressure and velocity distribution within the pipe respectively. The results provide a better understanding of the flow structure within the vertical pipeline transporting capsules. The effect of the presence of the capsules on the flow structure and the pressure drop within the pipe has been enumerated. Capsule pipeline designers need the pressure drop correlations in order to design such pipelines. In the present study, pressure drop values for various cases have been calculated in order to develop semi-empirical correlations that predict the pressure drop in a capsule transporting vertical pipeline for various aforementioned flow and geometric configurations. The development of such prediction models for the pressure drop, which includes the effects of different geometric parameters of a pipeline transporting capsules, is a major achievement of the present study. It has also been shown that these prediction models have a good accuracy.

Research Aim # 3: CFD Based Flow Diagnostics and Design of Bends Transporting Capsules

Achievement # 3: This study provides a detailed CFD based investigation on the design criteria and flow diagnostics of pipe bends, transporting capsules for both on-shore and off-shore applications as bends are an integral part of all types of pipelines. A numerical study on the flow of spherical and cylindrical capsules, having density both equal to and greater than water, has been presented. The experimental data available in the published literature regarding the flow of capsules in pipe bends is severely limited. Hence, a new methodology has been developed to predict the velocity of the capsule/s in the pipe bends which is a major achievement of this study. Discrete Phase Modelling (DPM) has been used numerically to simulate the flow of particle/s in pipe bends, where the shape of the capsule has been controlled by the shape factor of the particle/s. In addition of the capsule velocities, the DPM also provides with the trajectory of the capsules in the bends. Furthermore, using simple trigonometric functions, the orientation of cylindrical capsules in the bends has been formulated. The author is not familiar with any study which uses the combination of these techniques to predict the velocity, trajectory and orientation of capsules in pipe bends and considers this a significant achievement of the present study.

In order to cover a wide range of investigations for commercial purposes, flow of both equi-density and heavy-density spherical and cylindrical capsules in pipe bends has been numerically simulated for various (a) orientations of the bends (horizontal and vertical) (b) radius of curvature of the bends (c) diameters of the capsules (d) lengths of the capsules (e) average flow velocities (f) concentration/number of the capsules and (g) spacing between the capsules. No single study has considered such a wide range of investigations on the flow of capsules in pipe bends which is very important as far as the formulation of prediction models is concerned because more parameters and results leads towards more generic correlations.

A detailed investigation on the flow structure and behaviour has been presented which is a major achievement of this study. The pressure and velocity fields in a bends, transporting capsules have been critically analysed. It has been found out that a detailed quantitative analysis within the bend is quite difficult to conduct with the use of available techniques and software. A quantitative analysis based on the comparison between the different cases investigated is, however, included in the present study. Furthermore, the quantitative analysis regarding the pressure drop in the bends is included, which leads towards the development of prediction models. These analyses are a major achievement of this study. The results presented give a clear picture of the flow behaviour within the pipe and the effect of the presence of the capsule/s on the flow structure and the pressure drop within the pipe.

Research Aim # 4: Development of an Analytical Model for the Optimum Design of Pipelines Transporting Capsules

Achievement # 4: In the current study, an optimisation methodology for pipelines transporting capsules has been developed, based on the principle of least-cost, which is both robust and user-friendly. The optimisation methodology presented here makes use of the semi-empirical correlations, developed for the prediction of the pressure drop within pipelines, transporting capsules for diverse range of flow conditions. The models developed are unique in the sense that that they include all relevant parameters that affect pressure drop in a hydraulic capsule pipeline, which is a major

achievement of this study. Furthermore, a novel analytical model has been developed for optimal design of HCPs, which requires only the solid throughput as the input to the model. All other parameters needed for the design have been modelled mathematically.

The optimisation methodology developed not only provides with the optimal diameter of the pipeline but also accurately calculates the pumping power required for the system. Moreover, the optimisation model provides all relevant parameters such as the average velocity of the flow, velocity of the capsules, the flow rate of water within the pipeline etc. Hence, the optimisation model developed in this study can be used to design a commercial HCP and is a key achievement of this study. The model developed is easy to use and robust.

8.3. Thesis Conclusions

A comprehensive study has been carried out to support the existing literature regarding the flow of capsules in a pipeline and to provide novel additions to improve the current understanding of the design process, operational characteristics, geometry related effects and optimization methodology for the transport of capsules in pipelines. The major conclusions from each facet of this research study are summarized as follows:

Research Objective # 1: To determine the effect of the shape of the capsules on the flow structure and the pressure drop within the pipelines

Conclusion # 1: From the investigations regarding the effect of the shape of the capsules on the flow structure and the pressure drop within the pipelines, carried out in this study, it can be concluded that the cylindrical capsules result in an increased pressure drop in pipelines as compared to the flow of spherical capsules. This holds true for both straight pipes and pipe bends. As far as the flow structure is concerned, cylindrical capsules, due to their bluff body shape, creates a large wake region downstream of the capsules. Very low pressure within this wake region is one of the primary reasons behind the increase in the pressure drop within the pipeline for the flow of cylindrical capsules, in comparison with the flow of spherical capsules of the same size and at same average flow velocity. Furthermore, it has also been observed that the cylindrical capsules attain a considerably less velocity as compared to spherical capsules, at the same average flow velocity. Cylindrical capsules interact with the walls of the pipe bends more severely as compared to spherical capsules. While spherical capsules try to roll on the walls of the bends, cylindrical capsules, due to their shape, try to slide past the bends which generates complex flow patterns within the bends, increasing the pressure drop and wear and tear in the bends due to excessive frictional forces being generated. The results presented in this study regarding the flow of cylindrical capsules in pipelines is of great importance for the designers of HCPs as the prediction models developed for the friction factor of cylindrical capsules are directly used in the design and optimisation of HCPs.

Research Objective # 2: To analyse the effect of the density of the capsules on the flow distribution and the pressure drop within the pipes

Conclusion # 2: From the investigations regarding the effect of the density of the capsules on the flow structure and the pressure drop within the pipelines, carried out in this study, it can be concluded that heavy-density capsules result in an increased pressure drop in pipelines as compared to the flow of equi-density capsules. This holds true for both straight pipes and pipe bends. As far as the flow structure is concerned, heavy-density capsules propagate along the bottom wall of the pipe in case of horizontal pipelines. This disrupts the uniform flow structure, observed in case of equi-density capsules. This disruption of the flow structure gives rise to swirling flow due to adverse velocity gradients present on the top surface of the capsules. The addition of secondary flow structures increases the pressure drop within the pipeline. In case of heavy-density capsule flow in vertical pipes, although the capsules propagate along the central axis of the pipeline, due to the gravitational effects the velocity of the capsules decreases drastically. This effect strengthens the shear layers in the vicinity of the capsules and hence increases the pressure drop within the pipeline. Furthermore, it has also been observed that heavy-density capsules tend to strike the walls of the pipe bends more occasionally as compared to equi-density capsules. This effect further increases the pressure drop within the pipeline. The results presented in this study regarding the flow of heavy-density capsules in pipelines is of great importance for the designers of HCPs as the prediction models developed for the friction factor of heavy-density capsules are directly used in the design and optimisation process of HCPs.

Research Objective # 3: To establish the effect of the concentration of the capsules on the flow variations and the pressure drop within the capsule pipelines

Conclusion # 3: From the investigations regarding the effect of the concentration of the capsules on the flow structure and the pressure drop within the pipelines, carried out in this study, it can be concluded that an increase in capsule concentration results in an increased pressure drop within the pipelines. This holds true for both straight pipes and pipe bends. As far as the flow structure is concerned, more capsules in a pipeline decreases the effective flow area within the pipeline, offering more resistance to the flow and hence increasing the pressure drop. The effects of the concentration of the capsules within HCPs have been formulated explicitly to develop prediction models for the friction factor of capsules. These prediction models⁵ are then used to develop design equations for HCPs.

Research Objective # 4: To formulate the effect of the length of the cylindrical capsules on the flow distribution and the pressure drop within the pipes

Conclusion # 4: From the investigations regarding the effect of the length of the cylindrical capsules on the flow structure and the pressure drop within the pipelines, carried out in this study, it can be concluded that longer cylindrical capsules result in an increased pressure drop in straight pipes as compared to the flow of shorter cylindrical capsules. This is due to the fact that longer cylindrical capsules offer more resistance to the flow by blocking the effective flow area through the cross section of the pipeline, hence increasing the pressure drop. However, in case of pipe bends, longer cylindrical capsules result in reduced pressure drop within pipe bends. This happens due to reduced flow separation taking place in bends because the effective area for the flow to remain attached to increases.

Hence, longer cylindrical capsules show varying effects in pipes and bends. The results presented in this study regarding the effect of the length of cylindrical capsules in pipelines is of great importance for the designers of HCPs as the prediction models developed for the friction factor of cylindrical capsules are directly used in the design and optimisation of HCPs, where the friction factor expressions explicitly includes the effects of the length of the cylindrical capsules.

Research Objective # 5: To determine the effect of the spacing between the capsules in a train on the flow variations and the pressure drop within the capsule pipelines

Conclusion # 5: From the investigations regarding the effect of the spacing between the capsules on the flow structure and the pressure drop within the pipelines, carried out in this study, it can be concluded that increase in the spacing between the capsules results in an increased pressure drop in straight pipes except for heavy-density spherical capsules in horizontal pipes. The effect of spacing between the capsules is marginal in comparison with the effects of other parameters on the pressure drop investigated in this study. Furthermore, the effect of the spacing between the capsules in pipe bends is highly non-linear, i.e. in case of horizontal pipe bends; increase in the spacing between equi-density capsules increases the pressure drop within pipe bends. However, increase in the spacing between heavy-density capsules in horizontal pipe bends decreases the pressure drop. For the flow of capsules, both equi-density and heavy-density, in vertical pipe bends, increase in the spacing between the capsules increases the pressure drop within the pipe bends. All these effects are marginal when compared with the effects of other parameters taken into account in this study. The results presented in this study regarding the effects of spacing between the capsules in pipelines is of great importance for the designers of HCPs as the prediction models developed for the friction factor of capsules, with varying spacing, are directly used in the design and optimisation of HCPs.

Research Objective # 6: To establish the effect of the diameter of the capsules on the flow structure and the pressure drop within the pipelines

Conclusion # 6: From the investigations regarding the effect of the diameter of the capsules on the flow structure and the pressure drop within the pipelines, carried out in this study, it can be concluded that the capsules with larger diameters result in an increased pressure drop in pipelines as compared to the flow of capsules with smaller diameters. This holds true for both straight pipes and pipe bends. As far as the flow structure is concerned, larger sized equi-density capsules, which propagate along the central axis of the pipeline, attains higher velocities as compared to smaller equi-density capsules. This is due to the fact that larger sized equi-density capsules encounter more of the high velocity gradients within the pipeline. This holds true for heavy-density capsules as well for the same reason. Furthermore, larger diameter capsules have a large wake region downstream, which can interact with the trailing capsules in the train, hence generating further complexities within the flow. This further increases the pressure drop in the pipeline. Large sized capsules block the effective flow cross sectional area within the pipeline, increasing the flow velocity in the annulus region between the capsule and the pipe wall. The results presented in this study regarding the flow of capsules, having various diameters, is of great importance for the designers of HCPs as the prediction models developed for the friction factor of capsules of various diameters are directly used in the design and optimisation of HCPs.

Research Objective # 7: To formulate the effect of the average flow velocity on the flow variations and the pressure drop within the capsule pipelines

Conclusion # 7: From the investigations regarding the effect of the average flow velocity on the flow structure and the pressure drop within HCPs, carried out in this study, it can be concluded that higher average flow velocities result in an increased pressure drop in capsule pipelines as compared to lower average flow velocities. This holds true for both straight pipes and pipe bends. As far as the flow structure is concerned, both higher and lower average flow velocities exhibit the same flow variations in straight pipes. However, in pipe bends, due to the curvature, the average flow velocity affects the flow structure even for single phase flow. This is due to the centrifugal effects, which gets prominent as capsules are introduced within the pipe bends. Hence, secondary flow structures are generated which lead towards higher pressure drop within the bends. It has also been observed that the capsule velocity is a function of average flow velocity; hence, the pressure drop within HCPs gets affected by the average flow velocity. The results presented in this study regarding the effects of average flow velocity on pressure drop, are of great importance for the designers of HCPs because the prediction models developed for the friction factor of capsules are a function of the capsule velocities and hence average flow velocities. These prediction models are directly used in the design and optimisation of HCPs.

Research Objective # 8: Development of semi-empirical relations for the friction factor and pressure drop in pipelines transporting

Conclusion # 8: From the results presented in this study, and after analysing the effects of various geometric and flow-related variables on the flow structure and pressure drop within HCPs, semi-empirical relationships have been developed for the friction factor of capsules. Multiple regression analysis has been extensively used for the estimation of the effects of the various parameters on the friction factor of capsules. Furthermore, in order to design capsule pipelines, pressure drop expressions have been formulated based on the prediction models. The pressure drop expressions have been divided into two parts where the first part represents the effects of water flow and the second part represents the effects of the presence of capsules within the pipeline.

Research Objective # 9: Development of a robust optimisation model based on the least-cost principle

Conclusion # 9: From the optimisation methodology developed in Chapter 7 regarding pipelines transporting capsules, it can be concluded that in such a pipeline, for a fixed solid throughput, increase in the diameter of the pipeline increases the manufacturing costs. This is because a larger diameter pipe and capsules are more expensive than smaller diameter pipe and capsules. It can also be concluded that as the diameter of the pipeline increases, the pressure drop (or head loss) decreases, and in-turn, the required pumping power decreases. This is because an increase in the diameter of the pipeline, for a fixed solid throughput, decreases the average flow velocity within the pipeline. As the pressure drop has an inverse relationship with the diameter of the pipeline, and is directly proportional to the square of the average flow velocity, a decrease is observed in the pressure drop within the pipeline.

Furthermore, as the required pumping power for the system is a function of the pressure drop within the pipeline, increase in the pipeline diameter is associated with a decrease in the pumping power and hence decrease in the operational cost of the pipeline. It is noteworthy that the total cost of the pipeline is a sum of all the aforementioned costs of the pipeline. Hence, the total cost of the pipeline first decreases and then increases as the pipeline diameter increases for a fixed solid throughput. The pipeline diameter, for which the total cost is at minimum, corresponds to the optimal pipeline diameter. Furthermore, optimal pipeline diameter, for the flow of cylindrical capsules in the pipeline, is higher as compared to the flow of spherical capsules. Optimal pipeline diameter, for the flow of heavy-density capsules in horizontal pipelines, is higher as compared to the flow of equi-density capsules. Optimal pipeline diameter, for the flow of heavy-density capsules in vertical pipelines, is lower as compared to the flow of equi-density capsules. It has also been concluded that the optimisation methodology presented in the present study is both user-friendly and robust as the only input to the model is the solid throughput.

8.4. Thesis Contributions

The major contributions of this research study are summarized below in which novelties of this research are described:

Contribution # 1:

One of the major contributions of this study is detailed investigations on local and global flow characteristics within horizontal pipelines transporting capsules. The available literature does not provide any information on local flow structure within such pipelines. The availability of computational fluid dynamics tools along with experimental data has enabled the author to carry out this investigation. The pressure and velocity distributions within horizontal pipelines transporting capsules have been investigated over wide range of flow conditions. Effects of parameters such as capsule diameter, capsule shape, capsule density, capsule spacing, length of capsule, average flow velocity on pressure and velocity in near capsule region have clearly been enumerated. Furthermore novel pressure drop prediction models have been developed which include all the relevant parameters. The above modelling has been achieved through data generated from extensive numerical investigations. This pressure drop model is a novel contribution to the knowledge base that can be used to design hydraulic capsules pipeline transporting capsules of various shapes and densities.

Contribution # 2:

Another major contribution of this study is detailed investigations on local and global flow characteristics within vertical pipelines transporting capsules. The available literature does not provide any information on local flow structure within such pipelines as well. In this case as well, the availability of computational fluid dynamics tools along with experimental data has enabled the author to carry out this investigation. For vertical pipelines also, the pressure and velocity distributions within pipelines transporting capsules have been investigated over wide range of flow conditions. Effects of all the parameters as mentioned in contribution 1 on pressure and velocity in near capsule region have clearly been enumerated for vertical pipelines. Furthermore novel pressure drop prediction models have

been developed which include all the above mentioned relevant parameters. The above modelling has been achieved through data generated from extensive numerical investigations on vertical capsule pipelines. This pressure drop model is a novel contribution to the knowledge base that can be used to design hydraulic capsules pipeline transporting capsules of various shapes and densities.

Contribution # 3:

Bends are an integral part of pipeline networks. Unfortunately very limited information is available on flow through bends transporting capsules. Numerical investigation on flow through bends transporting capsules is a major contribution of this study. One of the most significant contributions of this research study is the development of a novel methodology, based on Discrete Phase Modelling of particles in a pipeline, to predict the velocity, trajectory and orientation of a capsule in pipeline bends. The effects of various geometric and flow-related parameters on the pressure drop within such bends have been evaluated for a wide range of investigations. In addition to effects of parameters mentioned in contributions 1 and 2, effects of an additional parameter namely the radius ratio of the bend have also been enumerated. Based on these investigations novel models have been developed for prediction of pressure drop for flow of capsules through bends under diverse flow conditions. Up until now no models were available for this purpose. The development of these pressure drop prediction models is a major step forward in modelling pipeline networks transporting capsules.

Contribution # 4:

Capsule pipelines are becoming increasingly important as a mode of freight transport. Unfortunately a coherent design methodology for designing hydraulic capsule pipelines is not available. This major gap in the knowledge base has been bridged through this study in which a novel design methodology for designing such pipelines is presented. The developed methodology is robust and user friendly and provides optimal solution for a given capsule throughput. The design methodology includes models for operating costs as well as cost of pipelines and capsules. These costs have been critically analysed, and their dependence on various factors has been quantified. This novel optimisation methodology, based on the least-cost principle, which makes use of the fact that the optimal pipeline size corresponds to the minimum total cost involved in the system, is a key contribution of this study.

8.5. Recommendations for Future Work

The design, operation and optimization of pipelines transporting capsules have been presented in the present study such that gaps identified in literature could be bridged. In light of the concluded remarks provided in the previous sections, a vast potential for further research in this particular area of transportation has been unlocked. The main areas identified for further work are described below which are associated to further performance-related analysis, design and optimization of pipelines transporting capsules.

Recommendation # 1:

Capsule flow in pipelines is a transient phenomenon where the capsules trajectory can vary under influence of the local flow structure. In order to accommodate these unsteady effects in the straight pipes and pipe bends, a numerical study on the transient behaviour of the capsules in the pipelines needs to be carried out. Such a study will provide precious information regarding the generation of complex flow structures in the pipelines transporting capsules in both space and time. This task requires additional computational power as the hydrodynamic forces on the capsules are calculated at each time step. Furthermore, transient analysis of pipelines transporting capsules provides information regarding the trajectory and the orientation of the capsules.

Recommendation # 2:

More advanced modelling techniques have now become available such as two degree of freedom model, six degree of freedom model etc. Using such models, the transport of solid bodies in pipelines can be analysed with much better accuracy. In these techniques, the capsules are treated as free bodies, partially or completely. These advanced models do not require any inputs in terms of the capsule velocity or orientation. The hydrodynamic forces acting on the capsules are enumerated on-the-fly and necessary modifications are carried out for the trajectory, velocity and orientations of the capsules in the pipeline. These advanced modelling techniques are indeed computationally very expensive and requires massive computational power. Furthermore, these tools require extra computational skills in terms of writing complex scripts to define the changing mesh structure and extraction of the data.

Recommendation # 3:

Numerical studies can be conducted on the flow of low-density capsules in the pipelines. Low density capsules are especially suitable for off-shore applications where the cargo needs to be transported from a point of lower elevation to a point of higher elevation. In such a scenario, the low-density of the capsules will have a huge impact on the pressure drop considerations in the vertical pipeline. Furthermore, studies can be conducted on the flow of capsules in inclined pipelines. Two-way capsule motion can also be analysed, i.e. capsules travelling down a vertical/inclined pipeline rather than being propagated vertically upwards only.

Recommendation # 4:

Different shapes and degree of rigidities of the capsules can be analysed using CFD, and the results compared with the one presented in this study for optimisation purposes. Last but not least, wear and tear analysis can be conducted on the flow of heavy-density capsules in horizontal pipelines. In addition to the translating motion of the heavy-density capsules in horizontal pipelines, the capsules travel along the wall of the pipe giving rise to static friction and increased pressure drop[within the pipeline. An estimation of the wear and tear can have significant effect on the design and optimisation of such pipelines. Furthermore, estimation of the effects of rolling motion of the capsules on the pressure drop within the pipeline will able to take the prediction models presented in this study to a higher level of accuracy.

REFERENCES

- [1] Needham, J. (1986) “Science and Civilization in China”, Physics and Physical Technology; Part 1, Physics, vol. 4
- [2] Liu, H. (1992) “Hydraulic Behaviours of Coal Log Flow in Pipe”, In the Proceedings of the 4th International Conference on Bulk Materials Handling and Transportation; Symposium on Fright Pipelines, Wollongong, Australia
- [3] Subramanya, K. (1998) “Pipeline transportation technology: An overview”, Current Science, vol. 75, pp. 824
- [4] Govier, G. W. Aziz, K. (2008) “Flow of Complex Mixtures in Pipes”, Society of Petroleum Engineers, 2nd ed., ISBN: 0882755471
- [5] Fay, J. A. (1994) “Introduction to Fluid Mechanics”, MIT Press, ISBN: 0262061651
- [6] Darcy, H. (1857) “Recherches Expérimentales Relatives au Mouvement de l’Eau dans les Tuyaux [Experimental Research on the Movement of Water in Pipes]”, Mallet-Bachelier, Paris
- [7] Moody, L. F. (1944) “Friction factors for pipe flow”, Transactions of the ASME, vol. 66, pp. 671– 684
- [8] Yasuki, N. Boucher, R. (1994) “Introduction to Fluid Mechanics”, Butterworth-Heinemann, 1st ed., ISBN: 0340676493
- [9] Mole Solutions Ltd. (2010) “Aggregate Strategic Research Programme Project 05: Assess the feasibility of using pipelines to transport aggregates in England”, Final Report
- [10] Round, G. F. (1992) “Pneumatic Capsule Pipeline Systems: A Short History and State-of-the-Art”, Bulk Solids Handling, vol. 12, pp. 67 – 72
- [11] Tubexpress Systems Inc. accessible at <http://www.capsu.org/library/documents/0005.html>
- [12] Jvarsheishvili, A. G. (1992) “Lilo-1 and Lilo-2 Systems for Pneumatic Transportation of Freight in Containers through Pipelines in Georgia”, In the Proceedings of the 4th International Conference on Bulk Materials Handling and Transportation; Symposium on Fright Pipelines, Wollongong, Australia
- [13] Kosugi, S. (1992) “A Capsule Pipeline for Limestone Transportation”, In the Proceedings of the 4th International Conference on Bulk Materials Handling and Transportation; Symposium on Fright Pipelines, Wollongong, Australia
- [14] Montgomery, B. Fairfax, S. Smith, B. (2001) “Capsule Pipeline Transport Using An Electromagnetic Drive”, Cement Industry Technical Conference, Salt Lake City, U.S.A.

- [15] Capsule Pipeline for Aggregate Transport accessible at <http://www.agg-net.com/resources/articles/capsule-pipelines-for-aggregate-transport>
- [16] Assadollahbaik, M. Liu, H. (1986) “Optimum Design of Electromagnetic Pump for Capsule Pipelines”, *Journal of Pipelines*, vol. 5, pp. 157 – 169
- [17] Vlasak, P. (1999) “An Experimental Investigation of Capsules of Anomalous Shape Conveyed by Liquid in a Pipe”, *Powder Technology*, vol. 104, pp: 207 – 213
- [18] Liu, H. (2003) “Pipeline Engineering”, Lewis Publishers, U.S.A., ISBN: 1587161400
- [19] Mishra, R. (1996) “Flow Characteristics for Multi-Sized Heterogeneous Slurries in Straight Pipe and Pipe Bends”, Ph.D. Thesis, Indian Institute of Technology, Delhi, India
- [20] Jacobs, B. E. A. (2005) “Design of Slurry Transport Systems”, Elsevier Science Publishers Ltd., U.K., ISBN: 1851666346
- [21] Ellis, H. S. (1964) “An Experimental Investigation of the Transport by Water of Single Cylindrical and Spherical Capsules with Density Equal to that of the Water”, *The Canadian Journal of Chemical Engineering*, vol: 42, Issue: 1, pp: 1 – 8
- [22] Mathur, R. Rao, C. R. Agarwal, V. C. (1989) “Transport Velocity of Equal Density Spherical Capsules in Pipeline”, In the Proceedings of the 4th Asian Congress of Fluid Mechanics, Hongkong, pp: 106 – 109
- [23] Mishra, R. Agarwal, V. C. Mathur, R. (1992) “Empirical Relations for Spherical Capsules of Various Densities”, In the Proceedings of the 19th National Conference on Fluid Mechanics and Fluid Power, Bombay
- [24] Mishra, R. Agarwal, V. C. (1998) “Prediction of Holdup in Transport of Spherical Capsules in Pipeline”, In the Proceedings of the 3rd International Conference on Fluid Mechanics, Beijing, pp: 681 – 686
- [25] Ulusarslan, D. Teke, I. (2005) “An Experimental Investigation of the Capsule Velocity, Concentration Rate and the Spacing between the Capsules for the Spherical Capsule Train Flow in a Horizontal Circular Pipe”, *Journal of Powder Technology*, vol: 159, pp: 27 – 34
- [26] Ulusarslan, D. (2010) “Effect of Capsule Density and Concentration on Pressure Drops of Spherical Capsule Train Conveyed by Water”, *Journal of Fluids Engineering*, vol: 132
- [27] Charles M. E. (1962) “Theoretical Analysis of the Concentric Flow of Cylindrical Forms”, *The Canadian Journal of Chemical Engineering*, vol: 41, Issue: 2, pp: 46 – 51
- [28] Newton, R. Redberger, P. J. Round, G. F. (1963) “Numerical Analysis of Some Variables Determining Free Flow”, *The Canadian Journal of Chemical Engineering*, vol: 42, Issue: 4, pp: 168 – 173

- [29] Kroonenberg, H. H. (1979) "A Mathematical Model for Concentric Horizontal Capsule Transport", *The Canadian Journal of Chemical Engineering*, vol: 57, Issue: 3, pp: 383
- [30] Tomita, Y. Yamamoto, M. Funatsu, K. (1986) "Motion of a Single Capsule in a Hydraulic Pipeline", *Journal of Fluid Mechanics*, vol: 171, pp: 495 – 508
- [31] Tomita, Y. Okubo, T. Funatsu, K. Fujiwara, Y. (1989) "Unsteady Analysis of Hydraulic Capsule Transport in a Straight Horizontal Pipeline", In the Proceedings of the 6th International Symposium on Freight Pipelines, Eds. H. Liu and G. F. Round, USA, pp: 273 – 278
- [32] Lenau, C. W. El-Bayya, M. M. (1996) "Unsteady Flow in Hydraulic Capsule Pipeline", *Journal of Engineering Mechanics*, vol: 122, Issue: 12, pp: 1168 – 1173
- [33] Khalil, M. F. Kassab, S. Z. Adam, I. G. Samaha, M. A. (2010) "Turbulent Flow around a Single Concentric Long Capsule in a Pipe", *Journal of Applied Mathematical Modelling*, vol: 34, pp: 2000 – 2017
- [34] Ellis, H. S. (1964) "An Experimental Investigation of the Transport by Water of Single Spherical Capsules with Density Greater than that of the Water", *The Canadian Journal of Chemical Engineering*, pp. 155 – 160
- [35] Round, G. F. Bolt, L. H. (1965) "An Experimental Investigation of the Transport in Oil of Single, Denser-than Oil, Spherical and Cylindrical Capsules", *The Canadian Journal of Chemical Engineering*, pp: 197 – 205
- [36] Ellis, H. S. Kruyer, J. Roehl, A. A. (1975) "The Hydrodynamics of Spherical Capsules", *The Canadian Journal of Chemical Engineering*, vol. 53, pp. 119 – 125
- [37] Ellis, H. S. (1964) "An Experimental Investigation of the Transport in Water of Single Cylindrical Capsule with Density Greater than that of the Water", *The Canadian Journal of Chemical Engineering*, pp. 69 – 76
- [38] Kruyer, J. Redberger, P. J. Ellis, H. S. (1967) "The Pipeline Flow of Capsules, Part 9", *Journal of Fluid Mechanics*, vol. 30, pp. 513 – 531
- [39] Ellis, H. S. (1974) "Minimising the Pressure Gradients in Capsule Pipelines", *The Canadian Journal of Chemical Engineering*, vol. 52, pp. 457 – 462
- [40] Kruyer, J. Snyder, W. T. (1975) "Relationship between Capsule Pulling Force and Pressure Gradient in a Pipe", *The Canadian Journal of Chemical Engineering*, vol. 53, pp. 378 – 383
- [41] Tomita, Y. Okubo, T. Funatsu, K. Fujiwara, Y. (1989) "Unsteady Analysis of Hydraulic Capsule Transport in a Straight Horizontal Pipeline", In the Proceedings of the 6th International Symposium on Freight Pipelines, Eds. H. Liu and G. F. Round, USA, pp: 273 – 278
- [42] Agarwal, V. C. Singh, M. K. Mishra, R. (2001) "Empirical Relation for the Effect of the Shape of the Capsules and the Nose Shape on the Velocity Ratio of Heavy Density Capsules in a Hydraulic

- Pipeline”, In the Proceedings of the Institute of Mechanical Engineers, Part E: Journal of Process Mechanical Engineering
- [43] Chow, K. W. (1979) “An Experimental Study of the Hydrodynamic Transport of Spherical and Cylindrical Capsules in a Vertical Pipeline”, M. Eng. Thesis, McMaster University, Hamilton, Ontario, Canada
- [44] Hwang, L. Y. Wood, D. J. Kao, D. T. (1981) “Capsule Hoist System for Vertical Transport of Coal and Other Mineral Solids”, The Canadian Journal of Chemical Engineering, vol. 59, pp. 317 – 324
- [45] Latto, B. Chow, K. W. (1982) “Hydrodynamic Transport of Cylindrical Capsules in a Vertical Pipeline”, The Canadian Journal of Chemical Engineering, vol. 60, pp. 713 – 722
- [46] Tachibana, M. (1983) “Basic Studies on Hydraulic Capsule Transportation, Part 2, Balance and Start-up of Cylindrical Capsule in Rising Flow of Inclined Pipeline”, Bulletin of the JSME, vol. 26, pp. 1735 – 1743
- [47] Tsuji, Y. Morikawa, Y. Chono, S. Hasegawa, T. (1984) “Fundamental Investigation of the Capsule Transport, 2nd Report, Wake of a Capsule and the Effect of Interaction between Two Capsules on the Drag”, Bulletin of JSME, vol. 27, pp. 468 – 474
- [48] Ohashi, A. Yanaida, K. (1986) “The Fluid Mechanics of Capsule Pipelines, 1st Report, Analysis of the Required Pressure Drop for Hydraulic and Pneumatic Capsules”, Bulletin of JSME, vol. 29, pp. 1719 – 1725
- [49] Bartosik, A. S. Shook, C. A. (1995) “Prediction of Vertical Liquid-Solid Pipe Flow Using Measured Concentration Distribution”, Particulate Science and Technology, vol. 13, pp. 85 – 104
- [50] Yanaida, K. Tanaka, M. (1997) “Drag Coefficient of a Capsule Inside a Vertical Angular Pipe”, Powder Technology, vol. 94, pp. 239 – 243
- [51] Swamee, P. K. (1999) “Capsule Hoist System for Vertical Transport of Minerals”, Journal of Transportation Engineering, pp. 560 – 563
- [52] Vlasak, P. and Myska, J. (1983) “The Effect of Pipe Curvature on the Flow of Carrier Liquid Capsule Train System”, In the Proceedings of the Institute of Hydrodynamics, Praha
- [53] Vlasak, P. Berman, V. (2001) “A Contribution to Hydro-transport of Capsules in Bend and Inclined Pipeline Sections”, Handbook of Conveying and Handling of Particulate Solids, pp. 521 – 529
- [54] Azzi, A. Friedel, L. (2005) “Two-Phase Upward Flow 90^o Bend Pressure Loss Model”, Forschung im Ingenieurwesen, vol. 69, pp. 120 – 130
- [55] Ulusarlan, D. (2007) “Determination of the Loss Coefficient of Elbows in the Flow of Low-Density Spherical Capsule Train”, Experimental Thermal and Fluid Science, vol. 32, pp. 415 – 422

- [56] Motamedian, E. Kasiri, N. Ghaemi, A. (2007) “Modelling Two-Phase Flow in Horizontal Pipe Bends”, *Hydrocarbon Processing*, pp. 145 – 150
- [57] Spedding, P. L. Benard, E. Crawford, N. M. (2008) “Fluid Flow through a Vertical to Horizontal 90° Elbow Bend III Three Phase Flow”, *Experimental Thermal and Fluid Science*, vol. 32, pp. 827 – 843
- [58] Silva, F. S. Resendiz, J. C. L. Mariscal, I. C. Eslava, R. T. (2010) “Pressure Drop Models Evaluation for Two-Phase Flow in 90 Degree Horizontal Elbows”, *Ingenieria Mecanica Tecnologia Desarrollo*, vol. 3, pp. 115 – 122
- [59] Ulusarlan, D. (2010) “Effect of Diameter Ratio on Loss Coefficient of Elbows in the Flow of Low-Density Spherical Capsule Trains”, *Particulate Science and Technology*, vol. 28, pp. 348 – 359
- [60] Mazumder, Q. H. (2012) “CFD Analysis of Effect of Elbow Radius on Pressure Drop in Multiphase Flow”, *Modelling and Simulation in Engineering*, vol. 2012
- [61] Mazumder, Q. H. (2012) “CFD Analysis of Single and Multi-Phase Flow Characteristics in Elbow”, *Engineering*, vol. 4, pp. 210 – 214
- [62] Polderman, H. G. (1982) “Design Rules for Hydraulic Capsule Transport Systems”, *Journal of Pipelines*, vol. 3, pp. 123 – 136
- [63] Assadollahbaik, M. Liu, H. (1986) “Optimum Design of Electromagnetic Pump for Capsule Pipelines”, *Journal of Pipelines*, vol. 5, pp. 157 – 169
- [64] Swamee, P. K. (1995) “Design of Sediment Transporting Pipeline”, *Journal of Hydraulic Engineering*, vol. 121
- [65] Swamee, P. K. (1999) “Capsule Hoist System for Vertical Transport of Minerals”, *Journal of Transportation Engineering*, pp. 560 – 563
- [66] Agarwal, V. C. Mishra, R. (1998) “Optimal Design of a Multi-Stage Capsule Handling Multi-Phase Pipeline”, *International Journal of Pressure Vessels and Piping*, vol. 75, pp. 27 – 35
- [67] Colebrook, C.F. (1939) “Turbulent Flow in Pipes with Particular Reference to the Transition Region between Smooth and Rough Pipe Laws” *Journal of the Institution of Civil Engineers*
- [68] Sha, Y. Zhao, X. (2010) “Optimisation Design of the Hydraulic Pipeline Based on the Principle of Saving Energy Resources”, In the Proceedings of Power and Energy Engineering Conference, Asia-Pacific
- [69] Versteeg, H. K. and Malalasekera, W. (1995) “An Introduction to Computational Fluid Dynamics”, Longman Scientific and Technical, U.K., ISBN: 0131274988
- [70] Pozrikidis, C. (2001) “Fluid Dynamics Theory, Computation and Numerical Simulation”, Kluwer Academic Publishers, U.S.A., ISBN: 038795869X

- [71] Cebeci, T. Shao, J. P. Kafyeke, F. and Laurendeau, E. (2005) “Computational Fluid Dynamics for Engineers”, Horizons Publishing, U.S.A., ISBN: 3540244514
- [72] Blazek, J. (2001) “Computational Fluid Dynamics Principles and Applications”, Elsevier, ISBN: 0080430090
- [73] Lomax, H. Pulliam, T. H. Zingg, D. W. (2001) “Fundamentals of Computational Fluid Dynamics”, Springer, ISBN: 3540416072
- [74] Hoffmann, K. A. and Chiang, S. T. (2000) “Computational Fluid Dynamics”, Engineering Education System, U.S.A., ISBN: 0962373133
- [75] Ansys 13.0.0 User Guide accessible at http://www1.ansys.com/customer/content/documentation/130/wb2_help.pdf
- [76] Munson, B. R. Young, D. F. Okiishi, T. H. (2002) “Fundamentals of Fluid Mechanics”, John Wiley & Sons Inc., 4th ed., U.S.A., ISBN: 0471675822
- [77] Ulusarlan, D. Teke, I. (2005) “An Experimental Determination of Pressure Drops in the Flow of Low Density Spherical Capsule Train Inside Horizontal Pipes, Journal of Experimental Thermal and Fluid Science, vol: 30, pp: 233 – 241
- [78] Industrial Accessories Company accessible at <http://www.iac-intl.com/parts/PB103001r2.pdf>
- [79] Morsi, S. A. Alexander, A. J. (1972) “An Investigation of Particle Trajectories in Two-Phase Flow Systems”, Journal of Fluid Mechanics, vol. 55, pp. 193 – 208
- [80] Agarwal, V. C. Singh, M. K. Mathur, R. (2001) “Empirical Relation for the Effect of the Shape of the Capsule and the Nose Shape on the Velocity Ratio of Heavy Density Capsules in a Hydraulic Pipeline”, In the Proceedings of the Institute of Mechanical Engineers, vol. 215, pp. 147 – 155
- [81] Khalil, M. F. Kassab, S. Z. Adam, I. G. Samaha, M. A. (2009) “Prediction of Lift and Drag Coefficients on Stationary Capsule in Pipeline”, CFD Letters, vol. 1, pp: 15 – 28
- [82] Menter, F. R. (1994) “Two-Equation Eddy-Viscosity Turbulence Models for Engineering Applications”, American Institute of Aeronautics and Astronautics, vol. 32, pp: 1598 – 1605
- [83] Patankar, S. V. Spalding, D. B. (1972), “A Calculation Procedure for Heat, Mass and Momentum Transfer in Three-Dimensional Parabolic Flows”, Heat and Mass Transfer, vol. 15, pp: 1787 – 1806
- [84] Rauch, R. D. Batira, J. T. Yang, N. T. Y. (1991) “Spatial Adaption Procedures on Unstructured Meshes for Accurate Unsteady Aerodynamic Flow Computations”, Technical Report, American Institute of Aeronautics and Astronautics, vol. 91, pp: 1106
- [85] Barth, T. J. Jespersen, D. (1989) “The Design and Application of Upwind Schemes on Unstructured Meshes”, 27th Technical Report, Aerospace Sciences Meeting, Nevada

- [86] Venkatakrishnan, V. (1993) "On the Accuracy of Limiters and Convergence to Steady State Solutions", Technical Report, American Institute of Aeronautics and Astronautics, vol. 93, pp: 880
- [87] Anderson, J. D. (2007) "Fundamentals of Aerodynamics", McGraw Hill, 4th ed., U.S.A., ISBN: 0071289089
- [88] Round, G. F. (1990) "Hydrodynamics of Capsule Pipelines", In the Proceedings of the 6th International Symposium on Freight Pipelines, Missouri, U.S.A.
- [89] Uluasarlan, D. (2008) "Comparison of Experimental Pressure Gradient and Experimental Relationships for the Low Density Spherical Capsule Train with Slurry Flow Relationships", Powder Technology, vol. 185, pp: 170 – 175
- [90] Uluasarlan, D. Teke, I. (2008) "Comparison of Pressure Gradient Correlations for the Spherical Capsule Train Flow", Particulate Science and Technology, vol. 26, pp: 285 – 295
- [91] Uluasarlan, D. Teke, I. (2009) "Relation between the Friction Coefficient and Re Number for Spherical Capsule Train – Water Flow in Horizontal Pipes", Particulate Science and Technology, vol. 27, pp: 488 – 495
- [92] Fujiwara, Y. Tomita, Y. Satou, H. Funatsu, K. (1994) "Characteristics of Hydraulic Capsule Transport", JSME International, vol. 37, pp: 89 – 95
- [93] Teke, I. Uluasarlan, D. (2007) "Mathematical Expression of Pressure Gradient in the Flow of Spherical Capsules Less Dense than Water", International Journal of Multiphase Flow, vol. 33, pp: 658 – 674
- [94] Cheremisinoff, P. N. Cheng, S. I. (1988) "Civil Engineering Practice", Technomies Publishing Co., Lancaster, P. A., U.S.A., ISBN: 0877625409
- [95] Davis, C. Sorensen, K. (1969) "Handbook of Applied Hydraulics", McGraw-Hill Book Co., New York, 3rd ed., U.S.A., ISBN: 0070730024
- [96] Russel, G. (1963) "Hydraulics", Holt, Rinehart and Winston, New York, 5th ed., U.S.A., EAN: BWB12771249
- [97] Koo, W. W. (1992) "Can a Capusle Pipeline System Compete with Truck, Rail and Barge in Shipping Agricultural Products?", In the Proceedings of the 4th International Conference on Bulk Materials Handling and Transportation; Symposium on Fright Pipelines, Wollongong, Australia
- [98] Liu, H. and Wu, J. (1992) "Economic Feasibility of Using Hydraulic Capsule Pipeline to Transport Grain in the Midwest of the United States", In the Proceedings of the 4th International Conference on Bulk Materials Handling and Transportation; Symposium on Fright Pipelines, Wollongong, Australia

- [99] Butler, T. Atkins, W. S. Jacobs, B. and Veasey, D. (1992) “Commercial Viability and Potential Market for Pneumatic Capsule Pipeline”, In the Proceedings of the 4th International Conference on Bulk Materials Handling and Transportation; Symposium on Fright Pipelines, Wollongong, Australia

APPENDICES

A-1: Computational Fluid Dynamics

➤ Introduction

Computational Fluid Dynamics or CFD is the analysis of systems involving fluid flow, heat transfer and associated phenomena such as chemical reactions by means of computer-based simulation. The technique is very powerful and spans a wide range of industrial and non – industrial application areas. From 1960s onwards, the aerospace industry has integrated CFD techniques into the design, R&D and manufacture of aircraft and jet engines. More recently, the method has been applied to the design of internal combustion engines, combustion chambers of gas turbines and furnaces. Furthermore, motor vehicle manufacturers now routinely predict drag forces, under – bonnet air flows and the in – car environment with CFD. CFD is becoming a vital component in the design of industrial products and processes.

The variable cost of an experiment, in terms of facility hire and/or person – hour costs, is proportional to the number of data points and the number of configurations tested. In contrast, CFD codes can produce extremely large volumes of results at no added expense, and it is very cheap to perform parametric studies, for instance, to optimise equipment performance.

➤ Working of CFD Codes

There are three distinct streams of numerical solution techniques. They are finite difference, finite element and spectral methods. Finite volume method, a special finite difference formulation, is central to the most well established CFD codes. The numerical algorithms include integration of the governing equations of fluid flow over all the control volumes of the domain, discretisation or conversion of the resulting integral equations into a system of algebraic equations and the solution of these equations by an iterative method.

CFD codes are structured around the numerical algorithms that can tackle fluid flow problems. In order to provide easy access to their solving power, all commercial CFD packages include sophisticated user interfaces to input problem parameters and to examine the results. Hence, all codes contain three main elements. These are:

- Pre – Processor
- Solver Execution
- Post – Processor

Pre – processing consists of the input of the flow problem to a CFD programme by means of an operator – friendly interface and the subsequent transformation of this input into a form suitable for use by the solver. The user activities at the pre – processing stage includes definition of the geometry of the

region of interest. It is called the computational domain. Grid generation is the sub – division of the domain into a number of smaller, non – overlapping sub – domains. It is also called Mesh. Selection of the physical or chemical phenomena that needs to be modelled, definition of fluid properties and the specification of appropriate boundary conditions at cells, which coincide with or touch the domain boundary, are also included in pre – processing.

The solver primarily consists of setting up the numerical model and the computation/monitoring of the solution. The setting up of the numerical model includes the following:

- Selection of appropriate physical models. These included turbulence, combustion, multiphase etc.
- Defining material properties like the fluid, solid, mixture etc.
- Prescribing operating conditions
- Prescribing boundary conditions
- Prescribing solver settings
- Prescribing initial solution
- Setting up convergence monitors

The computation of the solution includes:

- The discretized conservation equations are solved iteratively. A number of iterations are required to reach a converged solution.
- Convergence is reached when change in solution variables from one iteration to the next is negligible. Residuals provide a mechanism to help monitor this trend.
- The accuracy of the converged solution is dependent upon problem setup, grid resolution, grid independence, appropriateness and accuracy of the physical model.

Figure A-1.1 describes the working of the solver.

Post processing comprises the examination of the results obtained and revision of the model based on these results. These can be further elaborated into:

- Examine the results to view solution and extract useful data.
- Visualization tools can be used to extract the overall flow pattern, separation, shocks, shear layers etc.
- Numerical reporting tools are used to calculate quantitative results like forces, moments, and average heat transfer co-efficient, flux balances, surface and volume integrated quantities.
- Are physical models appropriate?
- Are boundary conditions correct?
- Is the grid adequate?
- Can grid be adapted to improve results?
- Does boundary resolution need to be improved?
- Is the computational domain large enough?

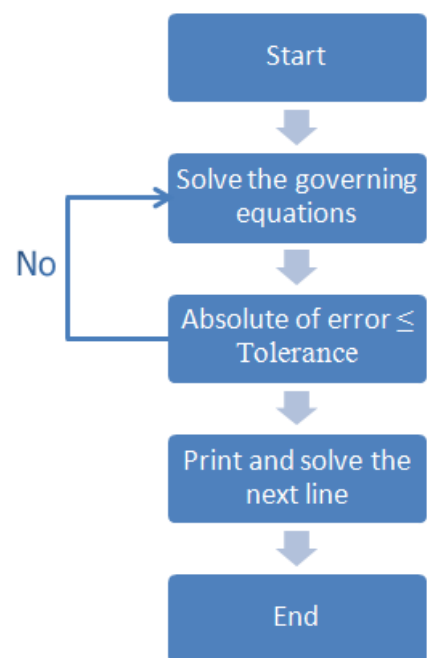


Figure A-1.1. CFD Solver

Due to the increased popularity of engineering workstations, many of which have outstanding graphic capabilities, the leading CFD packages are now equipped with versatile data visualisation tools. These include domain geometry, grid display, vector plots, line and shaded contour plots, 2D and 3D surface plots, particle tracking, view manipulations, colour post – script output etc. more recently these facilities may also include animation for dynamic result display, and in addition to graphics, all codes produce trustworthy alphanumeric output and have data export facilities for further manipulation external to the codes. As in many other branches of CAE, the graphics output capabilities of CFD codes have revolutionised the communication of ideas to the non – specialists. An overview of CFD modelling is presented in figure A-1.2.

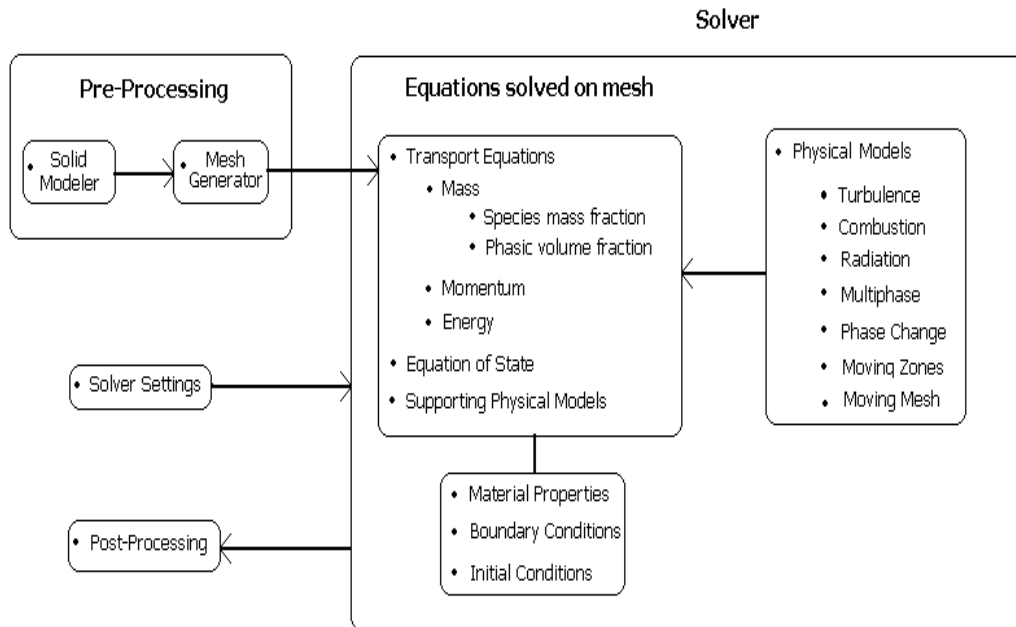


Figure A-1.2. Overview of CFD Modelling

➤ Numerical Formulation of Fluid Flow

The governing equation of fluid flow represents mathematical statements of the conservation laws of Physics:

- The mass of a fluid is conserved.
- The rate of change of momentum equals the sum of the forces on a fluid particle. (Newton's second law)
- The rate of change of energy is equal to the sum of the rate of heat addition to and the rate of work done on a fluid particle. (first law of thermodynamics)

The fluid is regarded as a continuum. For the flow diagnostics at macroscopic length scales, the molecular structure of matter and molecular motions may be ignored. The behaviour of the fluid is described in terms of macroscopic properties such as velocity, pressure, density and temperature etc.

These are averages over suitably large numbers of molecules. A fluid particle or point in a fluid is then the smallest possible element of fluid whose macroscopic properties are not influenced by individual molecules.

➤ Conservation of Mass

The mass balance equation for the fluid element can be written as:

$$\text{Rate of increase of mass in fluid element} = \text{Net rate of flow of mass into fluid element} \quad (\text{A-1.1})$$

For liquids, as the density is constant, the mass conservation equation is:

$$\text{Div } V = 0 \quad (\text{A-1.2})$$

This equation describes the net flow of mass out of the element across its boundaries. The above equation in longhand notation can be written as:

$$\frac{\partial u}{\partial x} + \frac{\partial v}{\partial y} + \frac{\partial w}{\partial z} = 0 \quad (\text{A-1.3})$$

This equation represents the steady, three dimensional mass conservation of the fluid or continuity at a point in an incompressible fluid.

➤ Conservation of Momentum

Newton's second law states that the rate of change of momentum of a fluid particle equals the sum of the forces on the particle:

$$\text{Rate of increase of Momentum of the fluid particle} = \text{Sum of forces acting on the fluid particle} \quad (\text{A-1.4})$$

There are two types of forces on fluid particles. These are surface forces and the body forces. Surface forces include pressure, viscous and gravity forces while body forces include centrifugal, coriolis and electromagnetic forces. It is a common practice to highlight the contributions due to the surface forces as separate terms in the momentum equations and to include the effects of body forces as source terms.

The x – component of the momentum equation is found by setting the rate of change of x – momentum of the fluid particle equal to the total force in the x – direction on the element due to surface stresses, plus the rate of increase of x – momentum due to sources. The equation is as follows:

$$\rho g_x + \frac{\partial \sigma_{xx}}{\partial x} + \frac{\partial \tau_{yx}}{\partial y} + \frac{\partial \tau_{zx}}{\partial z} = \rho \left(\frac{\partial u}{\partial t} + u \frac{\partial u}{\partial x} + v \frac{\partial u}{\partial y} + w \frac{\partial u}{\partial z} \right) \quad (\text{A-1.5})$$

The y and z – component of momentum equation are given by:

$$\rho g_y + \frac{\partial \tau_{xy}}{\partial x} + \frac{\partial \sigma_{yy}}{\partial y} + \frac{\partial \tau_{zy}}{\partial z} = \rho \left(\frac{\partial v}{\partial t} + u \frac{\partial v}{\partial x} + v \frac{\partial v}{\partial y} + w \frac{\partial v}{\partial z} \right) \quad (\text{A-1.6})$$

$$\rho g_z + \frac{\partial \tau_{xz}}{\partial x} + \frac{\partial \tau_{yz}}{\partial y} + \frac{\partial \sigma_{zz}}{\partial z} = \rho \left(\frac{\partial w}{\partial t} + u \frac{\partial w}{\partial x} + v \frac{\partial w}{\partial y} + w \frac{\partial w}{\partial z} \right) \quad (\text{A-1.7})$$

➤ Energy Equation

The energy equation is derived from the first law of thermodynamics which stated that the rate of change of energy of a fluid particle is equal to the rate of heat addition to the fluid particle plus the rate of work done on the particle:

$$\begin{aligned} & \text{Rate of increase of energy of fluid particle} = \\ & \text{Net rate of heat added to the fluid particle} + \text{Net rate of work done on the fluid particle} \end{aligned} \quad (\text{A-1.8})$$

Conservation of energy of the fluid particle is ensured by equating the rate of change of energy of the fluid particle to the sum of the net rate of work done on the fluid particle, the net rate of heat addition to the fluid and the rate of increase of energy due to sources. The energy equation is:

$$\begin{aligned} & \rho \frac{DE}{Dt} = \\ & -\text{div}(pu) + \left[\frac{\partial(u\tau_{xx})}{\partial x} + \frac{\partial(u\tau_{yx})}{\partial y} + \frac{\partial(u\tau_{zx})}{\partial z} + \frac{\partial(v\tau_{xy})}{\partial x} + \frac{\partial(v\tau_{yy})}{\partial y} + \right. \\ & \left. \frac{\partial(v\tau_{zy})}{\partial z} + \frac{\partial(w\tau_{xz})}{\partial x} + \frac{\partial(w\tau_{yz})}{\partial y} + \frac{\partial(w\tau_{zz})}{\partial z} \right] + \\ & \text{div}(k \text{grad } T) + S_E \end{aligned} \quad (\text{A-1.9})$$

➤ Equations of State

The motion of a fluid in three dimensions is described by a system of five partial differential equations, i.e. mass conservation, x, y and z momentum equations and energy equation. Among the unknowns are four thermodynamic variables, i.e. density, pressure, temperature and internal energy. Relationships between the thermodynamic variables can be obtained through the assumption of thermodynamic equilibrium.

The fluid velocities may be large, but they are usually small enough that, even though properties of a fluid particle change rapidly from place to place, the fluid can thermodynamically adjust itself to new conditions so quickly that the changes are effectively instantaneous. Thus, the fluid always remains in thermodynamic equilibrium. The only exceptions are certain flows with strong shockwaves, but even some of those are often well enough approximated by equilibrium assumptions. The state of a substance in thermodynamic equilibrium can be described by means of just two state variables. Equations of state relate the other variables to the two state variables, i.e. density and temperature. The equations of state are:

$$p = p(\rho, T) \quad (\text{A-1.10})$$

$$i = i(\rho, T) \quad (\text{A-1.11})$$

Liquids and gases flowing at low speeds behave as incompressible fluids. Without density variations, there is no linkage between the energy equation, mass conservation equation and momentum equations. The flow field can often be solved by considering mass conservation and momentum conservation equations only. The energy equation only needs to be solved alongside the others if the problem involves heat transfer.

➤ Navier – Stokes equations

In a Newtonian fluid, the viscous stresses are proportional to the rates of deformation. Liquids are incompressible; the viscous stresses are twice the local rate of linear deformation times the dynamic viscosity. The Navier – Stokes equations are:

$$\rho g_x - \frac{\partial p}{\partial x} + \mu \left(\frac{\partial^2 u}{\partial x^2} + \frac{\partial^2 u}{\partial y^2} + \frac{\partial^2 u}{\partial z^2} \right) = \rho \left(\frac{\partial u}{\partial t} + u \frac{\partial u}{\partial x} + v \frac{\partial u}{\partial y} + w \frac{\partial u}{\partial z} \right) \quad (\text{A-1.12})$$

$$\rho g_y - \frac{\partial p}{\partial y} + \mu \left(\frac{\partial^2 v}{\partial x^2} + \frac{\partial^2 v}{\partial y^2} + \frac{\partial^2 v}{\partial z^2} \right) = \rho \left(\frac{\partial v}{\partial t} + u \frac{\partial v}{\partial x} + v \frac{\partial v}{\partial y} + w \frac{\partial v}{\partial z} \right) \quad (\text{A-1.13})$$

$$\rho g_z - \frac{\partial p}{\partial z} + \mu \left(\frac{\partial^2 w}{\partial x^2} + \frac{\partial^2 w}{\partial y^2} + \frac{\partial^2 w}{\partial z^2} \right) = \rho \left(\frac{\partial w}{\partial t} + u \frac{\partial w}{\partial x} + v \frac{\partial w}{\partial y} + w \frac{\partial w}{\partial z} \right) \quad (\text{A-1.14})$$

A-2: Capsule Velocities

Table A-2.1. Velocities of Equi-Density Spherical Capsules in a Horizontal Pipeline

N/Lp	k	V_{av} (m/sec)	Sc (m)	V_c (m/sec)
1	0.5	1	1	1.1510
		2		2.3019
		3		3.4529
		4		4.6038
	0.7	1		1.1220
		2		2.2439
		3		3.3659
		4		4.4879
	0.9	1		1.0930
		2		2.1860
		3		3.2790
		4		4.3720
2	0.5	1	1 * d	1.1510
			3 * d	1.1510
			5 * d	1.1510
		2	1 * d	2.3019
			3 * d	2.3019
			5 * d	2.3019
		3	1 * d	3.4529
			3 * d	3.4529
			5 * d	3.4529
		4	1 * d	4.6038
			3 * d	4.6038
			5 * d	4.6038
	0.7	1	1 * d	1.1220
			3 * d	1.1220
			5 * d	1.1220
		2	1 * d	2.2439
			3 * d	2.2439
			5 * d	2.2439
		3	1 * d	3.3659
			3 * d	3.3659
			5 * d	3.3659
		4	1 * d	4.4879
			3 * d	4.4879
			5 * d	4.4879
0.9	1	1 * d	1.0930	
		3 * d	1.0930	
		5 * d	1.0930	
	2	1 * d	2.1860	

			3 * d	2.1860		
			5 * d	2.1860		
			3	1 * d	3.2790	
				3	3 * d	3.2790
					5 * d	3.2790
					4	1 * d
				4	3 * d	4.3720
					5 * d	4.3720
					3	0.5
3 * d	1.1510					
5 * d	1.1510					
2	1 * d	2.3019				
	3 * d	2.3019				
	5 * d	2.3019				
3	1 * d	3.4529				
	3 * d	3.4529				
	5 * d	3.4529				
4	1 * d	4.6038				
	3 * d	4.6038				
	5 * d	4.6038				
3	0.7	1	1 * d	1.1220		
			3 * d	1.1220		
			5 * d	1.1220		
		2	1 * d	2.2439		
			3 * d	2.2439		
			5 * d	2.2439		
		3	1 * d	3.3659		
			3 * d	3.3659		
			5 * d	3.3659		
4	1 * d	4.4879				
	3 * d	4.4879				
	5 * d	4.4879				
3	0.9	1	1 * d	1.0930		
			3 * d	1.0930		
		2	1 * d	2.1860		
			3 * d	2.1860		
		3	1 * d	3.2790		
			3 * d	3.2790		
		4	1 * d	4.3720		
			3 * d	4.3720		

Table A-2.2. Velocities of Equi-Density Cylindrical Capsules in a Horizontal Pipeline

N/Lp	Sc (m)	k	Lc (m)	Vav (m/sec)	Vc (m/sec)
1	1	0.5	1 * d	1	1.1215
				2	2.2430
				3	3.3645
				4	4.4860
			3 * d	1	1.1215
				2	2.2430
				3	3.3645
				4	4.4860
			5 * d	1	1.1215
				2	2.2430
				3	3.3645
				4	4.4860
		0.7	1 * d	1	1.0741
				2	2.1482
				3	3.2223
				4	4.2965
			3 * d	1	1.0741
				2	2.1482
				3	3.2223
				4	4.2965
			5 * d	1	1.0741
				2	2.1482
				3	3.2223
				4	4.2965
		0.9	1 * d	1	1.0249
				2	2.0499
				3	3.0748
				4	4.0998
3 * d	1		1.0249		
	2		2.0499		
	3		3.0748		
	4		4.0998		
5 * d	1		1.0249		
	2		2.0499		
	3		3.0748		
	4		4.0998		
2	1 * d	0.5	1 * d	1	1.1215
				2	2.2430
				3	3.3645
				4	4.4860
			3 * d	1	1.1215
				2	2.2430

				3	3.3645	
				4	4.4860	
				5 * d	1	1.1215
					2	2.2430
					3	3.3645
			4	4.4860		
			0.7	1 * d	1	1.0741
					2	2.1482
					3	3.2223
					4	4.2965
		3 * d		1	1.0741	
				2	2.1482	
				3	3.2223	
				4	4.2965	
		5 * d		1	1.0741	
			2	2.1482		
			3	3.2223		
			4	4.2965		
		0.9	1 * d	1	1.0249	
				2	2.0499	
3	3.0748					
4	4.0998					
3 * d	1		1.0249			
	2		2.0499			
	3		3.0748			
	4		4.0998			
5 * d	1		1.0249			
	2		2.0499			
	3		3.0748			
	4		4.0998			
3 * d	0.5	1 * d	1	1.1215		
			2	2.2430		
			3	3.3645		
			4	4.4860		
		3 * d	1	1.1215		
			2	2.2430		
			3	3.3645		
			4	4.4860		
		5 * d	1	1.1215		
			2	2.2430		
			3	3.3645		
			4	4.4860		
	0.7	1 * d	1	1.0741		
2			2.1482			
3			3.2223			
4			4.2965			

			3 * d	1	1.0741
				2	2.1482
				3	3.2223
				4	4.2965
			5 * d	1	1.0741
				2	2.1482
				3	3.2223
				4	4.2965
		0.9	1 * d	1	1.0249
				2	2.0499
				3	3.0748
				4	4.0998
	3 * d	1	1.0249		
		2	2.0499		
		3	3.0748		
		4	4.0998		
	5 * d	0.5	1 * d	1	1.1215
				2	2.2430
				3	3.3645
				4	4.4860
3 * d			1	1.1215	
			2	2.2430	
			3	3.3645	
			4	4.4860	
5 * d			1	1.1215	
			2	2.2430	
			3	3.3645	
			4	4.4860	
0.7		1 * d	1	1.0741	
			2	2.1482	
			3	3.2223	
			4	4.2965	
		3 * d	1	1.0741	
			2	2.1482	
0.9	1 * d	3	3.2223		
		4	4.2965		
		1	1.0249		
		2	2.0499		
	3 * d	3	3.0748		
		4	4.0998		

Table A-2.3. Velocities of Heavy-Density Spherical Capsules in a Horizontal Pipeline

N/Lp	k	V_{av} (m/sec)	Sc (m)	V_c (m/sec)
1	0.5	1	1	1.0352
		2		2.0704
		3		3.1056
		4		4.1408
	0.7	1		1.0437
		2		2.0873
		3		3.1310
		4		4.1747
	0.9	1		1.0521
		2		2.1043
		3		3.1564
		4		4.2086
2	0.5	1	1 * d	1.0352
			3 * d	1.0352
			5 * d	1.0352
		2	1 * d	2.0704
			3 * d	2.0704
			5 * d	2.0704
		3	1 * d	3.1056
			3 * d	3.1056
			5 * d	3.1056
		4	1 * d	4.1408
			3 * d	4.1408
			5 * d	4.1408
	0.7	1	1 * d	1.0437
			3 * d	1.0437
			5 * d	1.0437
		2	1 * d	2.0873
			3 * d	2.0873
			5 * d	2.0873
		3	1 * d	3.1310
			3 * d	3.1310
			5 * d	3.1310
		4	1 * d	4.1747
			3 * d	4.1747
			5 * d	4.1747
0.9	1	1 * d	1.0521	
		3 * d	1.0521	
		5 * d	1.0521	
	2	1 * d	2.1043	
		3 * d	2.1043	
		5 * d	2.1043	

		3	1 * d	3.1564	
			3 * d	3.1564	
			5 * d	3.1564	
		4	1 * d	4.2086	
			3 * d	4.2086	
			5 * d	4.2086	
	3	0.5	1	1 * d	1.0352
				3 * d	1.0352
				5 * d	1.0352
			2	1 * d	2.0704
				3 * d	2.0704
				5 * d	2.0704
3			1 * d	3.1056	
			3 * d	3.1056	
			5 * d	3.1056	
4			1 * d	4.1408	
			3 * d	4.1408	
			5 * d	4.1408	
0.7		1	1 * d	1.0437	
			3 * d	1.0437	
			5 * d	1.0437	
		2	1 * d	2.0873	
			3 * d	2.0873	
			5 * d	2.0873	
		3	1 * d	3.1310	
			3 * d	3.1310	
			5 * d	3.1310	
		4	1 * d	4.1747	
			3 * d	4.1747	
			5 * d	4.1747	
0.9	1	1 * d	1.0521		
		3 * d	1.0521		
	2	1 * d	2.1043		
		3 * d	2.1043		
	3	1 * d	3.1564		
		3 * d	3.1564		
	4	1 * d	4.2086		
		3 * d	4.2086		

Table A-2.4. Velocities of Heavy-Density Cylindrical Capsules in a Horizontal Pipeline

N/Lp	Sc (m)	k	Lc (m)	Vav (m/sec)	Vc (m/sec)
1	1	0.5	1 * d	1	0.9195
				2	1.8391
				3	2.7586
				4	3.6781
			3 * d	1	0.9112
				2	1.8224
				3	2.7336
				4	3.6448
			5 * d	1	0.9029
				2	1.8058
				3	2.7086
				4	3.6115
		0.7	1 * d	1	0.9784
				2	1.9568
				3	2.9352
				4	3.9136
			3 * d	1	0.9667
				2	1.9335
				3	2.9002
				4	3.8669
			5 * d	1	0.9551
				2	1.9101
				3	2.8652
				4	3.8203
0.9	1 * d	1	1.0372		
		2	2.0745		
		3	3.1117		
		4	4.1490		
	3 * d	1	1.0222		
		2	2.0445		
		3	3.0667		
		4	4.0890		
	5 * d	1	1.0073		
		2	2.0145		
		3	3.0218		
		4	4.0290		
2	1 * d	0.5	1 * d	1	0.9195
				2	1.8391
				3	2.7586
				4	3.6781
			3 * d	1	0.9112
				2	1.8224

				3	2.7336	
				4	3.6448	
				5 * d	1	0.9029
					2	1.8058
					3	2.7086
			4	3.6115		
			0.7	1 * d	1	0.9784
					2	1.9568
					3	2.9352
					4	3.9136
		3 * d		1	0.9667	
				2	1.9335	
				3	2.9002	
				4	3.8669	
		5 * d		1	0.9551	
				2	1.9101	
				3	2.8652	
				4	3.8203	
		0.9	1 * d	1	1.0372	
				2	2.0745	
				3	3.1117	
				4	4.1490	
			3 * d	1	1.0222	
				2	2.0445	
				3	3.0667	
				4	4.0890	
			5 * d	1	1.0073	
				2	2.0145	
3	3.0218					
4	4.0290					
3 * d	0.5	1 * d	1	0.9195		
			2	1.8391		
			3	2.7586		
			4	3.6781		
		3 * d	1	0.9112		
			2	1.8224		
			3	2.7336		
			4	3.6448		
		5 * d	1	0.9029		
			2	1.8058		
			3	2.7086		
			4	3.6115		
	0.7	1 * d	1	0.9784		
			2	1.9568		
			3	2.9352		
			4	3.9136		

			3 * d	1	0.9667
				2	1.9335
				3	2.9002
				4	3.8669
			5 * d	1	0.9551
				2	1.9101
				3	2.8652
				4	3.8203
		0.9	1 * d	1	1.0372
				2	2.0745
				3	3.1117
				4	4.1490
	3 * d	1	1.0222		
		2	2.0445		
		3	3.0667		
		4	4.0890		
	5 * d	0.5	1 * d	1	0.9195
				2	1.8391
				3	2.7586
				4	3.6781
3 * d			1	0.9112	
			2	1.8224	
			3	2.7336	
			4	3.6448	
5 * d			1	0.9029	
			2	1.8058	
			3	2.7086	
			4	3.6115	
0.7		1 * d	1	0.9784	
			2	1.9568	
			3	2.9352	
			4	3.9136	
		3 * d	1	0.9667	
			2	1.9335	
	3		2.9002		
	4		3.8669		
0.9	1 * d	1	1.0372		
		2	2.0745		
		3	3.1117		
		4	4.1490		
	3 * d	1	1.0222		
		2	2.0445		
3	3.0667				
4	4.0890				

Table A-2.5. Velocities of Equi-Density Spherical Capsules in a Vertical Pipeline

N/Lp	k	V_{av} (m/sec)	Sc (m)	V_c (m/sec)
1	0.5	1	1	1.2658
		2		2.5315
		3		3.7973
		4		5.0630
	0.7	1		1.1289
		2		2.2579
		3		3.3868
		4		4.5157
	0.9	1		1.0365
		2		2.0729
		3		3.1094
		4		4.1459
2	0.5	1	1 * d	1.2658
			3 * d	1.2658
			5 * d	1.2658
		2	1 * d	2.5315
			3 * d	2.5315
			5 * d	2.5315
		3	1 * d	3.7973
			3 * d	3.7973
			5 * d	3.7973
		4	1 * d	5.0630
			3 * d	5.0630
			5 * d	5.0630
	0.7	1	1 * d	1.1289
			3 * d	1.1289
			5 * d	1.1289
		2	1 * d	2.2579
			3 * d	2.2579
			5 * d	2.2579
		3	1 * d	3.3868
			3 * d	3.3868
			5 * d	3.3868
		4	1 * d	4.5157
			3 * d	4.5157
			5 * d	4.5157
0.9	1	1 * d	1.0365	
		3 * d	1.0365	
		5 * d	1.0365	
	2	1 * d	2.0729	
		3 * d	2.0729	
		5 * d	2.0729	

		3	1 * d	3.1094	
			3 * d	3.1094	
			5 * d	3.1094	
		4	1 * d	4.1459	
			3 * d	4.1459	
			5 * d	4.1459	
	3	0.5	1	1 * d	1.2658
				3 * d	1.2658
				5 * d	1.2658
			2	1 * d	2.5315
				3 * d	2.5315
				5 * d	2.5315
3			1 * d	3.7973	
			3 * d	3.7973	
			5 * d	3.7973	
4			1 * d	5.0630	
			3 * d	5.0630	
			5 * d	5.0630	
0.7		1	1 * d	1.1289	
			3 * d	1.1289	
			5 * d	1.1289	
		2	1 * d	2.2579	
			3 * d	2.2579	
			5 * d	2.2579	
		3	1 * d	3.3868	
			3 * d	3.3868	
			5 * d	3.3868	
		4	1 * d	4.5157	
			3 * d	4.5157	
			5 * d	4.5157	
0.9	1	1 * d	1.0365		
		3 * d	1.0365		
	2	1 * d	2.0729		
		3 * d	2.0729		
	3	1 * d	3.1094		
		3 * d	3.1094		
	4	1 * d	4.1459		
		3 * d	4.1459		

Table A-2.6. Velocities of Equi-Density Cylindrical Capsules in a Vertical Pipeline

N/Lp	Sc (m)	k	Lc (m)	Vav (m/sec)	Vc (m/sec)
1	1	0.5	1 * d	1	1.0928
				2	2.1856
				3	3.2783
				4	4.3711
			3 * d	1	1.2578
				2	2.5156
				3	3.7733
				4	5.0311
			5 * d	1	1.3428
				2	2.6855
				3	4.0283
				4	5.3711
		0.7	1 * d	1	1.0467
				2	2.0934
				3	3.1401
				4	4.1869
			3 * d	1	1.2048
				2	2.4095
				3	3.6143
				4	4.8190
			5 * d	1	1.2862
				2	2.5723
				3	3.8585
				4	5.1446
		0.9	1 * d	1	1.0136
				2	2.0272
				3	3.0407
				4	4.0543
3 * d	1		1.1666		
	2		2.3332		
	3		3.4999		
	4		4.6665		
5 * d	1		1.2454		
	2		2.4909		
	3		3.7363		
	4		4.9818		
2	1 * d	0.5	1 * d	1	1.0928
				2	2.1856
				3	3.2783
				4	4.3711
		3 * d	1	1.2578	
			2	2.5156	

		0.7	5 * d	3	3.7733
				4	5.0311
				1	1.3428
				2	2.6855
			3	4.0283	
			4	5.3711	
			1 * d	1	1.0467
				2	2.0934
				3	3.1401
				4	4.1869
			3 * d	1	1.2048
				2	2.4095
		3		3.6143	
		4		4.8190	
		5 * d	1	1.2862	
			2	2.5723	
			3	3.8585	
			4	5.1446	
		0.9	1 * d	1	1.0136
				2	2.0272
				3	3.0407
				4	4.0543
			3 * d	1	1.1666
				2	2.3332
				3	3.4999
				4	4.6665
			5 * d	1	1.2454
				2	2.4909
3	3.7363				
4	4.9818				
3 * d	0.5	1 * d	1	1.0928	
			2	2.1856	
			3	3.2783	
			4	4.3711	
		3 * d	1	1.2578	
			2	2.5156	
			3	3.7733	
			4	5.0311	
		5 * d	1	1.3428	
			2	2.6855	
			3	4.0283	
			4	5.3711	
	0.7	1 * d	1	1.0467	
			2	2.0934	
			3	3.1401	
			4	4.1869	

			3 * d	1	1.2048
				2	2.4095
				3	3.6143
				4	4.8190
			5 * d	1	1.2862
				2	2.5723
				3	3.8585
				4	5.1446
		0.9	1 * d	1	1.0136
				2	2.0272
				3	3.0407
				4	4.0543
	3 * d	1	1.1666		
		2	2.3332		
		3	3.4999		
		4	4.6665		
	5 * d	0.5	1 * d	1	1.0928
				2	2.1856
				3	3.2783
				4	4.3711
3 * d			1	1.2578	
			2	2.5156	
			3	3.7733	
			4	5.0311	
5 * d			1	1.3428	
			2	2.6855	
			3	4.0283	
			4	5.3711	
0.7		1 * d	1	1.0467	
			2	2.0934	
			3	3.1401	
			4	4.1869	
		3 * d	1	1.2048	
			2	2.4095	
	3		3.6143		
	4		4.8190		
0.9	1 * d	1	1.0136		
		2	2.0272		
		3	3.0407		
		4	4.0543		
	3 * d	1	1.1666		
		2	2.3332		
3	3.4999				
4	4.6665				

Table A-2.7. Velocities of Heavy-Density Spherical Capsules in a Vertical Pipeline

N/Lp	k	V_{av} (m/sec)	Sc (m)	V_c (m/sec)
1	0.5	2	1	0.5724
		3		1.8382
		4		3.1039
	0.7	1		0.1247
		2		1.2537
		3		2.3826
		4		3.5115
	0.9	1		0.7336
		2		1.7700
		3		2.8065
		4		3.8430
	2	0.5		2
3 * d			0.5724	
5 * d			0.5724	
3			1 * d	1.8382
			3 * d	1.8382
			5 * d	1.8382
4			1 * d	3.1039
			3 * d	3.1039
			5 * d	3.1039
0.7		1	1 * d	0.1247
			3 * d	0.1247
			5 * d	0.1247
		2	1 * d	1.2537
			3 * d	1.2537
			5 * d	1.2537
		3	1 * d	2.3826
			3 * d	2.3826
			5 * d	2.3826
		4	1 * d	3.5115
			3 * d	3.5115
			5 * d	3.5115
0.9		1	1 * d	0.7336
			3 * d	0.7336
			5 * d	0.7336
		2	1 * d	1.7700
			3 * d	1.7700
			5 * d	1.7700
		3	1 * d	2.8065
			3 * d	2.8065
			5 * d	2.8065
		4	1 * d	3.8430

			3 * d	3.8430
			5 * d	3.8430
3	0.5	2	1 * d	0.5724
			3 * d	0.5724
			5 * d	0.5724
		3	1 * d	1.8382
			3 * d	1.8382
			5 * d	1.8382
		4	1 * d	3.1039
			3 * d	3.1039
			5 * d	3.1039
	0.7	1	1 * d	0.1247
			3 * d	0.1247
			5 * d	0.1247
		2	1 * d	1.2537
			3 * d	1.2537
			5 * d	1.2537
		3	1 * d	2.3826
			3 * d	2.3826
			5 * d	2.3826
		4	1 * d	3.5115
			3 * d	3.5115
			5 * d	3.5115
	0.9	1	1 * d	0.7336
			3 * d	0.7336
		2	1 * d	1.7700
3 * d			1.7700	
3		1 * d	2.8065	
		3 * d	2.8065	
4		1 * d	3.8430	
		3 * d	3.8430	

Table A-2.8. Velocities of Heavy-Density Cylindrical Capsules in a Vertical Pipeline

N/Lp	Sc (m)	k	Lc (m)	Vav (m/sec)	Vc (m/sec)
1	1	0.5	1 * d	2	0.7230
				3	1.8157
				4	2.9085
			3 * d	3	1.2401
				4	2.4978
				5 * d	0.7579
		0.7	1 * d	3	2.1006
				4	2.1006
			1 * d	1	0.0941
				2	1.1408

				3	2.1875	
				4	3.2342	
			3 * d	2	0.7595	
				3	1.9643	
				4	3.1690	
				5 * d	2	0.4422
			3		1.7283	
				4	3.0145	
				0.9	1 * d	1
			2			1.6835
		3	2.6971			
		4	3.7106			
			3 * d	1	0.5714	
				2	1.7380	
				3	2.9046	
				4	4.0712	
			5 * d	1	0.4770	
				2	1.7224	
				3	2.9679	
				4	4.2133	
2	1 * d	0.5	1 * d	2	0.7230	
				3	1.8157	
				4	2.9085	
				3 * d	3	1.2401
			4		2.4978	
				5 * d	3	0.7579
		4			2.1006	
		0.7	1 * d	1	0.0941	
				2	1.1408	
				3	2.1875	
				4	3.2342	
				3 * d	2	0.7595
					3	1.9643
					4	3.1690
					5 * d	2
			3	1.7283		
			4	3.0145		
			0.9	1 * d		1
					2	1.6835
		3			2.6971	
4	3.7106					
	3 * d	1		0.5714		
		2		1.7380		
		3		2.9046		
		4		4.0712		
		5 * d		1	0.4770	

				2	1.7224		
				3	2.9679		
				4	4.2133		
	3 * d	0.5	1 * d	2	0.7230		
					3	1.8157	
					4	2.9085	
				3 * d	3	1.2401	
					4	2.4978	
					5 * d	3	0.7579
			4	2.1006			
			0.7	1 * d	1	0.0941	
						2	1.1408
						3	2.1875
						4	3.2342
					3 * d	2	0.7595
						3	1.9643
						4	3.1690
						5 * d	2
					3		1.7283
					4		3.0145
				0.9	1 * d		1
							2
						3	2.6971
						4	3.7106
					3 * d	1	0.5714
						2	1.7380
						3	2.9046
			4			4.0712	
	5 * d	0.5	1 * d	2	0.7230		
						3	1.8157
						4	2.9085
				3 * d	3	1.2401	
						4	2.4978
					5 * d	3	0.7579
			4	2.1006			
			0.7	1 * d	1	0.0941	
						2	1.1408
						3	2.1875
						4	3.2342
					3 * d	2	0.7595
						3	1.9643
						4	3.1690
				0.9		1 * d	1
					2		1.6835
					3		2.6971
					4		3.7106

			3 * d	1	0.5714
				2	1.7380
				3	2.9046
				4	4.0712

Table A-2.9. Velocities of Capsules in Horizontal Bends

N/Lp	r/R	Ψ	s	k	Lc (m)	Sc (m)	Vav (m/sec)	θ ($^{\circ}$)	Vcx1 (m/sec)	Vcy1 (m/sec)	Vcx2	Vcy2
1	4	1	1	0.5	1 * d	1	1	0	1.1126	0.0741	N/A	
								18	1.0736	0.3134		
								36	0.9477	0.5755		
								54	0.7279	0.8118		
								72	0.4216	0.988		
								90	0.1263	1.0996		
				4			0	4.3551	0.2978			
							18	4.1933	1.2633			
							36	3.6895	2.3088			
							54	2.8349	3.2306			
							72	1.653	3.9051			
							90	0.532	4.3299			
			1	0			1.0985	0.0739				
				18			1.06	0.3133				
				36			0.9356	0.5761				
				54			0.7183	0.8139				
				72			0.3838	1.0044				
				90			0.1222	1.1048				
			4	0			4.3144	0.298				
				18			4.1546	1.263				
				36			3.6548	2.3111				
				54			2.8079	3.2359				
				72			1.6327	3.9176				
				90			0.5198	4.333				
1	0	1.0959	-0.037									
	18	1.0175	0.096									
	36	0.7098	0.4117									
	54	0.5181	0.6607									
	72	0.0312	0.8899									
	90	-0.23	1.0228									
4	0	3.722	0.172									

8	1	1	0.5	0.5	18	3.2055	0.5955								
						36	2.5367	1.2705							
			54			1.7382	1.9103								
			72			0.8532	2.4129								
			90			-0.218	3.0014								
		1	36		0.9251	0.5929									
		4	36		3.6395	2.3595									
		1	36		0.9126	0.5925									
		4	36		3.6011	2.3598									
		1	0		1.0585	0.0162									
					18	1.0278	0.14								
					36	0.5161	0.7408								
					54	0.54	0.8917								
					72	0.392	0.967								
	4	0	4.1838	0.0694											
			18	4.0637	0.5676										
			36	1.896	2.8527										
			54	2.097	3.544										
			72	1.5501	3.8373										
	1	0	1.0374	0.0157											
			18	1.0074	0.1392										
			36	0.4928	0.7115										
			54	0.524	0.8799										
			72	0.3785	0.9527										
	4	0	4.1055	0.0698											
			18	3.9873	0.5659										
			36	1.8281	2.7645										
			54	2.0526	3.4887										
72			1.4917	3.7879											
1	36	0.9542	0.5859												
4	36	3.7193	2.3539												
1	36	0.9461	0.5916												
4	36	3.7022	2.3545												
1	0	1.1136	0.0175												
		18	1.0827	0.1453											
		36	0.5191	0.7419											
0.8094	1	0.5	0.7	2.7	0.5	0.7									
							36	0.7							
		72			0.7										
		90					0.7								
		1							0.7						
		4								0.7					
		1									0.7				
	4	0.7													
	1			0.7											
	4											0.7			
	1												0.7		
	4													0.7	
	1														0.7
	4														
1	0.7														
4			0.7												

		0.8094	2.7		1 * d	1 * d			1.0860	0.1137	0.9621	0.2408
						2 * d			1.0860	0.1137	0.5667	0.7779
		0.645			2 * d	1 * d			1.0860	0.1137	0.5818	0.7895
						2 * d			1.0860	0.1137	0.5924	0.8856

Table A-2.10. Velocities of Capsules in Vertical Bends

N/Lp	r/R	Ψ	s	k	Lc (m)	Sc (m)	Vav (m/sec)	θ ($^{\circ}$)	Vcx1 (m/sec)	Vcy2 (m/sec)	Vcx2 (m/sec)	Vcy2 (m/sec)	
1	4	1	1	0.5	1	1	1	36	1.8698	1.153	N/A		
							4	36	3.2184	2.183			
							0.7	1	36	1.8492			1.1532
								4	36	3.1659			2.2184
							0.5	1	0	1.8915			-0.102
									18	1.6775			0.6574
				36					0.9788	1.1771			
				54					1.006	1.2207			
				72					0.1837	1.3061			
				90					0.0223	1.2466			
				0.7			4	0	4.0673	0.2416			
								18	3.82	0.5578			
			36					2.1215	2.9183				
			54					2.0409	3.3215				
			72					1.533	3.5305				
			90					0.9261	3.5681				
			0.5	1			0	1.8657	-0.062				
							18	1.592	0.631				
							36	0.9496	1.1999				
							54	0.95	1.2333				
							72	0.104	1.2623				
							90	-0.007	1.2152				
			0.7	4			0	3.8889	-0.152				
							18	2.4212	1.7812				
							36	2.9237	2.3418				
							54	2.5381	2.6376				
							72	0.0134	3.5178				
							90	-0.293	3.7833				
0.8094	1	0.5	1	36	1.9183	1.1566							
			4	36	3.2408	2.1701							

			2.7	0.7			1	36	1.905	1.1638	
				4			36	3.2176	2.1611		
				1			0	1.6098	0.0431		
							18	1.2988	0.5585		
							36	1.0959	0.7169		
							54	0.5044	0.9479		
							72	0.1661	0.8407		
							90	0.0775	0.8794		
				4			0	3.4723	-0.367		
							18	3.2429	0.7234		
							36	2.8346	2.0081		
							54	1.6996	2.9096		
	72	1.3096	3.088								
	90	-0.216	3.59								
	1	0	1.6767	0.0258							
		18	1.4754	0.3598							
		36	1.2196	0.6499							
		54	0.8424	0.9294							
		72	0.3291	1.089							
		90	-0.153	0.82							
	4	0	4.0917	-0.067							
		18	3.4976	0.1652							
		36	2.8669	2.5737							
		54	2.5326	2.8892							
72		-0.006	3.1367								
90		-0.241	3.8395								
8	1	1	2.7	0.5			1	36	1.5837	1.1588	
				4			36	3.3834	2.3874		
				1			36	1.4975	1.1258		
				4			36	3.3513	2.3912		
				1			0	1.9493	-0.569		
							18	1.9443	0.6231		
	36	0.9864	1.5396								
	54	0.9125	1.3292								
	72	0.5874	0.9765								
	90	0.0037	0.8688								
	4	0	3.6046	-0.456							
		18	3.7017	0.9742							
36		2.913	2.5104								
54		2.3838	2.6527								
					0.7			1	36	1.4975	1.1258
					4			36	3.3513	2.3912	
	1				0			1.9493	-0.569		
					18			1.9443	0.6231		
					36			0.9864	1.5396		
					54			0.9125	1.3292		
72		0.5874	0.9765								
90		0.0037	0.8688								
4	0	3.6046	-0.456								
	18	3.7017	0.9742								
	36	2.913	2.5104								
	54	2.3838	2.6527								

								72	1.0609	3.6312		
								90	0.459	3.6649		
2	4	1	1	0.7	1 * d	2	N/A	1.8492	1.1532	0.8696	1.9487	
								2.0989	0.6287	0.4863	2.0903	
								1.5031	0.5558	0.8433	1.1761	
								1.5429	0.6298	0.6771	0.9244	
								1.5279	1.0762	1.2321	1.4642	
								1.4975	1.1258	0.8924	1.7377	
								0.9410	1.5594	0.8754	1.4352	
								0.9410	1.5594	0.7095	1.3155	
	8	1	2.7		1 * d	1 * d	3.8662	0.8606	2.7609	2.6831		
						2 * d	3.8662	0.8606	2.0012	3.2722		
						1 * d	4.1484	0.2010	2.7361	2.7081		
						2 * d	4.1484	0.2010	1.5084	3.5367		
		2.7	1 * d		2 * d	1 * d	3.8053	0.1314	2.8099	2.6837		
						2 * d	3.8053	0.1314	2.2257	2.9471		
						1 * d	4.0917	-0.0666	2.7391	2.7601		
						2 * d	4.0917	-0.0666	1.9462	2.7518		
	8	1	1		1 * d	1 * d	3.9562	1.2011	3.3929	2.3514		
						2 * d	3.9562	1.2011	3.1312	2.6939		
						1 * d	3.9562	1.2011	3.0183	2.8217		
						2 * d	3.9562	1.2011	2.4939	3.3093		
		2.7	1 * d		2 * d	1 * d	3.6025	0.2471	3.2030	2.3930		
						2 * d	3.6025	0.2471	3.0198	2.5229		
						1 * d	3.6025	0.2471	3.0320	2.5172		
						2 * d	3.6025	0.2471	2.5370	2.4154		

A-3: Pressure Drop in Horizontal HCPs

Table A-3.1. Pressure Drop variations in a Horizontal Pipe carrying Equi-Density Spherical Capsules

N/Lp	k	V_{av} (m/sec)	Sc (m)	ΔPm/Lp (Pa/m)	Difference w.r.t. k = 0.5 (%)
1	0.5	1	1	124	N/A
		2		431	
		3		905	
		4		1533	
	0.7	1		186	50
		2		657	52
		3		1385	53
		4		2360	54
	0.9	1		1450	1069
		2		5279	1125
		3		11246	1143
		4		19312	1160
2	0.5	1	1 * d	147	N/A
			3 * d	148	
			5 * d	149	
		2	1 * d	520	
			3 * d	524	
			5 * d	526	
		3	1 * d	1098	
			3 * d	1104	
			5 * d	1110	
		4	1 * d	1870	
			3 * d	1880	
			5 * d	1892	
	0.7	1	1 * d	274	86.39
			3 * d	277	87.16
			5 * d	281	88.59
		2	1 * d	978	88.08
			3 * d	987	88.36
			5 * d	1005	91.06
		3	1 * d	2075	88.98
			3 * d	2093	89.58
			5 * d	2133	92.16
		4	1 * d	3553	90.00
			3 * d	3579	90.37
			5 * d	3648	92.81
	0.9	1	1 * d	3105	2012.24
			3 * d	2765	1768.24
			5 * d	2772	1760.40

		2	1 * d	11457	2103.27		
			3 * d	10117	1830.73		
			5 * d	10019	1804.75		
		3	3	1 * d	24447	2126.50	
				3 * d	21758	1870.83	
				5 * d	21532	1839.82	
		4	4	1 * d	43283	2214.60	
				3 * d	37652	1902.77	
				5 * d	37220	1867.23	
		3	0.5	1	1 * d	172	N/A
					3 * d	175	
					5 * d	175	
2	2			1 * d	616		
				3 * d	627		
				5 * d	627		
3	3			1 * d	1304		
				3 * d	1331		
				5 * d	1327		
4	4			1 * d	2228		
				3 * d	2275		
				5 * d	2267		
0.7	1		1	1 * d	373	116.86	
				3 * d	386	120.57	
				5 * d	401	129.14	
	2		2	1 * d	1336	116.88	
				3 * d	1388	121.37	
				5 * d	1431	128.23	
	3		3	1 * d	2841	117.87	
				3 * d	2963	122.61	
				5 * d	3042	129.24	
	4		4	1 * d	4868	118.49	
				3 * d	5082	123.38	
				5 * d	5211	129.86	
0.9	1	1	1 * d	4527	2531.98		
			3 * d	4222	2312.57		
	2	2	1 * d	16602	2595.13		
			3 * d	15493	2370.97		
	3	3	1 * d	35806	2645.86		
			3 * d	33341	2404.96		
	4	4	1 * d	62996	2727.47		
			3 * d	57534	2428.97		

Table A-3.2. Pressure Drop variations in a Horizontal Pipe carrying Equi-Density Cylindrical Capsules

N/Lp	Sc	k	Lc	Vav	$\Delta Pm/Lp$	Difference w.r.t. k = 0.5
	(m)		(m)	(m/sec)	(Pa/m)	(%)
1	1	0.5	1 * d	1	414	N/A
				2	1600	
				3	3534	
				4	6208	
			3 * d	1	398	
				2	1512	
				3	3316	
				4	5799	
			5 * d	1	415	
				2	1571	
				3	3430	
				4	5998	
		0.7	1 * d	1	1532	270.05
				2	5990	274.38
				3	13354	277.87
				4	23575	279.75
			3 * d	1	1598	301.51
				2	6206	310.45
				3	13815	316.62
				4	24186	317.07
			5 * d	1	1912	360.72
				2	7439	373.52
				3	16531	381.95
				4	29160	386.16
		0.9	1 * d	1	20009	4733.09
				2	78143	4783.94
				3	173845	4819.21
				4	306886	4843.40
			3 * d	1	24348	6017.59
				2	92653	6027.84
				3	203477	6036.22
				4	356216	6042.71
5 * d	1		28974	6881.69		
	2		108359	6797.45		
	3		235889	6777.23		
	4		410603	6745.67		
2	1 * d	0.5	1 * d	1	439	N/A
				2	1691	
				3	3718	
				4	6466	
			3 * d	1	479	

				2	1817			
				3	3923			
				4	6863			
				1	530			
			5 * d	2	1986			
				3	4337			
				4	7554			
				1	1849		321.18	
			0.7	1 * d	2		7176	324.36
					3		15891	327.41
					4		27962	332.45
					1		2175	354.07
		3 * d		2	8596	373.09		
				3	19149	388.12		
				4	34085	396.65		
				1	2944	455.47		
		5 * d		2	10798	443.71		
				3	23260	436.32		
				4	41777	453.04		
				1	34339	7722.10		
		0.9	1 * d	2	133402	7788.94		
				3	296058	7862.83		
				4	523514	7996.41		
				1	44168	9120.88		
			3 * d	2	167120	9097.58		
				3	366405	9239.92		
				4	640272	9229.33		
				1	56992	10653.21		
			5 * d	2	212277	10588.67		
				3	457170	10441.16		
				4	798375	10468.90		
				1	553	N/A		
		1 * d	2	2119				
			3	4667				
			4	8181				
			1	568				
		3 * d	2	2155				
			3	4716				
			4	8238				
			1	624				
5 * d	2	2353						
	3	5141						
	4	8967						
	1	2402	334.36					
3 * d	0.7	1 * d	2	9296	338.70			
			3	20587	341.12			

			3 * d	4	36188	342.34
				1	2759	385.74
				2	10672	395.22
				3	23518	398.69
			4	41282	401.12	
			5 * d	1	3979	537.66
				2	15252	548.19
				3	33596	553.49
		4		58898	556.83	
		0.9	1 * d	1	39327	7011.57
				2	153695	7153.19
				3	342033	7228.76
				4	603879	7281.48
			3 * d	1	51976	9050.70
				2	198763	9123.34
				3	437585	9178.73
	4			767256	9213.62	
	5 * d	0.5	1 * d	1	603	N/A
				2	2317	
				3	5113	
				4	8971	
			3 * d	1	611	
				2	2327	
				3	5104	
				4	8925	
			5 * d	1	670	
				2	2537	
				3	5557	
4				9710		
0.7	1 * d	1	2696	347.10		
		2	10525	354.25		
		3	23366	356.99		
		4	41156	358.77		
	3 * d	1	3263	434.04		
		2	12654	443.79		
		3	28033	449.24		
		4	49371	453.18		
0.9	1 * d	1	40706	6650.58		
		2	159586	6787.61		
		3	355721	6857.19		
		4	628762	6908.83		
	3 * d	1	53192	8605.73		
		2	203620	8650.32		
		3	448530	8687.81		
		4	786724	8714.83		

Table A-3.3. Pressure Drop variations in a Horizontal Pipe carrying Heavy-Density Spherical Capsules

N/Lp	k	V_{av}	Sc	ΔPm/Lp	Difference w.r.t. k = 0.5	
		(m/sec)	(m)	(Pa/m)	(%)	
1	0.5	1	1	226	N/A	
		2		727		
		3		1818		
		4		3412		
	0.7	1		474	109.73	
		2		1990	173.73	
		3		4469	145.82	
		4		6418	88.10	
	0.9	1		4854	2047.79	
		2		18924	2503.03	
		3		42104	2215.95	
		4		73254	2046.95	
2	0.5	1	1 * d	351	N/A	
			3 * d	363		
			5 * d	346		
		2	1 * d	1316		
			3 * d	1334		
			5 * d	1320		
		3	1 * d	2697		
			3 * d	3307		
			5 * d	3261		
		4	1 * d	4826		
			3 * d	5533		
			5 * d	5758		
	0.7	1	1 * d	1240	253.28	
			3 * d	998	174.93	
			5 * d	1044	201.73	
		2	1 * d	5103	287.77	
			3 * d	4207	215.37	
			5 * d	4091	209.92	
		3	1 * d	11032	309.05	
			3 * d	8457	155.73	
			5 * d	8723	167.49	
		4	1 * d	22229	360.61	
			3 * d	16027	189.66	
			5 * d	14965	159.90	
		0.9	1	1 * d	11475	897.10
				3 * d	10269	992.59
				5 * d	10500	972.61
2	1 * d		44445	845.17		
	3 * d		40213	924.15		

			5 * d	40464	956.83
		3	1 * d	103600	914.64
			3 * d	91109	1038.22
			5 * d	93453	1033.96
		4	1 * d	170152	743.74
			3 * d	161621	973.91
			5 * d	175038	1131.17
3	0.5	1	1 * d	537	N/A
			3 * d	558	
			5 * d	483	
		2	1 * d	2056	
			3 * d	1948	
			5 * d	1784	
		3	1 * d	4244	
			3 * d	4345	
			5 * d	3935	
		4	1 * d	7893	
			3 * d	7964	
			5 * d	6911	
	0.7	1	1 * d	2176	305.21
			3 * d	1912	242.65
			5 * d	2020	318.22
		2	1 * d	7825	280.59
			3 * d	6561	236.81
			5 * d	8274	363.79
		3	1 * d	18376	332.99
			3 * d	15558	258.07
			5 * d	15952	305.39
		4	1 * d	34830	341.28
			3 * d	24554	208.31
			5 * d	30387	339.69
	0.9	1	1 * d	17644	3185.66
			3 * d	18146	3151.97
		2	1 * d	65114	3067.02
			3 * d	67670	3373.82
		3	1 * d	140896	3219.89
			3 * d	159069	3560.97
4		1 * d	253989	3117.90	
		3 * d	282792	3450.88	

Table A-3.4. Pressure Drop variations in a Horizontal Pipe carrying Heavy-Density Cylindrical Capsules

N/Lp	Sc	k	Lc	Vav	$\Delta P_m/L_p$	Difference w.r.t. k = 0.5
	(m)		(m)	(m/sec)	(Pa/m)	(%)
1	1	0.5	1 * d	1	430	N/A
				2	1705	
				3	3591	
				4	5649	
			3 * d	1	426	
				2	1718	
				3	3815	
				4	6741	
			5 * d	1	369	
				2	1342	
				3	3132	
				4	5109	
		0.7	1 * d	1	1820	323.26
				2	7005	310.85
				3	15725	337.90
				4	29651	424.89
			3 * d	1	1642	285.45
				2	6437	274.68
				3	14162	271.22
				4	24439	262.54
			5 * d	1	1788	384.55
				2	6978	419.97
				3	15383	391.16
				4	26488	418.46
		0.9	1 * d	1	15467	3496.98
				2	72471	4150.50
				3	162546	4426.48
				4	287444	4988.41
			3 * d	1	20483	4708.22
				2	79781	4543.83
				3	177241	4545.90
				4	312411	4534.49
5 * d	1		23874	6369.92		
	2		92006	6755.89		
	3		203124	6385.44		
	4		356183	6871.68		
2	1 * d	0.5	1 * d	1	425	N/A
				2	1608	
				3	3757	
				4	6579	

			3 * d	1	383		
				2	1587		
				3	3535		
				4	5313		
			5 * d	1	447		
				2	1724		
				3	3956		
				4	6154		
		0.7	1 * d	1	2018		374.82
				2	8628		436.57
				3	17099		355.12
				4	32888		399.89
			3 * d	1	2182		469.71
				2	8506		435.98
				3	17445		393.49
				4	30342		471.09
	5 * d		1	2740	512.98		
			2	11221	550.87		
			3	24998	531.90		
			4	42641	592.90		
	0.9	1 * d	1	22001	5076.71		
			2	86137	5256.78		
			3	195219	5096.14		
			4	346480	5166.45		
		3 * d	1	30731	7923.76		
			2	118479	7365.60		
			3	261319	7292.33		
			4	458273	8525.50		
5 * d		1	33963	7497.99			
		2	128632	7361.25			
		3	281606	7018.45			
		4	492858	7908.74			
3 * d	0.5	1 * d	1	540	N/A		
			2	2312			
			3	5512			
			4	9186			
		3 * d	1	511			
			2	1883			
			3	4317			
			4	8471			
		5 * d	1	536			
			2	2074			
			3	4397			
			4	7760			
	0.7	1 * d	1	2662		392.96	
			2	10545		356.10	

			3 * d	3	23643	328.94	
				4	40731	343.40	
				1	2786	445.21	
				2	10318	447.96	
				3	23539	445.26	
				4	40213	374.71	
			5 * d	1	3290	513.81	
				2	12897	521.84	
				3	28282	543.21	
				4	50014	544.51	
			0.9	1 * d	1	31000	5640.74
					2	116924	4957.27
	3	263176			4674.60		
	4	456841			4873.23		
	3 * d	1		35935	6932.29		
		2		140433	7357.94		
		3		313461	7161.08		
		4		553679	6436.17		
	5 * d	0.5	1 * d	1	632	N/A	
				2	2508		
3				5486			
4				9141			
3 * d			1	528			
			2	2353			
			3	4774			
			4	8759			
5 * d			1	614			
			2	2465			
			3	5075			
			4	10020			
0.7		1 * d	1	2916	361.39		
			2	11574	361.48		
			3	26503	383.10		
			4	45932	402.48		
	3 * d	1	3341	532.77			
		2	13171	459.75			
		3	28732	501.84			
		4	51640	489.57			
0.9	1 * d	1	36720	2.18			
		2	148096	5.46			
		3	331816	5.86			
		4	588755	6.34			
	3 * d	1	39349	6126.11			
		2	153083	6003.79			
		3	339547	6089.34			
		4	596617	6426.82			

A-4: Pressure Drop in Vertical HCPs

Table A-4.1. Pressure Drop variations in a Vertical Pipe carrying Equi-Density Spherical Capsules

N/Lp	k	V_{av} (m/sec)	Sc (m)	ΔP_m/Lp (Pa/m)	Difference w.r.t. k = 0.5 (%)
1	0.5	1	1	9929	N/A
		2		10237	
		3		10708	
		4		11335	
	0.7	1		9992	0.63
		2		10464	2.22
		3		11192	4.52
		4		12164	7.31
	0.9	1		11276	13.57
		2		15151	48.00
		3		21296	98.88
		4		29357	158.99
2	0.5	1	1 * d	9953	N/A
			3 * d	9954	
			5 * d	9955	
		2	1 * d	10325	
			3 * d	10328	
			5 * d	10329	
		3	1 * d	10901	
			3 * d	10905	
			5 * d	10911	
		4	1 * d	11669	
			3 * d	11678	
			5 * d	11687	
	0.7	1	1 * d	10082	1.30
			3 * d	10083	1.30
			5 * d	10087	1.33
		2	1 * d	10785	4.46
			3 * d	10792	4.49
			5 * d	10810	4.66
		3	1 * d	11882	9.00
			3 * d	11898	9.11
			5 * d	11937	9.40
		4	1 * d	13354	14.44
			3 * d	13383	14.60
			5 * d	13452	15.10
0.9	1	1 * d	12978	30.39	

			3 * d	12620	26.78	
			5 * d	12582	26.39	
			2	1 * d	21236	105.68
				3 * d	20059	94.22
				5 * d	19935	93.00
			3	1 * d	34527	216.73
		3 * d		31799	191.60	
		5 * d		31582	189.45	
		4	1 * d	52802	352.50	
			3 * d	47956	310.65	
			5 * d	47364	305.27	
		3	0.5	1	1 * d	9978
3 * d	9980					
5 * d	9980					
2	1 * d			10415		
	3 * d			10427		
	5 * d			10425		
3	1 * d			11098		
	3 * d			11122		
	5 * d			11119		
4	1 * d			12013		
	3 * d			12054		
	5 * d			12054		
0.7	1		1 * d	10183	2.05	
			3 * d	10193	2.13	
			5 * d	10208	2.28	
	2		1 * d	11147	7.03	
			3 * d	11197	7.38	
			5 * d	11238	7.80	
	3		1 * d	12650	13.98	
			3 * d	12764	14.76	
			5 * d	12846	15.53	
	4		1 * d	14677	22.18	
			3 * d	14883	23.47	
			5 * d	15013	24.55	
0.9	1	1 * d	14516	45.48		
		3 * d	14114	41.42		
	2	1 * d	26759	156.93		
		3 * d	25562	145.15		
	3	1 * d	46121	315.58		
		3 * d	43751	293.37		
	4	1 * d	74044	516.37		
		3 * d	67843	462.83		

Table A-4.2. Pressure Drop variations in a Vertical Pipe carrying Equi-Density Cylindrical Capsules

N/Lp	Sc	k	Lc	Vav	$\Delta Pm/Lp$	Difference w.r.t. k = 0.5
	(m)		(m)	(m/sec)	(Pa/m)	(%)
1	1	0.5	1 * d	1	10231	N/A
				2	11419	
				3	13356	
				4	16032	
			3 * d	1	10206	
				2	11313	
				3	13107	
				4	15574	
			5 * d	1	10219	
				2	11354	
				3	13194	
				4	15714	
		0.7	1 * d	1	11347	10.91
				2	15812	38.47
				3	23182	73.57
				4	33399	108.33
			3 * d	1	11401	11.71
				2	15979	41.24
				3	23492	79.23
				4	33914	117.76
			5 * d	1	11696	14.45
				2	17158	51.12
				3	26143	98.14
				4	38632	145.84
		0.9	1 * d	1	29823	172.66
				2	87967	484.11
				3	183684	734.74
				4	316739	900.35
			3 * d	1	34021	208.89
				2	102000	567.54
				3	212341	848.09
				4	364456	1028.73
5 * d	1		38426	241.17		
	2		116956	615.47		
	3		243237	879.94		
	4		416256	1036.81		
2	1 * d	0.5	1 * d	1	10258	N/A
				2	11508	
				3	13514	
				4	16299	
			3 * d	1	10287	

				2	11590		
				3	13750		
				4	16692		
				1	10333		
			5 * d	2	11767		
				3	14074		
				4	17245		
				1	11665		13.72
		0.7	1 * d	2	17004		47.76
				3	25721		90.33
				4	37808		131.97
				1	12022		16.87
			3 * d	2	18254		57.50
				3	28857		109.87
				4	43418		160.11
				1	12663		22.55
	5 * d		2	20882	77.46		
			3	33442	137.62		
			4	52536	204.64		
			1	44188	330.77		
	0.9	1 * d	2	143168	1144.07		
			3	306066	2164.81		
			4	532962	3169.91		
			1	53724	422.25		
		3 * d	2	176021	1418.73		
			3	374291	2622.12		
			4	647113	3776.79		
			1	66068	539.39		
		5 * d	2	219515	1765.51		
			3	463935	3196.40		
			4	799111	4533.87		
			1	10369	N/A		
3 * d	0.5	1 * d	2	11938			
			3	14489			
			4	18008			
			1	10377			
		3 * d	2	11948			
			3	14489			
			4	17981			
			1	10424			
	5 * d	2	12122				
		3	14860				
		4	18626				
		0.7	1 * d	1		12223	17.88
2	19123			60.19			
3	30423			109.97			

				4	46074	155.85
			3 * d	1	12574	21.17
				2	20411	70.83
				3	33189	129.06
				4	50845	182.77
			5 * d	1	13748	31.89
				2	24903	105.44
				3	43056	189.74
				4	68116	265.70
		0.9	1 * d	1	49136	373.87
				2	163508	1269.64
				3	351832	2328.27
				4	613642	3307.61
			3 * d	1	61508	492.73
				2	207632	1637.80
				3	445450	2974.40
				4	773794	4203.40
	5 * d	0.5	1 * d	1	10420	N/A
				2	12137	
				3	14936	
				4	18798	
			3 * d	1	10420	
				2	12120	
				3	14874	
				4	18664	
			5 * d	1	10469	
				2	12302	
				3	15271	
				4	19351	
		0.7	1 * d	1	12515	20.11
				2	20328	67.49
				3	33224	122.44
				4	51028	171.45
			3 * d	1	13056	25.30
				2	22384	84.69
				3	37669	153.25
				4	58874	215.44
	0.9	1 * d	1	50533	384.96	
			2	169431	1295.99	
			3	365594	2347.74	
			4	638664	3297.51	
		3 * d	1	62723	501.95	
			2	212481	1653.14	
			3	456385	2968.34	
			4	793272	4150.28	

Table A-4.3. Pressure Drop variations in a Vertical Pipe carrying Heavy-Density Spherical Capsules

N/Lp	k	V_{av}	Sc	ΔP_m/Lp	Difference w.r.t. k = 0.5		
		(m/sec)	(m)	(Pa/m)	(%)		
1	0.5	2	1	10255	N/A		
		3		10730			
		4		11361			
	0.7	1		10020	2.38		
		2		10499	4.69		
		3		11233	7.53		
	0.9	4		12216	N/A		
		1		11369	47.49		
		2		15125	96.21		
		3		21053	154.11		
	2	0.5		2	1 * d	10378	N/A
					3 * d	10370	
5 * d			10372				
3			1 * d	10956			
			3 * d	10951			
			5 * d	10961			
4			1 * d	11724			
			3 * d	11730			
			5 * d	11745			
0.7		1	1 * d	10211	5.17		
			3 * d	10169			
			5 * d	10154			
		2	1 * d	10915		5.00	
			3 * d	10888		5.09	
			5 * d	10900		9.71	
		3	1 * d	12020		9.73	
			3 * d	12017		9.99	
			5 * d	12056		15.20	
		4	1 * d	13506		15.29	
			3 * d	13524		15.82	
			5 * d	13603		N/A	
		0.9	1	1 * d		12954	103.19
				3 * d		12862	
				5 * d		12814	
2	1 * d		21087	97.15			
	3 * d		20444	95.23			
	5 * d		20249	216.33			
3	1 * d		34657	195.59			
	3 * d		32370	192.04			
	5 * d		32011				

		4	1 * d	54348	363.56
			3 * d	48523	313.67
			5 * d	48316	311.38
3	0.5	2	1 * d	10556	N/A
			3 * d	10522	
			5 * d	10510	
		3	1 * d	11266	
			3 * d	11243	
			5 * d	11221	
		4	1 * d	12217	
			3 * d	12201	
			5 * d	12174	
	0.7	1	1 * d	10445	
			3 * d	10313	
			5 * d	10330	
		2	1 * d	11487	8.82
			3 * d	11401	8.35
			5 * d	11417	8.63
		3	1 * d	13088	16.17
			3 * d	13029	15.89
			5 * d	13082	16.58
		4	1 * d	15293	25.18
			3 * d	15197	24.56
			5 * d	15305	25.72
	0.9	1	1 * d	14800	N/A
			3 * d	14500	
		2	1 * d	27655	161.98
			3 * d	26243	149.41
		3	1 * d	47281	319.68
			3 * d	44717	297.73
4		1 * d	75026	514.11	
		3 * d	69725	471.47	

Table A-4.4. Pressure Drop variations in a Vertical Pipe carrying Heavy-Density Cylindrical Capsules

N/Lp	Sc	k	Lc	Vav	$\Delta P_m/L_p$	Difference w.r.t. k = 0.5	
	(m)		(m)	(m/sec)	(Pa/m)	(%)	
1	1	0.5	1 * d	2	11456	N/A	
				3	13418		
				4	16117		
			3 * d	3	13260		
				4	15770		
				5 * d	3		13473
		0.7	1 * d	4	16062		
				1	11395		
				2	15909		
			3 * d	3	23302	38.87	
				4	33558	73.66	
				2	16237	108.21	
			5 * d	3	23835	N/A	
				4	34329	79.75	
				2	17667	117.69	
			0.9	1 * d	3	26829	N/A
					4	39517	99.13
					1	29935	146.03
		3 * d		2	88149	N/A	
				3	183927	669.46	
				4	317041	1270.75	
		5 * d		1 * d	1	34630	1867.12
					2	102998	N/A
					3	213691	1511.55
3 * d	4			366120	2221.62		
	1			39753	N/A		
	2			119123	N/A		
5 * d	1 * d	3	246107	1726.67			
		4	419876	2514.10			
		1	11566	N/A			
	0.5	1 * d	2	13612	N/A		
			3	16418	N/A		
			4	16991	N/A		
3 * d		3	13997	N/A			
		4	16991	N/A			
		5 * d	3	14480	N/A		
0.7	1 * d	4	17691	N/A			
		1	11746	N/A			
		2	17149	48.27			
	3 * d	3	25931	90.50			
		4	38025	131.61			
		2	18829	N/A			

				3	28546	103.94	
				4	43029	153.25	
				5 * d	2	21738	N/A
					3	35128	142.60
			0.9	1 * d	4	51369	190.37
					1	44431	N/A
					2	144045	1145.42
					3	306266	2149.97
		3 * d	3 * d	4	531966	3140.14	
				1	54907	N/A	
				2	178063		
				3	377076	2593.98	
		5 * d	5 * d	4	650084	3726.05	
				1	68682	N/A	
				2	224072		
				3	469608	3143.15	
	3 * d	0.5	1 * d	4	804323	4446.51	
				2	12010	N/A	
				3	14592		
			4	18139			
			3 * d	3	14776		
				4	18341		
			5 * d	3	15379		
				4	19250		
		0.7	1 * d	1	12320		60.76
				2	19307	110.06	
				3	30652	155.41	
				4	46328	N/A	
3 * d			2	20952	129.57		
			3	33921	182.12		
			4	51743	N/A		
			2	25945	188.59		
5 * d	5 * d	3	44383	262.20			
		4	69724	N/A			
		1	49373	1264.69			
		2	163899	2314.88			
0.9	1 * d	3	352379	3286.92			
		4	614353	N/A			
		1	62750				
		2	209677	2933.39			
	3 * d	3 * d	3	448214	4137.71		
			4	777239			
			2	12164	N/A		
			3	14925			
4	18818						
3 * d	3	15185					

				4	19062	
			5 * d	3	15846	
				4	20044	
				1	12614	
		0.7	1 * d	2	20522	68.71
				3	33430	123.99
				4	51327	172.75
				2	22974	N/A
			3 * d	3	38499	153.53
				4	59884	214.15
				1	50754	N/A
		0.9	1 * d	2	169753	1295.54
				3	366062	2352.68
				4	639243	3296.98
				1	63954	N/A
			2	214503		
			3 * d	3	459135	2923.61
				4	796684	4079.44

A-5: Pressure Drop in HCP Bends

Table A-5.1. Pressure Drop variations in Horizontal Bends carrying Equi-Density Capsules

Ψ	N/Lp	r/R	k	Lc (m)	Sc (m)	Vav (m/sec)	$\Delta P_m/L_p$ (Pa/m)
1	1	4	0.5	1 * d	1	1	169
			0.7			4	2010
						1	244
			4			3039	
	2	4	1 * d		1	378	
			3 * d			602	
	1	8	0.5		1	151	
						4	1846
			0.7			1	221
						4	2707
	2	4	1 * d		1	658	
			3 * d			654	
0.8094	1	4	0.5	1	1	522	
			0.7			4	7718
						1	1892
			4			29019	
	2	4	1 * d		1	3101	
			2 * d			3264	
0.645	2	4	2 * d	1	1 * d	2761	
			2 * d		3310		
0.8094	1	8	0.5	1 * d	1	463	
						4	6804

0.645	2	0.7			1	1742
					4	26749
					1 * d	2851
					2 * d	2742
	2 * d		1	1 * d	2056	
				2 * d	2189	

Table A-5.2. Pressure Drop variations in Horizontal Bends carrying Heavy-Density Capsules

Ψ	N/Lp	r/R	k	Lc (m)	Sc (m)	Vav (m/sec)	$\Delta P_m/L_p$ (Pa/m)
1	1	4	0.5	1 * d	1	1	246
						4	2899
			1			581	
			4			8523	
	2		0.7		1 * d	2365	
					3 * d	1203	
	1	8	0.5		1	4	3033
						1	520
			0.7			4	7522
						1 * d	1190
	2		0.7		3 * d	1148	
					548		
0.8094	1	4	0.5	1	4	7247	
					1	1819	
			0.7		4	25470	

					1 * d		6654
					2 * d		4247
0.645	2			2 * d	1 * d	1	3868
					2 * d		5009
			0.5				460
	1			1 * d	1	4	6589
0.8094						1	1584
		8				4	23612
			0.7		1 * d		1957
					2 * d		1897
	2			2 * d	1 * d	1	2400
0.645					2 * d		2667

Table A-5.3. Pressure Drop variations in Vertical Bends carrying Equi-Density Capsules

Ψ	N/Lp	r/R	k	Lc	Sc	Vav	$\Delta P_m/L_p$
				(m)	(m)	(m/sec)	(Pa/m)
			0.5			1	5995
	1				1	4	8612
		4				1	6280
			0.7			4	13997
1	2			1 * d	1 * d		6735
					3 * d	1	7328
			0.5				6773
	1				1	4	8881
		8				1	7986
			0.7			4	15253

	2				1 * d		11167
					3 * d	1	10274
			0.5				7407
	1				1	4	11556
0.8094		4				1	12461
						4	28570
			0.7		1 * d		28533
	2				2 * d		45627
0.645				2 * d	1 * d	1	20315
					2 * d		37333
			0.5				7523
	1				1	4	11545
0.8094		8		1 * d		1	10866
						4	28296
			0.7		1 * d		34232
	2				2 * d		37387
0.645				2 * d	1 * d	1	27002
					2 * d		38734

Table A-5.4. Pressure Drop variations in Vertical Bends carrying Heavy-Density Capsules

Ψ	N/Lp	r/R	k	Lc	Sc	Vav	$\Delta P_m/L_p$
				(m)	(m)	(m/sec)	(Pa/m)
			0.5			1	6312
						4	8562
1	1	4		1 * d	1	1	7370
			0.7			4	14094

	2	8	0.5		1 * d	1	10453
					3 * d		10419
	1		6642				
			4		9379		
			1		7416		
	2		0.7		4	14910	
			1 * d		1	8214	
						3 * d	8520
	6979						
	0.8094		1		4	0.5	
1		11318					
2		0.7	4	26685			
			1 * d	29058			
0.645	2	2 * d		1 * d	1	23476	
				2 * d		41899	
0.8094	1	8	0.5	1 * d	1	7511	
						4	12444
	1		11775				
0.645	2	0.7		2 * d	1	4	28560
						1 * d	24913
	2 * d					27346	
	1 * d					19598	
				2 * d		29969	

A-6: Expressions for Capsule Velocities and Friction Factor in HCPs

Table A-6.1. Holdup Data

Pipeline Orientation	Capsule Shape	Density of the Capsules	Holdup Expressions
Horizontal	Spherical	Equi-Density	$\frac{V_c}{V_{av}} = 1.22 - (0.15 * k)$
		Heavy-Density	$\frac{V_c}{V_{av}} = 1.067 - (0.0196 * s) + (0.042 * k)$
	Cylindrical	Equi-Density	$\frac{V_c}{V_{av}} = \left[\frac{1}{\left\{ \frac{7}{4} k (1 - k) + \frac{49}{60} (1 - k^2) + k^2 \right\}} \right]$
		Heavy-Density	$\frac{V_c}{V_{av}} = 0.77 - \left(0.008 * \frac{Lc}{d} \right) + (0.302 * k)$
Vertical	Spherical	Equi-Density	$\frac{V_c}{V_{av}} = \frac{1}{k^{0.34}}$
		Heavy-Density	$V_c = \frac{V_{av}}{k^{0.34}} \left(\frac{\left(\frac{4}{3} gD(s-1) \right)}{k} (1 - k^2) \left(1 - \frac{1}{s} \right)^{0.05} \right)$

	Cylindrical	Equi-Density	$\frac{Vc}{Vav} = \frac{1}{k^{0.128}} * \left(\frac{Lc}{d}\right)^{0.128}$
		Heavy-Density	$Vc = \frac{Vav}{k^{0.128}} \left(\frac{Lc}{d}\right)^{0.128} - \frac{\left(\sqrt{2gD \left(\frac{Lc}{d}\right)} (s-1) (1-k^2) \left(1-\frac{1}{s}\right)^{0.05}\right)}{k^{0.128}}$

Table A-6.2. f_c and K_{lc} Expressions

Pipeline Orientation	Capsule Shape	Density of the Capsules	f_c and K_{lc} Expressions
Horizontal	Spherical	Equi-Density	$f_c = \frac{\left(2.63 \left(\frac{N}{Lp} * d\right)^{1.069} k^{2.56} \frac{Sc + Lp^{0.218}}{Lp}\right)}{Re_c^{0.116}}$
		Equi-Density	$K_{lc} = \frac{\left(22387 \left(\frac{N}{Lp} * d\right)^{2.26} k^{3.5} \frac{Sc + Lp^{1.5}}{Lp}\right)}{Re_c^{0.38} \frac{r^{0.2}}{R}}$
		Heavy-Density	$f_c = \frac{\left(5.5 \left(\frac{N}{Lp} * d\right)^{0.87} k^{4.12}\right)}{Re_c^{0.004} \frac{Sc + Lp^{0.089}}{Lp}}$

			$K_{lc} = \frac{\left(138 \left(\frac{N}{Lp} * d\right)^{0.66} k^{3.5}\right)}{Re_c^{0.077} \frac{r^{0.2}}{R} \frac{Sc + Lp}{Lp}^{1.17}}$
	Cylindrical	Equi-Density	$f_c = \frac{\left(13.18 \left(\frac{N}{Lp} * Lc\right)^{0.178} k^{5.13} \frac{Lc^{0.1}}{d} \frac{Sc + Lp}{Lp}^{0.1}\right)}{Re_c^{0.117}}$
			$K_{lc} = \frac{\left(691 \left(\frac{N}{Lp} * Lc\right)^{1.63} k^{2.92} \frac{Sc + Lp}{Lp}^{1.05}\right)}{Re_c^{0.026} \frac{r^{0.2}}{R} \frac{Lc}{d}^{1.88}}$
		Heavy-Density	$f_c = \frac{\left(3.38 \left(\frac{N}{Lp} * Lc\right)^{0.016} k^{5.24} \frac{Lc^{0.1}}{d} \frac{Sc + Lp}{Lp}^{0.1}\right)}{Re_c^{0.019}}$
			$K_{lc} = \frac{\left(549 \left(\frac{N}{Lp} * Lc\right)^{0.5} k^{3.92}\right)}{Re_c^{0.14} \frac{Lc}{d}^{0.43} \frac{r^{0.2}}{R} \frac{Sc + Lp}{Lp}^{0.45}}$
Vertical	Spherical	Equi-Density	$f_c = \frac{\left(2.75 \left(\frac{N}{Lp} * d\right)^{1.058} k^{2.59} \frac{Sc + Lp}{Lp}^{0.2}\right)}{Re_c^{0.12}}$
			$K_{lc} = \frac{\left(33884 \left(\frac{N}{Lp} * d\right)^{1.19} k^{3.24} \frac{Sc + Lp}{Lp}^{1.39}\right)}{Re_c^{0.55} \frac{r^{0.2}}{R}}$
		Heavy-Density	$f_c = \frac{\left(5.58 \left(\frac{N}{Lp} * d\right)^{1.12} k^{2.64} \frac{Sc + Lp}{Lp}^{0.074}\right)}{Re_c^{0.146}}$
			$K_{lc} = \frac{\left(10^{5.6} \left(\frac{N}{Lp} * d\right)^{0.044} k^{4.33} \frac{Sc + Lp}{Lp}^{0.036}\right)}{Re_c^{0.83} \frac{r^{0.2}}{R}}$

	Cylindrical	Equi-Density	$f_c = \frac{\left(6.3 \left(\frac{N}{Lp} * Lc\right)^{0.13} k^{4.96} \frac{Lc^{0.1}}{d} \frac{Sc + Lp^{0.1}}{Lp}\right)}{Re_c^{0.07}}$
			$K_{lc} = \frac{\left(10^{6.8} \left(\frac{N}{Lp} * Lc\right)^{1.22} k^{4.5} \frac{Sc + Lp^{1.35}}{Lp}\right)}{Re_c^{0.81} \frac{r^{0.2}}{R} \frac{Lc^{1.5}}{d}}$
		Heavy-Density	$f_c = \frac{\left(4.16 \left(\frac{N}{Lp} * Lc\right)^{0.14} k^{4.8} \frac{Lc^{0.1}}{d} \frac{Sc + Lp^{0.1}}{Lp}\right)}{Re_c^{0.035}}$
			$K_{lc} = \frac{\left(10^8 \left(\frac{N}{Lp} * Lc\right)^{1.33} k^{4.5} \frac{Sc + Lp^{1.35}}{Lp}\right)}{Re_c^{0.96} \frac{r^{0.2}}{R} \frac{Lc^{1.58}}{d}}$

LIST OF PUBLICATIONS

- Asim, T. Mishra, R. Saqib, M. and Ubbi, K. (2011) “Optimisation of a Pipeline transporting capsules Carrying Spherical Capsules”, In the Proceedings of Maintenance Performance Measurement and Management Conference, Lulea, Sweden
- Asim, T. Mishra, Saqib, M. and Ubbi, K. (2011) “Pressure Drop in Pipeline transporting capsules Carrying Spherical Capsules”, In the Proceedings of the 38th National Conference on Fluid Mechanics and Fluid Power, Bhopal, India
- Asim, T. Mishra, R. and Pradhan, S. (2012) “A Study on Optimal Sizing of Pipeline Transporting Equi-sized Particulate Solid-Liquid Mixture”, Journal of Physics: Conference Series, vol. 364
- Asim, T. and Mishra, R. (2012) “Optimal Design of Pipeline transporting capsules carrying Spherical Capsules”, Journal of Physics: Conference Series, vol. 364
- Asim, T. Mishra, and R. Ido, I. (2012) “Pressure Drop in Bends, transporting capsules Carrying Spherical Capsules”, Journal of Physics: Conference Series, vol. 364
- Asim, T. Mishra, R. and Kollar, L. (2012) “Optimisation of a Horizontal Pipeline transporting capsules carrying Cylindrical Capsules”, Journal of Physics: Conference Series, vol. 364
- Asim, T. Mishra, R. Nearchou, A. and Ubbi, K. (2012) “Effect of the Length and Diameter of a Cylindrical Capsule on the Pressure Drop in a Horizontal Pipeline”, Journal of Physics: Conference Series, vol. 364
- Asim, T. Mishra, R. and Rao, V. (2012) “Effect of Eccentricity on Pipe Boundary Layer Growth for Flows in Annulus”, In the Proceedings of The Queen’s Diamond Jubilee Computing and Engineering Annual Researchers’ Conference, University of Huddersfield, UK
- Asim, T. Mishra, R. and Rao, V. (2012) “Spatiotemporal Growth of Laminar Boundary Layers in a Concentric Annulus”, In the Proceedings of The Queen’s Diamond Jubilee Computing and Engineering Annual Researchers’ Conference, University of Huddersfield, UK